Volume 13S, October 2020 ISSN 2352-1872

ELSEVIER

Abstracts of the ECTS Congress 2020

47th European Calcified Tissue Society Congress
ECTS 2020 Digital Congress
Live Prime Time: 22 - 24 October 2020
ECTS@Home weekly: 1 October - 8 December 2020

Bone Reports 13 (2020)

Contents lists available at ScienceDirect

Bone Reports

journal homepage: www.elsevier.com/locate/bonr

Volume 13S, October 2020

Abstracts of the ECTS Congress 2020

47th European Calcified Tissue Society Congress
ECTS 2020 Digital Congress
Live Prime Time: 22 - 24 October 2020
ECTS@Home weekly: 1 October - 8 December 2020

The publication of this Supplement is supported by the European Calcified Tissue Society.

Bone Reports 13 (2020)

Contents lists available at ScienceDirect

Bone Reports

journal homepage: www.elsevier.com/locate/bonr

Volume: 13S, October 2020

Contents page

Abstracts of the ECTS Congress 2020

47th European Calcified Tissue Society Congress
ECTS 2020 Digital Congress
Live Prime Time: 22 - 24 October 2020
ECTS@Home weekly: 1 October - 8 December 2020

2352-1872(202010)13:S;1-T

Bone Reports 13 (2020) 100710

Contents lists available at ScienceDirect

Bone Reports

journal homepage: www.elsevier.com/locate/bonr

Abstracts of the ECTS Congress 2020

47th European Calcified Tissue Society Congress
ECTS 2020 Digital Congress
Live Prime Time: 22 - 24 October 2020
ECTS@Home weekly: 1 October - 8 December 2020

Scientific Programme Committee

Chair:
Anna Teti (L'Aquila, Italy)
Co-Chairs:
Bo Abrahamsen (Holbæk, Denmark)
Clinical Co-Chair:
Christian Meier (Basel, Switzerland)
Pre-Clinical Co-Chair:
Christa Maes (Leuven, Belgium)

Members:
Bram Van der Eerden (Rotterdam, The Netherlands)
Eleni Douni (Vari, Greece)
Natalie Butterfield (London, UK), ECTS Academy
Pawel Pludowski (Warsaw, Poland)
Peter Pietschmann (Vienna, Austria)

Local Organising Committee
Chair:
Martine Cohen-Solal (Paris, France)
Members:
Roland Chapurlat (Lyon, Paris)
Eric Lespessailles (Orléans, France)
Anne Blangy (Montpellier, France)
Frederic Velard (Reims, France)
Thomas Funk-Brentano (Paris, France), New Investigator, ECTS Academy
Amelie Coudert (Paris, France), New Investigator

Abstract Review Panel
Each abstract was scored blind.
Abrahamsen, Bo (Denmark)
Alonso, Nerea (United Kingdom)
Arnett, Tim (United Kingdom)
Aspden, Richard (United Kingdom)
Athanas, Anastasilakis (Greece)
Baklacı, Korhan (Turkey)
Baleanu, Felicia (Belgium)
Baschant, Ulrike (Germany)
Bassett, Duncan (United Kingdom)
Bergwitz, Clemens (United States of America)
Bianchi, Maria Luisa (Italy)
Blin, Claudine (France)
Body, Jean-Jacques (Belgium)
Bonnet, Nicolas (Switzerland)
Borda, Ileana Monica (France)
Bouillon, Roger (Belgium)
Boyde, Alan (United Kingdom)
Briot, Karine (France)
Busse, Björn (Germany)
Butterfield, Natalie (United Kingdom)
Cancela, M.Leonor (Portugal)
Cappariello, Alfredo (Italy)
Capulli, Mattia (Italy)
Carmeliet, Gertrudis (Belgium)
Carsote, Mara (Romania)
Cenci, Simone (Italy)
Chapurlat, Roland (France)
Chenu, Chantal (United Kingdom)
Cipriani, Cristiana (Italy)
Clark, Emma (United Kingdom)
Cohen-Solal, Martine (France)
Colaianni, Graziana (Italy)
Colangelo, Luciano (Italy)
Coleman, Robert (United Kingdom)
Compston, Juliet (United Kingdom)
Cormier-Daire, Valerie (France)
Cosman, Felicia (United States of America)
Dawson-Hughes, Bess (United States of America)
de Vries, Teun (The Netherlands)
Delaisse, Jean-Marie (Denmark)
Diez-Perez, Adolfo (Spain)
Douni, Eleni (Greece)
Ducy, Patricia (United States of America)
Edwards, Claire (United Kingdom)
Elefteriou, Florent (United States of America)
Elson, Ari (Israel)
Estrada, Karol (United States of America)
Farquharson, Colin (United Kingdom)
Findaly, David (Australia)
Forlino, Antonella (Italy)
Fukumoto, Seiji (Japan)
Funck-Brentano, Thomas (France)
Galbusera, Fabio (Italy)
Gautvik, Kaare (Norway)
Gennari, Luigi (Italy)
Geoffroy, Valerie (France)
Gianfrancesco, Fernando (Italy)
Glueer, Claus (Germany)
Goldring, Mary (United States of America)
Gregory, Jenny (United Kingdom)

https://doi.org/10.1016/j.bonr.2020.100710

2352-1872

Grigoriadis, Agi (United Kingdom)
Grinberg, Daniel (Spain)
Guanabens, Nuria (Spain)
Guarnieri, Vito (Italy)
Hadji, Peyman (Germany)
Haffner-Luntzer, Melanie (Germany)
Hay, Eric (France)
Herrman, Marietta (Germany)
Hofbauer, Lorenz (Germany)
Ignatius, Anita (Germany)
Jafari, Abbas (Denmark)
Jähn, Katharina (Germany)
Jakob, Franz (Germany)
Kiviranta, Riku (Finland)
Klaushofer, Klaus (Austria)
Kornak, Uwe (Germany)
Lafage-Proust, Marie-Helene (France)
Langman, Craig (United States of America)
Lanske, Beate (United States of America)
Legeai-Mallet, Laurence (France)
Lems, Willem (The Netherlands)
Lerner, Ulf (Sweden)
Lips, Paul (The Netherlands)
Lorentzon, Mattias (Sweden)
Machuca, Irma (France)
Maurizi, Antonio (Italy)
Mazzaferro, Sandro (Italy)
McCabe, Laura (United States of America)
Menale, Ciro (Italy)
Merlotti, Daniela (Italy)
Milovanovic, Petar (Germany)
Minisola, Salvatore (Italy)
Misof, Barbara (Austria)
Müller, Ralph (Switzerland)
Nishimura, Riko (Japan)
Nuki, George (United Kingdom)
Oei, Ling (The Netherlands)
Ohlsson, Claes (Sweden)
Orriss, Isabel (United Kingdom)
Palermo, Andrea (Italy)
Paschalis, Eleftherios (Austria)
Peyruchaud, Olivier (France)
Pietschmann, Peter (Austria)
Pikner, Richard (Czech Republic)
Pitsillides, Andrew (United Kingdom)
Provot, Sylvain (France)
Ralston, Stuart (United Kingdom)
Ramasamy, Saravana (United Kingdom)
Rauner, Martina (Germany)
Reid, David (United Kingdom)
Rejnmark, Lars (Denmark)
Riminucci, Mara (Italy)
Roato, Ilaria (Italy)
Robey, Pamela Gehron (United States of America)
Rossi, Antonio (Italy)
Roux, Christian (France)
Rucci, Nadia (Italy)
Schäfer, Arne (Germany)
Schalin-Jantti, Camilla (Finland)
Schepelmann, Martin (Austria)
Schinke, Thorsten (Germany)
Schnabel, Dirk (Germany)
Schwarz, Peter (Denmark)
Siggelkow, Heide (Germany)
Sims, Natalie (Australia)
Sobacchi, Cristina (Italy)
Soe, Kent (Denmark)
Sommer, Nicole (Austria)
Staines, Katherine (United Kingdom)
Stenbeck, Gudrun (United Kingdom)
Szulc, Pawel (France)
Taipaleenmäki, Hanna (Germany)
Teti, Anna (Italy)
Tobias, Jon (United Kingdom)
Tsourdi, Elena (Germany)
Tuckermann, Jan (Germany)
Vacher, Jean (Canada)
van de Peppel, Jeroen (The Netherlands)
van der Eerden, Bram (The Netherlands)
van Driel, Marjolein (The Netherlands)
van Hul, Wim (Belgium)
Vestergaard, Peter (Denmark)
Vico, Laurence (France)
Villa, Anna (Italy)
Wagener, Raimund (Germany)
Weaver, Connie M (United States of America)
Williams, Graham (United Kingdom)
Yorgan, Timur (Germany)
Young, Marian (United States of America)
Zaucke, Frank (Germany)
Zhou, Hong (Australia)
Zwerina, Jochen (Austria)

Bone Reports 13 (2020) 100320

Contents lists available at ScienceDirect

Bone Reports

journal homepage: www.elsevier.com/locate/bonr

Plenary Oral Presentations

Plenary Oral Presentations 1: Cross talk between bone and metabolism

PLO07

Plasma sclerostin is associated with visceral adipose tissue but not subcutaneous adipose tissue in men and women in the Framingham Study

Douglas Kiel[a], Timothy Tsai[b], Ching-Ti Liu[c], Marian Hannan[a], Thomas Travison[a], Clifford Rosen[d], Sundeep Khosla[e], Mary Bouxsein[f]
[a]*Marcus Institute for Aging Research, Harvard Medical School/Hebrew SeniorLife, Boston, United States*
[b]*Marcus Institute for Aging Research, Hebrew SeniorLife, Boston, United States*
[c]*Biostatistics, Boston University School of Public Health, Boston, United States*
[d]*Maine Medical Center Research Institute, Scarborough, United States*
[e]*Endocrinology, Mayo Clinic, Rochester, United States*
[f]*Center for Advanced Orthopaedic Studies, Harvard Medical School, Boston, United States*

Sclerostin, a 190 amino acid protein secreted primarily by osteocytes, was initially identified due to mutations in the *SOST* gene associated with high bone mass through Wnt signaling. LRP5-Wnt signaling in the osteoblast is capable of regulating body adiposity, and mice expressing high sclerostin levels had progressive loss of white adipose tissue. Thus sclerostin may represent a link between adipose tissue depots and skeletal status, although no previous studies have defined a potential relation in humans. We therefore determined the association between plasma sclerostin, and both visceral (VAT) and subcutaneous (SAT) adipose tissue in 265 men [mean (SD) age 58 (6) yr] and 234 post-menopausal women [mean (SD) age 60 (5) yr] from the 3rd Generation of the Framingham Osteoporosis Study. Sclerostin was measured from blood collected between 2016-2019 using the DiaSorin assay that measures intact sclerostin (ICC = 0.902; CV = 5.7%) without inclusion of sclerostin fragments. Participants underwent abdominal CT scans using an 8-slice multidetector CT scanner (LightSpeed Ultra; GE, Milwaukee, WI) to measure VAT and SAT (cm^3) between 2008-2011. Multiple linear regression was used to quantify the association between sclerostin and VAT and SAT, adjusting for age, sex, height, BMI, and self-reported activity level. Mean sclerostin concentration was significantly higher in men [472 (116) pg/mL] than women [396 (107) pg/mL]. After adjustment for age, sex, BMI, height and physical activity, each SD (117.8 pg/ml) difference in sclerostin was associated with 82 cm^3 greater VAT on average (p=0.027) Sclerostin was not significantly associated with SAT (β=-60.0; p=0.13). These results suggest the possibility that sclerostin secretion from bone may result in increased VAT accumulation in men and women, although confirmation is needed with more optimal timing of the measures and replication in other studies. If confirmed, these results suggest the possibility of lowering VAT by inhibiting sclerostin pharmacologically.

doi:10.1016/j.bonr.2020.100327

PLO08

KIAA1199 (CEMIP), a novel secreted factor from bone and bone marrow influences body composition and metabolism by regulating bone and fat

Li Chen[a,b], Kaikai Shi[a], Louise H.D. Nielsen[a], Nicholas Ditzel[a], Weimin Qiu[a], Michaela Tencerova[a], Florence Figeac[a], Thomas Levin Andersen[c], Justyna Kowal[a], Alexander Rauch[a], Moustapha Kassem[a]
[a]*Dept. of Endocrinology, Odense University Hospital, Odense, Denmark*
[b]*Guilin Medical University, Guilin, China*
[c]*Dept. of Pathology, Odense University Hospital, Odense, Denmark*

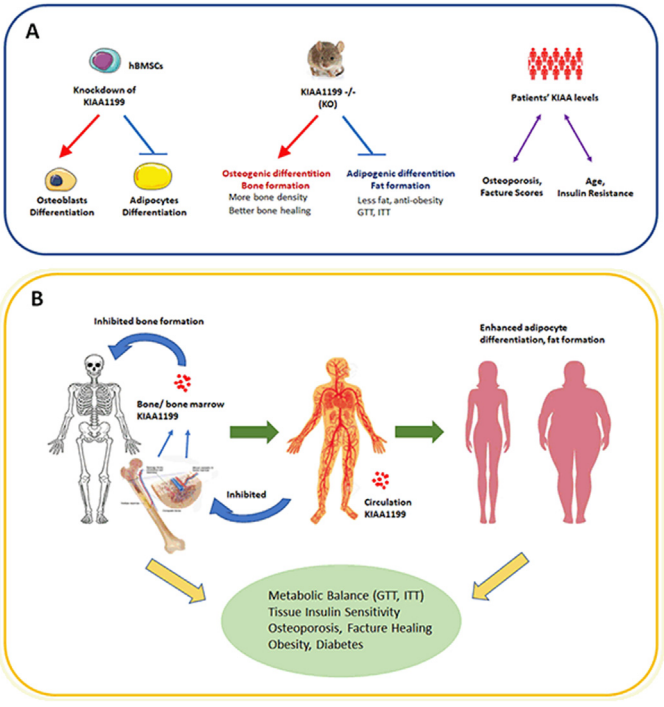

KIAA1199 influences body composition and metabolism by regulating bone and fat

2352-1872/$ – see front matter

Bone and bone marrow are realized as endocrinology organs, more and more secreted factors from bone or bone marrow had been identified to have roles in whole body metabolism and physiology. We have previously identified KIAA1199 as a novel secreted factor by human bone marrow stromal stem cells (hBMSCs). In the study, we further studied its roles in hBMSCs, knockout (KO) mice and clinical patients. *In vitro* induced deficiency of KIAA1199 in hBMSCs resulted to enhanced bone marrow osteoblast differentiation and impaired adipocyte differentiation, respectively. Consistently, *in vivo* KIAA1199^{KO} mice significantly enhanced trabecular and cortical bone density at BV/TV, Tb.N, Tb.den. and Ct.Th. ($p< 0.05$) and showed a faster bone healing in fracture models compare to the corresponding wild type (WT) mice ($p< 0.05$). On the other hand, the KIAA1199^{KO} mice exhibited significant decreases marrow adipose tissue (MAT), subcutaneous and visceral fat depots under both normal diet and high fat diet compared to WT controls ($p< 0.01$), they were also protected from glucose intolerance and insulin tolerance ($p< 0.05$) by increase the insulin sensitivity in different tissues. In clinical patients, bone marrow KIAA1199 levels is correlated to fracture predict factors and significant higher in osteoporosis patients ($p< 0.05$); while plasma KIAA1199 was correlated with the patients' age, plasma fasting glucose and fat mass ($p< 0.05$); furthermore, KIAA1199 levels in fat was significant higher in insulin resistance patients ($p< 0.05$). Our founding discovered KIAA1199 as a novel factor that play roles at bone and fat composition, and whole-body energy metabolism.

doi:10.1016/j.bonr.2020.100328

PLO09

αE-catenin deletion in skeletal stem and progenitor cells (SSPCs) increases their adipogenic potential and protects against diet- or age-induced obesity and hyperglycemia

Karen De Samblancx[a], Marion Mesnieres[a], Dana Trompet[a], Naomi Dirckx[a], Katrien Corbeels[b], Elena Nefyodova[a], Ruben Cardoen[a], Jolanda van Hengel[c], Frans van Roy[c], Greetje Vande Velde[d], Bart Van der Schueren[b], Chantal Mathieu[b], Christa Maes[a]

[a]*Laboratory of Skeletal Cell Biology and Physiology (SCEBP), Skeletal Biology and Engineering Research Center (SBE), KU Leuven, Leuven, Belgium*

[b]*Department of Chronic Diseases, Metabolism and Ageing, KU Leuven, Leuven, Belgium*

[c]*Department of Biomedical Molecular Biology, Ghent University; Inflammation Research Center, Flanders Institute for Biotechnology (VIB), Ghent, Belgium*

[d]*Molecular Small Animal Imaging Center (MoSAIC), Department of Imaging & Pathology, KU Leuven, Leuven, Belgium*

In this study, we generated conditional knock-out (cKO) mice in which the intracellular cell-cell adhesion complex component αE-catenin was deleted in Prx1-Cre-expressing skeletal stem/progenitor cells (SSPCs). MicroCT-analysis/histomorphometry showed that compared with control littermates, αE-catenin-cKO mice had a reduced trabecular bone mass (*BV/TV: 10.6±1.1% (control) versus 6.1±0.9% (αE-catenin-cKO); p=0.006;n=8; 18-week-old*) and excessive bone marrow adipose tissue (BMAT) (osmium-bound BMAT volume/TV: *0.15±0.05% (control) versus 1.71±0.61% (αE-catenin-cKO); p=0.02;n=11; 12-week-old)*. Increased adipogenesis in bone was exacerbated by high-fat diet (HFD), ageing or irradiation, and appeared a cell-autonomous consequence of αE-catenin loss, as mutant BMSCs *in vitro* showed increased adipogenic differentiation.

Changes in bone mass and BMAT can relate to altered systemic metabolism. Interestingly, when challenged by HFD for 16 weeks, control mice displayed increased glycemia and glucose-intolerance, whereas αE-catenin-cKO mice were largely protected against these adverse metabolic effects. Moreover, while the bodyweight of control mice on HFD doubled compared with genotype-matched littermates fed a normal diet (*51.6±5.3g on HFD versus 27.8±1.1g; p< 0.001;n=9-10*), αE-catenin-cKO animals on HFD did not develop obesity (*32.6±1.5g on HFD versus 25.4±0.7g; NS;n=9-10*). Indirect calorimetry revealed increased oxygen consumption and energy expenditure in αE-catenin-cKO mice (*p< 0.0001;n=9-10*), despite similar food intake and ambulatory activity as controls, suggesting increased burning and reduced peripheral accumulation of the dietary fat.

Notably, a similar beneficial metabolic phenotype was seen in αE-catenin-cKO mice upon ageing: 1-year-old mutant mice were significantly leaner and more glucose-tolerant than controls. Surprisingly, while increased BMAT was again pertinent, mutant mice at this age had more trabecular bone than controls. Thus, excessive BMAT rather than altered bone mass correlated consistently with the improved systemic metabolism in αE-catenin-cKO mice.

In conclusion, deletion of αE-catenin in Prx1-Cre+-SSPCs caused increased marrow adiposity while protecting the mice against challenged glucose homeostasis and obesity, implying novel links between SSPC fate control, BMAT and energy metabolism.

doi:10.1016/j.bonr.2020.100329

PLO10

Skin autofluorescence, a non-invasive biomarker for advanced glycation end-products, is associated with Sarcopenia: The Rotterdam study

Komal Waqas[a], Jinluan Chen[a,b], Katerina Trajanoska[a,b], M. Arfan Ikram[b], Fernando Rivadeneira[a,b], Andre Uitterlinden[a,b], M. Carola Zillikens[a]

[a]*Endocrinology, Internal Medicine, Erasmus Medical Center, Rotterdam, Netherlands*

[b]*Epidemiology, Erasmus Medical Center, Rotterdam, Netherlands*

Accumulation of advanced glycation end-products (AGEs) in skeletal muscle might be an underlying mechanism of primary sarcopenia. No studies have so far investigated the associations between skin AGEs, sarcopenia and its components namely appendicular skeletal mass index (ASMI), hand grip strength (HGS) and gait speed (GS) in a general Caucasian population.

In our cross-sectional analysis, 2744 participants with a mean age of 74.1 years (56% females, 13% diabetics) were included from the Rotterdam Study. Skin AGEs were measured with an AGE reader^{TM} as Skin autofluorescence (SAF), ASMI by insight dual energy X-ray absorptiometry, HGS by a hydraulic hand dynamometer and for a subgroup (n=2079), GS measured on an electronic walkway. We defined probable sarcopenia (low HGS) and sarcopenia (low HGS + low ASMI) based on European working group on Sarcopenia in older people revised criteria (EWGSOP2). Multivariate linear and logistic regression analysis were performed adjusting for age, sex, body fat percentage, height, renal function, diabetes and smoking status as covariates. Data was also analyzed in sex-stratified, age-adjusted SAF quartiles for comparison with the literature.

SAF was inversely associated with ASMI (β=-0.064, $p=3^{E-5}$), HGS (β=-0.054, $p=2^{E-5}$) and GS (β=-0.077, $p=3^{E-4}$). Prevalence of low ASMI was 7.7%, of probable sarcopenia 19% and of sarcopenia 3.5%. SAF was an independent predictor of low ASMI (odds ratio [OR]= 1.98, 95% confidence interval [CI] 1.47-2.67), probable sarcopenia OR=1.34 (95% CI: 1.07-1.67) and sarcopenia OR=1.98 (95% CI: 1.30-3.03). Comparing the bottom three SAF quartiles combined (Q1-3) with top quartile (Q4), the OR was 1.62 (95% CI: 1.18-2.23) for low

ASMI, 1.16 (95% CI: 0.91-1.47) for probable sarcopenia and 1.67 (95% CI: 1.06-2.65) for sarcopenia in the total population.

Higher skin AGEs are associated with low muscle mass, strength and function which is in line with the hypothesis that AGEs play a role in age-related sarcopenia.

doi:10.1016/j.bonr.2020.100330

PLO11

Cholesterol promotes myeloma cell viability and increases bone marrow myeloma tumour burden in vivo

Beatriz Gamez[a], Emma V. Morris[a], Sam W.Z. Olechnowicz[b], Sowman Aneka[b], Christina J. Turner[a], Seint T. Lwin[a], Matthew T. Drake[c], Claire M. Edwards[a,b]

[a]*Nuffield Department of Surgical Sciences, University of Oxford, Oxford, United Kingdom*

[b]*Nuffield Department of Orthopaedics, Rheumatology and Musculoskeletal Sciences, University of Oxford, Oxford, United Kingdom*

[c]*Department of Medicine, Divisions of Nephrology and Hypertension and Endocrinology, Mayo Clinic, Rochester, United States*

Multiple myeloma (MM) is characterized by expansion of malignant plasma cells in the bone marrow (BM) and destructive osteolysis. MM is preceded by the non-malignant condition monoclonal gammopathy of undetermined significance (MGUS). Understanding MGUS progression and MM bone disease development are key for patient management, and obesity is known to promote MM pathogenesis. Our aim was to determine the effect of cholesterol on MM development.

Supporting a role for cholesterol in MM progression, we found that MGUS patients had increased LDL-VLDL cholesterol (5.3%, $p< 0.05$) and decreased HDL cholesterol (58%, $p< 0.001$). Using a 2% cholesterol diet to increase circulating cholesterol in mice (34%, $p< 0.001$), mice were randomly assigned to a cholesterol diet 4 weeks prior to 5TGM1 MM inoculation that was either a) halted at time of tumour inoculation or b) continued for the entire experiment. Cholesterol diet had no effect on body weight but increased liver weight (8%, $p< 0.05$) and LDL levels (80%, $p< 0.01$). While pre-treatment with a cholesterol diet had no effect on tumour burden, mice remaining on the cholesterol diet for the entire experiment had increased tumour burden (87%, $p< 0.005$), associated with increased lipid droplet content in MM cells (cells with high lipid content 0 vs 3.4%). MM1s and JJN3 MM cells cultured with delipidized FBS had a 50% reduction in viability ($p< 0.001$), restored by LDL but not VLDL. 5TGM1 MM cells had reduced viability following culture with delipidized FBS that was restored with either LDL or VLDL.

Taken together, our results show that cholesterol promotes myeloma cell growth *both in vitro and in vivo.* Increased serum cholesterol results in higher myeloma cell lipid content, and ultimately increases BM tumour burden. These results identify cholesterol as a mediator of myeloma pathogenesis and provide new directions for dietary or pharmacological intervention strategies.

doi:10.1016/j.bonr.2020.100331

PLO12

PTH-induced bone anabolism promotes systemic breast cancer growth and metastasis

Yetki Aslan, Lea Hanna Doumit Sakr, Judith Luce, Sylvie Thomasseau, Rafailia Vakasiri, Claire-Sophie Devignes, Sylvain Provot

Université de Paris, INSERM, 1132, Paris, France

Clinical studies have shown that high bone mass correlates with increased risk of breast cancer. Using genetic mouse models, we previously demonstrated that increased bone formation upon activation of HIF signaling in osteoprogenitors, distantly promotes mammary tumor growth and systemic metastasis. Here, we evaluated whether mice treated with the anabolic agent PTH (parathyroid hormone) could increase the risk of breast cancer. Immune competent mice received daily injections of PTH (80μg/kg) for 3 weeks. MicroCT analyses showed that PTH treatment increased bone mass as expected. Two days after stopping PTH treatment, mice were inoculated with luciferase-expressing breast cancer cells derived from MMTV-PyMT tumors, by intracardiac injections to assess metastasis, or by orthotopic injections in mammary glands to assess primary tumor growth. We found that PTH-pretreated mice develop bigger primary tumors compared to control mice (average weight= 2.6g (n=8) versus 1.6g (n=7), p=0.0184, respectively). They also presented increased metastasis in multiple tissues outside the skeleton compared to controls (average luciferase signal (relative light unit)= 1.69x10^{9} RLU (n=10) versus 3.60x10^{8} RLU (n=8), p=0.0028). If PTH-induced systemic tumorigenesis worked through activation of the PTH receptor (PTH1R) in osteoblasts, expressing a constitutive active form of PTH1R specifically in osteoblasts (Col1-PTH1R^{ca} mice) would mimic the effect of PTH-pretreatment. We observed that Col1-PTH1R^{ca} mice, which have a high bone mass, develop significantly bigger primary mammary tumors (2.5g (n=7) versus 1.2g (n=5), p=0.0033), and more metastases in bones and soft tissues located away from the skeleton (1.18x10^{9} RLU (n=17) versus 3.20x10^{8} RLU (n=15), p=0.0617).

Together, our data demonstrate that PTH-induced bone anabolism promotes systemic breast cancer growth and metastasis in mice, and indicate that this effect is mediated by activation of PTH signaling in osteoblast lineage cells. This discovery is important since it suggests that patients treated with bone anabolic agents are at risk for breast cancer.

doi:10.1016/j.bonr.2020.100332

Plenary Oral Presentations 2: Osteoblasts and bone regulators

PLO13

The loss of Profilin 1 is associated with early-onset Paget's disease of bone degenerating into osteosarcoma

Federica Scotto di Carlo[a], Sharon Russo[a], Laura Pazzaglia[b], Teresa Esposito[a,c], Carmine Settembre[d], Fernando Gianfrancesco[a]

[a]*Institute of Genetics and Biophysics, Italian National Research Council, Naples, Italy*

[b]*Laboratory of Experimental Oncology, IRCCS Istituto Ortopedico Rizzoli, Bologna, Italy*

[c]*IRCCS INM Neuromed, Pozzilli, Italy*

[d]*Telethon Institute of Genetics and Medicine (TIGEM), Pozzuoli, Italy*

Paget's disease (PDB) is a late-onset bone remodelling disorder with variable phenotypic manifestations. Most PDBs harbour mutations in *SQSTM1* and show pain and fractures of affected bone(s). The most severe PDB patients display earlier onset and osteosarcoma transformation (PDB/OS) and are negative for *SQSTM1* mutations.

To disclose the genetics of PDB/OS, we investigated a pedigree with 14 PDB subjects showing early-onset (32±9 years) and osteosarcoma complication in 3 cases. We performed exome sequencing and identified a loss-of-function mutation in the *PFN1* gene (LOD score 3,38), encoding the Profilin 1, which leads to proteasome degradation of the mutant

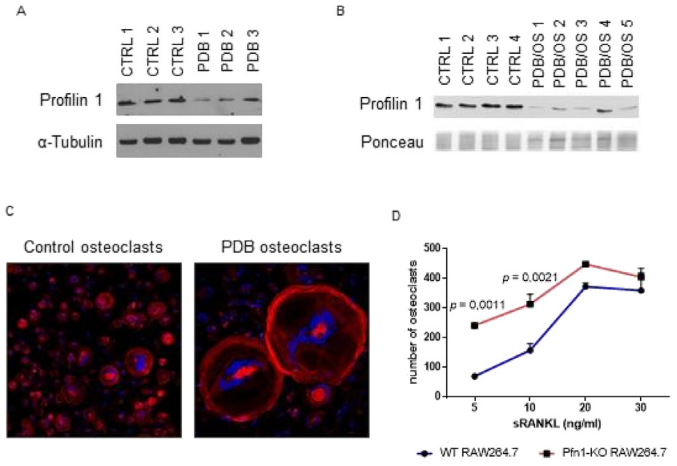

Profilin 1 is downregulated in both PDB **(A)** and PDB/OS **(B)** patients. Low PFN1 levels result in large and multinucleated osteoclasts **(C)** sensitive to lower doses of the stimulating cytokine RANKL **(D)**
Profilin 1 in PDB/OS

protein [A]. The screening conducted on 218 patients of our PDB biobank detected a germline deletion of *PFN1* in four, exhibiting early-onset PDB (36±14 years; two diagnosed at age 24 and 26). Interestingly, experiments on sporadic PDB/OS biopsies revealed that 8/14 tumours carried loss of *PFN1* and consequent protein downregulation [B].

Osteoclasts differentiated from *PFN1*-mutated patients displayed a surface area 4-fold larger than controls [C]. CRISPR-Cas9-mediated knock-out in RAW264.7 demonstrated that the *Pfn1*-KO led to monocytes sensitive to lower doses of RANKL compared to wild-type cells, and *Pfn1*-KO osteoclasts were more active [D]. Interestingly, μ-CT analysis on our *ad-hoc* generated *Pfn1*-knock-in model highlighted that heterozygous mice (n=9) as young as 4 months show a reduction of bone volume in their femurs by 25% (P=0,003), compared to wild-type (n=9). Conversely, *Pfn1*-KO MC3T3 failed to efficiently mineralise and acquired malignant features.

In conclusion, we identified the gene responsible for osteosarcoma predisposition in severe PDB patients.

doi:10.1016/j.bonr.2020.100333

PLO14

Slc38a10 is a novel regulator of osteoblastic bone formation

Andrea S. Pollard, Davide Komla Ebri, Penny Sparkes, Apostolos Gogakos, John G. Logan, Natalie C. Butterfield, Victoria Leitch, J.H. Duncan Bassett, Graham R. Williams
Imperial College London, London, United Kingdom

Slc38a10 is a highly conserved, evolutionarily ancient member of the Slc38 neutral amino acid transporter family. It lacks structural features common to other Slc38 family members and its function is unknown. In a skeletal phenotype screen of >1000 knockout mouse lines generated by the International Mouse Phenotyping Consortium, we identified low bone mineral content (BMC) and strength in *Slc38a10*-KO mice and hypothesised that SLC38A10 is a novel regulator of bone mass.

Detailed skeletal phenotyping of *Slc38a10*-KO mice (n=5 per sex, per age, per genotype; local ethics committee approval), primary bone cell culture and RNAseq were used to determine the mechanisms underpinning regulation of bone mass by SLC38A10. *Slc38a10*-KO mice exhibited short stature (P< 0.001, ANOVA) and reduced BMC (P< 0.01, Kolmogorov-Smirnov test) at all ages. Static and dynamic histomorphometry demonstrated markedly impaired bone formation (60% reduction, P< 0.05, t-test) but normal bone resorption relative to wild types. Accordingly, proliferation of SLC38A10-deficient osteoblasts *in vitro* was profoundly decreased (40% reduction, P< 0.05, t-test), whereas osteoclast function was normal. Differential gene expression and gene set enrichment analysis revealed decreased expression of chemokine signalling and cell adhesion associated genes in *Slc38a10*-KO osteoblasts. The chemokine receptors *Ccr1* (Log_2FC -10.6, p < 1.50E-08) and *Ccr5* (Log_2FC -4.3, p < 0.00077) and integrin subunits *Itgax* (Log_2FC -7, p< 9.19E-15), *Itgb2* (Log_2FC -5, p< 3.51E-11), *Itgam* (Log_2FC -4.4, p< 2.22E-06), *Itgal* (Log_2FC -3.7, p< 5.11E-07) and *Itga4* (Log_2FC -3.3, p< 1.92E-12) were all down-regulated in SLC38A10 deficient osteoblasts.

Integrins are essential for osteoblast proliferation, adhesion to extracellular matrix, differentiation and mineralisation, while CCR1 and CCR5 regulate integrin expression in multiple cell types. Here, we propose that SLC38A10 regulates integrin-mediated osteoblast proliferation and adhesion via a *Ccr1*/*Ccr5*-dependent mechanism. Defining this signalling pathway will facilitate the identification of novel drug targets and anabolic approaches for the treatment of osteoporosis.

doi:10.1016/j.bonr.2020.100334

PLO15

Bone tissue in murine atypical type VI osteogenesis imperfecta has changes in vascular pores and matrix organization, plus classic OI hypermineralization

Ghazal Hedjazi[a], Gali Guterman-Ram[b], Stéphane Blouin[a], Paul Roschger[a], Victoria Schemenz[c], Wolfgang Wagermaier[c], Peter Fratzl[c], Jochen Zwerina[a], Nadja Fratzl-Zelman[a], Joan C. Marini[b]
[a]*Ludwig Boltzmann Institute of Osteology at Hanusch Hospital of OEGK and AUVA Trauma Centre, Meidling,1st Med. Department Hanusch Hospital, Vienna, Austria*
[b]*Section on Heritable Disorders of Bone and Extracellular Matrix, NICHD, NIH, Bethesda, United States*
[c]*Max Planck Institute of Colloids and Interfaces, Dept. of Biomaterials, Potsdam, Germany*

Objectives: Osteogenesis imperfecta (OI) is a connective tissue disorder with high bone fragility. Very rare cases of atypical type VI OI result from loss-of-function mutation (p.S40L) in *IFITM5*,the causative gene for type V OI. Bone histology is similar to type VI OI, with extremely severe progressive phenotype. To obtain insights into bone material properties of this new OI entity, we investigated a knock-in (KI) murine model carrying aleucine substitution for the BRIL p.Serine42 residue.

Methods: We analyzed femurs of heterozygous male mutants of 4- and 8-week-old mice and wild-types (KI: n=5, and 10, WT: n=4 and 10, respectively) by qBEI, assessing bone mineralization density distribution, histomorphometric parameters and osteocyte lacunae sections (OLS). Vascularization was evaluated by micro-CT and collagen matrix orientation by second harmonic generation fluorescence microscopy. The effects of genotype and age were tested by two-way ANOVA.

Results: Independently of age, KI has increased average mineral content in trabecular bone (Ca Mean: +3.4%, P=0.003); decreased OLS mean area and perimeter (-17.1%, -10.4% respectively, both P< 0.0001), elevated pore volume (+12.8%, P=0.048) and a 2.6 fold increase (P< 0.0001) in the relative amount of disordered matrix versus WT.

Moreover, we observed in both genotypes, CaMean (metaphysis: +8.0%; cortical bone: +4.7%, both P< 0.0001), decreased mean OLS density, porosity, area, perimeter and vascular pore number and volume/TV (-44.2%, -53.1%, -16.7%, -12.8%, -30.47%, -47.1 respectively,

all: P< 0.0001) in 8-week versus the 4-week old littermates. BV/TV was not altered.

Conclusion: Our mouse model shows typical OI tissue levelproperties, such as hypermineralized matrix and altered osteocyte lacunae characteristics, but also significantly larger vascular pore volume consistent with defective PEDF secretion as in type VI OI. Increased proportion of disordered collagen might be a major contributor to the deterioration of mechanical competence in this OI mouse model and in affected patients.

doi:10.1016/j.bonr.2020.100335

PLO16

RhoA regulates the quiescence and cell fate of skeletal stem and progenitor cells (SSPCs)

Dana Trompet[a], Marian Dejaeger[a], Marion Mesnieres[a], Elena Nefyodova[a], Ruben Cardoen[a], Cord Brakebusch[b], Jos Tournoy[c], Frank Luyten[d], Christa Maes[a]

[a]*Laboratory of Skeletal Cell Biology and Physiology (SCEBP), Skeletal Biology and Engineering Research Center (SBE), KU Leuven, Leuven, Belgium*

[b]*Biomedical Institute, BRIC, Faculty of Health, University of Copenhagen, Copenhagen, Denmark*

[c]*Department of Chronic Diseases, Metabolism and Ageing, University Hospitals Leuven, Leuven, Belgium*

[d]*Skeletal Biology and Engineering Research Center (SBE), Department of Development and Regeneration, KU Leuven, Leuven, Belgium*

A better understanding of skeletal stem/progenitor cell (SSPC) biology, including the significance and regulation of cytoskeleton-centered processes as cell migration and adhesion, could provide novel osteo-anabolic therapies. Therefore, we generated conditional knock-out (cKO) mice lacking RhoA, a key cytoskeletal regulator, in SSPCs and osteolineage cells using Prx1-Cre and Osx-Cre:GFP mice.

MicroCT and histomorphometry revealed that loss of RhoA led to reduced trabecular bone mass in both mouse models (e.g. BV/TV 12-week-old Prx1-Cre;RhoA-cKO mice: 10.91±0.97% versus 15.57±0.40% in controls; n=8-9;p< 0.001). Interestingly, whereas the reduced BV/TV in Osx-Cre:GFP;RhoA mutants could be attributed to decreased osteoblast number and activity, Prx1-Cre;RhoA-cKO mice rather showed dominant effects in the earlier stem/progenitor cells. Firstly, we found that SSPC quiescence was reduced in Prx1-Cre;RhoA-cKO mice. Mutant BMSCs showed 2-fold increased proliferation *in vitro* (n=3;p< 0.05) and young Prx1-Cre;RhoA-cKO bones contained 40% more CFUs than controls (n=9;p< 0.05). Moreover, Prx1-Cre;RhoA-cKO mice grew wider bones, and generated larger calluses after fracture (n=16;p< 0.01), indicating an increased SSPC expansion capacity. Compromised stem cell quiescence upon RhoA-inactivation was further supported by reduced long-term EdU-label-retention *in vivo*, and associated with increased senescence (p16 qRT-PCR) and premature exhaustion of the SSPC pool, as CFUs were reduced in 1-year-old Prx1-Cre;RhoA-cKOs. Secondly, loss of RhoA affected the cell fate and differentiation profile of SSPCs, favoring adipogenesis and chondrogenesis. Cultured mutant BMSCs displayed increased adipogenic differentiation (n=4-5;p< 0.05) and Prx1-Cre;RhoA-cKO mice showed increased BM adiposity, which aggravated upon injury (e.g. post-fracture osmium-staining: 0.42±0.35% BMAT (control) versus 5.34±6.43% (cKO); n=8;p< 0.05). Increased chondrogenesis was seen upon fracture (7.1±3.6% cartilage (control) versus 12.3±1.5% (cKO); post-fracture-day7; n=4-5;p< 0.01) and in occasional enchondroma formation. Notably, RhoA-deficient cells showed changes in Wnt/β-catenin and YAP/TAZ-signaling consistent with these alterations.

Altogether, we conclude that loss of RhoA in SSPCs increases cellular expansion and alters differentiation, leading to premature SSPC exhaustion and osteopenia.

doi:10.1016/j.bonr.2020.100336

PLO17

Unique serum microRNA profile in monogenic osteoporosis caused by *PLS3* mutations

Riikka Mäkitie[a], Matthias Hackl[b], Moritz Weigl[b], Anders Kämpe[c], Alice Costantini[c], Johannes Grillari[d,e], Outi Mäkitie[f,g,h]

[a]*Faculty of Medicine, University of Helsinki, Folkhälsan Institute of Genetics and Research Program for Clinical and Molecular Metabolism, Helsinki, Finland*

[b]*TAmiRNA GmbH, Vienna, Austria*

[c]*Center for Molecular Medicine, Karolinska Institutet, and Clinical Genetics, Karolinska University Hospital, Stockholm, Sweden*

[d]*Christian Doppler Laboratory on Biotechnology of Skin Aging, Department of Biotechnology, BOKU-University of Natural Resources and Life Sciences Vienna, Vienna, Austria*

[e]*Ludwig Boltzmann Institute for Experimental and Clinical Traumatology, Austrian Cluster for Tissue Regeneration, Vienna, Austria*

[f]*Folkhälsan Institute of Genetics and Research Program for Clinical and Molecular Metabolism, Faculty of Medicine, University of Helsinki, Helsinki, Finland*

[g]*Center for Molecular Medicine, Karolinska Institutet and Clinical Genetics, Karolinska University Hospital, Stockholm, Sweden*

[h]*Children´s Hospital and Pediatric Research Center, University of Helsinki and Helsinki University Hospital, Helsinki, Finland*

Objective: Mutations in *PLS3*, encoding Plastin 3, result in severe, childhood-onset osteoporosis with prevalent peripheral and spinal compression fractures. Due to X chromosomal inheritance, mutation-positive males are typically more severely affected. Despite the manifest skeletal pathology, conventional bone metabolic markers are normal in affected patients. This study explored the circulating microRNA levels in patients with defective PLS3 function.

Subjects and Methods: A cross-sectional cohort study on 15 mutation-positive (5 males, median age 41 years, range 8-76 years) and 14 mutation-negative (6 males, median 40 years, range 6-69 years) subjects from four Finnish families with PLS3 osteoporosis due to *PLS3* mutations. We screened fasting serum samples with a custom-designed panel comprising 192 miRNAs using qPCR. Findings were compared between *PLS3* mutation-positive and mutation-negative subjects. All studies were approved by the Research Ethics Board of Helsinki University Hospital.

Results: We identified a unique pattern of circulating miRNAs in the mutation-positive subjects compared with the mutation-negative subjects. Of the 192 miRNAs, seven were significantly differentially expressed between the groups, with three upregulated (miR-301b-3p, miR-181c-5p, miR-203a-3p; *p*-values 0.015-0.035) and four downregulated (miR-93-3p, miR-532-3p, miR-133a-3p, miR-590-3p; *p*-values 0.004-0.039) in the *PLS3* mutation-positive subjects. All seven miRNAs have previously been linked to bone metabolism and two of them (miR-181c-5p and miR-203a-3p) can be bioinformatically predicted to target 3'UTR of *PLS3*, but none of the them have previously been associated with PLS3.

Conclusions: Our results indicate that *PLS3* mutations are reflected in an altered serum miRNA profile and suggest that specific miRNAs associate with PLS3 in bone metabolism and that their regulation is disrupted in defective PLS3 function. These findings provide new insight into the pathogenesis of PLS3-related bone disorders and may offer new

avenues for future diagnosis and treatment of osteoporosis. Further functional studies are warranted.

doi:10.1016/j.bonr.2020.100337

PLO18

Large-scale genomics and proteomics to identify novel circulating biomarkers for bone density

Sirui Zhou[a], John A. Morris[a], Erin Oerton[b], Vincenzo Forgetta[a], Claudia Langenberg[b], J. Brent Richards[a]
[a]*McGill University, Montreal, Canada*
[b]*Cambridge University Hospital, Cambridge, United Kingdom*

Rationale: Circulating causal protein biomarkers for osteoporosis may be helpful for risk prediction, diagnosis and can act as drug targets. Mendelian randomization (MR), a human genetics-based method can rapidly scan for such biomarkers when the genetic determinants of the protein biomarker are tested for their effect on osteoporosis outcomes.

Objective: To identify clinically relevant circulating biomarkers for bone mineral density (BMD).

Methods: We first used two-sample Mendelian randomization (MR) and co-localization methods to screen 922 circulating biomarkers for their causal effect on BMD. To do so we used five proteomic GWAS studies (N = 13,990) and an estimated BMD (eBMD) GWAS study (N=426,824), applying inverse-variance based MR methods. Prioritized biomarkers were then tested for their association with total body BMD (tBMD) in the Fenland cohort (N=476) by measurement on the Olink platform.

Results: The genetic determinants of 922 proteins, which explain up to 80% of variance in the protein levels, were tested for their association with eBMD using MR methods. We identified 83 candidate protein biomarkers for eBMD, after adjusting for multiple testing ($P < 4x10^{-5}$). Measuring 27 of these proteins in the Fenland cohort we found that 4 had associations with tBMD with P-values < 0.05 where direction of effect was that expected from the MR study. Amongst the most promising protein was ACAM, where increased levels were associated with increased eBMD in the MR study ($P = 2.96 \times 10^{-7}$) and by direct measurement (P = 0.009).

Conclusion: These results suggest that MR is able to prioritize circulating protein levels as biomarkers for BMD outcomes. The identified biomarkers have been tested through MR and direct measurement and may serve as causal biomarkers and consequently drug targets.

doi:10.1016/j.bonr.2020.100338

Plenary Oral Presentations 3: Osteoporosis: From cause to treatment

PLO01

Irisin treatment prevents dysregulation of osteoblast differentiation and activity in 3D *in vitro* bone cocultures exposed to microgravity during the space flight CRS-14 mission

Graziana Colaianni[a], Silvia Colucci[b], Giacomina Brunetti[b], Giorgio Mori[c], Maria Grano[a]
[a]*Department of Emergency and Organ Transplantation, University of Bari, Bari, Italy*
[b]*Department of Basic Medical Sciences, Neuroscience and Sense Organs, University of Bari, Bari, Italy*
[c]*Department of Clinical and Experimental Medicine, University of Foggia, Foggia, Italy*

We previously showed that irisin administration prevents the development of disuse-induced osteoporosis and muscular atrophy in HU mice, a murine model which mimics adverse effects on musculoskeletal system caused by prolonged bed rest and microgravity exposure. Astronauts experience bone loss at a rate of 0.5-1.5%/month, equally to postmenopausal women in 1 year. Understanding molecular mechanisms responsible for bone cells unbalance in microgravity would allow the development of better countermeasures, eventually advancing terrestrial osteoporosis treatments.

We conduct a unique investigation aboard the SpaceX Dragon cargo ferry to the ISS during the space flight CRS-14 mission. The aim of this study was to provide a controlled 3D *in vitro* cell coculture model to mimic the bone microenvironment in microgravity. Using the e-Osteo hardware equipped with bioreactors, osteoblast (OB), osteoclast (OC) and endothelial (EC) cells, seeded on Skelite™ discs, were cultured w/or w/o rec-Irisin and exposed to 14 days of microgravity. Gene expression analysis was assessed, and results were compared to ground controls treated within identical payloads.

Our results show that in OB/EC/OC coculture, three of the most relevant transcription factors responsible for OB differentiation were affected by microgravity (*Atf4* -75%, $p< 0.01$; *RunX2* -87%, $p< 0.001$; *Osterix* -95%, $p< 0.05$ Vs ground), whereas treatment with rec-Irisin fully prevented *Atf4* and *RunX2* mRNA decrease and, although not fully restored, it induced a 5-fold increase of *Osterix* mRNA ($p< 0.001$) Vs untreated cells. Moreover, microgravity-induced decreases of *Collagen I* (-84%; $p< 0.05$) and *Osteoprotegerin* (-94%; $p< 0.05$) were prevented by rec-Irisin. Despite it was not effective in preventing *Trap* mRNA increase, rec-Irisin induced a 2.8-fold increase of *Osteoprotegerin* ($p< 0.05$) that might compensate by reducing osteoclastogenesis in microgravity.

Our results provide evidence that Irisin protects OB differentiation and activity in microgravity and it might represent a countermeasure to prevent bone loss in astronauts.

doi:10.1016/j.bonr.2020.100321

PLO02

Additive effect of Act-RIIA-mFc and PTH in the prevention of disuse-induced bone loss

Mikkel Bo Brent[a], Frederik Duch[a], Andreas Lodberg[a], Ulf Simonsen[a], Bram C.J. van der Eerden[b], Jesper Skovhus Thomsen[a], Annemarie Brüel[a]
[a]*Department of Biomedicine, Aarhus University, Aarhus, Denmark*
[b]*Department of Internal Medicine, Erasmus Medical Center, Rotterdam, Netherlands*

Damage to or destruction of the lower motor neuron cell bodies or their axons results in reduced or abolished voluntary movement accompanied by a substantial loss of bone mass. Intermittent parathyroid hormone 1−34 (PTH) is one of the most potent bone anabolic drugs know. ActRIIA-mFc is a new and promising activin type IIA decoy receptor that increases bone and muscle mass. We investigated whether PTH and ActRIIA-mFc alone or in combination could prevent loss of bone mass after three weeks of Botulinum toxin A (BTX)-induced hindlimb disuse in mice. Seventy-two 16-week-old female C57-BL/6 mice were allocated to the following groups: Baseline, Control, BTX, BTX + ActRIIA-mFc, BTX + PTH, and BTX + ActRIIA-mFc + PTH. Disuse was achieved by injecting BTX directly into the right hindlimb. Mice in the treatment groups were

injected intraperitoneally with ActRII-mFc (10 mg/kg) twice weekly and PTH (100 μg/kg) subcutaneously five times a week. After three weeks the mice were sacrificed and the right femora were analysed using DXA, μCT, mechanical testing, and dynamic bone histomorphometry. Injections with BTX resulted in a loss of cortical (−12%, $p< 0.05$) and trabecular bone mass (−34%, $p< 0.05$), trabecular thickness (−30%, $p< 0.05$), and mid-diaphyseal bone strength (−17%, $p< 0.05$). Act-RIIA-mFc attenuated the disuse-induced loss of trabecular bone volume (+39%, $p< 0.05$) and trabecular thickness (+11%, $p< 0.05$) compared to BTX. Surprisingly, monotherapy with PTH did not attenuate the loss of trabecular thickness and trabecular bone volume. Finally, combination therapy with Act-RIIA-mFc and PTH were able to partly or completely prevent disuse-induced loss of trabecular bone volume (+118%, $p< 0.05$), trabecular thickness (+10%, $p< 0.05$), and mid-diaphyseal bone strength (+22%, $p< 0.05$) compared to BTX. Act-RIIA-mFc and PTH in combination was more efficient in preventing the disuse-induced bone loss of trabecular micro-architecture than either treatment alone.

doi:10.1016/j.bonr.2020.100322

PLO03

Older men with sarcopenia have rapid progression of abdominal aortic calcification - the prospective MINOS study

Pawel Szulc[a], Roland Chapurlat[b]
[a]Epidemiology of Osteoporosis, INSERM, Unit 1033, Université de Lyon, Lyon, France
[b]Hôpital Edouard Herriot, INSERM, Unit 1033, Université de Lyon, Lyon, France

Low muscle mass and strength (sarcopenia) are associated with high cardiovascular risk. Our aim was to assess the risk of rapid progression of abdominal aortic calcification (AAC) in older men with low relative appendicular lean mass (RALM) and poor physical performance.

A cohort of 621 men aged 50-85 was followed prospectively. Body composition was assessed by DXA (HOLOGIC QDR1500). Poor physical performance was defined as incapacity to perform ≥1 of 5 clinical tests (balance, muscle strength). AAC was assessed using Kauppila's semiquantitative score (baseline, after 3 and 7.5 years).

Rapid AAC progression (>0.5 point/year) was found in 167 men (27%). After adjustment for potential confounders including baseline AAC, the risk of rapid AAC progression increased with lower RALM (OR=1.37/SD, 95%CI: 1.09-1.74, $p< 0.01$) and was higher in the lowest (< 7.4kg/m^2) vs. the highest (>8.6kg/m^2) quartile (OR=1.99, 95%CI: 1.06-3.74, $p< 0.01$). Poor physical performance was associated with rapid AAC progression (OR=2.46, 95%CI: 1.16-5.21, $p< 0.05$). Men who had both low RALM and poor physical performance had higher risk of rapid AAC progression (OR=4.98, 95%CI: 1.72-14.43, $p< 0.01$) vs. men without these characteristics. Low RALM and poor physical performance were each associated with AAC progression mainly in men without other risk factors, e.g. 310 men aged < 70 with normal testosteronemia and without diabetes or heart disease (OR=2.33/SD decrease, 95%CI: 1.27-4.28, $p< 0.01$ and OR=6.01, 95%CI: 1.06-33.97, $p< 0.05$, respectively). Measures of adiposity (BMI, total, appendicular and central fat) were not associated with AAC progression. Other risk factors were associated with rapid AAC progression, e.g. age, ischemic heart disease, smoking (OR=3.53, $p< 0.005$), lower levels of testosterone (OR=1.25/SD, $p< 0.05$) and osteocalcin (OR=1.85, $p< 0.01$), high LDL-cholesterol.

Overall, low RALM and poor physical performance are associated with higher risk of rapid AAC progression and possibly represent another measure of cardiovascular risk.

doi:10.1016/j.bonr.2020.100323

PLO04

Bone resorption in mouse models of mitochondrial neurological diseases

Vasiliki-Iris Perivolidi[a,b], Foteini Violitzi[a], George Panayotou[a], Eleni Douni[a,b]
[a]Institute of Bioinnovation, Biomedical Sciences Research Center Alexander Fleming, Vari-Athens, Greece
[b]Department of Biotechnology, Agricultural University of Athens, Athens, Greece

Mitochondria are involved in diverse vital biological processes, while mitochondrial dysfunction causes metabolic disorders, neurodegenerative disease, and aging. Our group has recently identified two mitochondrial outer membrane proteins, SLC25A46 and DNAJC11, as novel genetic causals of neurological diseases in mice. SLC25A46, a mitochondrial transporter member, has been recently identified as a novel pathogenic cause in human neurological diseases. Impaired SLC25A46 function causes lethal neuropathology in mice (Slc25a46$^{atc/atc}$), characterized by ataxia, optic atrophy and cerebellar hypoplasia, similarly to human pathology. DNAJC11, a molecular co-chaperone, causes a lethal neuromuscular phenotype in mice (DnaJC11$^{spc/spc}$). In both models the mitochondrial structure and activity are impaired in the nervous system, while any effect to other systems remains unknown.

The objective of the current study was to investigate whether mitochondrial dysfunction also affects the skeletal system and bone homeostasis in mutant mice. Histological analysis demonstrated a dramatic loss of trabecular bone at femur metaphyseal region in both models compared to WT littermates. Micro-CT analysis showed that metaphysis of Slc25a46$^{atc/atc}$ mice displayed 77% reduction in trabecular bone volume fraction (WT: 5,37±0,8 vs Slc25a46$^{atc/atc}$: 1,22±0,28, $p< 0.001$), 76% reduction in trabecular number (WT: 1,38±0,2 vs Slc25a46$^{atc/atc}$: 0,33±0,12, $p< 0.001$) and significant increase in trabecular separation (WT: 0,50±0,06 vs Slc25a46$^{atc/atc}$: 0,72±0,03, $p< 0.05$). On the same context, DnaJC11$^{spc/spc}$ mice developed trabecular bone loss as shown by 92% decrease in trabecular bone volume fraction (WT: 5,24±0,46 vs DnaJC11$^{spc/spc}$: 0,43±0,09, $p< 0.001$), 92% decrease in trabecular number (WT: 1,38±0,13 vs DnaJC11$^{spc/spc}$: 0,12±0,02, $p< 0.001$) and significant increase in trabecular separation at femur metaphysis (WT: 0,51±0,03 vs DnaJC11$^{spc/spc}$: 0,81±0,04, $p< 0.001$). Interestingly, both models displayed approximately 8% reduction of cortical bone volume fraction at diaphysis compared to WT littermates. Deregulated expression of genes encoding bone markers and mitochondrial proteins are currently investigated through qPCR to correlate bone loss with mitochondrial biogenesis.

doi:10.1016/j.bonr.2020.100324

PLO05

Regular proton-pump inhibitor intake is associated with deterioration of tibial bone microarchitecture and strength in older patients as assessed via high-resolution peripheral quantitative computed tomography

Ursula Heilmeier[a], Ursina Meyer[a], Alexandra Siegenthaler[b], Marie Boensch[b], Lauren Abderhalden[a], Robert Theiler[a], Andreas Egli[a], Heike Annette Bischoff-Ferrari[a]

[a]Department of Geriatrics and Aging Research, Center on Aging and Mobility, University Hospital Zurich, University of Zurich, Zurich, Switzerland
[b]Center on Aging and Mobility, University of Zurich, Zurich, Switzerland

Introduction: Proton pump inhibitors (PPI) are widely used among older adults and have been found to increase fracture risk. However, the underlying pathophysiology of PPI-induced bone fragility is only partly known. In addition, their effect on bone microarchitecture remains unclear as prior clinical PPI-studies were limited to lower-resolution imaging techniques such as DXA or 3D-QCT. With the advent of high-resolution peripheral computed tomography (HR-pQCT), human bone microarchitecture and strength is now quantifiable in vivo at a spatial resolution of 130 µm. Using HR-pQCT, we investigated here prospectively, if PPI use is associated with changes in HR-pQCT-derived bone microarchitectural and strength parameters in older patients.

Methods: 189 patients aged ≥ 60 years, were enrolled as part of a 2-year Vitamin D RCT (NCT 00599807). Participants underwent HR-pQCT scanning of the tibia at baseline and after 2y. During the 2-year FU, 24 participants took PPIs for >50% of the time (PPI-users), while n=165 were PPIs-free (Non-PPI users). Bone microstructural parameters including bone strength estimates were computed using regression models adjusted for age, sex, BMI, VitD treatment, baseline bone parameters, and comorbidities.

Results: PPI-users exhibited similar baseline age, gender, and VitD treatment proportions compared to non-PPI users. During FU, PPI-users lost about 3.5 times more total tibial BMD (-8.6 vs -2.4 mg/cm3, p=0.0118), twice as much cortical BMD (-29.03 vs. -14.16 mg/cm3, p=0.0052), and around 10-times more cortical thickness (p=0.0034) than non-PPI users. These losses translated into a significantly higher loss in bone strength (tibial stiffness -4487.9 vs. 83.4 N/mm, p=0.048; failure load -193.6 vs. 18.8 N, p=0.0382) in PPI-users relative to Non PPI-users.

Conclusion: Our data suggest that PPI-intake is associated with deterioration of bone microarchitecture and bone strength in the tibia of older patients. This may partly explain the increased fracture risk observed in this large clinical patient group.

doi:10.1016/j.bonr.2020.100325

PLO06

Romosozumab improves lumbar spine BMD and bone strength greater than alendronate as assessed by quantitative computed tomography and finite element analysis in the ARCH trial

Jacques P. Brown[a], Arkadi Chines[b], Roland Chapurlat[c], Joseph Foldes[d], Xavier Nogues[e], Roberto Civitelli[f], Tobias De Villiers[g], Fabio Massari[h], Cristiano Zerbini[i], Wenjing Yang[b], Chris Recknor[j], Cesar Libanati[k]
[a]Laval University, Quebec City, Canada
[b]Amgen Inc., Thousand Oaks, United States
[c]INSERM UMR 1033, University of Lyon, Lyon, France
[d]Hadassah Hebrew University Medical Center, Jerusalem, Israel
[e]IMIM Institut Hospital del Mar d'Investigacions Mèdiques, Barcelona, Spain
[f]Washington University School of Medicine, St. Louis, United States
[g]Stellenbosch University, Stellenbosch, South Africa
[h]Instituto de Investigaciones Metabólicas, Buenos Aires, Argentina
[i]Centro Paulista de Investigação Clinica, São Paulo, Brazil
[j]United Osteoporosis Centers, Gainesville, United States
[k]UCB Pharma, Brussels, Belgium

Objective: Assess improvements in lumbar spine (LS) bone mineral density (BMD) and bone strength with romosozumab (Romo) vs alendronate (ALN) treatment in ARCH (NCT01631214) by quantitative computed tomography (QCT) and Finite Element Analysis (FEA).

Materials and methods: Postmenopausal women with osteoporosis and prior vertebral/hip fracture were randomised 1:1 to receive subcutaneous Romo 210mg monthly or oral ALN 70mg weekly for 12 months, followed by open-label oral ALN 70mg weekly. In an imaging substudy, LS BMD was assessed by QCT and vertebral-estimated bone strength by FEA using QCT images obtained at baseline and Months 6, 12, and 24. Correlation analyses evaluated the relationship between changes in FEA, QCT, and dual-energy X-ray absorptiometry (DXA).

Results: 90 patients (49 Romo, 41 ALN) with baseline and ≥1 post-baseline QCT/FEA assessment were included. Mean (SD) age at baseline was 73 (7) years; DXA T-scores were -3.08 (1.09), -2.70 (0.68), and -2.84 (0.45) at the LS, total hip, and femoral neck, respectively. Patients in both groups experienced significant gains in integral BMD and LS bone strength, with significantly greater increases on Romo compared with ALN at all time points (Figure). With treatment arms combined, correlation between change in FEA/BMD and DXA was similar (r=0.69-0.87, all p< 0.001).

Conclusion(s): Compared with ALN, Romo significantly improved LS BMD and bone strength. These effects occurred rapidly and were preserved upon transition to ALN through 24 months.

Acknowledgements: This study was funded by Astellas, UCB Pharma and Amgen Inc. Medical writing services were provided by Costello Medical.

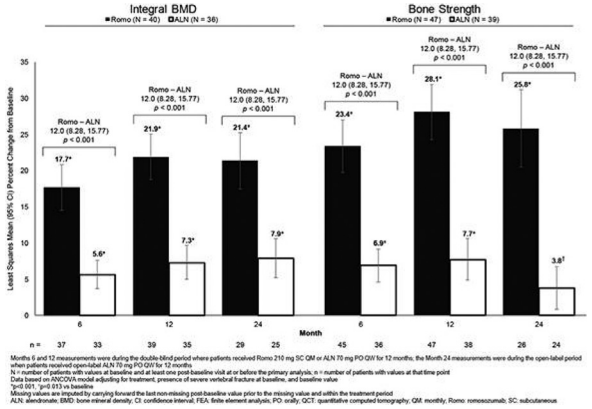

Figure. Percentage change from baseline and difference between romosozumab and alendronate treatment in integral BMD and bone strength at the lumbar spine through the primary analysis in ARCH

doi:10.1016/j.bonr.2020.100326

Bone Reports 13 (2020) 100620

Contents lists available at ScienceDirect

Bone Reports

journal homepage: www.elsevier.com/locate/bonr

Concurrent Oral Presentations

Concurrent Oral Presentations 1: Basic/Translational: Skeletal environment pathologies

COP19

Parallel platform for rapid functional screening of Osteoarthritis associated genes

Erika Kague[a], Francesco Turci[b], Yushi Yang[b], Stephen Cross[c], Elizabeth Lawrence[d], Lucy McGowan[d], Joanna Moss[d], Paddy Royal[b], Chrissy Hammond[d]

[a]*University of Bristol, Bristol, United Kingdom*
[b]*School of Physics, University of Bristol, Bristol, United Kingdom*
[c]*Wolfson Bioimaging Facility, University of Bristol, Bristol, United Kingdom*
[d]*School of Physiology, Pharmacology and Neuroscience, University of Bristol, Bristol, United Kingdom*

Genome Wide Association studies (GWAs) have recently boosted the number of genes associated to Osteoarthritis, which now sum to over 100 loci linked to the disease. As most GWAs hits fall in non-coding regions and frequently in enriched gene loci, the identification of the causal gene is a challenge. Therefore, platforms to rapidly test putative OA genes in parallel need to be developed. Here, we took advantage of the major predictor of OA (joint shape variation) and the rapid development of zebrafish to robustly develop a platform for rapid functional validation of OA associated genes. We primarily characterised OA in the aged zebrafish jaw joint by 3D morphometrics and histological analysis showing that zebrafish develop OA naturally. We compared joint alterations in cartilage and bone shape in OA mutants (*chsy1*, *col9a1*, *col11a2*, and *wnt16*) to aged osteoarthritic and found signs of premature OA. We tested a higher number of genes (*chsy1*, *col9a1*, *col11a2*, *gdf5*, *barx1*, *mcf2l*, *dot1l*, *wnt16* and *ncoa3*) in parallel by analysing shape and cellular behaviour during joint development (5dpf). Our findings suggest OA as a developmental disease. As a rapid toolkit to test OA genes we showed that CRISPR G0s display similar cellular and shape patterns in larvae and adults as those of homozygous. Furthermore, combining zebrafish rapid development with genetics and by customising computational tools towards the automation of 3D shape analysis we developed a robust, rapidly and parallel functional screening platform for OA associated genes which could boost identification of potential druggable targets.

doi:10.1016/j.bonr.2020.100633

COP20

Mice harbouring the minor allele of the human *DIO2* polymorphism (Thr92Ala) are protected against osteoarthritis

Natalie Butterfield[a], Naila Mannan[a], Katherine Curry[a], Elizabeth McAninch[b], Antonio Bianco[c], Graham Williams[a], Duncan Bassett[a]

[a]*Imperial College London, London, United Kingdom*
[b]*Division of Endocrinology and Metabolism, Rush University Medical Center, Chicago, United States*
[c]*Section of Adult and Pediatric Endocrinology, Diabetes and Metabolism, Department of Medicine, University of Chicago, Chicago, United States*

The type II deiodinase (DIO2) regulates thyroid hormone action in individual target tissues by converting the pro-hormone T4 to the active hormone T3. Expression of the minor Ala92 allele of a common *DIO2* polymorphism (Thr92Ala) results in decreased enzyme activity and impaired T3 action, and has been suggested to underlie continuing psychological and metabolic symptoms experienced by some hypothyroid patients despite T4 replacement. It has been proposed that patients with the Ala92 allele may thus benefit from increased doses of T4 or combination therapy with T4 and T3. Furthermore, the Thr92Ala polymorphism has been controversially associated with osteoarthritis susceptibility in human genetic studies. Since T3 stimulates hypertrophic chondrocyte differentiation and expression of cartilage matrix degrading enzymes, we hypothesised the *DIO2* Ala92 minor allele confers protection against osteoarthritis.

To investigate this hypothesis, we generated mice homozygous for the Ala92 and Thr92 *Dio2* variants by *Crispr/Cas9* genome editing. Analysis of joints from 16 week-old male mice ($Dio2^{Ala92/Ala92}$, n=10, and $Dio2^{Thr92/Thr92}$, n=9; approved by local ethics committee) demonstrated features of early-onset osteoarthritis only in $Dio2^{Thr92/Thr92}$ mice. $Dio2^{Thr92/Thr92}$ mice had decreased cartilage volume and thickness determined by contrast-enhanced micro-CT analysis ($Dio2^{Thr92/Thr92}$ vs $Dio2^{Ala92/Ala92}$, $^{*}P=0.019$ and $^{**}P=0.006$, respectively, Mann-Whitney) and increased articular cartilage surface damage determined by back-scattered electron scanning electron microscopy ($Dio2^{Thr92/Thr92}$ vs $Dio2^{Ala92/Ala92}$, $^{*}P=0.017$, Mann-Whitney). In contrast, $Dio2^{Ala92/Ala92}$ mutants had no signs of osteoarthritis. This provides the first functional evidence of a role for this candidate *DIO2* polymorphism *in vivo*, demonstrates a protective role for the Ala92 allele, and indicates that expression of $DIO2^{Ala92}$ may facilitate maintenance of cartilage integrity. These studies emphasise the need for caution and further research, as treatment of hypothyroid patients harbouring the Ala92 allele with increased doses of T4 or T4/T3 combination therapy could unintentionally enhance their susceptibility to osteoarthritis.

doi:10.1016/j.bonr.2020.100634

2352-1872/$ – see front matter

COP21

TAK1 inhibition effectively suppresses NLRP3 inflammasome-mediated inflammation and osteoclastic bone resorption in rheumatoid arthritis

Hirofumi Tenshin[a], Jumpei Teramachi[b], Masahiro Hiasa[a], Asuka Oda[c], Takeshi Harada[c], Masahiro Oura[c], Kimiko Sogabe[c], Mohannad Ashtar[a], Kotaro Tanimoto[a], So Shimizu[a], Yoshiki Higa[a], Eiji Tanaka[a], Toshio Matsumoto[d], Masahiro Abe[c]

[a]*Department of Orthodontics and Dentofacial Orthopedics, Institute of Biomedical Sciences, Tokushima University, Tokushima, Japan*
[b]*Department of Tissue Regeneration, Institute of Biomedical Sciences, Tokushima University, Tokushima, Japan*
[c]*Department of Hematology, Endocrinology and Metabolism, Institute of Biomedical Sciences, Tokushima University, Tokushima, Japan*
[d]*Fujii Memorial Institute of Medical Sciences, Tokushima University, Tokushima, Japan*

Aberrant NLRP3 inflammasome activation has been demonstrated in rheumatoid arthritis (RA), which may cause the debilitating joint inflammation and bone destruction. TGF-βactivated kinase-1 (TAK1) mediates a wide range of biological processes associated with inflammation. Here, we aimed to clarify the roles of TAK1 in joint inflammation and bone destruction in RA with special reference to NLRP3 inflammasome activation. Treatment with the TAK1 inhibitor LLZ1640-2 substantially alleviated pain as well as inflammatory scores and bone destruction in joints ($p< 0.01$ for one way ANOVA) in collagen-induced arthritis (CIA) as a mouse model for RA. Histological analyses revealed strong expression of NRLP3 inflammasome insynovial macrophages and cathepsin K-expressing osteoclasts while upregulating RANK ligand expression in synovial fibroblasts in joints in of CIA mice. Of note, the treatment with LLZ1640-2 substantially suppressed osteoclastogenesis as well as synovial hypertrophy and pannus formation along with almost complete inhibition of NRLP3 as well as RANK ligand induction in the synovial tissues. LLZ1640-2 or *TAK1* gene silencing almost completely suppressed NLRP3 and pro-IL-1β induction in bone marrow macrophages (BMMs) isolated from CIA mice upon stimulation with lipopolysaccharide, a TLR4 agonist, and subsequent their IL-1β production and caspase-1 activation by ATP. The TAK1 inhibition also downregulated IL-1β-induced *RANKL*mRNA expression in synovial fibroblasts, and suppressed osteoclast differentiation from BMMs in cocultures with the synovial fibroblasts. Furthermore, RANK ligand induced phosphorylation of TAK1 in BMMs or RAW264.7 preosteoclastic cells; however, LLZ1640-2 abolished the TAK1 phosphorylation and suppressed their osteoclast differentiation by RANK ligand. From these results, TAK1 inhibition can effectively block NLRP3 inflammasome-mediated inflammation, and RANK ligand expression and osteoclastic bone resorption. Therefore, TAK1 inhibition may become a novel treatment strategy targeting inflammasome priming and activation to effectively alleviate inflammation as well as bone destruction in RA.

doi:10.1016/j.bonr.2020.100635

COP22

Altered osteo-angiogenic development of fetal endochondral bones impacts hematopoietic stem cell homing during embryogenesis and B cell production in postnatal life

Marion Mesnieres[a], Anna-Marei Böhm[a], Manmohan Bajaj[b], Nicolas Peredo[a], Pieter Baatsen[c], Satish Khurana[d], Catherine Verfaillie[b], Christa Maes[a]

[a]*Laboratory of Skeletal Cell Biology and Physiology (SCEBP), Skeletal Biology and Engineering Research Center (SBE), KU Leuven, Leuven, Belgium*
[b]*Stem Cell Biology and Embryology Unit, Stem Cell Institute, KU Leuven, Leuven, Belgium*
[c]*Research Group Molecular Neurobiology, VIB-KU Leuven Center for Brain & Disease Research, KU Leuven/VIB, Leuven, Belgium*
[d]*School of Biology, Indian Institute of Science Education and Research (IISER), Thiruvananthapuram, India*

The bone marrow (BM) niche, including specific osteo- and angiogenic compartments, is crucial for hematopoiesis during life. However, little is known about the characteristics of the fetal BM-environment controlling initial homing and settlement of hematopoietic stem/progenitor cells (HSPCs) in bone.

We investigated hematopoietic development in mice with skeletal alterations induced by conditional overexpression of $VEGF_{164}$ in Osx-Cre:GFP+ cells. Skeletal preparations, microCT and histology showed that VEGF-upregulation induced an abnormal vascular pattern from E14.5 onwards and led to severely malformed limb bones, failing to form proper BM-cavities by E18.5. Flow-cytometry revealed a 2-fold decrease in the number of HSPCs ($Lin^-Sca1^+cKit^+$/LSK-cells) colonizing the mutant bones at E18.5 ($p=0.0014;n=5$). To functionally test the HSPC homing-supporting capacity, we created a non-lethal hypomorph model by postponing VEGF-overexpression until E13.5. These embryos displayed normal-sized BM-cavities while still exhibiting significant vascular and stromal alterations as well as a drastic, 5-fold reduction in HSPC number by P2 ($p< 0.0001;n=8/9$), unrelated to altered proliferation. Homing was effectively impaired, as twofold less injected labeled HSPCs reached the mutant skeleton (compared with WT recipients;$p=0.0006;n=8/9$). Detailed investigations of the BM-environment by immunohistochemistry with deep-tissue confocal imaging, EM, and flow-cytometry, exposed a drastically abnormal vascular network architecture and altered endothelial morphology in constitutive and induced VEGF-overexpression mutants, associated with a shift in sinusoidal/arteriolar endothelial phenotype. Additionally, the number of immature stromal cells characterized by PDGFRβ- or Osx-expression and closely intertwined with the vasculature, was significantly increased in both models ($p< 0.001;n=4-7$;flow-cytometry;E18.5-P2). Interestingly, surviving VEGF-mutants displayed a specific B cell deficit in their blood from 2-weeks of age ($p< 0.05;n=6/8$), attributed to a differentiation block at the pre-pro/pro-B cell stage in the BM ($p< 0.0001;n=6/8$).

Thus, impaired osteo-angiogenic development of fetal bones impacts HSC homing and settlement in the BM, while postnatal skeletal VEGF-upregulation causes niche alterations and a long-lasting B cell production defect.

doi:10.1016/j.bonr.2020.100636

COP23

Roles of Notch 1, Notch2 and CXCR4 in in-bone Breast Cancer (BrCa) cellular dormancy

Antonio Maurizi, Michela Ciocca, Cristiano Giuliani, Iona Norwood, Alfredo Cappariello, Nadia Rucci, Anna Teti

DISCAB, University of L'Aquila, L'Aquila, Italy

Dormant BrCa cells often home to the bone and, upon reactivation, relapse in bone and in other organs. BrCa cells that interact with Spindle-shaped N-cadherin$^+$ Osteoblasts (SNOs) are recognised to become dormant through a Notch2-dependent mechanism and to keep a stem-phenotype. In this work, systematic analysis of primary human BrCa and associated bone metastases revealed the presence of infrequent single cells (5.22 cells/mm^2) expressing high level of Notch1 ($Notch1^{HIGH}$), along with the already

known infrequent cells overexpressing Notch2 (Notch2^{HIGH}). FACS analysis of MDA-MB231 (MDA), ZR75D and T47D BrCa cell lines confirmed that Notch1^{HIGH} and Notch2^{HIGH} cells represented only 1-4% of the total population. In-vitro co-culture of Notch1^{HIGH} or Notch2^{HIGH} MDA cells were performed on SNOs and NON-SNOs and compared with Notch1/2^{LOW}-NON-SNO co-cultures. Notch1^{HIGH} or Notch2^{HIGH} MDA cells co-cultured with SNOs showed halved tumour cell proliferation (Notch1^{HIGH}:-49%; Notch2^{HIGH}:-51%;$p< 0.001$), indicating similar ability of Notch1^{HIGH} and Notch2^{HIGH} to induce SNO-mediated tumour cell dormancy. Consistently, Notch1^{HIGH} or Notch2^{HIGH} MDA cells co-cultured with NON-SNOs showed lower inhibition of tumour cell proliferation (Notch1^{HIGH}:-31%; Ntch2^{HIGH}:-30%;$p< 0.05$), similar to Notch1/2^{LOW} MDA cell co-cultured with SNOs (-25%;$p< 0.05$). Silencing Notch1 or Notch2 in MDA cells rescued BrCa cell proliferation when co-cultured with SNOs (Notch1^{HIGH}:+1.7; Nocth2^{HIGH}:+2.1-fold vs SCR-siRNA;$p< 0.05$), suggesting the relevance of MDA Notch1/Notch2-SNO partnership for BrCa dormancy. Notch1^{HIGH} and Notch2^{HIGH} MDA cells shared the overexpression of the HSC stem markers *CXCR4* and *TIE2* (Notch1^{HIGH}:+6.20;+3.65;$p< 0.05$; Notch2^{HIGH}:+1.34;+2.6;$p< 0.05$ vs Notch1/2^{LOW}). Luciferase-transfected CXCR4$^{HIGH/LOW}$ or TIE2$^{HIGH/LOW}$MDA cells were intratibially injected in immunocompromised CD1$^{nu/nu}$ female mice. In-bone tumour incidence was lower in CXCR4^{HIGH} MDA cell-injected mice (-80%vsCXCR4^{LOW};$p=0.001$), mimicking the results obtained injecting Notch1^{HIGH} or Notch2^{HIGH} MDA cells (-70%vsNocth1/2^{LOW};$p=0.02$). Conversely, tumour incidence was unremarkable in TIE2^{HIGH}vsTIE2^{LOW} MDA cell-injected mice ($p>0.05$). These results are consistent with a stem dormant phenotype of BrCa cells when co-expressing Notch1 or Notch2 and CXCR4, but not TIE2.

doi:10.1016/j.bonr.2020.100637

Concurrent Oral Presentations 1: Clinical/Public Health: Secondary Osteoporosis and osteoporosis management

COP01

Risk of acute myocardial infarction among new users of Bisphosphonates: a nested case-control study

Elisa Dieguez-Costa[a], Ramón Mazzucchelli[b], Alberto García Vadillo[c]
[a]*Diagnostic Radiology, Hospital Vithas Nuestra Señora de America, Madrid, Spain*
[b]*Hospital Universitario Fundación Alcorcón, Madrid, Spain*
[c]*Reumatología, Hospital U La Princesa, Madrid, Spain*

Background: Evidence suggest that bisphosphonates (BF) may inhibit atherosclerosis and vascular calcification. In several small-scale clinical trials, BF improved some intermediate targets of atherosclerosis. Observational studies found a lower risk of Acute Myocardial Infarction (AMI) or stroke among BF users compared to non-users. While this epidemiological evidence suggests that BF may protect against cardiovascular events a "prevalent user bias" cannot be excluded.

Objectives: To analyze the hypothesis that BF reduce de risk of AMI in new users and assess whether the effect depends on the duration of treatment.

Methods: Case-control study nested in a primary cohort composed of patients aged 40 to 99 years, with at least one year of follow-up in the BIFAP database during the 2002-2015 study period. From this cohort of patients, we identified incident cases of AMI and randomly selected five controls per case, matched by exact age, gender, and index date. Adjusted odds ratios (AOR) and their corresponding 95% confidence interval (CI) were calculated through an unconditional logistic regression. Only new users of BF were considered.

Results: A total of 23,590 cases of IAM and 117,612 controls were included. The mean age was 66.8 (SD 13.4) years and 72.52% were male, in both groups. 584 (2,47%) cases and 2,892 (2.46%) controls used or had used some bisphosphonate. The use of BF was not associated with a lower risk of IAM (AOR 0.97; 95%CI: 0.84-1.13). Nor was it associated with the duration of treatment (AOR less than 1 year = 0.91; 95%CI: 0.72-1.15); AOR more than 1 year= 1.01; 95%CI: 0.84-1.21). The stratified analysis by age and sex also did not show either a protective effect of BF.

Conclusion: Our results do not support a cardioprotective effect of BF, regardless of the duration of treatment, age, sex or background cardiovascular risk.

doi:10.1016/j.bonr.2020.100627

COP02

Fracture risk assessment in Canada: Bone mineral density reports and osteoporosis specialists do not agree

Shivraj Singh Riar[a], A. Lynne Feasel[b], Fariba Aghajafari[c], Elizabeth Freiheit[d], Gregory A. Kline[a,b], Christopher J. Symonds[a,b], Emma O. Billington[a,b]
[a]*Division of Endocrinology and Metabolism, University of Calgary Cumming School of Medicine, Calgary, Canada*
[b]*Dr. David Hanley Osteoporosis Centre, Alberta Health Services, Calgary, Canada*
[c]*Division of Family Medicine, University of Calgary Cumming School of Medicine, Calgary, Canada*
[d]*Biostatistics, University of Michigan, Ann Arbor, United States*

Background: Osteoporosis pharmacotherapy is generally recommended if ten-year risk of osteoporotic fracture is ≥20%. Canadian guidelines recommend risk calculation using either FRAX® or the CAROC tool. Although FRAX® is better at predicting fracture risk in the Canadian population, bone mineral density (BMD) reports present CAROC-derived risk estimates. We evaluated agreement between risk estimates calculated in an osteoporosis clinic (using FRAX®) with CAROC estimates reported on BMD.

Methods: Charts of postmenopausal women with age-associated osteoporosis, who attended a consultation at an osteoporosis clinic, were reviewed. Ten-year osteoporotic fracture risk was calculated using FRAX® with BMD (OC-FRAX risk), and categorized as being low (< 10.0%), moderate (10.0-19.9%), or high (≥20.0%). OC-FRAX estimates were compared to the radiologist's estimate, calculated using CAROC (BMD-CAROC risk) on each participant's BMD. Estimates were considered discordant when OC-FRAX and BMD-CAROC placed patients in different risk categories.

Results: Among 190 participants (mean [SD] age 63.2[6.4] years and OC-FRAX risk 13.6[7.7]%), OC-FRAX and BMD-CAROC risk estimates were discordant in 99 (52%). As shown in T1, 10.6% of patients were deemed high risk by OC-FRAX but considered low or moderate risk by BMD-CAROC, while 8.9% of patients were deemed high risk by BMD-CAROC but low or moderate risk by OC-FRAX. For the 20% treatment threshold, decisions to treat would differ in 19.5%, depending on whether OC-FRAX or BMD-CAROC was used.

Conclusion: In a large Canadian health region, fracture risk estimates on BMD reports frequently showed disagreement with FRAX® estimates calculated by an osteoporosis clinician. These findings highlight the need for implementation of a consistent and accurate fracture risk assessment process.

T1
Discordance between ten-year fracture risk calculated in an osteoporosis clinic using FRAX® (OC-FRAX) and CAROC estimates on BMD reports (BMD-CAROC

	BMD-CAROC Low Risk (<10%)	BMD-CAROC Moderate Risk (10-20%)	BMD-CAROC High Risk (≥20%)
OC-FRAX Low Risk (<10%)		57 (30.0%)	5 (2.6%)
OC-FRAX Moderate Risk (10-20%)	5 (2.6%)		12 (6.3%)
OC-FRAX High Risk (≥20%)	2 (1.1%)	18 (9.5%)	

doi:10.1016/j.bonr.2020.100628

COP03

Denosumab 10-year simulation of bone remodeling in human biopsies

Duncan C. Tourolle[a], Charles Ledoux[a], Daniele Boaretti[a], Mauricio Aguilera[b], Najma Saleem[c], Ralph Müller[a]
[a]*Institute for Biomechanics, ETH Zurich, Zurich, Switzerland*
[b]*Amgen Inc., Mexico City, Mexico*
[c]*Amgen Inc., Thousand Oaks, United States*

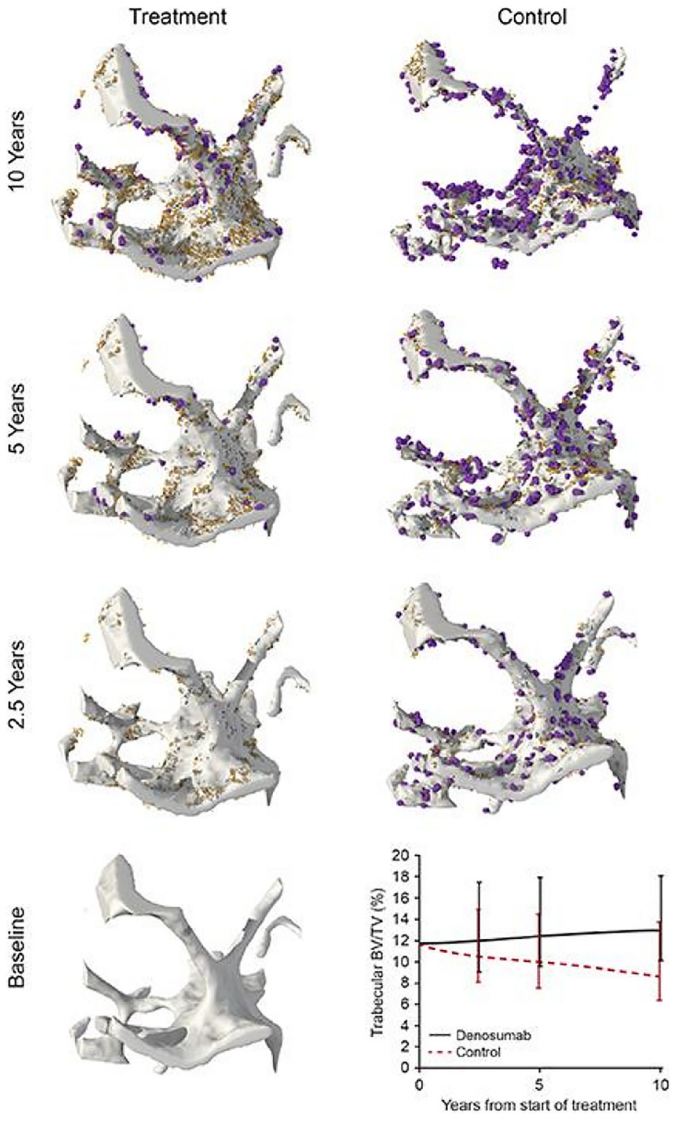

Figure. The evolution of the digitally twinned biopsies (treatment and control) over the study period (orange = osteoblasts; purple = osteoclasts). The simulation used a temporal multiscale approach: mechanical stimulation was calculated every 18 days, cell behaviour every 3.5 days, and the reaction-diffusion of molecules on a 20-minute timescale. Inset plot: Trabecular bone volume fraction (BV/TV) for treatment and control cases.

Denosumab is a potent antiresorptive that disrupts osteoclast formation, function, and survival. The effects of denosumab treatment (up to 10 years) on bone histomorphometry has provided insight into how denosumab influences cellular activity over time; however, histomorphometry is 2-dimensional and reflects a single timepoint. Here, we compare FREEDOM and Extension biopsy data with simulations using an agent-based model for cell activity coupled with a micro-multiphysics model to resolve the local mechanical environment and cell-cytokine-antibody reactions affecting bone remodeling.

Treatment and control models were run to model the FREEDOM trial protocol for a 10-year period using iliac crest bone biopsies matched to FREEDOM baseline by age and trabecular bone volume fraction (BV/TV); conditions were identical except the treatment group received virtual injections of denosumab at 6-month intervals. Marrow was filled with uniform distributions of mesenchymal and hematopoietic stem cells, bone surfaces were covered with lining cells, and mechanical loading was computed using micro-finite element analysis.

Treatment and control simulations matched the BV/TV observed in biopsies from denosumab and placebo groups through year 10 of the FREEDOM Extension. In the simulation, treatment decreased osteoclast number, which led to a modest increase in trabecular thickness as well as osteocyte stress shielding and concomitantly increased RANKL production, followed by a small increase in osteoclast number over the 10-year period (Figure). Lack of treatment led to a significant loss of bone mass and structure.

This micro-multiphysics model simulated denosumab cellular action over a 10-year period, matching static and dynamic morphometric measures assessed in clinical biopsies.biopsies.

doi:10.1016/j.bonr.2020.100629

COP04

Bone material strength index as measured by impact microindentation in vivo is altered in patients with primary hyperparathyroidism

Manuela Schoeb[a], Elizabeth M. Winter[a], Abbey Schepers[b], Marieke Snel[a], Natasha M. Appelman-Dijkstra[a]
[a]*Center for Bone Quality and Center for Endocrine Tumors, Department of Internal Medicine, Leiden University Medical Center, Leiden, Netherlands*
[b]*Center for Bone Quality and Center for Endocrine Tumors, Department of Surgery, Leiden University Medical Center, Leiden, Netherlands*

Background: Excess levels of parathyroid hormone (PTH) in primary hyperparathyroidism (PHPT) increase bone turnover in favor of resorption resulting in loss particularly of cortical bone with relative preservation of trabecular bone. Accordingly, Bone Mineral Density (BMD) is usually decreased at cortical sites and relatively preserved at trabecular sites. Despite these findings, fracture risk is increased at both non-vertebral and vertebral sites, and fractures occur at higher BMD than expected. We therefore hypothesized that components of bone quality other than BMD such as bone material properties also are affected.

Aim: To evaluate bone material properties using Impact Microindentation (IMI) in vivo in patients with PHPT.

Methods: We measured Bone Material Strength index (BMSi) by IMI at the midshaft of the tibia in 25 patients with PHPT(21 women), 10

of whom had prevalent fragility fractures(FF), and 25 euparathyroid controls matched for age, sex and FF status(21 women).

Results: Mean age of PHPT patients and controls was 63.7±13.7 and 62.6±12.5 years, respectively(p=0.64). Calcium and PTH levels were significantly higher in PHPT patients as expected. BMD was comparable in PHPT patients and controls at the lumbar spine (0.91±0.17 versus 0.86±0.10, p=0.22) and the femoral neck (0.69±0.12 versus 0.65±0.06, p=0.22). However, BMSi was significantly lower in PHPT patients compared to controls (76.7±5.5 versus 82.2±4.6, p< 0.001). In addition, BMSi was significantly lower in the 10 PHPT patients with FF compared to 15 PHPT patients without FF (74.0±5.5 versus 78.4±5.2, p=0.03).

Conclusion: BMSi was significantly lower in PHPT patients compared to euparathyroid matched controls, independently of BMD, and PHPT patients with fragility fractures had the lowest BMSi. Our data indicate that bone material properties are impaired in patients with PHPT, which might help explain their increased global fracture risk. IMI might be a valuable additional tool in the evaluation of bone fragility in patients with PHPT.

doi:10.1016/j.bonr.2020.100630

COP05

Treatments of osteoporosis increase bone material strength index in patients with low bone mass

Manuela Schoeb, Frank Malgo, Joséphine J.M. Peeters, Elizabeth M. Winter, Socrates E. Papapoulos, Natasha M. Appelman-Dijkstra
Center for Bone Quality, Leiden University Medical Center, Leiden, Netherlands

Background: Impact microindentation (IMI) is a minimally-invasive technique to assess tissue-level properties of bone in humans in vivo at the tibia. The resistance of cortical bone to indentation, measured as Bone Material Strength index (BMSi), is reduced in patients with fragility fractures, but there is no information about changes in values during long-term therapy. In the present study we assessed changes in BMSi in patients receiving anti-osteoporotic treatments for periods longer than 12 months.

Methods: We included treatment-naive patients with low bone mass who had a BMSi measurement with OsteoProbe® at presentation and consented to a repeat measurement after treatment.

Results: We studied 54 patients (34 women), median age 58 years, of whom 30 were treated with bisphosphonates or denosumab (treatment group) and 24 with vitamin D ± calcium alone (control group). There were no differences in clinical characteristics between the two groups with the exception of a higher number of previous fragility fractures in the treatment group (25 versus 4, p< 0.01) which also had lower baseline hip BMD (femoral neck 0.66±0.09 versus 0.70±0.09 g/cm^2, p=0.041; total hip 0.77±0.10 versus 0.84±0.12 g/cm^2, p=0.016), and lower baseline BMSi values (79.3±4.1 versus 82.2±4.1, p=0.014). After 23.1±6.6 months, BMSi increased significantly in the treatment group (82.4±4.3 versus 79.3±4.1, p< 0.001), but did not change in the control group (81.5±5.2 versus 82.2±4.1, p=0.35). Changes in BMSi with antiresorptives were inversely related with baseline BMSi values (r=-0.43, p=0.02), but not with changes in BMD. During the period of observation, two patients in the control group with large decreases in BMSi values (8.5 and 8.9%, respectively) sustained incident fractures.

Conclusion: In patients at increased fracture risk antiresorptive treatments induced BMD-independent improvement in bone material properties, the magnitude of which depended on pre-treatment values. Early identification of individuals with imminent fractures by IMI warrants further investigation.

doi:10.1016/j.bonr.2020.100631

COP06

Stable BMD after pregnancy and breast-feeding among women in their mid-thirties

Fiona E. McGuigan[a], Stefanie Untermann[a], Hanna Jensen[a], Kristina E. Akesson[a,b]
[a]*Clinical Sciences Malmö, Lund University, Malmö, Sweden*
[b]*Orthopaedics, Skåne University Hospital, Malmö, Sweden*

Attaining high bone mass in young adulthood may contribute to lower fracture risk later in life. However, this is also the principal period for child-bearing, and pregnancy and breast-feeding may lead to increased maternal bone resorption due to the nutritional demands of the foetus and neonate.

Objectives were first; to describe BMD and the association with pregnancy and duration of breast-feeding in young adult women; second to determine whether post-partum BMD recovery is partial or complete. In the population based PEAK-25 cohort (n=1061, age 25.5 ± 0.2) the majority (93%) were nulliparous at study entry with most having had a pregnancy by age 35.

BMD was measured at ages 25 and 35 (n=795 attended both assessments). Number of pregnancies was collated and duration of breast-feeding categorized; 1-6 months, >7-15 or >15 months. BMD and rate of change was analysed; adjusted for physical activity, BMI, alcohol and smoking. Written informed consent was obtained.

618 women (77.7%) had 1137 pregnancies (range 1-4). The majority (96%) breastfed (median accumulated duration 12 months). BMD was higher in those with at least one pregnancy, compared to nulliparous women, at the femoral neck (p_{adj}=0.039) and spine (p_{adj}=0.003). BMD was not significantly different with breast-feeding duration; but women breast-feeding for >15 months had higher rate of loss at the femoral neck.

In healthy, young northern European women with assumed calcium sufficiency, we observed no adverse effects from pregnancy and breast-feeding; with an overall positive effect on skeletal health at the spine.

	1. Nulliparous (n= 177)	2. Completed Pregnancy AND Breastfed (n=594)	3. Duration of Breast Feeding 1-6m (n=121)	4. Duration of Breast Feeding >7-15m (n=257)	5. Duration of Breast Feeding >15m (n=216)	ANOVA p-adj (group 3 v 4 v5)
Fem Neck BMD	1.013 (0.135)	1.015 (0.122)	1.021 (0.121)	1.012 (0.126)	1.016 (0.119)	0.267
Spine BMD	1.229 (0.154)	1.256 (0.137)	1.250 (0.140)	1.252 (0.139)	1.264 (0.133)	0.007
Change in Fem Neck	-0.327 (0.539)	-0.344 (0.627)	-0.188 (0.530)	-0.337 (0.528)	-0.440 (0.759)	0.004
Change in Spine	0.067 (0.517)	0.091 (0.461)	0.175 (0.494)	0.091 (0.462)	0.045 (0.436)	0.062

BMD, pregnancy & breast-feeding in young women

doi:10.1016/j.bonr.2020.100632

Concurrent Oral Presentations 2: Basic/Translational: Genetic and molecular control of bone cells

COP31

Mice carrying a ubiquitous R235W mutation of Wnt1 display a bone-specific phenotype

Timur Alexander Yorgan[a], Tim Rolvien[a], Julian Stürznickel[a], Nele Vollersen[a], Fabiola Lange[a], Anke Baranowsky[a], Irm Hermans-Borgmeyer[b], Jean-Pierre David[a], Ralf Oheim[a], Michael Amling[a], Thorsten Schinke[a]
[a]*Osteology and Biomechanics, University Medical Center Hamburg-Eppendorf, Hamburg, Germany*
[b]*Center for Molecular Neurobiology, University Medical Center Hamburg-Eppendorf, Hamburg, Germany*

Mutations of Wnt1, originally established as a key regulator of brain development through the generation of non-viable *Wnt1*-deficient mice, were recently found to cause either early-onset osteoporosis (EOOP) or osteogenesis imperfecta type XV (OI-XV). The deduced function of Wnt1 as an osteoanabolic factor has been confirmed in various mouse models with bone-specific inactivation or over-expression, however mice carrying disease-causing *Wnt1* mutations have not yet been described. Based on the clinical analysis of EOOP patients carrying a heterozygous *WNT1* mutation (p.R235W), we introduced this mutation into the murine *Wnt1* gene to address the question, whether this would cause a skeletal phenotype. $Wnt1^{+/R235W}$ and $Wnt1^{R235W/R235W}$ mice were born at the expected Mendelian ratio and did not display postnatal lethality or obvious non-skeletal phenotypes. At 12 weeks of age, the trabecular and cortical bone mass of $Wnt1^{R235W/R235W}$ mice was reduced, explained by a lower bone formation rate as compared to wildtype littermates (BV/TV: 5.7 vs. 8.6 %; Ct.Th: 146.2 vs. 168.9 μm; BFR/BS: 136.8 vs. 233.2 $\mu m^3/\mu m^2/y$). At 52 weeks of age, we also observed a moderate bone mass reduction in heterozygous $Wnt1^{+/R235W}$ mice (BV/TV: 2.7 vs. 5.2 %), thereby underscoring their value as a model of WNT1-dependent EOOP. Importantly, treatment of wildtype and $Wnt1^{+/R235W}$ mice by daily injection of parathyroid hormone (PTH), caused a similar osteoanabolic response in both groups. Our data demonstrate the pathogenicity of the *WNT1*-R235W mutation, confirm that controlling skeletal integrity is the primary physiological function of Wnt1, and suggest that osteoanabolic treatment with teriparatide should be applicable for individuals with *WNT1*-dependent EOOP.

doi:10.1016/j.bonr.2020.100645

COP32

Mitoguardin-2 deficiency results in severe osteoporosis

Davide Komla-Ebri, Andrea S. Pollard, Penny C. Sparkes, Elena J. Ghirardello, Apostolos Gogakos, John G. Logan, Graham R. Williams, J.H. Duncan Bassett
Imperial College London, London, United Kingdom

Miga2 encodes Mitoguardin-2, a key regulator of mitochondrial fusion, morphology and function. In a rapid-throughput skeletal phenotype screen of >1000 knockout lines generated by the International Knockout Mouse Consortium, we found that *Miga2* deficient mice had profoundly reduced bone mineralisation and strength and hypothesised that Mitoguardin-2 has an important and unrecognised physiological function in bone.

To investigate the role of *Miga2* in skeletal development and adult bone turnover, we performed detailed phenotyping of $Miga2^{-/-}$ mice (n≥10 per genotype, per age, per sex; approved by the local ethics committee). X-ray microradiography demonstrated reduced femur length (P14 -10.8% and P183 -3.9%: vs WT, $p< 0.001$ *t*-test) and impaired bone mineral content (P14 -11.2% and P183 -4.15%: vs WT, $p< 0.001$ Kolmogorov-Smirnov test). Furthermore, micro-CT analysis demonstrated reduced cortical thickness in both femur (P70 -5.9%; vs WT, $p< 0.05$ *t*-test) and caudal vertebrae (P70 -7.6%; vs WT, $p< 0.05$ *t*-test). Consistent with these findings, femur 3-point bend testing demonstrated severely reduced bone strength (P183 -25.2%; vs WT, $p< 0.05$ *t*-test) and stiffness (P183 -19.8%, vs WT $p< 0.001$ *t*-test), while vertebral compression testing also revealed markedly reduced strength (P183 -12.8% vs WT, $p< 0.05$ *t*-test) and stiffness (P183 -16.3%, vs WT $p< 0.05$ *t*-test). Histomorphometric analysis at P14 and P70 demonstrated no difference in growth plate and osteoclast parameters between $Miga2^{-/-}$ and WT mice, suggesting the abnormal phenotype in $Miga2^{-/-}$ mice results from a defect in the osteoblast lineage.

These data demonstrate that Mitoguardin-2 is required for growth during development and bone mineral accrual, and is essential for the maintenance of adult bone structure and strength. These studies indicate that precise regulation of mitochondrial fusion and function is essential for skeletal homeostasis and may represent a novel target for anabolic therapy.

doi:10.1016/j.bonr.2020.100646

COP33

Novel *RPL13* variants and evidence for incomplete penetrance in a human ribosomopathy with spondyloepimetaphyseal dysplasia

Alice Costantini[a], Jessica J. Alm[a], Francesca Tonelli[b], Helena Valta[c], Céline Huber[d], Anh N. Tran[e], Valentina Daponte[b], Nadi Kirova[a], Yong-Uk Kwon[f], Jung Yun Bae[g], Woo Yeong Chung[h], Shengjiang Tan[i], Yves Sznajer[j], Gen Nishimura[k], Tuomas Näreoja[e], Alan J. Warren[i], Valérie Cormier-Daire[d], Ok-Hwa Kim[l], Antonella Forlino[b], Tae-Joon Cho[m], Outi Mäkitie[a,c,n]
[a]*Department of Molecular Medicine and Surgery and Center for Molecular Medicine, Karolinska Institutet, Stockholm, Sweden*
[b]*Department of Molecular Medicine, University of Pavia, Pavia, Italy*
[c]*Metabolic Bone Clinic, University of Helsinki and Helsinki University Hospital, Helsinki, Finland*
[d]*Department of Clinical Genetics, Imagine Institute, Paris, France*
[e]*Department of Laboratory Medicine, Karolinska Institutet, Stockholm, Sweden*
[f]*Department of Orthopaedic Surgery, Inje University College of Medicine, Busan, Republic of Korea*
[g]*Department of Orthopaedic Surgery, Pusan National University Yangsan Hospital, Yangsan, Republic of Korea*
[h]*Department of Pediatrics, Busan Paik Hospital, Busan, Kosovo, Republic of*
[i]*Department of Haematology, University of Cambridge, Cambridge, United Kingdom*
[j]*Center for Human Genetic, Cliniques universitaires Saint-Luc, UCLouvain, Cliniques universitaires St. Luc, Brussels, Belgium*
[k]*Center for Intractable Diseases, Saitama Medical University Hospital, Saitama, Japan*
[l]*Pediatric Radiology Section, Woorisoa Children's Hospital, Seoul, Republic of Korea*
[m]*Division of Pediatric Orthopaedics, Seoul National University Children's Hospital, Seoul, Republic of Korea*
[n]*Folkhälsan Institute of Genetics, Helsinki, Finland*

Spondyloepimetaphyseal dysplasias (SEMD) are a heterogeneous group of skeletal disorders with short stature and major skeletal impairments. We report four unrelated families with SEMD in which we identified two monoallelic missense variants and one splice site variant in *RPL13*, encoding the ribosomal protein eL13. Notably, two of the families featured incomplete penetrance and variable expressivity of the disease, with phenotypes ranging from normal to severe SEMD. *In vitro* studies on primary dermal fibroblasts demonstrated normal eL13 expression, with proper subcellular localization but reduced colocalization with eL28 in patients (n=3) compared to healthy controls (n=3) ($p< 0.001$). Polysome profiling revealed a 1.3-fold increase in the ratio of 60S subunits to 80S ribosomes, suggesting impaired ribosomal function. Our *rpl13* mutant zebrafish model, generated by CRISPR-Cas9 editing, showed cartilage deformities in line with human phenotype (Figure 1). These findings extend the genetic spectrum of RPL13-related SEMD, underscore incomplete penetrance with wide phenotypic variability, and model the human disease *in vivo*, thus confirming the role of eL13 in skeletogenesis.

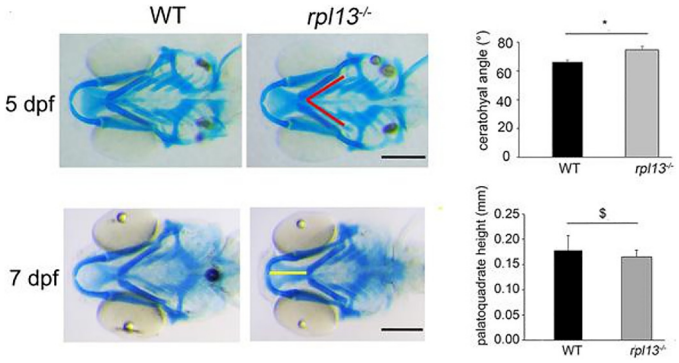

Figure 1. The *rpl13*-/- zebrafish model
Alcian Blue staining of control (WT) and *rpl13*$^{-/-}$ zebrafish at 5 and 7 days post fertilization (dpf). At 5 dpf, *rpl13*$^{-/-}$ show increased ceratohyal angle (red line) compared to WT (*p=0.006), and at 7 dpf, reduced palatoquadrate height (yellow line) ($ p=0.02). P-values from Student's T test. Scale bar: 200 μm.

doi:10.1016/j.bonr.2020.100647

COP34

Ablation of *Slc20a1/PitT1* and *Slc20a2/PiT2* in mice in the osteogenic lineage causes dentin dysplasia and formation of ectopic enamel islands

Sampada Chande[a], Caroline Zeiss[b], Joëlle Vézier[c,d], Nicholas W. Chavkin[e], Nati Hernando[f], Cecilia M. Giachelli[e], Carsten A. Wagner[f], Laurent Beck[c,d], Sarah Beck-Cormier[c,d], Clemens Bergwitz[a]
[a]*Medicine/Section Endocrinology, Yale School of Medicine, New Haven, United States*
[b]*Comparative Medicine, Yale School of Medicine, New Haven, United States*
[c]*5INSERM, U1229, RMeS, Nantes, France*
[d]*UMR_S1229, UFR Odontologie, Université de Nantes, Nantes, France*
[e]*Bioengineering, University of Washington, Seattle, United States*
[f]*Institute of Physiology, University of Zürich, Zürich, Switzerland*

Global *PiT2*-deficient mice display abnormal dentinogenesis, but tooth development is normal. To further evaluate the role of the two house-keeping phosphate (Pi) transporters *PiT1* and *PiT2* we generated a double knockout *(Osx-DKO)*in the osteogenic lineage using *osterix-GFP:Cre (Osx-Cre)*. *Osx-Cre* is not expressed in ameloblasts.

Evaluation of *Osx-DKO* mice using alcian blue/alizarin red whole mount staining at P22 showed normal skeletal development and uCT analysis of their femurs showed normal bone volume/total volume and cortical tissue density, but reduced cortical thickness (mean+/- SEM: 0.058+/-0.0035 mm (*PiT1*$^{flox/flox}$;*PiT2*$^{flox/flox}$, n=3); 0.046+/-0.0022 mm (*Osx-DKO*, n=3); p=0.0364). However, *Osx-DKO* mice failed to thrive and died shortly after weaning due to incisor fractures. None of the *Osx-Cre* controls (n>100) died or showed dental fractures, although we observed a subtle growth and craniofacial phenotype as previously reported.

Gross evaluation of *Osx-DKO* jaws showed greater wear of the incisors while molar teeth appeared normal. Histology of demineralized jaws revealed multifocal ameloblast dysplasia characterized by periodic abnormal proliferation of ameloblasts, which generate islands of enamel matrix detached from the tooth itself at P10 and P22. This manifests as multifocal enamel hypoplasia. Odontoblast pathology was not seen in these sections, however there is dentin dysplasia at P22.

Micro-CT analysis showed a decreased dentin volume/tooth volume (mean+/-SEM: 46.32+/-0.62 (*PiT1*$^{flox/flox}$;*PiT2*$^{flox/flox}$, n=8), 40.43+/-0.15 (*Osx-Cre* control, n=2) and 35.34+/-1.88 (*Osx-DKO*, n=8); p=0.0001) accompanied by an increased pulp volume/tooth volume (20.24+/-0.51 (*PiT1*$^{flox/flox}$;*PiT2*$^{flox/flox}$, n=8), 20.39+/-0.68 (*Osx-Cre* control, n=2) and 24.84+/-0.76 (*Osx-DKO*, n=8); p=0.0003) as described in the global *PiT2* KO. Further histomorphometric and SEM/EDX evaluation of non-demineralized jaws will be performed to analyze the pre-dentin and ectopic enamel areas.

Our findings confirm involvement of *PiT2* during the tooth mineralization as suggested by the dentin dysplasia. Additionally, *PiT1* may be involved in mesenchymal-epithelial signaling during tooth development as suggested by formation of ectopic enamel islands.

doi:10.1016/j.bonr.2020.100648

COP35

Postnatal expression of DLX5 and DLX6 promotes final osteoblast differentiation and the maintenance of cortical bone

Morgane Bourmaud[a], Camille Blandin[a], Eric Hay[b], Mylene Zarka[a], Caroline Marty[a], Giovanni Levi[c], Martine Cohen-Solal[a]
[a]*Hopital Lariboisiere, Inserm U1132 and Université de Paris, Paris, France*
[b]*Inserm U1132 and Université de Paris, Paris, France*
[c]*Museum National d'Histoire Naturelle, UMR CNRS/MNHN 7221, Paris, France*

Introduction: Low bone formation and reduction of osteoblast progenitors and/or the commitment of mesenchymal stem cells towards osteoblast differentiation is a cause of osteoporosis. The transcription factors DLX5 and DLX6 regulate the specification of osteoblasts in bone development. This project aims to analyze the role of DLX5/6 in bone remodeling.

Methods: We first generated Dlx5/6 $^{\Delta/\Delta\ Osx\text{-}Cre}$ mice and found they were all lethal. Subsequently, we generated Dlx5/6 $^{+/+\ Osx\text{-}Cre}$ and Dlx5/6 $^{\Delta/\Delta\ Osx\text{-}Cre}$ in which *Dlx5/6* knocked-out was induced by doxycycline administration 4 weeks after birth. Bone phenotype was analyzed at 3 and 6 months in male mice. Osteoblastic gene expression was assessed during the osteoblastic differentiation from murine osteoblastic progenitors.

Results: Compared to Dlx5/6 $^{+/+\ Osx\text{-}Cre}$, 3 month-old Dlx5/6 $^{\Delta/\Delta\ Osx\text{-}Cre}$ mice showed a higher tissue volume ($1.60x10^9\pm3.73x10^7$ vs $2.27x10^9\pm2.39x10^7\mu m^3$, p< 0.01) and BV/TV (14.83±0.66 vs 22.43± 2.82%, p< 0.05). Tb.Sp (193.37±5.47 vs 150.49±9.61μm, p< 0.01) and BFR (0.346±0.06 vs 0.208±0.007 $\mu m^3/\mu m^2$/day, p=0.08) were lower. Cortical bone analysis revealed lower cortical thickness (Ct.Th, 195.13±3.46 vs 141.78±4.21μm, p< 0.0001), along with higher medullary volume ($8.77x10^8\pm1.94x10^7$ vs $1.55x10^9\pm8.79x10^6\mu m^3$, p< 0.01). Cortical porosity was increased (1.26±0.11 vs 2.89±0.5%, p< 0.01) without any effect in osteocyte number. Similar results were observed at 6 months. *Dlx5/6* KO cells derived from calvaria and bone marrow as well as total bone tissue showed decreased expression of Col1, alkaline phosphatase and osteocalcin levels.

Discussion: Deletion of *Dlx5/6* resulted in high total and trabecular bone volume along with lower trabecular bone resorption and formation. Moreover, lack of *Dlx5/6* impaired cortical thickness and porosity, suggesting a differential role of *Dlx5/6* in the regulation of trabecular and cortical bone remodeling.

Conclusion: *Dlx5/6* plays a crucial role in postnatal bone remodeling. These data highlight that the activation of *Dlx5/6* complex could be a potential target to reduce osteoporosis

doi:10.1016/j.bonr.2020.100649

COP36

New *Ifitm5* S42L mouse model for atypical type VI OI connects types V and VI Osteogenesis Imperfecta

Gali Guterman-Ram[a], Ghazal Hedjazi[b], Chris Stephan[c], Stéphane Blouin[b], Paul Roschger[b], Klaus Klaushofer[b], Jochen Zwerina[b], Kenneth M. Kozloff[c], Nadja Fratzl-Zelman[b], Joan C. Marini[a]
[a]*Section on Heritable Disorders of Bone and Extracellular Matrix, Eunice Kennedy Shriver National Institute of Child Health and Human Development, National Institutes of Health, Bethesda, United States*

[b]Ludwig Boltzmann Institute of Osteology at Hanusch Hospital of OEGK and AUVA Trauma Centre Meidling, 1st Med. Dept. Hanusch Hospital, Vienna, Austria
[c]Departments of Orthopaedic Surgery and Biomedical Engineering, University of Michigan, Ann Arbor, United States

Osteogenesis Imperfecta (OI) is a rare collagen-related bone disorder. Type V OI, caused by recurrent dominant mutation in *IFITM5*/BRIL, and type VI OI, caused by recessive null mutations in *SERPINF1*/PEDF, have distinct features. *IFITM5* S40L, reported in 8 patients, causes severe dominant OI with phenotype, bone histology and decreased cellular secretion of PEDF similar to type VI OI, rather than Type V OI. Our objective is understanding the role of the pathways connecting *IFITM5* and *SERPINF1* in bone development.

We generated an *Ifitm5* S42L knock-in mouse model with NICHD-ACUC research approval.

Our investigations focused on validating that the new model recapitulates patients. First, newborn *Ifitm5* S42L mice, both heterozygous and homozygous, are non-lethal, have flared rib cage, shoulder and knee dislocations, and homozygotes have rib fractures and unmineralized calvaria. Radiographically, heterozygous mice exhibit »50% humeral fractures at 1,2-and 6-months, while homozygotes incur fractures in 96% of humerii, femora and pelvis. Like aVI OI patients, young heterozygous males have increased serum ALP and unchanged serum PEDF level ($p< 0.01$) vs. WT. Mechanical testing of 2-month heterozygous males showed reduced stiffness, yield and ultimate load, with markedly increased brittleness. Biomechanics are not explained by change in bone size, suggesting material differences. Vascular pore volume/BV was increased on μCT. Whole-body DXA-aBMD was significantly decreased in 1,2-and 6-month-old mice with a step effect, suggesting homozygotes are more severe than heterozygotes($p< 0.01$). qBEI revealed hypermineralization in 1 and 2-month heterozygous vs. WT males, with increased CaMean, CaPeak ($p< 0.05$) and tripling of CaHigh in cortical bone($p=0.0133$ in 1-month-old, $p=0.0027$ in 2-month-old mice). Cultured calvarial osteoblasts from heterozygous mice deposit increased mineralization by alizarin red staining ($p< 0.05$) and expression of osteoblast differentiation markers.

This validated model with physiologic levels of *Ifitm5* S42L expression will be used to understand mechanisms and pathways involving *Ifitm5* and *Serpinf1*.

doi:10.1016/j.bonr.2020.100650

Concurrent Oral Presentations 2: Clinical/Public Health: Bone strength and structure

COP13

Sphingosine 1-phosphate is a likely important factor exacerbating vascular calcification in chronic kidney disease

Najwa Skafi[a,b], Solenne Pelletier[c], Christophe Soulage[d], Sophie Reibel[e], Nicolas Vitale[f], Eva Hamade[a], Bassan Badran[a], Rene Buchet[b], David Magne[b], Dennis Fouque[g], Saida Mebarek[b], Leyre Brizuela[b]
[a]PRASE-EDST Campus Rafic Hariri-Hadath, Beirut, Lebanon
[b]CNRS UMR 5246 ICBMS MEM2 team, Villeurbanne, France
[c]Nephrology, CHU, Lyon Sud Inserm 1033, Pierre Benite, France
[d]UMR INSERM U.1060 - Université Lyon-1, Villeurbanne, France
[e]Chronobiotron UMS3415, Strasbourg, France
[f]UPR-3212 CNRS - Université de Strasbourg, Strasbourg, France
[g]Nephrology, CHU, Lyon Sud UCBL Carmen, Pierre Benite, France

Patients with chronic kidney disease (CKD), and particularly those under hemodialysis (HD), experience a dramatically increased risk of developing cardiovascular complications, mostly due to the exacerbation of vascular calcification (VC). VC likely relies on the trans-differentiation of vascular smooth muscle cells (VSMCs) into osteochondrocyte-like cells, which start an ossification-like process.

Sphingosine 1-phosphate (S1P) is a pleiotropic sphingolipid that regulates biological processes as proliferation, differentiation or angiogenesis. Sphingosine kinases 1 and 2 (SK1, SK2) catalyze the conversion of sphingosine into S1P. Because of the implication of S1P in cardiovascular and bone physiopathology, we explored if SK/S1P metabolism participates in CKD-associated VC.

The study involved 53 HD patients recruited in France from AURAL (*Association pour l'Utilisation du Rein Artificiel à Lyon*). This study was approved by a local ethical committee (*Lyon Sud Est IV*), and all HD patients were volunteers who gave informed consent after written information. Twelve healthy volunteers with no known kidney disease served as controls.

We demonstrated for the first time that serum S1P is significantly increased in CKD patients with mild aortic abdominal calcification (AAC) compared to healthy donors (2.4 ± 1.4 μM versus 1.3 ± 0.8 μM, $p=0.005$) or to patients without AAC (1.2 ± 0.9 μM, $p=0.005$). S1P serum content was correlated to sclerostin, an independent marker of VC in CKD ($p=0.04$).

Serum S1P was indeed significantly augmented in a rat model of CKD with VC. In addition, SK2 expression and activity were upregulated in the media of an *ex-vivo* model of aorta calcification. SK2 activity and S1P secretion were furthermore significantly enhanced in a VSMC line during trans-differentiation into calcifying cells. Finally, specific blockade of SK2/S1P signalling strongly inhibited calcification in these cells.

Taken together our results open an unexplored therapeutic option, targeting S1P metabolism, for the prevention and treatment of VC in CKD patients under HD.

doi:10.1016/j.bonr.2020.100639

COP14

Muscle density is better than bone density in the discrimination of incident hip fracture: a propensity score matching study

Ling Wang[a], Lu Yin[b], Xiaoguang Cheng[a], Glen M. Blake[c], Klaus Engelke[d]
[a]Department of Radiology, Beijing Jishuitan Hospital, Beijing, China
[b]National Center for Cardiovascular Disease, China, Beijing, China
[c]King's College London, St Thomas' Hospital, London, United Kingdom
[d]FAU, University Hospital, Erlangen, Germany

Objective: Muscle weakness might also play a significant role in the increased risk of hip fracture. The aim of the study is to explore the value of muscle parameters for the discrimination of acute hip fractures and to compare discriminating capabilities with bone variables.

Methods: 438 low-energy acute hip fracture cases and 316 healthy controls from the China Action on Spine and Hip Status (CASH) study were included in the study. Muscle cross sectional area (CSA) and density were measured for the gluteus maximus (G.max) and gluteus medius and minimus (G.med/min). Areal BMD (aBMD) of the femoral neck (FN) and total hip (TH) were measured. Using propensity score matching (PSM), we generated two samples with cases and controls matched for age, BMI and sex. Logistic models were used to evaluate the odds ratio (OR) of fracture per SD increase of muscle and bone parameters.

Results: After PSM, 159 femoral neck fracture cases were matched with 159 non-fracture controls, and 101 intertrochanteric fracture cases with 101 controls. G.max muscle Hounsfield unit (HU) value (FN fracture: OR 0.39, CI% 0.28-0.54, TR fracture: OR 0.23, CI% 0.13-0.39) and G.med/min muscle HU value (FN fracture: OR 0.11, CI% 0.07-0.19, TR fracture: OR 0.05, CI% 0.02-0.13) were strongly associated with hip fracture after adjustment for FN aBMD. At both fracture sites G.med/min muscle density showed the best discrimination (AUC 0.882 for FN fractures, 0.945 for TR fractures).

Conclusion: Muscle density performs better than aBMD and muscle size in the discrimination of hip fracture.

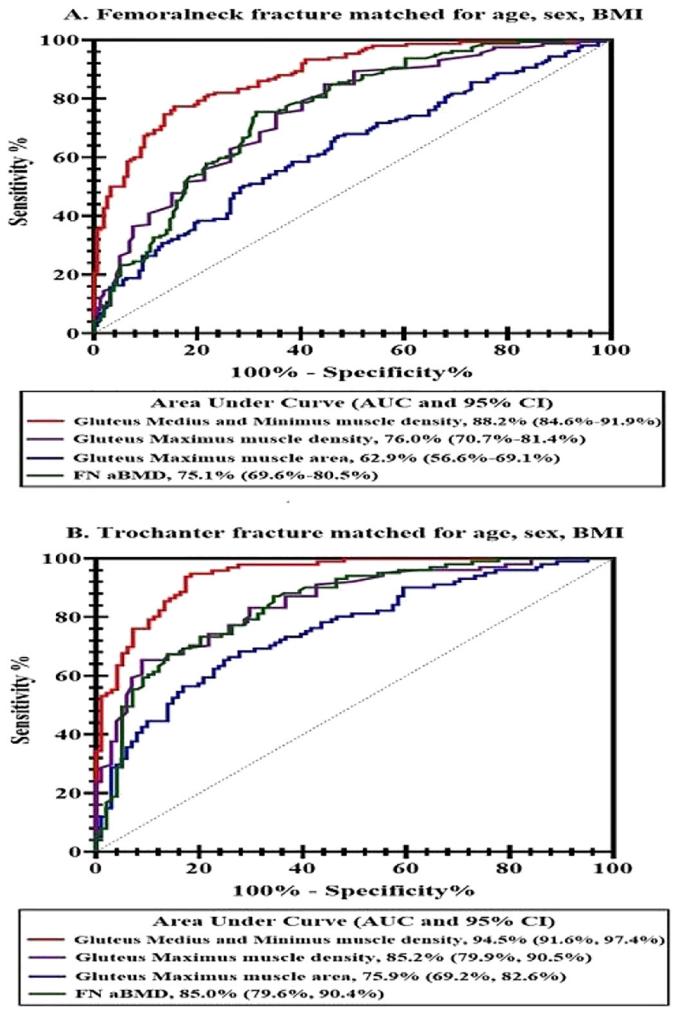

Figure 1. ROC curves: Comparison of fracture predication abilities using various indices in matched

doi:10.1016/j.bonr.2020.100640

COP15

Bone mass, structure and turnover in EOOP patients with LRP5/LRP6 mutations - Case series of 33 patients

Julian Stürznickel[a], Tim Rolvien[a,b], Alena Delsmann[a], Sebastian Butscheidt[b], Florian Barvencik[a], Uwe Kornak[c], Michael Amling[a], Ralf Oheim[a]

[a]*Department of Osteology and Biomechanics (IOBM), University Medical Center Hamburg-Eppendorf, Hamburg, Germany*

[b]*Department of Orthopedics, University Medical Center Hamburg-Eppendorf, Hamburg, Germany*

[c]*Institute of Medical Genetics and Human Genetics, Charité-Universitätsmedizin Berlin, Berlin, Germany*

Background and aim: Reduced bone mineral density (BMD; i.e., Z-score ≤-2.0) occurring already in young age (i.e., premenopausal women, men < 50 years) in the absence of secondary osteoporosis is considered as early-onset osteoporosis (EOOP). Regarding hereditary causes of EOOP, mutations affecting Wnt signaling pathways are of special interest due to its key role in bone mass regulation. Here, we analyze the effects of *LRP5*- and *LRP6*-variants on BMD, bone microstructure and turnover.

Materials and methods: EOOP patients with suspected hereditary cause were analyzed by a SureSelect XT gene panel comprising bone affecting genes. Assessment of skeletal status included turnover parameters (n=33), BMD by dual-energy X-ray absorptiometry (DXA; n=33) and microstructure *via* high-resolution peripheral quantitative computed tomography (HR-pQCT; n=25) compared to age- and sex-matched reference values. Values are presented as mean ± standard deviation (SD).

Results: We detected 28 *LRP5*- and 5 *LRP6*-variants in 33 EOOP patients (49.5 ± 17.0 years), including 8 novel variants. Biochemical analysis revealed low formation in all patients. Vertebral and peripheral fractures occurred in 11/33 and 16/33 patients, respectively, whereas 12/33 patients had no history of fractures. Z-score ≤-2.0 was detected in 22/33 and values in the spine were significantly lower compared to the hip (-2.3 ± 1.3 vs. -1.8 ± 0.7; p< 0.05). HR-pQCT analysis revealed moderately impaired microstructure in both trabecular and cortical parameters. Moreover, a significant correlation between DPD levels and Z-score was detectable (r=0.412, p< 0.05). No significant difference between patients with *LRP5*- or *LRP6*-variants was detectable.

Conclusion: LRP5-/LRP6-variants represent a relevant proportion of genetic alterations in EOOP patients. These show low bone formation, reduced Z-scores and impaired bone microstructure, leading to an increased risk of fractures. This detailed skeletal characterization improves the interpretation of novel variants, while the effect of other variants remains to be elucidated.

doi:10.1016/j.bonr.2020.100641

COP16

Bone peripheral microarchitecture in type 1 diabetes with and without neuropathy; a cross-section study

Tatiane Vilaca[a], Margaret Paggiosi[a], Jennifer Walsh[a], Dinesh Selvarajah[b], Richard Eastell[a]

[a]*Academic Unit Bone Metabolism, University of Sheffield, Sheffield, United Kingdom*

[b]*Department of Oncology and Metabolism, University of Sheffield, Sheffield, United Kingdom*

Fracture risk is increased in diabetes, especially in type 1 diabetes. The mechanisms involved are not established. Some evidence suggests that abnormalities in microarchitecture might be involved, especially in patients with microvascular disease.

We assessed bone microarchitecture using high resolution peripheral quantitative computed tomography in patients with type 1 diabetes with (T1DN+, n=20) and without (T1DN-, n=20) distal symmetric polyneuropathy and in controls (n=20). Participants were scanned at the standard site and at 14% bone length at the radius and tibia. We used non-parametric tests to compare the groups.

At the 14% length site, favourable trabecular microarchitecture was found in diabetes at both sites (table). At the standard site, tibial cortical porosity was 56% higher (p=0.009) and tibial connectivity was 120% higher (p=0.001) in T1DN+ compared to T1DN-.

Diabetes is associated with low bone turnover; the low bone turnover likely preserved trabecular microarchitecture, resulting in favourable findings at the 14% site.

At distal sites, the major feature was the increase in cortical porosity which was found only at the tibia and in patients with neuropathy. This finding suggested that microvascular complications, especially neuropathy, could affect bone vascularization and innervation and impact on cortical porosity. Overall, impaired microarchitecture is unlikely to be the main mechanism of bone fragility in diabetes.

	Radius			
	T1DN- vs control (%)	p	T1DN+ vs control (%)	p
Trabecular density (mgHA/cm3)	↑50	0.006**	↑14	0.057
Inner trabecular density (mgHA/cm3)	↑113	0.002**	↑29	0.031*
Trabecular number	↑27	0.002**	↑11	0.072
Trabecular BV/TV (no units)	↑50	0.006**	↑14	0.064
Meta/Inn trabecular density (no units)	↓45	0.002**	↓32	0.035*
Trabecular separation	↓23	0.001**	↓9	0.076
Trabecular inhomogeneity	↓24	0.001**	↓17	0.118

	Tibia			
	T1DN- vs control (%)	p	T1DN+ vs control (%)	p
Trabecular density (mgHA/cm3)	↑43	0.003**	↑35	0.046*
Inner trabecular density (mgHA/cm3)	↑53	0.002**	↑64	0.034*
Trabecular number	↑15	0.005**	↑15	0.023*
Trabecular BV/TV (no units)	↑43	0.003**	↑36	0.047*
Meta/Inn trabecular density (no units)	↓19	0.002**	↓19	0.044*
Trabecular separation	↓15	0.005**	↓18	0.021*
Trabecular inhomogeneity	↓25	0.001**	↓22	0.008**

Percentage differences in trabecular features between T1DN- and T1DN+ and control
*p<0.05 **p<0.017

doi:10.1016/j.bonr.2020.100642

COP17

Cortical porosity does not predict incident fractures in postmenopausal women

Frida Igland Nissen[a,b], Camilla Andreasen[a,c], Åshild Bjørnerem[a,b], Ann Kristin Hansen[a,c]
[a]*Department of Clinical Medicine, UiT The Arctic University of Norway, Tromsø, Norway*
[b]*Department of Gynecology and Obstetrics, University Hospital of North Norway, Tromsø, Norway*
[c]*Department of Orthopedic Surgery, University Hospital of North Norway, Tromsø, Norway*

Fracture risk is frequently assessed measuring areal bone mineral density (aBMD) or using Fracture Risk Assessment Tool (FRAX) including clinical risk factors. However, these tools have limitations and additional bone measurements may enhance the predictive ability of these tools. In cross-sectional studies, higher cortical porosity is found in women with fractures, and cortical porosity and cortical thickness are associated with fracture risk independent of aBMD and FRAX. Whether cortical porosity predicts incident fractures, is still elusive. In this prospective study, we examined whether cortical porosity of the proximal femur predicts incident fractures independent of aBMD in postmenopausal women. We pooled 211 postmenopausal women with fractures aged 54-94 years at baseline (cases) and 232 fracture-free age-matched controls in a nested case-control study. The cases had prevalent fractures (181 forearm, 26 proximal humerus and 4 hip). We assessed femoral neck (FN) aBMD, calculated FRAX 10-year probability of major osteoporotic fracture, and quantified femoral subtrochanteric cortical porosity, thickness, and cross-sectional area (CSA) from CT images using StrAx software. During a mean follow-up of 6.4 years, 114 of all 443 women suffered an incident fracture (33 forearm, 11 proximal humerus, 13 hip, 10 ankle, 15 vertebral, 32 others). Per SD higher total cortical porosity, thinner cortices, and smaller cortical CSA, hazard ratio (HR) (95% confidence interval) for fracture were 1.09 (0.91-1.30), 0.99 (0.82-1.20), and 1.08 (0.90-1.29), respectively, all $p > 0.100$. Cortical porosity of the inner transitional zone predicted incident fractures adjusted for prior fracture, HR 1.22 (1.00-1.48), $p = 0.045$, but not after additionally adjusted for FN aBMD, HR 1.15 (0.95-1.39), $p = 0.160$. Per SD higher FN aBMD and FRAX, HRs were 1.42 (1.14-1.76) and 1.39 (1.14-1.68), respectively, both $p \leq 0.001$. Based on this data, FN aBMD and FRAX predicted incident fractures in women, while cortical porosity did not.

doi:10.1016/j.bonr.2020.100643

COP18

Bone matrix mineralization increases with age and remains elevated after Teriparatide treatment in *WNT1* or *PLS3* mutation-related low-turnover osteoporosis: A transiliac bone biopsy study

Nadja Fratzl-Zelman[a], Katherine Wesseling-Perry[b], Riika E. Mäkitie[c], Paul Roschger[a], Jochen Zwerina[a], Ville-Valtteri Välimäki[d], Christine M. Laine[e,f], Matti J. Välimäki[g], Renata C. Pereira[b], Outi Mäkitie[c,e]
[a]*Ludwig Boltzmann Institute of Osteology at the Hanusch Hospital of OEGK and AUVA Trauma Centre Meidling, 1st Medical Department Hanusch Hospital, Vienna, Austria*
[b]*Department of Pediatrics, David Geffen School of Medicine at UCLA, Los Angeles, United States*
[c]*Folkhälsan Institute of Genetics and University of Helsinki, Helsinki, Finland*
[d]*Department of Orthopaedics and Traumatology, University of Helsinki and Jorvi Hospital, Helsinki University Hospital, Espoo, Finland*
[e]*Children's Hospital, University of Helsinki and Helsinki University Hospital, Helsinki, Finland*
[f]*Department of Endocrinology, Institute of Medicine, Sahlgrenska University Hospital and University of Gothenburg, Gothenburg, Sweden*
[g]*Division of Endocrinology, Department of Medicine, Helsinki University Central Hospital, Helsinki, Finland*

Introduction: Patients with defects in *WNT1* or *PLS3* have severe progressive osteoporosis characterized by low bone turnover, low bone mineral density, and fractures. Teriparatide increases serum bone formation and resorption markers but has only modest effects on iliac crest histomorphometry in these patients. We thus analyzed bone material properties in transiliac biopsy samples to further evaluate the effects of PTH on bone quality in these patients.

Subjects and Methods: Quantitative backscattered electron imaging (qBEI) was performed on iliac crest samples from 11 patients (9-75 years old) from two families (6 with *WNT1* mutation and 5 with *PLS3* mutation). A subset of 6 adults (*WNT1*patients: n=3; *PLS3* patients: n=3) underwent re-biopsy after 24 months of treatment with teriparatide (20μg/day). qBEI measures of bone mineralization density distribution were correlated with age, histomorphometric indices, and osteocyte-specific protein expression.

Results: Prior to teriparatide, the average calcium content of the bone matrix (CaMean) in the 6 adult patients with *PLS3* and *WNT1* mutations was 4% above reference values. The fraction of highly mineralized bone matrix (CaHigh) was 4.5-fold increased. Teriparatide further increased CaHigh in cortical bone (+15.69%, p=0.03) and the number of FGF23-expressing osteocytes in trabecular bone (+3.1%, p=0.03). In both pediatric and adult patients, CaMean was negatively correlated with histomorphometric measures of bone formation (versus OS/BS: R=-0.920; p< 0.0001; versus MS/BS: R=-0.897, p=0.0002) and positively with patient age, both in trabecular (R=0.878, p=0.0004) and in cortical bone (R=0.826, p=0.0017).

Conclusions: Bone matrix mineralization is elevated in patients with *WNT1* or *PLS3* mutations and increases with age as bone formation decreases. Matrix mineralization is unaffected by teriparatide in these patients. This departure from the typical response suggests that *WNT1* and *PLS3* may interfere with catabolic mechanisms of PTH and further studies are warranted to determine the precise mechanisms of these changes.

doi:10.1016/j.bonr.2020.100644

Concurrent Oral Presentations 3: Basic/Translational: Mechanisms of osteoporosis

COP07

TGF-β induced senescence is a novel therapeutic target for treating osteoporosis in Gerodermia Osteodysplastica

Wing Lee Chan[a], Jonathan Goldes[a], Magdalena Steiner[a], Alvin C. Ma[b], Stefan Mundlos[a], Uwe Kornak[a]

[a]*Institute for Medical Genetics and Human Genetics, Charité-Universitätsmedizin Berlin, Berlin, Germany*

[b]*Department of Health Technology and Informatics, The Hong Kong Polytechnic University, Hong Kong, China*

Gerodermia osteodysplastica (GO) is a rare hereditary disorder characterized by lax skin and osteoporosis. GO is caused by loss of function mutations in the gene *GORAB*, which is essential in mediating the COPI-mediated retrieval of trans-Golgi enzymes. Loss of Gorab caused defective protein glycosylation and reduced glycosaminoglycan contents. This leads to immature collagen network and elevated activation of TGF-β signaling. In this study, we used patient fibroblasts and a conditional mouse model in which *Gorab* is inactivated in the long bones (*Gorab^{Prx1}*) to study the role of overactivated TGF-β signaling in the pathomechanism of GO. We report that excessive TGF-β signaling elevated Nox4 expression in *Gorab*^{Prx1} (2.00 ± 0.23 fold, N=6, p< 0.01) and in patient fibroblast (2.05 ± 0.07 fold, N=4, p< 0.01), resulting in increased mitochondrial superoxide (1.74 ± 0.14 fold, N=4, p< 0.01 in *Gorab^{Prx1}*; 1.20±0.06 fold in patient fibroblast, N=6, p< 0.01). The increased oxidative stress is correlated with DNA damage accumulation in *Gorab^{Prx1}* (2.35±0.24 fold increased γH2AX level, N=3, p=0.015) and in patient fibroblast (1.52±0.05 fold increase in cells with 53BP1 nuclear foci; N=3, p< 0.01). This led to significant upregulation of the cell cycle inhibitor Cdkn2a (p16) expression (4.02±0.50 fold in *Gorab^{Prx1}*, N=5, p< 0.001; 6.32± 1.03 in patient fibroblasts, N=4, p< 0.01) and cellular senescence. Targeting this TGF-β induced senescence axis with either anti-TGF-β antibody 1D11, the antioxidant N-acetylcysteine (NAC), or inactivation of Cdkn2a ameliorated the osteoporosis phenotype. These results demonstrated the crucial role and therapeutic potential of targeting TGF-β-induced senescence in GO.

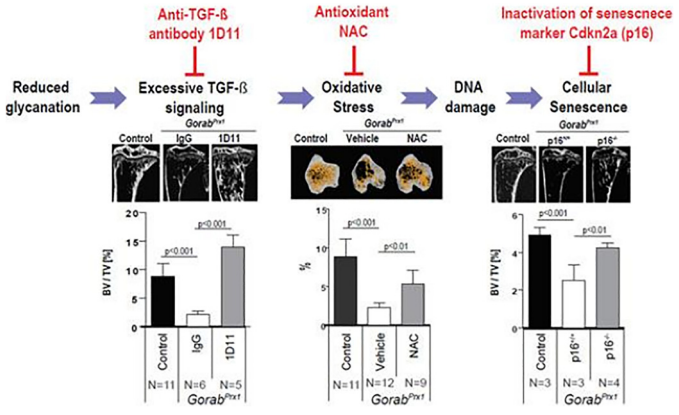

Summary Figure

doi:10.1016/j.bonr.2020.100621

COP08

Protective effect of *Saccharomyces boulardii* CNCM I-745 on the development of inflammatory osteoclasts and inflammatory bone destruction

Maria-Bernadette Madel[a], Lidia Ibáñez[b], Thomas Ciucci[c], Antoine Boutin[a], Rodolphe Pontier-Bres[d], Christophe Hue[e], Majlinda Topi[a], Henri-Jean Garchon[e,f], Matthieu Rouleau[a], Dorota Czerucka[d], Abdelilah Wakkach[a], Claudine Blin-Wakkach[a]

[a]*Université Côte d'Azur, CNRS UMR 7370, Laboratoire de PhysioMédecine Moléculaire, Nice, France*

[b]*Cardenal Herrera-CEU University, Department of Pharmacy, Valencia, Spain*

[c]*National Cancer Institute, National Institutes of Health, Laboratory of Immune Cell Biology, Center for Cancer Research, Bethesda, United States*

[d]*Centre Scientific de Monaco, Monaco, Monaco*

[e]*Université Paris-Saclay, UVSQ, INSERM, Infection et inflammation, Montigny-le-Bretonneux, France*

[f]*Genetics Division, Ambroise Paré Hospital, AP-, HP, Boulogne-Billancourt, France*

Pathological bone destruction is characterized by the emergence of inflammatory osteoclasts (i-OCLs) that differ from steady-state tolerogenic osteoclasts (t-OCLs) by their progenitors and opposite immune functions. However, the mechanisms controlling their emergence are poorly understood. Recent findings showed that bone loss in osteoporosis strongly correlates with gut microbiota dysbiosis, through inflammatory response modulation. Thus, our aim was to better characterize these two OCL subsets and identify new potential specific targets for i-OCLs focusing on gut eubiosis restoration.

Comparative RNA-sequencing of purified i-OCLs and t-OCLs revealed an upregulation of pattern recognition receptors (PRRs) involved in anti-fungal responses including Dectin-1 (p=0.07; log2FC -1.19), Mincle (p=0.06; log2FC -0.87) and TLR2 (p< 0.0001; log2FC -1.86) in i-OCLs. *In vitro*, PRR-specific agonists significantly reduced i-OCLs formation (p< 0.0001) without affecting t-OCLs or the phagocytic capacity and viability of OCLs. Similar results were observed *in vitro* in the context of osteoporosis where agonists blocked OCL differentiation from ovariectomized (OVX), but not SHAM control mice (p< 0.0001). Thus, to modulate i-OCLs *in vivo*, we used *Saccharomyces boulardii* CNCM I-745 (*Sb*), a well-studied probiotic known for its anti-inflammatory effects. *Sb* administration in OVX-mice significantly reduced bone destruction compared to untreated mice (BV/TV,p< 0.0001) (Fig. 1) and the proportion of i-OCLs (p< 0.0001) without affecting t-OCLs.

Our results demonstrate that specific i-OCL inhibition is highly promising to combat inflammatory bone destruction. Moreover, our findings highlight the protective effect of *Saccharomyces*

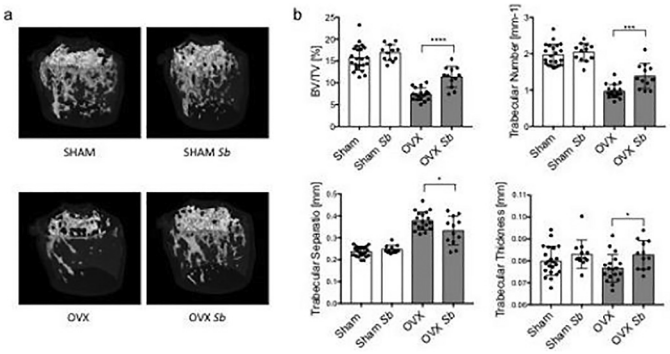

Fig. 1. Saccharomyces boulardii CNCM I-745 has a protective effect on osteoporosis. MicroCT analysis of OVX and SHAM control mice treated with the probiotic yeast Saccharomyces boulardii (Sb). **a** Representative μCT images of femurs from SHAM OVX mice treated with Sb. **b** Histograms indicate mean ± S.D. of bone volume fraction (BV/TV), trabecular number, thickness and separation (n = 12.). *p<0.05; **p<0.01; ***p<0.001; ****p<0.0001; n.s. no significant difference.

boulardii CNCM I-745 on bone destruction and provide novel regulatory mechanisms as new therapeutic targets for inflammatory bone loss.

doi:10.1016/j.bonr.2020.100622

COP09

Enpp1 enzyme replacement restores bone mass in murine model of Enpp1 associated osteoporosis

Demetrios Braddock[a], Dillon Kavanagh[a], Ralf Oheim[b], Kristin Zimmerman[a], Simon V. Kroge[b], Paul Stabach[a], Steven Tommasini[c], Michael Levine[d], Thomas Carpenter[e], Mark Horowitz[c]

[a]*Pathology, Yale School of Medicine, New Haven, United States*
[b]*Department of Osteology and Biomechanics, University Medical Center Hamburg-Eppendorf, Hamburg, Germany*
[c]*Orthopaedics and Rehabilitation, Yale School of Medicine, New Haven, United States*
[d]*Pediatric Endocrinology, University of Pennsylvania, Philadelphia, United States*
[e]*Pediatric Endocrinology, Yale School of Medicine, New Haven, United States*

Human heterozygous ecto-nucleotide pyrophosphatase/phosphodiesterase (ENPP1) deficiency results in mild elevation of FGF23, mild phosphate wasting, intermediate levels of plasma pyrophosphate, and early onset osteoporosis (EOOP), a phenotype recapitulated in homozygous Enpp1 deficient mice (*Enpp1*$^{asj/asj}$). To determine whether Enpp1 enzyme replacement would affect bone mass, we compared the skeletal phenotype of WT and *Enpp1*$^{asj/asj}$ mice treated with Enpp1-Fc or vehicle on a low magnesium, high phosphate diet to exacerbate the mineralization deficiency ('acceleration diet'). We found that, like *Enpp1*$^{asj/asj}$ mice fed normal chow for 10 weeks, *Enpp1*$^{asj/asj}$ mice fed the acceleration diet for 5 weeks exhibit decreased trabecular bone mass (Tb. BV/TV 70%, Tb.Sp 125%, and TbN 82% of WT) and reduced cortical bone mass (Ct. BV/TV 90% and Ct. Thickness 72% of WT). Also similar to 10-week *Enpp1*$^{asj/asj}$ mice fed normal chow, tibias of 5-week *Enpp1*$^{asj/asj}$ mice fed acceleration diet exhibited less favorable biomechanics (maximum load, stiffness, and total work of 52%, 45%, and 27% of WT, respectively). Treating the *Enpp1*$^{asj/asj}$ mice between weeks 2-5 with Enpp1-Fc normalized trabecular bone mass parameters, and normalized or improved bone biomechanical properties (normalized maximum load compared to WT, improved stiffness to 74% and total work to 63% of WT) and cortical bone mass (improved Ct. BV/TV to 92% and Ct.Th to 81% of WT). Furthermore, qBEI showed no significant differences in BMDD or osteocyte lacunae of mice on 'acceleration diet' (treated or untreated). Finally, a consequence of the acceleration diet was renal failure due to tissue mineralization in untreated *Enpp1*$^{asj/asj}$ mice, which appeared after week 4 and was prevented with ENPP1-Fc. However, no histological findings specific for renal osteodystrophy, including histomorphometry and qBEI, were detected, suggesting that renal osteodystrophy did not develop in the untreated mice. Our results suggest that bone mass in Enpp1 deficiency may respond to Enpp1 enzyme replacement therapy.

doi:10.1016/j.bonr.2020.100623

COP10

Loss of glucocorticoid rhythm induces an osteoporotic phenotype in mice

Maaike Schilperoort[a], Jan Kroon[a], Sander Kooijman[a], Cheraine Bouten[a], Ilse Gille[a], Kathrin Mletzko[b], Felix Schmidt[b], Hetty Sips[a], Leo van Ruyven[c], Bjorn Bosse[b], Alberto Pereira[a], Natasha Appelman-Dijkstra[a,d], Nathalie Bravenboer[a], Patrick Rensen[a], Onno Meijer[a], Elizabeth Winter[a,d]

[a]*Department of Internal Medicine, Division of Endocrinology, Einthoven Laboratory for Experimental Vascular Medicine, Leiden University Medical Center, Leiden, Netherlands*
[b]*Department of Osteology and Biomechanics (IOBM), University Medical Center Hamburg-Eppendorf, Hamburg, Germany*
[c]*Department of Functional Anatomy, Academic Centre for Dentistry Amsterdam (ACTA), Academic Centre for Dentistry Amsterdam (ACTA), Amsterdam, Netherlands*
[d]*Department of Internal Medicine, Division of Endocrinology, Einthoven Laboratory for Experimental Vascular Medicine, Center for Bone Quality, Leiden University Medical Center, Leiden, Netherlands*

Glucocorticoid (GC)-induced osteoporosis is a widespread health problem that is accompanied with increased fracture risk. Detrimental effects of GC therapy on bone have been ascribed to the excess in GC exposure, but it is unknown whether disruption of the endogenous GC rhythm inherent to GC therapy also plays a role. To investigate this, we subcutaneously implanted female C57Bl/6J mice with either vehicle pellets or slow-releasing corticosterone (CORT) pellets to blunt CORT rhythm without inducing hypercortisolism (n=10 mice/group). This experiment was approved by the Central Animal Experiments Committee. Flattening of the CORT rhythm for 7 weeks reduced cortical and trabecular bone volume (-8.1%, P=0.0009 and -25.5%, P=0.017 respectively), cortical and trabecular thickness (-6.9%, P< 0.0001 and -8.7%, P=0.03 respectively), and cortical BMD (-3.4%, P=0.032), as determined by micro-CT analysis. Furthermore, TRAP levels were increased (+42%, P=0.008) while P1NP levels were decreased (-37%, P< 0.0001) in plasma of mice with a flattened CORT rhythm compared to vehicle, indicative of a negative balance in bone remodelling. Double calcein labeling of bone *in vivo* revealed a reduced bone formation, as reflected by a reduced mineral apposition rate (MAR; -20%, P=0.018), mineralizing surface per bone surface (MS/BS; -23%, P=0.014) and bone formation rate per bone surface (BFR/BS; -39%, P=0.002). Collectively, these perturbations in bone turnover and structure decreased bone strength (-14.7%, P=0.003) and stiffness (-11.1%, p=0.003), as determined by mechanical testing. In conclusion, we demonstrate for the first time that flattening of the GC rhythm results in an osteoporotic phenotype in mice. Our findings indicate that at least part of the fracture risk associated with GC therapy may be the consequence a disturbed GC rhythm, rather than an excess in GC dose alone.

doi:10.1016/j.bonr.2020.100624

COP11

Protein Kinase G II signaling is osteoprotective in dexamethasone-treated mice

Shyamsundar Pal China[a], Hema Kalyanaraman[a], Julian J. Garcia[b], John Tat[a], Robert L. Sah[b], Renate B. Pilz[a]

[a]*Department of Medicine, University of California, San Diego, United States*
[b]*Department of Bioengineering, University of California, San Diego, United States*

Glucocorticoid-induced osteoporosis (GIOP) is the most common form of secondary osteoporosis, occurs due to suppressed osteogenesis. Anti-resorptive bisphosphonates are first-line treatment for GIOP, but they further suppress bone turnover. We previously showed that pharmacological activation of Protein kinase G (PKG) with cGMP-elevating agents (Cinaciguat) and transgenic overexpression

of a constitutively active PKGII (*prkg2*^{RQ}) have bone-anabolic effects. We hypothesized that increased PKGII signaling may prevent dexamethasone-induced bone loss.

Twelve-week old male C57BL/6 wild-type (WT) mice (IACUC-approved protocol S10121) were randomized to receive Vehicle, dexamethasone (DX, 2.5mg/kg, s.c. on alternative days) or DX+ cinaciguat (Cin, 10μg/kg, daily) for five weeks. Osteoblast specific (Col1a1-promoter) *prkg2* transgenic mice (Tg) and their WT littermates were treated similarly with Vehicle or DX. Bone micro-architecture and strength were measured ex-vivo by μCT and three-point-bending, respectively. Primary osteoblasts (POBs) were used for *in vitro* studies. Data (mean±SEM) were analyzed using t-test or ANOVA followed by Dunnett´s multiple comparisons tests.

Dexamethasone decreased cortical bone volume and femoral strength, reduced cross-sectional thickness (Cs.Th.), cross-sectional bone-area (B.Ar) and ultimate load to failure; Cinaciguat prevented DX-induced bone deterioration. Cortical bone quality in dexamethasone-treated *prkg2*^{RQ} Tg mice was comparable to that of vehicle-treated WT littermates, and superior to dexamethasone-treated WT littermates. DX treatment (5μM) of WT POB reduced proliferation (MTT), and expression of osteocalcin, β-catenin and CyclinD1 mRNAs; Cinaciguat (500nM) prevented these glucocorticoid effects in WT POBs, and *prkg2*^{RQ} Tg POBs were resistant to dexamethasone.

Enhanced PKGII signaling prevents Dx-induced bone loss and PKGII may represent a novel treatment target for GIOP.

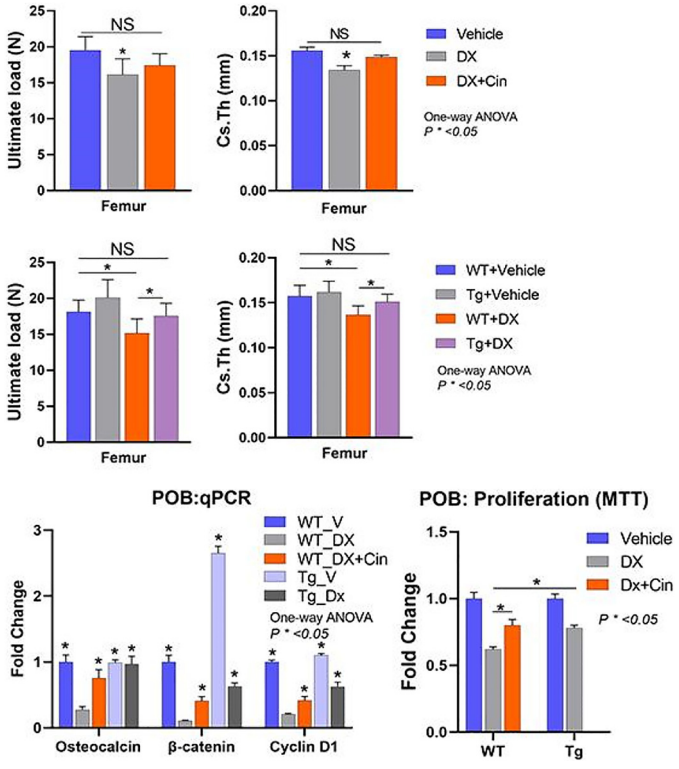

Bone quality assessments and in vitro results

doi:10.1016/j.bonr.2020.100625

COP12

Delayed fracture healing in *Mmp10* (Stromelysin 2) knockout mice: Molecular and cellular mechanism

José Valdés-Fernández[a], Tania López-Martínez[a], Purificación Ripalda-Cemboráin[b], Isabel Calvo[c], Borja Sáez[c], Juan Antonio Romero-Torrecilla[a], Josune Orbe[d], José Antonio Rodríguez[d], José Antonio Páramo[d], Felipe Prósper[a,e], Froilán Granero-Moltó[a,b]

[a]*Cell Therapy, Clínica Universidad de Navarra, Pamplona, Spain*
[b]*Orthopaedic Surgery and Traumatology, Clínica Universidad de Navarra, Pamplona, Spain*
[c]*Myeloid Pathology, Center for Applied Medical Research (CIMA), Pamplona, Spain*
[d]*Atherothrombosis, Center for Applied Medical Research (CIMA), Pamplona, Spain*
[e]*Haematology, Clínica Universidad de Navarra, Pamplona, Spain*

Background: After an injury bone develops a healing response recovering its structure and function without forming a scar tissue. Matrix metalloproteinases play a leading role in the remodeling of the extracellular matrix during this process, in consequence, disorders affecting MMPs activity could impair the fracture-healing process. MMP-10 is a matrix metalloproteinase highly similar to MMP-3 (Stromelysin 1) with a wide spectrum of protein targets *in vitro*.

Purpose: To determine the role of MMP-10 during fracture repair.

Methods: All animal procedures were approved by our institutional committee for the use in animals in research. A closed fracture was performed in wild type (WT) and *Mmp10* knockout (Mmp10^{KO}) C57BL/6 mice. Repair process was analyzed at 7-, 10-, 14- and 21-days post fracture (-dpf) by histology, immunohistochemistry and micro computed tomography (mCT).

Results: By mCT analysis we found a significant increase of the callus volume at 14-dpf in Mmp10^{KO} mice (WT, 17.13±4.56 mm^3; Mmp10^{KO}, 27.64±11.82 mm^3, p=0.023). Interestingly, at 21-dpf the callus volume between both groups was similar (WT, 13.59±3.48; Mmp10^{KO}, 17.50±4.99, p=0.1564). Segmentation of the callus at 14-dpf indicates that the differences in callus volume were located in soft tissue accumulation (WT, 6.375±3.839 mm^3; Mmp10^{KO}, 12.270±8.100 mm^3, p=0.0433) without significant differences in bone tissue content. Histomorphometric analysis showed increased content of cartilage in Mmp10^{KO} mice (WT, 5.995±6.256 mm^2; Mmp10^{KO}, 18.290±10.770 mm^2, p=0.0124) together with osteoclast accumulation as detected by TRAP staining at 14-dpf, suggesting a deficient osteoclast activity. Indeed, the observed phenotype was rescued by a non-competitive WT bone marrow (BM) transplant. Conditioned medium derived from BM cultures derived from Mmp10^{KO} mice presented accumulation of unprocessed proMMP-9 that could be rescued by addition of recombinant MMP-10.

In conclusion, lack of MMP-10 activity results in transient fracture healing impairment with delayed cartilage resorption derived from reduced MMP-9 activity in macrophages/osteoclasts.

doi:10.1016/j.bonr.2020.100626

Concurrent Oral Presentations 3: Clinical/Public Health: Novel targets in managing bone diseases

COP25

Prolongation of the reversal-resorption phase leads to increased cortical porosity in men and women

Bilal M. El-Masri[a,b,c], Majken I. Kejser[a,b,c], Line L. Sørensen[a,b,c], Xenia G. Borggaard[a,b,c], Malene H. Nielsen[a,b,c], Lene W.T. Boel[d], Kaja S. Laursen[d], Jesper S. Thomsen[e], Christina M. Andreasen[a,b,c], Thomas L. Andersen[a,b,d]

[a]Clinical Cell Biology, Department of Pathology, Odense University Hospital, Odense, Denmark
[b]Department of Clinical Research, University of Southern Denmark, Odense, Denmark
[c]Department of Molecular Medicine, University of Southern Denmark, Odense, Denmark
[d]Department of Forensic Medicine, Aarhus University, Aarhus, Denmark
[e]Department of Biomedicine, Aarhus University, Aarhus, Denmark

Our recent studies of cortical bone of aging women show an age-related accumulation of enlarged eroded pores, reflecting a prolonged reversal-resorption phase and delayed bone formation, contributes substantially to the age-induced cortical porosity in women. The study investigates age-induced cortical porosity and thinning in men and women, responsible remodeling events, and whether the cumulative eroded pores in aging women reflect prolongation of the reversal-resorption phase. 2D-histomorphometric analysis was performed on iliac crest autopsies from 35 women and 35 men (aged 20-95 years), approved by the Danish Medical Ethical Committee (1506824). Intracortical pores were classified according to remodeling type, stage, and positioning. 20 eroded pores from the 2D-analysis were 3D-traced in 6 young and 6 old women and classified in 200 consecutive sections above and below the central section. The study illustrates an increase in cortical porosity with age (r_s=0.40, p< 0.05) in women. An increased mean pore diameter with age (r_s=0.46, p< 0.01)and porosity (r_s=0.80, p< 0.0001) in women, and with porosity (r_s=0.80, p< 0.0001) in men was illustrated. An increase in the fraction of type 2 pores with age (r_s=0.34,p<0.05) and porosity (r_s=0.34, p<0.05) and a decrease in the fraction of type 1 pores with age (r_s=-0.34, p<0.05) and porosity in women (r_s=0.34, p<0.05) was illustrated. Additionally, eroded, coalescent type 2 pores contributed significantly to porosity in men (r_s=0.38, p< 0.05)and women (r_s=0.62, p< 0.0001). 3D-tracing of eroded type 2 pores in elderly are part of an extended, branched and complex network of eroded canals with limited transition to formation, resulting from coalescing remodeling events with a prolonged reversal-resorption phase. We confirm, porosity in both genders is mainly the cumulative result of enlarged and merged type 2 pores. 3D-tracing supports that these pores reflect prolongation of the reversal-resorption phase, delaying initiation of bone formation.

doi:10.1016/j.bonr.2020.100651

COP26

Leveraging data from bivariate genome-wide association meta-analysis to unravel novel pleitropic pathways of bone-muscle crosstalk

Katerina Trajanoska[a], Niki L. Dimou[b], David Karasik[c], Fernando Rivadeneira[a], Gefos Consirtia[d]
[a]Internal Medicine, Erasmus University Medical Center, Rotterdam, Netherlands
[b]Department of Hygiene and Epidemiology, University of Ioannina School of Medicine, Ioannina, Greece
[c]Bar-Ilan University, Azrieli Faculty of Medicine, Safed, Israel
[d]Genetics, Rotterdam, Netherlands

Background: The intimate relationship between bone and muscle is governed by various mechanical and biochemical interactions; regulated by a complex network of pleiotropic genes within common biological pathways. We aimed to assess pleiotropy between bone and muscle by performing a bivariate genome-wide association study (GWAS).

Methods: We included 15 cohorts from populations across Europe, the US and Australia (N_{total}=30,531). Total body BMD (TB-BMD; g/cm2) and lean mass (TB-LM; kg) were measured in all cohorts using DXA. SNPs were imputed to the Haplotype Reference Consortium (HRC) reference panel. Each cohort performed univariate GWAS adjusted for age, gender, height, fat percentage and principal components using 8,027,751 SNPs. After GWAS meta-analysis genome-wide significance (GWS) was set at P< 5×10^{-8}. We used a sum rank method to test for pleiotropic loci influencing both TB-BMD and TB-LM.

Results: The univariate TB-BMD GWAS identified 18 signals all mapping to known BMD loci. Only four loci were associated with TB-LM, two of which were novel associations mapping to *SPEG* (rs1810144-C, beta=0.05SD; P=6.2×10^{-10}) and *MYPN* (rs12415105-G,beta=0.04SD; P=3.7×10^{-8}). Both *SPEG* and *MYPN* have evidence from animal models for implication in muscle biology. Notably, the bivariate meta-analysis yielded 17 pleiotropic signals from 15 different loci mapping in or near *MEF2C*, XYLB/ACvr2B, *PPP6R3/LRP5*, *LRP4* and *SLC27A6* among others (Figure 1), linked with both bone and muscle biology.

Conclusion: Our findings provide basis for future functional assessments aimed at unravelling biological mechanisms underlying complex bone-muscle interactions; with the potential of pinpointing strategies for the joint prevention and intervention of osteoporosis and sarcopenia.

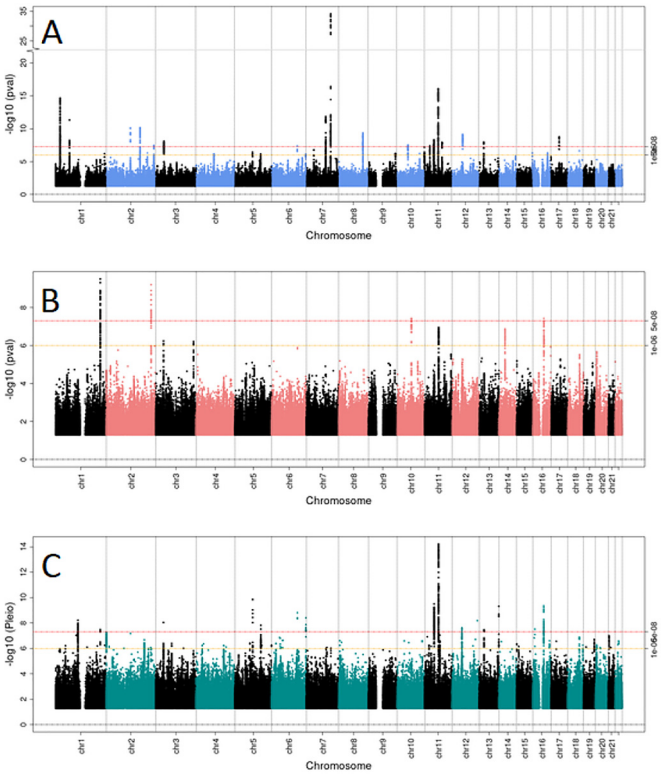

Manhattan plots: A) Univariate TB-BMD, B) Univariate TB-LM and C) Bivariate GWAS

doi:10.1016/j.bonr.2020.100652

COP27

Membrane palmitoylated protein 7 (MPP7) and anaphase promoting complex subunit 1 (ANAPC1) associate with bone remodelling and osteoporosis

Petra Malavašič[a], Ajda Ogrin[b], Iryna Khrystoforova[c], Einav Wircer[c], Chen Shochat[c], Janja Marc[b], David Karasik[c], Nika Lovšin[b]
[a]General Hospital Novo mesto, Novo mesto, Slovenia
[b]Clinical Biochemistry, Faculty of Pharmacy, University of Ljubljana, Ljubljana, Slovenia
[c]Bar Ilan University, Safed, Israel

Genome-wide association studies (GWAS) are one of the most common approaches to identify genetic loci that are associated with bone

mineral density (BMD). Such novel genetic loci represent new potential targets for the prevention and treatment of fragility fractures. GWAS have identified hundreds of associations with BMD; however, only few have been functionally evaluated, and functional characterization remains a challenge. Two loci significantly associated with femoral neck BMD at genome-wide level are intronic SNPs rs3905706, ($p = 2.4 \times 10^{-16}$) located in MPP7 gene and SNP rs17040773 ($p = 1.5 \times 10^{-9}$) located in ANAPC1 gene. We therefore examined the expression of these candidate genes in human tissues, cultured cells, and in animal model (zebrafish). Human bone tissue samples were obtained from 47 osteoporotic, and healthy controls. The expression of MPP7 was significantly 2-fold decreased in bone tissues from osteoporotic patients as compared to osteoarthritic and control tissues. On the contrary, the expression of ANAPC1 gene did not significantly differ between osteoporotic, osteoarthritic and control human bone and muscle tissues. Next, we examined mpp7a and anapc1 expression in whole fish during zebrafish development and adulthood, by in situ hybridisation and qPCR. mpp7a was highly significantly expressed in zebrafish scales (ossified tissue) than in muscle, whereas anapc1 expression was equally high in both zebrafish tissues. anapc1 expression increased in the newly formed zebrafish fins (2,6-fold, p=0,009), thereby indicating a role in adult tissue regeneration, while mpp7a expression remained unchanged during fin regeneration. In addition, we also investigated expression of MPP7 and ANAPC1 during osteogenic and adipogenic differentiation of human mesenchymal stem cells. Altogether, our findings suggest that MPP7 and ANAPC1 play an important role in bone remodelling and osteoporosis susceptibility in humans.

doi:10.1016/j.bonr.2020.100653

COP28

Long-term safety in adults with X-linked Hypophosphatemia (XLH) treated with Burosumab, a fully human monoclonal antibody against FGF23: Final results of a phase 3 trial

Peter Kamenický[a], Anthony A. Portale[b], Tom Carpenter[c], Karine Briot[d], Erik A. Imel[e], Thomas Weber[f], Pisit Pitukcheewanont[g], Hae Il Cheong[h], Suzanne Jan de Beur[i], Yasuo Imanishi[j], Nobuaki Ito[k], Robin Lachmann[l], Hiroyuki Tanaka[m], Farzana Perwad[b], Lin Zhang[n], Alison Skrinar[n], Linda Rees[n], Karl L. Insogna[c], On behalf of the AXLES 1 Investigators

[a]*Université Paris-Sud, Le Kremlin Bicêtre, Paris, France*
[b]*University of California San Francisco, San Francisco, United States*
[c]*Yale School of Medicine, New Haven, United States*
[d]*Centre d'Evaluation des Maladies Osseuses, Hôpital Cochin, Paris, France*
[e]*Indiana University School of Medicine, Indianapolis, United States*
[f]*Duke University Medical Center, Durham, United States*
[g]*Children's Hospital Los Angeles, University of Southern California Keck School of Medicine, Los Angeles, United States*
[h]*Seoul National University Children's Hospital, Seoul, Republic of Korea*
[i]*Johns Hopkins University, Baltimore, United States*
[j]*Osaka City University Graduate School of Medicine, Osaka, Japan*
[k]*The University of Tokyo Hospital, Tokyo, Japan*
[l]*University College London Hospitals, London, United Kingdom*
[m]*Okayama Saiseikai General Hospital, Okayama, Japan*
[n]*Ultragenyx Pharmaceutical Inc, Novato, United States*

Burosumab, a fully human IgG1 monoclonal antibody to FGF23, is approved in Canada and Brazil to treat XLH in patients ≥1 year of age and in the US to treat XLH in patients ≥6 months of age. Burosumab has also received conditional marketing authorization in Europe to treat XLH with radiographic evidence of bone disease in children ≥1 year of age and in adolescents with growing skeletons. Burosumab significantly improved serum phosphorus, fracture/pseudofracture healing, stiffness, and physical functioning in a phase 3, double-blind, multicenter study (CL303, NCT02526160). In this trial, adult subjects with XLH were randomized 1:1 to receive burosumab or placebo subcutaneously every 4 weeks. At Week 24, subjects in the placebo group crossed over to receive burosumab (total duration ≥96 weeks). Here, we report final long-term safety results from this trial.

Most (119/134, 89%) subjects completed 96 weeks and received 1 mg/kg burosumab; protocol-specified dose reductions were required for 11/134 (8.2%) subjects to effectively manage hyperphosphatemia (all mild [Grade 1]). Mean (±SE) baseline serum phosphorus was 1.98 (±0.03) mg/dL and was 2.97 (±0.05) mg/dL at Week 94 (midpoint of dose interval). Mean (±SE) iPTH level was 96 (±3.8) pg/mL at baseline and progressively declined to 79 (±3.3) pg/mL at Week 96. Nephrocalcinosis score at Week 96 changed by 0 in 101 subjects, -1 in 9 subjects, +1 in 10 subjects (14 subjects not available). There were no meaningful changes in ectopic mineralization. There were no neutralizing antibodies. No treatment-emergent adverse events led to study or treatment withdrawal.

Serum phosphorus was maintained with long-term burosumab treatment, with no evidence of loss of effect in adults with XLH. Burosumab dose reductions effectively managed mild hyperphosphatemia. Frequency, severity, and types of AEs reported were consistent with previous burosumab trials.

doi:10.1016/j.bonr.2020.100654

COP29

Highlighting the bone cells alterations in Gorham-Stout Disease

Michela Rossi, Ippolita Rana, Giulia Battafarano, Eda Mariani, Viviana De Martino, Rita De Vito, Matteo D'Agostini, Marina Macchiaiolo, Michaela V. Gonfiantini, Alessandro Jenkner, Paola Sabrina Buonuomo, Andrea Bartuli, Andrea Del Fattore
Bambino Gesu' Children's Hospital, Rome, Italy

Gorham-Stout Disease (GSD) is characterized by progressive osteolysis and angiomatous proliferation without new bone formation. The etiology is unknown, the diagnosis is challenging and there are no set therapeutic approaches for patients. Our work aims to identify the cellular and molecular alterations leading to bone loss in GSD.

Patients and controls bone cells were cultured *in vitro* to analyze differentiation, morphology and activity. Gene and miRNA expression was evaluated by transcriptomic and Real-Time RT-PCR analysis.

Bone biopsy analysis revealed in patients fibrous tissue, increased number of osteoclasts and vessels, and enlarged osteocyte lacunae. In GSD sera high levels of ICTP, VEGF-A, IL-6 and Sclerostin and a reduction of TGFβ were detected. GSD-PBMC had a 2-fold increased ability to differentiate into osteoclasts, that displayed a more motile phenotype and enhanced bone resorption activity (Resorbed Area/cell μm^2, HD: 886.7±61.2, GSD: 4100.0±938.8. p=0.01). Gene expression analysis of GSD osteoclasts revealed 106 modulated transcripts, 40 and 66 under- and over- expressed, respectively. These transcripts are involved in Beta-arrestin, PI3 Kinase and EGF receptor pathways. Moreover, large microRNA array of GSD osteoclasts revealed the upregulation of 3 miRNA involved in Metallopeptidase and PI3K activity. MSC from a patient did not show defect of osteogenic differentiation, whereas GSD-osteoblasts had impaired activity as shown by reduced mineralization and by altered pathways of bone morphogenesis and ossification modulation identified by transcriptomic analysis. GSD-osteoblasts had also an increased osteoclastogenic potential. miRNA analysis of GSD osteoblasts revealed a modulation of 12 miRNA involved in PDGFB signalling and NF-kB activity pathway.

Our results highlighted the molecular alterations in GSD patients and pave the way for the identification of molecular pathways that could be the target for new therapeutic approaches for GSD.

doi:10.1016/j.bonr.2020.100655

COP30

LIGHT as regulator of bone homeostasis during osteolytic bone metastasis formation in non-small cell lung cancer patients

Giacomina Brunetti[a], Dimas C. Belisario[b], Giuseppina Storlino[c], Graziana Colaianni[a], Lucio Buffoni[d], Giuseppe Ingravallo[c], Carl F. Ware[e], Silvia Colucci[a], Riccardo Ferracini[f], Maria Grano[c], Ilaria Roato[b]

[a]*Department of Basic and Medical Sciences, Neurosciences and Sense Organs, University of Bari, Bari, Italy*

[b]*Center for Experimental Research and Medical Studies (CeRMS), A.O.U. Città della Salute e della Scienza di Torino, Torino, Italy*

[c]*Department of Emergency and Organ Transplantation, University of Bari, Bari, Italy*

[d]*Department of Oncological Sciences, University of Torino, Torino, Italy*

[e]*Infectious and Inflammatory Disease Center, Sanford Burnham Prebys Medical Discovery Institute, La Jolla, United States*

[f]*Department of Surgical Sciences (DISC), IRCCS, A.O.U. San Martino, Genoa, Italy*

Tumor necrosis factor superfamily member 14 (*TNFSF14*), LIGHT is one of the cytokines produced by tumor and immune cells, which promotes homeostasis of lymphoid organs, liver and bone. Non-small cell lung cancer (NSCLC) commonly metastasizes bone, altering bone homeostasis and causing osteolysis. Here we investigated the role of LIGHT in NSCLC-induced osteolytic bone disease.

The LIGHT expression in monocytes was higher in patients with metastatic bone lesions than in non-bone metastatic ones (66.5 ± 24.5 vs 43.3 ± 25.2 mean ± SD, $p = 0.001$), in healthy donors (66.5 ± 24.5 vs 8.5 ± 4.6 $p = 0.0002$), and in non-bone metastatic patients than in healthy donors (43.3 ± 25.2 vs 8.5 ± 4.6, $p = 0.0001$). Serum LIGHT levels were also significantly higher in bone metastatic patients than in non-bone metastatic ones (186.8 ± 191.2 pg/ml vs 115.8 ± 73 pg/ml, $p = 0.04$) and in healthy donors (186.8 ± 191.2 pg/ml vs 85.7 ± 38.4 pg/ml, $p = 0.04$).

A neutralizing mAb anti-LIGHT added to osteoclast (OC) cultures of both bone and non-bone metastases inhibited osteoclastogenesis, but the decrease was statistically significant only for bone metastatic patients (272 ± 98 vs 132 ± 74, $p = 0.01$). To investigate the role of LIGHT in NSCLC- induced bone lesion *in vivo*, we performed an intratibial injection of a mouse lung cancer cell line LLC-1, in wild-type (WT) and LIGHT KO mice. The WT-injected mice displayed a significant reduction of about 20% for BV/TV, Tb.N, Tb.Th, and Tb.Sp compared to the WT-vehicle mice ($p< 0.01$). These parameters did not show significant variation for KO-injected mice vs vehicle or for WT-injected mice vs KO-injected mice. These data indicate LIGHT as a regulator of bone homeostasis during NSCLC metastatic invasion, thus it may be a novel therapeutic target in osteolytic bone metastases.

doi:10.1016/j.bonr.2020.100656

Concurrent Oral Poster Presentations 1: Basic/ Translational

P001

Transcriptome analysis reveals potential biomarkers of *CLCN7*-dependent Autosomal Dominant Osteopetrosis Type 2 (ADO2)

Iona Norwood, Denis Szondi, Nadia Rucci, Anna Teti, Antonio Maurizi

DISCAB, University of L'Aquila, L'Aquila, Italy

ADO2 is a rare genetic disease characterized by dense yet fragile bones. To date, the radiological approach remains the gold standard for ADO2 diagnosis. However, recent observations unveiled that ADO2 is a systemic disease affecting various organs beyond bone, including lung, kidney, muscle and brain. Monitoring disease status and progression would greatly benefit from specific biomarkers shared by the affected organs. In this work, data derived from RNA deep sequencing (RNA-dSeq) of bone, lung, kidney, muscle, brain and osteoclasts isolated from wildtype and *Clcn7*^{G213R} ADO2 mice was subjected to Gene Ontology analyses, which identified shared modulated biological processes, molecular functions and cellular components, with Response to stimulus ($p=4.26E-19$), Cell communication ($p=7.41E-17$) and Extracellular space ($p=3.34E-41$) overrepresented in all ADO2 organs tested and in osteoclasts, and RNA processing ($p=1.14E-06$), Nucleic acid binding ($p=3.70E-05$) and Microtubule cytoskeleton ($p=7.11E-04$) underrepresented. KEGG pathway analysis also revealed the presence of common pathways altered in ADO2 organs and in osteoclasts, including Cytokine-cytokine receptor interaction ($p=6.72E-06$), Hematopoietic cell lineage ($p=3.04E-05$), JAK-STAT signaling pathway ($p= 0.004$), Chemokine signaling pathway ($p=0.04$), Protein processing in endoplasmic reticulum ($p=0.006$) and Ubiquitin mediated proteolysis ($p=0.01$). A deep analysis of the altered pathways allowed us to extrapolate a list of genes modulated in all ADO2 organs, including *Epor*, *Ccl8* and *Cd38* ($p< 0.05$), encoding the erythropoietin receptor, the monocyte chemoattractant protein 2 and the cyclic ADP ribose hydrolase, respectively. These genes were modulated also in circulating ADO2 monocytes ($p< 0.05$), thus representing potential candidate biomarkers of the disease. Given that monocytes give rise to osteoclasts and macrophages and that these two cell types are involved in ADO2 pathogenesis in bone and in visceral organs, respectively, we conclude that these transcriptional biomarkers could represent useful and inexpensive tools for ADO2 diagnosis and monitoring of disease status.

doi:10.1016/j.bonr.2020.100657

P004

Extracellular vesicles are new bone turnover diagnostic tools to discriminate osteoporosis induced by estrogen deprivation or by unloading

Alfredo Cappariello[a,b], Argia Ucci[b], Maurizio Muraca[c], Anna Teti[b], Nadia Rucci[b]

[a]*Children Hospital Bambino Gesù, Rome, Italy*

[b]*Biotechnological and Applied Clinical Sciences, University of L'Aquila, L'Aquila, Italy*

[c]*Department of Women's and Children's Health, University of Padova, Padova, Italy*

EVs are released from cells and transport cargos to establish cell-to-cell communication. Osteoblasts are sources of membrane-bound RANKL-enriched EVs, promoting osteoclast survival and inducing osteoclast formation when injected into the circulation of RANKL-deleted mice. Here, we hypothesised that circulating EVs could represent biological tools to monitor bone turnover, thus providing new diagnostic biomarkers of osteoporosis. In primary murine osteoblasts subjected to oestrogen deprivation by charcoal-stripped foetal calf serum, or to microgravity by culture in the Rotating Wall Vessel bioreactor, we observed an increased release of membrane-bound RANKL-enriched EVs (4- and 1.6-fold, respectively;$p< 0.04$). Circulating EVs isolated from the sera of female CD1 mice also expressed surface RANKL along with *alp* and *runx2* mRNAs. Serum EVs from ovariectomised (OVX) or female hind-limb tail-suspended (HLTS) mice showed distinct molecular profiles. They expressed higher RANKL compared to control mouse EVs, with a different kinetics detected from 5 to 10 weeks from OVX or HTLS (OVX-EVs, bell-shaped;$p< 0.02$; HLTS-EVs, sustained;$p< 0.03$). Transcriptomic and proteomic profiles uncovered shared (mRNAs=4, proteins=5) and unshared (OVX-EV-specific: mRNAs=5, proteins=1; HLTS-EV-specific: mRNAs=4, proteins=4) molecular signatures, including cytokines, growth factors, adipokines, adhesion molecules and

osteoblast-specific factors, that discriminated OVX versus HLTS conditions. Furthermore, OVX-EVs were enriched in *adenylate-cyclase-10* mRNA (+14664.1;p=0.031), while *signal-transducer-and-activator-of-transcription-1* was the most distinctive mRNA (+209.38;p=0.049) in HLTS-EVs. Amongst the differentially modulated proteins there were P-selectin and Lipocalin 2, which were barely detectable in control mouse EVs. In contrast, while P-selectin remained low in HTLS-EVs, it progressively increased up to 2.225-fold(p=0.0081) in OVX-EVs. On the contrary, Lipocalin-2 remained low in OVX-EVs and increased up to 13.665-fold(p=0.0431) in HTLS-EVs. These results suggest that circulating EVs collected by liquid biopsy could allow i)the differential diagnosis of OVX- (post-menopausal) versus HLTS-induced (disuse) osteoporosis and ii)the exploitation of their exclusive molecular profiles to monitor changes of bone turnover over time.

doi:10.1016/j.bonr.2020.100658

P015

RNA-based bone histology and histomorphometry

Elena Makareeva, Laura Gorrell, Shakib Omari, Edward L. Mertz, Sergey Leikin
NICHD, National Institutes of Health, Bethesda, United States

Traditional histological staining identifies many cell types in bone sections, but subjective morphological evaluation of these cells limits the information content and ambiguity of such analysis. To develop a more objective approach to bone histopathology and characterize cell differentiation, functional state, and crucial molecular pathways, we replaced the traditional staining with fluorescent labeling of RNA transcripts. We adapted commercial tape-transfer cryo-sectioning (Section Lab) and fluorescent RNA labeling (RNAScope™) technologies for simultaneous imaging of multiple transcripts in the same cryosection of a fully mineralized mouse bone. We developed automated analysis procedures for counting different bone cells and evaluating relative expression of key RNA transcripts within these cells. For instance, we identify active osteoclasts and osteoblasts as bone surface cells with high *Ctsk* and *Col1a1* expression, respectively. We characterize osteoblast differentiation by visualizing expression of *Bglap*, *Dmp1*, *Sost*, and other transcripts relative to *Col1a1*. To test this approach, we utilized a G610C mouse model of osteogenesis imperfecta (OI). RNA-based histological analysis combined with RNA-based histomorphometry demonstrated altered differentiation of G610C osteoblasts and resolved multiple inconsistencies between histopathological, micro-CT, and biomechanical measurements in this animal model. We found that reduced mineral apposition rate in G610C mice is likely caused by deficient osteoblast maturation. The animals appear to compensate for this deficiency and normalize their bone formation rate by recruiting additional osteoblasts without an accompanying increase in the number of active osteoclasts, explaining an otherwise puzzling increase in trabecular thickness. We are currently developing approaches to identifying molecular mechanisms of bone cell pathology by combining single cell transcriptomic analysis with visualization of key RNA transcripts in histological sections.

doi:10.1016/j.bonr.2020.100659

P064

Advanced 3D-confocal microscopy of cleared mouse bones reveals the architecture and quantitative interrelationship of the stromal and vascular compartments in bone

Nicolas Peredo[a], Anna-Marei Bohm[a], Elena Nefyodova[a], Nikky Corthout[b], Sebastian Munck[b], Christa Maes[a]
[a]*Laboratory of Skeletal Cell Biology and Physiology (SCEBP), Skeletal Biology and Engineering Research Center (SBE), Department of Development and Regeneration, KU Leuven, Leuven, Belgium*
[b]*VIB Bio Imaging Core and VIB-KU Leuven Center for Brain & Disease Research, Department of Neurosciences, KU Leuven/VIB, Leuven, Belgium*

Advanced imaging methodologies enabling visualization of cellular components and morphological structures at high resolution are an absolute necessity to study complex structures as skeletal blood vessels and stromal cell networks and their alterations upon ageing, disease and trauma. In our lab, we use 3D-confocal microscopy to further our knowledge on how skeletal stem/progenitor cells (SSPCs) and blood vessels interact. For studying their spatial relationship in 3D and quantitatively, we here optimized extended bone imaging procedures achieving improved depth and quality.

We co-immunostained thick sections from mouse bones for leptin receptor (LepR/SSPCs) and endomucin (Emcn/blood vessels) and imaged the diaphyseal marrow using laser-scanning confocal microscopy, after applying a tissue-clearing protocol. By adding Z-intensity laser-correction during imaging and post-processing denoising, we achieved 60µm-increased depth of homogenous signal and an improved signal-to-noise-ratio along the Z-axis (Figure, top). To distinguish endothelial and stromal cells individually and quantify and map their distribution, we segmented the LepR/Emcn/Hoechst signals using an ImageJ/FIJI-macro developed in-house, and skeletonized the segmented signals. Emcn+ analysis delivered vascular traits such as diaphyseal blood vessel density, number, volume, surface and diameter, as well as the density of endothelial cells and intravascular blood cells. The technology also exposed the 3D-architecture of a high-density stromal meshwork of LepR+ cells, displaying a multitude of cellular projections. About half of these LepR+ cells tightly localized onto the sinusoidal blood vessels, covering almost 80% of their abluminal surface (Figure,bottom).

In conclusion, we developed a high-resolution 3D-imaging and image-processing/analysis pipeline to characterize and measure vessel and stromal compartments within bone.

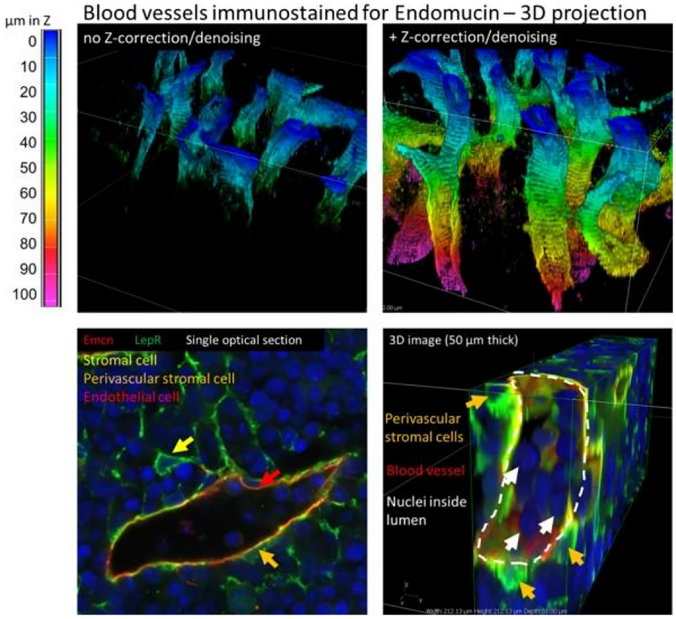

A method for skeletal blood vessels and stromal cell networks imaging at high quality in 3D.

doi:10.1016/j.bonr.2020.100660

P099

Glutamine metabolism in osteoprogenitors governs bone mass accrual and PTH-induced bone anabolism

Steve Stegen[a], Sophie Torrekens[a], Riet Van Looveren[a], Peter Carmeliet[b], Geert Carmeliet[a]
[a]Clinical & Experimental Endocrinology, KU Leuven, Leuven, Belgium
[b]Angiogenesis & Vascular Metabolism, KU Leuven/VIB, Leuven, Belgium

Skeletal homeostasis highly depends on osteoprogenitor proliferation and matrix synthesis, which are two biosynthetically and bioenergetically demanding processes that require sufficient and appropriate nutrient supply. Osteoprogenitors likely use glucose via glycolysis for energy production, but which nutrients support biosynthesis is unknown.

We first characterized the nutritional control of osteoprogenitor function, by culturing FACS-isolated Osterix positive (Osx^+) cells in decreasing glucose, fatty acid or glutamine concentrations. Glutamine withdrawal significantly decreased Osx^+ cell viability, proliferation and osteogenic differentiation, whereas the effect of glucose or fatty acid deprivation was less profound. To validate the *in vivo* role of glutamine metabolism, we deleted glutaminase 1 (GLS1), the rate-limiting enzyme, in osteolineage cells of 8-week-old male mice using doxycycline-inducible *Osx*-Cre mice ($Gls1^{ob-}$). MicroCT analysis showed that mutant mice displayed a low bone mass phenotype (60% reduction vs wild-type, $p< 0.05$), caused by decreased bone formation without affecting resorption, assessed by histological and serum analysis. More specifically, osteolineage cell number and activity was decreased in $Gls1^{ob-}$ mice. Mechanistically, proliferation, protein synthesis and redox homeostasis was impaired in cultured GLS1-deficient osteoprogenitors. Metabolomics showed that glutamine is catabolized via different pathways to generate nucleotides, amino acids and glutathione. Consequently, supplementation of these metabolites fully restored the anabolic defects in GLS1-deficient osteoprogenitors.

Finally, we confirmed the pro-anabolic role of glutamine metabolism using a model of parathyroid hormone (PTH)-induced bone formation. In wild-type mice, the osteo-anabolic response to intermittent PTH was associated with increased expression of glutamine transporters and GLS1, resulting in enhanced glutamine uptake and flux in anabolic and redox pathways. In contrast, GLS1 inactivation in Osx^+ cells prevented the PTH-driven adaptations in glutamine metabolism and fully blunted the PTH-induced increase in bone mass.

Taken together, GLS1-mediated glutamine flux in biosynthetic and redox pathways is critical for bone mass accrual and stimulation of glutamine metabolism supports PTH-induced bone formation.

doi:10.1016/j.bonr.2020.100661

P122

Evidence that teriparatide regulates osteoclast differentiation and survival in mice via Cxcr4 activity

Beatriz Larraz-Prieto[a], Javier Bonsón[a], Oude D. Zhu-Huang[a], Sachin Wani[a], Omar Albagha[a,b], Colin Farquharson[c], Stuart Ralston[a], Nerea Alonso[a]
[a]Rheumatology and Bone Disease Unit, CGEM-IGMM, University of Edinburgh, Edinburgh, United Kingdom
[b]College of Health and Life Sciences, Hamad Bin Khalifa University, Doha, Qatar
[c]Division of Functional Genetics and Development, Roslin Institute, University of Edinburgh, Edinburgh, United Kingdom

CXCR4 has been identified by GWAS as a response gene to the anabolic agent teriparatide (an agonist for PTH1R), which increases osteoblast activity and indirectly activates osteoclasts. We confirmed by mRNAseq that primary murine osteoclasts also express *Pth1r* during differentiation, especially at early stages. However, the direct role of teriparatide in osteoclasts is still unknown. Our aim is to investigate the involvement of *CXCR4* in the osteoclast response to teriparatide.

Macrophage-derived osteoclasts from murine bone marrow were treated with 50nM teriparatide and/or the Cxcr4 inhibitor AMD3100 at 100μM for 5 days. Vehicle-treated osteoclasts were used as controls. TRAcP-positive cells ≥3 nuclei were considered osteoclasts.

Teriparatide increased osteoclast numbers at early stages to (mean percentage ± SEM) 227±23% on day 2, p=0.005; 187±10% on day 3, p=0.001; and 123±9% on day 4, p=0.04, compared to control. However, their lifespan was shorter: by day 5, there was a 74±12% reduction in osteoclast number compared to vehicle-treated cells (p=0.003). AMD3100-induced inhibition of Cxcr4 activity caused a reduction in the number of osteoclasts, especially at late stages (55±7% on day 4, p=0.003; 28±12% on day 5, p=0.004). This reduction could not be rescued by teriparatide since cultures treated with AMD3100+ teriparatide showed a decrease in osteoclast number on day 2 (151± 17%; p=0.01); day 3 (107±10%; p=0.02), and day 4 (80±7%; and p=0.02), compared to teriparatide-treated cells. Visual inspection of the cultures also showed that teriparatide increased the size of osteoclasts, whilst AMD3100 reduced osteoclast size dramatically.

In summary, teriparatide increases osteoclastogenesis and limits osteoclast lifespan, by activating Cxcr4. This initial boost in bone resorption could be crucial for triggering bone formation associated with treatment. Further functional analysis of the role of *CXCR4* in osteoclasts in response to teriparatide are currently ongoing, to address its clinical value in personalising treatment options for osteoporotic patients.

doi:10.1016/j.bonr.2020.100662

P132

Secondary ossification center protects growth plate chondrocytes from mechanical stress

Meng Xie[a], Lei Li[a], Phillip Newton[a], Lauren Shumate[b], Shigeki Nishimori[b], Henry Kronenberg[b], Murat Bastepe[b], Igor Adameyko[a,c], Andrei Chagin[a,d]
[a]Karolinska Institutet, Solna, Sweden
[b]Harvard Medical School, Boston, United States
[c]Medical University of Vienna, Vienna, Austria
[d]Sechenov University, Moscow, Russian Federation

The secondary ossification center (SOC), which later forms a bony epiphysis, is a skeletal element with largely unknown functions. Recently, we have shown that the SOC creates a stem cell niche in the underlying growth plate, but whether this is the main function of SOC remains unknown. Based on evolutionary observations, we hypothesized that the SOC may shield the growth plate from mechanical stresses caused by locomotion. To test this hypothesis, we first applied external loading to bones with and without SOC and revealed that SOC allows the epiphyseal chondrocytes to withstand a 7 folds higher load (1N versus 7N, $P< 0.0001$) before chondrocytes undergo caspase-dependent apoptosis in a YAP-p73-associated manner. Importantly, this protective function of SOC was particularly vivid for hypertrophic chondrocytes, which turned out to be extremely sensitive to mechanical loading and the SOC allows these cells to withstand 25 folds higher load (0.2N versus 5N, $P< 0.0001$) prior undergoing apoptosis. The protective role of the SOC was further verified in *in vivo* mouse models, where we inhibited SOC development genetically, by activation of the Gsa signaling pathway or inactivation of SIK3; or pharmacologically, by blocking angiogenesis. Our results show that one of the main functions of

the SOC is to protect the epiphyseal chondrocytes, especially the hypertrophic cells from mechanical stress generated by locomotion.

doi:10.1016/j.bonr.2020.100663

P133

Inhibition of HMGA2 abolishes articular cartilage regeneration induced by Lin28a in mice

Yohan Jouan[a], Benoit Bardeche-Trystram[a], Yohan Lionne[a], Augustin Latourte[a,b], Pascal Richette[a,b], Hang-Korng Ea[a,b], Martine Cohen-Solal[a,b], Eric Hayÿ[a]
[a]BIOSCAR U1132, Université de Paris, INSERM 1132, Paris, France
[b]Rheumatology, Hopital Lariboisière, AP-, HP, Paris, France

Cartilage loss characterizes osteoarthritis (OA) along a poor regeneration capacity. We previously showed that re-expression of Lin28a (RNA-binding protein) is involved in cartilage maintenance. Chondrocyte Lin28a deletion worsens cartilage degradation, while it's inhibited by Lin28a overexpression in OA mice along with an increase osteophyte volume. In chondrocytes, Lin28a inhibits Let7b/c miRNAs and increases HMGA2 expression (chromatin remodeling protein). HMGA2 binds to Sox9 promoter, therefore promoting its re-expression and chondrocyte reprogramming. Our aim was to demonstrate the mediation of HMGA2 in Lin28a regenerative effect in mice.

OA was induced in Col2CRE^{er} (WT) and Col2CRE^{er}TG Lin28a (TG) mice and then overexpression of Lin28a was induced after 4 weeks to promote cartilage regeneration. Intra-articular administration of scrambled or HMGA2 siRNA are performed weekly for 4 weeks. We analyzed subchondral bone and osteophyte formation (μCT) and cartilage indices (OA score and cartilage remodeling factors (MMP13, Lin28a, HMGA2, Sox 9)).

Subchondral bone BV/TV and osteophyte volume are increased in OA mice compared to sham, but genotype and treatment has no impact on BV/TV. OA increases osteophyte volume in TG mice compare to WT. However, HMGA2 inhibition significantly reduced osteophyte volume compared to scrambled si administration (0.17±0.02 vs 0.11± 0.03 mm^3, $p< 0.01$). TG mice showed a higher HMGA2 expression in chondrocytes which was reduced with siHMGA2. Lin28a overexpression blocked cartilage degradation (OA score 5.3±0.45 vs 2.8±0.3 $p< 0.05$) which was abolished with siHMGA2 (3.2±0.22 vs 5.3±0.45 $p< 0.01$). SiHMGA2 treated TG mice revealed increased MMP13(+)cells and apoptotic cells compared to TG mice treated with scrambled si (39%±2% vs 45%±3% $p< 0.05$). In TG mice, immunohistochemistry revealed that 80% of the Lin28a(+)cells expressed also HMGA2 and Sox9, whereas siHMGA2 strongly reduced Lin28a/Sox9 co-labeling.

Altogether, these results confirm that HMGA2/Sox9 axis mediate chondrocyte reprogramming induced by Lin28a in mice. This identifies potential targets for cartilage regeneration in OA.

doi:10.1016/j.bonr.2020.100664

P134

Synovial cells secrete a temperature-stable protein that inhibits hypertrophic differentiation and induces articular cartilage differentiation of chondrocytes *in vitro*

Marta Baroncelli[a], Zelong Dou[a], Ellie Landman[a], Michael Chau[a,b], Lars Ottosson[a], Ola Nilsson[a,c]
[a]Department of Women's and Children's Health, Karolinska Institutet, Stockholm, Sweden
[b]Department of Orthopedic Surgery, University of Minnesota, Minneapolis, United States
[c]School of Medical Sciences, Örebro University and Örebro University Hospital, Örebro, Sweden

Osteoarthritis (OA) is a degenerative joint disease resulting from articular cartilage disruption with limited therapeutic options. From the original cartilaginous template, all but chondrocytes closest to synovial joint undergo hypertrophic differentiation, indicating that articular chondrocytes are protected from hypertrophic differentiation and remodelling into bone.

We hypothesized that synovial microenvironment inhibits hypertrophic differentiation and promotes articular cartilage formation.

We cultured rat epiphyseal chondrocytes in high-density pellets, with or without synoviocyte-conditioned medium, and quantified and localized expression of differentiation markers using quantitative RT-PCR and *in situ* hybridization (Ethical Approval: Dnr N12/16). Chondrocytes in regular media underwent reproducible hypertrophic differentiation, with increasing expression of Collagen type 10 (*Col10*) *($p< 0.05$)*, Alkaline phosphatase (*Alp*) *($p< 0.001$)*, and Indian hedgehog (*Ihh*) *($p< 0.01$)*, whereas articular cartilage-marker Lubricin *(Prg4)* remained low. However, with synoviocyte-conditioned medium, hypertrophic markers remained low (*Col10, Ihh, $p< 0.05$*; *Alp, $p< 0.001$)*, whereas *Prg4* increased (18-fold; $p< 0.05$).

We aimed to characterize this synovial factor(s) that promote articular cartilage formation and inhibit hypertrophic differentiation. We used an *in vitro* bioassay that quantifies hypertrophic and articular differentiation and found that the putative factor is inactivated by proteinase-K digestion ($p< 0.01$), heat-resistant (90°C; $p< 0.001$), with size between 50-100 kDa.

Our findings show that chondrocytes in pellets undergo a sequential differentiation program similar to chondrocytes *in vivo*, and suggest that synoviocytes secrete a heat-resistant, large protein that inhibits hypertrophic differentiation while promoting articular cartilage differentiation. This finding may have important implications for OA pathogenesis and treatment, and for articular cartilage development and tissue engineering.

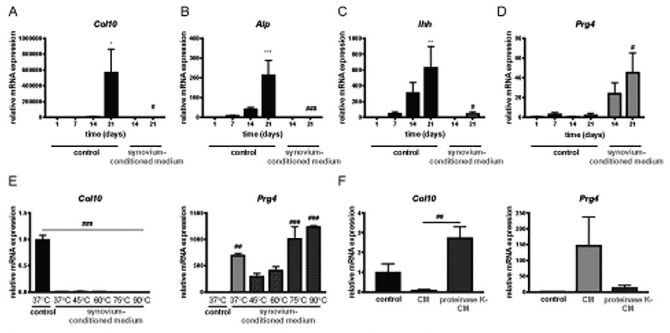

Synovium-conditioned medium induces articular cartilage-like phenotype *in vitro*. Gene expression of *Col10* (A), *Alp* (B), *Ihh* (C) measured by qPCR significantly increased in chondrocytes over time, whereas *Prg4* expression is induced by synovium-conditioned medium (D). *Col10* and *Prg4* expression in chondrocytes at day 14 of culture, treated with chondrogenic medium (control), synoviocyte-conditioned medium (CM), untreated or temperature-treated (E), and proteinase K-treated (F). Bars represent average ± SEM. All values are displayed as relative to control at day 1. (*, relative to control at day 1; #, relative to control at same time point. *, # $p<0.05$; **, ## $p<0.01$; ***, ### $p<0.001$).

Figure.

doi:10.1016/j.bonr.2020.100665

P136

Probiotics prevent cartilage damage and progression of osteoarthritis in mice

Antonia Sophocleous[a,b], Asim Azfer[b], Carmen Huesa[c], Eleni Stylianou[a], Giovanny Rodriguez Blanco[d], Stuart H. Ralston[b]
[a]Department of Life Sciences, European University Cyprus, Nicosia, Cyprus
[b]Rheumatology and Bone Diseases Unit, MRC Institute of Genetics and Molecular Medicine, University of Edinburgh, Edinburgh, United Kingdom

[c]Centre for Reproductive Health, The Queen's Medical Research Institute, University of Edinburgh, Edinburgh, United Kingdom
[d]Cancer Research UK Beatson Institute, Glasgow, United Kingdom

Background: In recent years, increasing interest has focused on the role of the microbiome in the pathogenesis of various diseases including inflammatory disease, osteoporosis, and osteoarthritis. Here we examined the role of intestinal microbiome and probiotics in the development and progression of osteoarthritis in mice subjected to destabilisation of medial meniscus (DMM).

Methods: The intestinal microbiome was depleted by broad-spectrum antibiotics from one week before birth until the age of 6 weeks when mice were subjected to DMM following microbiome reconstitution or sham reconstitution. Mice with reconstituted microbiome were also treated with a mixture of probiotic strains or vehicle. Cartilage damage and inflammation at the knee joint were evaluated by histological analyses. Changes in circulatory concentrations of inflammatory cytokines were assessed in serum samples using the MILLIPLEX® MAP Mouse Cytokine/Chemokine Magnetic Bead Panel. Differences were assessed by one-way ANOVA All experiments had ethical approval by the University of Edinburgh.

Results: Probiotic treatment in mice with reconstituted microbiome significantly inhibited osteoarthritis progression at the femoral condyle compared to mice with sham reconstitution and vehicle treatment (36.5% ±4.3 [mean±SEM] less cartilage damage; $p< 0.001$). Histological assessment showed that probiotic treatment following microbiome reconstitution reduced joint inflammation score, to a similar degree as it inhibited cartilage damage compared to sham reconstitution/vehicle treatment (34.1%±12.4) but this did not reach statistical significance ($p=0.161$). Out of the twenty-five inflammatory cytokines/chemokines investigated only keratinocyte chemoattractant chemokine circulating levels were slightly reduced in serum samples from mice subjected to microbiome reconstitution and probiotic treatment, but this was not statistically significant (31.9%±7.7 reduction compared to sham reconstitution/vehicle treatment; $p=0.03$ [adjusted p-value of multiple comparisons=0.002]).

Conclusion: Treatment with probiotics prevents DMM-induced cartilage damage progression at the femoral condyle, with evidence of local inhibitory effects on inflammation. Further studies to elucidate the mechanism of action of probiotics in osteoarthritis pathogenesis are warranted.

doi:10.1016/j.bonr.2020.100666

P324

Mice with deletion of PKA regulatory subunit1A in osteoblasts show severe bone pathology

Carole Le Henaff[a], Brandon Finnie[a], Joshua Johnson[a], Yasaman Nahaei[a], Zhiming He[a], Krishnakali Dasgupta[a], Juhee Jeong[a], Johanna Warshaw[a], Henry M. Kronenberg[b], Lawrence S. Kirschner[c], Nicola C. Partridge[a]
[a]Basic Sciences and Craniofacial Biology, New York University Dental School, New York, United States
[b]Endocrine Unit - Massachussett General Hospital, Harvard Medical School, Boston, United States
[c]Department of Cancer Biology and Genetics, Ohio State University, Columbus, United States

Parathyroid hormone (PTH) was the first osteoanabolic hormone for treating osteoporosis. We have previously shown that PTH acts through PTHR1 and protein kinase A (PKA) activation to regulate osteoblastic gene expression. Our study aimed to elucidate the effects of increased PKA activity and better understand the actions of PTH (1-34) in bone. Tamoxifen (1mg/10g) was injected weekly to 1 or 5 month-old C57Bl/6J male *col1*CRE^{ERT}/*Prkar1a*$^{fl/fl}$ mice or *Prkar1a*$^{fl/fl}$ mice as controls for 3-4 weeks to delete the PKA regulatory subunit 1A in osteoblasts and increase PKA activity. At both ages, *col1*CRE^{ERT}/*Prkar1a*$^{fl/fl}$ mice demonstrated bone pathologies in their skulls, femurs and vertebrae and tumors in their tails (Figure 1). MicroCT showed cortical bone breakdown with apparent trabecular bone in the cortical area in femurs and vertebrae and expansion of bone in skulls. Deletion of Prkar1a increased bone turnover with a huge increase in osteoblast activity shown by serum-P1NP levels (6.5-13 fold), only single fluorescent labeling and a substantial increase in osteoclast activity shown by CTX levels (4.4-12 fold) and TRAP staining. Surprisingly, the *col1*CRE^{ERT}/*Prkar1a*$^{fl/fl}$ skulls showed thicker calvariae, shown by alizarin red staining and μCT but no changes in mandibles or teeth. *Col1*CRE^{ERT}/*Prkar1a*$^{fl/fl}$ mice had tumors in their tails evident by an invasion of stromal and osteoclastic cells but with intact growth plate, cartilage and intervertebral discs. In conclusion, high PKA activity in osteoblasts appears to be involved with high bone turnover and pathological events mimicking hyperparathyroidism, Jansen's metaphyseal chondrodysplasia or McCune-Albright syndrome.

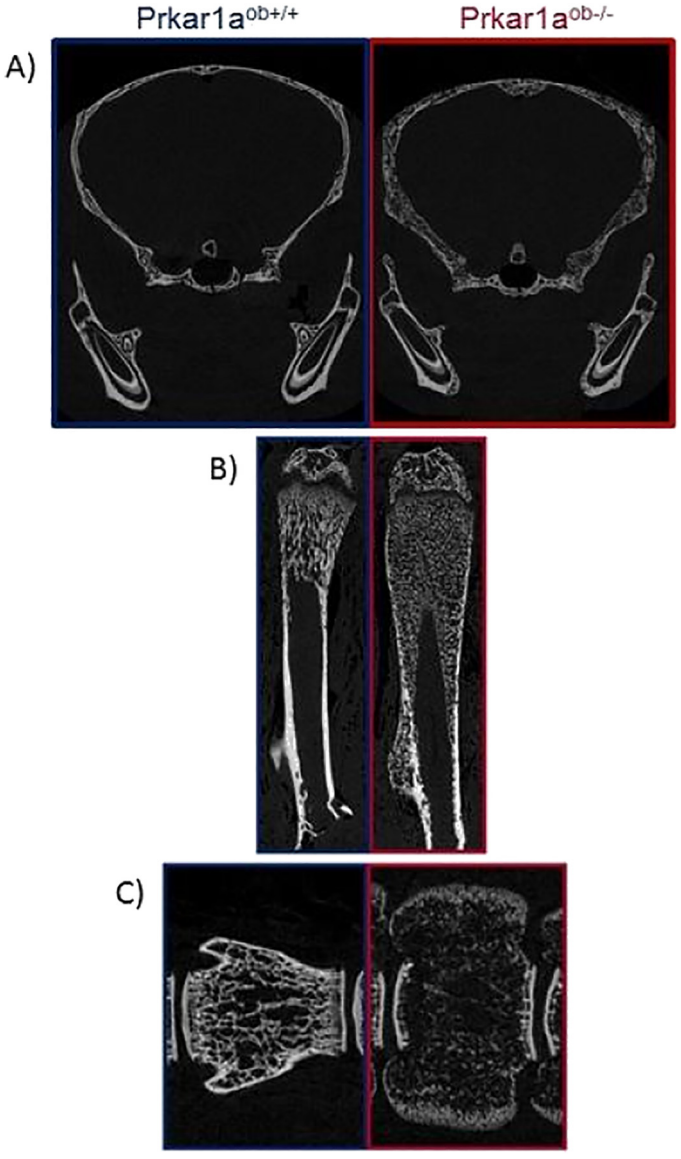

Fig. 1. uCT analysis of skulls (A), femurs (B) and vertebrae (C) in 7 week-old col1CREERT/Prkar1a

doi:10.1016/j.bonr.2020.100668

Concurrent Oral Poster Presentations 1: Clinical/ Public Health

P005

Serum biomarkers for antiresorptives-related osteonecrosis of the jaw: In vivo and clinical validation studies

Hye-Yeon Kim[a], Jinwoo Kim[b]
[a]*Graduate School of Medicine, Ewha Womans University, Seoul, Republic of Korea*
[b]*Oral and Maxillofacial Surgery, Ewha Womans University, Seoul, Republic of Korea*

Introduction: There have been many efforts to assess the risk for ARONJ by using bone biomarkers, especially for serum CTX as a useful predictor. However, the results of other clinical studies that used serum markers have been controversial, and no conclusive opinions have been reached about other bone biomarkers. Therefore, the aim of the study was to identify novel biomarkers for ARONJ.

Materials and Methods: This study includes 3 parts; (1) Establishment of animal ARONJ model with precedent metabolic bone disease (*Bone* 2015:442) (2) Detection of biomarkers for ARONJ in animal model (3) Clinical trial for biomarker validation. Our ARONJ model showed deteriorated bone architectures, and TRACP_5b and RANKL/OPG ratio in ONJ animal model were significantly decreased over time compared with the non-ONJ group (*CIDRR* 2016:281) Clinical validation study was set as cohort design with patients who administrating antiresorptives and all the patients got blood sampling 4 times. Serum bone ALP, calcitonin, intact PTH, osteocalcin, P1NP, vitamin D, osteoprotegerin, sRANKL, SOST, TRACP_5b and Dkk-1 were analysed, mainly with ELISA. Statistical analysis included bivariate, diagnostic statistics and repeated measures ANOVA.

Results: Serum intact PTH and TRACP_5b were significantly decreased in the case group compared with the control group (n=72; $P< 0.05$) and DKK-1 was increased in case group at T0. ($P< 0.05$) These results were consistent over time. (RM-ANOVA; $P< 0.05$) AUC of Intact PTH was 0.625 and DKK-1 was 0.676. ($P< 0.05$)

Conclusions: These results show that serum intact PTH, DKK-1 and TRACP_5b could be possible biomarkers for ARONJ.

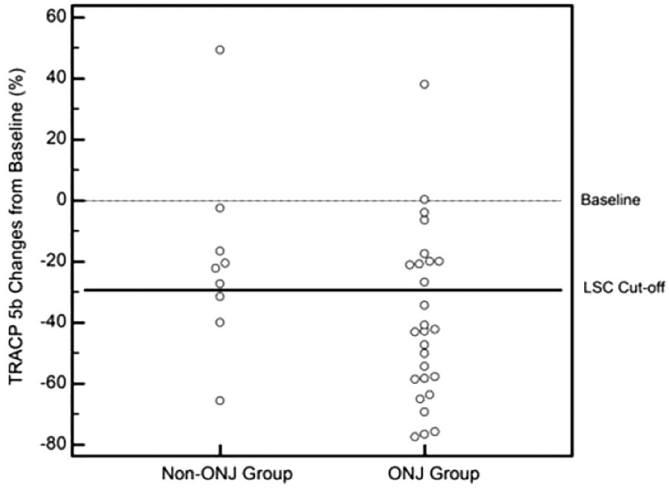

Individual biomarker change from baseline

doi:10.1016/j.bonr.2020.100669

P006

The relationship between bone regulatory markers and bone turnover in renal osteodystrophy

Syazrah Salam[a,b], Orla Gallagher[c], Fatma Gossiel[b], Arif Khwaja[a], Richard Eastell[b]
[a]*Sheffield Kidney Institute, Sheffield Teaching Hospitals NHS Foundation Trust, Sheffield, United Kingdom*
[b]*Academic Unit of Bone Metabolism, University of Sheffield, Sheffield, United Kingdom*
[c]*Oncology and Metabolism, University of Sheffield, Sheffield, United Kingdom*

Introduction: Renal osteodystrophy is common in advanced chronic kidney disease (CKD) patients and is characterized by abnormal bone turnover and mineralization. Parathyroid hormone (PTH) increases bone turnover through osteoblast and osteoclast activation. Osteoprotegerin (OPG) is a decoy receptor of receptor activator of nuclear factor kappa-β ligand and thus, inhibits osteoclast maturation. Meanwhile, sclerostin is an inhibitor of the Wnt signalling pathway and thus, inhibits osteoblast maturation. We aimed to assess the relationship between these bone regulatory markers and bone turnover as assessed by bone histomorphometry.

Methodology: We recruited 43 CKD patients with eGFR< 30ml/min/1.73m^2 or on dialysis. Fasting serum samples were analysed using Immunodiagnostic Systems automated assays for intact PTH (iPTH) and bone turnover markers (bone alkaline phosphatase [bALP], intact procollagen type 1 N-terminal propeptide [intact PINP] and tartrate-resistant acid phosphatase 5b [TRAP5b]). OPG and sclerostin were analysed using manual ELISA by Biomedica. Trans-iliac bone biopsy was performed for quantitative histomorphometry. Normal bone turnover was defined as bone formation rate/bone surface (BFR/BS) of 18-38μm^3/μm^2/year. Spearman rank correlation was used to test the relationship between the variables.

Results: Median BFR/BS was 32.12 (IQR 17.76 - 48.25) um^3/um^2/year. 26% of patients had low and 40% had high bone turnover. iPTH and OPG were positively correlated with BFR/BS (rho=0.42, p< 0.01 and rho=0.36, p< 0.05 respectively). Sclerostin was not correlated with BFR/BS. Furthermore, sclerostin did not correlate with bALP and intact PINP whereas OPG correlated with TRAP5b (rho=0.43, p< 0.01). iPTH correlated with bALP (rho=0.62, p< 0.001), intact PINP (rho=0.62, p< 0.001) and TRAP5b (rho=0.50, p = 0.001).

Conclusions: Circulating levels of iPTH and OPG were modestly associated with bone turnover but sclerostin was not. There are likely to be bone regulators other than iPTH, OPG and sclerostin which regulate bone turnover in renal osteodystrophy.

Keywords: Renal osteodystrophy, iPTH, OPG, sclerostin, bone histomorphometry.

doi:10.1016/j.bonr.2020.100670

P008

Relatively higher bone formation markers during puberty are correlated with more bone mass accrual independent of longitudinal growth in boys

Thiberiu Banica, Sara Vandewalle, Hans-Georg Zmierczak, Stefan Goemaere, Jean De Schepper, Jean-Marc Kaufman, Bruno Lapauw
Department of Internal Medicine and Pediatrics Research group Endocrinology, Unit for Osteoporosis and Metabolic Bone Diseases, Ghent University, Gent, Belgium

Introduction: Almost half of the peak bone mass is accumulated during puberty. It is however unclear to what extent bone turnover markers (BTMs) reflect the rate of bone modelling and bone mass accrual during puberty and longitudinal growth.

Objective: Determine whether BTMs reflect bone mass accrual in boys independent of longitudinal growth.

Methods: Procollagen type 1 N-terminal propeptide (P1NP) and carboxy-terminal collagen crosslinks (CTX) levels were analyzed on fasting serum samples using ECLIA in 118 peri-pubertal boys from the NINIOS cohort (12.5±2.8 years). Dual-energy x-ray absorptiometry determined bone mineral content (BMC) at the whole-body. Tibial cortical bone geometry was measured using pQCT. Measurements were taken at baseline and after two years.

Results: Serum concentrations of P1NP and CTX both peaked at Tanner stage 3 and 4 (see table). The P1NP/CTX ratio did not differ in Tanner stages 1-4, but was significantly lower in Tanner stage 5 ($p< 0.001$) due to stronger decreases in P1NP vs. CTX concentrations. Baseline P1NP levels were positively associated with increases in BMC, height and cortical thickness (all $p< 0.016$). Baseline CTX levels were positively associated with increases in BMC, height and periosteal circumference (all $p< 0.023$). After correction for longitudinal growth these findings remained significant. Multivariate analyses showed a positive association between P1NP but not CTX levels and changes in BMC ($r=0.451; p< 0.001$).

Conclusion: Serum P1NP and CTX reflect total bone mass accrual, modelling and longitudinal growth during puberty. The relation with bone mass accrual and modelling appeared independent of longitudinal growth. Further, the relation with bone mass accrual is mostly driven by P1NP.

	Tanner 1 (n=38)	*Tanner 2 (n=24)*	*Tanner 3 (n=12)*	*Tanner 4 (n=32)*	*Tanner 5 (n=12)*
P1NP (µg/l)	532.12 (387.48, 676.76)	685.60 (561.37, 809.94)	1185.03 (1059.04, 1311.01)	1142.64 (1040.43, 1244.84)	577.79 (421.31, 734.27)
CTX (ng/ml)	0.60 (0.44, 0.77)	0.76 (0.62, 0.91)	1.43 (1.29, 1.58)	1.32 (1.20, 1.44)	1.12 (0.94, 1.30)
P1NP/CTX ratio	979.49 ± 288.31	1049.51 ± 449.28	971.31 ± 393.59	1063.08 ± 570.43	443.48 ± 133.40

Results for P1NP and CTX are represented as the estimated mean with 95% confidence interval. The Ratio is represented as the mean +/- stdev

doi:10.1016/j.bonr.2020.100671

P016

Diurnal and weekly variability in serum levels of bone-related circulating microRNAs

Patryk Zarecki[a], Johannes Grillari[b,c,d], Miguel Debono[a], Matthias Hackl[e], Richard Eastell[a]

[a]*Oncology & Metabolism, University of Sheffield, Sheffield, United Kingdom*
[b]*Department of Biotechnology, University of Natural Resources and Life Sciences, Vienna, Austria*
[c]*Christian Doppler Laboratory on Biotechnology of Skin Aging, Department of Biotechnology, BOKU–University of Natural Resources and Life Sciences Vienna, Vienna, Austria*
[d]*Ludwig Boltzmann Institute for Experimental and Clinical Traumatology, Austrian Cluster for Tissue Regeneration, Vienna, Austria*
[e]*TAmiRNA GmbH, Vienna, Austria*

MicroRNA is involved in post-transcriptional regulation of gene expression. Due to its regulatory role, microRNA is differently expressed during certain conditions in healthy and diseased individuals. We hypothesize that microRNA biomarkers for bone diseases could have different expression patterns during the day or over an extended period of time, and in response to food intake.

In 2 separate longitudinal studies, a panel of 19 bone-related miRNAs was measured using the osteomiR™ RT-qPCR assay in serum samples of:

1) 29 postmenopausal Caucasian women with (n=14) and without osteoporosis (n=15). Blood samples were taken on 7 occasions after overnight fasting: 08:30, 09:00, 09:30, 11:00, 12:00, 14:00, 15:00, with meals provided at 10:00 and 13:00.

2) 35 postmenopausal women divided into 3 groups: vertebral fractures (n= 12), low BMD (n= 14) and healthy controls (n = 9). Blood samples were collected once per week for 8 weeks at designated times.

We have analysed the data using a mixed model analysis of variance approach and we found:

1) statistically significant (P-value< 0.05) fixed effect between measured time-points during the day for 9 miRNAs: hsa-miR-375, hsa-miR-214-3p, hsa-miR-143-3p, hsa-miR-335-5p, hsa-miR-23a-3p, hsa-miR-133b, hsa-miR-141-3p, hsa-miR-127-3p, hsa-miR-152-3p;

2) no significant changes between weekly time-points. The overall variability between weekly time-points was between CV of 40% to 90%.

Circulating microRNAs measured in serum seem to be highly variable on inter- and intra-individual levels, but even with high variability there are large diurnal changes in some miRNA levels, especially from early morning to later hours (between 40 and 70%). At a practical level, it is appropriate to standardise conditions and collection time to ensure reliable results in diagnostics.

doi:10.1016/j.bonr.2020.100672

P049

How the nanoscale composition and collagen fiber orientation affect osteonal mechanical competence

Kilian Stockhausen[a], Felix Schmidt[a], Mahan Qwamizadeh[a], Eva Wölfel[a], Haniyeh Hemmatian[a], Imke Greving[b], Daniel Laipple[b], Björn Busse[a]

[a]*Department of Osteology and Biomechanics, University Medical Center Hamburg-Eppendorf, Hamburg, Germany*
[b]*Institute of Materials Research, Helmholtz-Zentrum Geesthacht, Outstation at German Electron Synchrotron DESY, Geesthacht, Germany*

The mechanical integrity of bone is strongly dependent on its collagen fiber orientation (CFO). During remodeling fibers are aligned to better resist specific strain modes. While the structural properties of osteons with longitudinal and transverse CFO have been explored in the past, the composition and its impact on the mechanical competence remain understudied. Bone specimen were acquired during autopsy from a healthy 44-year old man. Based on *Circularly Polarized Light Microscopy* ten longitudinal and ten transverse osteons were selected. A set of established methods were performed to assess local compositional and mechanical properties (Fig. 1) and a *finite element model* was generated to predict the mechanical behaviour at different length scales. QBEI revealed a higher mean calcium content in osteons with longitudinal CFO. FTIR results were supportive of the qBEI data indicated by a correlation of the mineral-to-matrix ratio with Ca_{mean} ($r=0.729$, $p< 0.0001$). Osteons with longitudinal CFO were characterized by a higher elastic modulus and hardness signifying an increased stiffness. Our study shows that osteons differ not only in their preferential CFO but also in their mineralization profile. The stiffness mismatch between contrasting osteon types might further elucidate the

underlying mechanisms of crack initiation and propagation at the nanoscale.

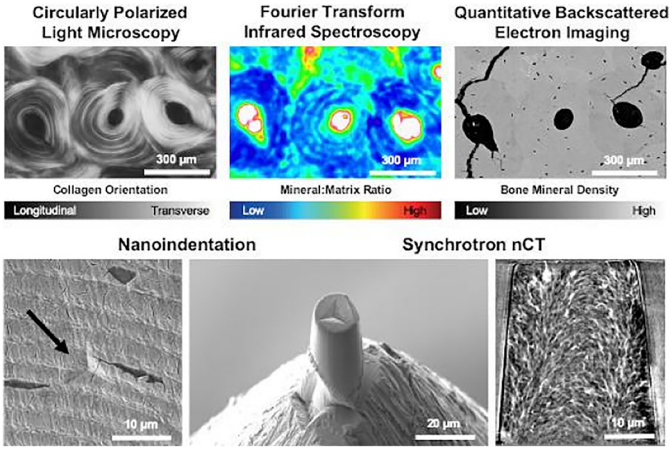

Structural, compositional and mechanical parameters were obtained by established methods

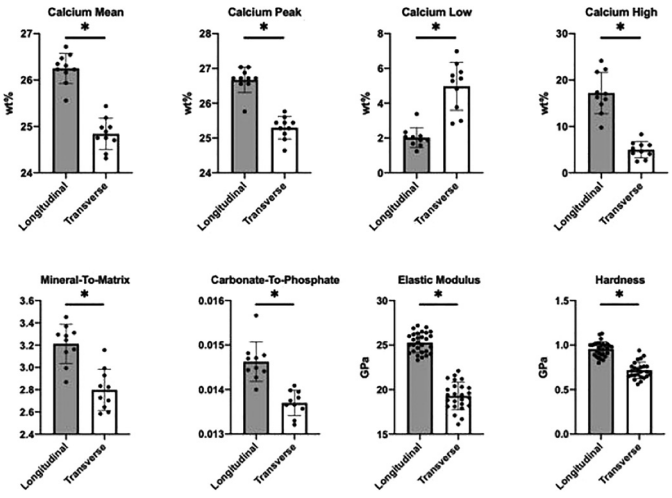

Significant compositional and mechanical differences were detected for contrasting CFOs

doi:10.1016/j.bonr.2020.100673

P121

Zoledronic acid is not equally potent on osteoclasts generated from different individuals - osteoclasts from smokers are less sensitive

Anais M.J. Møller[a,b], Jean-Marie Delaissé[c,d], Jacob B. Olesen[c], Troels Bechmann[b,e], Jonna S. Madsen[a,b], Luisa M. Canto[f], Silvia R. Rogatto[b,f], Kent Søe[c,d,g]

[a]*Department of Clinical Immunology and Biochemistry, Lillebaelt Hospital, University Hospital of Southern Denmark, Vejle, Denmark*

[b]*Department of Regional Health Research, University of Southern Denmark, Odense, Denmark*

[c]*Clinical Cell Biology, Dept. of Pathology, Odense University Hospital, Odense, Denmark*

[d]*Department of Clinical Research, University of Southern Denmark, Odense, Denmark*

[e]*Department of Oncology, Lillebaelt Hospital, University Hospital of Southern Denmark, Vejle, Denmark*

[f]*Department of Clinical Genetics, Lillebaelt Hospital, University Hospital of Southern Denmark, Vejle, Denmark*

[g]*OPEN, Odense Patient data Explorative Network, Odense University Hospital, Odense, Denmark*

Zoledronic acid (Zol) is used to treat e.g. osteoporosis and cancer induced bone disease, but patients show a highly variable sensitivity to Zol. What may be the reason for this difference in sensitivity?

Objective: Do osteoclasts from different individuals show a variable sensitivity to Zol in vitro and why?

Method: Osteoclasts were generated using monocytes from 46 healthy female blood donors (40-66 years) (ethical approval 20150059). Matured osteoclasts were reseeded onto bone slices pre-coated with Zol (0.03-50 µM) and IC50 values determined based on total eroded bone surface.

Results: IC50 values varied from 0.06 to 12.57 µM Zol (median: 0.26 µM). Analyses showed that IC50 correlated with: 1) smoking (Table), 2) nuclei/osteoclast (Table), 3) DNA methylation of CTSK gene promotor (r_s=0.37, p=0.0118), 4) active cathepsin K levels (r_s=0.33, p=0.0311), and 5) trench-forming were more sensitive than pit-forming osteoclasts (p< 0.0001). Surprisingly, neither gene nor protein expression of FDPS correlated with IC50.

Conclusions: Osteoclasts from smokers are less sensitive to Zol, osteoclasts with high nuclearity are less sensitive to Zol, epigenetics and activity levels of cathepsin K alter the sensitivity to Zol, and osteoclasts making trenches are most sensitive. These findings could be of clinical relevance - this is currently investigated.

Table
Multiple linear regression analysis

Dep. variable	R2	Indep. variable	Coef.	SE	t	p
IC50_log - ES/BS	0.30	CTX in vivo (ng/ml)	-0.964	1.52	-0.63	0.530
		PINP in vivo (µg/l)	0.022	0.02	1.39	0.174
		Height (m)	-2.213	3.10	-0.71	0.480
		Weight (kg)	-0.002	0.01	-0.15	0.880
		Age (years)	-0.001	0.03	-0.01	0.997
		Menopause status (pre/post)	0.613	0.46	1.34	0.190
		Smoking (no/yes)	**1.289**	0.47	2.73	**0.010**
		#osteoclasts in vitro	0.002	0.01	0.41	0.686
		#nuclei/osteoclast in vitro	**0.314**	0.14	2.28	**0.029**

doi:10.1016/j.bonr.2020.100674

P128

Osteocyte lacunae characteristics in iliac crest bone samples of aged adults

Stéphane Blouin[a], Barbara M. Misof[a], Markus A. Hartmann[a], Andrea Berzlanovich[b], Gerlinde M. Gruber[c], Sonja Lueger[a], Phaedra Messmer[a], Petra Keplinger[a], Paul Roschger[a]

[a]*Ludwig Boltzmann Institute of Osteology at Hanusch Hospital of OEGK and AUVA Trauma Centre Meidling, 1st Med. Dept. Hanusch Hospital, Vienna, Austria*

[b]*Center of Forensic Science, Medical University of Vienna, Vienna, Austria*

[c]*Department of Anatomy, Center for Anatomy and Cell Biology, Medical University of Vienna, Vienna, Austria*

Objectives: Osteocytes characteristics assessment is important to understand bone pathology since osteocytes play a major role in bone metabolism as mechanosensors, key regulators of osteoblast and osteoclast activity and of the mineral homeostasis. Therefore we propose to analyze quantitative backscattered electron images of bone samples and to quantify sectioned osteocyte lacunae number, size and shape as indirect 2D-characteristics of the osteocytes.

Methods: Twelve iliac crest necropsy samples were obtained from control women under 65 years (median=62 yrs; n=6) or over 90 years (median=94 yrs; n=6) without known bone pathology.

Calcium concentration maps (pixel resolution 0.9 μm) were obtained by quantitative backscattered electron imaging (Field Emission SEM Supra40, Zeiss, Oberkochen, Germany). Grey-level (value corresponding to 5.2 weight% calcium content) and size (range of 5 μm² to 80μm²) thresholds were used to obtain binary images of osteocyte lacunae sections (OLS). We measured OLS-density, OLS-porosity and the average values resulting from the frequency distributions of OLS area, perimeter and aspect ratio between major and minor axes (AR).

Results: Cortical bone in the adults had a higher OLS-porosity (+29%, p< 0.01) due to a higher OLS-density (+49%, p< 0.001), while the OLS-area, OLS-perimeter & OLS-AR (rounder OLS) were lower (-13%, -12%, -21%, respectively, all: p< 0.001) compared to trabecular bone

Interestingly no statistical difference in OLS size and number were observed in trabecular bone between both age groups, while in cortical bone OLS-density (-13%, p< 0.05) was lower and OLS-perimeter (+5%, p< 0.05) and OLS-AR (+13%, p< 0.01) were higher for the older age group.

Conclusion: Quantitative backscattered electron imaging reveals different osteocyte lacunae section density and size between cortical and trabecular bone in adults and also changes occurring with ageing in cortical bone. These data from an adult cohort will serve as reference to characterize bone pathologies in adults with respect to age.

doi:10.1016/j.bonr.2020.100675

P223

Associations between prenatal indicators of mechanical loading and proximal femur shape: Findings from the UK Avon Longitudinal Study of Parents and Children (ALSPAC)

Monika Frysz[a,b], Jon Tobias[a,b], Deborah Lawlor[b,c,d], Richard Aspden[e], Jenny Gregory[e], Alex Ireland[f]

[a]*Musculoskeletal Research Unit, Translational Health Sciences, Bristol Medical School, University of Bristol, Bristol, United Kingdom*

[b]*MRC Integrative Epidemiology Unit, University of Bristol, Bristol, United Kingdom*

[c]*Population Health Science, Bristol Medical School, University of Bristol, Bristol, United Kingdom*

[d]*Bristol NIHR Biomedical Research Centre, Bristol, United Kingdom*

[e]*Aberdeen Centre for Arthritis and Musculoskeletal Health, School of Medicine, Medical Sciences and Nutrition, University of Aberdeen, Aberdeen, United Kingdom*

[f]*Musculoskeletal Science and Sports Medicine Research Centre, Department of Life Sciences, Manchester Metropolitan University, Manchester, United Kingdom*

Hip development is influenced by mechanical loading during fetal movement, which increases with gestation length and is lower in oligohydramnios (OH) and breech presentation. However, associations between prenatal loading and hip shape in later life remain unexplored.

We examined associations between prenatal loading indicators (gestation length, OH and breech) obtained from obstetric records and hip shape modes (HSMs) generated using dual-energy X-ray absorptiometry images taken at age 14- and 18-years in participants from ALSPAC. These associations were examined in 2453 (30 OH, 105 breech) and 2330 (27 OH, 95 breech) participants with complete data at age 14- and 18-years respectively using confounder-adjusted models.

At 14 years HSM2 was 0.59SD (95%CI -0.96 to -0.12) lower in OH males, and HSM5 (-0.31SD, 95%CI -0.71 to -0.07) and HSM9 (-0.32SD, 95%CI -0.59 to -0.05) were lower in OH in both sexes. At 18 years HSM1 (-0.44SD, 95%CI -0.18 to -0.69) and HSM2 (-0.71SD, 95%CI -1.18 to -0.24) were lower and HSM6 (0.51SD, 95%CI 0.02 to 1.01) and HSM8 (1.06SD, 95%CI 0.51 to 1.60) were higher in OH males, whilst HSM5 was lower in OH in both sexes (-0.35SD, 95%CI -0.67 to -0.03). On modelling the combined effect of these associations, OH appeared to be associated with a wider femoral neck and head, and larger lesser/greater trochanters particularly in males (Figure 1). Only weak associations were observed between gestation length/breech and HSMs.

These results suggest that prenatal skeletal loading, in particular oligohydramnios, may influence adolescent joint shape with associations generally stronger in males.

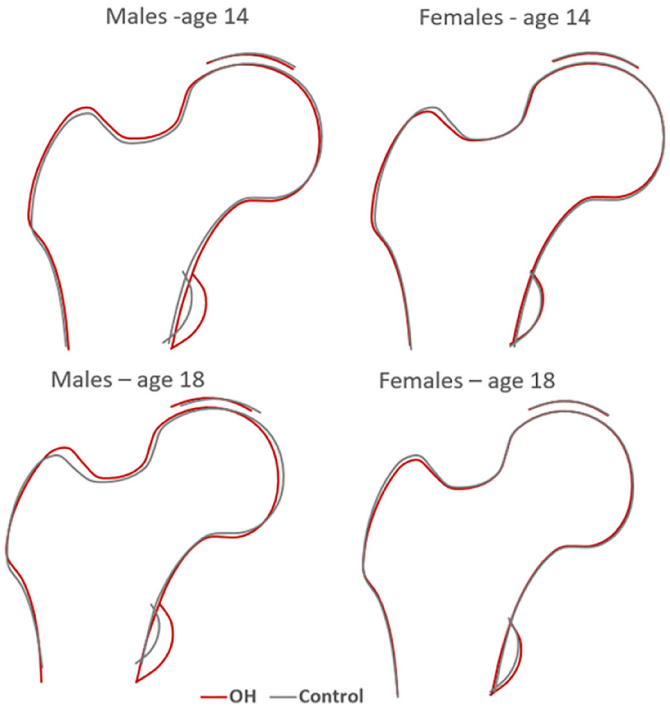

Figure 1. Composite hip shape at age 14 and 18 in individuals with and without OH, stratified by sex

doi:10.1016/j.bonr.2020.100676

P269

Comparison of treatment responder rates for three oral bisphosphonates: The TRIO study

Margaret A. Paggiosi[a], Nicola Peel[b], Eugene McCloskey[a], Jennifer S. Walsh[a], Richard Eastell[a]

[a]*Oncology and Metabolism, The University of Sheffield, Sheffield, United Kingdom*

[b]*Metabolic Bone Centre, Northern General Hospital, Sheffield Teaching Hospitals NHS Foundation Trust, Sheffield, United Kingdom*

Bone mineral density (BMD) is used to assess bisphosphonate treatment efficacy however it is unclear whether the response rate is similar for all oral bisphosphonates.

The TRIO study is a 2-year, randomized, open-label, parallel, trial of three oral bisphosphonates. We recruited 172 postmenopausal women (53-84 years) with a BMD T-score, of ≤-2.5 at the spine and/or total hip, or ≤ -1.0 plus a previous fragility fracture. Participants were randomized to receive either ibandronate (A), alendronate (B) or risedronate (C). at the licenced dose together with calcium (120 mg/day) and vitamin D (800 IU/day). Lumbar spine, total hip and femoral neck BMD were

measured at baseline, weeks 12 (in duplicate), 48 and 96.

We calculated individual BMD changes between baseline and weeks 12, 48 and 96. Duplicate week 12 results were used to calculate the least significant change (LSC) for lumbar spine (4.4%), total hip (4.2%) and femoral neck BMD (8.0%). Women were classified as treatment responders if their individual BMD increase was greater than the site-specific LSC. Differences in the number of responders by weeks 12, 48 and 96 were examined using chi-squared tests.

The LSC for femoral neck BMD was larger than that for lumbar spine and total hip BMD. Lumbar spine BMD identified more treatment responders than total hip BMD and femoral neck BMD. The number of treatment responders was dependent on the bisphosphonate type. By week 96, more women had responded to alendronate than ibandronate and risedronate.

Anatomical site	Responders by week 12 (n/total n (%))	Responders by week 48 (n/total n (%))	Responders by week 96 (n/total n) (%))
Lumbar spine	A=10/49 (20.4), B=11/55 (20.0), C=7/48 (14.6), All=28/152 (18.4)	A=24/45 (53.3), B= 25/50 (50.0), C=12/46 (26.1), All=61/141 (43.3)	A=20/29 (69.0)*, B=29/34 (85.3)*, C=13/30 (43.3)*, All=62/93 (66.7)
Total hip	A=6/48 (12.5), B=10/55 (18.2), C=3/48 (6.3), All=19/151 (12.5)	A=10/44 (22.7), B=12/50 (24.0), C=4/46 (8.7), All=26/140 (18.4)	A=9/28 (32.1)**, B=18/34 (52.9)**, C=6/30 (20.0)**, All=33/92 (35.9)
Femoral neck	A=6/48 (12.5)*, B=1/55 (1.8)*, C=1/48 (2.1)*, All=8/151 (5.3)	A=5/44 (11.4), B=2/50 (4.0), C=3/46 (6.5), All=10/140 (7.1)	A=0/28 (0), B=3/34 (8.8), C=2/30 (6.7), All=5/92 (5.4)

Responders by treatment duration, bisphosphonate type and anatomical site. Difference between bisphosphonates (A, B, and C) *p=0.04 and **p=0.03.

doi:10.1016/j.bonr.2020.100677

P276

Fracture rates in patients discontinuing alendronate treatment in real-life: A pharmaco-epidemiological study

Anne Sophie Sølling[a], Diana Hedevang Christensen[b], Bianka Darvalics[b], Torben Harsløf[a], Reimar Wernich Thomsen[b], Bente Langdahl[a]

[a]*Department of Endocrinology and Internal Medicine, Aarhus University Hospital, Aarhus, Denmark*

[b]*Department of Clinical Epidemiology, Aarhus University Hospital, Aarhus, Denmark*

Purpose: Based on the FLEX trial it has become clinical practice to discontinue alendronate (ALN) after 5 years of treatment, however, information on the fracture risk in these patients in a real-life setting is sparse. We aimed to examine ALN discontinuation patterns, to compare the fracture rates in patients discontinuing ALN after 5 to 5.5 years to patients continuing ALN for more than 5.5 years and to determine predictors of fractures after ALN discontinuation.

Methods: A nationwide population-based cohort study using Danish health registry data. Our source population was patients living in Denmark who had redeemed at least two ALN prescriptions between January 1st 1995 and September 1st 2018 (n=186,219). We used similar exclusion and inclusion criteria as in the FLEX trial.

Results: We found that 25% of ALN initiators used ALN for less than one year and 43% continued treatment for 5 years. Comparing patients who discontinued ALN after 5 to 5.5 years with continuers, we observed no increase in the risk of vertebral fractures (incidence rate ratios (IRR) 0.59, 95% CI 0.33-1.06), hip fractures (IRR 1.04, 95% CI 0.75-1.45) or major osteoporotic fractures (IRR 1.05, 95% CI 0.88-1.25). High age (>80 vs. 50-60 years, IRR 2.59, 95% CI 1.01-6.49) was a predictor for fractures following ALN discontinuation.

Conclusion: Less than 50% continued ALN treatment for 5 years. We did not find an increased risk of fractures in patients discontinuing ALN after 5 to 5.5 years compared to patients continuing ALN for more than 5.5 years.

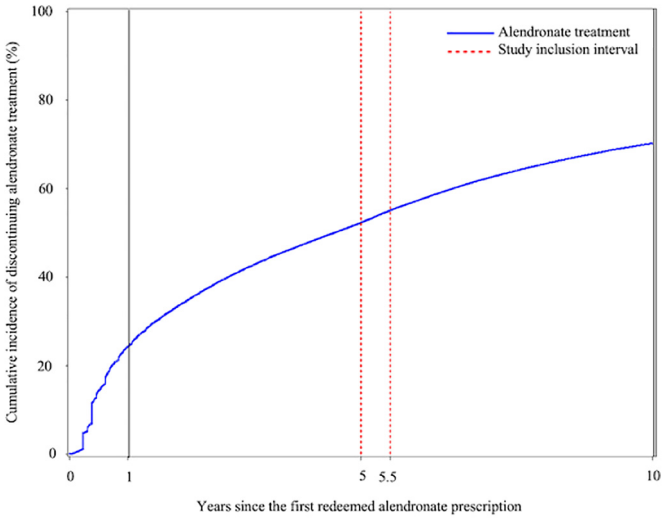

The cumulative incidence of discontinuing alendronate starting from the first redeemed alendronate prescription treating death as competing risk
n=176671

Figure 1.

doi:10.1016/j.bonr.2020.100678

P280

Systematic review and quality appraisal of cost-effectiveness analyses of drugs for postmenopausal osteoporosis

Md Azharuddin[a], Mohammad Adil[b], Pinaki Ghosh[c], Prem Kapur[d], Manju Sharma[a,b]

[a]*Pharmaceutical Medicine, Division of Pharmacology, School of Pharmaceutical Education and Research, Jamia Hamdard, New Delhi, India*

[b]*Pharmacology, School of Pharmaceutical Education and Research, Jamia Hamdard, New Delhi, India*

[c]*Pharmacology, Poona College of Pharmacy, Bharati Vidyapeeth, Pune, India*

[d]*Medicine, Hamdard Institute of Medical Sciences and Research, Jamia Hamdard, New Delhi, India*

Background: Worldwide, osteoporosis in postmenopausal women remains a substantial public health burden with extensive socioeconomic impact. The cost-effectiveness analyses of these drugs has been commonly assessed but the studies have neglected the treatment sequence impact. Therefore, aim of this study was to critically appraise the published study assessing cost-effective analysis of drugs for postmenopausal osteoporosis.

Methods: A systematic search was conducted in PubMed and CEA Registry, included all relevant English articles published between 2008 and 2019. Study characteristics, methods and outcomes were critically assessed. The Quality of included studies were assessed by using QHES (Quality of Health Economic Studies) and CHEERS (Consolidated Health Economic Evaluation Reporting Standards) instrument. Resulting scores of these instruments were then transformed into percentages to allow the comparison between QHES and CHEERS.

Results: A total 49 studies were included, Markov model was used across the studies. A healthcare payer, societal perspective was used in most of the studies, and others studies were addressed respective countries specific payer perspective. QALY as an outcome was used across the studies. Majority of studies were funded by the industry and reported favorable cost effectiveness. Based on QHES total score, 35 studies were found to be industry-funded with higher QHES mean (80.38±8.69) as compared with 14 non-industry funding studies with mean 72.22±17.67. The overall mean QHES scores were 78.38,

represents high quality (75-100). Additionally, overall mean CHEERS score (%) was found to 74.72± 11.21.

The statistical pairwise comparison between CHEERS mean (74.72± 11.21) and QHES mean (78.38± 11.84) did not found statistically significant ($p< 0.10$) whereas, QHES score found higher mean as compared to CHEERS.

Conclusions: Majority of the studies reported that drugs used for postmenopausal osteoporosis were cost effective among older population. Moreover, this study could be useful in health intervention decision making and development of future health economics studies.

doi:10.1016/j.bonr.2020.100679

P313

A novel *HSPG2* splice site mutation causing Schwartz-Jampel syndrome is associated with an impaired lacunocanalicular system

Simon von Kroge[a], Uwe Kornak[b], Michaela Schweizer[c], Ralf Oheim[a], Michael Amling[a], Tim Rolvien[a,d]

[a]*Department for Osteology and Biomechanics, University Medical Center Hamburg-Eppendorf, Hamburg, Germany*

[b]*Institute for Medical Genetics and Human Genetics, Charité-Universitätsmedizin Berlin, Berlin, Germany*

[c]*Core Facility of Morphology and Electron Microscopy, Center for Molecular Neurobiology Hamburg, Hamburg, Germany*

[d]*Department of Orthopedics, University Medical Center Hamburg-Eppendorf, Hamburg, Germany*

Perlecan, a heparan sulfate proteoglycan encoded by the heparan sulfate proteoglycan 2 (*HSPG2*) gene, is a matrix and cell surface protein found in numerous tissues at interfaces where a barrier is required. Specifically, it is abundant in the extracellular matrix of cartilage and the osteocyte lacunocanalicular space of bone. In mice, perlecan deficiency has been associated with decreased bone quality as well as decreased osteocyte canalicular density. Clinically, pathological mutations in the *HSPG2* gene lead to Schwarz-Jampel syndrome (SJS), which is characterized by chondrodysplasia, osteoporosis and myotonia.

Here, we present a patient with multiple vertebral fractures and early-onset osteoporosis (EOOP), myotonia and blepharophimosis. In this patient, compound heterozygous mutations in the *HSPG2* gene were detected indicating the presence of SJS. While the first variant (c.5743G>A) is reported to be common in the general population, the second variant (c.11993-3DelG) was predicted to influence splicing. RT-PCR using RNA isolated from skin fibroblasts from the patient confirmed the splice site mutation in the *HSPG2* gene causing complete retention of intron 87 within exon 87 and 88. In an obtained transiliac crest biopsy, we investigated bone micromorphology, matrix mineralization and the lacunocanalicular system using histomorphometry, quantitative backscattered electron imaging (qBEI) and scanning electron microscopy. QBEI analysis revealed a marked reduction of the mean mineralization (21.8 wt% vs. 24.0±0.7 wt%) compared to age- and sex-matched healthy controls (n=5). Interestingly, while the osteocyte number per bone area was not altered, osteocyte lacunae were smaller (29.8 μm^2 vs. 33.3±2.5 μm^2) and canaliculi were less frequent per lacuna (13.2 vs. 18.7±1.9) pointing to impaired mechanotransduction due to obstructed fluid movement in the lacunocanalicular system. Clinically, these findings may result in the respective phenotype of EOOP. In conclusion, this is the first human case of SJS underlining the effect of *HSPG2* on osteocyte canaliculi and matrix mineralization.

doi:10.1016/j.bonr.2020.100680

Concurrent Oral Poster Presentations 2: Basic/ Translational

P077

Preventative metformin treatment increases myeloma tumour burden and bone disease in vivo

Beatriz Gamez[a], Emma V. Morris[a], Sam W.Z. Olechnowicz[b], Aneka Sowman[b], Christina J. Turner[a], Claire M. Edwards[a,b]

[a]*Nuffield Department of Surgical Sciences, University of Oxford, Oxford, United Kingdom*

[b]*Nuffield Department of Orthopaedics, Rheumatology and Musculoskeletal Sciences, University of Oxford, Oxford, United Kingdom*

Multiple myeloma (MM) is a B cell malignancy associated with osteolytic bone lesions. MM arises from an asymptomatic state known as monoclonal gammopathy of undetermined significance (MGUS). Metformin has been reported to have anti-cancer properties, including reducing the risk of progression from MGUS to MM. Our aim was to determine whether pretreatment with metformin, could alter the bone microenvironment to reduce development of MM in vivo.

C57Bl/KaLwRij mice were treated with metformin for 4 weeks prior to MM inoculation, when metformin treatment was halted. In contrast to our hypothesis, pretreatment with metformin induced a two-fold increase in tumour burden (101%, $p< 0.001$), associated with an increase in osteolytic bone lesions (57%, $p< 0.05$). 2T3 preosteoblasts were treated with metformin, prior to addition of MM cells, increasing MM cell adhesion to preosteoblasts (118%, $p< 0.05$), quiescent MM cells ($p< 0.01$) and p21 expression. Short-term metformin pretreatment increased the osteogenic capacity of osteoblasts in vitro (92%, $p< 0.05$). Metformin increased osteopontin (OPN) gene ($p< 0.01$) and protein expression in osteoblasts. Silencing OPN expression in osteoblasts reduced MM cell attachment in response to metformin. In vivo, MM-bearing mice pretreated with metformin had elevated expression of OPN in the bone marrow as detected by immunohistochemistry.

Altogether our results show that metformin pre-treatment induces changes in the bone microenvironment, increasing the capacity to harbour MM cells. This can be partially explained by the increase in osteoblastic OPN expression which may act as chemoattractant for MM cells. In addition, metformin increases the osteogenic capacity of osteoblasts, potentially expanding the endosteal niche where MM dormant cells reside. Overall these results highlight the need for caution when considering the use of metformin in non-diabetic patients with MGUS as an approach to reduce progression towards MM.

doi:10.1016/j.bonr.2020.100681

P078

Pyridazinone scaffold-based molecules decrease osteosarcoma cells growth

Aurélie Moniot[a], Julien Braux[a], Christine Guillaume[a], Ingrid Allart-Simon[b], Sandra Audonnet[c], Sarah Renault[d], Françoise Rédini[d], Janos Sapi[b], Sophie C. Gangloff[a], Stéphane Gérard[b], Frédéric Velard[a]

[a]*EA 4691 BIOS, Biomatériaux & inflammation en site osseux, Université de Reims Champagne Ardenne, Reims, France*

[b]*UMR CNRS 7312 ICMR, Institut de Chimie Moléculaire de Reims, Université de Reims Champagne Ardenne, Reims, France*

[c]*URCACyt, Université de Reims Champagne Ardenne, Reims, France*

[d]*INSERM UMR1238 Phy.Os Sarcomes osseux et remodelage des tissus calcifiés, Université de Nantes, Nantes, France*

Primary osteosarcoma is a rare bone cancer mostly encountered in children and adolescents, with a second incidence peak in older patients

over 65 and an incidence about 0.4/100,000 per year [Mirabello, 2009; Jawad, 2011]. It has been evidenced that there was no significant improvement in treatments for these patients since 1990s [Perkins, 2014]. Pyridazinone derivatives, through their ability to target type 4 phosphodiesterases (PDE4), have been described as potential anti-cancer therapeutics [Akhtar, 2016]. Using two different pharmacomodulated pyridazinone scaffolds, we evidenced their cytotoxic effect on 4 human (MG-63, Saos-2, MNNG/HOS and K-HOS) and 1 murine (MOS-J) osteosarcoma cell lines through a reduction in cell mitochondrial activity [Moniot, ECTS 2019]. Focusing on both Saos-2 and MNNG/HOS cell lines, we observed a decrease of cell layer density up to 53% ($p < 0.05$) compared to controls by DNA measurement and numbering cells after 4 days of treatment. Such a reduced cell number was explained by both an increase of apoptosis (Annexin V+/PI- cells) up to 19% ($p < 0.05$) and a decrease of cell proliferation up to 22% ($p < 0.05$) without inducing senescence. Cell motility evaluated in wound healing assay at 24h, was decreased by 34% ($p < 0.05$) as compared to controls. Anti-tumor effect of the best hit candidate was assessed in a murine syngenic osteosarcoma model. After tumor development (between 150 and 500 mm^3 when starting the treatment), injections of 50 mg/kg of our hit candidate twice a week for 2 weeks decreased tumor growth by 28% ($p < 0.05$) as compared to untreated animals. Treatment with our drug also decrease ectopic bone formation in the vicinity of the tumor. These results suggested that pyridazinone scaffold-based molecules could be promising anti-osteosarcoma agents when coupled in a polytherapy.

Keywords: Osteosarcoma, pyridazinone, cytotoxicity, migration, tumor growth

doi:10.1016/j.bonr.2020.100682

P082

RANKL promotes the expansion of mammary epithelial cells in osteoporotic TgRANKL mouse models

Anthi Kolokotroni[a,b], Vagelis Rinotas[a], Evi Gkikopoulou[a,b], Eirini Efstathiou[a,b], Eleni Dermitzaki[a,b], Thanasis Rentis[a,b], Danae Zareifi[c], Ilias Lymperopoulos[d], Martina Samiotaki[a], Leonidas Alexopoulos[c], George Panayotou[a], Eleni Douni[a,b]

[a]*Institute of Bioinnovation, Biomedical Sciences Research Center Alexander Fleming, Vari-Athens, Greece*

[b]*Department of Biotechnology, Agricultural University of Athens, Athens, Greece*

[c]*Department of Mechanical Engineering, National Technical University of Athens, Athens, Greece*

[d]*1rst Breast Clinic, Iaso Hospital, Athens, Greece*

Receptor activator of nuclear factor-κB ligand (RANKL), a master regulator in osteoclastogenesis and bone resorption, is critically involved in the proliferation of mammary epithelial cells during pregnancy and lactation, as well as in the initiation of breast cancer. Given that RANKL mediates the paracrine effect of progesterone in the expansion of mammary epithelial cells, RANKL is considered as a highly promising therapeutic target for the prevention and treatment of breast cancer.

In this study, we investigated the expression of RANKL in the mammary glands of osteoporotic transgenic mice expressing human RANKL (TgRANKL), demonstrating expression of both mouse and human RANKL at the luminal epithelial cells in ductal and alveolar structures that was further upregulated during pregnancy or upon exogenous progesterone administration. We also identified an epithelial expansion in the mammary glands of TgRANKL mice compared to wild-type (WT) mice as quantified by whole-mount carmine staining (WT: 3.803 ± 1.661 vs TgRANKL: 10.20 ± 2.800, p< 0.01) and hematoxylin/eosin staining (WT: 2.355 ± 1.074 vs TgRANKL: 10.87 ± 1.959 p< 0.05), which was analogous to local RANKL levels and was reversed upon anti-human RANKL inhibition (Denosumab). Moreover, we developed a method to quantify mammary ductal branches using microCT (DV/TV% WT: 5.476 ± 0.3504 vs TgRANKL: 7.875 ± 0.2775 p< 0.001). Immunocytochemical analysis revealed increased proliferation in epithelial cells, as shown by the proliferative markers Ki67, Cyclin D1 and BrdU. Analysis of TgRANKL mammary glands with RNA sequencing, proteomic analysis and multi-plex analysis for phosphoproteins supported increased cell proliferation, and revealed upregulated genes and signaling molecules activated during carcinogenesis. Collectively, our results demonstrate that increased expression of RANKL in the mammary glands of osteoporotic TgRANKL mice is correlated with enhanced proliferation of mammary epithelial cells.

doi:10.1016/j.bonr.2020.100683

P156

Impaired bone healing in type 2 diabetes is caused by defective bone microenvironment functions of skeletal progenitor cells

Florence Figeac[a], Michaela Tencerova[a,b], Dalia Ali[a], Thomas L. Andersen[c,d,e], Dan Rémi Christiansen Appadoo[a], Nicholas Ditzel[a], Justyna Magdalena Kowal[a], Moustapha Kassem[a,f]

[a]*Molecular Endocrinology, KMEB University of Southern Denmark and Odense University Hospital, Odense, Denmark*

[b]*Molecular Physiology of Bone, Institute of Physiology, Czech Academy of Sciences, Prague, Czech Republic*

[c]*Pathology, Clinical Cell Biology- Odense University Hospital, Odense, Denmark*

[d]*Clinical Research, University of Southern Denmark, Odense, Denmark*

[e]*Molecular Medicine, University of Southern Denmark, Odense, Denmark*

[f]*Cellular and Molecular Medicine, Danish Stem Cell Center (DanStem)- University of Copenhagen, Copenhagen, Denmark*

The cellular mechanisms of obesity and type 2 diabetes (T2D)-associated impaired fracture healing are poorly studied. In a murine model of T2D reflecting both hyperinsulinemia due to HFD and insulinopenia induced by streptozotocin (STZ:40mg/kg), we examined the cellular dynamics of bone fracture healing in a tibia cortical bone defect model. A delayed bone healing as evaluated by μCT-scanning, was observed in HFD compared to ND (Bone Volume BV: -31.6% at day (D)14 and -38.7% at D21). Defect area histomorphometric analysis revealed decreased newly formed bone (7.03%±1.6 vs 14.44%±2.8 HFD vs ND, p< 0.05), accumulation of adipocytes (13.04%±2.2 vs 5.82%±0.4 HFD vs ND, p< 0.05) and both parameters were inversely correlated (R^2=0.49; p< 0.02). The number of osteoprogenitor cells *Runx2*+ and SCA1+ cells was unchanged or increased (189.5±26,0 vs 108.3 17.9 cells/mm^2 in HFD vs ND, p< 0.05), respectively. An accelerated senescence phenotype as shown by a 101.8% increase of ROS production and senescence gene expression was detected. Also, the number of senescent cells as evaluated by LAMIN $B1^-$ was increased (11.02%±1.3 vs 3.39%±0.6 HFD vs ND, p< 0.0001). In HFD+STZ animals, a more pronounced delayed bone healing was observed (BV:-39.7% at D14) and inversely correlated with glucose tolerance (R^2=0.48, p< 0.004) and marrow adiposity (R^2=0.37,p< 0.01). Senescent phenotype presents in hyperinsulinemic condition was absent in insulinopenic condition. To test for the human relevance, we observed that sera from obese and T2D patients exerted inhibitory effects on osteoblastic differentiation of human marrow stromal MSC. Our data suggest that T2D exerts negative effects on bone healing through inhibitory effects of differentiation of osteoblastic stem cells and that the degree of hyperglycaemia and not insulin levels per se, are detrimental to bone healing.

doi:10.1016/j.bonr.2020.100684

P157

Low protein diet compromises the recovery of lactation-induced bone loss in female mouse dams with no effects on skeletal muscles

Ioannis Kanakis[a], Moussira Alameddine[a], Mattia Scalabrin[a], Rob van 'tHof[a], Susan Ozanne[b], Katarzyna Goljanek-Whysall[a,c], Aphrodite Vasilaki[a]

[a]*Institute of Lifecourse and Medical Sciences, University of Liverpool, Liverpool, United Kingdom*

[b]*MRC Metabolic Diseases Unit and Metabolic Research Laboratories, University of Cambridge, Cambridge, United Kingdom*

[c]*Department of Physiology, School of Medicine, NUI Galway, Galway, Ireland*

The maternal musculoskeletal system rapidly adapts to fetal growth requirments during gestation and lactation. High calcium demands cause lactation-induced maternal bone loss but skeletal recovery is achieved promptly post-weaning. Dietary protein is vital for both offspring and mother but protein undernutrition effects on maternal skeleton and skeletal muscles is largely unknown. Our aim was to evaluate the effects of protein restriction during gestation and lactation on the maternal musculoskeletal system in mouse dams and during the post-weaning recovery. We first compared mouse dams fed with normal (N, 20% crude protein) or low (L, 8% crude protein) protein diet during gestation (19d) and lactation (21d) (Lac-N and Lac-L). For the 4-week post-weaning recovery period, another cohort of dams maintained on the same diets (Rec-NN and Rec-LL) or switched from low to normal (Rec-LN); aged-matched Virgin females were used as controls. At the end of lactation, skeletal muscle morphology and neuromuscular junctions (NMJs) integrity were found unaffected as assessed by histology; microCT analysis detected changes in bone microarchitecture of tibiae and spines, showing extensive bone loss in Lac-L mouse dams as compared with Lac-N (44.3% and 22.7% reduction in tibial and L5 BV/TV, $p< 0.001$ and $p< 0.01$, respectively). Full skeletal recovery was achieved only in Rec-NN dams at 4-weeks post-lactation, comparable to nulliparous, but partial in Rec-LN. In Rec-LL dams, there was a clear delay in bone recovery with elevated bone resorption and reduced formation as assessed by bone histomorphometric analyses of osteoclasts and osteoblasts. Low protein intake-derived primary osteoblasts showed decreased *in vitro* bone-forming capacity and osteogenic marker (Runx-2, Alp, Col1a1) gene suppression which was related to differential expression of selected bone-related microRNAs, such as miR-26a, -34a and -125b. We conclude that normal protein intake during the gestation and lactation and also post-weaning is indispensable for maternal musculoskeletal health.

doi:10.1016/j.bonr.2020.100685

P158

PiT2/SLC20A2: a new regulator of the bone marrow adipose tissue homeostasis?

Giulia Frangi[a,b], Greet Kerckhofs[c], Jérémy Boulestreau[a,b], Florent Autrusseau[a,b], Joëlle Veziers[a,b,d], Boris Halgand[a,b,d], Jérôme Guicheux[a,b,d], Xavier Prieur[e], Laurent Beck[a,b], Sarah Beck-Cormier[a,b]

[a]*INSERM, UMR 1229, Regenerative Medicine and Skeleton (RMeS), Université de Nantes, Ecole Nationale Vétérinaire, Agroalimentaire et de l'Alimentation, Nantes-Atlantique (ONIRIS), Nantes, France*

[b]*Université de Nantes, Unité de Formation et de Recherche (UFR) Odontologie, Nantes, France*

[c]*Skeletal Biology and Engineering Research Center, Department of Development and Regeneration, KU Leuven, Leuven, Belgium*

[d]*Centre Hospitalier Universitaire (CHU) Nantes, Pôles Hospitalo-Universitaires (PHU4) - Ostéo-articulaire - Tête et Cou - Odontologie - Neurochirurgie - Neuro-traumatologie (OTONN), Nantes, France*

[e]*INSERM UMR_S 1087/CNRS UMR 6291, l'Institut du Thorax, Université de Nantes, Nantes, France*

A great interest has lately emerged in the bone marrow adipose tissue (BMAT) and its intimate relationship with skeletal health. Our recently published work identifies the sodium-phosphate co-transporter PiT2/SLC20A2 as an important genetic determinant for bone quality and strength. Given the strong relationship between bone and BMAT, we decided to characterize the BMAT in PiT2-deficient mice (PiT2KO) (French Ethical approval n°02286.01).

We examined BMAT volume in the proximal part of PiT2WT and PiT2KO tibias by Contrast-Enhanced high-resolution μCT (CE-CT) analyses at P21 and P112. At P21, CE-CT analyses showed a dramatic BMAT volume increase in PiT2KO mice compared to the WT ($n=6$ per genotype, $p=0.0050$). These data are consistent with the 3-fold increase in Perilipin positive adipocytes quantified in the BMAT at P16 ($n=6$-8 per genotype, $p< 0.0036$), and with the increased expression of *Adiponectin* ($p=0.0061$) and *FABP4* ($p=0.0424$) at P21 in PiT2KO tibias compared to the WT ($n=4$-7 per genotype). Western blot ($n=9$-18 per genotype) and Elisa ($n=5$-9 per genotype) tests indicated that the absence of PiT2 enhanced Adiponectin secretion from the BMAT in PiT2KO mice without altering its serum level. At P112, CE-CT analyses showed an absence of BMAT volume increase with age that is normally observed in WT mice, leading to a decreased BMAT volume compared to PiT2WT mice ($n=11$ per genotype, $p=0.0086$).

To determine whether the increased BMAT in PIT2KO mice was caused by a cell autonomous or a paracrine effect, the adipogenic differentiation of Bone marrow Mesenchymal Stromal Cells (BMSCs) from P21 PiT2WT and PiT2KO mice was evaluated. We showed that the adipogenic differentiation capacity of PiT2KO BMSCs is identical to the PiT2WT BMSCs, suggesting that the increased BMAT observed in P21 PiT2KO mice *in vivo* may come from cells of a non-adipogenic origin.

Overall, our results reveal PiT2 as a new regulator of BMAT.

doi:10.1016/j.bonr.2020.100686

P205

A novel laser-induced lesion paradigm to image osteoblast - immune cell interactions in vivo

Karina Geurtzen[a], Franziska Knopf[b]

[a]*CRTD - Center for Regenerative Therapies Dresden, CMCB, TU Dresden, Dresden, Germany*

[b]*Center for Healthy Aging and CRTD - Center for Regenerative Therapies TU Dresden, CMCB, TU Dresden, Dresden, Germany*

Crosstalk between bone and immune cells, in particular osteoblasts and macrophages, has the potential to trigger bone formation and regeneration but also to impair both processes, if disturbed. In vivo models to image such interactions in real time are sparse. Zebrafish have become a powerful model to study bone formation and regeneration, also in the context inflammation and leukocyte recruitment. Zebrafish larvae are ideally suited to perform live cell imaging. Here, we report on a novel laser-induced lesion paradigm to in vivo image osteoblast-immune cell interactions in a developing skull bone in zebrafish. Using the fact that macrophages get attracted by cell debris, we established a sterile wounding assay, in which approx. 10 % of osteoblasts are killed by laser-assisted cell ablation. Recovery of the osteoblast population occurs by proliferation of the remaining cells within a single day. Using spinning disc confocal microscopy, we tracked the immediate migration of

macrophages into the site of ablation within minutes. A significant proportion of the respective cells display an inflammatory phenotype, characterized by enhanced *tnf-α* and *irg1* expression. The macrophages´ recruitment is potentially triggered by release of ROS at the injury site. Finally, during pharmacological glucocorticoid exposure, which impairs bone formation, we found reduced macrophage migration into the region of interest. Altogether, our novel lesion paradigm presents a valuable tool to further study the interaction between bone and immune cells, and can be used to elucidate the signals driving appropriate and disturbed macrophage recruitment in vivo.

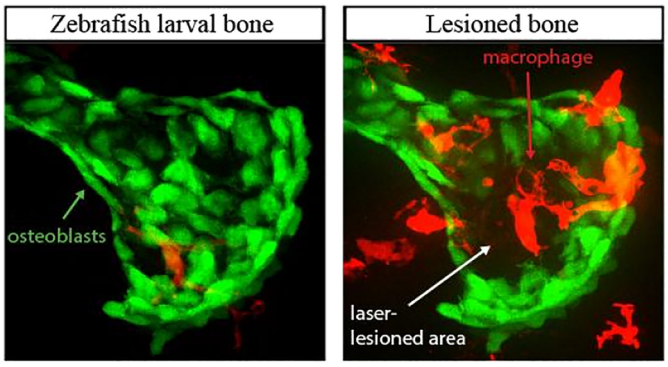

Laser-induced lesion paradigm to ablate zebrafish larval osteoblasts

doi:10.1016/j.bonr.2020.100687

P206

Thermoneutral temperature mitigates hind-limb unloading-induced bone loss by preserving energetic metabolism

Laura Peurière, Carmelo Mastrandrea, Marie-Hélène Lafage-Proust, Laurence Vico
INSERM U1059-SAINBIOSE, Université de Lyon, Saint-Priest-en-Jarez, France

Hind-Limb Unloading (HLU) induces both bone loss and expansion of bone marrow adipose tissue (BMAT). However, BMAT depends on energetic metabolism, which may be challenged by HLU, since experimental conditions may alter body temperature. Therefore, we compared the effects of HLU on bone, at 22°C, the current standard experimental temperature, to those at 28°C, a thermoneutral temperature in mice.

16 week-old male C57BL/6J mice were acclimatized for 4 weeks (1 mouse/cage) and then submitted to HLU or kept, pair-fed with respective HLU mice, in control cages (CONT) for 14 days at either 22°C or 28°C (201611231457342-V6, CEEAL-UJM#98). *In vivo* μCT was performed at Days 0 and 14. Femora were collected for histomorphometry, osmium-stained BMAT quantification and RT-qPCR mRNA analyses of cortical bone.

In HLU, body weight and food consumption were respectively lower and higher at 22°C than at 28°C. Moreover, HLU22°C showed 5.6-times lower leptin serum levels and higher BMAT volume compared to CONT22°C and both 28°C groups. Trabecular bone loss amplitude was respectively 3.7 and 1.5-times greater in CONT22°C and HLU22°C compared to the respective 28°C groups (Fig.1). Similar results were found in cortical bone. Femur trabecular osteoclastic surfaces were higher at 22°C (6.6% and 8.0% in CONT and HLU) than at 28°C (2.3% and 3.9% in CONT and HLU), respectively. Interestingly, we found higher cortical expression of apoptosis genes (DDIT3, P27) and RANKL at 22°C than at 28°C, regardless of loading condition.

We conclude that HLU effects on bone at 22°C are strongly influenced by energetic metabolic challenge.

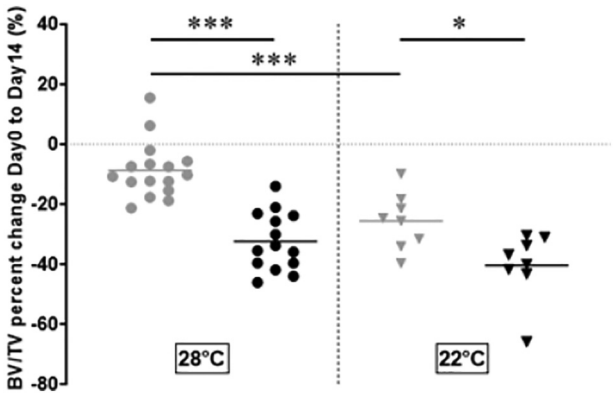

Figure 1. Femur trabecular volume percent change in control (grey) and HLU mice (black).

doi:10.1016/j.bonr.2020.100688

P207

How the skeleton adapts to an extremely short lifespan: Revealing compositional and biomechanical features of the bone matrix in the shortest-lived vertebrate model killifish *(N.furzeri)*

Imke A.K. Fiedler[a], Felix N. Schmidt[a], Eva M. Wölfel[a], Anton Davydok[b], Katharina Jähn[a], Dario R. Valenzano[c], Björn Busse[a]
[a]*Department of Osteology and Biomechanics, University Medical Center Hamburg-Eppendorf, Hamburg, Germany*
[b]*Institute of Material Research, Helmholtz-Zentrum Geesthacht, Outstation at German Electron Synchrotron DESY, Hamburg, Germany*
[c]*Max Planck Institute for Biology of Ageing, Cologne, Germany*

Introduction: Musculoskeletal research is reliant on vertebrate organisms to unravel the mechanisms of bone aging and fragility. While most model organisms including mice and zebrafish can have a lifespan of up to 5 years, killifish complete their life cycle in only 3-9 months. Yet, they show aging-related decay similar to humans, including decreased brain function, regenerative capacity, and spinal integrity. We thus hypothesize that the killifish can foster new insights into skeletal aging and aim to provide a comprehensive understanding of its skeletal system.

Methods: A total of 12 adult killifish (GRZ strain) underwent *ex vivo* bone quality analyses (6 male/6 female, 11±1 weeks old). Micro-computed tomography was performed for whole-bone morphometry (4 μm voxel size). Histology, energy dispersive spectroscopy, Raman spectroscopy, synchrotron X-ray scattering, and mechanical testing was performed to assess vertebral bone matrix composition and mechanical properties.

Results: Killifish showed a vertebral body length of 924±134 μm, bone volume/tissue volume of 44±6 %, and vertebral thickness of 46±11 μm. The vertebral bone matrix featured osteoblastic appositional bone growth but was anosteocytic (reflecting an inherent trait of advanced bony fish). The matrix was composed of carbonated hydroxyapatite and collagen and had an elastic modulus of 19.4±2.8 GPa. The mineral crystal thickness was 2.1±0.3 nm and the Ca/P ratio was 1.85±0.03 (1.82±0.01 in males, 1.88±0.02 in females, p=0.05).

Discussion: Bone analyses of killifish indicate that, despite the extremely short lifespan, their bone matrix is designed to reach similar degrees of mineralization and biomechanical performance compared to much longer-lived species, e.g. humans. Moreover, the lack of

osteocytes in this species did not imply an impairment of bone quality measures. This study underlines the killifish as an intriguing vertebrate model to rapidly assess alterations in bone formation capacity and fragility as a function of age and intervention.

doi:10.1016/j.bonr.2020.100689

P318

Fgfr3 gain-of-function mutation impacts bone homeostasis in hypochondroplasia mouse model

Léa Loisay[a], Davide Komla Ebri[b], Nabil Kaci[a], J.H. Duncan Bassett[b], Graham R. Williams[b], Laurence Legeai Mallet[a]
[a]*Institut IMAGINE and Hôpital Necker-Enfants Malades, Paris, France*
[b]*Molecular Endocrinology Laboratory, Department of Metabolism, Digestion and Reproduction, Imperial College London, London, United Kingdom*

Hypochondroplasia (HCH) is a moderate rhizomelic dwarfism induced by a Fibroblast Growth Factor Receptor 3 (Fgfr3) gain-of-function (GOF) mutation. We generated the first mouse model of HCH (*Fgfr3*$^{Asn534Lys/+}$) expressing the most common missense mutation (p.Asn540Lys). Macroscopic analysis of *Fgfr3*$^{Asn534Lys/+}$ mice displayed progressive dwarfism throughout development with shortened limbs (e.g. -13% femoral length at P14 (n≥7 per group p< 0.0001 t-test) compared to control mice thus indicating that endochondral ossification is impaired.

To estimate the impact of *Fgfr3* GOF mutation on bone formation, we performed micro-computed tomography analyses of *Fgfr3*$^{Asn534Lys/+}$ mice hindlimbs at three age points: P42, P70, P180 (n≥10 males per group). As in human pathology, we observed reduced trabecular bone mineral density (BMD) (e.g. P70 femur -3.15% p=0.0183 t-test), trabecular number (e.g. P70 femur -24.59% p=0.0004 t-test) and thickness (e.g. P70 femur -12.89% p=0.0004 t-test) in *Fgfr3*$^{Asn534Lys/+}$ mice compared to controls. We next investigated cortical bone of femur and tibia. Unexpectedly, our studies revealed a marked increase in BMD at P42 (+6.12% p=0.0006 t-test), P70 (+5.67% p=0.0166 t-test), P180 (+10.17% p< 0.0001 t-test), in *Fgfr3*$^{Asn534Lys/+}$ femurs mice compared to controls. In opposite, in tibial cortical bone, the BMD is equivalent to the *Fgfr3*$^{+/+}$ at P42 (p=0.3277 t-test), decreased at P70 (-4.60% p< 0.0001 t-test) and increased at P180 (+6.18% p= 0.0002 t-test). These findings suggest that an increase in cortical BMD may be a novel pathological feature of HCH. Moreover, our study shows that activating Fgfr3 mutation 1) affects trabecular and cortical bone differently 2) impacts the cortical osteogenesis of the limb with a prominent severity in its proximal than distal section 3) increases its effects with ageing.

Altogether, these results indicate that Fgfr3 regulation is essential for normal bone development and bone mass maintenance. All these data will improve our understanding of the hypochondroplastic bone features during adulthood.

doi:10.1016/j.bonr.2020.100691

P322

ENPP1 regulates bone mass via an unidentified catalytically independent mechanism

Demetrios Braddock[a], Kristin Zimmerman[a], Ralf Oheim[b], Simon V. Kroge[b], Paul Stabach[a], Dillon Kavanagh[a], Steven Tommasini[c], Thomas Carpenter[d]
[a]*Pathology, Yale School of Medicine, New Haven, United States*
[b]*Department of Osteology and Biomechanics, University Medical Center Hamburg-Eppendorf, Hamburg, Germany*
[c]*Orthopaedics and Rehabilitation, Yale School of Medicine, New Haven, United States*
[d]*Pediatric Endocrinology, Yale School of Medicine, New Haven, United States*

Heterozygous ENPP1 deficiency is associated with early onset osteoporosis, a phenotype faithfully reproduced in mice. ENPP1 hydrolyzes extracellular nucleotide triphosphates to generate nucleotide monophosphates and pyrophosphate (PPi), however the mechanism of ENPP1 associated osteoporosis is not readily apparent given that PPi is a strong inhibitor of mineralization.

Current murine models reduce both Enpp1 catalytic activity and protein expression via disruption of protein folding and stability. A single catalytic site, a Threonine at position 238 in Enpp1, is responsible for the hydrolysis of the high-energy nucleoside phosphate bond via an SN2 reaction mechanism. Accordingly, we converted the Threonine nucleophile to an Alanine in C57BL/6 mice using Crispr/Cas techniques to eliminate Enpp1 catalytic activity without disrupting protein expression, and compared the skeletal and tissue mineralization phenotype in *Enpp1*$^{T238A/T238A}$ mice with WT sibling pairs, and to *Enpp1*$^{asj/asj}$ mice which exhibit both disrupted protein expression and catalysis.

Similar to *Enpp1*$^{asj/asj}$ mice, *Enpp1*$^{T238A/T238A}$ mice exhibited markedly decreased plasma PPi (13% of WT), increased intact FGF23 (180% of WT), phosphate wasting (70% of WT), and increased extra-skeletal calcifications in the soft tissues and joints. Of note, bone mass in *Enpp1*$^{T238A/T238A}$ mice was better preserved than in *Enpp1*$^{asj/asj}$ mice at both 10 and 23 wks of age, with normal trabecular bone volume and trabecular number (by both microCT and histomorphometry). Moreover, *Enpp1*$^{T238A/T238A}$ mice had a consistently more favorable biomechanical profile (stiffness, maximum load, and total work in tibias on 4-point bending) than *Enpp1*$^{asj/asj}$ mice. Furthermore, in contrast to *Enpp1*$^{asj/asj}$ mice, *Enpp1*$^{T238A/T238A}$ mice exhibited no evidence of osteomalacia - MAR and MLT were normal at both 10 and 23 weeks. Finally, similar to *Enpp1*$^{asj/asj}$ mice, qBEI analysis demonstrated decreased osteocyte lacunar area at both time points. Overall, this constellation of findings suggests that Enpp1 contributes to skeletal mass through an unidentified mechanism independent of its catalytic activity.

doi:10.1016/j.bonr.2020.100692

Concurrent Oral Poster Presentations 2: Clinical/ Public Health

P044

Role of bone nano-mechanics in age-related fragility fractures

Richard Abel[a], Ulrich Hansen[b], Justin Peter Cobb[a]
[a]*Medicine, Surgery and Cancer, Imperial College London, London, United Kingdom*
[b]*Mechanical Engineering, Imperial College London, London, United Kingdom*

Nanoscale building blocks of bone including collagen fibrils and mineral apatite may be important determinants of whole-bone mechanical properties and contribute to the risk of age-related fractures. Yet there are few studies of bone nanoscale mechanics in patients with a known fracture history, thereby limiting research into fracture prevention.

Tensile nano- and tissue-level mechanics were measured in trabecular sections from proximal femora of three groups: ageing non-fractured donors (Controls) and ageing fracture patients, both untreated (Fx-Untreated) and bisphosphonate-treated (Fx-BisTreated) (n = 10 per group). Tissue-level mechanics were recorded using a mechanical testing rig, whilst collagen and mineral strains were measured simultaneously with synchrotron-derived X-ray diffraction. Tissue- and nano-level mechanics were compared across the donor groups, and macro-mechanical data were regressed against nano.

Irrespective of treatment, fracture patients exhibited significantly lower tensile strength, critical strain and max strain in comparison to

the control group, in combination with lower peak collagen and mineral strain (Kruskal Wallis all $p< 0.001$). The Fx-BisTreated group, exhibited the lowest properties in every comparison (Mann Whitney U Test $p< 0.001$). In all three groups, peak strain in the mineral coincided with the critical stress at the tissue scale, whilst peak fibril strain occurred afterwards (i.e. higher strain). Tensile strength and critical tissue strain were positively correlated with both peak fibril and mineral strains (all $r^2 \geq 0.80$).

Age-related fractures are associated with lower peak fibril and mineral strain irrespective of treatment. Lower strains indicate earlier mineral disengagement and subsequent onset of fibril sliding, which appear to be the underlying mechanisms leading to fracture. Fibril sliding represents an early stage in the cascade of events that lead to fracture but ultimately, the mineral governs macroscopic bone strength. Fracture prevention treatments could target collagen-mineral interactions to restore the onset of mineral disengagement and fibril sliding to that of healthy bone.

doi:10.1016/j.bonr.2020.100693

P159

In type 2 diabetes mellitus collagen fibril plasticity is altered along with higher glyco-oxydative damage and non-osteoporotic bone mineral density

Eva Maria Wölfel[a], Katharina Jähn[a], Anna Kornelia Siebels[a], Liang-Yu Ma[a], Grazyna E. Sroga[b], Annika Vom Scheidt[a], Felix Nikolai Schmidt[a], Birgit Wulff[c], Herbert Mushumba[c], Klaus Püschel[c], Michael Amling[a], Deepak Vashishth[b], Eric Schaible[d], Petar Milovanovic[a,e], Elizabeth Zimmermann[a,f], Björn Busse[a]

[a]*Department of Osteology and Biomechanics, University Medical Center Hamburg-Eppendorf, Hamburg, Germany*
[b]*CBIS, Department of Biomedical Engineering, Rensselaer Polytechnic Institute, Troy, United States*
[c]*Department of Forensic Medicine, University Medical Center Hamburg-Eppendorf, Hamburg, Germany*
[d]*Advances Light Source, Lawrence Berkeley National Laboratory, Berkeley, United States*
[e]*Laboratory for Anthropology and Skeletal Biology, University of Belgrade, Belgrade, Serbia*
[f]*Shriners Hospitals for Children Canada, Montreal, Canada*

Type 2 diabetes mellitus (T2DM) is associated with increased fracture risk, despite presenting with normal to high BMD. This points to an impaired bone quality, which among others, is determined by microstructure, osteocyte function, and advanced glycation end-product (AGE) accumulation. We hypothesize that the intrinsic bone properties at fibrillar length scale are impaired in diabetic bone while presenting with normal BMD and higher AGE level.

From 21 T2DM-diagnosed cases (74±7 yrs) and 23 age-matched controls (74±8 yrs), the mid-diaphyseal femoral cortex and 12th thoracic vertebra were collected during autopsy with IRB approval. DXA measured vertebral osteoporotic fracture risk based on areal BMD (aBMD). HR-pQCT measured femoral cortical volumetric BMD (Ct.vBMD). Mechanical deformations at multiple length-scales were determined by synchrotron small angle x-ray scattering (SAXS) during simultaneous tensile testing (12 controls, 9 T2DM). The osteocytic expression of sclerostin and connexin43 was determined by immunohistochemistry, while fluorescent AGEs were analyzed via fluorescent assay and carboxymethyl-lysine (CML) with CML-ELISA (11 controls, 12 T2DM).

aBMD did not differ between the groups, while HR-pQCT showed a tendency to lower Ct.vBMD in T2DM (1032.13±42.28 vs. 1061.86±30.2 mgHA/cm³,$p=0.061$). Tensile tests during SAXS measurements showed that T2DM cases present with a lower fibril strain compared to controls. Between the groups we found no differences in osteocytic expression of sclerostin and connexin43. Compared to controls, T2DM was associated with 18% higher fluorescent AGE levels (309±72 vs. 263±66 ngQuinine/mgCollagen), and significantly higher CML (1456±293 vs. 909±298 ngCML/mgProtein, $p=0.003$).

Taken together, our results highlight changes in plasticity in diabetic bone. While osteocytic function seems to be preserved, accumulation of AGEs is higher in T2DM. The observed changes at the fibrillar length scale combined with increase in glycoxidative damage of bone protein provide possible mechanisms leading to the increased fracture risk observed in T2DM individuals independent of BMD.

doi:10.1016/j.bonr.2020.100694

P172

Hyperglycaemia is not associated with higher volumetric bone mineral density in a Chinese health check-up cohort

Ling Wang[a], Kaiping Zhao[b], Xiaoguang Cheng[a], Annegreet G. Veldhuis-Vlug[c], China Biobank study group

[a]*Department of Radiology, Beijing Jishuitan Hospital, Beijing, China*
[b]*Department of Medical Record Management and Statistics, Beijing Jishuitan Hospital, Beijing, China*
[c]*Center for Bone Quality, Department of Internal Medicine, Division of Endocrinology, Leiden University Medical Center, Leiden, Netherlands*

Objective: Diabetes mellitus (DM) patients have an increased fracture risk despite having higher areal bone mineral density (aBMD) measured by DXA. This apparent paradox might be explained by the overestimation of BMD by DXA due to the higher fat mass in diabetes patients. This study investigated the relation between volumetric BMD (vBMD) measured by quantitative computed tomography (QCT) in subjects with or without diabetes and impaired fasting glucose (IFG).

Methods: 9643 healthy participants (5501 men and 4142 women, mean age 53 years range 30-96) from the China Biobank project, underwent QCT based on chest low dose CT to compute vBMD of L1 and L2 vertebrae. The study was approved by the Beijing Jishuitan Hospital IRB. Data was analyzed using linear regression models. Age and glycaemia had an interaction effect, therefore we stratified the analyses by age (age cut point 55 years).

Results: Of the 9643 participants, 829 had diabetes (559men, 270 women) and 994 had IFG (672 men, 322 women). vBMD was associated with FPG both in women ≥55 years ($r=-0.072$, $p=0.008$) and < 55 years ($r=-0.109$, $p< 0.001$) and not in men, but this association did not remain significant after adjustment for age.

In subjects ≥55y, women with DM were older than healthy women (mean age 68.5 vs 63.3 y, $p< 0.001$), and vBMD was lower (86.1 vs. 96.3 mg/cm^3, $p< 0.001$), and not in men, but this association did not remain significant after adjustment for age ($p=0.606$). In subjects < 55y, no differences were found in vBMD between DM and healthy subjects after adjustment for age. There were no difference in vBMD between IFG and healthy subjects.

Conclusion: Compared to aBMD, vBMD is not higher in subjects with diabetes compared to healthy subjects. Therefore, vBMD measured with QCT might be a more reliable measurement than aBMD in subjects with diabetes.

doi:10.1016/j.bonr.2020.100695

P200

Interest of texture analysis and neural networks for the characterization of knee osteoarthritis radiographic progression in OAI and MOST cohorts

Khac Lan Nguyen[a,b], Andy Xavier[a,b], Ahmad Almhdie[a,b], Nada Ibrahim[a,c], Hechmi Toumi[a,b], Rachid Jennane[a], Eric Lespessailles[a,b]
[a]*EA 4708-I3MTO, Université d'Orléans, Orléans, France*
[b]*PRIMMO-CHR d'Orléans, Orléans, France*
[c]*Rheumatology, CHR d'Orléans, Orleans, France*

Characterize knee osteoarthritis (OA) progression combining both trabecular bone texture (TBT) analysis and convolutional neural networks (CNNs) on computed radiographs (CR) and radiographic imaging (RG).

OA progression was defined as an increase in Kellgren-Lawrence (KL) grade over 48 months (OAI, 1182 patients) and 60 months (MOST, 607 patients). A fractal texture analysis was performed on different regions of interest under the tibial plateau. Baseline knee OA images (KL4) were automatically graded by the CNN. Characterization of the progression was explored using logistic regression models evaluated by the area under the ROC curves (AUC).

Obtained AUCs of clinical covariates (Cov: age, gender, BMI) were 0.56 and 0.52 in the OAI and MOST cohorts, respectively. TBT was more efficient than CNNs whatever the cohort, the modality and the quality of radiographs (AUC > 0.6). Combining TBT and CNNs improved the global prediction results (Figure). For each cohort, the full model (TBT + CNN + Cov) improved AUC results up to 0.68 (RG, OAI). The lowest AUC was obtained with the MOST cohort and the RG modality. AUCs using each radiograph modality were similar for both MOST (0.64 CR, 0.63 RG, 0.62 CR & RG, p-value > 0.05) and OAI (0.66 CR, 0.68 RG, 0.66 CR&RG, p-value > 0.05).

These results suggest that combining CNNs and TBT might improve AUC scores for the characterization of knee OA progression. The inclusion of all radiographs (CR & RG and also poor-quality radiographs) may minimize AUC scores.

Keywords: Knee osteoarthritis, Radiography, Trabecular Bone Texture,Convolutional Neural Networks

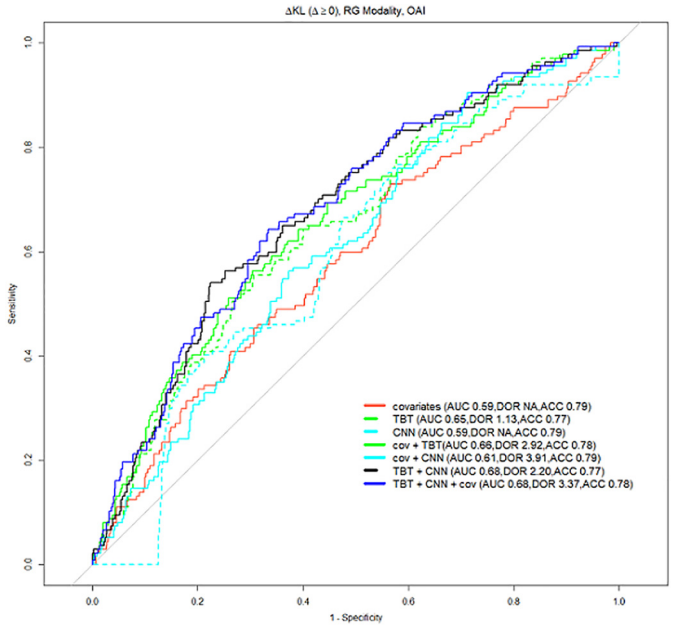

ROC curves obtained for knee OA progression prediction on RG radiographs in OAI cohort

doi:10.1016/j.bonr.2020.100696

P210

Lipocalin-2 (LCN2) increases after acute exercise but is dispensable for muscle physiology

Marco Ponzetti, Argia Ucci, Antonio Maurizi, Anna Teti, Nadia Rucci
Biotechnological and Applied Clinical Sciences, University of L'Aquila, L'Aquila, Italy

Lipocalin 2 (Lcn2) is an adipokine carrying out a variety of functions, however its importance in muscle physiology is barely known. We had the opportunity to collect sera from 15 healthy individuals before and after uphill running, which subjected their muscles to an acute high-intensity aerobic exercise (speed=75-80m/min, slope=30% time=40-50min). Interestingly, we observed an increase of LCN2 levels (1.3-fold, p=0.0005), along with an increase of muscle damage markers creatine kinase (1.4-fold, p=0.0013) and myoglobin (6.5-fold, p=0.015). The Wnt antagonist DKK1 was also slightly increased after exercise (1.1-fold, p=0.04), positively correlating with LCN2 (R=0.38, P=0.04). To understand the relevance of LCN2 in muscle physiology, we next investigated the muscle phenotype in Lcn2 knock out (*Lcn2*$^{-/-}$) mice at different ages. First, we checked LCN2 in muscle of WT mice, finding that it was expressed at transcriptional and protein level in diaphragm, quadriceps and *soleus*. Moreover, histological analysis showed 12-20% smaller muscle fibres (p< 0.001), but no fibrosis or muscle damage in quadriceps of *Lcn2*$^{-/-}$ mice compared to WT. Muscle weight and grip strength were also similar between the two genotypes. Consistently, serum myoglobin and CK were comparable to WT, while serum interleukin-6 ranged from 3.9±6.8pg/ml to 17.13±14.93pg/ml in WT but was undetectable in *Lcn2*$^{-/-}$ mice (n.mice/genotype=15-19). Transcriptionally, *Lcn2*$^{-/-}$ quadriceps showed an increase of the myogenic factor *Myogenin* (2.5-fold, p=0.02), and reduction of *Interleukin-1b* (0.5-fold, p=0.04) at 3 months, which became unremarkable at 12. Finally, treatment with recombinant Lcn2 reduced myogenic differentiation in C2C12 cells (-22%, p=0.02) and primary mouse myoblasts (-27%,p=0.001), evaluated as % myonuclei/total cells. Taken together, we found that Lcn2 is increased after high-intensity exercise and is dispensable for normal muscle physiology, while its deletion reduces inflammatory cytokines in mouse muscle. Furthermore, treating muscle cells with Lcn2 reduces myogenic differentiation, suggesting that Lcn2 may be detrimental in inflammatory muscle conditions.

doi:10.1016/j.bonr.2020.100697

P218

Association between muscle strength and body composition in osteoporotic patients with vertebral fractures

Larisa Marchenkova, Ekaterina Makarova, Mikhail Eryomushkin, Ekaterina Chesnikova, Elena Styazhkina
Rehabilitation Department for Somatic Patients, National Medical Research Center for Rehabilitation and Balneology of Ministry of Health of Russian Federation, Moscow, Russian Federation

The aim was to evaluate the relationship between muscle strength and body composition in patients with osteoporotic vertebral fractures (VFs).

Methods: Study comprised 90 men and women 40-80 y.o. with primary osteoporosis. Study group (n=60) included patients with at least 1 VF, control group (n=30) consisted of subjects of the same age, BMI and BMD without any fracture. Muscles strength was assessed

using tenzodynamometry, Up-and-go test, 10-m walk test, back and abdomen static and dynamic muscle endurance tests. Body composition was evaluated using DXA Total Body program.

Results: Patients with VFs had a muscle strength deficiency -40.9% in trunk flexors (TF) and -18.1% in extensors (TE) with an adequate function of the left (LLF) and right lateral flexors (RLF). Patients in study group had lower muscle strength vs controls in TF (15.6±9.8 vs 27.7±9.9 kg, p< 0.001), TE (14.6±8.9 vs 21.3±8.4 kg, p< 0.001), LLF (13.1±7.2 vs 24.1±8.9 kg, p< 0.001) and RLF (13.4±7.4 vs 24.3±7.7 kg, p< 0.0001). No difference in functional tests results were registered (p>0.05). Body composition analyses showed differences between study and control groups in relative skeletal muscle index (RSMI, 6.5±1.2 vs 7.5±2.1 kg/m^2, p=0.02) and fat mass (29717±8367.4 vs 35464±9127.4 g, p=0.01). There was no significant difference in soft tissue and lean (muscle) mass between groups. Strength of all studied trunk muscles strongly negatively correlated with the number of VFs (p < 0.001) and positively correlated with femoral neck BMD (g/m^2), fat mass, soft tissue mass and lean mass (p< 0.001), but not with age and RSMI (p>0.05).

Conclusions: Patients with VFs have a decrease in muscles strength and lower RSMI, mass and % of body fat vs patients without fractures. Number of VFs, low BMD, decreased fat, soft tissue and lean mass are associated with muscle dysfunction in osteoporotic patients with VFs.

doi:10.1016/j.bonr.2020.100698

P235

The effectiveness of the Fracture Risk Evaluation Model (FREM) in predicting major osteoporotic fractures and hip fractures: A register-based cohort study

Michael Kriegbaum Skjødt[a,b], Sören Möller[b], Mette Bliddal[b], Nana Hyldig[b], Jens Søndergaard[c], Bo Abrahamsen[a,b,d], Katrine Hass Rubin[b]

[a]*Department of Medicine, Holbæk Hospital, Holbæk, Denmark*
[b]*OPEN, Open Patient data Explorative Network, Department of Clinical Research, University of Southern Denmark and Odense University Hospital, Odense, Denmark*
[c]*The Research Unit of General Practice, Department of Public Health, University of Southern Denmark, Odense, Denmark*
[d]*NDORMS, Nuffield Department of Orthopaedics, Rheumatology and Musculoskeletal Sciences, Oxford University, Oxford, United Kingdom*

Background: The FREM tool was developed for automated case finding of individuals at high imminent risk of osteoporotic fractures using health registry data. The aim of this study was to test longer-term performance of the model and the effect of applying a shorter look-back period.

Methods: Using Danish national health registers we generated consecutive general population cohorts for 2014 to 2018. Within each year and across the full time period we estimated the individual risk scores and determined the actual occurrence of major osteoporotic fractures (MOF) and hip fractures. Risk scores were calculated with 15- and 5-year look-back periods. Negative predictive value (NPV) and positive predictive value (PPV) were estimated, applying a calculated risk cut-off of 2% for MOF and 0.3% for hip fractures.

Results: Applying a 15-year look-back, AUC C-statistics was 0.75-0.76 for MOF and 0.84-0.87 for hip fractures in 2014 (table 1). Results were comparable across each year and for a five year outcomes period. Applying a 5-year look-back generated similar results, with slightly lower C-statistics.

Conclusion: C-statistics and predictive values where similar across the years, and only marginally lower when using 5- instead of 15-year look-back periods. The FREM tool can be used in contexts with shorter look-back for predicting one- and five-year fracture risk.

Table 1
Performance and predictive capabilities of FREM using 15-year look-back

		Women		Men	
		Year 2014	Year 2014-2018	Year 2014	Year 2014-2018
MOF	**C-statistic (95% CI)**	0.76 (0.75-0.76)	0.72 (0.72-0.72)	0.75 (0.74-0.75)	0.71 (0.71-0.72)
	PPV (95% CI)	4.3 (4.2-4.4)	22.0 (21.0-23.1)	3.8 (3.7-4.0)	17.3 (15.6-19.2)
	NPV (95% CI)	99.2 (99.1-99.2)	93.4 (93.3-93.4)	99.5 (99.5-99.5)	97.2 (97.2-97.2)
HIP	**C-statistic (95% CI)**	0.87 (0.86-0.87)	0.84 (0.84-0.84)	0.84 (0.84-0.85)	0.82 (0.82-0.82)
	PPV (95% CI)	1.4 (1.3-1.4)	9.9 (9.8-10.1)	1.0 (0.9-1.0)	7.4 (7.1-7.8)
	NPV (95% CI)	99.9 (99.9-99.9)	98.9 (98.9-98.9)	99.9 (99.9-99.9)	99.0 (99.0-99.0)

doi:10.1016/j.bonr.2020.100699

P254

Using machine learning approaches and genomic data for fracture risk prediction in the US older men

Qing Wu
University of Nevada, Las Vegas, United States

Predicting an individual's fracture risk from genomic variants remains a challenge because of the complexity in the data. Numerous Single Nucleotide Polymorphisms (SNPs) associated with bone density and fracture have been discovered by GWASs. However, how to best utilize these genetic variants to predict an individual's fracture risk remain unclear. Conventional statistical approaches do not have the flexibility or the adequacy to model complex genomic data. Thus our aims to 1) develop different machine learning (ML) models from genomic data; 2) to identify the best ML model for fracture prediction. Genomic data of Osteoporotic Fractures in Men cohort Study (N=5,133) were analyzed. Genotype imputation was performed at the Sanger Imputation Server. 1,103 fracture-associated SNPs were identified, and corresponding weighted genetic risk scores were derived for each man in the data. Convention osteoporosis risk factors and identified genomic variants were including for analysis and modeling. Data were normalized and split into a training set (80%) and validation set (20%). For model training, the synthetic minority over-sampling technique was employed to account for low fracture rate, and 10-fold cross-validation was employed for hyper-parameters optimization. In the testing set, the area under the ROC curve (AUC) and accuracy were used to assess the model performance. We found that the performance of gradient boosting in predicting fracture was the best among the four models with AUC of 0.71 and the accuracy of 0.88. We found that random forest and neural network have the AUC of 0.70 and 0.69, and the accuracy of 0.80 and 0.84. Logistic regression had the worst performance with the AUC of 0.65 and an accuracy of 0.69. Each pairwise comparison between models was significant (p<0.0001). Thus the ML algorithms have better performance than logistic regression in fracture prediction, and gradient boosting performed the best for the prediction in the men.

doi:10.1016/j.bonr.2020.100700

P259

Opposite associations for trabecular and cortical volumetric bone mineral density with Coronary Artery Calcification score: The SCAPIS Pilot study

Thomas Funck-Brentano[a,b], Louise Grahnemo[b], Ola Hjelmgren[c], John Brandberg[d], Göran Bergström[e], Claes Ohlsson[b]
[a]*Rheumatology, Universite de Paris, Paris, France*
[b]*Department of Internal Medicine and Clinical Nutrition, Center for Bone and Arthritis Research, Institute of Medicine, the Sahlgrenska Academy, University of Gothenburg, Gothenburg, Sweden*
[c]*Department of Molecular and Clinical Medicine, the Sahlgrenska Academy, University of Gothenburg, Gothenburg, Sweden*
[d]*Department of Radiology, Institute of clinical Sciences, Sahlgrenska Academy, University of Gothenburg, Gothenburg, Sweden*
[e]*Department of Clinical Physiology, Sahlgrenska University Hospital, University of Gothenburg, Gothenburg, Sweden*

Previous epidemiological studies show an inverse association between trabecular bone volumetric bone mineral density (Tb.vBMD) in the spine and coronary artery calcification score (CACS). However, the association between cortical vBMD (Ct.vBMD) in long bones and CACS remains unknown.

To compare the associations for Tb.vBMD and Ct.vBMD with CACS, we used the cross-sectional population-based SCAPIS pilot cohort, consisting of randomly selected participants aged 50 to 64 years. CACS expressed as Agatston score, Tb.vBMD in the vertebral body of Th12, and Ct.vBMD at the right midshaft femur were assessed in 519 men and 541 women using computed tomography.

The correlation between Tb.vBMD and Ct.vBMD was modest. The base logistic model was adjusted for age, sex, and body mass index (and menopausal status in women), while the full model was further adjusted for smoking status, diabetes, hypertension, physical activity and family history of cardiovascular event. In sex-combined models, Tb.vBMD was independently inversely (per SD increase, OR= 0.77 95% CI 0.66 to 0.90), while Ct.vBMD was independently directly (per SD increase, OR= 1.27 95% CI 1.09 to 1.48) associated with CACS > 0 in the base model. Sex-stratified analyses revealed that these associations were only significant in women. All these associations remained significant after further adjustments for cardiovascular risk factors.

A high Ct.vBMD/Tb.vBMD ratio was associated with an increased risk of CACS > 0 in women (above vs below the median, OR = 1.87 95% CI 1.21 to 2.90). This association remained significant after further adjustments for cardiovascular risk factors.

In conclusion, this study provides the first demonstration of opposite associations for trabecular and cortical vBMD with CACS, suggesting a yin/yang role of trabecular and cortical vBMD on the risk of coronary artery calcification, mainly in women. We propose that distinct pathophysiological mechanisms exist for the trabecular vs cortical bone in the bone-vascular axis.

doi:10.1016/j.bonr.2020.100701

P261

Causal assessment of the association between bone mineral density and the risk of dementia

Samuel Ghatan[a], Katerina Trajanoska[a], Petra Proitsi[b], M. Afran Ikram[c], Andre Uitterlinden[a], Angela Hodges[d], Ling Oei[a], Fernando Rivadeneira[a]
[a]*Internal Medicine, Erasmus University Medical Center, Rotterdam, Netherlands*
[b]*Maurice Wohl Clinical Neuroscience Institute, Institute of Psychiatry, Psychology and Neuroscience, King's College London, London, United Kingdom*
[c]*Epidemiology, Erasmus University Medical Center, Rotterdam, Netherlands*
[d]*Institute of Psychiatry, King's College London, London, United Kingdom*

Introduction: Evidence for an association between BMD and cognitive decline has been postulated for many years. As both dementia and osteoporosis are prominent age-related diseases the association is expected to be driven by shared comorbid factors, until proven otherwise. The aim of this study was to establish if there is a causal association between bone mineral density (BMD) and dementia.

Methods: We included 5,545 participants (58% females) from a prospective population-based cohort (age:66.3±10.3). All participants underwent DXA to measure femoral neck (FN) and lumbar spine (LS) BMD. We assessed dementia at the time of DXA measurement and during a follow-up of maximum 12 years. We used time-to-event analysis to determine the observational relationship between BMD and incident dementia, including Alzheimer's disease (AD) adjusted for age, sex, cohort effect, smoking, education, apoE (genotype) and hormone use. Next, we applied a two-sample bidirectional Mendelian Randomization approach, leveraging genetic data from large-scale genome-wide association studies (GWAS) of Alzheimer disease (N_{cases}=17,008 cases; $N_{controls}$= 37,154 controls; and of FN- and LS-BMD (n=~32,000) seeking to provide robust evidence of causality.

Results: Among the 5,545 non-demented participants included in in the study 397 (7.2%) developed dementia (n=264 Alzheimer's cases) during a mean follow-up of 7 years. Lower levels of FN-BMD were associated with higher risk of dementia (HR:1.20, 95%CI: 0.72-0.92) and Alzheimer disease (HR:1.27, 95%: 0.68-0.92). In contrast, LS-BMD was not associated with incidence dementia (HR:1.07, 95%: 0.84-1.04) or Alzheimer disease (HR:1.10, 95%: 0.80-1.04). These observational results were not supported by the MR analysis (FN-BMD: effect=0.04, 95%CI:-0.09, 0.17).

Conclusion: There is no evidence supporting that the replicated observational association between higher BMD and lower AD incidence is causal. While increasing BMD won't be by itself an effective intervention to modify the risk of dementia, its prognostic ability as early maker of cognitive decline needs to be established.

doi:10.1016/j.bonr.2020.100702

P300

Trabecular bone score in subjects with normocalcemic hyperparathyroidism

Anda Mihaela Naciu[a], Gaia Tabacco[a], Stefania Falcone[b], Assunta Santonati[c], Silvia Irina Briganti[a], Diana Lelli[d], Claudio Pedone[d], Andrea Fabbri[b], Iacopo Chiodini[e], John Paul Bilezikian[f], Nicola Napoli[a], Silvia Manfrini[a], Roberto Cesareo[g], Andrea Palermo[a]
[a]*Unit of Endocrinology, Campus Bio-Medico, Rome, Italy*
[b]*Unit of Endocrinology and Metabolic Diseases, CTO A. Alesini Hospital, University Tor Vergata, Rome, Italy*
[c]*Department of Endocrinology, San Giovanni Addolorata Hospital, Rome, Italy*
[d]*Unit of Geriatric, Campus Bio-Medico, Rome, Italy*
[e]*Unit for Bone Metabolism Diseases and Diabetes & Laboratory of Endocrine and Metabolic Research, Istituto Auxologico Italiano, IRCCS, Milan, Italy*
[f]*Metabolic Bone Diseases Unit, Division of Endocrinology, Department of Medicine, College of Physician and Surgeons, Columbia University, New York, United States*
[g]*Thyroid and Metabolic Bone Diseases Center, Santa Maria Goretti Hospital, Latina, Italy*

Background and objective: The effects of normocalcemic hyperparathyroidism(NHPT) on bone quality remain quite limited. The study aims were to assess the trabecular bone score (TBS) of NHPT patients versus hypercalcemic hyperparathyroidism

(PHPT) patients and to evaluate if TBS may identify vertebral fractures(VF).

Methods: Multicentric cross-sectional study, including 47 consecutive patients with NHPT and 41 PHPT. 39 BMI and age matched control subjects were consecutively recruited. All patients underwent a biochemical examination, lumbar spine, total hip, femoral neck, and non-dominant forearm bone mineral density (BMD) and TBS. Morphometric VF were assessed by DXA-scan. Sensitivity, specificity and overall accuracy were calculated for all the markers of interest; for the combination of TBS with femoral neck Z score we used the c statistic (that is equivalent to the AUC) derived from a logistic regression model.

Results: All study groups presented similar age, BMI and kidney function. TBS did not differ between the three groups. The prevalence of VF was 28% in NHPT group, 59% in PHPT group and 23% in controls. In NHPT group, TBS or Z-score*TBS did not show a better performance in individuating VF (TBS: Threshold 1.254, specificity 68%, sensitivity 54%, accuracy 64%; Z-score*TBS: Threshold -0.15, specificity 56%, sensitivity 54%, accuracy 55%) compared to femoral neck Z-score (Threshold -0.05, specificity 76%, sensitivity 69%, accuracy 74%). Conversely, in PHPT group, TBS showed better performance compared to femoral neck Z-score (Threshold 1.292, specificity 44%, sensitivity 74%, accuracy 61% vs Threshold -0.65, specificity 56%, sensitivity 61%, accuracy 59%). The combination femoral neck Z-score and TBS was comparable to femoral neck Z-score alone for the prediction of VF in both NHPT (c statistic 0.683 vs 0.678, P=0.715) and PHPT(c statistic 0.569 vs 0.548, P=0,830).

Conclusion: NHPT does not show a significant impairment of TBS and this tool does not perform better than femoral neck Z-score in individuating VF.

doi:10.1016/j.bonr.2020.100703

P326

A natural history study in patients with ENPP1 deficiency

Yvonne Nitschke[a], Kristina Kintzinger[a], Mary Hackbarth[b], Ulrike Botschen[a], Sisi Wang[c], Rachel Gafni[d], Kerstin Mueller[c], Gus Khursigara[e], William Gahl[b], Frank Rutsch[a], Carlos Ferreira[b]

[a]*Muenster University Children's Hospital, Münster, Germany*
[b]*National Human Genome Research Institute, National Institutes of Health, Bethesda, United States*
[c]*ICON plc, Vancouver, Canada*
[d]*National Institute of Dental and Craniofacial Research, National Institutes of Health, Bethesda, United States*
[e]*Inozyme Pharma, Boston, United States*

Deficiency in ENPP1 activity, an enzyme that generates extracellular pyrophosphate (PPi) from ATP and modulates adenosine metabolism, results in life threatening disorders. Infants present with Generalized Arterial Calcification of Infancy (GACI), characterized by arterial calcifications and stenosis with approximately 50% mortality within the first 6 months of life. Surviving patients will develop Autosomal Recessive Hypophosphatemic Rickets type 2 (ARHR2).

To better characterize ENPP1 Deficiency, data was obtained from chart reviews of GACI and ARHR2 patients with mutations in ENPP1 or ABCC6 from the National Institutes of Health (NCT03478839) and Münster University Children's Hospital (NCT03758534).

Analysis revealed a diagnosis of GACI in 115 patients and ARHR2 in 36. Twenty-five survived GACI and later developed ARHR2. Of 109 probands with genetic confirmation, 88 had mutations in ENPP1 and 21 in ABCC6. There were 25 of 76 patient deaths in the ENPP1 cohort. Consistent with past observations, arterial calcification (88%, 95%), joint calcification (64%, 33%), hypertension (65%, 67%) and short stature (stature-for-age less than third centile; 42%; 33%) were prevalent and consistent in ENPP1 and ABCC6 cohorts, respectively. Organ calcification (78%; 85%) cardiac dysfunction (78%, 85%), renal dysfunction (47%: 40%) and gastrointestinal dysfunction (63%; 58%) were also observed in both ENPP1 and ABCC6 cohorts, respectively. A higher prevalence of neurological complications was observed in the ABCC6 cohort (58% to 40%) while hearing loss (53%; 7%) and rickets (48%; 17%) was higher in the ENPP1 cohort.

This natural history study reveals the significant mortality and morbidity due to calcification of arteries and multiple organs, as well as organ dysfunction. Similar symptom prevalence was found in both ENPP1 and ABCC6 deficiencies suggesting that these disorders are founded in low PPi levels. Further analysis will further support and elucidate the progression of the disease.

Disclosure: Grant support and consulting fees from Inozyme Pharma.

doi:10.1016/j.bonr.2020.100704

Bone Reports 13 (2020) 100339

Contents lists available at ScienceDirect

Bone Reports

journal homepage: www.elsevier.com/locate/bonr

NI Seminar & Gathering

P047

Micro-architectural changes of lumbar vertebrae in patients with alcoholic liver cirrhosis

Jelena Jadzic[a], Danica Cvetkovic[b], Petar Milovanovic[a], Nada Tomanovic[c], Marija Djuric[a], Danijela Djonic[a]

[a]*Laboratory for Anthropology and Skeletal Biology, Institute for Anatomy, Faculty of Medicine, University of Belgrade, Belgrade, Serbia*

[b]*Institute of Forensic Medicine, Faculty of Medicine, University of Belgrade, Belgrade, Serbia*

[c]*Institute of Pathology, Faculty of Medicine, University of Belgrade, Belgrade, Serbia*

Although it's well known that vertebral fractures incidence in alcoholic liver cirrhosis (ALC) patients is increased, data about bone micro-structural changes are limited. The aim of this study was to compare trabecular and cortical micro-architecture of lumbar vertebrae from ALC patients and healthy age-matched controls. According to our knowledge, this is first up-to date study that includes patohistological confirmation of ALC. Our study comprised 38 lumbar vertebrae samples of male participants divided into ALC (n=20) and control group (n=18). This study was carried out in accordance with the Directive of the European Parliament and the Council of Europe and ethic approval was granted.

Micro-CT evaluation of the trabecular bone in lumbar vertebrae showed significant decrease in bone volume density (9.82±3.35 vs. 13.42±4.21), trabecular thickness (0.13±0.03 vs. 0.16±0.03) and trabecular number (0.67 ± 0.24 vs. 0.89±0.16), while total porosity (90.18±3.52 vs. 86.58±4.21) and inversed connectivity parameter (4.06±1.80 vs. 2.54±1.32) was increased ($p< 0.01$, t test). However, prominent alteration in cortical parameters and bone mineralization wasn't observed in lumbar vertebrae of ALC patients ($p>0.05$, t test). Our data indicate that increased bone fragility and susceptibility for non-traumatic fractures in ALC patients could be predominantly explained by micro-structural alterations in trabecular bone quality and quantity. Taking into consideration all limitations of the DXA scans, we genuinely recommend screening of the lumbar spine for ALC patients in order to estimate individual fracture risk and implement base rules of personalized medicine in common clinical practice.

Keywords: Alcoholic liver cirrhosis, Trabecular micro-architecture, Vertebral fractures, Micro-CT

doi:10.1016/j.bonr.2020.100340

2352-1872/$ – see front matter

P208

Mice with a heterozygous microdeletion in the aggrecan gene exhibit a growth disorder similar to that of humans with heterozygous aggrecan mutations

Ameya Bendre, Ola Nilsson

Department of Women's and Children's Health, Karolinska Institutet, Stockholm, Sweden

Background: In humans, heterozygous Aggrecan (*Acan*) mutations cause autosomal short stature (ISS) with advanced bone age, early-onset osteoarthritis and intervertebral disc disease (OMIM#165800). The cartilage matrix deficiency mouse (*Acan*^{cmd}) has a naturally occurring 7bp microdeletion in the *Acan* gene. Heterozygous mice reportedly are born with a normal size and show proportional dwarfism and

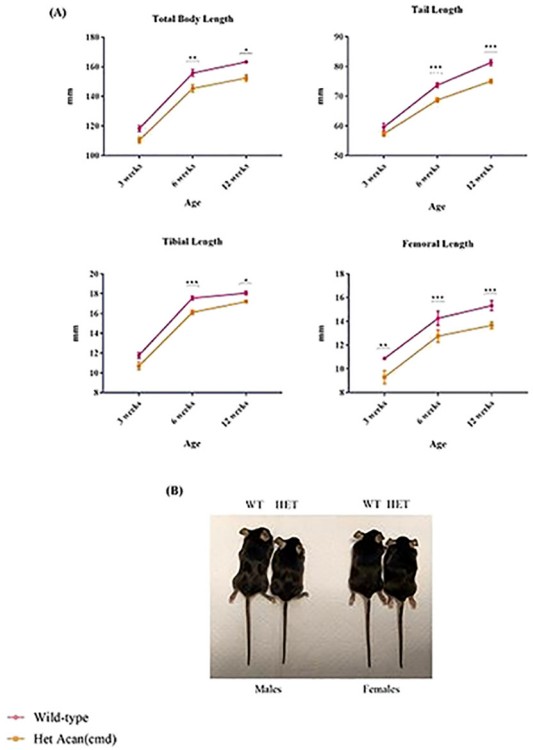

Fig.1(A): Total Body, Tail, Tibial and Femoral length measurements (Mean and +/- SEM) in 3, 6 and 12 week male mice. Two way ANOVA followed by Sidak's multiple comparisons test was employed for statistical analysis ($p < 0.001$: ***; $p < 0.01$: **; $p < 0.05$: *). **Fig.1(B):** 6 week old Wild-type and Heterozygous Acan(cmd) mice.

Fig. 1. Total body, Tail, Tibial and Femoral length measurements in WT and HET Acan (cmd) mice.

degenerative disc disease with increasing age. However, the phenotype has not been assessed in detail.

Objective: To characterize growth pattern, growth plate histology and function in the heterozygous ($Acan^{cmd}$) mouse.

Methods: Ethical approval was duly obtained from Stockholm animal ethics committee. Heterozygous *Acan*^{cmd} and wild-type (WT) mice were assessed for skeletal and body growth at different ages.

Results: At 3 weeks of age, Heterozygous *Acan*^{cmd} mice were smaller in overall size evident by smaller total body length ($p< 0.01$) and tail length measurements ($p< 0.001$) and also had shorter tibiae ($p< 0.03$) and femora ($p< 0.004$) than WT littermates (Fig.1). The difference in growth was even more obvious at 6 and 12 weeks of age. Additionally, the magnitude of the growth deficit was similar to that seen in patients with heterozygous aggrecan mutations.

Conclusions: The heterozygous ($Acan^{cmd}$) mice have a growth disorder that is similar to the human growth disorder of heterozygous *ACAN* mutations in terms of progression with age as well as in magnitude (10 - 15% smaller). The findings suggest that this strain is a suitable model to study the underlying pathogenic mechanisms of this disorder and to test therapeutic strategies.

doi:10.1016/j.bonr.2020.100341

P251

Early effects of androgen deprivation on bone and mineral homeostasis: A prospective cohort study

Rougin Khalil[a], Leen Antonio[a], Michaël R. Laurent[b], Karel David[a], Na Ri Kim[a], Pieter Evenepoel[a], Anton Eisenhauer[c], Alexander Heuser[c], Etienne Cavalier[d], Sundeep Khosla[e], Frank Claessens[a], Dirk Vanderschueren[a], Brigitte Decallonne[a]

[a]*KU Leuven, Leuven, Belgium*
[b]*University Hospitals Leuven, Leuven, Belgium*
[c]*GEOMAR Helmholtz Center for Ocean Research, Kiel, Germany*
[d]*University of Liège, Liège, Belgium*
[e]*Mayo Clinic, Rochester, United States*

Background: Long-term androgen deprivation therapy (ADT) negatively influences bone. The short-term effects are less known.

Objectives: To prospectively investigate the early effects of ADT on calcium/phosphate homeostasis and bone turnover.

Methods: A morning blood sample was taken from eugonadal male sex offenders, prior to ADT (cyproterone acetate) and at first clinical visit post-initiation as part of standard clinical care.

Outcome measures: Change in markers of calcium/phosphate homeostasis and bone turnover.

Results: The median age was 44 (range 20-75) years. The median time interval between baseline and first follow-up was 13 (range 6-27) weeks. Compared to baseline, a more than 5-fold and 3 fold-fold decrease was observed for total testosterone (to 3.4 nmol/L) and estradiol (to 17.6 pmol/L), respectively ($P< 0.0001$). Serum calcium and phosphate increased, with decreased PTH and $1,25(OH)_2D3$ (see table). The stable calcium isotope ratio ($\delta^{44/42}Ca$) decreased, indicating increased net calcium loss from bone. Bone formation markers decreased whereas sclerostin increased, indicating suppressed bone formation. Bone resorption markers (TRAcP5b, CTX) were unaltered.

Conclusion: Calcium release from the skeleton occurs early following ADT in adult men. The increase of sclerostin and reduction of bone formation markers, without changes in resorption markers, suggests a dominant negative effect on bone formation.

	BEFORE ADT median	BEFORE ADT range	AFTER ADT median	AFTER ADT range	p-value
Calcium (mmol/L)	1.88	1.60-2.38	2.03	1.71-2.50	<0.0001
Phosphate (mmol/L)	1.02	0.82-1.49	1.20	1.01-1.48	0.0016
PTH (ng/L)	33.7	20.8-92.9	23.2	15.4-60.7	0.0156
1,25(OH)2D3 (ng/L)	53.8	22.3-70.9	48.9	27.4-64.3	0.0134
BAP (µg/L)	17.7	11.3-35.3	12.7	6.2-20.7	<0.0001
Osteocalcin (ng/mL)	20.7	9.5-63.0	18	7.0-37.4	0.0056
Periostin (nmol/L)	0.91	0.76-1.46	0.87	0.56-1.09	0.0500
Sclerostin (ng/mL)	0.55	0.29-1.02	0.63	0.27-1.28	<0.0001
δ44/42Ca (‰)	-0.77	-0.94- -0.58	-0.88	-1.08- -0.56	0.0458

Effect of androgen deprivation on bone and mineral homeostasis.

doi:10.1016/j.bonr.2020.100342

P285

Melatonin alleviates vascular calcification and ageing through exosomal miR-204/miR-211 cluster in a paracrine manner

Feng Xu[a], Jia-Yu Zhong[b], Ling-Qing Yuan[a]

[a]*Department of Metabolism and Endocrinology, Hunan Provincial Key Laboratory of Metabolic Bone Diseases, National Clinical Research Center for Metabolic Diseases, the Second Xiangya Hospital of Central South University, Changsha, China*
[b]*Department of Geriatrics, Institute of Aging and Age-related Disease Research, the Second Xiang-Ya Hospital, Central South University, Changsha, China*

Vascular calcification has now been demonstrated to be an active systematic process that highly resembles mineralisation of skeleton and goes along with aging. Melatonin (MT) has been demonstrated to regulate the cardiovascular diseases but its effects on arterial calcification and aging are scarely reported. In the present study, we found 10 μM MT significantly inhibited osteogenic differentiation and senescence of vascular smooth muscle cells (VSMCs) in a MT membrane receptor-dependent manner. By using the 5/6-nephrectomy plus high phosphate diet treated (5/6 NTP) mice as *in vivo* calcification models, we also demonstrated that daily injection of MT alleviated arterial calcification and aging when compared with vehicle groups ($n=5$ per group, $p< 0.05$). Moreover, exosomes isolated from MT treated VSMCs ($VSMCs^{MT}$-exos) could be uptaken by VSMCs both *in vitro and in vivo*. Interestingly, $VSMCs^{MT}$-exos attenuated the osteogenic differentiation and senescence of VSMCs *in vitro* and also exhibited inhibition effects on arterial calcification and aging of the NTP mice *in vivo* ($n=5$, $p< 0.05$). Further, the transwell assay showed that MT decreased osteogenic differentiation and senescence of VSMCs through a paracrine mechanism. However, inhibition of exosomes release by GW4869 blocked the effects. Then, we found that MT elevated the expression level of miR-204/miR-211 in both VSMCs and exosomes derived from VSMCs. Overexpression of miR-204/miR-211 in VSMCs exosomes inhibited osteogenic differentiation and senescence of VSMCs in vitro while knockdown of miR-204/miR-211 reversed partially the inhibition effects of $VSMCs^{MT}$-exos in mice. Finally, we demonstrated that miR-204 and miR-211 inhibited expression of BMP2 and luciferase activity of BMP2 promoter. Knockdown of BMP2 decreased the level of calcification and senescence of VSMCs. In summary, our present study revealed that exosomes from MT-treated VSMCs could attenuate arterial calcification and aging in a paracrine manner through an exosomal miR-204/miR-211/BMP2 signaling pathway.

doi:10.1016/j.bonr.2020.100343

P314

The role of cytoplasmic mRNA polyadenylation in the pathogenesis of *Osteogenesis imperfecta*

Olga Gewartowska[a], Seweryn Mroczek[b], Goretti Aranaz Novaliches[c], Monika Kusio-Kobiałka[b], Jan Prochazka[c], Andrzej Dziembowski[a]

[a]*Laboratory of RNA Biology, International Institute of Molecular and Cell Biology in Warsaw, Warsaw, Poland*

[b]Faculty of Biology, University of Warsaw, Warsaw, Poland
[c]Laboratory of Transgenic Models of Diseases, Institute of Molecular Genetics of the Czech Academy of Sciences, Prague, Czech Republic

TENT5A is a non-canonical, cytoplasmic poly(A) polymerase, able to post-transcriptionally regulate expression of certain genes. Mutations in TENT5A has been found in several pediatric patients suffering from Osteogenesis imperfecta (OI).

To study the link between TENT5A and pathogenesis of the disease, we have generated TENT5A knock-out mouse line. TENT5A KO display skeletal malformations, frequent ribs fractures and a high level of serum alkaline phosphatase (KO: 311,5 [U/ml] ± 31,71, n=10], WT: 163,5 [U/ml] ± 11,46, n=13; p< 0,0010). MicroCT scan revealed severe hipomineralisation of TENT5A KO bones. Furthermore, we have discovered that pro-collagen I alpha 1 in significantly decreased in the serum of TENT5A KO (Fig.1)

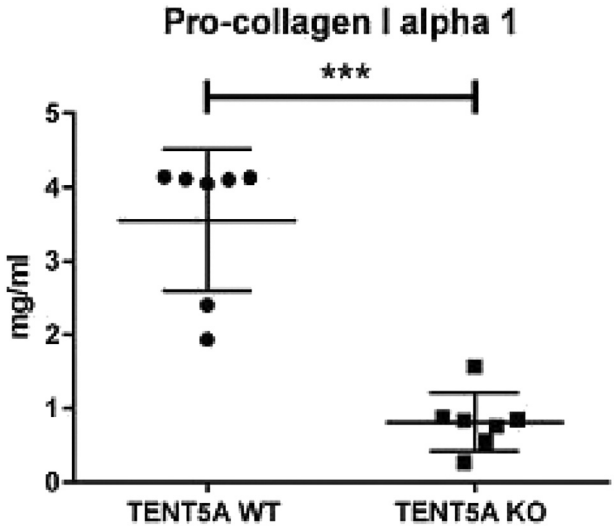

Fig. 1. Decreased pro-collagen I alpha 1 serum level in TENT5A KO mice.

We have performed Nanopore Direct RNA sequencing to measure lengths of poly(A) tails in primary osteoblast cultures. The analysis revealed that poly(A) tails of Col1a1 and Col1a2 transcripts are significantly shorter in TENT5A KO (p< 0,0001), therefore collagen I transcripts are targets of TENT5A and upon *TENT5A* mutation their polyadenylation is compromised (Fig.2)

Therefore, for the first time, we propose the elucidation of the role of TENT5A in the pathogenesis of OI.

Ethical approval for the procedures on animals was obtained from I Local Ethical Commission in Warsaw (decisions no 176/2016, 781/2018, 783/2018).

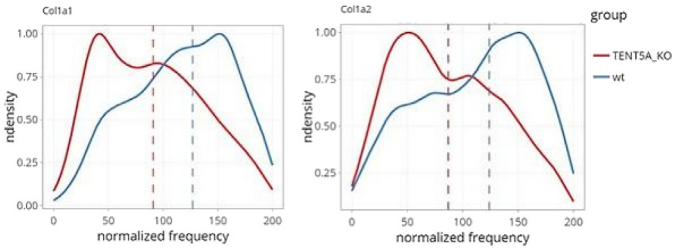

Fig. 2. ONT direct sequencing reveals pro-collagen I mRNAs polyadenylation by TENT5A

doi:10.1016/j.bonr.2020.100344

Bone Reports 13 (2020) 100345

Contents lists available at ScienceDirect

Bone Reports

journal homepage: www.elsevier.com/locate/bonr

Poster Focus 1 Basic/Translational

P075

Osteosarcoma cells release factors that enhance RANKL-positive extracellular vesicle discharge by osteoblasts

Alfredo Cappariello[a,b], Marta Colletti[a], Angela Di Giannatale[a], Maurizio Muraca[c], Nadia Rucci[b], Anna Teti[b]

[a]*Children Hospital Bambino Gesù, Rome, Italy*

[b]*Biotechnological and Applied Clinical Sciences, University of L'Aquila, L'Aquila, Italy*

[c]*Department of Women's and Children's Health, University of Padova, Padova, Italy*

Extracellular Vesicles (EVs) shuttle ligands and transcription factors affecting target cells. Osteoblasts communicate with other bone cells through the release of EVs enriched in RANKL, a pivotal cytokine regulating osteoclastogenesis, angiogenesis and tumour progression. Hence, we hypothesize that primary bone tumours perturb the release of RANKL-positive EVs by osteoblasts to promote tumour expansion. We incubated primary murine osteoblasts for 48h with conditioned medium from human osteosarcoma cell lines. Cytofluorimetry revealed an increase of osteoblast RANKL-positive EVs after incubation with MNNG-HOS ($+1.99\pm0.29$; $p=0.005$), U2OS ($+2.84\pm0.87$; $p=0.028$) and MG63 ($+3.177\pm0.55$; $p=0.0006$) conditioned media. We screened by real-time PCR array the MNNG-HOS cell transcriptome, noting high expression of genes encoding osteoblast regulatory proteins, including *bmp7*, *pthrp*, *vegfα* and *tgfβ*. Liquid Chromatography-tandem Mass Spectrometry of MNNG-HOS EVs uncovered a panel of 447 proteins. Bioinformatics analysis (false discovery rate = 0.01) revealed that 28.8% of proteins were associated with signal transduction and 25.4% with cell communication processes. Some transcription factors were quantified to be present with a significant abundance (Sp1, 62.8%; KLF7, 41.7%; EGR1, 29.3%), while VEGF/VEGFR network (33.5%), Syndecan (33.5%) and LKB1 signalling (33.3%), IGF1 pathway (32.8%) and Integrin interactions (35.5%), reported to support the RANKL axis, were the most represented biological pathways. Finally, cell surface proteins enhancing RANKL signalling were recognized, including CD109 (18% peptide coverage), Ephrin type-A receptor 2 (11% peptide coverage), Matrix metalloproteinase-14 (3% peptide coverage) and Thrombospondin-1 (7% peptide coverage). Our data suggest that MNNG-HOS cells release a complex array of EV-shuttled proteins involved in RANKL signalling that is likely to induce the release of RANKL-enriched EVs from osteoblasts and to support tumour progression in the bone marrow.

doi:10.1016/j.bonr.2020.100353

P092

Vitamin C epigenetically controls osteogenesis and bone mineralization

Roman Thaler[a], Farzaneh Khani[b], Janet M. Denbeigh[b], Ines Sturmlechner[c,d], Xianhu Zhou[b], Oksana Pichurin[b], Amel Dudakovic[b], Jiang Zhong[e], Jeong-Heon Lee[e], Ramesh Natarajan[f], Ivo Kalajzic[g], David R. Deyle[h], Eleftherios P. Paschalis[i], Barbara Misof[i], Tamas Ordog[j], Andre J. van Wijnen[a]

[a]*Department of Orthopedic Surgery, Department of Biochemistry & Molecular Biology, Center for Regenerative Medicine, Mayo Clinic, Rochester, United States*

[b]*Department of Orthopedic Surgery, Mayo Clinic, Rochester, United States*

[c]*Departments of Pediatric and Adolescent Medicine, Mayo Clinic, Rochester, United States*

[d]*Department of Pediatrics, University of Groningen, University Medical Center Groningen, Groningen, Netherlands*

[e]*Epigenomics Program, Center for Individualized Medicine, Mayo Clinic, Rochester, United States*

[f]*Department of Internal Medicine, Virginia Commonwealth University, Richmond, United States*

[g]*Department of Reconstructive Sciences, UConn Health, Farmington, United States*

[h]*Department of Medical Genetics, Mayo Clinic, Rochester, United States*

[i]*1st Medical Department, Ludwig Boltzmann Institute of Osteology at the Hanusch Hospital of Social Health Insurance Vienna (WGKK) and Austrian Social Insurance for Occupational Risk (AUVA), Vienna, Austria*

[j]*Epigenomics Program, Center for Individualized Medicine, Department of Physiology and Biomedical Engineering and Division of Gastroenterology and Hepatology, Department of Medicine, Mayo Clinic, Rochester, United States*

Malnutrition-induced conditions such as scurvy, impaired wound healing, bone pain and bone fracture risk revealed the requirement of Vitamin C (VitC) to the integrity and homeostasis of connective tissue including bone. Although this function has been attributed to VitC as cofactor to proline hydroxylation during collagen formation, recent studies recognize VitC also as cofactor for a series of epigenetic modulators. Here, we report that primary to collagen maturation, VitC orchestrates bone cell differentiation and function epigenetically via stimulating TET enzymes and DNA hydroxymethylation at promoters and enhancers of bone-specific genes ($p< 0.001$) permitting their coordinated expression. Bone tissue and osteogenic cells at all stages of differentiation are tightly dependent on sustained VitC administration, and promptly lose their osteogenic properties after withdrawal of VitC. This VitC dependence is selective for the osteogenic lineage and is dispensable for the differentiation of primary bone-marrow derived mesenchymal stem cells during adipogenic lineage commitment. Mechanistically, VitC stimulates active DNA demethylation by TET enzymes, in particular TET2, thus specifically prompting the accumulation of hydroxymethyled Cytosine at select promoters, enhancers and super-enhancer-like

2352-1872/$ – see front matter

elements which can bind key osteogenic transcription factors including SMAD4 and RUNX2. This epigenetic circuit permits the expression of all major pro-osteogenic genes, including Bglap2, Col1a1, Alpl, Sost (all p>0.01), and consequently warrants osteogenic lineage commitment and differentiation. In conclusion, we reveal the epigenetic functions of VitC as the key determining property during bone formation. These data suggest that after bone-degenerative conditions the bone equilibrium could be re-established by the administration of VitC or by targeting DNA hydroxymethylation pathways.

doi:10.1016/j.bonr.2020.100346

P182

Functional assessment of coding and regulatory variants from the DKK1 locus

Núria Martínez-Gil[a], Neus Roca-Ayats[a], Nurgül Atalay[a], Marta Pineda-Moncusí[b], Natàlia Garcia-Giralt[b], Wim Van Hul[c], Eveline Boudin[c], Sergi Vives[a], Mireia Vinardell[a], Leonardo Mellibovsky[b], Xavier Nogués[b], Diana Ovejero[b], Adolfo Díez-Pérez[b], Daniel Grinberg[a], Susanna Balcells[a]

[a]*Department of Genetics, Microbiology and Statistics, Faculty of Biology, Universitat de Barcelona, CIBERER, IBUB, IRSJD, Barcelona, Spain*

[b]*Musculoskeletal Research Group, IMIM (Hospital del Mar Medical Research Institute), Centro de Investigación Biomédica en Red en Fragilidad y Envejecimiento Saludable (CIBERFES), ISCIII, Barcelona, Spain*

[c]*Center of Medical Genetics, University of Antwerp & University Hospital Antwerp, Antwerp, Belgium*

The *DKK1* gene encodes a protein with the same name, which acts in the extracellular space as an inhibitor of the Wnt signaling pathway. This is an important protein in bone tissue development, in bone homeostasis, and in different critical aspects of bone biology. For these reason, it is important to know the functionality of coding and regulatory variants in the *DKK1* gene. In this sense, in the present work we have studied the functionality of different DKK1 variants with specific approaches for each one. Seven of them were missense, one belongs into the 3´UTR, and another is intronic and could affect splicing. We have also analysed a downstream region where genome-wide significant variants from different GWAS studies are located. Through a luciferase reporter assay, we have determined that variants p.Met16Leu, p.Ala41Thr, p.Tyr74Phe and p.Arg120Leu display a reduced DKK1 inhibitory capacity (Figure 1). This result agrees with the High Bone Mass (HBM) phenotype of 2 women from our cohort who carry mutations p.Try74Phe and p. Arg120Leu, respectively. Besides, by means of a 4C-sequencing

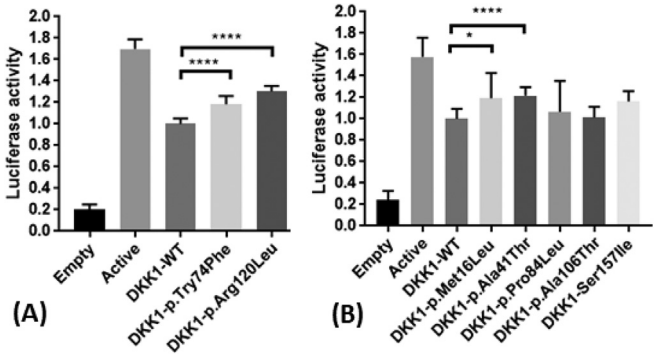

Fig. 1. Relative luciferase activity of the Wnt pathway activity for the endogenous pathway (Empty), for the active pathway (Wnt1: LRP5, mesdc2) and the inhibited pathway with the WT DKK1 or the mutated DKK1. **(A)** Variants present in the general population **(B)** Variants present in the HBM patients. Significant differences are indicated as ****P < 000.1; *P<0.05.

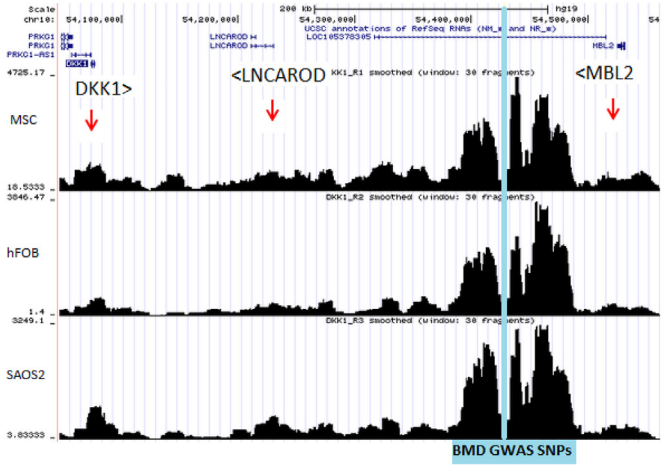

Fig. 2. 4C-seq using the BMD GWAS SNPs region as viewpoint (blue line) in human fetal osteoblast (hFOB), mesenchymal stem cells (MSC) and Saos-2 cell line.

experiment, we have detected that the region containing several genome-wide significant variants interacts both with *DKK1*, *MBL2* and *LNCAROD* (LncRNA Activating Regulator Of *DKK1*; Figure 2).

doi:10.1016/j.bonr.2020.100348

P187

Early onset idiopathic osteoporosis: digenism of wnt signaling pathway

Carollne Caetano[a], Manon Ricquebourg[a,b], Philippe Orcel[a,b], Stéphanie Fabre[a,b], Thomas Funck Brentano[a,b], Martine Cohen Solal[a,b], Corinne Collet[a,c]

[a]*Inserm U1132 and université de Paris, Paris, France*

[b]*Rheumatology, Hôpital Lariboisière, AP-, HP, Paris, France*

[c]*UF de Biologie Moléculaire, Hôpital Lariboisière, AP-, HP, Paris, France*

Juvenile idiopathic osteoporosis is defined by low BMD and fractures since childhood. Its prevalence is unknown and the main differential diagnoses are imperfect osteogenesis moderate form (type 1, OMIM 166200) whose genetic etiology is based on the presence of pathogenic variants in the *COL1A1* and *COL1A2* genes; early onset osteoporosis (OMIM 615221, *WNT1*gene) and, more exceptionally, X-linked osteoporosis (OMIM 300910, *PLS3* gene). In addition, heterozygous pathogenic variants in *LRP5* gene are responsible for primary osteoporosis.

Our study focused on the molecular determination of adult patients with idiopathic osteoporosis using targeted gene sequencing panel responsible for bone fragility. This approach has identified severe forms due to two pathogenic variants, one in *LRP5* gene associated with one heterozygous variant in gene encoding a regulator of the wnt signalling pathway.

In detail, among 69 patients with idiopathic osteoporosis, 16 patients had a "probably pathogenic" or "pathogenic" variant in *LRP5*. The positivity rate was 23% (16/69). Amongst 16 patients, 3 patients had a heterozygous "probably pathogenic" variant in *LRP5* gene associated with a heterozygous "probably pathogenic" variant in *DKK1* (NM_012242.4: c.359G>T, p.(Arg120Leu)) or *WNT3A* (NM_033131.3: c.377G>A, p. (Arg126His)) or*EN1* (NM_001426. 3: c.1168G>A, p. (Glu390Lys).

Both patients with two variants in two different genes DKK1 and LRP5 or WNT3A and LRP5 had multiple fractures and displayed significantly lower BMD compared to patients with a single variant of the LRP5 gene.

In conclusion, our study showed that predominantly vertebral primary osteoporosis displayed a high positive rate of variants in LRP5. Our results suggest that an association of two variants in two different genes such as *LRP5*/*WNT3A*and *LRP5*/*DKK1* is responsible for severe juvenile idiopathic osteoporosis.

doi:10.1016/j.bonr.2020.100354

P190

Effects of a ketogenic diet on the progression of osteoarthritis in obese mice - *in vivo* characterization and analysis of underlying epigenetic mechanisms

Thomas Solé[a,b], Sara Delon[a], Margaux Digonnet[a], Luciano Pirola[c], Emiline Groult[d], Jérôme Lafont[d], Thierry Thomas[a,b], Laurence Vico[a], Maura Strigini[a]

[a]*INSERM U1059 SAINBIOSE and UdL/UJM Saint-Etienne, Saint-Priest-en-Jarez, France*
[b]*University Hospital CHU Saint-Etienne, Saint-Etienne, France*
[c]*INSERM U1060 CARMEN and UdL/UCBL1 Lyon, Lyon, France*
[d]*LBTI UMR5305, CNRS and UdL/UCBL1 Lyon, Lyon, France*

Low-grade metabolic inflammation, damaging adipokine profile and weight-related joint overload increase osteoarthritis (OA) incidence in obese subjects.

Histone deacetylase (HDAC) inhibitors slow-down OA progression *in vitro* and *in vivo*. Levels of the ketone body beta-hydroxybutyrate (BHB) increase following a low carb/high fat ketogenic diet (KD). BHB, a putative HDAC inhibitor, affects histone modifications and gene expression *in vitro* and *in vivo*, but the exact molecular mechanisms remain controversial.

KD can simultaneously induce weight-loss, decrease metabolic inflammation and increase circulating BHB, and could thus be beneficial in obesity-linked OA treatment.

We induced knee OA in obese mice on a high fat diet (HFD) by medial meniscus destabilization, then fed mice one of three diets *ad libitum:* HFD; KD; Standard Diet (STD) for 8 weeks (licence 12127-2017110911058255v2).

BHB levels increased tenfold in KD group only. Glycemia remained high in HFD mice, but decreased in STD and even more in KD ($p< 0{,}001$). HFD mice continued gaining weight, while STD and KD lost weight. OA progression was particularly slowed down in KD: MMP13 expression in cartilage was two-fold lower in KD compared to HFD ($p=0.005$) and to STD ($p=0.02$); osteophytes were smaller (HFD: 101247 AU; STD: 61863 AU; KD: 4325 8AU, $p< 0.001$); severe OA cases (OARSI score>2.5) were less frequent (HFD>STD>KD, $p=0.037$).

To understand the underlying molecular mechanisms, we turned to an *in vitro* model of OA (IL1 treated chondrocytes). While classic HDAC inhibitors (TSA, butyrate) greatly diminished the induction of MMP13, BHB (up to 40 mM) had only a very mild effect.

As KD increased histone beta-hydroxy-butyrylation of peripheral tissues, this novel histone modification may contribute to the beneficial effects of KD on obesity-linked OA.

doi:10.1016/j.bonr.2020.100349

P317

Gene set enrichment analysis reveals a first somatic mutation in the catalytic domain of *MAP2K1* in a melorheostosis patient

Raphaël De Ridder[a], Eveline Boudin[a], Joe Ibrahim[a], M. Carola Zillikens[b], Bram C.J. van der Eerden[b], Wim Van Hul[a], Geert Mortier[a]

[a]*Center of Medical Genetics, University and University Hospital of Antwerp, Antwerp, Belgium*
[b]*Division of Endocrinology, Department of Internal Medicine, Erasmus Medical Center, Rotterdam, Netherlands*

Melorheostosis is a very rare sclerosing bone dysplasia characterized by asymmetrical progressive cortical hyperostosis. In addition, surrounding soft tissues are usually also affected. The localized lesions and the usual sporadic occurrence suggest that melorheostosis is caused by a somatic mutation in early development. Recently, somatic mosaicism was identified for mutations (p.Q56P, p.K57N, or p.K57E) in the negative regulatory domain of MAP2K1, resulting in increased signalling in affected tissues. In this study, we screened for *MAP2K1* mutations in both affected and unaffected tissues from four sporadic melorheostosis patients. For three patients, we performed whole exome sequencing on DNA extracted from affected bone and unaffected tissues. In two patients, we identified mutations in affected tissues (p.K57N and p.K57E), previously described by Kang *et al.*. For a fourth patient, DNA and RNA extracted from both an affected and an unaffected skin biopsy was available, on which whole genome sequencing (WGS) and RNA sequencing was performed. WGS did not reveal a pathogenic mutation in *MAP2K1*. However, gene set enrichment analysis of the transcriptome data demonstrated upregulation of proliferative pathways. Interestingly, increased proliferation of MAP2K1$^{p.K57N}$-positive osteoblasts has been reported by Kang *et al.* In-depth analysis of the RNA-seq data revealed a novel variant (p.C121S) in the catalytic domain of MAP2K1, only present in the affected skin. Using allele-specific PCR, we confirmed the presence of this variant in both DNA and RNA from the affected skin. Affected bone tissue was unfortunately not available for further confirmation. Interestingly, both the p.K57N and the p.C121S mutations have been reported before in melanoma patients. *In vitro* characterisation has shown that both mutations increase phosphorylation of the MAP2K1 downstream effector Erk. In conclusion, our study strongly suggests that not only variants (p.K57N and p.K57E) in the regulatory domain of MAP2K1 but also in the catalytic domain (p.C121S) may cause melorheostosis.

doi:10.1016/j.bonr.2020.100357

Bone Reports 13 (2020) 100352

Contents lists available at ScienceDirect

Bone Reports

journal homepage: www.elsevier.com/locate/bonr

Poster Focus 1 Clinical/Public Health

P145

Albumin-adjusted calcium equation and reference interval for adjusted calcium. Data from the UK Biobank

Marian Schini[a], Fadil Hannan[b], Jennifer Walsh[a], Richard Eastell[a]
[a]The University of Sheffield, Sheffield, United Kingdom
[b]The University of Oxford, Oxford, United Kingdom

Introduction: UK Biobank (UKBB) is a health resource, with data on half a million participants aged 40-69 years, mainly white, equally represented from both sexes and is being used for various research projects.

When studying calcium metabolism, it is recommended to use the albumin-adjusted calcium, ideally with an equation based on the local population. However, UKBB did not provide an equation for this calculation. Moreover, the recommended range for calcium in the UK is the Pathology Harmony Range (2.20-2.60 mmol/L) but the best approach would be to calculate the range based on this large population.

Aims: To provide an equation for calculating the albumin-adjusted calcium. To calculate the reference interval for adjusted calcium.

Methods: We selected 374,565 patients based on available laboratory criteria (albumin, urea, creatinine, ALT, ALP) and a plot was created of total calcium against albumin. The regression equation was used to establish the adjusted calcium equation. In order to establish the UKBB reference interval, all participants with a measurement of calcium at the time of recruitment were included. Exclusion criteria were the same as above plus low eGFR (<60 ml/min/m^2) and/or low vitamin D (<50 nmol/L).

Results: The calculated equation was:

Adjusted calcium = Total calcium + 0.0177 (46.3 - albumin)

In total, 178,377 patients were involved in the reference interval calculation and the result was 2.25 to 2.56 mmol/L (9.0-10.24 mg/dl); the confidence intervals did not include the upper and lower ranges of the Pathology Harmony range.

Conclusions: We have provided an equation which can be used in future projects on calcium metabolism using UKBB data. We have established a population-based reference interval for albumin-adjusted calcium.

Discussion: The use of the correct equation and reference interval is essential when studying calcium metabolism. The UKBB interval remains to be validated in elderly and non-white populations.

doi:10.1016/j.bonr.2020.100347

P222

Muscle density, but not size, correlates well with muscle performance

Ling Wang[a], Lu Yin[b], Giuseppe Guglielmi[c], Xiaoguang Cheng[d], Glen M. Blake[e], Klaus Engelke[f]
[a]Department of Radiology, Beijing Jishuitan Hospital, Beijing, China
[b]National Center for Cardiovascular Disease, China, Beijing, China
[c]University of Foggia, Foggia, Italy
[d]Beijing Jishuitan Hospital, Beijing, China
[e]King's College London, St Thomas' Hospital, London, United Kingdom
[f]FAU, University Hospital, Erlangen, Germany

Objective: To determine the associations of handgrip strength (HGS) and the Timed Up and Go test (TUG) with muscle size and density of different muscle levels.

Methods: 301 healthy participants were enrolled in this study and recruited for QCT imaging of the lumber, hip and mid-thigh. We also test muscle strength (HGS) and physical performance (TUG). Gluteus maximus muscle(GMaxM) and gluteus medius/minimus muscle(GM/MinM), trunk muscle at vertebrae L2 level and mid-thigh muscle were measured for cross-sectional areas and attenuations. Health-related covariates included blood pressure, diabetes mellitus, fracture history, fast serum glucose and the EuroQol five-dimension score (EQ-5D). General linear models were fitted using method of least squares to evaluate associations of TUG and handgrip strength with muscle CSA and density.

Results: None of the associations between muscle area and TUG was significant after adjustment for age, height and weight. The same result was observed in men for associations between muscle density and TUG. In contrast, in women GMaxM and trunk muscle density showed a significant association with TUG even after adjustment for age, height and weight, although slopes were rather small. Interestingly the slope was even negative in females (β -0.06, $p = 0.001$, adjusted). In men but not in women muscle area of the gluteus maximus and of the mid-thigh were significantly associated with HGS but results were not significant for the trunk muscle. Gluteus maximus and trunk muscle density were significantly associated with HGS in men and women. Mid-thigh muscle density was significantly associated with HGS in men only.

Conclusion: Our study results show that muscle density performs better than muscle size in associating with muscle performance and seems to be as a surrogate for the role of physical performance as hip fracture risk factors.

doi:10.1016/j.bonr.2020.100350

P241

Deep learning spine segmentation to get accurate and relevant BMD and TBS values: The OsteoLaus study

François De Guio[a], El Hassen Ahmed[a], Enisa Shevroja[b], Olivier Lamy[b], Franck Michelet[a], Didier Hans[c]
[a]*Medimaps, Canéjan, France*
[b]*Lausanne University Hospital, Lausanne, Switzerland*
[c]*Lausanne University Hospital and Medimaps, Lausanne, Switzerland*

Optimal spine segmentation (SpS) is the basis for the clinical accuracy of BMD and TBS DXA-based computations.

We aimed at implementing and optimizing a deep learning (DL) method for an automatic and accurate SpS in AP spine DXA; compare BMD and TBS obtained after expert, DL or default automatic segmentation provided by the DXA manufacturer.

1,162 women (OsteoLaus cohort) with DXA scans (GEHC Lunar) and validated reference bone masks done by bone imaging experts were included. 50% of the scans were used for training, 25% for validation, 25% for testing. We adapted a U-net architecture to use the low-energy and high-energy images as inputs. Parameters included the ReLU activation function, ADAM optimizer for gradient descent and minimization of Dice Coefficient (DC) as loss function. Segmentation`s accuracy was evaluated by the DC. BMD and TBS obtained after DL or manufacturer segmentations were compared to the expert segmentation with: correlation coefficients, root mean square deviation (RMSD), classification of osteoporosis by BMD T-score.

The model rapidly converged. Comparison of metrics in training and validation datasets revealed no model overfitting. Mean DC was >0.97 in the training and test datasets. There was a good agreement for BMD or TBS values between AI and expert segmentation in comparison to the manufacturer segmentation. AI segmentation yielded to better correlations, lower RMSD and higher accuracy to classify patients by BMD T-score (Table 1).

We propose a DL-based segmentation that performs significantly better than the segmentation proposed by the DXA manufacturer. This segmentation enables a quick (3s), reproducible and accurate bone mask to get clinically meaningful bone scores (BMD, TBS).

Table 1

	Correlation coefficient BMD-BMD expert	RMSD BMD-BMD expert (%)	Accuracy BMD T-score<-2.5 vs BMD expert	Correlation coefficient TBS-TBS expert	RMSD TBS-TBS expert (%)
AI segmentation	0.996	0.028 (2.56%)	97.9 %	0.989	0.017 (1.31%)
Manufacturer segmentation	0.994	0.040 (3.70%)	94.5%	0.960	0.034 (2.55%)

doi:10.1016/j.bonr.2020.100355

P278

Effect of denosumab on circulating markers of atherosclerosis in women with postmenopausal osteoporosis

Cristiana Cipriani[a], Sara Piemonte[a], Luciano Colangelo[a], Federica Ferrone[a], Valeria Fassino[a], Marco Occhiuto[a], Luciano Nieddu[b], Salvatore Minisola[a], Jessica Pepe[a]
[a]*Department of Clinical Internal Medicine, Cardiovascular and Anesthesiological Sciences, Sapienza University of Rome, Rome, Italy*
[b]*Faculty of Economics, UNINT University, Rome, Italy*

The study was aimed at evaluating the effect of denosumab on circulating levels of the main markers of atherosclerosis in women with postmenopausal osteoporosis.

The study was approved by the Policlinico Umberto I Ethics Committee. Denosumab was administered at the dose of 60 mg subcutaneously every 6 months (m) in 28 women (mean age 75±5 years) with postmenopausal osteoporosis and low cardiovascular risk. Zoledronic acid (ZA) was administered in a control group of 6 age-matched women as a single intravenous dose. Serum levels of vascular cell adhesion protein 1 (*VCAM*-1), intercellular adhesion molecule 1 (*ICAM-1*), E and P selectin, CD-40 ligand, interleukin-6, m*atrix metalloproteinase (MMP) 1* and 9, fibrinogen (FBG), monocyte chemoattractant protein-1 and C-reactive protein (CRP) were measured at baseline, 15 days (d), 2 and 6 m after any dosing with a total follow-up of 24 m in denosumab and of 12 m in ZA group.

We observed a significant increase in serum FBG and CRP in both groups at 12 m (denosumab: +2.2±0.2% and +50.3±1.6%; ZA: +9.4± 0.1 and +81.8±0.8%, p< 0.01 for all). Serum ICAM-1 levels showed significant increase in the ZA group (+18±0.1%, p< 0.01) at 12 months. In the denosumab group, we observed a significant increase in serum *MMP-1* (+11±0.4%, p< 0.02) and MMP-9 (+39.4±0.8%, p< 0.01) at 24 m. No changes in serum levels of any other molecule were observed.

Our results demonstrate that there is no significant effect of denosumab on the circulating markers of atherosclerosis in women with osteoporosis. Fluctuation of FBG and CRP can be ascribed to the well-known perturbation of immunological mechanisms stimulated by denosumab and zoledronic acid. As far as results on serum MMPs, a late-onset action of denosumab on macrophages and/or fibroblasts could be implicated, and effect of these molecules on bone and other systems need future evaluation.

doi:10.1016/j.bonr.2020.100356

P338

The recommended starting dose of 0.4mg/kg burosumab is insufficient for most children with X-linked hypophosphatemia (XLH) - Results from the first treated patients in Sweden

Sigrun Hallgrimsdottir[a,b], Ola Nilsson[a,b,c]
[a]*Division of Pediatric Endocrinology, Department of Women's and Children's Health, Karolinska Institute and University Hospital, Stockholm, Sweden*
[b]*Center for Molecular Medicine, Karolinska Institute and University Hospital, Stockholm, Sweden*
[c]*School of Medical Sciences, Örebro University and University Hospital, Örebro, Sweden*

Background: In XLH elevated FGF23 levels cause phosphate wasting and decreased activation of vitamin D leading to hypophosphatemia and rickets. Burosumab is a human monoclonal antibody that neutralizes FGF23. Previous phase 2 and 3 clinical trials showed that a dose of approximately 1.0 mg/kg is required to maintain serum phosphorus in the low normal reference range. However, an international consensus statement recommends a starting dose of 0.4 mg/kg (Haffner *et al.* Nat Rev Nephrol 2019).

Objective: To evalute the efficacy of the recommended starting dose of Burosumab and observe required doses for optimal response.

Methods: Five pediatric patients with genetically verified XLH and overt rickets despite optimized conventional therapy were treated with burosumab at a starting dose of 0.4 mg/kg. Treatment response was monitored with biweekly blood and urine samples. Doses were increased if 2 consecutive serum phosphorus were below the reference level. These were the first five patients started on Burosumab at our center.

Results: Serum phosphorus and TmP/GFR increased significantly and ALP decreased during treatment in all patients. However, all patients continued to have plasma phosphorus levels below the reference interval during treatment with the starting dose.

Conclusions: This finding is consistent with previous dose-finding studies and indicates that the a dose of 0.4 mg/kg will be insufficient to maintain plasma phosphorus in the low normal range in most children with XLH. Starting at a suboptimal dose will result in increased numbers of blood draws and may delay recovery of rickets.

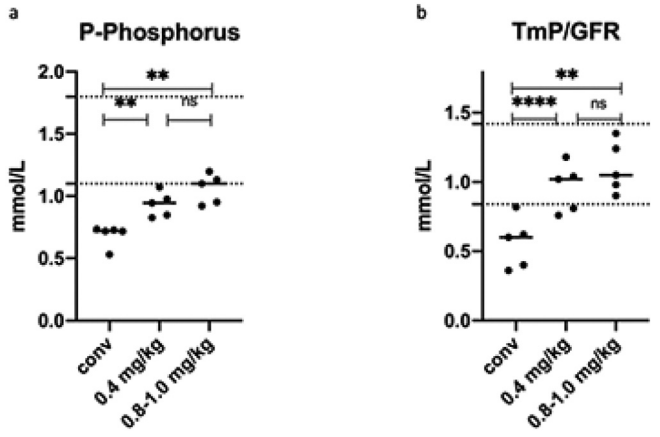

Fig. 1. P-Phosphorus (a) and TmP/GFR (b) during conventional treatment and burosumab treatment with starting dose and after a dose increase. Fasting samples, taken before dose administration. Graph plotted with average values for each participants during different treatment/dose. One way ANOVA and Tukey's multiple comparison test was employed for statistical analysis ($p < 0.05$: *; $p < 0.01$: **; $p < 0.001$: ***, $p < 0.0001$: ****).

[Average phosphorus (a) and TmP/GFR (b) before and during burosumab treatment with different doses.]

doi:10.1016/j.bonr.2020.100358

P341

Design and topline results of TransCon PTH, a long-acting PTH, phase 2 trial in patients with hypoparathyroidism

David B. Karpf[a], Sanchita Mourya[a], Aliya Khan[b], Lars Rejnmark[c], PaTH Forward Trial Investigators

[a]*Clinical Development, Ascendis Pharma, Inc., Palo Alto, United States*
[b]*Division of Endocrinology and Metabolism and Geriatrics, McMaster University, Oakville, Canada*
[c]*Department of Endocrinology, Aarhus University Medical School, Aarhus, Denmark*

Background: PTH deficiency in hypoparathyroidism (HP) leads to hypocalcemia and hyperphosphatemia. Standard of care (SoC), ie, large doses of calcium (Ca) and active vitamin D, worsens hypercalciuria and increased sCa x sP product. Studies have shown that continuous SC infusion of PTH(1-34) normalizes sCa, sP, sMg, uCa and bone turnover better than SoC or once- or twice-daily injections of PTH in HP patients.

TransCon™ PTH is an investigational long-acting prodrug of PTH (1-34). PTH(1-34) is transiently bound to an inert carrier via a linker, applying TransCon (transient conjugation) technology. Under physiological conditions, linker auto-cleavage occurs, releasing active PTH at a controlled rate with a flat, infusion-like profile. Phase 1 trial results demonstrated that TransCon PTH provided physiologic levels of PTH 24 hours per day, increasing sCa while controlling uCa and decreasing sP, with no evidence of bone anabolic activity.

Phase 2 Design: Adult patients with HP treated with SoC were randomized at sites worldwide to daily TransCon PTH 15, 18 or 21 μg PTH or daily blinded placebo via pen-injector for 4 weeks. The primary composite endpoint requires 1) normal sCa **and** 2) normal FECa (or ≥50% decrease from baseline), **and** 3) not taking active D, **and** 4) taking ≤1000 mg/d of Ca. All subjects enter a long-term extension trial where the TransCon PTH dose will be individually optimized.

Preliminary Results: Approximately 55 subjects are expected to be randomized and dosed. Top-line data (proportion of subjects meeting the composite primary endpoint) will be presented, as well as preliminary results from the long-term extension portion of the trial. Preliminary diary data on the initial 8 subjects completing 4 weeks of follow-up in the extension trial show that all have discontinued SoC. The Phase 2 trial is designed to support the TransCon PTH target profile as a "true" PTH replacement therapy.

doi:10.1016/j.bonr.2020.100351

Bone Reports 13 (2020) 100359

Contents lists available at ScienceDirect

Bone Reports

journal homepage: www.elsevier.com/locate/bonr

Poster

P002

Low serum osteocalcin levels are associated with the presence of diabetes mellitus in glucocorticoid treated patients

Helena Florez[a], José Hernández-Rodríguez[b], Josep Lluís Carrasco[c], Sergio Prieto-González[b], Xavier Filella[d], Ana Monegal[a], Núria Guañabens[a], Pilar Peris[a]

[a]Metabolic Bone Diseases Unit. Department of Rheumatology, Hospital Clinic, University of Barcelona, Barcelona, Spain

[b]Vasculitis Research Unit, Department of Autoimmune Diseases, Hospital Clínic, Barcelona, Spain

[c]Biostatistics, Department of Basic Clinical Practice, University of Barcelona, Barcelona, Spain

[d]Biochemistry and Molecular Genetics Department, Hospital Clinic, Barcelona, Spain

Increasing evidence indicates that osteocalcin (OC) is involved in the regulation of glucose homeostasis. Glucocorticoid (GC) treatment is associated with impaired osteoblast function and decreased OC levels and also with the development of CG-induced diabetes mellitus (GIDM). However, whether decreased OC levels in GC-treated subjects contribute to GIDM is not well known.

Objectives: To analyse whether OC levels in GC-treated patients are associated with the presence of GIDM.

Methods: 127 patients (aged 62±18years, 63% women) on GC treatment for autoimmune diseases (≥5mg/day,>3 months) were included. Clinical and anthropometric data were analysed, including the GC dose and treatment duration, presence of GIDM, fragility fractures, densitometric osteoporosis and bone formation (OC, bone alkaline phosphatase [BAP], PINP) and resorption markers (urinary NTX, serum CTX). The cut-offs of each bone marker for the presence of GIDM were estimated and optimized with the Youden index and included in the logistic regression analysis (adjusted for BMI, age and GC doses).

Results: 17.3% of patients presented GIDM. Diabetic subjects were older (70.5±12.2 vs. 59.6±18.4;p=0.001) and had a higher BMI than non-diabetics (30±5.2 vs. 26±4.2;p=0.002). No differences were observed in GC dose or duration or in the presence of vertebral fractures. Diabetics showed lower levels of OC (7.57±1.01 vs. 11.56±1; p< 0.001), PINP (21.48±1.01 vs. 28.39±1;p=0.0048), NTx (24.91±1.01 vs. 31.7±1;p=0.036) and CTX (0.2±1.01 vs. 0.3±1;p=0.0016) with similar BAP values. The best discriminating cut-offs for GIDM presence were: < 9.25ng/mL for OC, < 24ng/mL for PINP, < 27.5nMol/mM for NTX and < 0.25ng/mL for CTX. On multivariate analysis OC (< 9.25) was the only marker related to the presence of GIDM (OR 6.1;CI95% 1.87-19.89; p=0.001).

Conclusions: Decreased OC levels in GC-treated patients are associated with an increased risk of GIDM, a finding that was not observed with other bone turnover markers, further confirming the involvement of OC in the glucose homeostasis regulation in this entity.

doi:10.1016/j.bonr.2020.100360

P003

Highly sensitive quantification of human total VEGF-A with a novel ELISA

Andreea Ana-Maria Suciu[a], Elisabeth Gadermaier[a], Jacqueline Wallwitz[a], Gabriela Berg[b], Gottfried Himmler[a]

[a]The Antibody Lab, Vienna, Austria

[b]Biomedica Medizinprodukte GmbH, Vienna, Austria

Purpose: Vascular endothelial growth factor A (VEGF-A) is one of the most important regulators of vascular development and angiogenesis. It also plays critical roles in skeletal development as osteoblastic cells represent a major source of VEGF in the bone environment. Moreover, VEGF regulates osteoclastic differentiation and migration in bone repair. Thus, VEGF represents a relevant therapeutic target. The sensitive measurement of low amounts of circulating VEGF-A found in control cohorts of healthy individuals proves to be a challenge. Hence, there is a need for a highly sensitive assay that enables the reliable quantification of low VEGF-A concentrations.

Methods: We developed a highly sensitive sandwich ELISA for the detection of human total VEGF-A using high quality, well-characterized recombinant monoclonal and polyclonal anti-human VEGF-A antibodies. The linear epitopes of the polyclonal detection antibody were mapped with microarray technology. Analyte stability was determined and in accordance with international guidelines, assay parameters like specificity, dilution linearity, and spike recovery were assessed.

Results: We demonstrate that human VEGF-A can reliably be measured in plasma preparations. In contrast, some samples show a clear increase, indicating that serum preparation might have an influence on the results, as VEGF can be released from platelets during sample manipulation. Most importantly, we show that samples of apparently healthy individuals are measurable over background. The assay covers a calibration range between 0 and 2000 pg/ml and assay characteristics as well as analyte stability meet the international standards of acceptance. The recombinant capture antibody recognizes a structural epitope in the conserved receptor binding-site of VEGF-A and thus, specifically binds to all VEGF-A isoforms. The polyclonal detection antibody recognizes linear epitopes in the first 120 amino acids of the VEGF-A molecule

Conclusion: Our novel VEGF-A ELISA provides a reliable and accurate tool for the quantitative determination of all VEGF-A isoforms with high sensitivity.

doi:10.1016/j.bonr.2020.100361

P007

Novel assay for uncarboxylated osteocalcin (ucOC) demonstrates an association between plasma glucose and ucOC levels in humans

Milja Arponen[a], Eeva-Christine Brockmann[b], Riku Kiviranta[a], Urpo Lamminmäki[b], Kaisa K. Ivaska[a]
[a]Institute of Biomedicine, University of Turku, Turku, Finland
[b]Department of Biotechnology, University of Turku, Turku, Finland

Osteocalcin (OC) is an osteoblast-secreted protein containing three glutamic acid residues (Glu) which undergo post-translational carboxylation into gamma-carboxyglutamic acids. Uncarboxylated form of osteocalcin (ucOC) may participate in the regulation of glucose homeostasis and measurement of ucOC could be useful in evaluating interactions between bone and glucose metabolism.

We developed specific antibodies and an immunoassay to detect ucOC in human blood samples. ucOC-specific recombinant antibodies were screened from an antibody library and four candidates were selected for cloning and characterization. Then, we developed immunoassay for ucOC with selected antibody and validated it with blood samples from healthy volunteers. We then measured plasma ucOC levels in subjects with normal fasting blood glucose (< 6 mmol/L, N=49) or with hyperglycemia (>7 mmol/L, N=31). Further, we analyzed ucOC in age- and gender-matched patients with diagnosed type 2 diabetes (T2DM, N=49). All samples were collected in accordance to Helsinki declaration.

Antibodies recognized ucOC with Glu at all carboxylation sites without cross-reaction to fully carboxylated osteocalcin. Antibodies had unique binding sites at carboxylation site and thus different characteristics. Immunoassay was sensitive to detect ucOC in serum and plasma analyzed, with levels in plasma on average 1.5 fold higher than in serum. Assay characteristics, such as limit of detection (0.18ng/ml), between-run (8.5%) and within-run variability (6.1%), were determined. ucOC concentrations were significantly lower in subjects with hyperglycemia (median 0.58ng/ml, p=0.007) or with T2DM diagnosis (0.68ng/ml, p=0.024) when compared to subjects with normal blood glucose (1.05ng/ml). There was no difference between subjects with hyperglycemia and T2DM (p=0.74). ucOC negatively correlated with fasting plasma glucose in subjects without T2DM (r= -0.30, p=0.007) but not in patients with T2DM (p=0.26).

Immunoassay based on novel recombinant antibody is a sensitive method to detect ucOC in human circulation. Correlation between ucOC and plasma glucose further suggests interactions between osteocalcin and glucose metabolism.

doi:10.1016/j.bonr.2020.100362

P009

The PoCOsteo cohort - deep bone phenotyping for fracture risk prediction

Christoph Haudum[a,b], Barbara Luegger[a], Kerstin Koschka[a], Hans Peter Dimai[a], Barbara Obermayer-Pietsch[a]
[a]Division of Endocrinology and Diabetology, Medical University Graz, Graz, Austria
[b]CBmed GmbH - Center for Biomarker Research in Medicine, Graz, Austria

Objective: Risk predictors for osteoporotic fractures are important research tools addressing bone fragility in an ageing population. The EU project PoCOsteo ("in-office device for identifying individuals at high risk of osteoporosis and osteoporotic fracture", H2020-NMPB 767325) aims to define these risk factors based on cohorts via deep phenotyping for the identification of blood- and urine-based biomarkers and bone characteristics, but also machine learning approaches for a point-of-care tool to predict fracture probability in elderly patients - one of these cohorts is built at the Medical University Graz.

Methods: Patients are recruited at the local Outpatient Clinic and followed via visits after one year. For future specialized genomic, proteomic and epigenetic analyses, a multitude of samples including various blood, serum, plasma, DNA and urine samples are taken. Besides routine lab and bone markers, DXA (GE Lunar, iDXA) including TBS (trabecular bone score) as well as VFA (vertebral fracture assessment) and spinal X-rays, a high-resolution peripheral quantitative CT analysis (XtremeCTII, Scanco) is performed. Past and prospective fractures, a standardized EQ-5D-5L form and other questionnaires, and muscular parameters including grip strength (dynamometer, Jamar) are documented.

Results: 699 (92 male, 607 female) out of 1000 planned patients have been recruited so far. Their mean age was 64.9 ± 5.3 years. Follow-up visits of 200 patients have already been analysed. In addition to the documented prevalent fractures, 8 incident fractures have been assessed (3 vertebral and 5 non-vertebral).

Summary and Conclusions: This Horizon-2020-funded PoCOsteo cohort presents a valuable source of clinical data and biobanking for further fracture risk prediction research. The current number of incident fractures is in line with the previously published age-adjusted incidence rates in the Austrian population. The dataset will be used as basis for a predictive model to determine 10 year-fracture risk including biochemical, genetic, epigenetic and imaging data.

doi:10.1016/j.bonr.2020.100363

P010

Rheumatoid arthritis treatment associated changes in circulating bone-turnover markers

Gitte Lund Christensen[a], Trine W. Jensen[b], Michael Sejer Hansen[c,d], Kim Hørslev-Petersen[e], Lars Hyldstrup[f], Bo Abrahamsen[g,h,i], Bente Langdahl[j], Bo Zerahn[k], Jan Pødenphanth[c], Kristian Stengaard-Petersen[l], Peter Junker[m], Mikkel Østergaard[n,o], Tine Lottenburger[e], Torkell Juulsgaard Ellingsen[l], Lis Smedegaard Andersen[l], Ib Tønder Hansen[l], Henrik Skjødt[n], Jens K. Pedersen[e], Anders Jørgen Svendsen[p,q], Ulrik Tarp[l], Hanne M. Lindegaard[m], Merete Lund Hetland[n,r], Niklas Rye Jørgensen[s], The CIMESTRA study group
[a]Dept. of Clinical Biochemistry, Copenhagen University Hospital Rigshospitalet, Glostrup, Denmark
[b]Dept. of Endocrinology, Copenhagen University Hospital, Denmark, Hvidovre, Denmark
[c]Dept. of Rheumatology, Copenhagen University Hospital, Gentofte, Denmark
[d]ReumaKlinik Roskilde, Roskilde, Denmark
[e]Dept. of Rheumatology, Gigthospitalet, University of Southern Denmark, Graasten, Denmark
[f]Dept. of Endocrinology, Copenhagen University Hospital, Hvidovre, Denmark
[g]OPEN, University of Southern Denmark, Odense, Denmark
[h]Department of Medicine, Holbaek Hospital, Holbaek, Denmark
[i]NDORMS, University of Oxford, Oxford, United Kingdom
[j]Dept. of Endocrinology and Internal Medicine THG, Aarhus University Hospital, Aarhus, Denmark
[k]Dept. of Clinical Physiology, Copenhagen University Hospital, Herlev, Denmark
[l]Dept. of Rheumatology, Aarhus University Hospital, Aarhus, Denmark
[m]Dept. of Rheumatology, Odense University Hospital, Odense, Denmark
[n]Copenhagen Center for Arthritis Research, Center for Rheumatology and Spine Disease, Glostrup, Denmark

[o]Department of Clinical Medicine, Faculty of Health and Medical Sciences, University of Copenhagen, Copenhagen, Denmark
[p]Department of Internal Medicine, Odense University Hospital, Svendborg, Denmark
[q]Dept. of Public Health, University of Southern Denmark, Odense, Denmark
[r]Department of Clinical Medicine, University of Copenhagen, Copenhagen, Denmark
[s]Dept. of Clinical Biochemistry, Copenhagen University Hospital, Glostrup, Denmark

Rheumatoid arthritis (RA) is associated with focal articular bone erosions and development of osteoporosis. The aim of this study was to describe treatment-associated changes in circulating bone-turnover markers (BTM) and their correlation to changes in bone mineral density (BMD).

Methods: 160 newly diagnosed RA-patients (67% women, mean age 53 (42-62) years) were randomized to a) Methotrexate (7.5-20 mg weekly) plus Cyclosporin A (2.5-4.5 mg/kg) (MTX+CyA) or b) Methotrexate plus placebo (MTX). Patients with an initial negative BMD Z-score had Alendronate (10 mg/day) added. The BTMs C terminal telopeptide of type I collagen (CTX), pro-collagen type1 N-terminal peptide (P1NP), osteocalcin (OC) and bone-specific alkaline phosphatase (BAP) were determined using an IDS-iSYS automated immunoassay at 0, 2, 4, 6, 8, 12, 24, 36 and 52 weeks. DXA scan was performed at baseline and after 1 year. Ethical approval was obtained by Danish health authorities.

Results: Regulation of BTMs by MTX or MTX+CyA, in patients that did not receive Alendronate, is shown in figure 1.

Alendronate naive patients in both treatment-groups showed a similar decrease in BMD after 1 year. This was not correlated with changes in BTMs from 0-24 weeks. Alendronate treatment slightly increased BMD. This correlated with reduced levels of all four BTMs after 24 weeks.

Conclusion: The investigated treatments induced minor changes in the circulating levels of OC and BAP. Significant correlations between BTM and BMD were only observed in the Alendronate treated group. Changes in BMD due to RA disease-progression or treatment are not reflected in BTM changes.

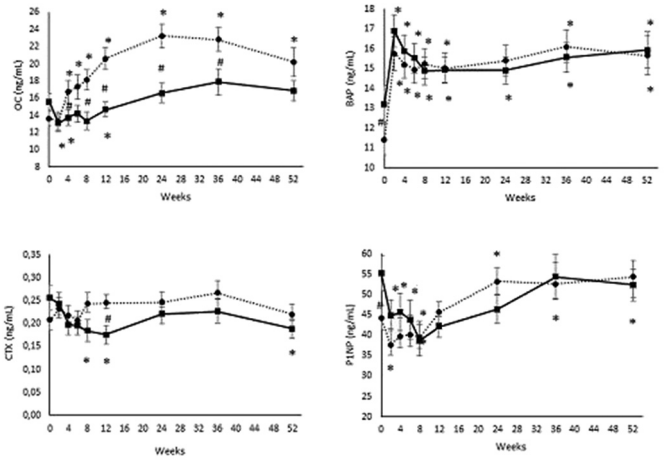

Figure 1
Temporal bone turnover marker changes in alendronate naive patients with early RA. —●— MTX ····●···· MTX+CyA
OC was significantly increased from week 8 by MTX+CyA compared to MTX, while BAP was increased after 2 weeks by both treatments. Significanct difference from initial value was tested with repeated measures ANOVA * p<0.05. Difference between treatments was tested with one-way between groups ANOVA # p<0.05

doi:10.1016/j.bonr.2020.100364

P011

Towards understanding therapeutic failures in Masquelet surgery: First evidences that defective induced membrane properties are associated with clinical failures

Marjorie Durand[a], Laure Barbier[a], Laurent Mathieu[b], Thomas Poyot[a], Thomas Demoures[c], Jean-Baptiste Souraud[c], Alain-Charles Masquelet[d], Jean-Marc Collombet[a]
[a]Military Biomedical Research Institute (IRBA), Brétigny sur Orge, France
[b]Percy Military Hospital, Clamart, France
[c]Bégin Military Hospital, Saint Mandé, France
[d]Saint-Antoine Hospital, Paris, France

The two-stage Masquelet induced-membrane technique (IMT) consists of cement spacer-driven membrane induction followed by an autologous cancellous bone implantation in this membrane to promote large bone defect repairs. For the first time, this study aims at correlating IMT failures with physiological alterations of the induced membrane (IM) in patients. For this purpose, we compared various histological, immunohistochemical and gene expression parameters obtained from IM collected in patients categorized lately as successfully (Responders; n = 8) or unsuccessfully (Non-responders; n = 3) treated with the Masquelet technique (6 month clinical and radiologic post-surgery follow-up). While angiogenesis or macrophage distribution pattern remained unmodified in non-responder IM as compared to responder IM, we evidenced an absence of mesenchymal stem cells and reduced density of fibroblast-like cells in non-responder IM. Furthermore, non-responder IM exhibited altered extracellular matrix (ECM) remodeling parameters such as an increase in metalloproteinase-9 (MMP-9) and a decrease in tissue inhibitor of metalloproteinases (TIMP-1) gene expression as well as an important collagen overexpression as shown by picrosirius-red staining. In summary, this study is the first to report evidence that IMT failure can be related to defective IM properties while underlining the importance of ECM remodeling parameters, particularly MMP-9/TIMP-1 gene expression ratio, as early predictive biomarkers of the IMT outcome regardless of the type of bone, fracture or patient characteristics.

doi:10.1016/j.bonr.2020.100365

P012

Segmentation of the fascia lata and reproducible quantification of intermuscular adipose tissue and fat fraction of the thigh

Klaus Engelke[a,b], Oliver Chaudry[b], Andreas Friedberger[b], Wolfgang Kemmler[b], Armin Nagel[c]
[a]Department of Medicine 3, FAU University Erlangen-Nürnberg, Erlangen, Germany
[b]Inst. of Medical Physics, FAU Erlangen-Nürnberg, Erlangen, Germany
[c]Department of Radiology, FAU University Erlangen-Nürnberg, Erlangen, Germany

Background: Osteoporosis and sarcopenia are associated with declined muscle function and increased intermuscular adipose tissue (IMAT). The quantification of IMAT is challenging because it requires a segmentation of the fascia lata (FL).

Objectives: To develop a semiautomated segmentation method for the fascia lata of the thigh and to quantify reanalysis precision of IMAT volume in T1w and fat fraction in Dixon MR images.

Methods: MRI Scans were acquired on a 3T Siemens MAGNETOM Skyra at the mid-thigh (length 10cm, 34 slices, voxel size T1w 0.5x0.5x3.0mm³, Dixon 0.8x0.8x3.0mm³). T1wTSE images were used for segmentation, starting with a fuzzy c-mean clustering followed

by filtering steps to enhance 3D surface like structures representing the FL. Finally, a level set algorithm was applied to obtain the closed 3D surface of the FL. Results could be corrected manually. Segmented masks were transferred from the T1w to the FF images by rigid registration. IMAT was segmented using a threshold determined from the histogram of the FF values within the intra-fascia region. 15 sarcopenic (80±5y) and 5 healthy (28±4y) male subjects were analyzed by three operators once (inter-operator reproducibility) and three times by one operator (intra-operator reproducibility).

Results: Inter- and intra-operator variability results of IMAT and FF are shown in the table as mean / root mean square of the standard deviation (RMS-SD) in units of the measured variable / coefficient of variation (RMS-CV) in %. Overall precision was excellent with almost all errors < 1.5[%.

Conclusion: A semi-automatic 3D segmentation for the fascia of the thigh was developed. Operator impact on IMAT was almost negligible.

Young Healthy male subjects	FF [%]	5.7/0.11/1.17	5.7/0. 04/0.38
Elderly sarcopenic male subjects	FF [%]	14.9/0.12/0.16	15.0/0.08/0.10
Young Healthy male subjects	Volume IMAT [cm³]	18.1/1.75/5.80	18.0/0.25/0.82
Elderly sarcopenic male subjects	Volume IMAT [cm³]	66.8/0.96/0.29	66.7/0.58/0.17

Inter- (column 3) and Intraoperator (column 4) precision. Values are shown as Mean/ RMS-SD/RMS-CV%.

doi:10.1016/j.bonr.2020.100366

P013

Assessment of senescence in adipose mesenchymal stem cells for optimized ex vivo expansion and therapeutic potential

Nicolas Theys[a], Hara Episkopou[a], Céline Pierard[a], Anabelle Decottignies[b]
[a]*Novadip Biosciences, Mont Saint Guibert, Belgium*
[b]*Université catholique de Louvain, Brussels, Belgium*

Bone tissue engineering using osteoblastic differentiated adipose mesenchymal stem cells (AMSCs) is tested in clinical trials to heal critical size bone defects. For such therapies, a high number of cells is desirable for bioactivity, requiring extensive *ex vivo* cell expansion. However, adult MSC proliferation is limited as culture causes continuous changes resulting in induction of replicative senescence. Replicative senescence is a complex process whereby stem cells grow old and is related to dysfunction of telomeres, the end part of eukaryotic chromosomes that are shortened after each replication cycle. The changes in stem cell functions related to aging of the donor, can be attributed to a decline in the effectiveness of regenerative capability. We present the results of a study where specific markers in the physiology of the AMSCs from 6 adults subjects of different ages were monitored during long-term *ex vivo* expansion as surrogates of their proliferation, differentiation and therapeutic potential. Telomere dysfunction, defects of Lamin-A and expression levels of the senescence markers *p16, p21* genes and several Senescence-Associated Secretory Phenotype markers (*IL6, IL8, MCP1*) were evaluated during early, intermediate and late passages. We show that, independent of the age of the donor, the senescence rate increases steadily for all cell samples reaching a senescent phenotype after numerous passages. The population doubling time is significantly increased with proliferation. Interestingly, higher senescence rate is observed at early passages in cells derived from older donors paralleling the slower proliferation potential of their cells which may have an impact on the potency and efficacy or product derived therefrom. For each donor, the expression levels of specific tested senescence markers correlates with to the senescence status of the corresponding cell samples. In conclusion, our study provides new insights to understand the AMSC senescence mechanisms for the improvement of cellular therapies and quality control processes.

doi:10.1016/j.bonr.2020.100367

P014

Changes in protein profile in bone marrow extracts before and one year after gastric bypass surgery

Safiyye Süslü[a], Ingvild Kristine Blom-Høgestøl[b], Erik Fink Eriksen[b,c], Janne Elin Reseland[a]
[a]*Biomaterials, University of Oslo, Oslo, Norway*
[b]*Department of Endocrinology, Oslo University Hospital, Oslo, Norway*
[c]*Institute of Clinical Medicine, University of Oslo, Oslo, Norway*

The long-term skeletal changes after bariatric surgery are largely unknown, and identifying molecular mechanisms related to reduced bone health after long-term weight loss may reveal novel approaches for reducing the burden of these changes.

For better knowledge about bone status, we aimed to identify changes in the protein profile in bone marrow aspirates after weight loss due to gastric bypass surgical intervention.

Methods: Proteins in bone marrow aspirates from 9 patients before and 1 year after gastric bypass surgery (2013/1159/REK Sør-Øst B), were isolated using Trizol (Thermo Fisher Scientific). Total protein content was identified using the BCA Assay (Thermo Scientific). The amounts of specific proteins, such as cytokines (HCYP2MAG-62K;Millipore Merck) and bone markers (HBNMAG-51K) in various samples, were determined by the Luminex 200 system where acquired fluorescence data were analyzed using the 3.1 xPONENT software (Luminex).

Results: Bariatric surgery resulted in reduced bone mineral density ($p = 0.018$) and enhanced levels of osteocalcin ($p = 0.001$).

In the bone marrow aspirates a reduction in the level of vascular endothelial growth factor (VEGF) ($p = 0.046$) and enhanced levels of osteopontin (OPN) ($p = 0.021$) and interleukin-1β (IL-1β) ($p = 0.025$) were observed.

Conclusion: The bone marrow protein profile indicate an enhanced resorption and bone turnover following the loss of weight and reduction in BMD after surgery.

doi:10.1016/j.bonr.2020.100368

P017

Calcium and vitamin D status in postmenopausal women with scoliosis

Nikola Kirilov, Elena Kirilova, Svilen Todorov, Martin Nikolov, Nikolay Nikolov
UMBAL Dr Georgi Stranski, Pleven, Bulgaria

Introduction: Different studies have suggested a link between vitamin D and scoliosis. Most of them have been focused on the relation of serum vitamin D levels to adolescent scoliosis. However, there is no other study which has compared the calcium and vitamin D status between the women with- and without scoliosis aftermenopause. The aim of this study is to establish the association between serum levels of 25-OH-Vit D and calcium and the presence of scoliosis in postmenopausal women.

Methods: We investigated calcium and vitamin D serum levels of 35 postmenopausal women. Lumbar scoliosis was assessed from DEXA scans, which was available for all of the women and was defined as Cobb angle >10°. Women were divided into two groups-with scoliosis and without scoliosis and both calcium and vitamin D serum levels were assessed for the women in each group.

Results: The mean age of all postmenopausal women was 61 years ± 9 SD (range 40-79 years). 8 of 35 women (22.8%) had scoliosis and 27 of 35 women (77.2%) were without scoliosis. Women with scoliosis had significantly lower vitamin D serum level (12.85nmol/l) compared to those without scoliosis (30.24nmol/l), (p=0.000).Calcium serum level (2.18 mmol/L) was also significantly lower in the women with scoliosis than those without scoliosis (2.38 mmol/L), (p=0.020).

Conclusion: Postmenopausal women with scoliosis showed lower calcium and vitamin D levels as compared to those without scoliosis.

doi:10.1016/j.bonr.2020.100369

P019

Bone neoformation in calvaria bone defects after the association of PVDF membrane and photobiomodulation therapy in ovariectomized rats: microtomographic evaluation

Fernanda Cristina Toloi Rufato[a], Luiz Gustavo Sousa[a], Priscilla Hakime Scalize[a], Marcio Mateus Beloti[a], Adriana Luisa Gonçalves Almeida[a], Rossano Gimenes[b], Adalberto Luiz Rosa[a], Karina Fittipaldi Bombonato-Prado[a], Simone Cecilio Hallak Regalo[a], Selma Siessere[a]

[a]*University of São Paulo - School of Dentistry of Ribeirão Preto, Ribeirão Preto, Brazil*

[b]*Federal University of Itajubá, Itajubá, Brazil*

Politetrafluoretilene membranes (PTFE) are considered the best for guided bone regeneration, but photobiomodulation therapy (PT) and poly(vinylidene fluoride)/PVDF membranes associated to barium titanate may represent good alternatives. This study evaluated bone architecture by means of computadorized microtomography after the association of PT with PTFE and P(VDF-TrFE)/BT membranes in calvaria bone defects of ovariectomized rats. The experimental protocol was approved by Ethics Committee for Animal Experimentation of the University of São Paulo (n. 2018.1.417.58.0). Twenty Wistar Hannover rats (300g) were submitted to bilateral ovariectomy (OVX) and 5 just submitted to ovary exposition (Sham). After 90 days, there were performed 5-mm calvaria bone defects in all animals. Ovariectomized rats were distributed in the following groups: 1) OVX (n=5); 2) OVX + P(VDF-TrFE)/BT membrane (n=5); 3) OVX + P(VDF-TrFE)/BT membrane + PT (n=5) and 4) OVX + PTFE membrane + PT (n=5). There were performed 12 sessions with gallium-aluminum-arsenate diode (780 nm) laser with energy density of 30 J/cm^2. Thirty days after euthanasia, samples were fixed and analyzed by means of micro-CT SkyScan 1172 (SkyScan, Belgium) for bone volume (BV/mm^3), bone surface (BS/mm2), trabecular number (TN/1/mm), trabecular thickness (TT/mm), trabecular separation (TS/mm) and connectivity density (CD/1/mm^3).There was observed a significant increase in the values of BV, BS, TN and CD when comparing the groups 2, 3 e 4 with sham and group 1 ($p< 0.05$). Groups 3 and 4 showed higher values of CD when compared to group 5. Trabecular separation was decreased in groups 3, 4 and 5 when compared to sham and group 1 ($p< 0.05$). There were no statistical differences either between groups 3 and 4 or for trabecular thickness parameter. It is concluded that all treatments with the membranes improved bone architecture when compared to sham and OVX animals, regardless the association with photobiomodulation therapy.

Fapesp - 2017/25683-4

doi:10.1016/j.bonr.2020.100370

P020

Mesenchymal stromal cells' secretome enhances osteoclastogenesis but reduces multinucleated giant cells formation *in vitro*

Paul Humbert, Julien De Lima, Meadhbh Á. Brennan, Frédéric Blanchard, Pierre Layrolle

UMR 1238 - Phy-OS, INSERM, Université de Nantes, Nantes, France

Human Mesenchymal Stromal Cells (hMSCs), when transplanted in combination with Calcium Phosphate materials (CaPs), lead to effective fracture healing in patients. Studies in Nude mice showed that implanted hMSCs are not contributing directly to bone-matrix deposition as they die rapidly and that efficient bone formation by host cells was associated with early osteoclast formation. We hypothesized that hMSCs paracrine effect alleviates the foreign body reaction against the biomaterial, restraining Multi-Nucleated Giant Cells (MNGCs) formation to the benefit of osteoclasts, thus initiating locally a bone remodeling cycle.

We investigated *in vitro* if hMSCs could secrete pro-osteoclastogenic and/or anti-MNGCs factors, especially under apoptotic stress using Staurosporine (STS). Osteoclasts and MNGCs were differentiated from hCD14$^+$ monocytes in the presence of Conditioned Media (CM) from hMSCs' culture. CM from 4 donors of hMSCs (untreated-CM, UNT-CM) consistently increased the size of osteoclasts by 20% while having no effect on MNGCs. After STS treatment of hMSCs, the CM obtained (STS-CM) significantly decreased the number of MNGCs by 20% (p-value< 0.001 by paired t-test). Further RNA expression analysis in osteoclasts revealed that three major differentiation markers (*NFATC1*, *cathepsin K* and *calcitonin receptor*) were consistently up-regulated by STS-CM compared to UNT-CM from 5 different donors (p-value< 0.05 by paired t-test). A proteomic analysis by LC-MS for 3 donors of hMSCs found 90 proteins enriched and 96 proteins depleted in the CM after STS treatment. A complementary multiplex immunoassay detected the overexpression of three cytokines (GROα, PDGF-AA and IL-8) and the reduced expression of two (Eotaxin and MCP-1, p-value< 0.05 by paired t-test). Additional tests are ongoing using neutralizing antibodies directed towards key cytokines or receptors based on these results.

This novel work supports the known immunomodulatory effect of hMSCs' secretome, suggests the impact of apoptosis and reinforces the hypothetical mechanisms of hMSC-CaP based bone regeneration through osteoclast recruitment.

doi:10.1016/j.bonr.2020.100371

P021

Glucose promotes transplanted human mesenchymal stem cell paracrine function pertinent to angiogenesis

Guotian Luo, Cyprien Denoeud, Nathanael Larochette, Esther Potier, Hervé Petite

Université de Paris, CNRS, INSERM, B3OA, Paris, France

Ecole Nationale Vétérinaire d'Alfort, B3OA, Maisons-Alfort, France

Objective: Massive cell death post-implantation is a roadblock for the use of human mesenchymal stem cell (hMSC) for cell-based regeneration of large bone defects. We previously established that glucose is instrumental for hMSC survival post-implantation. Because osteogenesis and angiogenesis are tightly coupled in the process of bone repair, we hereby investigate whether glucose affects hMSC-mediated angiogenic paracrine functions.

Methods: *In vitro* experiment: Release of bioactive factors and chemo-attractive potential of conditioned media (CM) from hMSCs towards human umbilical vein endothelial cells (HUVECs) were performed. The CM was obtained by exposure of hMSC to near-anoxia in the presence of glucose at 0, 1 or 5 g/L for 3 days.

In vivo experiment: hMSC pro-angiogenic potential was investigated using hMSC-containing hydrogels loaded with either 0,

1, 5, 10, or 20 g/L glucose and hMSC-free hydrogels loaded with 20 g/L glucose, which were implanted ectopically in nude mice. The newly-formed blood vessels at 21 days post-implantation was quantified using micro-CT scanner after microfil® injection.

Results: CM collected from hMSCs cultured with 1 or 5 g/L glucose promoted significant ($p < 0.05$) increased HUVECs migration when compared to the one collected from hMSCs cultured without glucose. hMSCs cultured in the presence of glucose released significantly ($p < 0.05$) higher amounts of Angiogenin, VEGF-A, a VEGF-C, Angiopoietin-1, Endostatin, and CCL2 when compared to hMSCs cultured without glucose. Most importantly, implanted hMSC-containing hydrogels loaded with either 5, 10, and 20 g/L glucose exhibited a 2.4-, 2.8-, and 2.4-fold increase ($p < 0.05$) in the volume of newly-formed blood vessels when compared to hMSC-containing hydrogels without glucose, respectively($n=8$). The volume of newly-formed blood vessels in cell-containing hydrogels without glucose and in cell-free hydrogels loaded with glucose were similar and minimal.

Conclusion: These data demonstrate that glucose promotes hMSC paracrine functions pertinent to angiogenesis.

Keywords: MSC, glucose, angiogenesis

doi:10.1016/j.bonr.2020.100372

P022

Towards in situ monitoring of *in vitro* 3D bone models

Donata Iandolo[a], Mikhael Hadida[a], Guénaëlle Bouët Chalon[a], Róisín M. Owens[b], Laurence Vico[a], David Marchat[a]
[a]*SAINBIOSE, INSERM U1059, Saint-Priest-en-Jarez, France*
[b]*Department of Chemical Engineering and Biotechnology, University of Cambridge, Cambridge, United Kingdom*

Cells are sensitive to numerous chemical and physical cues, imparted by both the fluid they are living in (*e.g.,* pH, glucose, O_2 and CO_2 concentration, flow speed and distribution, shear stress, hydrostatic pressure, reactive species), and the surface they are cultivated on (*e.g.,* surface chemistry and stiffness, wettability, micro and macro-architecture, release of chemical agents). Trying to recapitulate a physiologically relevant environment and control its parameters is thus a complex and fundamentally interdisciplinary challenge. We will develop a fully integrated platform comprising a perfusion system and purposely designed bioceramic scaffolds as they will guarantee to control the investigated fluidic environment with a high degree of confidence. This platform will allow us to carry out an extensive screening of cell responses to a range of reproducible mechanical and chemical environments and to suggest a map of the relationship of the mechanical environment and the induced cell response. The key innovative aspect of this project is the integration of innovative bioelectronics sensors within the perfusion system that will allow the continuous monitoring of cell proliferation and differentiation, leading to key insights in the underlying mechanism. A temporal profile of the secretion of the target analytes will be drawn and will be a relevant outcome of the project.

doi:10.1016/j.bonr.2020.100373

P024

Mesenchymal stem cells overexpressing BMP9 through CRISPR-Cas9 activation increase bone formation in rat calvarial defects

Gileade Freitas[a], Helena Lopes[a], Alann Souza[a], Isabella Santos[a], Adriana Almeida[a], Coralee Tye[b], Jane Lian[b], Janet Stein[b], Gary Stein[b], Marcio Beloti[a], Adalberto Rosa[a]
[a]*Bone Research Lab, University of São Paulo - School of Dentistry of Ribeirão Preto, Ribeirão Preto, Brazil*
[b]*The University of Vermont, Burlington, United States*

Cell therapy with mesenchymal stem cells (MSCs) induces bone formation in critical-size defects without resulting in complete regeneration. Cell therapy based on genetically edited MSCs is still underexplored. In this study we evaluated the in vivo effects of MSCs genetically edited by the CRISPR/Cas9 technique to overexpress BMP9. Mouse bone marrow MSCs were edited by lentiviral transduction with a dCas9-VPR-Puro vector and single guide RNA to target the BMP9 gene ($MSCs^{BMP9+}$). Cell editing was confirmed by increased gene expression of BMP9 and its targets Alk2, BMPR1 and 2, Hey1 and Dlx5. Calvarial defects 5mm in diameter were created in rats, and after 2 weeks the defects were injected with $MSCs^{BMP9+}$ or MSCs ($5x10^6$ cells in 50mL of PBS/defect), under approval of the Local Committee of Ethics in Animal Research. Four weeks post-injection, the newly formed bone was evaluated by micro-tomography (micro-CT) and the data were compared by Student's t-test ($p< 0.05$, $n=12$). The morphometric parameters generated from 3D-reconstructed micro-CT images indicated that bone volume, percentage of bone volume, bone surface and trabecular number were all higher in defects injected with $MSCs^{BMP9+}$ compared with control MSCs, while trabecular thickness and trabecular separation were lower (Fig. 1). These results indicate that MSCs with CRISPR/Cas9-mediated BMP9 overexpression increase bone repair. Our findings open new therapeutic possibilities for the treatment of bone defects based on genetically edited cells.

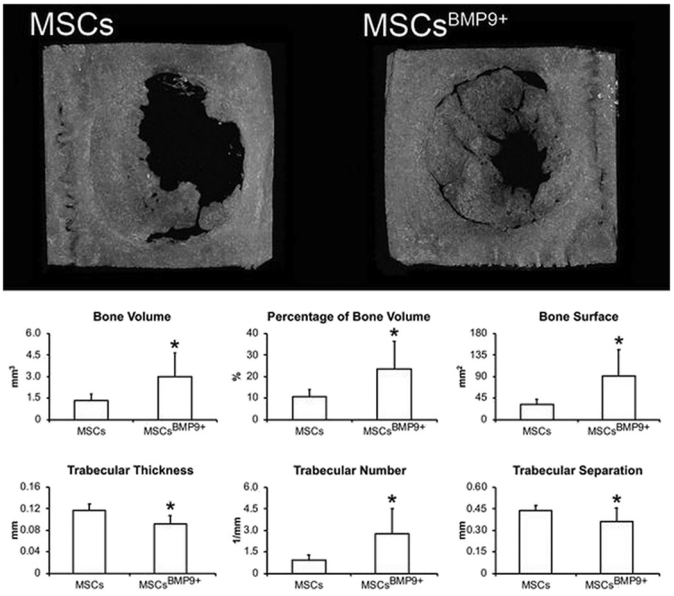

Fig. 1. 3D images and morphometry of bone tissue induced by MSCsBMP9+ and MSCs. * $p<0.05$.

doi:10.1016/j.bonr.2020.100374

P025

3D-printed cobalt-chromium porous metal implants showed enhanced bone-implant interface and bone in-growth in a rabbit epiphyseal bone defect model

Yu Ning Chim[a], Simon Kwoon Ho Chow[a], Sze Yi Mak[b], Michelle Meng Chen Li[a], Bob Ching Hang Yung[b], Edmond Wing Fung Yau[b], Elvis Chun Sing Chui[a]
[a]*The Chinese University of Hong Kong, Hong Kong, China*
[b]*Koln 3D Technology (Medical) Limited, Hong Kong, China*

Introduction: Cobalt-chromium(CoCr) alloys has the advantage over titanium implants in high hardness, wear-resistance, and biocompatibility without the risk of bone growth on the articulating surfaces, ideal for joint

prostheses. Utilization of additive manufacturing (3D-printing) to incorporate porous lattice structures in CoCr implants to enhance bone-implant interface is rarely reported and therefore investigated in this study.

Methodology: 16-weeks-old female rabbits were randomly divided into 3 groups: control (Porosity=0), group A (Porosity=0.25) and group B (Porosity=0.55) at n=3 per group. A 5-mm defect was drilled on the patellofemoral groove and 3D-printed CoCr implants were implanted (Figure 1). *Ex vivo* radiography and non-decalcified histology were performed at end-point of week 8. Bone-implant interface and bone in-growth were evaluated by histomorphometry. ANOVA was used to detect difference between groups with post-hoc Bonferroni test considered at $p< 0.05$.

Results: Bone in-growth were observed in small and large lattice unit group and both with higher bone-implant interface at 918.5 ± 40.3 μm and 590.5 ± 105.4 μm, respectively versus the control group at 218 ± 4.2 μm. Histomorphometry evaluation also showed that group A and B had 1.9 times and 5.2 times higher osteoid area fraction, respectively, compared with the control group.

Discussion and conclusion: Larger lattice units with larger porosity allowed more cavities for osteoid and bone formation in the CoCr implants as demonstrated by enhanced bone-implant interface and osteo-integration versus a solid implant. This study proves the concept and applicability of 3D-printed porous structure in CoCr implant to achieve better bone and implant integration.

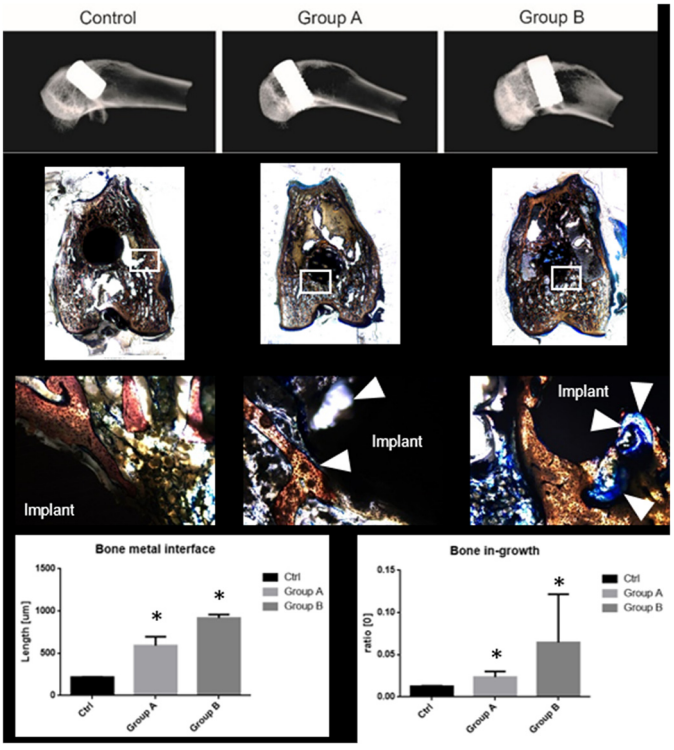

Fig. 1.

doi:10.1016/j.bonr.2020.100375

P026

Bone potential heterogeneity in hBMSCs is associated with their immunomodulatory capacity

Najat Raddi[a], Laura Coquelin[a], Luciano Vidal[b], Sanae Zazou[a], Gabriel Windels[a], Miryam Mebarki[a], Mathieu Manassero[c], Hélène Rouard[a], Nathalie Chevallier[a]

[a]*Unité d'Ingénierie et de Thérapie Cellulaire-EFS, IMRB U955-E10, INSERM, Faculté de Médecine, UITC-EFS, Université Paris-Est, Créteil, France*

[b]*UMR-1238, INSERM, laboratoire « Sarcomes osseux et remodelage des tissus calcifiés », Université de Nantes, Nantes, France*

[c]*B2OA UMR 7052, CNRS, INSERM, Université Paris Diderot; Ecole Nationale Vétérinaire d'Alfort, Université Paris-Est, Paris, France*

Human bone-marrow mesenchymal stromal cells (hBMSCs) associated to biomaterials are currently used in clinic for bone repair. However, their use may be hindered by a donor-dependent heterogeneity for bone formation. To evaluate this heterogeneity cells from 50 donors were amplified and grafted subcutaneously in a mouse model. Our results confirmed that the bone potentials of the cells is donor-dependent with bone gradient going from no to high bone potential. The differences in bone potential was confirmed in an orthotopic model indicating that the ectopic model is relevant to study hBMSCs behaviour. We next wanted to understand the differences which underline this heterogeneity. To do so, we focused on the behaviour of hBMSCs after graft. We observed that hBMSCs with high bone potential were associated with higher cell survival in vivo. In order to understand how cell survival is controlled after graft, a transcriptomic analysis was performed. Our results indicated that 24h after graft the high bone cells are in high metabolic activity whereas low bone cells enter in a bioenergetic crisis and this is associated with a higher neutrophil activity ($p< 0.01$). In order to evaluate whether inflammatory cells are involved in cells survival and cells energetic crisis, we evaluated the bone potential of hBMSCs in mice depleted or not in neutrophils. At 4 and 6 weeks post graft our results showed an increased bone formation by more than 3 times ($p< 0.01$) when low bone hBMSCs were graft in neutrophil-depleted mice. We then confirmed the enhancement of hBMSCs survival in absence of neutrophils. This was significant at 24h ($p< 0.01$) and still visible 2 weeks after graft. In conclusion, our results show that part of hBMSCs heterogeneity is due to their ability to regulate the inflammatory response which has an impact on their survival and therefore their bone potential.

doi:10.1016/j.bonr.2020.100376

P027

Dicalcium silicate modulates differential expression of circRNAs and mRNAs in BMSCs and promotes osteogenesis via circ_1983-miR-6931-Gas7 interaction

Wenchao Zhong[a], Xingyang Li[a], Wei Cao[a,b], Liangjiao Chen[a], Janak L. Pathak[a], Qingbin Zhao[a]

[a]*Key Laboratory of Oral Medicine, Guangzhou Institute of Oral Disease, Affiliated Stomatology Hospital of Guangzhou Medical University, Guangzhou, China*

[b]*Academic Centre of Dentistry Amsterdam (ACTA), Vrije Universiteit Amsterdam and University of Amsterdam, Amsterdam, Netherlands*

Dicalcium cilicate (C_2S) is a potent biomaterial for bone regeneration application. Circular-RNA (circRNAs) plays crucial role in osteogenic differentiation of mesenchymal stem cells (MSCs) and bone defect healing. This study aimed to elucidate the differential expression of circ_RNAs and mRNAs in C_2S-treated MSCs, the role of circ_1983 in C_2S-mediated bone regeneration, and its mechanism. The effect of C_2S on bone marrow-derived MSCs (BMSCs)-derived osteogenesis and rat cranial bone defect healing were analyzed. Differential expression of circ-RNAs and mRNAs in C_2S-treated BMSCs were profiled by RNA-sequencing. The interaction between circ_1983 and miR-6931 was confirmed by pull-down and dual luciferase reporter assays. ceRNA interaction circ_1983-miR-6931-Gas7 in BMSCs was analyzed by miRanda and GO data analysis. Role of circ_1983 in C_2S-induced osteogenic differentiation of BMSCs was analyzed by shRNA-mediated knockdown of circ_1983. Ethical approval for animal study was obtained. The selected significance

level was P< 0.05. C_2S (50 μg/ml) enhanced osteogenic differentiation of BMSCs and bone defect healing. Total 1410 circRNAs and 2246 mRNAs were differentially upregulated in C_2S-treated BMSCs. Upregulated circRNAs and ceRNA-interaction were associated with osteogenesis-related pathways. Circ_1983 was upregulated by 2-fold in C_2S-tretaed BMSCs, and showed ceRNA-interaction circ_1983-miR-6931-Gas7 that enhanced Runx2 expression and promoted osteogenesis. And, this effect was abolished in circ_1983 knockdowned BMSCs. In conclusion, for the first time, we reported the role of cicr_1983-miR-6931-Gas7 ceRNA-interaction in C_2S-induced osteogenic differentiation of BMSCs and bone defect healing. This study opens a new research stream "the role of circRNAs-mediated ceRNA-interaction in biomaterials and stem cell-based bone tissue engineering".

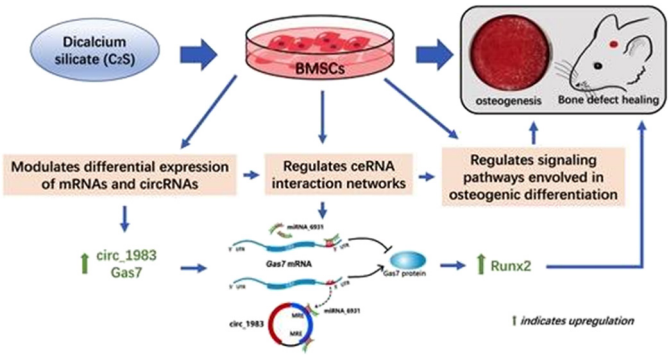

Scheme showing the role of C2S on bone regeneration and its mechanism.

doi:10.1016/j.bonr.2020.100377

P028

Mineral composition of the skeletal bones after tibia fracture modeling and intravenous injection of mesenchymal stem cells at early stage of bone regeneration

Ekaterina Zinchenko, Vladyslav Luzin, Dmitry Astrakhantsev, Nadezhda Mosyagina
State Establishment of Lugansk People's Republic Saint Luka Lugansk State Medical University, Lugansk, Ukraine

Aim: Of the study is to test chemical composition of the bones in rats after tibia fracture modeling and IV injection of mesenchymal stem cells (MSC) at early stage of bone regeneration

Material and methods: The experiment involved 105 adult rats distributed into the groups like the following: group A consistedted of intact animals, group B comprised animals with 2 mm holes in both tibiae, and in group C animals with the same tibia injury received intravenous MSC in dosage of $5x10^6$. For testing purposes we selected humerus, hipbone, and L3 vertebra. Testing of bone mineral was performed by means of weighing.

Results: Fracture modeling leads to instability of mineral composition in undamaged bones observed mostly in the period from the 7th to the 60th day of the experiment. Manifestations peak was observed by the 30th day. In the group C in comparison with the group B share of organic substances in the hipbone was higher by 3.55%, 6.67%, 4.59% and 3.60% (in the period from the 15th up to the 90th day); in the vertebra the same values were higher than those of group B by 3.29%, 5.13% and 5.09% (in the period from the 15th up to the 60th day) and in the humerus by 3.46% by the 30th day. Further, in comparison with the group B in the hipbone and the vertebra minerals share increased by 3.77% and 3.80%, and 3.40% and 5.98% respectively (both by the 30th and the 60th days) and in humerus - by 3.61% and 3.50% by the 60th and 90th days.

Conclusion: Administration of MSC on the 3rd day after fracture-modeling results in two-phase changes of mineral composition in undamaged bones: imbalance grows up to the 15th day and from the 15th day up to the 90th day it exhibits rapid restoration.

doi:10.1016/j.bonr.2020.100378

P029

The effects of tibia fracture and intravenous stem cells injected at the first stage of bone regeneration on morphology of the adrenal glands

Irina Solovyova, Vladyslav Luzin, Yuliya Venidiktova, Natal'ya Zabolotnaya
State Establishment of Lugansk People's Republic Saint Luka Lugansk State Medical University, Lugansk, Ukraine

Aim: Of the study is to test adrenal glands (AG) morphology changes after tibia fracture modeling and intravenous injection of mesenchymal stem cells (MSC) at the first stage of osteoreparation.

Material and methods: 90 male rats with the body weight of 190-225 grams were distributed into three groups like the following: group 1 - controls, group 2 - animals with tibia fracture (modeled as 2.2 mm reach-through round hole between proximal metaphysic and shaft), and group 3 for the animals with the same tibia fracture that received intravenous injections of 5 million MSC per injection. Bone marrow cells previously sampled from the tibia were placed into Eagle's MEM with L-glutamine and 10% bovine embryonic serum and antibiotic and were cultured and phenotyped according to standard methods. Upon expiration of observation terms (7, 15, 30, 60 and 90 days) the animals were withdrawn from the experiment; the AG were excised and measured by means of sliding calipers.

Results: In animals with fracture volume of the AG was bigger than that of the group 2 by 8.32%, 13.28%, 12.72%, and 7.32% (with respect to the period from the 7th to the 60th day), which may testify for compensatory hypertrophy. In animals with fracture that received MSC bigger volume of the AG (by 6.77% in comparison with group 2) was found only by the 7th day while in the period from the 15th to the 60th days volume values decreased by 5.86%, 9.34% и 7.67% respectively. This may be an evidence of faster restoration of the AG functionality under influence of stem cells.

Conclusion: Injury to the tibia results in hypertrophy of the AG observed nearly throughout the whole observation period, while MSC reduce effects of fracture on the AG, which is well observed from the 15th up to the 60th day.

doi:10.1016/j.bonr.2020.100379

P030

Bone tissue engineering: A bioelectronics approach

Donata Iandolo[a,b], Jonathan Sheard[c], Galit Katarivas Levy[d], Charalampos Pitsalidis[b], Francesca Santoro[e], Athina E. Markaki[d], Darius Widera[c], Róisín M. Owens[b]
[a]*INSERM U1059, Saint-Priest-en-Jarez, France*
[b]*Department of Chemical Engineering and Biotechnology, University of Cambridge, Cambridge, United Kingdom*
[c]*School of Pharmacy, University of Reading, Reading, United Kingdom*
[d]*Department of Engineering, University of Cambridge, Cambridge, United Kingdom*
[e]*CABHC@CRIB, Napoli Istituto Italiano di Tecnologia, Naples, Italy*

Osteoporosis is a skeletal disease characterized by bone loss and bone microarchitectural deterioration. The increasing life expectancy calls for innovative and effective approaches to compensate for bone

loss.[1] Due to their well-documented regenerative and anti-inflammatory potential, stem cells represent a promising option. The knowledge of bone piezoelectricity and of bioelectricity as a further cue to influence cell fate, in addition to biochemical and mechanical ones, has elicited for the use of physical stimulation together with electroactive materials as smart alternatives for bone tissue engineering.[2-4] The combination of smart substrates, stem cells and physical stimulation to induce cell differentiation is therefore a new avenue in the field. Biomimetic scaffolds were prepared by combining the conducting polymer PEDOT:PSS with collagen type I, the most abundant protein in bone. Pores sizes, mechanical and impedance properties were measured as a function of scaffold composition. Two populations of stem cells, namely human adipose-derived stem cells and neural crest-derived stem cells were used to understand the impact of scaffold composition on cell behaviour. Osteogenic differentiation studies were run for 21days and the different compositions were assessed for their impact on stem cell fate. SEM coupled with FIB was used as a powerful tool to look into the fine interaction between material and cells, highlighting an intimate contact of the cells lining the pores walls.

Preliminary electrical stimulation experiments were run using human adipose-derived stem cells and the adopted capacitive coupling protocol proved to positively affect stem cell osteogenic differentiation with an increase in the mineralised matrix deposited by cells at d21 after 4 days of electrical stimulation.

doi:10.1016/j.bonr.2020.100380

P031

Impact of a caspase inhibitor on alveolar shape changes following tooth extraction

Uwe Yacine Schwarze[a,b,c], Franz Josef Strauss[b,d], Reinhard Gruber[b,c,e]
[a]*Department of Dental Medicine and Oral Health, Department of Orthopaedics and Trauma, Medical University of Graz, Graz, Austria*
[b]*Department of Oral Biology, Medical University of Vienna, Vienna, Austria*
[c]*Austrian Cluster for Tissue Regeneration, Vienna, Austria*
[d]*Department of Conservative Dentistry, School of Dentistry, University of Chile, Santiago, Chile*
[e]*Department of Periodontology, School of Dental Medicine, University of Bern, Bern, Switzerland*

Background: Controlling resorption of the alveolar bone following tooth extraction is a challenge in implant dentistry. Accumulating evidence suggests that dying osteocytes induced the formation of bone-resorbing osteoclasts. Thus, blocking apoptosis might reduce resorption of the alveolar bone following tooth extraction.

Methods: To test this hypothesis, we extracted the first and second molar on each contralateral site of the mandible using 16 inbred rats. Rats received a cell permeable pan caspase inhibitor or the diluent for 9 days. We evaluated the shape change of the alveolar ridge with geometric morphometrics and the height of the alveolar ridge by linear measurements.

Results: Principle component analysis of geometric morphometrics data revealed a complete separation of the group suggesting that the pan caspase inhibitor caused significant shape changes of the alveolar bone. Linear measures showed that the pan caspase inhibitor reduced the resorption of the alveolar bone following tooth extraction on position M1 compared to the diluent controls (-0.24 mm versus -0.53 mm; $p=0.002$). There was no considerable resorption of the alveolar bone on position M2.

Conclusion: Resorption of the alveolar bone following tooth extraction is partially controlled by apoptotic mechanisms.

doi:10.1016/j.bonr.2020.100381

P032

Engineered extracellular matrix enhances the bone regeneration potential of aged human bone marrow stromal cells

Dominik Hanetseder, Tina Levstek, Heinz Redl, Darja Marolt Presen
Ludwig Boltzmann Institute for Experimental and Clinical Traumatology, Austrian Cluster for Tissue Regeneration, Vienna, Austria

Introduction: Regeneration of bone defects in elderly patients is limited due to the decreased function of bone forming cells and compromised tissue physiology. Previous studies suggested that the regenerative capacity of stem cells from aged tissues can be enhanced by exposure to young systemic and tissue microenvironments. We investigated whether extracellular matrix (ECM) engineered from human induced pluripotent stem cells (hiPSCs) can enhance the bone regeneration potential of aged human bone marrow stromal cells (hBMSCs).

Methods: ECM was engineered *in vitro* from hiPSC-derived mesenchymal progenitors (hiPSC-MPs), as well as young (< 30 years) and aged (>70 years) hBMSCs. ECM structure and composition were characterized before and after decellularization (immunofluorescence, biochemical assays). Growth and differentiation responses of BMSC strains (female 20 and 71 years, male 89 years) on ECMs were compared to tissue culture plastic, as well as to collagen and fibronectin coatings.

Results: Decellularized ECMs contained collagens type I and IV, fibronectin, laminin and < 5% residual DNA, suggesting efficient cell elimination. Cultivation of hBMSCs strains on the hiPSC-ECM in osteogenic medium significantly increased hBMSC growth (days 5 to 42) and osteogenesis, including collagen deposition (day 21), alkaline phosphatase activity (day 21), bone sialoprotein expression (day 21) and matrix mineralization (day 42) compared to plastic controls ($p< 0,05$). In aged BMSCs, matrix mineralization (Alizarin stain, calcium content) was only detected in ECM cultures in osteogenic medium. Comparison of ECMs engineered from hiPSC-MPs and hBMSCs of different ages suggested similar structure, composition and potential to enhance osteogenic responses in aged BMSCs.

Conclusions: Our studies suggest that aged BMSCs regenerative activity can be enhanced by culture on engineered ECM. Contribution of ECM components and underlying mechanisms need to be further elucidated. hiPSCs represent a scalable cell source, and tissue engineering strategies employing engineered ECM could potentially enhance bone regeneration in elderly patients.

doi:10.1016/j.bonr.2020.100382

P033

Novel autologous bone graft substitute containing rhBMP6, autologous blood coagulum and bioceramics in a rabbit posterolateral lumbar spine fusion study

Nikola Štoković[a], Natalia Ivanjko[a], Marko Pećin[b], Igor Erjavec[a], Ana Smajlović[b], Hrvoje Capak[b], Jadranka Bubić Špoljar[c], Dražen Vnuk[b], Dražen Matičić[b], Slobodan Vukičević[a]
[a]*Laboratory for Mineralized Tissues, University of Zagreb School of Medicine, Scientific Center of Excellence for Reproductive and Regenerative Medicine, Zagreb, Croatia*
[b]*University of Zagreb School of Veterinary Medicine, Zagreb, Croatia*
[c]*University of Zagreb School of Medicine, Zagreb, Croatia*

The aim of this study was to investigate ectopic bone formation and osseointegration in the posterolateral spinal fusion (PLF) model in New Zealand white rabbits using a novel innovative autologous bone graft substitute (ABGS) containing recombinant human Bone Morphogenetic Protein 6 (rhBMP6), autologous blood coagulum

(ABC) and tricalcium-phosphate (TCP) or biphasic (composed of 80% TCP and 20% hydroxyapatite) granulate bioceramics as compression resistant matrix (CRM). Blood samples were collected from rabbit ear marginal vein into tubes without an anticoagulant substance in a volume of 2500 µl. rhBMP6 (125 µg) was mixed with blood and bioceramics. The ABGS implants (n=6 per group) were implanted bilateraly between tranverse processes of the lumbar vertebrae L5-L6 following exposition and decortication of transverse processes. All animals were euthanized on day 50 after surgery. To visualize new ectopic bone formation, lumbar spine was scanned by µCT. The success of spinal fusion was analysed on µCT sections through the anterior and posterior transverse process. Furthermore, lumbar spine was palpated and the mobility of fused transverse processes was tested. Total fusion success rate was 90,9% and the same result was obtained by both analysis of spinal fusion on µCT sections and by palpatory mobility testing. µCT analyses revealed that an extensive amount of newly formed bone was present in both experimental groups and that there was no significant difference (p>0,05) among experimental groups regardless the type of bioceramics used (biphasic bioceramics vs tri-calcium phosphate bioceramics). Bone formation and osseointegration were confirmed on histological sections through newly formed bone between transverse processes. Successful spinal fusion between adjacent transverse processes was confirmed radiologically, by palpatory segmental mobility test and on histological sections. Therefore, an ABGS containing rhBMP6, ABC and bioceramic granulate might be an innovative and original biological approach for achieving a successful lumbar spine fusion.

doi:10.1016/j.bonr.2020.100383

P034

Effects of modified and bone surface mimicked PDMS membranes and protein modifications on osteoblast cell behaviour

Sedat Odabas[a], Berkay Erenay[b], Bora Garipcan[b]
[a]Chemistry Department Faculty of Science, Ankara University, Ankara, Turkey
[b]Institute of Biomedical Engineering, Boğaziçi University, Istanbul, Turkey

Bone tissue engineering is considered to be a sustainable alternative to regular bone grafting procedures. In this study, bone surface mimicked (BSM) PDMS membranes were produced and modified with extracellular matrix proteins, such as Fibronectin (FN) and Collagen-I (Col-I) to investigate the effects of topography and modification on cell proliferation. Here, bone surface topography was transferred onto PDMS membranes using soft lithography. Negative molds were sputter coated with gold and these negative patterns were once more transferred onto PDMS membranes to obtain positive surface topography. These surfaces were chemically modified with FN and Col-I to further mimic bone tissue microenvironment. To evaluate cell proliferation andmorphology; alamarBlue cell proliferation assay and F-actin/DAPI stainings were performed on adherent cells (Human fetal osteoblast) on Plain and BSM PDMS membranes. Results showed that, BSM membranes increased cell proliferation on both protein modifications. Col-I coated plain membranes had increased proliferative capability compared to FN coated ones. Both Col-I coated membranes reached confluency between days 7 and 14. Comparing their day 7 data shows, cells proliferation on BSM membranes are significantly increased (Plain FN PDMS membranes were behind this trend and BSM FN PDMS membranes are significantly different than plain membranes on day 21 ($P< 0.01$). Col-I coated PDMS membranes being more proliferative than FN coated ones already reported in literature. Our study shows that the increased roughness resulted from pattern transfer of bone surface under periosteum, along with Col-I protein modifications, which is abundant inside natural bone matrix significantly increased cell growth and resulted in more natural filament organization and behavior.

doi:10.1016/j.bonr.2020.100384

P035

Monitoring bone ingrowth after implantation of magnesium alloy implants: Longitudinal microCT in vivo data from the MgBone study

Timo Damm[a], Olga Will[a], Jana Humbert[a], Mirko Gerle[b], Claus-C. Glüer[a]
[a]Department of Biomedical Imaging, Clinic of Radiology, University-Hospital Schleswig-Holstein, Kiel, Germany
[b]Department of Oral and Maxillofacial Surgery, University-Hospital Schleswig-Holstein, Kiel, Germany

Introduction: Magnesium alloy bone implants degrade in vivo, turning them into an attractive implant material because it may obviate the need for a second surgery for implant removal. Alloy composition is essential to optimize the degradation process: Detrimental side effects like gas formation can be avoided. Optimal degradation rate should neither be too fast (before bone stability in the healing process is achieved) nor too slow (to return to a normal bone within a reasonable time period). Importantly, it has been reported that Mg may exert an osteoinductive effect which would support the bone healing process. In order to study these aspects in vivo we performed longitudinal µCT imaging.

Methods: Bone implant screws made of Mg5Gd and Mg10Gd are implanted into 16 rats. µCT scans with 26µm voxel size were acquired directly post-OP and at week 1, 4, 8, 14 and 18. Evaluation is performed in equidistant shells around the implant´s central axis to study both the degradation and the bone healing adjacent to the implant. Since x-ray absorption of magnesium alloys elements cannot be differentiated from bone related absorption directly, results are expressed as bone mineral comtent or density equivalent units (BMCe or BMDe).

Results: For the implant cores, we calculate degradation rates of (-0.021±0.012)BMCe/week and (0.002±0.011) BMCe/week (ns), whereas for the first hollow cylinder ring adjacent to the thread we find highly significant rates of (0.240±0.023) BMCe/week and (0.219±0.020) BMCe/week for Mg5Gd and Mg10Gd.

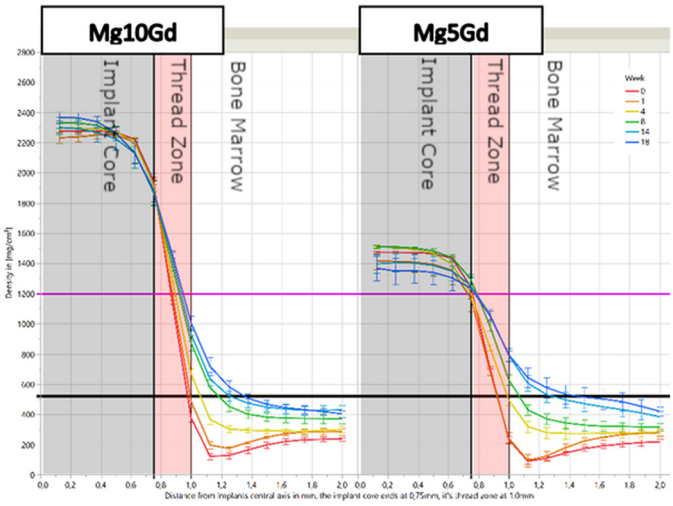

Fig. 1. Colorcoded temporal change of BMD over distance from the implant's center axis in mgHA/cm³.

Conclusion: A strongly positive net apposition with strongest gain at implant´s surface was observed.

doi:10.1016/j.bonr.2020.100385

P036

Tissue engineered scaffolds for mimetic autografts

Juan Antonio Romero-Torrecilla[a], Luis Riera[b], José Valdés-Fernández[a], Tania López-Martínez[a], Purificación Ripalda-Cemboráin[a], Vineetha Jayawarna[c], Peter Childs[c], Manuel Salmerón-Sánchez[c], Felipe Prósper-Cardoso[a], Froilán Granero-Moltó[a]
[a]*Terapia Celular, Clínica Universidad de Navarra, Pamplona, Spain*
[b]*Orthopedic Surgery and Traumatology, Clínica Universidad de Navarra, Pamplona, Spain*
[c]*Biomedical Engineering, University of Glasgow, Scotland, United Kingdom*

Introduction: Despite its regenerative capacity, bone healing can be compromised, leading to delayed fracture regeneration and nonunion. Due to the scarcity of bone tissue that can be used as autograft, novel tissue engineering strategies arise as a promising solution by using biocompatible materials.

Methods: Our objective is the development of engineered autografts capable of efficiently treat fracture nonunion. For this purpose, we designed polycaprolactone (PCL) autografts surrounded by a porous membrane mimicking periosteum. To assess their regenerative capacity, these scaffolds were tested in critical size femur defect for ten weeks carrying out μCT and histological analysis. Additionally, we are focusing on the generation of PCL biocomposites, such as poly ethyl-acrylate (PEA) covered PCL membranes which can enhance morphogen functionalization, reducing the effective BMP dose.

Results: At the mCT level, structural mimetic PCL scaffolds, showed no significant difference in bone healing (Empty group, 11.47±4.93 mm^3; MA, 14.95±3.09 mm^3, p=0.1711). Histological analysis demonstrates that MEW PCL mimicking periosteum enhances bone growth, but insufficient for successful healing. However, once functionalized with PEA and BMP-2, these implants showed highly improved regeneration (CTL group, 11,47±4,93 mm^3; BMP-2 group, 49,24±13,20 mm^3, p = 0.0001). Figure 1. These implants were loaded with BMP-2 solutions previously studied in vitro to estimate morphogen dose, which resulted in 55.64±14.83 ng (n=6).

Conclusions and discussion: In conclusion, PEA functionalized mimetic autografts show an important increase in bone healing, enhancing BMP-2 effects, which provide representative regeneration with a 100 folds lower dose than typically described in literature.

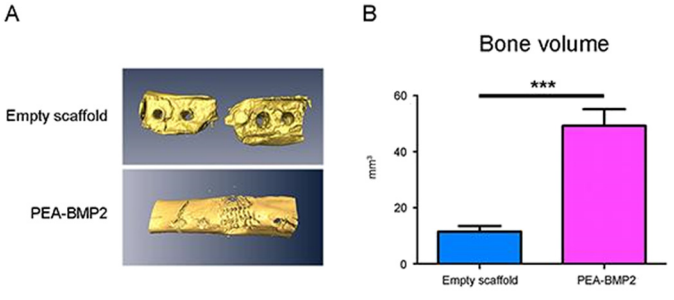

Figure1. A) 3D bone reconstruction from μCT analysis data of empty critical size femur defect and treated with PEA-BMP2 coated PCL scaffold using 10ug/ml morphogen solution. B) BMP2 treatment along with PEA coated PCL scaffolds significantly increases bone volume formed in these critical size defects (p = 0.0001,***).

doi:10.1016/j.bonr.2020.100386

P037

Mechanical impact of X-ray- and gamma-irradiation on the mechanical parameters of cortical human bone

Felix N. Schmidt[a], Kilian E. Stockhausen[a], Michael Hahn[a], Tim Rolvien[a,b], Christian Schulze[c], Klaus Püschel[d], Michael Amling[a], Björn Busse[a]
[a]*Department of Osteology and Biomechanics, University Medical Center Hamburg-Eppendorf, Hamburg, Germany*
[b]*Department of Orthopedics, University Medical Center Hamburg-Eppendorf, Hamburg, Germany*
[c]*Institute for Synaptic Physiology, Center for Molecular Neurobiology Hamburg, Hamburg, Germany*
[d]*Department of Forensic Medicine, University Medical Center Hamburg-Eppendorf, Hamburg, Germany*

For very high dosages of dozens of kGy, X-ray- and gamma-irradiation is known to cause a mechanical degradation of the mineralized bone tissue. Both in clinical and research applications, bone can be subject to many different sources of irradiation. However, data about the influence of irradiation on the mechanical properties of bone at dosages of clinical applications are lacking. Hence, we investigated the influence of irradiation in clinical relevant dosages on the mechanical parameters of bone with respect to material parameters and crack characterization.

Beam-shaped bone samples were irradiated at dosages of mGy, Gy and kGy and subsequently tested via three-point-bending. Additionally, to quantify the cracking behavior, tomographic fractometry was carried out to quantify the fracture surface.

Our results of the mechanical investigation point to a severe decrease of the mechanical performance at high dosages of 31.2 kGy quantifying the work to maximum stress (control: 39.98 ± 9.22 Nmm vs. 31.2 kGy: 12.75 ± 1.76 Nmm, $p < 0.05$) whereas no changes in mechanical parameters were detected for 30 Gy, 0.008 Gy and 6.4 mGy (44.15 ± 9.53 Nmm, 35.27 ± 7.17 Nmm and 41.01 ± 7.94 Nmm $p > 0.05$). These results are supported and in agreement with the fracture surface texture with a more tortious crack surface in the control group (control: 1.51 ± 0.15, 1.310 ± 0.086, $p < 0.005$).

Our findings suggest that synchrotron imaging (utilizing dosages of several kGy) does severely alter the mechanical properties of the bone material. Effects of synchrotron irradiation need to be considered in the bone quality framework. Clinically relevant radiation dosages of 30 Gy and less do not alter the mechanical behavior of bone primarily.

doi:10.1016/j.bonr.2020.100387

P038

Osteogenic potential of periodontal cells is dependent on Notch signaling

Polina Klauzen, Natella Enukashvili, Anna Malashicheva
Laboratory of Regenerative Biomedicine, Institute of Cytology, Russian Academy of Sciences, Saint-Petersburg, Russian Federation

Periodontal ligament stem cells (PDLSC) represent a perspective resource for regenerative medicine. Notch is an important signaling participating in embryonic patterning and in particular in osteogenesis. The role of Notch in osteogenesis is not defined. In this work, we sought to find out how Notch signaling affects osteogenic potential of periodontal ligament stem cells (PDLSC).

We activated Notch in PDLSC by addition of various amounts of lentiviruses bearing activated intracellular domain of the Notch1 receptor, NICD. Using real-time PCR, we analysed the dependence of changes in the expression levels of osteogenic markers (*RUNX2, COL1A1, OGN, POSTN*). Activation of Notch was confirmed by expression of Notch target gene *HEY1*. To quantify the intensity of mineralization of

periodontal MSCs at the final stage of osteogenic differentiation we used Alizarin red extraction technique.

We demonstrate that activation of Notch signaling leads to an increased expression of osteogenic markers at early stages of osteogenic induction of PDLSC, which in turn leads to the development of the final stage of osteogenic differentiation, characterised by the formation of calcium deposits. Moreover, the more intensive the initial level of Notch was, the stronger and more effective were the processes of osteogenesis.

In conclusion, activation of Notch signaling leads to an increase of the osteogenic potential of periodontal ligament stem cells in a dose-dependent manner. Thus Notch is able to modulate osteogenic differentiation of these cells affecting its effectiveness, apparently due to the strength of the signal that is transmitted to the cells.

doi:10.1016/j.bonr.2020.100388

P039

Sinus floor elevation using a new bovine bone grafting material: Case report

Gretel Pellegrini[a], Andrea S. Mattiuzzi[b], Miguel A. Pellegrini[c], Luis A. Corso[b], Cintya P. Contreras Morales[b], Elizabeth Arandia Osinaga[b], Susana N. Zeni[a,d]

[a]*Institute of Immunology, Genetics and Metabolism - Osteopathies Laboratory, CONICET, Buenos Aires, Argentina*

[b]*Department of Clinical Operative and Prosthesis II, University of Buenos Aires, School of Dentistry, Buenos Aires, Argentina*

[c]*INIGEM (UBA/CONICET), Buenos Aires, Argentina*

[d]*Department of General and Oral Biochemistry, University of Buenos Aires, School of Dentistry, Buenos Aires, Argentina*

Bone grafting aims to preserve the alveolar bone ridge height and volume for dental implant placement. While implant-supported overdentures present successful outcomes, the cost of the treatment attempts against its acceptance. The purpose of this case report is to provide preliminary clinical evidence of the efficacy of a new bovine bone graft [Synergy Bone Matrix (SBM), Odontit Implant Systems, Argentine] in the bone healing process when used for sinus floor elevation. A 54-year-old female with edentulous maxilla was referred to the Department of Clinical Operative and Prosthesis, Dental School, University of Buenos Aires, Argentine for rehabilitation. Bilateral sinus lifting and guided bone regeneration were performed using SBM. CBCT scans and panoramic x-rays were obtained at T=0, 6 months after the bone grafting (T1) and 4 months after placing dental implants (T2). A biopsy of each treated area was taken during the implant surgery. No discomfort, pain or inflammation was reported. Post-operative CBCT (T2), exhibited increase in the alveolar crest height (10.7 mm and 10.8 mm) and width (3.5 mm and 2.8 mm) in the right and left side, respectively. Dental implants achieved primary stability, indicating that there was an accurate bone quality after SBM placement. Histological evaluation showed that SBM particles were osteoconductive. All particles were surrounded by new bone formation. The bone formation pattern was lamellar and trabecular, and osteoblasts at the surface of the trabeculae, as well as osteocytes, were also observed. This is the first study that provides clinical and histological evidence of the efficacy of SBM in the healing process of alveolar bone when used for sinus floor elevation. This results evidence that SBM is biocompatible and osteoconductive. Comparative studies with greater number of patients and histomorphometrical analysis are needed to assess the survival of implants placed in sinuses grafted with SBM.

doi:10.1016/j.bonr.2020.100389

P040

A biomechanical study of the role of sitagliptin on the bone characteristics of diabetic rats

Arezoo Abdi[a], Ermioni Pasiou[b], Stavros Kourkoulis[b], Despina Perrea[a], John Vlamis[a]

[a]*Medical School, National and Kapodistrian University of Athens, Athens, Greece*

[b]*Unit of Biomechanics, National Technical University of Athens, Athens, Greece*

Sitagliptin is an antidiabetic drug that prolongs the action of incretin hormones by inhibiting the action of DPP-4 and seems to have protective effects to the bone. We tried to further elucidate elements of the relationship between sitagliptin and bone metabolism.

28 adult male Wistar rats were divided in three groups. Group 1 was the control group (n=8), group 2 was be the control diabetic group (n=8) and group 3 was the diabetic- sitagliptin group (n=12). Groups 2,3 were rendered diabetic with the use of a fructose/streptozotocin protocol. After confirming diabetes, Group 3 started receiving sitagliptin per os (10 mg/kg/day) and after 5 weeks their right femurs were harvested and sent for mechanical testing (three-point bending test). Their blood serum was tested for basic bone biomarkers. All experiments were approved by the National Bioethics Council of the Greek Ministry of Education.

The cross-sectional area of the diabetic femora was comparatively smaller and thinner than the control group. Surprisingly, both the cross-sectional area and the thickness of the animals treated with sitagliptin were even smaller compared to the diabetic group. The diabetic femora were more brittle than the control ones (deflection 13% smaller p=0,04) and the treatment with sitagliptin did not reverse the effect. Concerning the maximum load, the diabetic femora sustained larger (7% p=0,04) load compared to the maximum load sustained by the control femora and the maximum load recorded for the sitagliptin group was only slightly (1.5% p) higher. The ELISA results suggested a smaller expression of osteocalcin (p=0,008) in the sitagliptin group and no statistically significant differences in TRAP-5 and in GLP-1 expression.

This data suggests a reduced bone turnover rate in the diabetic group that is not reversed by the sitagliptin treatment. Anti-diabetic treatment may further reduce bone turnover, thus protecting bone from age related brittleness.

doi:10.1016/j.bonr.2020.100390

P041

A comparison, using Micro-CT, of the architecture of cancellous bone from the cervical, thoracic and lumbar spine using 480 vertebral bodies from 20 body donors

Guido Schröder[a], Laura-Marie Vivell[b], Sven Spiegel[b], Reimer Andresen[c], Claus Maximilian Cullen[c], Andreas Wree[d], Marko Schulze[e], Olga Sahmel[f], Heiner Martin[f], Hans-Christof Schober[g]

[a]*Internal Medicine, Municipal Hospital Acedemic Teaching Hospital University of Rostock, Rostock, Germany*

[b]*University of Rostock, Rostock, Germany*

[c]*Institute of Diagnostic and Interventional Radiology/Neuroradiology, Westkuestenklinikum Heide, Academic Teaching Hospital of the Universities of Kiel, Luebeck and Hamburg, Heide, Germany*

[d]*Institute of Anatomy University of Rostock, Rostock, Germany*

[e]*Institute of Anatomy, Univerity of Rostock, Rostock, Germany*

[f]*University of Rostock, Institute for Biomedical Engineering, Rostock-Warnemünde, Rostock, Germany*

[g]*Municipal Hospital Acedemic Teaching Hospital University of Rostock, Rostock, Germany*

Introduction: Structure of vertebral column alters with increasing age. Material and structural properties are both important for bone strength.Despite having numerous data from thoracic and lumbar spine (TS and LS), there is a paucity of data from cervical spine (CS) relating to these parameters. We examined bone cylinders from the centres of vertebral bodies C1 to L5 from elderly subjects with respect to their bone volume (BV/TV), trabecular thickness (Tb. Th.), separation (Tb.Sp.), trabecular orientation (SMI) and degree of anisotropy (DA).

Methods: 480 core samples (Jamshidi needle 8G) were stabilised in wet gauze and prepared in 1.5ml Eppendorf reaction vessels. The examination was made using a μ-CT (SKYSCAN 1172, RJL Micro &Analytic Company, Germany). A flat field correction, and generation of phantoms (reference), with density of 0,25 g/cm^{3}and 0,75 g/cm^{3}was carried out. This study received the approval of the ethics committee of the University of Rostock(Nr. A 2017-0072).

Data was analysed using SPSS, Version 24.0 (SPSS Inc., Chicago, USA). Comparisons between the groups utilized the Kruskal-Wallis test, followed by a pairwise comparison.The Shapiro-Wilk-test was used to test for normal distribution.

Results: BV/TV (%;M±SD) for CS: 25.45±2.30; TS:18.13±1.38; LS:16.25±0.60.

Regarding BV/TV ($p< 0.001$), Tb.Th. ($p=0.001$), Tb.Sp. ($p< 0.001$), SMI ($p< 0.001$) there were statistically significant differences between the segments of the vertebral column..A pairwise comparison yielded the following: BV/TV, CS vs. TS, $p=0.010$, CS vs. LS, $p< 0.001$. Tb.Th., CS vs. TS, $p=0.045$, CS vs. LS, $p< 0.001$,; Tb.Sp., CS vs. TS, $p=0.004$, CS vs. LS, $p=0.001$; SMI, CS vs. TS, $p=0.006$, CS vs. LS, $p< 0.001$. Between TS and LS there were no differences.

Conclusion: Cervical vertebrae have a unique microarchitecture which gives them their strength. Specifically, this entails a higher BV/TV, Tb.Th. and lower Tb.Sp. In addition, the SMI demonstrates more plates than rods.

doi:10.1016/j.bonr.2020.100391

P042

Analysis of cortical bone quality in long-term bisphosphonate users with atypical femur fracture (AFF)

Delphine Farlay[a], Sébastien Rizzo[a], Louis-Georges Ste-Marie[b], Laetitia Michou[c], Suzanne N. Morin[d], Shijing Qiu[e], Roland Chapurlat[a], Sudhaker D. Rao[e], Jacques Brown[c]

[a]*INSERM, UMR 1033, Univ Lyon, Université Claude Bernard Lyon 1, Lyon, France*

[b]*Université de Montreal, Montreal, Canada*

[c]*Division of Rheumatology, Department of Medicine, CHU de Québec-Université Laval, Quebec City, Canada*

[d]*McGill University, Montreal, Canada*

[e]*Bone & Mineral Research Laboratory, Henry Ford Health Syste, Detroit, United States*

Purpose: Atypical Femur Fractures (AFF) are associated with long-term bisphosphonates (BPs) therapy, but it is unclear if cortical bone quality is altered in AFF. Accordingly, we analyze cortical bone quality in BPs-treated patients with or without AFF.

Material and methods: Two groups of 26 transiliac bone biopsies from postmenopausal women treated with BPs with AFF and without AFF were analyzed. Histomorphometry revealed low remodeling in all patients. Degree of mineralization of bone (DMB) and heterogeneity index (HI) of mineralization were measured using digitized microradiography. Microhardness (Hv) was calculated with a Vickers microindenter. Quality of mineral phase and organic matrix were assessed using Fourier transform infrared microspectroscopy (FTIRM). Mann-Whitney and Spearman correlation tests were performed.

Results: Women with AFF were treated significantly longer (9.7±3.3yrs) than women without AFF (7.9±2.7yrs, $p=0.026$). Cortical DMB was significantly higher in AFF than in non-AFF ($p=0.001$) and HI was significantly lower ($p=0.050$) implying a denser and more homogeneous cortical bone in AFF vs non-AFF. Increase in cortical DMB persisted even after adjustment for treatment duration ($p=0.007$). Hv and quality of mineral phase and organic matrix (FTIRM) were not modified. Cortical DMB was positively correlated with treatment duration ($r'=0.468$; $p< 0.020$) in AFF group only. In contrast, denosumab, a more potent antiresorptive, lead to higher cortical DMB and lower HI as reported by us with the same methodology in 2-3 years denosumab treated women (Dempster et al. JCEM, 2018). However, Hv was significantly increased (unpublished) leading to beneficial effect on bone resistance.

Conclusions: Cortical DMB was higher and HI lower in AFF than in non-AFF, but these results do not appear to be solely due to a lower bone turnover in AFF. Therefore, the combination of a higher DMB (and lower HI) and absence of higher hardness could explain the propensity for AFF in long-term BP users.

doi:10.1016/j.bonr.2020.100392

P043

Local adaptation of bone micro-structure and canal network to tendon insertion investigated by image-based micro-FE simulations

Alexandra Tits[a], Peter Varga[b], Jean-François Kaux[c], Erwan Plougonven[d], Justin Fernandez[e], Pierre Drion[f], G. Harry Van Lenthe[g], Davide Ruffoni[a]

[a]*Department of Aerospace and Mechanical Engineering, University of Liège, Liège, Belgium*

[b]*AO Research Institute Davos, Davos, Switzerland*

[c]*Department of Physical Medicine and Sports Traumatology, University of Liège, Liège, Belgium*

[d]*Chemical Engineering Department, University of Liège, Liège, Belgium*

[e]*Auckland Bioengineering Institute, Auckland, New Zealand*

[f]*Department of Biomedical and Preclinical Sciences, University of Liège, Liège, Belgium*

[g]*Department of Mechanical Engineering, KU Leuven, Leuven, Belgium*

Tendons anchor to bone through a multi-material region called enthesis, showing several strategies to cope with the challenging task of joining dissimilar tissues. Less understood is whether bone microstructure also displays specific features to facilitate force transmission from tendon to bone. Such knowledge is of clinical relevance as local mechanical stresses play a crucial role in avulsion fractures and interface pathologies.

Here we characterized the microstructure of bone close to tendon insertion in calcanei of adult rats ($n=5$) with micro-computed tomography (SkyScan, Bruker; 5 to 1.2 micrometer voxel size). After aligning the virtual bones along the main axes of inertia, we investigated a bony tuberosity connecting the Achilles tendon with the plantar fascia ligament. We performed a spatially resolved analysis of trabecular microstructure, indicating that trabecular network (BV/TV and anisotropy) is not significantly influenced by the tendon insertion ($P = 0.69$). Conversely, high resolution images revealed that bone beneath the attachment region exhibits a highly oriented canal network, aligned with the pulling direction of the tendon ($P < 0.005$). Image-based micro-finite element analysis was used to calculate stresses within the bone induced by tendon loading. Simulations highlighted a non-trivial stress pattern within the bone with high stresses mainly flowing within the tuberosity (27% higher than in the rest of the bone, $P < 0.005$).

Our work suggests that not only the enthesis but also the underlying bone is well-adapted to accommodate tendon loading.

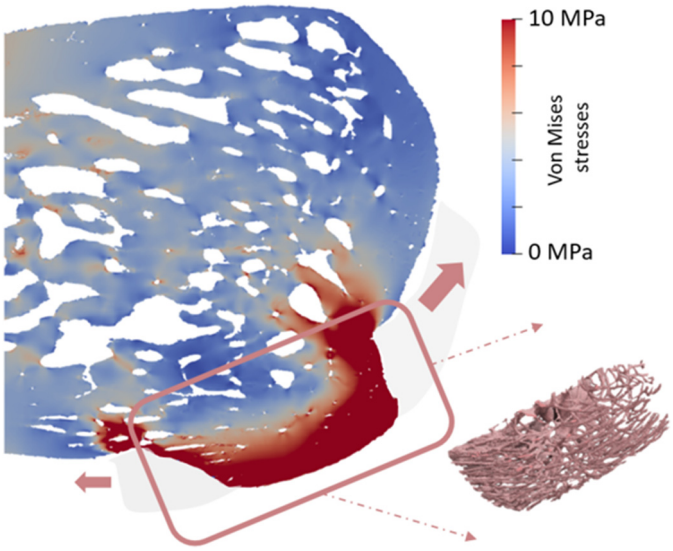

Von Mises stresses flowing in the tuberosity and corresponding highly oriented canal network.

doi:10.1016/j.bonr.2020.100393

P045

Effect of administration of azithromycin and/or probiotic bacteria on bones of estrogen-deficient rats

Urszula Cegieła, Maria Pytlik, Aleksandra Janas, Piotr Londzin, Joanna Folwarczna

Department of Pharmacology, School of Pharmaceutical Sciences in Sosnowiec, Medical University of Silesia, Katowice, Sosnowiec, Poland

Gut microbiota plays an important role in maintaining homeostasis, including that of the skeletal system. Probiotic bacteria were reported to favorably affect bones in conditions of estrogen deficiency. Antibiotics may affect the skeletal system directly or indirectly by influencing the microbiota. The aim of the study was to investigate the effects of azithromycin administered alone or with probiotic bacteria (*Lactobacillus rhamnosus*) on bone mechanical properties in estrogen-deficient (bilaterally ovariectomized) rats.

The experiments were carried out on mature female Wistar rats, divided into 5 groups (n=10-12): non-ovariectomized (NOVX) control rats, ovariectomized (OVX) control rats, OVX rats treated with: probiotic, azithromycin and azithromycin with probiotic. The drugs were administered for 4 weeks, starting one week after the surgery. Azithromycin (50 mg/kg p.o.) was administered once daily for one week and then 3 times a week, and probiotic ($3x10^8$ CFU/kg p.o.) was administered once daily. Serum concentrations of CTX-I, osteocalcin, ALP, calcium and phosphorus, and mechanical properties of cancellous (the proximal tibial metaphysis), compact (femoral and tibial diaphysis) and compact and cancellous (femoral neck) bone were determined. The results were statistically evaluated by ANOVA tests.

Estrogen deficiency induced typical osteoporotic changes in the OVX control rats, with increased bone resorption and formation, and worsening of mechanical properties of the tibial metaphysis; the other bones were not significantly affected. In OVX rats, probiotic alone decreased the ALP concentration, counteracted the changes in the tibial metaphysis at the yield point, and tended to increase the strength of the tibial and femoral diaphysis. Azithromycin alone and with probiotic slightly increased the strength of compact bone, and increased the phosphorus concentration. Only azithromycin alone slightly favorably affected the femoral neck and tibial metaphysis, and further increased the osteocalcin level.

In conclusion, changes in the skeletal system induced by azithromycin in ovariectomized rats seem not to be microbiota-mediated.

doi:10.1016/j.bonr.2020.100394

P046

Impact microindentation assesses cortical bone material properties in humans

Stamatia Rokidi[a], Natalie Bravenboer[b], Sonja Gamsjaeger[a], Pascale Chavassieux[c], Jochen Zwerina[a], Eleftherios Paschalis[a], Socrates Papapoulos[b], Natasha Appelman-Dijkstra[b]

[a]*Ludwig Boltzmann Institute of Osteology at Hanusch Hospital of OEGK and AUVA Trauma Centre Meidling, 1st Med. Dept. Hanusch Hospital, Vienna, Austria*

[b]*Leiden Center for Bone Quality, Leiden University Medical Center, Leiden, Netherlands*

[c]*INSERM UMR 1033, University of Lyon, Lyon, France*

Bone Material Strength index (BMSi) measured by Impact Microindentation is decreased in subjects with fragility fractures independently of BMD values. We recently reported that in humans, BMSi values are strongly associated with material properties of subperiosteal mineralized bone surface (SMBS). In the present study we investigated the relationship of BMSi with material properties of the whole cortex, by analyzing thin sections from iliac crest biopsies (N=12) from patients with different skeletal disorders and a wide range of BMD with or without fractures, by Fourier transform infrared imaging (FTIRI).

The calculated parameters were: i) mineral and organic matrix content and their ratio (MM) ii) mineral maturity/crystallinity and iii) the ratio of pyridinoline (Pyd) and divalent collagen cross-links (XLR). Results were expressed as images, which were converted to histogram distributions. For each histogram the characteristics recorded were: mean value, mode (most often occurring value), skewness, and kurtosis. These were subjected to correlation analysis (Pearson coefficient of correlation) with BMSi values. Statistical significance was assigned to $p< 0.05$.

BMSi significantly correlated with MM mean values ($p = 0.0063$, $r = 0.736$), as well as MM ($p = 0.0004$, $r = 0.855$), and XLR ($p = 0.0274$, $r = -0.632$) mode values.

The results of the present study demonstrate that BMSi values depend on MM, a metric that corrects the mineral content for the organic matrix content. They are also dependent on the XLR, thus strongly associate with organic matrix quality. Both observations are in agreement with our previous results on the immediate SMBS and strongly suggest that BMSi assesses cortical bone material properties.

doi:10.1016/j.bonr.2020.100395

P048

The effect of a deteriorated architecture of the lacunocanalicular network on the organization and mineralization of the extracellular matrix

Andreas Roschger[a,b], Alexander F. van Tol[a], Michael Thelen[c,d,e], Anne Seliger[e,f], Haisheng Yang[g,h], Wing Lee Chan[c,d,e], Tobias Thiele[f], Paul Roschger[i], Georg N. Duda[e,f], Paul Zaslansky[j], Uwe Kornak[c,d,e], Bettina M. Willie[f,g], Richard Weinkamer[a]

[a]*Department of Biomaterials, Max Planck Institute of Colloids and Interfaces, Potsdam, Germany*

[b]*Department of Chemistry and Physics of Materials, Paris-Lodron-University of Salzburg, Salzburg, Austria*

[c]Institut für Medizinische Genetik und Humangenetik, Charité-Universitätsmedizin Berlin, corporate member of Freie Universität Berlin, Humboldt-Universität zu Berlin, and Berlin Institute of Health, Berlin, Germany
[d]Max Planck Institute for Molecular Genetics, Berlin, Germany
[e]Berlin Institute of Health Center for Regenerative Therapies, Charité-Universitätsmedizin Berlin, corporate member of Freie Universität Berlin, Humboldt-Universität zu Berlin, and Berlin Institute of Health, Berlin, Germany
[f]Julius Wolff Institute, Charité-Universitätsmedizin Berlin, corporate member of Freie Universität Berlin, Humboldt-Universität zu Berlin, and Berlin Institute of Health, Berlin, Germany
[g]Department of Pediatric Surgery, Research Centre, Shriners Hospital for Children-Canada, McGill University, Montreal, Canada
[h]Department of Biomedical Engineering, College of Life Science and Bioengineering, Beijing University of Technology, Beijing, China
[i]Ludwig Boltzmann Institute of Osteology at the Hanusch Hospital of OEGK and AUVA Trauma Centre Meidling, 1st Med. Dept., Hanusch Hospital, Vienna, Austria
[j]Department for Operative and Preventive Dentistry, Centrum für Zahn-, Mund- und Kieferheilkunde, Charité - Universitätsmedizin Berlin, Berlin, Germany

The network of osteocytes and the surrounding extracellular matrix (ECM) are intricately interlinked in their spatial arrangement. The lacunocanalicular network (LCN) density housing the osteocytes was measured to be an amazing 74 kilometers of canaliculi in a cubic centimeter of human osteonal bone [1]. Bone regions with a denser network displayed a higher mineral content pointing towards an interaction between osteocytes and the surrounding matrix [2]. Our study focuses on this interaction with the aim to detect changes in the organization and mineralization of the ECM in a mouse model with a deteriorated LCN architecture. Tibias of 12 weeks old female C57BL/6 Gorab^{Prx1} (mouse model for the progeroid disorder gerodermia osteodysplastica) and wild type mice (n=6 for both groups) were characterized using (i) confocal microscopy to quantify the LCN architecture and the vascular channels, (ii) quantitative backscattered electron imaging (qBEI) to obtain the local calcium content, (iii) second-harmonic generation (SHG) microscopy of collagen to image the organization of the fibrous matrix, (iv) microCT to evaluate porosity. Gorab^{Prx1} mice had a 56% reduction in canalicular density, which is due to a decrease of canaliculi per lacuna and per canalicular junction, and an increase of regions without detectable network. In contrast, in Gorab^{Prx1} mice the number of vascular channels was 5.6-fold increased ($p< 0.0001$). The arrangement of the collagen matrix was disordered over the whole tibia cortex. However, the Ca content was very similar between Gorab^{Prx1} and control animals with no significant differences in the average Ca content and heterogeneity. Based on an analysis of the accessibility of the ECM via bone porosities, we conclude that the deteriorated canalicular network architecture in Gorab^{Prx1} mice is compensated by an improved access via lacunae and vascular channels.

[1] Repp et al., Bone reports 6, 101 (2017).
[2] Roschger et al., Bone 123, 76 (2019).

doi:10.1016/j.bonr.2020.100396

P050

Post mortem microstructure analysis on jaw bones of individuals with Type 2 Diabetes Mellitus

Teodora Rodic[a], Eva Maria Wölfel[b], Petar Milovanovic[a,b], Imke A.K. Fiedler[b], Danica Cvetkovic[c], Katharina Jähn[b], Michael Amling[b], Jelena Sopta[d], Slobodan Nikolic[c], Vladimir Zivkovic[c], Björn Busse[b], Marija Djuric[a]
[a]Department of Anatomy, University of Belgrade, Faculty of Medicine, Belgrade, Serbia
[b]University Clinic Eppendorf, Institute for Osteology and Biomechanics, Hamburg, Germany
[c]Institute for Forensic Medicine, University of Belgrade, Faculty of Medicine, Belgrade, Serbia
[d]Institute for Pathology, University of Belgrade, Faculty of Medicine, Belgrade, Serbia

Despite the frequent need for dental implant placement, and failure of up to 14% implants in Type 2 Diabetes Mellitus (T2DM) patients, no research on the microstructural and cellular level has been performed in jaw bone, which is a common site for dental implants and fixation screws.

The aim of this study was to examine the hypothesis that the jaw bone microstructure of individuals with T2DM differs significantly from healthy controls.

To examine bone quality of human jaw bone samples from the edentulous lower 1st molar region and the region of the mandibular angle, samples were extracted from male individuals with T2DM (n=10, age: 70.6±4.5 years) and healthy controls (n=11, age: 71.5±3.8 years) during autopsy (IRB approval present). Within the T2DM a subgroup treated with oral antidiabetics (OAD) (n=5, age: 70.2±5.5) and treated with insulin (n=5, age: 71±4.1) were identified. For microstructural analysis microcomputed tomography (micro-CT) was performed. Bone matrix mineralization and composition were assessed with quantitative Backscattered Electron Imaging (qBEI) and Raman spectroscopy. Additionally, cellular activity was determined via histomorphometry.

The results showed lower porosity in the lingual cortex (T2DM 1.89±1.37%; control 3.92±1.42%) (p=0.004) and increased trabecular thickness in the angulus in T2DM cases (0.32±0.05mm) compared to the controls (0.25±0.06mm) (p=0.008). qBEI showed more highly mineralized bone packets in the buccal cortex in the mandibular angle in insulin-treated (8.85±4.46 wt%) compared to OAD-treated T2DM group (2.81±1.93 wt%) (p=0.034). T2DM was associated with 20.68% lower lacunar size on average than in controls (p=0.03) in the trabecular bone of the angulus region. Raman and histomorphometry parameters showed marginal differences between the groups.

To conclude, T2DM jaw bone microstructure slightly differs from the healthy controls, showing more highly mineralized bone in some regions, with pore filling and trabecular thickening in other regions.

Keywords: type 2 diabetes, jaw, bone, microstructure

doi:10.1016/j.bonr.2020.100397

P051

Influence of LDFA and MPTA angles values of patients with varus deformity on the structural properties of bone tissue, obtained by computer microtomography measurements

Anna Nikodem[a], Miroslaw Kulej[b], Jaroslaw Filipiak[a], Szymon Ł. Dragan[b], Justyna Wolicka[a], Szymon F. Dragan[b]
[a]Mechanical Department, Wroclaw University of Science and Technology, Wroclaw, Poland,
[b]Department and Clinic of Orthopaedic and Traumatologic Surgery, Wroclaw Medical University, Wroclaw, Poland

The goal of the study was an analysis of the impact of LDFA and MPTA angles on the structural properties of bone tissue for patients qualified for knee replacement surgery due to the osteoarthritis, intensified by significant varus deformity. The research material consisted of tibia plateu from 65 patients undergoing knee replacement surgery who had significant varus (MDTA angle ranging from 76 to 88 degree). Tests of structural properties of bone tissue were carried out using the 1172 SkyScan, Bruker® X-ray microtomograph. The image

registration was carried out with a resolution of 12,5μm, with the 89kV/112mA lamp parameters. This study determines the parameters of geometry, structure and BMD. Analysis of structural parameters obtained with microCT showed changes in the structure and number of bone trabeculae. These changes concern both the geometry of the trabeculae themselves, the number, thickness, but also their character (SMI). The studies have also shown the strong correlation between structural properties and the MDFA angle. This is undoubtedly related to the asymmetrical loading of the knee joint, which is characterized by an significant increase in the value of stress in the medial region and its decrease on the lateral part of the tibia These changes, taking into account the loss of cartilage causes rapid changes in the structure, and, mechanical properties of the bone tissue. These changes cause problems with the selection of parameters related to the type and the method of implant placement during this type of patients. The ability to estimate the appropriate thickness of the bone layer removed for the knee joint endoprosthesis is therefore crucial from the point of view of its stability. Therefore, knowledge of the extent of changes in structural and mechanical properties of bone and cartilage in the area of the knee joint with degenerative changes is so important.

doi:10.1016/j.bonr.2020.100398

P052

A new osteoporotic animal model for implant-related infected non-unions after intramedullary fixation of the femur

Ronald Man Yeung Wong[a], Jie Li[a], Tsz Kiu Li[a], Simon Kwoon Ho Chow[a], Margaret Ip[b], Wing-Hoi Cheung[a]
[a]*Orthopaedics & Traumatology, The Chinese University of Hong Kong, Sha Tin, Hong Kong*
[b]*Microbiology, The Chinese University of Hong Kong, Sha Tin, Hong Kong*

Introduction: Infections after fracture fixation is one of the most challenging complications in trauma surgery. 20% of open fractures now occur in patients 65 years or older. Recent literature showed that circulating estrogen levels are strongly related with infection resistance. There is currently a lack of a single osteoporotic animal model with implant-related infection.

Methodology: 32 6-month old Sprague-Dawley rats were randomized to 4 groups: ovariectomized (OVX), OVX with infection (OVX+I), sham (S), sham with infection (S-I). An open femoral diaphysis fracture was performed at 9 months and stabilized with a k-wire. OVX-I and S-I were induced with methicillin-sensitive Staphylococcus aureus ($1x10^3$ CFU/mL) at fracture site. Rats were assessed clinically, healing with X-rays (callus width and area), micro-CT, bone and implant for bacterial load. Rats were euthanized at 2 and 4 weeks. ANOVA test was performed.

Results: Clinically 2 OVX-I rats died from sepsis. X-rays showed infected non-union for OVX-I rats at 4 weeks. 50% of S-I achieved union. This was supported with micro-CT, showing higher bone volume (BV) formation ($p=0.05$). Significantly more osteolysis was observed in OVX-I compared to S-I rats ($p=0.05$). Periosteal reaction was significantly higher in infected groups compared to respective control ($p=0.00$). All rats in OVX and S healed with normal callus formation. Callus area was significantly higher for S rats at $12.8\pm2.0mm^2$ compared with OVX at $7.57\pm3.3mm^2$ ($p=0.03$). Micro-CT also showed significantly higher BV ($p=0.05$). Microbiology results of bone showed significantly higher bacterial load in OVX-I group (4.3×10^6 CFU/g) compared to Sham-I group (1.0×10^6 CFU/g). No significant difference was detected on implant bacterial load.

Conclusion: With the aging population, research in implant-related fractures is needed for potential interventions. This study introduces a new animal model and shows evidence of potential poorer bone healing in implant-related osteoporotic fractures compared to normal bone.

doi:10.1016/j.bonr.2020.100399

P053

Vibration treatment modulates inflammatory response via the p38 MAPK pathway in osteoporotic rat fracture healing

Yu Ning Chim, Wing Hoi Cheung, SImon Kwoon Ho Chow
The Chinese University of Hong Kong, Hong Kong, China

Objective: To investigate if p38 MAPK pathway is involved in the enhancement effect of inflammatory response by Low-Magnitude High-Frequency Vibration (LMHFV) in osteoporotic fracture healing.

Methods: Ovariectomy-induced osteoporotic closed-femoral fracture SD-rats (Ethics Ref. No. 15/158/MIS-5-C) were randomized into control (OVX-C), control with p38 specific inhibitor, SB203580 (OVX-C-SB), vibration (OVX-V) or vibration with SB203580 (OVX-V-SB) groups ($n=48$, $n=6$/group/time-point). LMHFV (35Hz, 0.3g) was given 20 min/day and 5 days/week to vibration groups. Local expressions of total p38, phosphorylated p38 (p-p38), and pro-inflammatory marker of TNF-α at weeks 1 and 2 post-fracture were evaluated by immunohistochemistry and quantified by colour threshold in ImageJ. Callus width was measured by weekly radiography. Significant difference among groups was considered at $p< 0.05$ by one-way ANOVA.

Results: Immunohistochemistry results showed lower relative p-p38 level in OVX-C compared to OVX-V group at weeks 1 and 2 ($p< 0.03$ for both) (Figure 1A). Compared to OVX-C-SB and OVX-V-SB groups, OVX-V rats showed higher expression of TNF-α ($p=0.02$, $p=0.048$ respectively) at weeks 1 and 2(Figure 1B). Callus width was higher in OVX-V group compared to all other groups at week 1 ($p< 0.03$ for all) (Figure 1C).

Conclusion: LMHFV could activate p38 MAPK and enhance TNF-α expression at fracture site in OVX bone, leading to better callus formation. With the inhibition of p38 MAPK pathway, TNF-α expression at fracture site was suppressed and callus formation capacity was poorer. These suggest that enhancement in inflammatory response by mechanical stimulation in OVX bone is via p38 MAPK pathway.

Acknowledgement: OTC(2015-SCNT), NSFC(81472097)

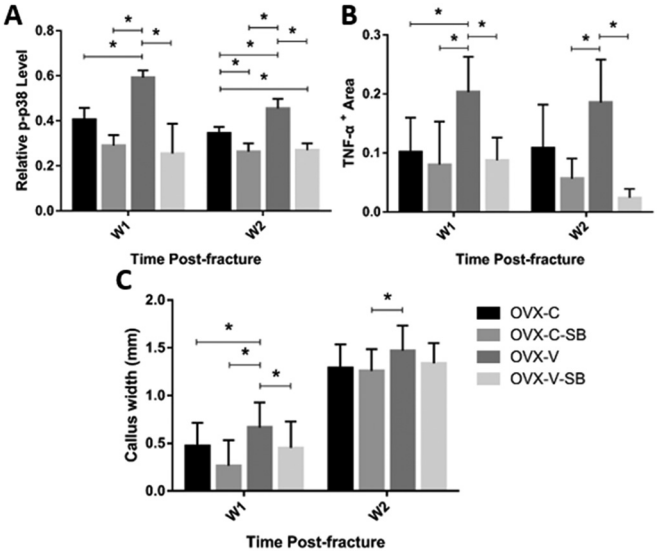

Fig. 1.

doi:10.1016/j.bonr.2020.100400

P054

Notoginsenoside R1 facilitates stem cell-based bone tissue engineering via inducing osteogenesis, angiogenesis and cell adhesion

Haiyan Wang[a], Janak Lal Pathak[a], Richard T. Jaspers[b], Gang Wu[c]
[a]*Affiliated Stomatology Hospital of Guangzhou Medical University, Guangzhou, China*
[b]*Faculty of Behavioural and Movement Sciences, Vrije Universiteit Amsterdam, Amsterdam Movement Sciences, Amsterdam, Netherlands*
[c]*Academic Centre for Dentistry Amsterdam (ACTA), University of Amsterdam and Vrije Universiteit Amsterdam, Amsterdam Movement Sciences, Amsterdam, Netherlands*

Cell adhesion, osteogenesis, and angiogenesis are essential phenomena for effective stem cell-based bone tissue engineering. Growth factors BMP2 and VEGF promote osteogenesis and angiogenesis, but their clinical application is still controversial due to the adverse effects and various shortcomings. Notoginsenoside R1 (NGR1) is a natural triterpene saponin compound extracted from traditional Chinese herb *Panax notoginseng*. Since NGR1 has high bioactivity, minimum adverse effects, and osteogenic potential, it could be used in bone regenerative application. This study aimed to investigate the effect of NGR1 on osteogenic/angiogenic differentiation and cell-adhesion of precursor cells, as well as bone regeneration during stem cell-based bone tissue engineering. We used 0-5 μg/ml of NGR1 to analyze the osteogenic and angiogenic differentiation of hASCs and HUVECs, respectively. Osteogenic/angiogenic gene expression, ALP activity, alizarin red matrix mineralization, and matrigel-based tube formation assay were performed in vitro. Western blot analysis tested the expression of p38 and JNK. NGR1 pretreated hASCs were seeded on 3D-printed TCP scaffold, and cell-adhesion in vitro and bone regeneration in the ectopic site of nude mice were analyzed. The animal study was approved by the ethical committee of Guangzhou Medical University. The selected significance level was $P< 0.05$. NGR1 promoted OCN expression, ALP activity, and matrix mineralization in dose-dependent manner, as well as activated the p38 and JNK signaling pathway. Higher numbers of the tube-like structures were observed in NGR1 treated hASCs or HUVECs matrigel culture. Actin staining revealed the increased adhesion of NGR1-pretreated hASCs to a glass slide and TCP-scaffold. Micro-CT analysis revealed the more bone formation in ectopically grafted NGR1-pretreated hASCs-seeded 3D-printed TCP-scaffolds. In conclusion, NGR1 enhanced osteogenic/angiogenic and cell-adhesion potential of precursor cells, as well as ectopic bone formation in hASCs-loaded 3D-printed TCP-scaffolds, suggesting it as a possible therapeutic agent to enhance the efficacy of stem cell-based bone tissue engineering.

doi:10.1016/j.bonr.2020.100401

P055

Exosomes released from osteogenically differentiating SHEDs carry miRNAs that promote osteogenic differentiation of osteoblast precursor cells

Yongyong Yan[a], Janak L. Pathak[a], Richard T. Jaspers[b], Gang Wu[c]
[a]*Key Laboratory of Oral Medicine, Guangzhou Institute of Oral Disease, Affiliated Stomatology Hospital of Guangzhou Medical University, Guangzhou, China*
[b]*Faculty of Behavioural and Movement Sciences, Vrije Universiteit Amsterdam, Amsterdam Movement Sciences, Amsterdam, Netherlands*
[c]*Academic Centre for Dentistry Amsterdam (ACTA), University of Amsterdam and Vrije Universiteit Amsterdam, Amsterdam Movement Sciences, Amsterdam, Netherlands*

Mesenchymal stem cells (MSC)-derived exosomes, or extracellular vesicles are cargo of mRNAs, miRNAs, and signaling proteins that promote osteogenesis and angiogenesis. Exosomes from different sources of MSCs such as bone marrow, placenta, adipose tissue, and dental tissue have different osteogenic potential. Stem cells from human exfoliated deciduous teeth (SHEDs) are easy to obtain and highly proliferative. This study aimed to develop osteogenically functional exosomes from SHEDs for bone regenerative application. SHEDs were isolated and characterized using the established protocol, and cultured in ± osteogenic medium (OM). Exosomes were isolated from the conditioned medium by ultracentrifugation and characterized by western-blot assay (WB), nanoparticle tracking, (NPT) and transmission electron microscopy (TEM). The effect of exosomes on the osteogenic differentiation of BMSCs was extensively analyzed. The differential expression pattern of miRNAs in exosomes was analyzed by Exos MicroRNA array analysis. Differentially upregulated miRNAs in OM-exosomes were further verified by RT-qPCR. The selected significance level was $P< 0.05$. We successfully isolated exosomes with the size 105 nm ± 72 nm from SHEDs, exosomes expressing surface markers CD9, CD63, ALIX, and TSG101. PKH26-tagged exosomes were easily uptaken by BMSCs at 4h. Exosomes from OM treatment (OM-exos) enhance BMSCs proliferation, and expression of osteogenic markers, RUNX2, ALP, and OCN at day 4 and 7 compared to exosomes from proliferation medium (PM-exos). Similarly, a higher intensity of ALP staining was observed in OM-Exos treated BMSCs. Total of 200 miRNAs were expressed in OM-Exos. Among them, 9 were upregulated, and 55 were downregulated compared to PM-exos. RT-qPCR results confirmed the higher expression of miR-122-5p (13-fold), miR486-5p (46-fold) and underexpression of miR26a-5p (4-fold), miR199a-3p (4-fold), and miR-23b-3p (5-fold) in OM-Exos compared to PM-Exos. In conclusion, exosomes released from osteogenically differentiating SHEDs carry miRNAs that promote osteogenic differentiation of BMSCs, indicating the possible use of OM-Exos for bone tissue regeneration application.

doi:10.1016/j.bonr.2020.100402

P056

The effects of sodium benzoate on structure of the proximal growth plate of the humerus and the thyroid gland

Vitaly Morozov[a], Elena Morozova[a], Vladyslav Luzin[b], Irina Belik[b]
[a]*Federal State Autonomous Educational Institution of Higher Education Belgorod State University", Belgorod, Russian Federation*
[b]*State Establishment of Lugansk People's Republic Saint Luka Lugansk State Medical University, Lugansk, Ukraine*

Aim: Of the study is to examine morphology of humeral proximal epiphyseal cartilage and thyroid gland in rats after 60-day sodium benzoate (SB) intake in various concentrations.

Material and Methods: The experiment involved 105 male rats with initial body weight of 200-210 grams. The 1st group (K) comprised animals that received daily *per os* 1 ml of 0.9% solution of NaCl, the 2nd and the 3rd groups (SB1 and SB2) received *per os* 1 ml of SB in dosage of 500 or 1000 mg per kg of body weight daily. Upon expiration of observation terms the frontal sections of the humeral proximal epiphysis and thyroid gland were hematoxylin-eosin stained.

Results: By the third day after SB discontinue, width of osteogenesis zone in SB1 group was lower than the control values by 8.32% and amount of primary spongiosa with related osteoblasts - by 6.98% and 6.03%. In SB2 group same values constituted 9.80%, 8.57%, and 8,75% respectively. By the 45th day only few significant changes were discovered.

In SB1 group the subcapsular portion of thyroid gland is characterized by large irregular-shaped follicles filled with colloid. The follicles were lined with simple squamous or cuboidal epithelium. Central portion of the

gland contained small or middle-sized follicles lined with simple cuboidal epithelium. The formation of lobules in thyroid gland was impaired and thickened connective tissue septae were found. In SB2 group the number of large irregular-shaped follicles lined with simple squamous epithelium in the peripheral portion of thyroid gland increased, some of them were found in central portion among small and middle-sized follicles. The thickened connective tissue septae and capsule contained dilated blood vessels fully filled with blood.

Conclusion: SB affects both bone formation and functionality of the thyroid gland. Manifestations and restoration rates in these organs well depend on dosage of SB.

doi:10.1016/j.bonr.2020.100403

P057

Growth and formation of the skeletal bones in rats with streptozocin-induced diabetes after tibia fracture

Alexandr Torba, Vladyslav Luzin, Dmitry Lugovskov, Nicolaj Botnar', Valeriya Shekhovtsova
State Establishment of Lugansk People's Republic Saint Luka Lugansk State Medical University, Lugansk, Ukraine

Aim: Of the study is to investigate growth and formation of the skeletal bones in rats with diabetes after fracture of the tibia.

Material and methods: In the study we used 420 rats: immature (45-50 g), adult (135-145 g), and old (290-310 g). Each age group was separated into the following groups: group 1 - controls, group 2 - animals with 2 mm round hole in the tibiae; group 3 - animals with streptozocin-induced diabetes (55 mg/kg). In the group 4 animals with diabetes received the same tibia injury. Upon expiration of observation terms (7, 15, 30, 60, and 90 days) animals were euthanized and bones (humeri, hipbones, and L3 vertebra) were excised. Osteometry was performed by means of a sliding caliper.

Results: Animals with diabetes exhibited slower bone growth as compared to the controls in all age groups. In group 4 significant changes in comparison with the group 2 began manifesting from the 15th day for young animals, and from the 60th day for the adults and old ones. By the 90th day, longitudinal dimensions of the bones in immature animals were lower than those of the group 2 by 5.19-6.24% and transverse dimensions decreased by 5.11-7.72%. In adults, width of hipbone and vertebra was lower than that of the group 2 by 4.87% and 5.26%, and both lateral and antero-posterior sizes of the humerus shaft decreased by 5.48% and 5.08%. In old animals, thickness of the hipbone and the vertebral body was lower than that of the group 2 by 5.54% and 3.50%.

Conclusion: Injury to the tibia in animals with diabetes has an adverse effect on bone growth rate already affected by diabetes. The most expressed alterations are observed in immature animals while in old animals these alterations on the contrary, are not well expressed.

doi:10.1016/j.bonr.2020.100404

P058

Growth of the skeletal bones under effect of formaldehyde vapors in different age periods

Vladimir Nizhel'sky, Vladyslav Luzin, Yuliya Sumtsova, Yuliya Chistyakova, Denis Novokhatsky
State Establishment of Lugansk People's Republic Saint Luka Lugansk State Medical University, Lugansk, Ukraine

Aim of the study is to investigate age features of bone growth in rats after inhalation of formaldehyde vapors.

Material and methods: 144 male rats (immature and adult) were distributed into 2 groups - the controls (K) and the experimental animals (F). Animals of the group F were exposed to formaldehyde vapors in dosage of 2.776 mg per cubic meter with exposure length of 60 minutes daily. Osteometry of the tibiae, the hipbones and the L3 vertebra was performed by means of sliding calipers. The osteometric data was analyzed by means of variation statistics using standard software.

Results: In immature rats of f-group length of the tibia decreased by 4.12%, 4.67%, 6.23%, 7.87%, and 9.86%, length of hipbone also decreased by 3.64%, 4.34%, 4.89%, 5.82%, and 7.28%, and body height of the vertebra decreased by 4.50%, 4.28%, 6.72%, 7.36%, and 8.14% (all in comparison with the controls with respect to the 10th, the 20th, the 30th, the 60th, and the 90th day of observation terms). In adults alterations started manifesting later - beginning from the 20th day. Tibia length then decreased by 4,20%, 5.65%, 6.87%, and 8.23%, hipbone length decreased by 3.81%, 4.13%, 4.98%, and by 6,78%, and height of the vertebral body decreased by 4.56%, 4.84%, 6.38%, and 7.46%. In animals that passed readaptation period, length of the tibia and the hipbone, and the vertebral body height increased by 4.27-6.46% in immature animals and by 3,72-5,19% in. Transverse dimensions of the same bones in the animals of the group F changed in a similar way.

Conclusion: Inhalation of formaldehyde results in inhibition of bone growth, which increases with the experiment duration. Immature animals are more susceptible to formaldehyde vapors than the adult ones. Animals that pass 30-day readaptation period after formaldehyde discontinue exhibit signs of restoration of bone growth.

doi:10.1016/j.bonr.2020.100405

P059

Myb deficiency impacts Rank-Rankl-Opg system

Veronika Oralova[a], Sabina Stouracova[a,b], Mary Clarke[c], Jon Frampton[c], Petr Benes[d], Eva Matalova[a,b]
[a]*Institute of Animal Physiology and Genetics CAS, Brno, Czech Republic*
[b]*University of Veterinary and Pharmaceutical Sciences, Brno, Czech Republic*
[c]*Institute of Cancer and Genomic Sciences, University of Birmingham, Birmingham, United Kingdom*
[d]*Department of Experimental Biology, Faculty of Sciences, Masaryk University, Brno, Czech Republic*

The Myb transcription factor has been intensely investigated in normal and disease haematopoiesis. Recently, the spectrum of tissues in which Myb has a crucial role has considerably broadened. For example, in bone there are indications that Myb is engaged in osteogenic pathways. Hence, we have employed Myb deficient mice to investigate this further. Since the Myb knockout is embryonic lethal, we focused on the survival limit, namely day (E) 15.5.

At E15.5, the ossification centre has just formed in long (endochondral) bones, although a kind of complex bone tissue is already present in the (intramembranous) mandible. E15.5 mandibular sections related to the first molar were analysed because the bone encapsulating the tooth has been shown to contain osteoblasts, osteoclasts, and first osteocytes at this stage of development. We focussed on one of the most important signalling systems related to osteoblast-osteoclast cross-talk, namely Rank-Rankl-Opg. Wild type and Myb knockout mandibles were dissected from samples collected in RNALater. After RNA isolation, cDNA was prepared and qPCR performed. In the Myb knockout, there was a lower expression of Rank (60 % of the wild type level) and Rankl (50 % of the wild type level), whereas Opg expression was higher (120 % of the wild type level). These initial results clearly point to an effect of Myb deficiency

on expression of Rank-Rankl-Opg components, which potentially could affect both osteoblasts and osteoclasts.

Supported by AZV (NV18-07-00073) and GACR (19-15272Y).

doi:10.1016/j.bonr.2020.100406

P060

Histomorphometric analysis of the alveolar trabecular bone using dentin as biomaterial

Matko Oguić[a], Sanja Zoričić Cvek[b], Ana Terezija Jerbić Radetić[b], Tanja Ćelić[b], Dragica Bobinac[c], Olga Cvijanović Peloza[b]
[a]*Dental Polyclinic Rident, Rijeka, Croatia*
[b]*Department of Anatomy, Medical Faculty of the University of Rijeka, Rijeka, Croatia*
[c]*Juraj Dobrila University of Pula, Pula, Croatia*

Different graft materials are used in implant dentistry. It has been proposed that teeth has regenerative potential, since dentin and cementum contain osteoinductive proteins similar to bone, which include BMP-2, TGF-β, osteocalcin. Histological data of rare human studies has revealed newly formed bone bridging over dentin and cementum fragments.

Nevertheless, histomorphometric data of the newly formed bone has not been documented yet.

The aim was to assess the values of the histomorphometric parameters and to analize the expression of the Osterix, TGF-β and TNF-α of the alveolar bone samples.

Dentin particles sized between 300 and 1,200 μm were used to fill extraction socket on 8 patients. 24 weeks after extraction, a bone cylinder was harvested from the grafted site using 2 mm diameter trephine. Immunohistochemical staining was performed on paraffin embedded bone samples and VAMS software was used for image analysis.

Results showed that BV/TV of the newly formed bone amounted 29% ±10,2, while dentin and soft tissue amounted 24, 14% and 46, 86%, respectively. Tb.Th amounted 971,74 ± 96,56 μm, Tb.Sp 396,01 ± 56,45 μm and Tb.N 4,18 ± 1,02/mm. Osterix is expressed in Obl and young Ocy (Figure 2). TNF-α expression was the highest in the cells of the connective tissue, while TGF-β showed positive expression in the osteocytes (Figure 3 and 4).

The evidence of the newly formed bone, which has amounted 29%, indicates that dentin stimulates bone regeneration and should be used as autograft in guided bone regeneration.

Keywords: Histomorphometry, Maxilla, Trabecular bone, Immunohistochemistry

doi:10.1016/j.bonr.2020.100407

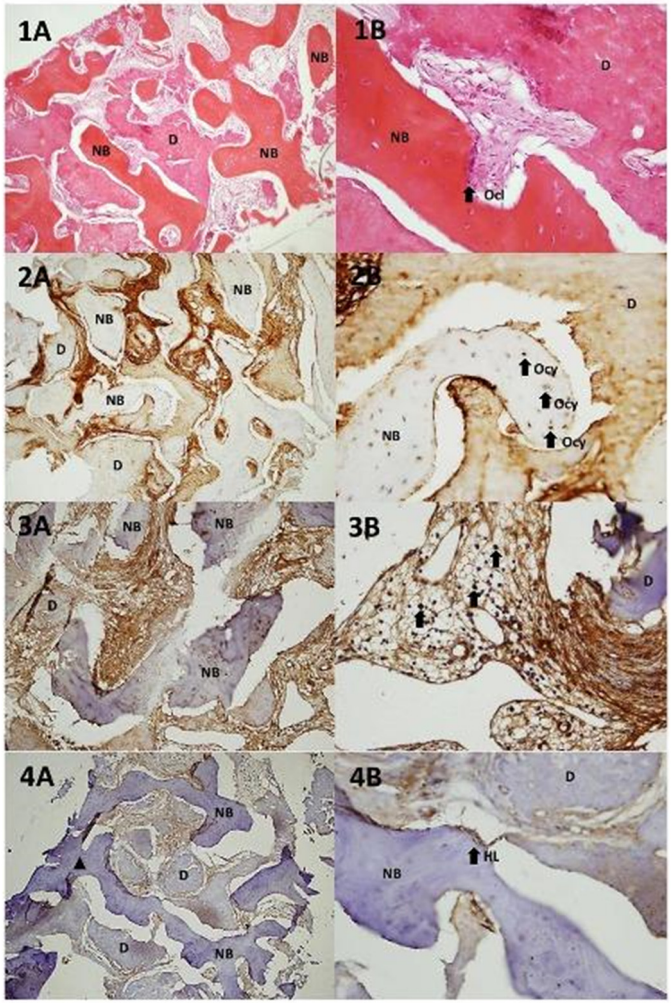

Figure 1A and 1B: HE staining
Figure 2A and 2B: Immunohistochemical staining for Osterix
Figure 3A and 3B: Immunohistochemical staining for TGF-α
Figure 4A and 4B: Immunohistochemical staining for TGF-β
NB – newly formed bone, **D** – dentin, **Ocl** – osteoclast, **Ocy** – osteocytes, **HL** – Howship's lacunae

Osterix, TGF-alpha and TGF-beta expression in alveolar bone samples.

P061

Characteristics of micro-fracture healing events in trabecular bone (microcalli) from human vertebrae remain unaffected by bisphosphonate treatment

Annika vom Scheidt[a], Eric F. Grisolia Seifert[a], Imke A.K. Fiedler[a], Christine Plumeyer[a], Kilian Stockhausen[a], Kathrin Mletzko[a], Pallavi Pandit[b], Matthias Schwartzkopf[b], Stephan V. Roth[b], Michael Amling[a], Björn Busse[a]
[a]*Department of Osteology and Biomechanics, University Medical Center Hamburg-Eppendorf, Hamburg, Germany*
[b]*Deutsches Elektronen-Synchrotron DESY, Hamburg, Germany*

Introduction: While conflicting observations regarding bisphosphonates´ influence on fracture healing exist for cortical bone of humans and animal models (non-union risk after atypical femoral fractures, increased callus size), effects on fracture healing in trabecular bone are understudied.

Previously, we quantified micro-fracture healing events in trabecular bone (microcalli) and found an accumulation of microcalli in bisphosphonate-treated osteoporosis patients compared to treatment-naïve. Here, we investigated morphological, cellular, and compositional characteristics of microcalli following bisphosphonate treatment to explore potential reasons for accumulation.

Methods: We analyzed lumbar vertebrae (L3) from osteoporotic women (83±7y; bisphosphonate-treated (BP): n=5, treatment-naïve (OP): n=7). Morphological characteristics of 92 microcalli were quantified using micro-computed tomography. After PMMA-embedding, horizontal sections from a subset of microcalli (BP: n=8, OP: n=8) were used for histology (toluidine blue, 4μm-sections) and synchrotron-based small angle x-ray scattering (16μm-sections) quantifying cellular and compositional characteristics.

Results: 3D morphology and histology of microcalli were similar in treatment-naïve and bisphosphonate-treated groups. Although the bisphosphonate group showed more microcalli (p=0.004, Fig.1A), their outer diameter, porosity, height, and cellular indices corresponded to treatment-naïve ones (p>0.05, Fig.1B). 50% of bisphosphonate-treated

microcalli showed eroded surfaces, but only 12.5% of untreated. Synchrotron-based mineral platelet thickness was similar (OP: 3.468± 0.107nm, BP: 3.474±0.055nm, p>0.05; Fig.1F).

Discussion: Despite bisphosphonate treatment, morphological and cellular characteristics of microcalli seem uninfluenced. The observed thickness of mineral platelets is adequate for healthy bone. While further investigation of cellular activity is required to explain the accumulation of microcalli under bisphosphonate treatment, these results indicate micro-fracture healing initiation is unaffected in bisphosphonate-treated trabecular bone.

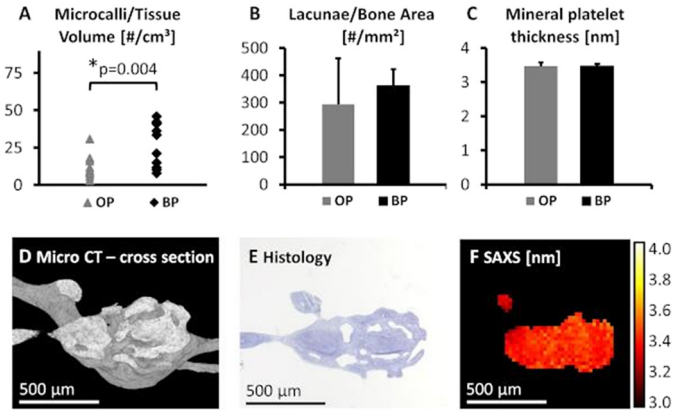

Fig. 1. Characterization of bisphosphonate influence on microcalli in human vertebrae.

doi:10.1016/j.bonr.2020.100408

P062

The secretome of mesenchymal stromal cells drives functional heterogeneity

Andrew Stone[a], Rachel Crossland[b], Emma Rand[a], Alasdair Kay[a], Gabriel Thornes[a], Amanda Barnes[a], Savvas Ioannou[a], Xiao-Nong Wang[b], Ian Hitchcock[a], Paul Genever[a]
[a]*Department of Biology, University of York, York, United Kingdom*
[b]*Haematological Sciences, Newcastle University, Newcastle, United Kingdom*

The use of mesenchymal stem/stromal cell (MSC) in regenerative therapies for skeletal disorders is hampered by heterogeneity within cell preparations intended for clinical use. We identified biomarker CD317, which discriminates elongated, migratory, regenerative MSCs ($CD317^{neg}$) from flattened/spread, non-migratory, differentiation-incompetent MSCs ($CD317^{pos}$), and investigated how their secreted outputs determined MSC phenotype.

LC-MS/MS identified significant increases in 44 soluble and 162 extracellular vesicle (EV) proteins from $CD317^{neg}$ versus $CD317^{pos}$ MSCs ($p< 0.05$) (Fig.1A, B). Gene-set enrichment analysis (GSEA) revealed enrichment for $CD317^{neg}$ upregulated proteins in "Focal Adhesion" and "Extracellular Matrix (ECM)-receptor interaction" KEGG pathways (Fig.1C, D).

$CD317^{neg}$ MSCs were enriched in fibronectin, type-VI collagen, periostin, aggrecan, biglycan, decorin and thrombospondin-1. Nanostring revealed 12 differentially expressed miRNAs between $CD317^{neg}$ and $CD317^{pos}$ MSC EVs ($p=0.0066$-0.0438); 10 miRNAs (mir376a-3p, mir29a-3p, mir221-3p, mir145-5p, mir630, mir21-5p, mir100-5p, mir320e, mir125b-5p and mir29b-3p) were upregulated in $CD317^{neg}$ EVs. GSEA of cumulative TargetScan predicted targets highlighted significant enrichment for "ECM-receptor interaction" and "Focal Adhesion" ($q=1.48e^{-8}$ and $3.92e^{-9}$ respectively). Focused ion-beam SEM of ECM substrates from 2-week cultures revealed a thicker matrix with more globular topography from $CD317^{neg}$ MSCs. $CD317^{neg}$ ECM or conditioned medium converted $CD317^{pos}$ MSCs to a $CD317^{neg}$ phenotype

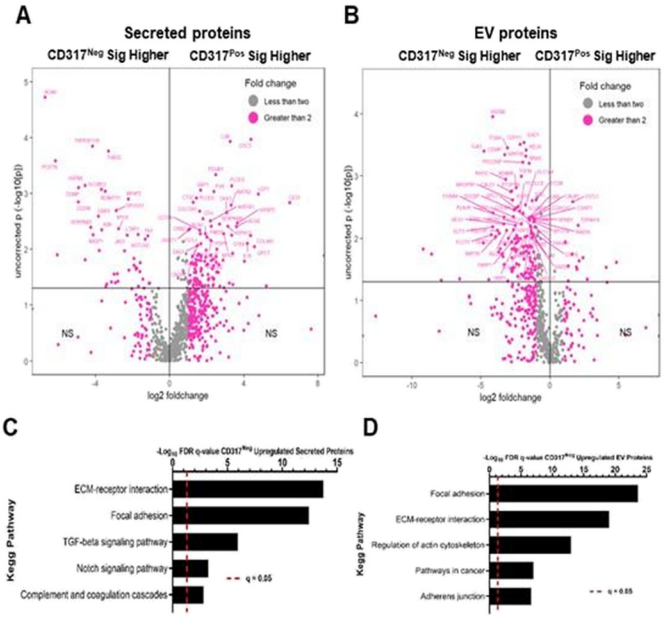

Fig. 1.

with significant reduction in cell volume and area but increased length: width ratio, migration speed and distance determined by PhaseFocus ptychography.

Plasticity within MSC subtypes is driven by secreted factors including soluble proteins, EVs and matrix substrata. Our findings also have implications for the selection and treatment of heterogeneous MSCs before clinical application.

Keywords: Extracellular vesicles, secretome, MSC

doi:10.1016/j.bonr.2020.100409

P063

Growth plate cartilage transplanted to the articular surface remodels into articular-like cartilage in a process promoted by the synovial joint microenvironment

Zelong Dou[a], Michael Chau[a], Marta Baroncelli[a], Ameya Bendre[a], Ellie Landman[a], Lars Ottosson[a], Ola Nilsson[a,b]
[a]*Pediatric Endocrinology Unit & Center for Molecular Medicine, Department of Women's and Children's Health, Karolinska Institutet and University Hospital, Stockholm, Sweden*
[b]*School of Medical Sciences, Örebro University, Örebro, Sweden*

Growth plate and articular cartilage are structurally similar yet functionally distinct skeletal tissues. During embryogenesis, both of them derive from the same pool of mesenchymal stem cells that form the cartilaginous templates of endochondral bones. Except for chondrocytes adjacent to joint cavities, most chondrocytes of the cartilaginous templates undergo hypertrophic differentiation starting at the center. We therefore hypothesized that the joint microenvironment inhibits hypertrophic differentiation.

To test this hypothesis, osteochondral allografts consisting of articular cartilage, epiphyseal bone, and growth plate cartilage from distal femoral epiphyses of inbred EGFP transgenic Lewis rats were transplanted in inverted or original (control) orientation to matching sites in wild-type Lewis rats and harvested on postoperative day 3, 7 and 28. The study was approved by the Stockholm Animal Ethics Committee.

Histological analysis revealed that growth plate cartilage transplanted to the articular surface gradually remodeled into an articular-like structure and at 4 weeks had attained a thickness and morphology

similar to the surrounding nascent articular cartilage (Fig 1). In contrast, superficial zone chondrocytes of articular cartilage ectopically placed inside the epiphysis changed morphology and migrated out of the superficial zone (Fig 1). In situ hybridization showed that that growth plate chondrocytes transplanted to the articular surface decreased type X collagen (*Col10a1*) and increased lubricin (*Prg4)*, whereas transplanted growth plate chondrocytes further from the articular surface enlarged and upregulated *Col10a1*.

These findings suggest that the synovial joint microenvironment inhibits hypertrophic differentiation and promote articular cartilage differentiation.

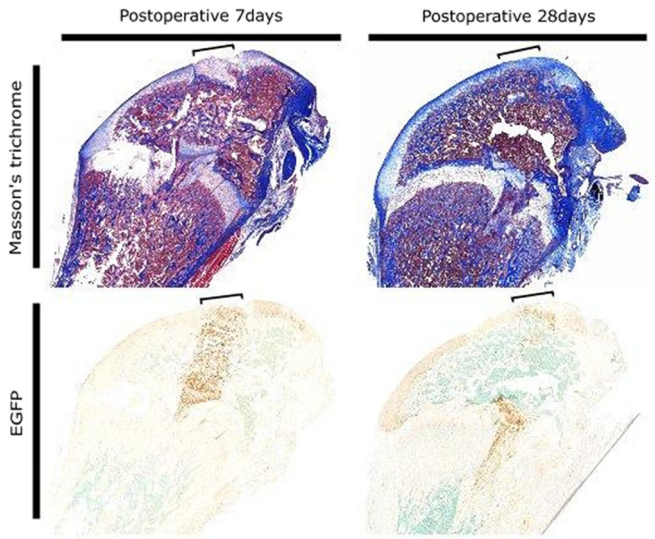

Figure 1. Histology and allografts tracing. Osteochondral allografts consisting of articular cartilage, epiphyseal bone, and growth plate cartilage from distal femoral intercondylar articular surfaces of inbred *EGFP*-expressing rats were transplanted to matching sites in *EGFP*--negative rats in original (control) (data not shown) or inverted orientation (shown here). Donor and recipient animals were 4 weeks of age. Histology was examined using Masson's trichrome stain (row 1), and allografts were localized by EGFP immunohistochemistry (row 2). Brackets delineate the osteochondral allografts.

Histological staining and allografts tracing on postoperative day 7 and 28 respectively.

doi:10.1016/j.bonr.2020.100410

P065

Role of hydrolyzed collagen in bone regeneration of adult zebrafish

Nili Vasserman, Chen Shochat Carvalho, David Karasik
Medical Sciences, Bar-Ilan University, Safed, Israel

Bone regeneration is an important process that allows healing of bone tissue after trauma, fractures, or surgical removal. There are clinical cases in which bone regeneration is needed in large quantity. Therefore, there is a need to develop novel, more potent, drugs, especially of anabolic nature. Due to fast bone regeneration, zebrafish (*Danio-rerio*-ZF) is a popular model for regeneration process study.

The aim of this study was to assess the *in-vivo* and *in-vitro* effect of a collagen hydrolysate (CH) supplementation on bone regeneration. Thus, *in-vivo* - ZF jawbone regeneration model was used to study the effect of CH on bone regeneration.

Three doses of CH: 40, 80 and 160mg/kg, were given daily with the fish food.

CH enhanced ZF bone regeneration measured by the resection gap closure. At 14 days, gap closure was 149μm in 160mg/kg group while it was only 238 μm in the untreated.

In-vitro- the effect of CH on MC3T3-E1 osteoblast and RAW264.7 osteoclast lines, was studied with 3 concentrations of CH: 0.25, 0.5 and 1mg/ml, followed by alkaline phosphatase, Alizarin red and TRAP staining. The expressions of osteogenic genes were measured by qPCR. 0.5mg/ml CH increased ALP activity and calcium deposition and decreased the size of osteoclasts which also contained less nuclei. Additionally, gene expression of osteocalcin and RUNX2 (Runt-related transcription factor 2) were increased.

Our results indicate an anabolic therapeutic potential of CH in bone regeneration with potential application for fracture healing. The gap closes after resection in a shorter time depending on the concentrations of CH. Our findings demonstrate that CH can upregulate osteoblast and down regulate the osteoclast. Further, this study affirms the advanced bone regeneration ability of CH in a ZF jawbone regeneration model. Our findings suggest that CH could represent a promising treatment in case of bone healing.

doi:10.1016/j.bonr.2020.100411

P066

Endothelial cell physiology in a microfluidic device and their response to mesenchymal stromal cells in vitro

Shuang Zhang[a], Bastiaan Tuk[b], Marijke Koedam[a], Johannes W. van Neck[b], Volkert van Steijn[c], Johannes P.T.M. van Leeuwen[d], Bram C.J. van der Eerden[a]
[a]*Internal Medicine, Erasmus Medical Center, Rotterdam, Netherlands*
[b]*Plastic and Reconstructive Surgery, Erasmus Medical Center, Rotterdam, Netherlands*
[c]*Chemical Engineering, Delft University of Technology, Delft, Netherlands*
[d]*Erasmus Medical Center, Rotterdam, Netherlands*

Introduction: Fracture healing involves a complex sequence of physiological events. Adequate blood supply is the most critical step as disturbed angiogenesis often causes nonunions. Paracrine factors derived from human bone mesenchymal stromal cells (hBMSCs) may have beneficial effects on angiogenesis during fracture healing but conventional cell culture models do not reflect the dynamic situation in vivo.

Objective: Study the effect of hBMSC secretome on endothelial cells and set up a microfluidic device to study endothelial cells under shear stress.

Methods: Conditioned medium was collected from hBMSCs (hBMSC-CM). The effect of hBMSC-CM on human umbilical vein endothelial cell (HUVEC) adhesion, proliferation and migration was evaluated by crystal violet staining, Ki67 immunostaining and wound healing assay, respectively. The mRNA expression of specific angiogenic biomarkers was determined by qPCR. Following fluid flow in microfluidic devices, cell viability and cell morphology was detected and monitored by live/dead assay, fluorescent cell tracker and CD31 immunofluorescent staining.

Results: Different proangiogenic and antiangiogenic factors including platelet-derived growth factor (PDGF-BB; 10-fold) and vascular endothelial growth factor (VEGF; 15-fold), were elevated in the hBMSC-CM by an angiogenic protein array. hBMSC-CM significantly accelerated HUVEC adhesion (P-value< 0.001), and increased their proliferation (P-value< 0.05) and migration (P-value< 0.01). hBMSC-CM also altered angiogenic marker gene expression including angiopoietin ANGPT1/2 (P-value< 0.01), VEGF-A (P-value< 0.01) and von Willebrand Factor (vWF). Initial studies under continuous fluid flow in microfluidics devices using live/dead assays and cell tracker staining showed that endothelial cell viability was excellent and showed abundant CD31 staining under physiological shear stress.

Conclusion: Trophic factors released by hBMSCs are able to stimulate the angiogenic response in static cultures. Our generated microfluidic device will benefit investigating the paracrine effect of hBMSCs on skeletal angiogenesis under physiological conditions.

doi:10.1016/j.bonr.2020.100412

P067

Dynamics of immunomodulatory roles of skeletal progenitors during hematoma phase of bone healing

Drenka Trivanovic[a], Theresa Kreuzahler[a], Ana Rita Pereira[a], Maximilian Rudert[b], Marietta Herrmann[a]
[a]*University Hospital Wuerzburg, Wuerzburg, Germany*
[b]*Department of Orthopaedic Surgery, König-Ludwig-Haus, University of Wuerzburg, Wuerzburg, Germany*

The aim of the study was to evaluate critical events during bone healing, particularly investigating the functions of bone marrow (BM) mesenchymal stromal cells (MSC) exposed to hematoma factors *in vitro* and *in vivo*.

Plate-fixed segmental femoral defects were created in female mice (C57BL/6J, n=62) (ethical approval 55.2.2-2532-2-580-23) and tissues (spleen, draining lymph nodes, bone and BM cells from defect and distal sites) were harvested 1, 3, and 7 days afterwards. Non-operated or sham-operated mice (no bone defect) served as controls. Human MSC (n=7) were isolated from BM of patients (ethical approval 187/18) and cultured in platelet rich plasma (PRP) to mimic the hematoma environment or fibrin hydrogels as control for 3 days. Along with cellular assays, protein and gene expression were analyzed. Values are given as mean ± standard deviation and significance was analyzed by Mann-Whitney and two-way ANOVA.

Femoral defects were associated with decreased frequency, of $CD3^+CD4^+$ (from 0.82±0.2% to 0.39±0.15% at day3, p=0.0047) and $CD3^+CD8^+$ cells (from 1.55±0.38 to 0.69±0.18% (p=0.0017) at day3 and 1.06±0.23% (p=0.0186) at day 7) in BM. A similar trend was observed in lymph nodes, but not in spleen. The frequency of $FOXP3^+$ within $CD3^+CD4^+CD25^+$ cells (Treg) increased at day1 (20.2±2.4%, p=0.04) and day3 (18.3±2.5%, p=0.062) in comparison to control (12.1±0.89%). Although cultured BM and bone cells isolated at day3 and day7, showed higher clonogenicity compared to non-operated or sham-operated mice, their subcultured progenies showed immunomodulatory potential *in vitro*, but declined clonogenicity in long-term culture. This was in accordance with promoted immunomodulatory capacity and reduced clonogenicity of human PRP-exposed MSC, which showed among other indications increased gene expression of *Ptgs2* (15-fold) and *HIF-1α* (4-fold), similarly as in day7 mouse BM cells.

Results suggest that immunomodulatory and stem cell roles of skeletal progenitors during bone healing are temporally controlled by the hematoma microenvironment.

doi:10.1016/j.bonr.2020.100413

P068

Bmp2 overexpression effects over appendicular skeleton development

José Valdés-Fernández[a], Juan Antonio Romero-Torrecilla[a], Tania López-Martínez[a], Purificación Ripalda-Cemboráin[a], Belén Prados[b], José Luis de la Pompa[b], Felipe Prósper[a], Froilán Granero-Moltó[a]
[a]*Terapia Celular, Clínica Universidad de Navarra, Pamplona, Spain*
[b]*Señalización Intercelular durante el Desarrollo y la Enfermedad Cardiovascular, CNIC (Centro Nacional de Investigaciones Cardiovasculares), Madrid, Spain*

Background: The development of the vertebrate skeleton is a complex biological event where diverse highly coordinated processes take place. In the skeletal morphogenesis signalling network, it has been reported that bone morphogenetic proteins (BMPs) play pivotal roles. BMPs are multifunctional growth factors which belong to the TGF-b superfamily of proteins, and knockout mouse models for diverse components of the BMP signalling pathway result in important skeletal abnormalities. Among the BMP family, BMP-2 has important roles in joint development, endochondral bone formation and bone maintenance and repair. *Bmp2* expression during early stages of fracture healing is compulsory for starting the reparative process.

Objective: Here we evaluate the effects of the overexpression of *Bmp2* over osteochondral development.

Methods: Transgenic mice conditionally overexpressing *Bmp2* (Rosa26-$Bmp2^{GOF}$) were crossed with transgenic mice expressing Cre recombinase under the control of Prrx1 promoter (Prrx1-Cre). With this strategy, mice offspring ($Bmp2^{GOF}$) would overexpress *Bmp2* in their limb buds, calvaria and sternum. Appendicular skeleton structure was analyzed employing micro CT, while articular tissue will be analyzed by histology.

Results: *Bmp2* overexpression originates a skeletal phenotype postnatally (Figure 1). Morphometric analysis showed that over-expressing *Bmp2* results in enlarged diaphyseal bone diameter (WT, 1.91±0.18 mm^3; $Bmp2^{GOF}$, 5.25±0.15 mm^3) with reduced mineral density (WT, 1320±31 mm^3; $Bmp2^{GOF}$, 997±8 mm^3). Histological staining shows that *Bmp2* overexpression produces a total remodeling of knee joint structure. Whereas articular cartilage was not affected, the growth plate of $Bmp2^{GOF}$ mice seems reduced and does not present hypertrophic chondrocytes or detecting levels of type X collagen by immunohistochemistry.

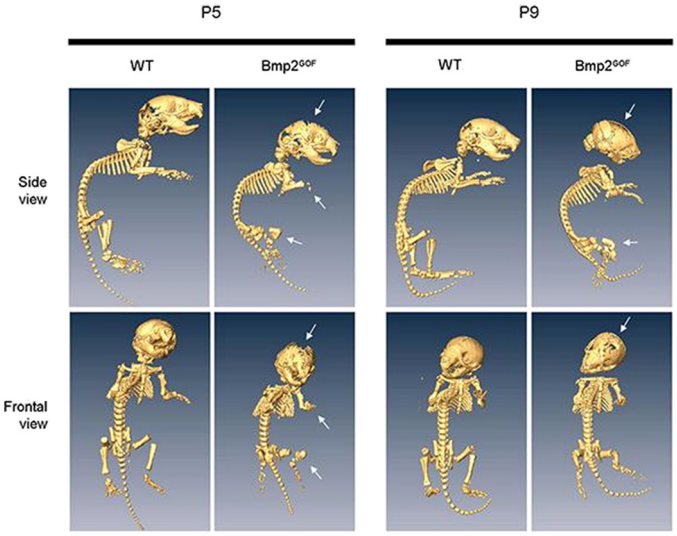

Fig 1. $Bmp2^{GOF}$ mice present skeletal abnormalities in their limbs. BMP2 overexpression causes the fusion of the radius and the ulna, as well as tibia and fibula. Femur is shorter than his WT counterpart, the tibia is folded over itself and the toe is embedded in the knee joint. $Bmp2^{GOF}$ mice also present a delay in calvaria bone fusion.

doi:10.1016/j.bonr.2020.100414

P069

Habitual loading measured in individual mice one week post surgery predicts fracture callus stiffness progression in a femur defect model

Graeme R. Paul, Esther Wehrle, Jianhua Zhang, Gisela A. Kuhn, Ralph Müller
Institute for Biomechanics, ETH Zurich, Zurich, Switzerland

Objective: Fracture healing is driven by mechanical forces within both soft tissue and newly formed bone. While longitudinal imaging has shown strong links between the mechanical environment and

bone formation, linking habitual loading, the mechanical environment and its effect on healing has not yet been investigated. In a mouse femur defect model, we have measured mechanical forces caused by habitual loading in each defect and used this parameter as a predictive measure for future healing outcomes.

Method: Twelve female CB57/BL6J mice received a femur osteotomy and were externally fixated using a calibrated strain-gauge setup. Strains in the defect were recorded (day 7-post surgery) during locomotion and converted to force in the defect as a percentage of bodyweight per mouse (BW). Micro-computed tomography images were acquired weekly and finite element analysis was used to determine tissue level strains and global defect stiffness, which was taken as a proxy for fracture healing progression.

Results: Habitual loading at day 7 correlated (Spearman's correlation coefficient) positively and significantly with callus stiffness for day 14-42 with a peak correlation at day 21 ($r=0.85$, $p< 0.001$). This indicates that the amount of mechanical stimulation self-induced by the mouse prior to bone formation is a leading factor in the fracture healing outcome. When incorporating habitual loading with individualised tissue level mechanical information (95^{th} percentile strain, median strain and 5^{th} percentile strain) and individualised mechanical information (defect volume and fixation stiffness), a linear regression model fit (r) of 0.88 was achieved.

Conclusion: Individualised habitual loading, one week post-surgery, predicts the outcome of fracture healing. The development of individualised models will allow quantified mechanical loading interventions to prevent non-union fractures and may therefore improve clinical outcomes of fracture healing.

doi:10.1016/j.bonr.2020.100415

P070

Role of macrophages in bone marrow cavity formation

Benjamin Tosun, Christine Fabritius, Christine Hartmann
Department for Bone and Skeletal Research, Institute of Musculoskeletal Medicine, University Hospital Münster, Germany, Münster, Germany

Introduction: During endochondral bone formation, chondrocytes differentiate into hypertrophic chondrocytes, which need to be removed in order to form the bone marrow cavity. According to the text books, osteoclasts and also blood vessels are essential for bone marrow cavity formation. Additional cell-types involved are chondroclasts and septoclasts. Osteoclasts differentiate from the hematopoietic lineage and require transcription factors including Pu.1 for their differentiation. Mice deficient for Pu.1 or the Rankl-receptor Rank lack osteoclasts but still form a bone marrow cavity.

Material and methods: Here, we analyzed long bones from mice (E14.5 to P0) to examine whether bone marrow cavity formation proceeds normally in mutant animals lacking Rank or Pu.1. Lineage tracing experiment using Vav1-Cre (hematopoietic-derived) and Cx3Cr1-Cre (yolk-sac derived) in combination with a RosaYFPStopflox allele were performed to identify the macrophage origin. All animal experiments were performed in accordance with local and national regulations under the licenses (84-02.04.2016.A369 and 2015.A128).

Results: Comparing the humeri of different embryonic stages, we observed a similar delay in bone marrow cavity formation in Rank and Pu.1 deficient mice. In Rank mutant bone marrow cavities, we detected a 3.5-fold increase ($P< 0.0001$) in the number of macrophages. Lineage tracing revealed that these were of hematopoietic origin. In contrast, Pu.1 deficient mice lack macrophages and osteoclasts.

Conclusion: Initiation of bone marrow cavity formation depends on osteoclasts and macrophages but proceeds independent of both cell-types. Further, in the absence of osteoclast differentiation hematopoietic derived macrophages accumulate in the bone marrow cavity.

Keywords: Macrophages, bone marrow cavity, Rank, Pu.1

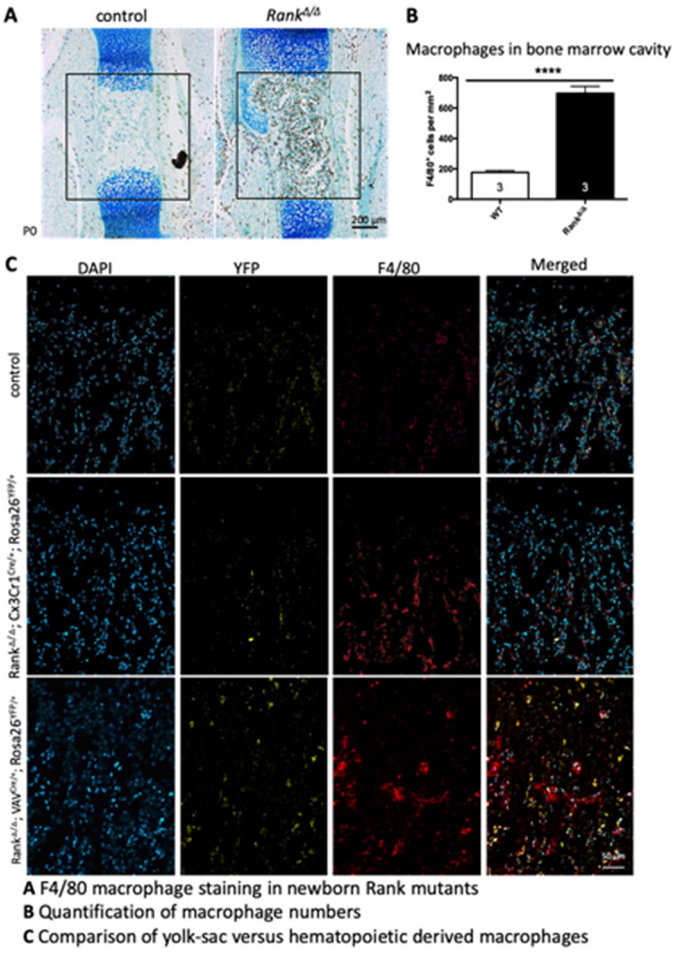

Bone marrow cavity analysis of newborn mutants.

doi:10.1016/j.bonr.2020.100416

P071

Role of beta-catenin on chondrocyte- and perichondrial-derived osteoblast differentiation

Lena Wolff, Christine Fabritius, Christine Hartmann
Bone- und Skeletal Research, Westfalian Wilhelms University, Institute of Musculoskeletal Medicine, Muenster, Germany

During endochondral ossification, a cartilaginous template is remodeled into bone involving perichondrial- and transdifferentiated chondrocyte-derived osteoblast precursors. Conditional deletion of beta-catenin in hypertrophic chondrocytes leads to a severe reduction of the chondrocyte- and perichondrial-derived osteoblast precursors, and to increased *Rankl* expression and, subsequently, more osteoclasts. Beta-catenin is a dual-function protein, functioning in Wnt-signaling as a transcriptional co-activator together with members of the Tcf/Lef transcription factor family. In addition, it is part of adherens junctions. Single knock-outs of either *Lef1*, *Tcf7* or *Tcf7l2* (conditional) did not affect osteoblast numbers or trabecular bone formation.

In a limb organ culture system, we addressed whether trans-differentiation occurs and whether it is compromised by the loss of

beta-catenin. For this, E13,5 wt and mutant forelimbs were cultivated for up to 10 days. In contrast to the *in vivo*situation, transdifferentiation of chondrocyte-derived osteoblast was not affected in beta-catenin mutants and, interestingly, no increase in osteoclasts was observed *in vitro*. Importantly, blood vessel invasion is absent in this system. As osteoclast precursors enter the bone marrow cavity via blood vessels this might explain why osteoclast numbers are not changed. To address, whether altered osteoclast numbers influence osteoblast differentiation, we analyzed mutants deficient for the transmembrane protein, Rank, essential for osteoclast differentiation. Our data suggest that the number of chondrocyte- and perichondrial-derived osteoblasts is increased in *Rank* mutants.

In conclusion, the alteration in osteoclast numbers and not beta-catenin itself influences osteoblast differentiation during bone development.

Ethical approval was obtained for all animal experiments (84-02.05.50.15.022; 81-02.04.2018.A036 and 84-02.04.2015.A128).

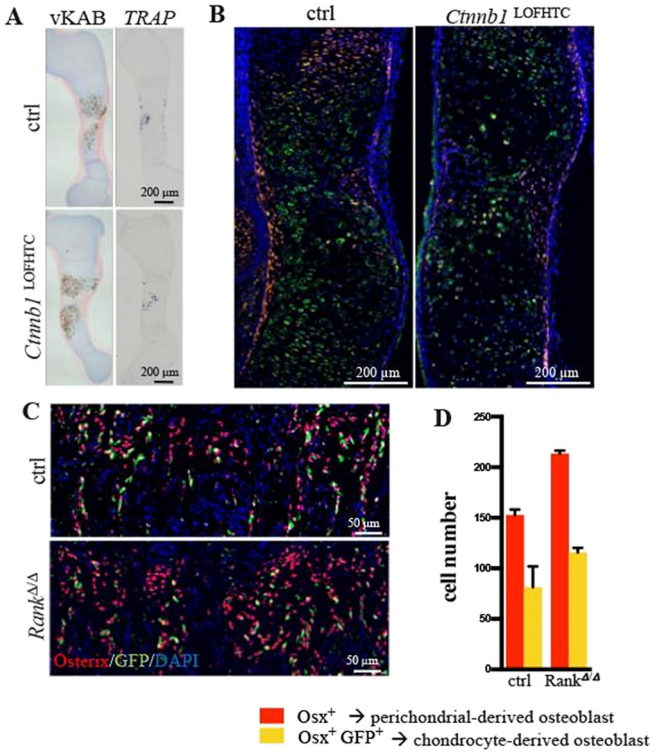

Figure: **A**, **B** Limb organ culture. **A** Trap staining revealed similar osteoclast numbers in beta-catenin conditional mutants and ctrls *in vitro*.
B Transdifferentiation is not affected in beta-catenin mutants *in vitro* .
C, D Increase in chondrocyte- and perichondrial-derived osteoblasts in *Rank* mutants compared to control.

Chondrocyte- and perichondrial-derived osteoblast.

doi:10.1016/j.bonr.2020.100417

P073

The effect of ADAR2 in osteosarcoma

Michela Rossi[a], Viviana De Martino[a], Giulia Battafarano[a], Eda Mariani[a], Valeriana Cesarini[a], Salvatore Minisola[b], Angela Gallo[a], Andrea Del Fattore[a]
[a]*Bambino Gesu' Children's Hospital, Rome, Italy*
[b]*Policlinico Umberto I, Sapienza, Rome, Italy*

Objectives: Osteosarcoma is the most common primary malignancy of bone in children and young adults. The clinical outcomes for osteosarcoma patients with recurrence and metastasis are devastating. The mechanism of RNA editing was recently shown to play a central role in the development of cancer and metabolic disorders. In this study we investigated the role of A-to-I editing enzyme ADAR2 (Adenosine Deaminase Acting on RNA 2) in osteosarcoma cell lines.

Methods: Empty vector transfected and ADAR2-overexpressing Saos2 and 143b cells were tested for their proliferation, migration, adhesion and mineralization ability. Gene expression was evaluated by Real-Time RT-PCR analysis.

Results: Saos2 cells express low levels of ADAR2 as revealed by Real-Time expression and immunofluorescence analysis. The overexpression of ADAR2 in this cell line reduced the proliferation, as confirmed by G1 arrest of cell cycle, and migration ability (wound healing µm, Empty: 189.5±16.8, ADAR2: 103.2±8.2. p=0.01) compared to control cells. Moreover, ADAR2-Saos2 cells displayed an adhesion defect at 1, 3 and 6 hours (number of cells/field, 1h Empty: 25.29±1.19, ADAR2: 14.96±2.88; 3h Empty: 49.70±5.21, ADAR2: 22.82±3.43; 6h Empty: 58.54±6.14, ADAR2: 34.30±3.95). An enhanced ability to form mineralized nodules was observed in ADAR2-overexpressing cells as shown by Alizarin Red (Arbitrary Unit, Empty: 1.02±0.36, ADAR2: 3.53±1.42) and Von Kossa stainings (Arbitrary Unit, Empty: 1.01±0.21, ADAR2: 2.81±0.26). Real-Time expression and western blot analysis revealed high levels of *Osterix* and *ALP*.

Interestingly, very low expression of ADAR2 was observed in the most aggressive 143b cell line. The overexpression of ADAR2 in these cells reduced the proliferation ability and increased *RUNX2*, *Osterix* and *ALP* expression compared to control cells.

Conclusion: To conclude, our results showed that ADAR2 acts as tumor suppressor in osteosarcoma cell lines and may represent a novel therapeutic target for treating osteosarcoma.

doi:10.1016/j.bonr.2020.100418

P074

Senolytic cocktail dasatinib+quercetin (D+Q) ameliorate irradiation-induced bone loss in mice through inhibiting osteocyte senescence and SASP

Qinghe Geng[a], Shen Wang[b], Han Huan[c], Huabei Sun[a], Juan Zhai[a], Kaijin Guo[a], Huaiyuan Zhai[a], Ke Heng[d], Hongwei Li[a], Jun Liu[d], Yiru Geng[a], Guoqiang Huang[a], Feiyuan Zhang[a], Jian Li[a], Yingle Li[a]
[a]*Xuzhou Medical University, Xuzhou, China*
[b]*Guangxi Medical University, Nanning, China*
[c]*Nanjing University of Chinese Medicine, Nanjing, China*
[d]*Nanjing Medical University, Nanjing, China*

Senolytic agents target selectively senescent cells. The senolytic cocktail, dasatinib (D) plus quercetin (Q), which causes selective elimination of senescent cells, reduced the number of naturally-occurring senescent cells and their secretion of frailty-related pro-inflammatory cytokines. The previous study demonstrated that the senolytic drugs D+Q combine therapy reduced senescent osteocytes accumulation and alleviated estrogen-deficiency induced osteoporosis in mice. Our previous studies have reported that radiation exposure mice developed osteoporosis as a result of increased osteocyte senescence and senescence-associated secretory phenotype (SASP). This study hypothesized that D+Q combined treatment improved bone mass and microarchitecture in radiation exposure mice. Here we report that radiation exposure mice developed reduced bone mass, microarchitecture, as well as mechanical strength. Additionally, increased osteocyte senescence was found in these radiation exposure mice, as indicated by increased protein expression of p16, p27, p53, mRNA expression of SASP, and decreased sirt1 and BMI-1. D+Q combined therapy significantly ameliorated bone loss by improving bone formation, alleviating bone resorption, through decreasing

osteocyte senescence and SASP. These findings suggest that D+Q combined therapy ameliorated the deleterious effects on the bone in radiation exposure mice, through inhibiting osteocyte senescence and SASP. Thus, our findings establish that radiation-induced osteoporosis is mediated, in part, by senescent cells, which can be targeted by senolytic to improve health and function.

doi:10.1016/j.bonr.2020.100419

P076

Effects of soybean isoflavone genistein and daidzein on proliferation and viability of human osteogenic sarcoma cell Saos-2

Hana Wakou, Kyoko Nakata, Hiromi Hagiwara
Biomedical Engineering, Toin University of Yokohama, Yokohama, Japan

Background: Soybeans abundantly contain genistein and daidzein in isoflavones. Difference of its structure is with or without hydroxyl group at 5-position. It has been reported that these isoflavones have anti-oxidant and anti-cancer effects. In this study, we investigated effects of genistein and daidzein on proliferation and viability of human osteogenic sarcoma cell Saos-2.

Methods: Saos-2 cells were gifted from Riken Cell Bank (Tsukuba, Japan). Genistein and daidzein were purchased from Tokyo Kasei Co., Japan. We monitored the proliferation of Saos-2 cells treated with 0 to 100 μM genistein and daidzein under a microscope for 5 days. We also examined viability of Saos-2 cells, at 48 h and 72 h, treated with 0 to 100 μM genistein and daidzein by using Cell Counting kit-8 (Dojindo).

Results: Genistein significantly inhibited proliferation and viability of Saos-2 cells in a dose-dependent manner. At 100 μM genistein, viability of Saos-2 cells was reduced by 50%. By contrast, daidzein weakly inhibited proliferation and viability of Saos-2 cells.

Conclusions: We found that 5-position hydroxyl group of genistein play a critical role on inhibitory effects of proliferation and viability of Saos-2 cells.

doi:10.1016/j.bonr.2020.100420

P079

Exposure of primary bone tumor-associated stromal cells to multi-pesticides at low doses and paracrine effects on osteoclast differentiation

Valérie Trichet[a], Louis-Romée Le Nail[a], Régis Brion[a], Françoise Rédini[a], François Vallette[b], Olivier Hérault[c], Christophe Olivier[b]
[a]*INSER UMR1238, Nantes University, Nantes, France*
[b]*INSERM UMR 1232, Nantes University, Nantes, France*
[c]*CNRS UMR 7292, Tours University, Tours, France*

Introduction: Effects of chronic poly-exposure at low doses of pesticides are poorly studied. Seven pesticides have been found simultaneously on fruits or vegetables; each one at doses that do not exceed the safety threshold, the acceptable daily intake (ADI). Previously, we have shown that a mixture of those 7 pesticides at ADI doses induced senescence of mesenchymal stromal cells (MSCs) derived from bone marrow and changed their secretome towards inflammation. Pesticide mixture did not induce transformation of MSC but revealed *in vivo* tumorigenicity of MSCs modified with 4 mutations. Osteosarcomas (OS) and giant cell tumors (GCT) are primitive bone tumors whose progression and therapeutic résistance involve interactions with non-tumor cells, including MSCs and osteoclasts. Our hypothesis is that the induction of a senescent stroma could aggravate pathologic osteolysis.

Methods: MSCs derived from OS and GCT were treated with the 7 pesticides mixture for 7 to 21 days. Doubling time and morphological change were measured (DAPI and phalloidin staining). Culture conditioned media were collected without serum during 24 hours, for multi-cytokine quantification and for osteoclast differentiation assays (CD14 positive cells derived from human blood).

Results: Pesticide exposure induced a 2-fold increase of the doubling time of stromal cells derived from OS or GCT, associated to an increase of cell size (30%). Pesticide exposure induced an increased secretion of IL6, MCP1, OPN, DKK1 and VEGF. Conditioned media obtained from 3-fold ADI-exposed stroma cells, induced a 20% to 50% increase of osteoclasts in *in vitro* assays (7 different primary stromal cell lines tested in 3 independent experiments).

Conclusion: Pesticides exposure induced senescence in OS and TCG-derived stromal cells. Following long exposure to pesticide mixture at the 3-fold ADI doses, secretomes of OS/GCT-derived stromal cells favor the osteoclastic differentiation of monocyte precursors.

doi:10.1016/j.bonr.2020.100421

P080

Eldecalcitol (ED-71) alleviates oral squamous cell carcinoma progression by suppressing GPX1 expression through NF-κB pathway

Yuan Gao, Yupu Lu, Minqi Li
Department of Bone Metabolism, School and Hospital of Stomatology, Shandong University & Shandong Key Laboratory of Oral Tissue Regeneration & Shandong Engineering Laboratory for Dental Materials and Oral Tissue Regeneration, Jinan, China

Background: Oral squamous cell carcinoma (OSCC) which the five year survival rate is only about 50%, accounts for about 90% of oral cancer. 1,25-dihydroxyvitamin D3 (1,25 - (OH)2D3) is the active form of vitamin D, which regulates many signal pathways related to cancer prognosis. Eldecalcitol (ED-71) is a new type of active vitamin D3 analog, which has been rarely reported as a potential anticancer agent for OSCC. Glutathione peroxidase-1 (Gpx1) gene is closely related to cell invasion and migration of many malignant tumors, while the research report on the relationship between Gpx1 and OSCC is rare.

Objective: To investigate the role of ED-71 in the progression of OSCC, and to determine whether ED-71 can down regulate Gpx1 expression through NF-κB signaling pathway, so as to reduce the biological behavior of OSCC, and then inhibit the development of OSCC.

Methods: SCC-15 and CAL-27 cell lines were selected. CCK-8 was used to observe the effect of drug concentration (0.04/0.4/4/40nM) and action time (12/24/36/48h) on cell viability and to explore the optimal drug concentration of ED-71. The effect of ED-71 on the tumorigenicity of cells in vitro was observed by colony formation test. Flow cytometry was used to observe the effect of ED-71 on the apoptosis and cell cycle of OSCC. Wound healing test and Transwell invasion assay were used to understand the effect of ED-71 on the migration and invasion of these two cell lines.

Existing results: Until now, interim results have been finished. ED-71 could increase the proportion of G2/M cells, inhibit cell proliferation, migration, invasion and colony formation singnificantly ($P< 0.05$), and the drug effect was time-dose-dependent. The relationship between ELD and GPX1 expression would be dected in the next step.

Conclusion: In general, this study showed that ED-71 can be used as a potential anticancer agent for OSCC.

doi:10.1016/j.bonr.2020.100422

P081

Vitamin D affects extracellular vesicle communication in bone metastasis

Joëlle Klazen[a], Iris Robbesom[a], Resti Rudjito[a], Thomas Hartjes[a], Martin van Royen[a], Sten Libregts[b], André van Wijnen[c], Carola Zillikens[a], Hans van Leeuwen[a], Marjolein van Driel[a]
[a]*Erasmus Medical Center, Rotterdam, Netherlands*
[b]*Utrecht University, Utrecht, Netherlands,*
[c]*Mayo Clinic, Rochester, United States*

Background: Bone metastases are currently incurable, resulting in death from bone-related events. Before primary cancer cells metastasize, they release nano-sized extracellular vesicles (EVs). EVs transfer information from the cancer cell to the bone. thereby preparing a metastatic niche. This makes them a target for new therapies. A potentially promising therapeutic in bone metastasis that restores bone integrity and induces tumor cell death is vitamin D. However, the effect of vitamin D on the communication between cancer cells and bone cells via EVs is unknown.

Objective: Unravel the role of vitamin D in bone metastatic prostate cancer cell EV interaction with osteoblasts.

Methods: EVs from vitamin D (10^{-7} M 1α,25-OH_2D_3) treated and untreated GFP-expressing human bone metastatic prostate cancer (PCa) cells (PC-3) were isolated by differential ultracentrifugation and counted by high-resolution flowcytometry (BD influx) and microscopy-image-guided counting (EVQuant). mRNA content was analyzed by high throughput sequencing. EV uptake by human osteoblasts (SV-HFO) was measured by flowcytometry (BD Accuri C6).

Results: Treating bone metastatic PCa cells with vitamin D strongly increased the number of EVs produced per cell (increase of 82%, p=0.0008). A different set of distinct genes was preferentially packaged in the EVs derived from vitamin D treated PCa cells [MvD1]. These genes also showed many mutual networks, which was not observed in the EVs derived from untreated cancer cells. Interestingly, the uptake of these EVs by osteoblasts was reduced (decreased by 43%, p=0.0260).

Conclusion: Vitamin D treatment of bone metastatic PCa cells affects their extracellular vesicle count, content and contact with bone. Our data identify new mechanisms by which vitamin D may alter the EV communication from metastatic cells to bone cells, and thereby unravel one of the mechanisms behind the therapeutic potential of vitamin D.

doi:10.1016/j.bonr.2020.100423

P083

Establishment of progesterone-induced mammary carcinogenesis in a humanized TgRANKL osteoporotic mouse model

Anthi Kolokotroni[a,b], Vagelis Rinotas[a], Evi Gkikopoulou[a,b], Lydia Ntari[c], Maritina Rouchota[d], Eirini Fragogeorgi[d], Danae Zareifi[e], Christos Fotis[e], Ilias Lymperopoulos[f], Leonidas Alexopoulos[e], George Loudos[d], Maria Denis[c], Niki Karagianni[c], Eleni Douni[a,b]
[a]*Institute of Bioinnovation, Biomedical Sciences Research Center Alexander Fleming, Vari-Athens, Greece*
[b]*Department of Biotechnology, Agricultural University of Athens, Athens, Greece*
[c]*Biomedcode Hellas SA, Vari-, Athens, Greece*
[d]*Bioemission Technology Solutions (BIOEMTECH), Athens, Greece*
[e]*Department of Mechanical Engineering, National Technical University of Athens, Athens, Greece*
[f]*1rst Breast Clinic, Iaso Hospital, Athens, Greece*

Receptor activator of nuclear factor-κB ligand (RANKL) mediates the paracrine effect of progesterone-induced proliferation of mammary epithelial cells during pregnancy and lactation. Moreover, RANKL is involved in the initiation of breast cancer and bone metastasis. To investigate the role of RANKL in breast carcinogenesis and bone metastasis we established a hormone-induced mouse model in C57BL/6 wild-type (WT) mice through implantation of pellets containing synthetic progestin (medroxyprogesterone acetate, MPA) followed by oral administration of 7,12-dime-thylbenz(a)anthracene (DMBA) for a period of 8 weeks. Palpable tumors appeared between 2-10 weeks after the last DMBA administration. Mice were analyzed through *in vivo* whole-body positron emission tomography (PET) scanning (β-eye™, BIOEMTECH) with the clinically approved tracer [^{18}F]-2-deoxy-D-glucose (FDG) in order to monitor tumor development and progression. Uptake and metabolism of FDG is higher in cancer than in normal cells due to increased glycolysis and overexpression of glucose membrane transporters (GLUTs). Mammary tumors isolated from treated mice were analyzed through histology, immunocytochemistry and multiplex protein assays. To investigate the involvement of RANKL in progesterone-induced breast carcinogenesis we compared tumor incidence among WT mice, transgenic mice expressing human RANKL (TgRANKL) or a humanized transgenic model expressing only human RANKL and not endogenous mouse RANKL (TgRANKL/RANKL$^{tles/tles}$). Our results showed tumor development in all groups, which was attenuated through pharmaceutical RANKL inhibition as confirmed by histological and immunohistochemical analysis. PET images showed accumulation of FDG in palpable and non-palpable tumors even at a very early stage of occurrence. Conclusively, we have established a novel preclinical platform for drug evaluation in a progesterone induced RANKL-dependent breast cancer model, and next steps include the strengthening of the platform through more in depth studies.

doi:10.1016/j.bonr.2020.100424

P084

Mechanical unloading enhances bone destruction and tumor expansion in multiple myeloma: Critical roles of osteocytic RANKL induction

Kotaro Tanimoto[a,b], Masahiro Hiasa[a,b], Hirofumi Tenshin[a,c], Jumpei Teramachi[b,d], Asuka Oda[b], Takeshi Harada[b], Mohannad Ashter[a,b], Kimiko Sogabe[b], Masahiro Oura[b], Itsuro Endo[b], Toshio Matsumoto[e], Eiji Tanaka[a], Masahiro Abe[b]
[a]*Department of Orthodontics and Dentofacial Orthopedic, Tokushima University, Tokushima, Japan, Tokushima, Japan*
[b]*Department of Hematology, Endocrinology and Metabolism, Tokushima University, Tokushima, Japan, Tokushim, Japan*
[c]*Department of Hematology, Endocrinology and Metabolism, Institute of Biomedical Sciences, Tokushima Univeersity, Tokushim, Japan*
[d]*Department of Tissue Regeneration, Tokushima University, Tokushima, Japan, Tokushima, Japan*
[e]*Fujii Memorial Institute of Medical Sciences, Tokushima University, Tokushima, Japan*

Multiple myeloma (MM), a malignancy of plasma cells, preferentially expands in the bone marrow, while inducing debilitating osteoclastic bone destruction to cause immobilization by bone fractures and/or paralysis by spinal compression. However, it is unclear whether immobilization or mechanical unloading affects MM tumor progression and bone destruction. Because osteocytes are master regulatory cells of bone remodeling by sensing mechanical stress, we explored the impacts of immobilization or mechanical unloading on MM tumor expansion in bone with special reference to osteocytes. Right hind legs of mice were unilaterally immobilized by sciatic denervation or casting with adhesive bandage. MicroCT revealed substantial volume reduction of not only muscles ($p < 0.05$) but also trabecular bone in the immobilized legs.

Histological analyses on the tibiae in the immobilized legs showed that osteoclast numbers were increased on the surface of the trabecular bone along with RANK ligand upregulation in osteocytes. Interestingly, when luciferase-transfected mouse 5TGM1 MM cells were inoculated into the tibiae in mice, 5TGM1 tumor expanded more rapidly in immobilized hind legs with the denervation or casting than in intact hind legs as shown by IVIS images($p< 0.05$). The acceleration of MM tumor growth by mechanical unloading was further confirmed by simultaneous MM cell inoculation into tibiae in both unloaded (right) or intact (left) hind legs in the same mice ($p< 0.05$). The acceleration of MM tumor growth by the mechanical unloading was mostly suppressed by injection of the anti-resorptive agents, zoledronic acid or the TAK1 inhibitor LLZ1640-2($p< 0.05$). In addition, MM cell growth was enhanced in cocultures with osteoclasts generated from bone marrow cells by RANK ligand. These results collectively demonstrate that mechanical unloading aggravates bone destruction and MM tumor expansion, and suggest the causative role of osteocytic RANK ligand induction and thereby osteoclastogenesis in promotion of MM tumor expansion by mechanical unloading.

doi:10.1016/j.bonr.2020.100425

P085

Risk of osteoporotic fracture in patients with breast cancer; meta-analysis

Young-Kyun Lee[a], Deog-Yoon Kim[b], Yong-Chan Ha[c], Dong Won Byun[d], Ha-Young Kim[e], Ho-Yeon Chung[b], Youjin Lee[f], SNUBH-KSBMR
[a]*Orthopedic Surgery, Seoul National University Bundang Hospital, Seongnam, Republic of Korea*
[b]*Kyung Hee University Medical Center, Seoul, Republic of Korea*
[c]*Orthopedic Surgery, Chung-Ang University College of Medicine, Seoul, Republic of Korea*
[d]*Soonchunhyang University Hospital, Seoul, Republic of Korea*
[e]*Gangneung Asan Hospital, Gangneung, Republic of Korea*
[f]*National Cancer Center, Goyang, Republic of Korea*

Background: The fracture risk induced by anti-estrogen therapy in patients with breast cancer remains controversial. The aim of this study was to perform a meta-analysis and systematic review to evaluate the risk of osteoporotic fracture in patients with breast cancer.

Methods: A systematic search was performed to identify studies that included any osteoporotic fracture (hip fracture and vertebral fracture) in patients breast cancer. Main outcome measures were occurrence and risk of osteoporotic fractures including hip and vertebral fractures in patients and controls.

Results: A systematic search yielded a total of four studies that included osteoporotic fracture outcomes in patients with breast cancer. Meta-analysis showed a higher risk of osteoporotic fracture in patients with breast cancer. Analysis of these four studies involving a total of 127,722 (23,821 cases and 103,901 controls) patients showed that the incidence of osteoporotic fractures was higher in the breast cancer group than in the control group. The pooled estimate of crude RR for osteoporotic fracture was 1.35 (95% CI: 1.29-1.42, $p < 0.001$).

Conclusions: Although studies were limited by a small number, results suggested a possible association between anti-estrogen therapy and increased risk of osteoporotic fractures in patients with breast cancer.

doi:10.1016/j.bonr.2020.100426

P086

The change of bone mineral density and bone metabolism after gastrectomy for gastric cancer: A meta-analysis

Young-Kyun Lee[a], Deog-Yoon Kim[b], Yong-Chan Ha[c], Youjin Lee[d], Dong Won Byun[e], Ho-Yeon Chung[b], Ha-Young Kim[f], SNUBH-KSBMR
[a]*Seoul National University Bundang Hospital, Seongnam, Republic of Korea*
[b]*Kyung Hee University Medical Center, Seoul, Republic of Korea*
[c]*Orthopedic Surgery, Chung-Ang University College of Medicine, Seoul, Republic of Korea*
[d]*National Cancer Center, Goyang, Republic of Korea*
[e]*Soonchunhyang University Hospital, Seoul, Republic of Korea*
[f]*Gangneung Asan Hospital, Gangneung, Republic of Korea*

Purpose: Survivorship care, including bone health, has become an important issue in gastric cancer. We performed a metaanalysis of the available observational studies to determine whether and how osteoporosis risk is increased after gastrectomy in patients with gastric cancer.

Methods: A total of 1204 patients (802 men) from 19 cohort studies were included.We evaluated the prevalence of osteoporosis in postgastrectomy patients, comparing the incidence according to the type of gastrectomy and sex. Additionally, we evaluated changes in bone mineral density (BMD) and bone metabolism-related markers pre- to postoperatively and between patients who underwent gastrectomy and matched controls. Proportion meta-analysis was performed and pooled odds ratios (ORs) were calculated.

Results: The pooled incidence estimate was 36% [95% confidence interval (CI), 32-40]. The incidence of osteoporosis was significantly higher in women than in men ($OR = 1.90$, $p < 0.001$) but was similar between partial and total gastrectomy groups ($OR = 0.983$, $p = 0.939$). BMD was significantly decreased, and calcium, phosphorous, and parathyroid hormone levels were significantly increased in patients after gastrectomy compared to those before gastrectomy. BMD and calciumand 25OH-vitamin D levels were significantly decreased, and parathyroid hormone and 1,25OH-vitamin D levels were significantly increased in the gastrectomy group compared to that in the control group.

Conclusion: We found that BMD is significantly decreased after gastrectomy in patients with gastric cancer. Vitamin D deficiency and secondary hyperparathyroidism are suggested to be common mechanism underlying BMD impairment. After resection, patients should undergo long-term nutritional and bone health surveillance, in addition to their oncological follow-up.

doi:10.1016/j.bonr.2020.100427

P088

Adipocytes and osteoporosis inhibit osteoblast differentiation by downregulating histone acetylation

Rodrigo P.F. Abuna, Luciana O. Almeida, Alann T.P. Souza, Roger R. Fernandes, Thales F.V. Sverzut, Bruna Scaf, Julia Lima, Adalberto L. Rosa, Marcio M. Beloti
School of Dentistry of Ribeirão Preto, University of Sao Paulo, Ribeirão Preto, Brazil

Osteoporosis induces low bone mass and adipocyte accumulation in bone marrow. Here, we investigated the effect of conditioned medium (CM) by osteoblasts previously co-cultured with adipocytes on osteoblasts grown in non-conditioned medium and compared them with osteoblasts from osteoporotic rats. All animal procedures were approved by Ethics Committee in Animal Research. Mesenchymal stem cells (MSCs) from bone marrow and adipose tissue of rats were cultured

under osteogenic and adipogenic conditions to differentiate into osteoblasts and adipocytes, respectively. Then, they were co-cultured for 3 days, and osteoblasts were cultured for another 24 hours in serum-free medium to produce CM. New osteoblasts were cultured for 3 days in this CM. Osteoporosis was induced by orchiectomy (ORX) and osteoblasts differentiated from bone marrow MSCs of ORX and Sham rats were compared. The inhibitory effect of CM on osteoblast differentiation was similar to that induced by osteoporosis (Fig. 1A-D) as well as decreased histone H3 acetylated (AcH3) protein expression (Fig. 1E-F). Trichostatin A (TSA), an inhibitor of histone deacetylase, was used to increase AcH3, which reverted the deleterious effect of CM and osteoporosis on osteoblast differentiation (Fig. 2A-F). In conclusion, adipocytes recapitulate the inhibitory effect of osteoporosis on osteoblast differentiation by downregulating histone acetylation.

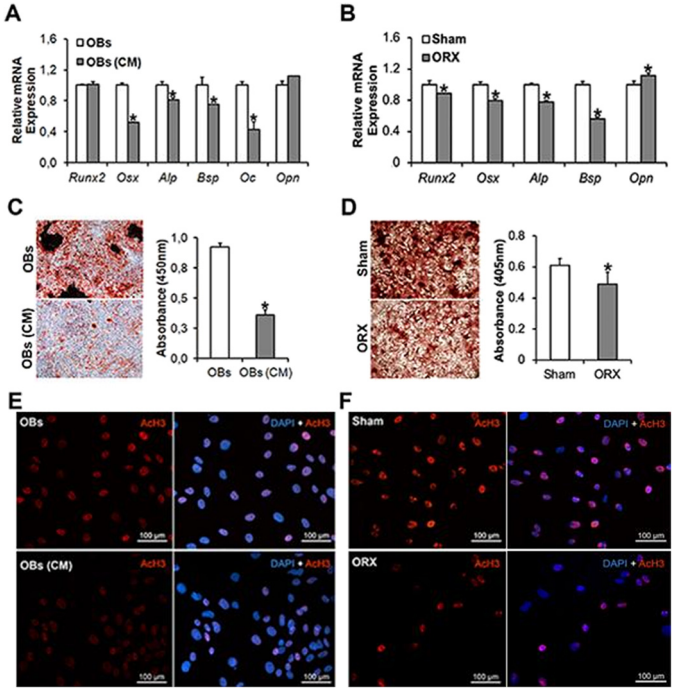

Fig. 1. Effect of CM and ORX on osteoblast differentiation. *Student's t-test, n=3, p≤0.05).

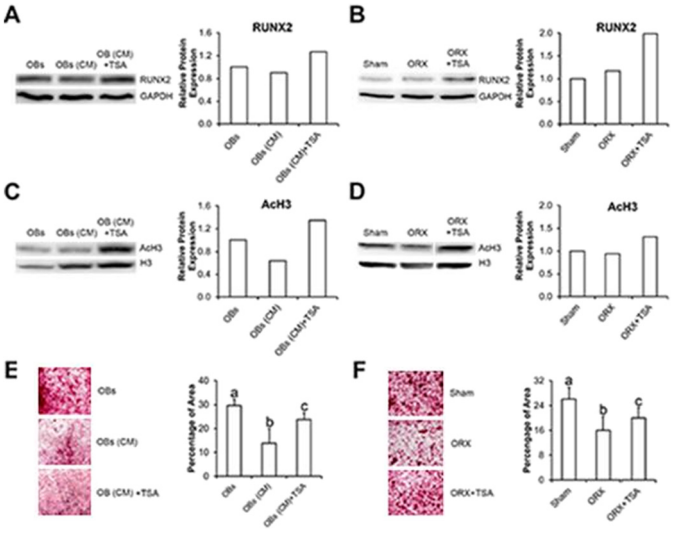

Fig. 2. Effect of CM and ORX on osteoblast differentiation involves AcH3. ANOVA, n=3, p≤0.05.

doi:10.1016/j.bonr.2020.100429

P089

Positive effects of mesenchymal stem cells from healthy rats on the impaired osteoblast differentiation of mesenchymal stem cells from osteoporotic and diabetic rats

Alann T.P. Souza, Gileade P. Freitas, Helena B. Lopes, Denise Weffort, Fabiola S. Oliveira, Marcio M. Beloti, Adalberto L. Rosa
School of Dentistry of Ribeirao Preto, University of Sao Paulo, Ribeirao Preto, Brazil

Osteoporosis and diabetes mellitus are systemic diseases that impaired the osteoblast differentiation of mesenchymal stem cells (MSCs). Considering cell therapy applications to treat bone defects under osteoporotic and diabetic conditions, we hypothesized that MSCs from healthy rats (HE-MSCs) have positive effects on the ability of MSCs from osteoporotic (ORX-MSCs) and diabetic (DM-MSCs) rats to differentiate into osteoblasts. Thus, the aim of this study was to evaluate the influence of HE-MSCs on the osteoblast differentiation of both ORX-MSCs and DM-MSCs, using an indirect co-culture model. All animal procedures were approved by Ethics Committee in Animal Research. Osteoporosis and diabetes mellitus were induced by orchiectomy surgery and streptozotocin injection, respectively. Then, MSCs were isolated from bone marrow of healthy, osteoporotic and diabetic rats, co-cultured under osteogenic condition and *Runx2* gene expression (n=3) and alkaline phosphatase (ALP) activity (n=5) were evaluated on day 10 and extracellular matrix mineralization (n=5), on day 14. Co-cultures of cells at the same condition (healthy, osteoporotic or diabetic) were used as controls. The data were compared by ANOVA (p≤0.05) and indicate that MSCs derived from healthy rats partially recovered the osteogenic potential of MSCs from rats with osteoporosis and diabetes mellitus (Fig. 1). These findings suggest that the use of MSCs from healthy donors may be an interesting strategy in cell therapy approaches to repair bone tissue under osteoporotic and diabetic conditions.

doi:10.1016/j.bonr.2020.100430

P090

Revealing the localization of Annexin A6 in matrix vesicles during physiological mineralization

Ekeveliny Amabile Veschi[a], Mayte Bolean[a], Agnieszka Strzelecka-Kiliszek[b], Joanna Bandorowicz-Pikula[b], Slawomir Pikula[b], Yubo Wang[c], Thierry Granjon[c], Saida Mebarek[c], David Magne[c], Ana Paula Ramos[a], José Luis Millán[d], Rene Buchet[c], Massimo Bottini[e], Pietro Ciancaglini[a]
[a]*Chemistry, Faculdade de Filosofia, Ciências e Letras de Ribeirão Preto (FFCLRP) da Universidade de São Paulo (USP), Ribeirao Preto, Brazil*
[b]*Nencki Institute of Experimental Biology, Warsaw, Poland*
[c]*Institut de Chimie et Biochimie Moléculaires et Supramoléculaires ICBMS UMR 5246 - Université Lyon 1 - CNRS - INSA Lyon - CPE Lyon Batiment Raulin, Lyon, France*
[d]*Sanford Burnham Prebys Medical Discovery Institute, La Jolla, San Diego, United States*
[e]*Department of Experimental Medicine, University of Rome Tor Vergata, Rome, Italy*

Annexin A6 (AnxA6, ~68 kDa) is the largest member of the annexin family of proteins present in matrix vesicles (MVs). MVs serve as nucleation sites for crystal deposition during physiological mineralization.

Here, we assess the localization of AnxA6 in the MV membrane using native MVs and MVs biomimetics. Biochemical analyses revealed that AnxA6 is present in three distinct regions of the MV membrane. The first, corresponds to Ca^{2+}-bound AnxA6 interacting with the inner leaflet of MV membrane, the second, is AnxA6 localized on the surface of the outer leaflet of MV membranes, and the third, is AnxA6 inserted in the membrane's hydrophobic bilayer and co-localized with cholesterol. Using monolayers and proteoliposomes composed of either dipalmitoylphosphatidylcholine (DPPC) to mimic the outer leaflet of the MV bilayer or a 9:1 DPPC:dipalmitoylphosphatidylserine (DPPS) mixture to mimic the inner leaflet, we confirmed that AnxA6 interacts differently with MV membranes in agreement with the biochemical data. Thermodynamic analysis based on the measurement of the surface pressure exclusion, enthalpy and phase transition cooperativity ($\Delta t_{1/2}$) showed that AnxA6 interacts with both the lipid models and that this interaction increases in the presence of cholesterol. The selective recruitment of AnxA6 by cholesterol molecules was observed in MVs as probed by the addition of methyl-β-cyclodextrin (MβCD). AnxA6-lipid interaction was Ca^{2+}-dependent as evidenced by the greater increase in surface pressure in negatively charged 9:1 DPPC:DPPS monolayers and a larger decrease in enthalpy in 9:1 DPPC:DPPS proteoliposomes caused by the addition of AnxA6 in presence of Ca^{2+} compared to zwitterionic bilayers composed of DPPC. We conclude that the different localizations and ways of interaction of AnxA6 with the lipid membrane suggest distinct functions in MV during biomineralization.

Financial supports: FAPESP, CAPES and CNPq

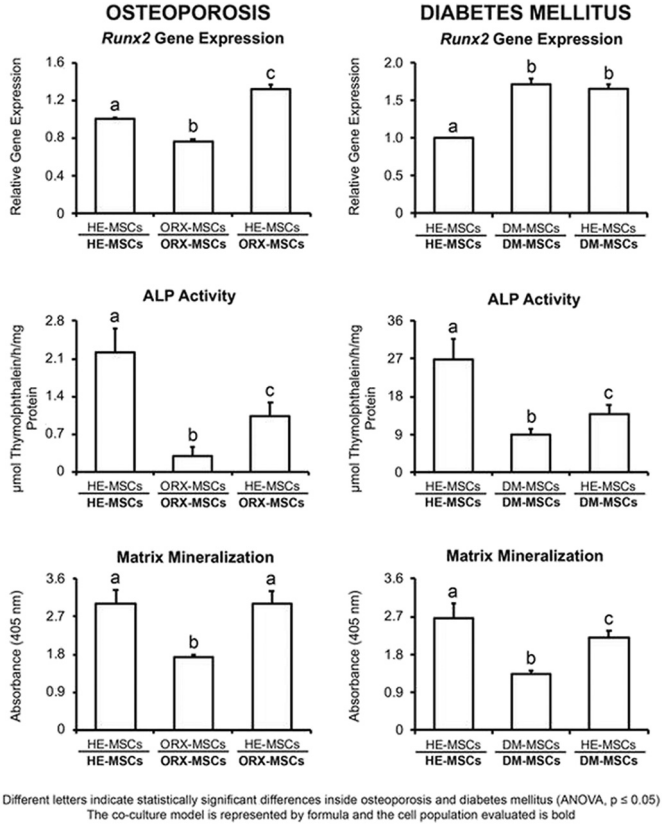

Fig. 1. Runx2 gene expression (n=3), ALP activity (n=5), and matrix mineralization (n=5).

doi:10.1016/j.bonr.2020.100431

P091

The type 1 lysophosphatidic acid receptor is involved in osteoblastogenesis up to osteocytogenesis

Adebayo Candide Alioli[a], Léa Demesmay[b], Sara Laurencin[a], Nicolas Beton[a], Delphine Farlay[b], Helene Follet[b], Jerold Chun[c], Richard Rivera[c], Daniel Bouvard[d], Irma Machuca-Gayet[b], Jean-Pierre Salles[a], Isabelle Gennero[a], Olivier Peyruchaud[b]

[a]*Centre de Physiopathologie de Toulouse Purpan INSERM UMR 1043, Toulouse, France*
[b]*INSERM, Unit 1033, Université Claude Bernard Lyon 1, Lyon, France*
[c]*Department of Molecular Biology, Dorris Neuroscience Center, The Scripps Research Institute, San Diego, United States*
[d]*Institute for Advance Biosciences, Grenobles, France*

Multiple factors, systemic and local, participate in the regulation of bone cell activity. One of those factors is lysophosphatidic acid (LPA). LPA is a natural bioactive lipid exhibiting growth factor-like activities on a large range of normal and neoplastic cells. LPA activates at least six different G-coupled receptors (LPA1-6). LPA_1 is ubiquitous Gi coupled GPCR and is the most interesting for bone homeostasis. Indeed, our team have shown that global deletion of *Lpar1* (the LPA_1 gene) alters the growth of mice as a consequence of a bone formation defects. The aim of this study was to better understand the specific role of LPA via its receptor LPA_1 in the accrual of bone mass during puberty. Thus, we generated *Lpar*1flox/flox;Osx:GFP-Cre/+ mouse lines, in which the *Lpar*1 was specifically invalidated from preosteoblats to osteocytes. Our results show that LPA_1 is essential for bone mineralization. We also found that the absence of LPA_1 slowdown osteocytogenesis and disturbs osteocyte maturation. Osteocytes are mechanosensor cells that control bone formation. Our results suggest a new role for LPA in bone mass control through osteocyte activity.

doi:10.1016/j.bonr.2020.100432

P093

Effects of ginsenoside Rb2 on osteogenic differentiation of C2C12 cells

Tahoo Park[a], Heesu Lee[b,c], Seong-Hee Ko[c,d]

[a]*Natural Product Research Center, Korea Institute of Science and Technology, Gangneung, Republic of Korea*
[b]*Oral anatomy, Gangneung-Wonju National University, College of Dentistry, Gangneung, Republic of Korea*
[c]*Research Institute of Oral Science, Gangneung, Republic of Korea*
[d]*Pharmacology, Gangneung-Wonju National University, College of Dentistry, Gangneung, Republic of Korea*

The most current therapies for osteoporosis have focused on inhibiting bone resorption by osteoclasts. Although the conventional drugs have therapeutic benefits, they also have disadvantages such as breast cancer and osteonecrosis of jaw. The purpose of this study is to develop the new anabolic agents for treatment of osteoporosis that have fewer risks compared to conventional therapies. *Panax Ginseng* is one of the most commonly used herbal medicines. Most of the biological activities of ginseng are derived from main components, ginseng saponins (ginsenosides). To determine the effect of ginsenosides on bone formation, we examined the effect of ginsenosides Rb2(G-Rb2) on C2C12 cell proliferation and osteogenic differentiation.

For determining the effects of ginsenosides on proliferation of C2C12 cells, we did MTT assay of C2C12 cells with ginsenoside Rb1, Rb2, Rc, Rd, Rg1 and Rg3 at 0.5, 5 and 50 μM. To evaluate whether ginsenoside Rb2(G-Rb2) could promote the osteogenic differentiation of C2C12 cells, nonosteogenic precursors, mRNA expression of runt-related transcription factor-2 (Runx2) was determined. mRNA of Runx2 expression was analyzed by quantitative real time PCR. And we examined the effects of G-Rb2 on mRNA expression of estrogen receptor α and β.

G- Rb1, Rb2, Rc and Rd significantly increased C2C12 cell proliferation. G-Rg3 decreased C2C12 cell proliferation at 5, 50 μM. G-Rb2 significantly increased mRNA expression of Runx2 after 24 hours culture in osteogenic media. In addition, G-Rb2 increased mRNA expression estrogen receptor α and β both. However G-Rb2 upregulated expression of estrogen receptor β to a greater extent than that of estrogen receptor α.

These results suggest that G-Rb2 may promote osteogenic differentiation of osteoblasts and may have bone protective effect through estrogen receptor upregulation.

doi:10.1016/j.bonr.2020.100433

P094

MiR-155 negatively regulates osteogenic differentiation of mMSCs, bone regeneration and bone mass

Zhichao Zheng[a], Janak Lal Pathak[a], Richard T. Jaspers[b], Gang Wu[c]
[a]*Affiliated Stomatology Hospital of Guangzhou Medical University, Guangzhou, China*
[b]*Faculty of Behavioural and Movement Sciences, Vrije Universiteit Amsterdam, Amsterdam Movement Sciences, Amsterdam, Netherlands*
[c]*Academic Centre for Dentistry Amsterdam (ACTA), University of Amsterdam and Vrije Universiteit Amsterdam, Amsterdam Movement Sciences, Amsterdam, Netherlands*

MicroRNA-155 (miR-155) inhibits BMP9-induced osteogenesis and stimulates TNF-α-mediated osteoclastogenesis. However, the role of miR-155 on bone regeneration and bone mass has not been investigated yet. This study aimed to examine the role of miR-155 on osteogenic differentiation of mMSCs in vitro, and bone regeneration and bone mass in vivo. miR-155$^{-/-}$ mice were obtained from The Jackson laboratory. While miR-155^{KI} mice were constructed by the CRISPR method. We analyzed femoral bone mass in miR-155$^{-/-}$, and miR-155^{KI} mice (7 weeks, n=4) by micro-CT. miR-155 was silenced with sponged-lentivirus in mouse BMSCs (mBMSCs), then cell migration and osteogenic differentiation were analyzed in vitro. BMP-2 (2 μg) loaded collagen film was ectopically transplanted in miR-155 transgenic mice and ectopic bone regeneration was evaluated by micro-CT. Ethical approval was obtained for animal study. The selected significance level was $P< 0.05$. Micro-CT data and quantification of bone parameters (BMD, BV/TV, Tb. N, Tb. Th, and Tb. Sp) showed that the bone mass was decreased in miR-155^{KI} mice and increased in miR-155$^{-/-}$ male mice. In miR-155^{KI} mice BMD, BV/TV, Tb.N, and Tb. Th were reduced by 0.8-, 0.7-, 0.8-, and 0.9-fold, respectively, compared to wildtype mice. In miR-155$^{-/-}$ mice, BMD, BV/TV, and Tb.N were increased 1.7-, 1.6-, and 1.6-fold, respectively, compared to wildtype mice. Matrix mineralization (Alizarin red staining, ARS) was enhanced in miR-155 knockdown mBMSCs culture. mBMSCs migration was significantly increased in the miR-155 knockdown group. Micro-CT images and quantification showed that the ectopic bone formation was reduced in miR-155^{KI} mice and enhanced in miR-155$^{-/-}$ mice. In conclusion, miR-155 showed an inhibitory effect on migration and osteogenic differentiation of mMSCs, bone regeneration, and bone mass. Therefore, miR-155 could be the possible therapeutic target to improve stem cell-based bone defect healing and to treat the diseases with low bone mass phenotype.

doi:10.1016/j.bonr.2020.100434

P095

Molecular players in biogenesis of mineralization-competent matrix vesicles

Sandeep Chaudhary[a], Massimo Bottini[b], Sana Khalid[c], José Luis Millán[d], Dobrawa Napierala[c]
[a]*University of Alabama at Birmingham, Birmingham, United States*
[b]*University of Rome Tor Vergata, Rome, Italy*
[c]*University of Pittsburgh, Pittsburgh, United States*
[d]*Sanford Children's Health Research Center, Sanford Burnham Prebys Medical Discovery Institute, La Jolla, United States*

Matrix vesicles (MVs) are a specific type of extracellular vesicles with a unique function of supporting the initiation of the mineralization process of the skeletal and dental tissues. Although it has been proposed that MVs are formed by shedding off the cell membrane, the molecular mechanisms driving formation of mineralization-competent MVs are not fully understood. The goal of our studies is to identify molecular mechanisms regulating MVs biogenesis during the initiation of the mineralization process. We hypothesized that molecular stimuli of the mineralization process are involved in the MVs biogenesis. Using cellular in vitro models of mineralization and nanoparticle tracking analyses, we have demonstrated that committed osteogenic cells rapidly increase release of MVs upon stimulation with inorganic phosphate (P_i). Western blot and immunostaining analyses identified that the P_i-induced release of MVs requires activation of Erk1/2 kinases and is associated with activation of Rac1 and cdc42 small GTPases, and reorganization of the actin cytoskeleton. Comparative mass spectrometry and protein profiling analyses of MVs released from osteogenic cells cultured under normophosphatemic (0.8mM P_i) and hyperphosphatemic (5mM P_i) conditions revealed that high P_i changes protein composition of MVs. Interestingly, while tissue-nonspecific alkaline phosphatase was highly abundant in both groups of MVs, neither of these groups was highly positive for markers of exosomes. In summary, our studies demonstrate that P_i is a potent stimulator of MVs biogenesis and regulates the protein composition of MVs.

doi:10.1016/j.bonr.2020.100435

P096

The integrin α2β1-dependent collagen upregulation is linked to the TGF-β superfamily

Melanie Brand[a], Daniel Kronenberg[a], Jens Everding[b], Beate Eckes[c], Richard Stange[a]
[a]*Department of Regenerative Musculoskeletal Medicine, Institute of Musculoskeletal Medicine, University Hospital Münster, Münster, Germany*
[b]*Department of Trauma, Hand and Reconstructive Surgery, University Hospital Münster, Münster, Germany*
[c]*Department of Dermatology, University of Cologne, Cologne, Germany*

Integrins are a family of transmembrane receptors, cell adhesion and signal transduction proteins with important roles in the interplay of

cells with extracellular matrix. Integrin α2β1 is one of four collagen-binding integrins and an important receptor for collagen I in bone tissue. Our group showed that integrin α2β1 deficiency in mice enhances the expression of collagen I and accelerates fracture healing. We will identify the basic mechanisms by which integrin α2β1 influences the bone metabolism.

Based on the well characterized roles of members of the TGFb family in collagen deposition and tissue repair, we investigated TGF-β1 and BMP-2 and their SMAD signaling cascades as these are prominent factors in the regulation of collagen gene expression and mineralization of bone tissue. By immunofluorescence staining and western blot analysis we identified the localization and level of phospoSMAD2,3 *in-vitro* in wild type (WT) and integrin α2-deficient ($ITGA2^{(-/-)}$) cells.

The western blot analysis showed an elevated basal level of phosphoSMAD2,3 in $ITGA2^{(-/-)}$ cells. Additionally, we detected different localization of phosphoSMAD2,3 in $ITGA2^{(-/-)}$ and WT cells. In WT cells signals for phosphoSMAD2,3 were detected in the cytosol, at the nucleus and ER as well as at the cell membrane. In the $ITGA2^{(-/-)}$ cells most of the signal was located at the ER and nucleus where phoshoSMAD2,3 binds to the promotor region of collagen type I and activates gene expression.

We could show that the loss of integrin α2β1 regulates collagen gene expression by increasing phosphorylation of SMAD2,3. Therefore, we hypothesize that integrin α2β1 influences collagen synthesis and the mineralization process by modulating the activity of members of the TGF-β superfamily and can be considered as therapeutic application for dysfunctions in the bone metabolism like non-union fractures.

doi:10.1016/j.bonr.2020.100436

P097

Osteogenic effect of the association of VEGF-A and BMP-9 on mesenchymal stem cells

Helena Lopes, Maria Paula Gomes, Julia Lima, Georgia Quiles, Gabriela Totoli, Gileade Freitas, Marcio Beloti, Adalberto Rosa
Bone Research Lab, University of São Paulo - School of Dentistry of Ribeirão Preto, Ribeirão Preto, Brazil

Mesenchymal stem cells (MSCs) can differentiate into several cell types, including osteoblasts. The bone morphogenetic protein 9 (BMP-9) and vascular endothelial growth factor A (VEGF-A) play a role in osteogenesis, both increasing osteoblast differentiation of MSCs. However, the effect of combining BMP-9 and VEGF-A on osteogenesis is unknown. Thus, the aim of this study was to evaluate the *in vitro* effect of the association of VEGF-A and BMP-9 on the osteogenic potential of MSCs derived from bone marrow (BM-MSCs) and adipose tissue (AT-MSCs). All animal procedures were approved by the Local Committee of Ethics in Animal Research. Firstly, we determined that 100 ng/mL of VEGF-A and BMP-9 is the most effective concentration to induce osteoblast differentiation of MSCs. Then, BM-MSCs and AT-MSCs from male Wistar rats were grown in culture medium supplemented with VEGF-A (100 ng/mL), BMP-9 (100 ng/mL) and VEGF-A + BMP-9 (100 ng/mL of both) for 7 days. Cells grown in non-supplemented medium were used as controls. The gene expression of osteoblastic markers (n=3) and alkaline phosphatase (ALP) activity (n=5) were evaluated and the data were compared by One-Way ANOVA and Tukey's test ($p< 0.05$). In general, VEGF-A did not induce osteoblast differentiation while BMP-9 alone and BMP-9+VEGF-A enhanced this differentiation with the later exhibiting the most pronounced effect (Fig. 1). The association of BMP-9 and VEGF-A increased the osteoblast differentiation of MSCs from both sources; however, this effect was more intense on AT-MSCs suggesting that these cells are more responsive to such combination of growth factors.

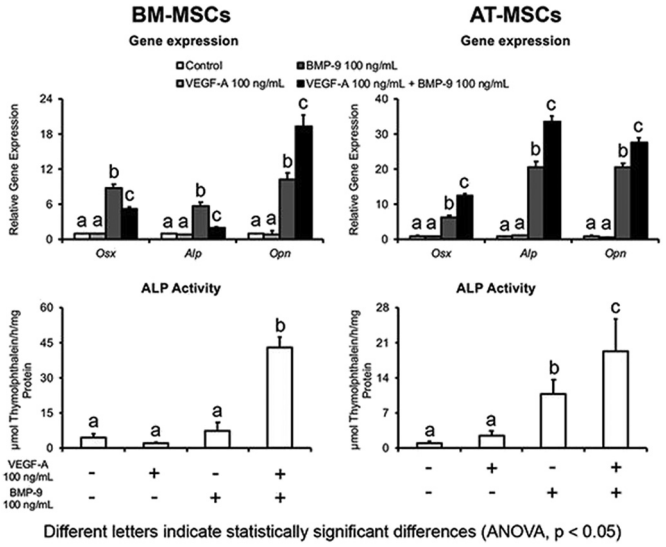

Fig. 1. Osteoblast differentiation of BM-MSCs and AT-MSCs induced by VEGF-A and BMP-9.

doi:10.1016/j.bonr.2020.100437

P098

Serotonin promotes osteogenic differentiation of MC3T3-E1 cells

YuRi Song[a], Si Yeong Kim[a], Hyun Ah Lee[a], Jeong-Hwa Baek[b], Hyun Jeong Kim[c], Hee Sam Na[a], Jin Chung[a]
[a]*Department of Oral Microbiology, Pusan National University School of Dentistry, Yangsan-si, Republic of Korea*
[b]*Department of Molecular Genetics, School of Dentistry, Seoul National University, Seoul, Republic of Korea*
[c]*Department of Dental Anesthesiology, School of Dentistry, Seoul National University, Seoul, Republic of Korea*

Background: Periodontitis is characterized with structural bone destruction of periodontium. Bone resorption was caused by the imbalance of bone homeostatis by osteoclast and osteoblast. Serotonin (SER; 5-hydroxytrypamine [5-HT]), a neurotransmitter involved in mood control, is involved in bone metabolism. However, the effect of serotonin on bone metabolism is still controveral and remains to be elucidated. Thus, the aim of this study was to investigate the effects of serotonin on osteoblastogenesis.

Method: To examine the effect of serotonin on cellular proliferation, MC3T3-E1 cells were treated with serotonin and MTT assay was performed. To evaluate whether serotonin promotes the osteogenic differentiation, the expression of RUNX2, osteocalcin (OCN), RANKL and osteoprotegerin (OPG) was observed by real-time PCR. The effect on mineralization was assessed by the alkaline phosphatase (ALP) acitivity assay.

Results: Serotonin treatment increased MC3T3-E1 cell proliferation until 3 days to 5 days. The mRNA expression of RUNX2 was increased after 72 hour culture with serotonin. In addition, serotonin enhanced the mRNA expression of OPG and RANKL. Serotonin increased OPG mRNA expression more than that of RANKL and then, it upregulated the OPG/RANKL ratio. Furthermore, serotonin enhanced osteogenic mineralization with ALP mRNA expression of and ALP activitiy.

Conclusion: These results suggest that serotonin up-regulates osteogenic differentiation of osteoblasts and increases osteoblast formation.

doi:10.1016/j.bonr.2020.100438

P100

Deletion of miR-675 in hMSC-TERTs leads to increased ALP activity

Ines Foessl[a], Marijke Koedam[b], Moustapha Kassem[c], Bram van der Eerden[b], Barbara Obermayer-Pietsch[a], Jeroen van de Peppel[b]
[a]*Department of Internal Medicine, Medical University of Graz, Graz, Austria*
[b]*Department of Internal Medicine, Erasmus MC, Rotterdam, Netherlands*
[c]*Department of Endocrinology and Metabolism, University Hospital of Odense, Odense, Denmark*

Introduction: MicroRNA-675 (miR-675) is located within the first exon of H19, a large intergenic non-coding RNA locus on chromosome 11. The host gene H19 is well conserved, paternally imprinted and thought to be transcribed to regulate the expression of insulin-like-growth-factor 2. H19 is strongly upregulated during osteogenic differentiation of human mesenchymal stem cells (hMSCs). The function of miR-675 in hMSCs is not well documented. In order to investigate miR-675 during osteoblast differentiation, we created miR-675 knockout cells to study their performance during osteogenic differentiation.

Methods: CRISPR/Cas9 knock-outs of miR-675 in hMSCs expressing telomerase (hMSC-TERTs) and the enzyme Cas9 were created. Two days after seeding in alpha-MEM medium, clonally expanded knock-out cells were differentiated in osteogenic medium for 14 days. Samples for standard biochemistry were harvested at 0, 7, 10 and 14 days. Alkaline phosphatase (ALP) activity was measured colorimetrically. Protein content was determined using a BCA-assay and DNA concentration was determined via ethidium bromide.

Results: miR-675 knock-out was confirmed by PCR and sequencing analyses. ALP activity in miR-675 knock-out cells was increased both at d7 (54,5 ±17mU/cm^2) compared to control cells (11,1 ± 3 mU/cm^2, p=0,0012) and at d10 (299,5 ±105 mU/cm^2) compared to control cells (47,0 ± 30,1 mU/ cm^2, p=0,0019). When normalized to DNA concentration, ALP activity was still significantly higher in the knock-out cells compared to controls (p=0,0046 at d7, p= 0,0005 at d10).

Discussion: The increased ALP activity of cells lacking miR-675 suggests an enhanced osteogenic differentiation with an earlier onset. Further research should indicate the mechanism and target genes of miR-675 during osteogenic differentiation and the implications on the function of H19. The establishment of cells lacking miR-675 is a first and promising step towards elucidating the function of miR-675 in the osteoblastic differentiation of hMSCs and is ready for further investigation.

doi:10.1016/j.bonr.2020.100439

P101

Extensive modeling-based bone formation after 2 months of romosozumab treatment: Results from the FRAME clinical trial

Erik F. Eriksen[a,b], Roland Chapurlat[c], Rogely Boyce[d], Jacques P. Brown[e], Stéphane Horlait[f], Cesar Libanati[g], Yifei Shi[d], Rachel B. Wagman[d], Pascale Chavassieux[c]
[a]*Department of Clinical Endocrinology, Oslo University Hospital, Oslo, Norway*
[b]*Institute of Clinical Medicine, Oslo University, Oslo, Norway*
[c]*INSERM UMR 1033, University of Lyon, Lyon, France*
[d]*Amgen Inc., Thousand Oaks, United States*
[e]*CHU de Quebec Research Centre and Laval University, Quebec City, Canada*
[f]*Amgen, Boulogne Billancourt, France*
[g]*UCB Pharma, Brussels, Belgium*

Objective: Assess the effect of two months of romosozumab vs placebo on the surface extant of modeling- and remodeling-based bone formation (MBBF/RBBF) in the FRAME trial (NCT01575834).

Materials and methods: Women aged ≥55 years with osteoporosis were randomized 1:1 to 210mg romosozumab or placebo SC QM for 12 months, followed by 60mg denosumab SC Q6M for 12 months. Unstained, 7 μm bone sections from patients with a Month 2 transiliac biopsy were analyzed by fluorescence microscopy. Histomorphometric parameters were measured at cancellous, endocortical and periosteal envelopes using an ocular linear test system. At each line intersection of the ocular sampling grid with single or double tetracycline labels administered at Month 2, the underlying cement line was classified as smooth (signifying bone modeling) or scalloped (remodeling). The effect of treatment on MBBF/RBBF at each envelope referent to bone and labeled surface was compared using the Wilcoxon rank-sum test, without multiplicity adjustment.

Results: After two months of romosozumab, MBBF referent to bone surface was significantly increased on endocortical and cancellous surfaces with no significant difference in surface extent of RBBF vs placebo (Figure). Romosozumab at Month 2 reversed proportions of MBBF/RBBF from approximately 33%/66% (placebo) to 66%/33% in endocortical and cancellous envelopes.

Conclusion: These data show that bone formation in the first two months of romosozumab treatment is predominately due to increased MBBF on the endocortical and cancellous surfaces.

Acknowledgements: This study was funded by UCB Pharma, Amgen Inc. and Astellas. Medical writing services were provided by Costello Medical.

Fig. Bone Modeling and Remodeling After 2 Months of Romosozumab vs Placebo

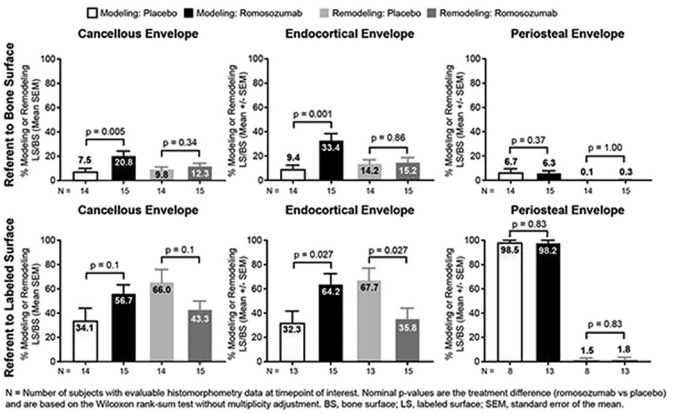

N = Number of subjects with evaluable histomorphometry data at timepoint of interest. Nominal p-values are the treatment difference (romosozumab vs placebo) and are based on the Wilcoxon rank-sum test without multiplicity adjustment. BS, bone surface; LS, labeled surface; SEM, standard error of the mean.

doi:10.1016/j.bonr.2020.100440

P102

Syndecan 3 stimulates bone formation through stabilisation of Frizzled 1

Andrew Butcher[a], Gemma Charlesworth[a], Amanda Prior[a], Katherine Sperinck[a], Adolorata Pisconti[b], George Bou-Gharios[a], Anna Daroszewska[a], Rob Van 'THof[a]
[a]*Liverpool University, Liverpool, United Kingdom*
[b]*Stony Brook University, New York, United States*

Syndecan 3 (Sdc3), a transmembrane heparan-sulphate proteoglycan, is important in embryonic development, however its role in the adult skeleton is unknown. We previously showed premature osteoporosis associated with high marrow fat and blunted anabolic response to mechanical loading in young adult Sdc3 knockout (Sdc3KO) mice, associated with reduced β-catenin in osteoblasts. Whilst canonical Wnt-signalling induces osteogenesis, Sdc3-Wnt interaction has not been studied. We hypothesised that Sdc3 stabilises the Frizzled1 (Fzd1) receptor, key for canonical Wnt-signalling.

We generated mice expressing *Sdc3* driven by the *Col1a1* promoter in osteoblasts. Femoral bone parameters were analysed by μCT (WT n=11, $WT^{Col1a1+}$ n=4, Sdc3KO n=10, $Sdc3KO^{Col1a1+}$ n=2). Sdc3KO and WT BMSCs were grown in osteogenic vs osteo-adipogenic conditions, and osteoblast vs adipocyte formation was quantified. Sdc3KO vs WT osteoblasts were treated with Bafilomycin for 6h and Fzd1 quantified by Western Blot (n=2).

There was an 84% increase in BV/TV in the $Sdc3KO^{Col1a1+}$ vs Sdc3KO ($p< 0.001$) and a 37% increase in the $WT^{Col1a1+}$ vs WT ($p< 0.001$). BV/TV in the $Sdc3KO^{Col1a1+}$ was also increased by 32% vs the WT mice ($p< 0.001$).

Sdc3KO BMSC cultured in osteo-adipogenic conditions showed a 2-fold increase in adipocyte numbers compared to WT cells ($p< 0.05$). Under osteogenic conditions, bone nodule formation was reduced by 60% in the Sdc3KO cultures ($p< 0.05$).

The Fzd1 level was reduced by 66% in osteoblasts from Sdc3KO mice compared to WT. Bafilomycin treatment increased Fzd1 protein by 20% in WT cells and 3.5-fold in Sdc3KO cells, restoring Fzd1 protein in Sdc3KO to levels equivalent to WT.

Our results indicate that Sdc3 enhances osteogenesis through stabilisation of Fzd1, which allows for increased Wnt-signalling in osteoblasts. Moreover, overexpression of Sdc3 in normal WT osteoblasts leads to increased bone formation in vivo. Thus, targeting Sdc3 could lead to development of bone anabolic therapeutics in the future.

Keywords: Bone, Osteoblasts, Syndecan3, Frizzled1

doi:10.1016/j.bonr.2020.100441

P103

FasL deficiency impacts the developing mandibular bone in an age-dependent manner

Eva Svandova[a,b], Barbora Vesela[a,b], Alice Ramesova[a,b], Herve Lesot[a], Anne Poliard[c], Jeremy Sadoine[c], Amina Djoudi[c], Eva Matalova[a,b]
[a]*Institute of Animal Physiology and Genetics, Academy of Sciences of the Czech Republic, Brno, Czech Republic*
[b]*University of Veterinary and Pharmaceutical Sciences, Brno, Czech Republic*
[c]*Laboratory of Orofacial Pathologies, Université Paris Descartes, Paris, France*

FasL (CD178), traditionally associated with apoptotic signalling, displays much broader spectrum of functions including those in osteogenesis. To reveal more details, FasL deficient (*gld*) mice were analysed with focus on the developing mandibular bone. This bone, as other intramembranous bones, includes osteoblasts differentiating directly from condensed mesenchymal cells. In the mouse model, the condensation appears around prenatal day 13 and two days later, a bone tissue containing osteoblasts, osteoclasts and osteocytes can be observed in proximity of the first molar tooth germ.

Immunohistochemistry identified presence of FasL already at prenatal day 13 and also in later prenatal stages, mostly in osteoblastic cells. However, postnatally, expression of FasL was ceasing, perhaps due to changing proportion of osteoblasts (FasL positive) vs. osteocytes (FasL mostly negative). To analyse this observation further, microCT technique was applied to compare bone quantity and quality at early postnatal stages, namely day 6, 12 and 24. The ratio of bone volume/tissue volume was decreased in the *gld* bone at postnatal day 6 but increased at postnatal day 12. The same changes applied for the trabecular thickness and were even more evident in 24-day-old *gld* mice. This study, therefore, pointed to the age-dependent alterations in the *gld* bone phenotype.

Acknowledgement: Supported by the Czech Science Foundation, project GAČR/FWF/19-29667L

doi:10.1016/j.bonr.2020.100442

P105

Homeodomain transcription factor MEIS1 inhibits differentiation of immortalised human MSCs

Yuan Guo[a], Rosinda Mies[a], Moustapha Kassem[b], Hans van Leeuwen[a], Jeroen van de Peppel[a]
[a]*Erasmus University Medical Center, Rotterdam, Netherlands*
[b]*University of Southern Denmark and Odense University Hospital, Odense, Denmark*

MEIS1 is an important transcriptional regulator in hematopoietic development. Previous studies illustrated that *MEIS1* was silenced by DNA methylation during differentiation of hematopoietic progenitors, suggesting a critical role of MEIS1 during the maintenance of the undifferentiated state of HSCs. Gene expression studies from our lab indicated that *MEIS1* was upregulated upon osteogenic and adipogenic differentiation of human BMSCs. The objective of this study is to investigate the role of MEIS1 during differentiation and ECM mineralization of hMSC-TERTs.

Homozygous MEIS1 disruption mutants ($MEIS1^{-/-}$) were generated in $hMSC\text{-}TERTs^{Cas9}$. Cells were differentiated into osteoblasts and extracellular matrix (ECM) mineralization was determined using Alizarin Red Staining. ALP, DNA, protein and calcium concentration were measured at day 7, 10, 12, 14 and 21 after osteogenic induction. The mRNA expression of osteocalcin was quantified by RT-PCR after 14 days osteoblast induction. Cells were differentiated into adipocytes and at multiple time-points Nile Red Staining and Hoechst staining were applied.

ALP activity in $MEIS1^{-/-}$ osteoblast differentiating cells was significantly increased (1.5-2-fold; $p< 0.05$) at each time point compared to $MEIS1^{+/+}$ $hMSC\text{-}TERTs^{Cas9}$. Moreover, Alizarin Red staining of the mineralized matrix and Ca^{2+} measurement in the media illustrated that the ECM mineralization in $MEIS1^{-/-}$ cells was enhanced during osteoblast mineralization (two days earlier). Additionally, $MEIS1^{-/-}$ $hMSC\text{-}TERTs^{Cas9}$ have an increased capacity to differentiate into adipocytes (4-6-fold; $p< 0.0001$). Osteocalcin expression was 15-fold higher expressed in $MEIS1^{-/-}$ cells compared to wild type ($p< 0.005$). Interestingly, a single nucleotide mutation (NM_002398:c.7533_7535delG) resulted in the expression of 4 different splice variants that were not observed in wild type cells.

Our findings illustrate that the transcription factor MEIS1 is involved in the inhibition of differentiation of hMSC-TERTs. We speculate a role for MEIS1 in hMSC-TERTs controlling osteoblastic genes expression signature regulated by different splice variants, and which is differentially between differentiated or non-differentiated hMSC-TERTs.

doi:10.1016/j.bonr.2020.100443

P106

Unravelling the role of phosphatidylserine on the precipitation of calcium phosphate by mineralizing-extracellular vesicles

Marcos Antonio Cruz[a], Claudio Ferreira[a], Saida Mebarek[b], Rene Buchet[b], Luciano Caseli[c], Pietro Ciancaglini[a], Ana Paula Ramos[a]
[a]*Department of Chemistry, University of Sao Paulo, Ribeirao Preto, Brazil*
[b]*UFR Chimie Biochimie, Universite Lyon 1, Lyon, France*
[c]*Instituto de Ciências Ambientais Químicas e Farmacêuticas, Federal University of Sao Paulo, Sao Paulo, Brazil*

Bone biomineralization is an exquisite process by which cells control the deposition of a hierarchically mineralized matrix. There is growing evidence about the involvement of extracellular vesicles in the formation and delivery of the very first mineral nuclei to the bone growth front. Our aim is to unravel the molecular mechanisms behind phospholipid-mediated calcium phosphate nucleation and to get insight on how phospholipid-mineral complexes are involved in the mineralization of collagen. To this end, we used self-assembled lipid monolayers mimicking the lipidic composition of matrix vesicles (MVs). We evidenced that the enrichment of phosphatidylserine (PS) on MVs is responsible to control the nucleation of the mineral. Using self-assembled monolayers mimicking the lipid composition of MVs, we noticed by *in situ* characterization techniques (vibrational spectroscopy, transmission electron microscopy and potentiometric measurements of free Ca^{2+}) that mineralization was achieved within 4 h on supersaturated solutions only when PS was present (Fig. 1). Amorphous calcium phosphate nucleated by PS was able to further convert to apatite after 24 h. Moreover, we also evidenced that phospholipid-mineral complexes were able to deliver a precursor mineral phase to type I-collagen fibrils after 24 h, attesting that these vesicles can act as a confined medium to specifically nucleate calcium phosphate in a PS-mediated manner. PS is localized in the inner leaflet of MVs, where calcium phosphate complexes and apatites are formed. Our findings indicated that PS is enough to induce apatite precipitation. We believe that this mechanism is not exclusive to MVs but universal to other mineralizing-EVs.

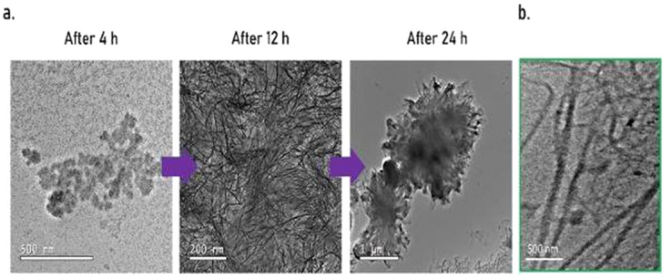

(a) TEM of mineralized PS-rich monolayers (b) Collagen fibrils infiltrated by the mineral after 24h.

doi:10.1016/j.bonr.2020.100444

P107

Fra1 is dispensable for the function of Runx2-expressing osteoblasts

Julia Luther, Mona Neven, Olga Winter, Lana Rosenthal, Michael Amling, Jean-Pierre David
Institute for Osteology and Biomechanics (IOBM), University Medical Center Hamburg-Eppendorf, Hamburg, Germany

Ubiquitous overexpression of the transcription factor activator protein-1 (AP-1) member Fra1 causes progressive osteosclerosis, a phenotype due to a cell-autonomous accelerated osteoblast differentiation resulting in an increased number of mature osteoblasts. In addition to the bone phenotype, Fra1 overexpression opposes adipocyte differentiation by an adipocyte-specific inhibition of Cebpa expression. Conversely, epiblast-specific deletion of Fra1 by *More-Cre* causes an osteopenic phenotype most likely due to a cell autonomous decreased bone formation by osteoblasts. Moreover, Fra1 has additionally been shown to enhance osteoclastogenesis in vitro.

To confirm the cell autonomous bone phenotype, we generated osteoblast-, as well as osteoclast-specific *Fra1*ko mice. Cell-specific deletion of Fra1 in osteoclasts by *LysM-Cre* did not affect trabecular bone mass in 12 week-old nor in 1 year old-mice (BV/TV: 14.23±3.49% (control) versus 12.85±2.733% (*LysM-Cre*;$Fra1^{fl/fl}$) at the age of 1 year). Deletion of Fra1 in osteoblasts by *Runx2-Cre* did not significantly change bone mass in young as well as in aged *Runx2-Cre*;$Fra1^{fl/fl}$ mice compared to control (trabecular BV/TV: 15.53±2.243% (control) versus 13.36± 0.7766% (*Runx2-Cre*;$Fra1^{fl/fl}$), cortical thickness: 0.2011±0.02263 mm (control) versus 0.1923±0.02356 mm (*Runx2-Cre*;$Fra1^{fl/fl}$) at the age of 1 year). In addition, we could not observe a significant change in the number of osteoblasts in these mice. However, interestingly, osteoblast specific deletion of Fra1 causes reduced adipose tissue mass accrual and reduced maturation of adipocytes in the epididymal fat tissue.

Therefore, expression of Fra1 in the later stage of osteoblast differentiation is not required for bone mass acquisition of adult mice but regulates adipose tissue metabolism. These data suggest that the bone anabolic function of Fra1 would be driven by its expression in early mesenchymal osteoblast progenitors rather than in commited Runx2-positive pre-osteoblasts.

doi:10.1016/j.bonr.2020.100445

P108

Epigenetic priming of BMP-mediated osteogenesis and bone repair

Amel Dudakovic[a], Rebekah Samsonraj[a], Christopher Paradise[a], Catalina Galeano-Garces[a], Merel Mol[b], Daniela Galeano-Garces[a], Pengfei Zan[a], M. Lizeth Galvan[a], Mario Hevesi[a], Oksana Pichurin[a], Roman Thaler[a], Dana Begun[a], Peter Kloen[b], Marcel Karperien[c], A. Noelle Larson[a], Jennifer Westendorf[a], Simon Cool[d], Andre van Wijnen[a]
[a]*Mayo Clinic, Rochester, United States*
[b]*Amsterdam University Medical Center, Amsterdam, Netherlands*
[c]*University of Twente, Enschede, Netherlands*
[d]*Institute of Medical Biology, Singapore, Singapore*

Bone formation can be enhanced by bone morphogenetic proteins (e.g., BMP2), parathyroid hormone (PTH), and targeting of WNT inhibitors. Previously, we established that the inhibition of the epigenetic enzyme Ezh2 (i.e., reduction in methylation of histone H3 at lysine 27) is bone anabolic and osteo-protective. These biological effects are linked to the ability of Ezh2 inhibition to enhance bone-stimulatory signaling pathways. For example, Ezh2 loss stimulates Wnt ligand (e.g., Wnt10b and Wnt10a) expression, enhances PTH receptor (Pthr1h) expression, and increases Smad1/5 phosphorylation (i.e., BMP2 signaling cascade activation). Because of high cost and side-effects associated with clinical use of BMP2, we investigated whether BMP2 dosing can be reduced by concurrent Ezh2 inhibition. Co-administration of BMP2 and GSK126, a selective Ezh2 inhibitor, enhances MC3T3 osteoblast differentiation. Interestingly, GSK126 and BMP2 co-administration results in synergistic activation of osteogenic genes, alkaline phosphatase activity, and alizarin red staining. Dual BMP2 (10ng/ml) and GSK126 (5μM) administration is synergistic and as effective as 50ng/ml BMP2 at inducing MC3T3 osteoblastogenesis. mRNA-Seq analysis reveals robust increases in osteoblast/osteocyte markers with BMP2 and GSK126 co-administration. In support of the findings with MC3T3 osteoblasts, dual GSK126 and BMP2 administration enhances osteogenic gene expression (e.g., SP7 and IBSP) in human BMSCs undergoing osteogenic differentiation. BMP2 (300ng local) and

GSK126 (5μg local + 50mg/kg systemic five days) combination was also assessed in an established murine calvarial critical-sized defect model. While we did not observe significant difference between BMP2 and BMP2 plus GSK126, our analyses (e.g., μCT, histomorphometry, and surgical grading) reveal more consistent healing in the combination treatment group. Together, our results suggest that Ezh2 inhibition enhances BMP2-mediated induction of osteogenic differentiation of progenitor cells (human BMSCs) and maturation of committed osteoblasts (murine MC3T3s). Thus, Ezh2 inhibition may be combined with BMP2 in clinical scenarios that require stimulation of bone formation.

doi:10.1016/j.bonr.2020.100446

P109

Deciphering the role of non-coding RNAs in osteogenesis and osteoclastogenesis

Sara Moura[a,b], Mario Barbosa[a,b], Susana Santos[a,b], Maria Ines Almeida[a,b]
[a]*i3S/INEB, Porto, Portugal*
[b]*ICBAS, Universidade do Porto, Porto, Portugal*

Introduction: Over the past years non-coding RNAs (ncRNAs), including microRNAs (miRNAs) and long ncRNA (lncRNAs), have emerged as important new therapeutic tools. We aim to investigate the impact of micro(mi)RNAs and long ncRNAs in osteogenic differentiation and osteoclastogenesis.

Methods: To achieve this goal, ncRNA expression profile was evaluated during osteogenic differentiation in primary human Mesenchymal Stem/Stromal Cells (MSC), MC3T3 cell line, and during osteoclast differentiation in human monocytes and RAW264.7 cell line, by RT-qPCR. Next, the biological effect of the most differently expressed ncRNAs was assessed using ncRNA mimics and inhibitors. To evaluate osteoblast-osteoclast crosstalk, osteoblast-derived culture media at day 7 of differentiation was cultured with osteoclasts and it effect was determined.

Results: The results showed that miRNAs (miR-195, miR-99a) are differently expressed during osteogenic differentiation of both human primary MSC and MC3T3 cells ($p < 0.05$). Moreover, miR-99a family is altered during osteoclastogenesis of human monocytes and RAW 264.7 ($p < 0.05$). Modulation of miRNA levels, specifically miR-195 and miR-99a inhibition, in MC3T3 pre-osteoblast cell line lead to an 2-fold increase of osteogenic differentiation markers and ALP and Alizarin Red O staining (mineralization). Moreover, supernatant from MC3T3-miRNA transfected cells at day 7 of osteogenic differentiation impaired osteoclastogenesis differentiation of RAW 264.7, by altering the number of multinucleated cells (>20%) and the expression of the osteoclast markers dendritic cell-specific transmembrane protein, C-C Motif Chemokine Ligand, and Cathepsin K ($p < 0.05$).

Conclusion: Taken together, our data indicate that ncRNAs have the ability to regulate osteogenic differentiation and osteoclastogenesis and are potential candidates for bone regenerative therapies.

Acknowledgements: This project is supported by FCT in the framework of the project POCI-01-0145-FEDER-031402 (PORTUGAL 2020/Programa Operacional da Competitividade e Internacionalização).

doi:10.1016/j.bonr.2020.100447

P110

BMP-7 improves cells sheets-like from human dental pulp stem cells: Expression of osteogenic markers, gap junction, and ECM remodeling

Leticia Gasparoni, Cristiane Bronzeri, Katiucia Paiva
Anatomy, University of Sao Paulo, São Paulo, Brazil

Cell Sheet is a technology developed for creating cell layers applied for tissue repair, where cells are stimulated to secrete extracellular matrix (ECM) to provide a more homogeneous microenvironment due to increase cell-ECM and cell-cell interactions. Furthermore, ECM remodeling is a crucial process to ensure matrix integrity, which is maintained by the balance between matrix metalloproteinases (MMPs) and their inhibitors (TIMPs and RECK). Cell Sheet may be an engineered alternative for bone repair. Bone Morphogenetic Proteins (BMPs) are well known to induce bone formation. This work aimed to evaluate the influence of BMP-7 on ECM remodeling proteins and osteogenic markers in cell sheets-like structures from human Dental Pulp Stem Cells (DPSCs) under osteogenic stimulation. DPSCs (passage 4-6) were kept under osteogenic media (a-MEM + 10% FBS, + 10 mM L-ascorbic acid phosphate + 1 mM dexamethasone + 10 mM b-glicerolphosphate + antibiotics) or BMP-7 media (osteogenic media + 50 ng/mL rhBMP-7). Real-time PCR (Collagen type I/Coll, Connexin 46/CX43, Runx2, Bone Sialoprotein/BSP, Dlx5, MMPs, TIMPs, and RECK genes), alkaline phosphatase activity quantification (ALP), and alizarin red stain (AR) were conducted after 1, 7, 14, 21, 28, and 35 days post-induction. BMP-7 induced ALP and AR detection earlier than osteogenic group. The expression of osteogenic markers, CX43, most of ECM remodelling enzymes and their inhibitors were upregulated throughout all experimental periods in both groups. BMP-7 induces early expression in most of the genes evaluated. Here, we showed for the first time a long-term follow-up of DPSCs undergoing to osteoblast differentiation associated with BMP-7. We suggest that BMP-7 can improve osteogenic cell sheet-like structure from DPSCs.

Financial Support: FAPESP

doi:10.1016/j.bonr.2020.100448

P111

Glucocorticoids induce osteoporosis mediated by glucocorticoid receptor-dependent and -independent pathways

Yu Jiang
The Affiliated Wuxi No.2 People's Hospital of Nanjing Medical University, Wuxi, China

Clinically, glucocorticoids (GCs) are widely used to treat inflammation-related diseases, but their long-term use can cause side effects such as osteoporosis and fracture, known as glucocorticoid-induced osteoporosis (GIOP). Nr3c1 is the major glucocorticoid receptor, and its mediated signaling pathway is involved in regulating various intracellular physiological processes, including bone cells; however, its mechanism in glucocorticoid-induced osteoporosis remains unclear. In this study, a zebrafish nr3c1 mutant was successfully generated using CRISRP/Cas9 technology to investigate the role of nr3c1 in glucocorticoid-induced osteoporosis. Mutation of nr3c1 mutant altered cartilage development and significantly decreased bone mineralization compared to in wild-type (WT) zebrafish. Additionally, qRT-PCR results showed that the expression of extracellular matrix (ECM), osteoblast, and osteoclast-related genes was altered in the mr3c1 mutant. The GCs-Nr3c1 pathway regulates bone-metabolic-related gene expression via Nr3c1-dependent and Nr3c1-independent pathways. A dual luciferase reporter assay further revealed that GCs and Nr3c1 transcriptionally regulated matrix metalloproteinase 9 (mmp9), alkaline phosphatase (alp), and acid phosphatase 5a (acp5a). This study reveals that GCs-Nr3c1 affects the expression of genes involved in bone metabolism and provides a basis for determining the role of GIOP and Nr3c1 in bone metabolism and development. We also identified a new effector target for clinical treatment of GIOP.

doi:10.1016/j.bonr.2020.100449

P113
ZBTB20 positively regulated titanium particle-induced macrophage inflammatory response and osteolysis

Yue Ding, Junxiong Qiu
Department of Orthopaedic Surgery, Sun Yat-Sen Memorial Hospital, Sun Yat-Sen University, Guangzhou, China

Aseptic Loosening caused by wear particles liberating from implant surfaces is one of the main causes for failure of artificial joint replacements. Wear particles play a critical role in osteolysis, which can be phagocytized by macrophages and other local cells, activating osteoclasts, and inciting an adverse immunoreaction. Therefore, it's pivotal to find potential therapeutic targets to suppress macrophages' pro-inflammatory functions.

This study was designed to explore the effect of ZBTB20, a member of BTB/POZ family, on titanium particle-induced osteolysis (TPIO). We performed H&E staining and IHC on synovial membranes of aseptic loosening patients, then RNA-Seq transcriptome analysis of RAW264.7 macrophages were carried out to explore potential key molecules. Cluster analysis showed that TNF-α and IL-6 mainly associated with other differentially expressed genes, and IκBα on upstream may be a potential suppressing target. It's reported that ZBTB20 contains transcriptional repressor activity to IκBα, so we hypothesized that ZBTB20 functions as a regulator in TPIO. By constructing shRNA and overexpression lentivirus, we observed that ZBTB20 regulated the Ti particle-induced inflammatory reaction by adjusting NF-kB pathways, IRF-3 and stabilizing TGN. We performed in vivo studies, using local lentivirus injection, local macrophage injection and bioluminescence imaging to illuminate the effect of ZBTB20 on particle-induced mouse cranial osteolysis. The results were consistent with in vitro experiments.

Collectively, our data suggested that ZBTB20 played a positive role in macrophage activation and osteoclastic bone loss induced by Ti particles *in vitro* and *in vivo*, and therefore a potential therapeutic target for the prevention of aseptic joint loosening.

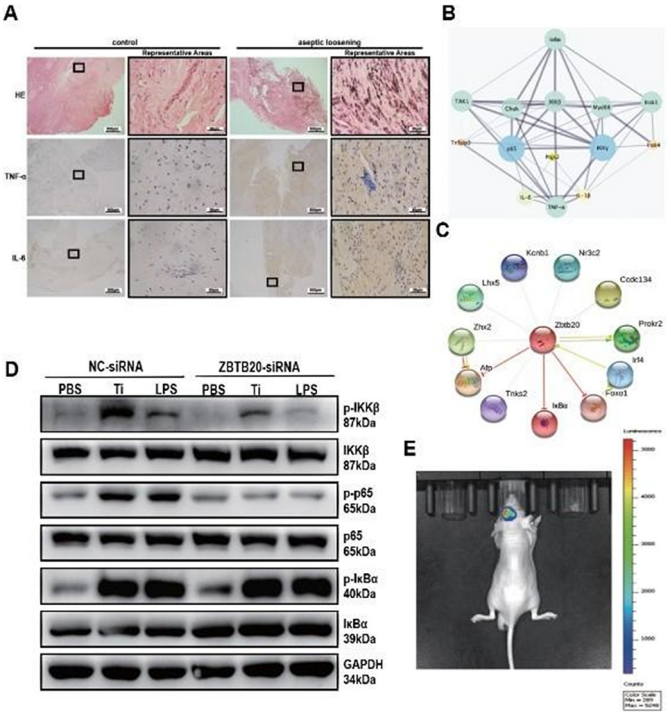

ZBTB20 positively regulated titanium particle-induced macrophage inflammatory response.

doi:10.1016/j.bonr.2020.100450

P114
Idebenone induces bone loss via increasing osteoclastogenesis

O.J. Sul, H.S. Choi
University of Ulsan, Ulsan, Republic of Korea

Coenzyme Q10 (CoQ10), an essential component of mitochondrial respiratory chain, is an endogenous fat-soluble antioxidant. Oxidative stress has been highly associated with ovariectomy-induced bone loss via action in osteoclasts (OCs). We hypothesized that idebenone, an analog of CoQ10 might protect against OVX-induced bone loss through the action in OCs. To test this idea, mice were subjected to OVX surgery and we examined the effect of idebenone on ovariectomy (OVX)-induced bone loss in vivo by μCT. In vitro, the effect of idebenone on differentiation of OC were analyzed by tartrate-resistant acid phosphatase staining. Administration of idebenone decreased bone density in SHAM mice, but it did not exacerbate OVX-induced bone loss any further in vivo. In vitro Idebenone increased the number and activity of OC when added at later stage. Idebenone also increased mitochondrial ROS. Our data demonstrates that that increased osteoclastogenesis by idebenone was at least partly due to increased mitochondrial ROS, suggesting a distinct role of mitochondria in OC and bone metabolism.

doi:10.1016/j.bonr.2020.100451

P115
Role of Tubulin β6 on microtubule dynamics and podosome belt organization

Justine Maurin, Guillaume Bompard, David Guérit, Anne Blangy
CRBM, CNRS, Montpellier, France

Bone is a dynamic tissue constantly renewed through the activity of osteoclasts, which resorb bone and of osteoblasts, which form the new bone. Osteoporosis is caused by excessive activity of osteoclasts. Their unique ability to resorb bone dependents on the formation of an actin-rich belt (sealing zone). It is composed of podosomes. Our goal is to characterize new actors and mechanisms regulating bone resorption. We showed that the inhibition of the exchange factor Dock5, prevents the organization of the podosome belt, osteoclast activity and bone loss in mice. Thus, preventing the organization of the podosome belt could be a novel approach to decrease bone resorption in patients with osteoporosis. The dynamics of the actin and microtubule cytoskeleton plays an essential role in the organization of osteoclast podosomes. In order to find new molecular mechanisms controlling the activity of osteoclasts, we performed global transcriptomic and proteomic approaches. Those data compared osteoclasts to monocytes and dendritic cells. These three myeloid cell types have podosomes, but only the osteoclast can organize them into a belt. Thus, we looked for genes induced in osteoclasts as compared to both other types. We found that osteoclasts express two tubulin β isotypes: β6 and β5, but only tubulin β6 gene is overexpressed in osteoclasts. Recently, we showed that the inhibition of tubulin β6 in osteoclasts affects microtubule dynamics, prevents the organization of the podosome belt and the bone resorption activity. Different papers showed that tubulin isoform composition can affects microtubule dynamics. Thus, we want to understand how tubulin β6 can affect the podosome belt organization. For this, the first aim is to study in vitro the intrinsic properties of microtubules according to their tubulin β6 and β5 content. The second goal will be to how tubulin β6 and β5 can impact on microtubule associated proteins in osteoclasts.

doi:10.1016/j.bonr.2020.100452

P116

TSPAN7 as a novel anti-resorptive target for the treatment of osteoporosis

Doori Park, Jingjing Lin, Soo Young Lee
Life Science and the Research Center for Cellular Homeostasis, Ewha Womans University, Seoul, Republic of Korea

Tspan7, a member of tetraspanin superfamily proteins, is expressed in a specific membrane microdomain, called "TEM", and is important for osteoclast fusion and function. Tspan7 expression can be up-regulated by RANKL signaling in the late stage of osteoclastogenesis. Overexpression or knock-down of Tspan7 in BMMs did not affect RANKL-mediated osteoclastogenesis but attenuated mature osteoclast fusion and morphology which suggest a guess in Tspan7 that act as an osteoclast function regulator. The Tspan7-CT is related to pososome belt composed actin ring structure formation. Inhibition of Tspan7 C-terminal by Tspan7-CT peptide inhibitor successfully blocked the c-Src and Syk activation in response to b3 integrin ligand vitronectin stimuli, and controlled b3 integrin mediated bone resorption. (Fig1,2,3)

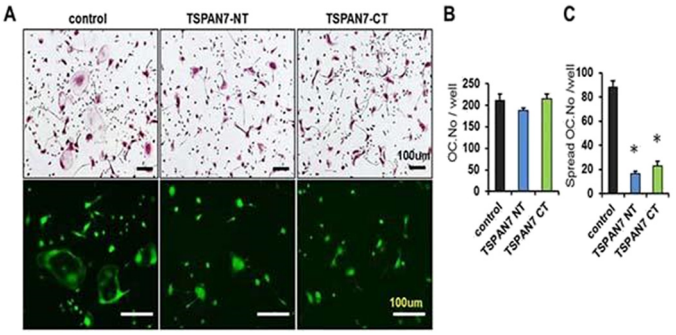

Tspan7 peptide regulates cytoskeleton integrity and cell survival of OCs.

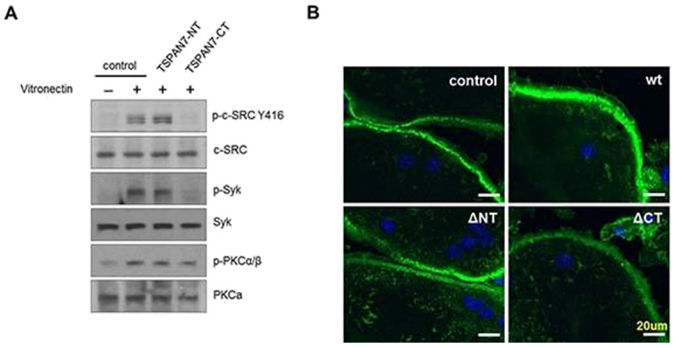

Tspan7 C-terminal regulates bone resorption signal proteins and podosome belt formation.

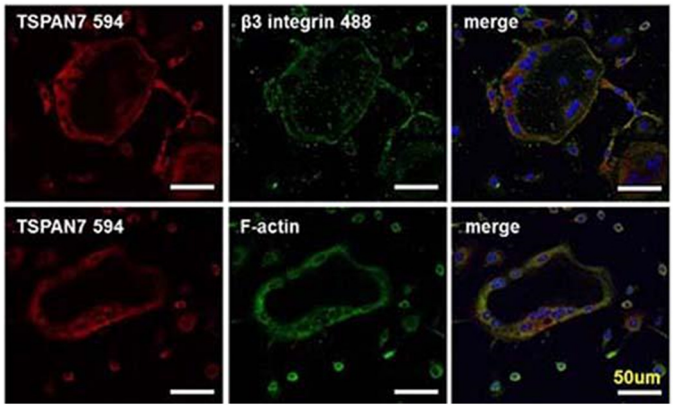

Tspan7 interacts with b3 integrin but not av integrin.

Thus, specific inhibition of Tspan7 may represent a promising new type of anti-resorptive drugs for treatment of bone diseases associated with increased OC formation and function.

doi:10.1016/j.bonr.2020.100453

P117

Density and function of actin-microdomains in healthy and NF1 deficient osteoclasts revealed by combined use of AFM and STED-microscopy

Takahiro Deguchi[a], Elnaz Fazeli[b], Sami Koho[c], Paula Pennanen[d], Maria Alanne[d], Mayank Modi[e], John Eriksson[e], Kari Vienola[f], Pekka Hänninen[d], Juha Peltonen[d], Tuomas Näreoja[g]
[a]*Nanoscopy and Nikon Centre@IIT, Nanobiophotonics, Italian Institute of Technology, Genova, Italy*
[b]*University of Turku, Turku, Finland*
[c]*Molecular Microscopy and Spectroscopy, Italian Institute of Technology, Genova, Italy*
[d]*Institute of Biomedicine, University of Turku, Turku, Finland*
[e]*Cell Biology, Faculty of Science and Engineering, Åbo Akademi University, Turku, Finland*
[f]*Department of Ophthalmology and Vision Science, UC Davis Eye Center, Sacramento, United States*
[g]*Department of Laboratory Medicine, Karolinska Institutet, Huddinge, Sweden*

Actin and myosins generate mechanical forces in osteoclasts (OC) that drive functions such as migration and membrane trafficking. In

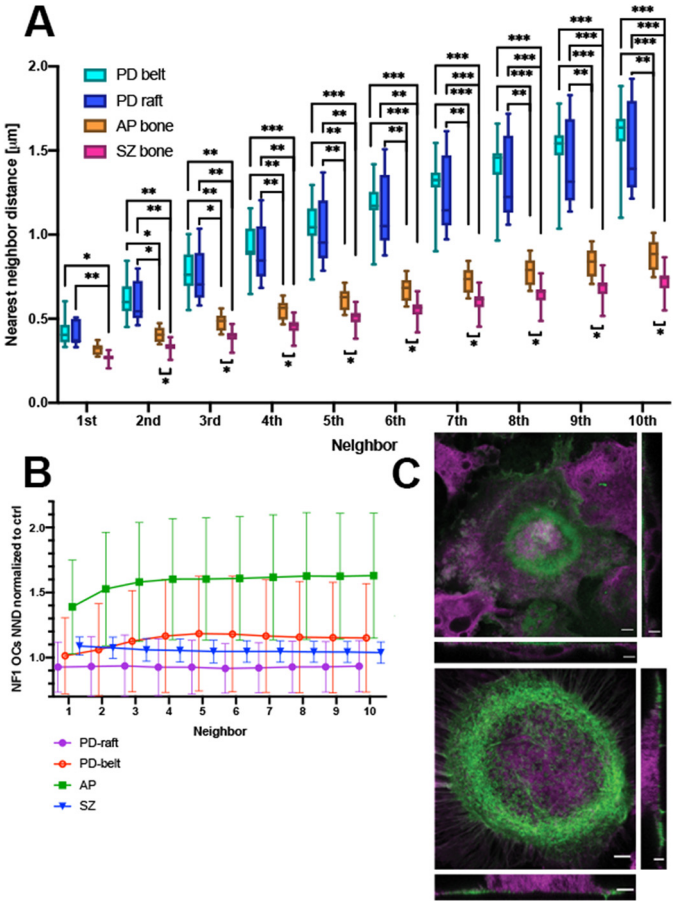

Density of f-actin clusters as nearest neighbor distances in OCs and accumulation of membrane compartments.

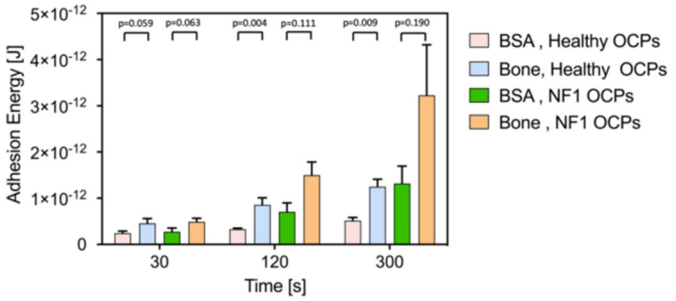

Adhesion energy of NF1 and healthy OCs to bone and BSA coated AFM-probe.

neurofibromatosis, these processes are perturbed due to a mutation in *NF1* gene. This mutation leads to generation of hyperactive bone-resorbing osteoclasts that increases incidence of skeletal dysplasia *e.g.* early-onset osteoporosis in patients suffering from neurofibromatosis.

Densities of actin-cores in OC-specific structures were higher on bone and the high density of facilitated accumulation of vesicular material at the center of a sealing zone. In NF1 deficient OCs, the NNDs at SZs were only slightly longer, nevertheless, we measured higher intensity of membrane staining within the SZs compared to healthy controls (Figure 1). However, actin patches appeared to be less dense than in healthy counterparts. It would appear that these observations could reflect the higher resorption capacity of NF1 OCs.

In healthy OCs adhesion to bone was significantly stronger than to BSA, while in NF1 OCs such a difference was not present (Figure 2). This loss of specificity implies that regulation of resorption has been lost to some extent while resorptive capacity has increased. In conclusion, this loss of regulation may explain skeletal dysplasia associated with neurofibromatosis.

doi:10.1016/j.bonr.2020.100454

P118

Altered osteoclastogenesis in Fanconi Anemia: A role for the hematopoietic niche in the bone marrow failure of the syndrome?

Alessia Oppezzo, Filippo Rosselli
Université Paris-Saclay, Institut Gustave Roussy, CNRS, Villejuif, France

Fanconi Anemia (FA) is a DNA repair deficiency syndrome, characterized by bone marrow failure (BMF), skeletal abnormalities and increased predisposition to cancer. We recently showed that cells from a majority of FA patients and mouse models present a constitutive expression of the Microphtalmia-associated transcription factor (MiTF) downstream several aberrantly activated stress signaling pathways. We demonstrated that MiTF overexpression has a major role in BMF in FA, affecting Hematopoietic Stem Cells (HSC) self-renewal capacity leading to their attrition (Oppezzo, 2019). MiTF is also a master regulator of osteoclasts (OCs) differentiation. OCs together with osteoblasts (OBs) are key elements of the hematopoietic niche. Thus, we wondered if altered MiTF expression is also present in FA OCs and if such abnormality has an impact on OCs differentiation, OCs/OBs crosstalk and niche homeostasis, participating to the skeletal abnormalities and BMF of the syndrome. We observed that the differentiation of *Fanca*$^{-/-}$ mouse-derived OCs is deeply altered. At the morphological level, FA OCs are smaller, less numerous and with a decreased number of nuclei compared to their WT counterpart, while at the molecular level they are characterized by a reduced expression of NFATc1 and DC-STAMP, two master regulators of osteoclastogenesis. Finally, while MiTF progressively increases during osteoclastogenesis in WT mice, it is stably highly expressed in FA osteoclasts progenitors, without changing during the progression from precursors to mature OCs, indicating that MiTF dysregulation can be responsible for the HSCs impairment and for the skeletal abnormalities in FA. Co-culture experiments mixing different combinations of WT and FA OBs and OCs with/without WT or FA HSCs to analyze their crosstalk and differentiation process and their ability to sustain HSCs proliferation are ongoing, with the final goal to determine the impact of the niche environment on HSCs attrition.

doi:10.1016/j.bonr.2020.100455

P119

MiR-188-5p negatively regulates titanium particle-induced macrophage inflammation and osteolysis by targeting BTK

Yue Ding, Sipeng Lin
Department of Orthopaedic Surgery, Sun Yat-Sen Memorial Hospital, Sun Yat-Sen University, Guangzhou, China

Wear particle-induced osteolysis and the consequent aseptic loosening remain the main causes of artificial joint replacements failure and revision. Previous studies have demonstrated that wear particles can be phagocytized by macrophages, which in turn activates osteoclasts and incites an adverse immunoreaction. MicroRNAs are considered as therapeutic targets for aseptic loosening, and in this study, the molecular mechanisms of miR-188-5p that regulate titanium particle-induced osteolysis (TPIO) were detected. In the present study, we characterized miRNAs and mRNA expression profiling in mouse bone marrow-derived macrophages (BMDM) cells exposed to titanium particle by microarray, which demonstrated that miR-188-5p was down-regulated. Moreover, overexpression of miR-188-5p downregulated the level of pro-inflammatory cytokines produced by BMDM, as well as M1 polarization, whereas knockdown of miR-188-5p exerted opposite effects. Here we also report that a dual luciferase reporter assay confirms the negative targeting regulatory relationship between miR-188-5p and Bruton´s tyrosine kinase (BTK). Overexpression of BTK, promoted the titanium particle-induced inflammatory reaction by adjusting NF-kB pathways, activation of NLRP3 inflammasome and M1 polarization, and interestingly rescued the effects of miR-188-5p overexpression in BMDMs. Furthermore, we set up a mouse model with local injection of agomiR-188-5p to confirm that miR-188-5p overexpression could rescue TPIO, and the results of micro-CT and immunofluorescence staining were consistent with the *in vitro* experiments. The finding reveals that high expression of miR-188-5p inhibits the titanium particle-induced macrophage inflammation and osteolysis by targeting BTK *in vitro* and *in vivo*, and therefore a potential therapeutic target for the prevention of aseptic joint loosening.

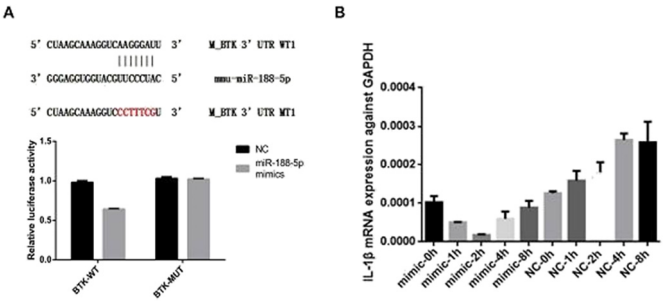

MiR-188-5p negatively regulates titanium particle-induced osteolysis by targeting BTK.

doi:10.1016/j.bonr.2020.100456

P120

The effect of denosumab treatment on osteoclast precursor cells in postmenopausal osteoporosis

Andreas Fontalis, Fatma Gossiel, Marian Schini, Jennifer Walsh, Richard Eastell
Department of Oncology and Metabolism, University of Sheffield, Sheffield, United Kingdom

Concerns have been raised about a rebound phenomenon in bone turnover upon discontinuation of denosumab in osteoporotic patients. Findings from the FREEDOM and FREEDOM Extension post hoc analysis encompassing 1475 patients, unveiled an increase in the fracture risk following denosumab cessation to similar levels observed in untreated patients. Our aim was to investigate the effect of denosumab on the osteoclast precursor cell population in order to elucidate the cellular mechanisms of this phenomenon.

Blood samples were obtained from 10 osteoporotic postmenopausal women, 6 months following the last dose of denosumab (60mg SC). Peripheral mononuclear cells were initially isolated and stained for CD14, M-CSFR, CD11b and TNFRII receptors. Osteoclast precursors were identified utilising fluorescent-activated cell sorting (FACS) analysis, as cells expressing CD14+/MCSFR+, CD14+/CD11b+ or CD14+/TNFR-II+. Our control group comprised a historical cohort of 69 postmenopausal women previously recruited for the TRIO study, investigating the effect of bisphosphonate treatment on osteoclast precursor cells (pre-treatment baseline measurements were utilised for comparisons).

Results are presented in Table 1. Data are presented as Mean ± Standard Deviation (SD) or median (IQR, interquartile range) based on whether a normal distribution was observed.

Median duration of denosumab administration was 3 years (range 0.5 to 8 years).

Denosumab administration resulted in an increase in the number of CD14+/CD11b+ cells indicating a block in the differentiation of osteoclast precursors to osteoclasts during denosumab therapy. This could explain the offset of treatment upon discontinuation and the reason a rebound increase in bone turnover is observed.

Table 1
Comparison of the CD14+ cells which were positive for M-CSFR, CD11b, TNFR-II between the two groups.

	Denosumab (N=10)	TRIO cohort (N=69)	p-value
%CD14+/MCSFR+	2.57 ± 1.87	1.7 (1.7)	0.361*
%CD14+/CD11b+	5.65 (23.08)	3.07 ± 1.73	0.001*
%CD14+/TNFRII+	1.93 ± 1.6	2.56 ± 1.47	0.224$
*Independent samples Mann Whitney U test	$Independent Samples t-test		

doi:10.1016/j.bonr.2020.100457

P123

Mir-342-3p regulates ostoclastogenesis in arthritis-associated osteoclast precursors

Claire Lozano[a], Valentin Estibals[a], Gabriel Courties[a], Hortense Courot[a], Claudine Blin-Wakkach[b], Maria-Bernadette Madel[b], Christophe Hue[c], Hendrick Mambu Mambueni[c], Henri-Jean Garchon[c], Virginie Escriou[d], Florence Apparailly[a], Isabelle Duroux-Richard[a]
[a]*IRMB, INSERM UMR 1183, Montpellier, France*
[b]*CNRS UMR 7370, Université Cote d'Azur, Laboratoire de PhysioMédecine Moléculaire, Nice, France*
[c]*Université Paris-Saclay, UVSQ, INSERM, Infection et inflammation, Montigny-Le-Bretonneux, France*
[d]*UTCBS, CNRS, INSERM, Université Paris Descartes, Sorbonne-Paris-Cité, Chimie ParisTech, PSL Research University, Paris, France*

Background: Rheumatoid arthritis is associated with bone destruction mediated by osteoclasts (OC), which originate from blood-derived myeloid precursors. MicroRNAs (miRNA) are key regulators of cellular processes, including osteoclastogenesis. Aiming at identifying key regulators of pathogenic OC in the context of arthritis, we have investigated the role of miR-342-3p in osteoclactogenesis.

Methods: OC were derived from $CD11b^+$ and $CD11c^+$ cells isolated from mouse bone marrow. In vitro studies were performed using the murine RAW264.7 cell line transfected with either miR-342-3p mimics or inhibitors. Cell survival and motility were assessed. We used Illumina RNA-Seq and in silico approach to identify putative targets of miR-342-3p, and dual luciferase assay to validate the binding. Anti-miR-342-3p was delivered in vivo to circulating $Ly6C^{high}$ monocytes using the DMAPAP/DOPE cationic liposome upon intravenous injection of mice with K/BxN serum-transfer arthritis (STA). Arthritis severity and bone histomorphometric parameters were analyzed.

Results: The expression level of miR-342-3p was increased in OC from STA mice, and transiently up-regulated in the early phase of osteoclastogenesis. Using the RAW264.7 cell line, we showed that miR-342-3p neutralization significantly inhibits the motility, proliferation and survival of OC precursors, resulting in decreased OC numbers and resorption activity. Upon miR-342-3p neutralization, 1185 genes were significantly deregulated, which were associated with locomotion and apoptosis pathways. In vitro assays validated ADAM17 as a target for miR-342-3p. Neutralization of miR-342-3p in $Ly6C^{high}$ precursors of STA mice increased ADAM17 expression level in OC progenitors.

Conclusions: Our data suggest that the miR-342-3p/*ADAM17* axis promotes the early phase of osteoclastogenesis by enhancing the cell survival and motility of OC precursors. The up-regulation of miR-342-3p in OC may also represents a biomarker of increased osteoclastogenic potential of inflammatory precursors in arthritis.

doi:10.1016/j.bonr.2020.100458

P124

The non-erythropoietic analogue cibinetide inhibits osteoclastogenesis *in vitro* and increases bone density in mice

Zamzam Awida[a], Albert Kolomansky[a], Sahar Hiram-Bab[b], Nathalie Ben-Califa[a], Hussam Saad[a], Tamar Liron[b], Maria Ibrahim[a], Michael Brines[c], Yankel Gabet[b], Drorit Neumann[a]
[a]*Department of Cell and Developmental Biology, Sackler Faculty of Medicine, Tel-Aviv University, Tel Aviv, Israel*
[b]*Department of Anatomy and Anthropology, Sackler Faculty of Medicine, Tel-Aviv University, Tel Aviv, Israel*
[c]*Araim Pharmaceuticals, Tarrytown, United States*

Erythropoietin (Epo), the master regulator of erythropoiesis, has also been implicated in a wide range of non-erythroid activities, including tissue protection. These functions are mediated *via* two receptors: hematopoiesis *via* the Epo receptor (EpoR) homodimer and tissue protection *via* a heteromer composed of EpoR and CD131. Cibinetide (ARA290) is a non-erythropoietic analogue of Epo, acting selectively on the heteromer complex. Our published findings that Epo stimulates osteoclast precursors and entrains a decrease in bone density, raise questions regarding the underlying molecular mechanisms.

Unexpectedly, we found that cibinetide injections in 12-week-old female mice (120 μg/kg thrice weekly for one month) resulted in a significant increase in tissue mineral density in cortical bone by 5.8% (1416.4 ± 39.27 vs 1338.74 ± 16.56 mgHA/cm^3) and in trabecular bone by 5.2% (1056.52 ± 30.94 vs 1004.13 ± 16.91 mg HA/cm^3) ($p< 0.05$), as measured using microCT.

In vitro, LPS as well as Epo administration to bone marrow derived macrophages (BMDM) enhanced osteoclastogenesis, whereas cibinetide administration had the opposite effect in a dose dependent manner. Combining cibinetide with either LPS or Epo treatment inhibited osteoclastogenesis in BMDM, suggesting that cibinetide overrides the pro-osteoclastogenic effect of LPS and Epo (Figure 1).

Our findings demonstrate the increasing complexity of EpoR signaling in bone, and pave the way for clinical translation through potential combination therapy of Epo and cibinetide in anemic patients in an attempt to preserve the erythropoietic actions of Epo, while preventing/attenuating the associated bone loss.

Keywords: Erythropoietin, Cibinetide, Osteoclasts, BMDM.

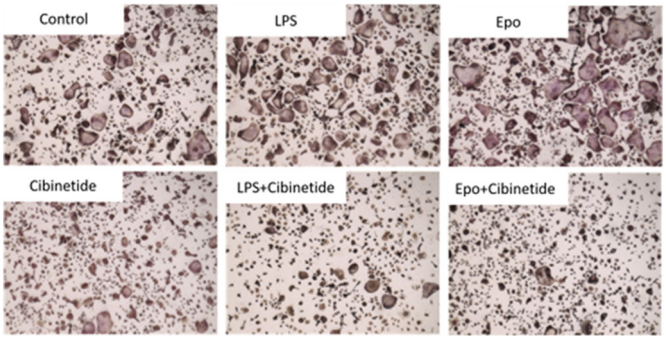

Cibinetide counteracts the pro-osteoclastogenic effect of LPS and Epo *in vitro*.
BMDMs were treated with RANKL (50ng/ml) along with Epo (10U/ml), Cibinetide (150nM) or Epo+ Cibinetide. After 48 hours LPS (10ng/ml) was introduced to the RANKL or RANKL+ Cibinetide stimulated cultures. On the 4th day multinucleated osteoclasts were stained for TRAP.

Fig. 1.

doi:10.1016/j.bonr.2020.100459

P125

Noggin as a regulator of bone remodelling

Fatemeh Safari[a,b], Mark Siegrist[a], Silvia Dolder[a], Eliza Hartmann[c], Frank Klenke[c], Willy Hofstetter[a]
[a]*Bone Biology & Orthopaedic Research, Department for BioMedical Research (DBMR), University of Bern, Bern, Switzerland*
[b]*Graduate School for Cellular and Biomedical Sciences, University of Bern, Bern, Switzerland*
[c]*Clinics of Orthopaedic Surgery & Traumatology, Inselspital, University Hospital Bern, Bern, Switzerland*

Bone Morphogenetic Protein 2 (BMP2) is used in orthopaedic surgery to promote bone healing. The endogenous synthesis of BMP-2 antagonist family members, however, may limit the efficacy of exogenous BMP2. Noggin is one of these inhibitors that blocks the effects of BMP on the differentiation and activation of osteoblast (OB) *in vitro* and *in vivo* and inhibits OB-mediated osteoclast (OC) development. Furthermore, Noggin was found to modulate osteoclastogenesis through a direct effect on OC lineage cells. The present study aimed at elucidating the underlying mechanisms of these effects. Direct (conventional culture dishes) and indirect (transwell culture dishes) co-cultures of murine OB/OPC (Osteoclast Progenitor Cells) and cultures of OPC alone were supplemented with combinations of Noggin, BMP2, L51P (engineered, inactive variant of BMP2) and DMH1 (BMP receptor 1 inhibitor). In cultures of OPC, Noggin but not DMH1 caused an increase in the number of OC by a factor of 3 ($p< 0.01$). This effect could not be reversed by BMP2 and L51P, respectively. In contrast, in co-cultures of OB/OPC, exposure to Noggin attenuated OC development. In direct co-cultures, this inhibitory effect of Noggin was blocked by BMP2 and L51P. In both direct and indirect co-culture systems, exposure to Noggin induced the release of GM-CSF, a potent inhibitor of osteoclastogenesis, by a factor of 6 and 4, respectively ($p< 0.01$). Treatment of the cultures with αGM-CSF Ab, however, restored OC development in the indirect co-culture system only. The data suggests a previously unknown function of Noggin directly acting pro-differentiation on OC lineage cells independently of BMP signalling. In co-cultures, besides GM-CSF, cell-cell contact between OB and OPC is required for mediation of the maximal inhibitory effects of Noggin on OC development. The nature of potential interaction partners for Noggin, however, remains to be elucidated.

doi:10.1016/j.bonr.2020.100460

P126

Bone remodeling mechanisms in osteoporotic TgRANKL transgenic mouse models

Vagelis Rinotas[a], Panagiotis Nikolaou[a,b], Konstantinos Kritikos[a,b], Apostolos Papadopoulos[a,b], Lenka Plestilova[c], Astrid Jüngel[c], Martina Samiotaki[a], George Panayotou[a], Eleni Douni[a,b]
[a]*Institute of Bioinnovation, Biomedical Sciences Research Center Alexander Fleming, Vari-Athens, Greece*
[b]*Department of Biotechnology, Agricultural University of Athens, Athens, Greece*
[c]*Center of Experimental Rheumatology, University Hospital Zürich, Zurich, Switzerland*

Osteoporosis is a multifactorial metabolic disease which is characterized by low bone density, reduced bone quality, and increased risk of fractures. We have recently established genetic osteoporosis models by expression of human RANKL in transgenic mice (TgRANKL). To investigate the pathogenic mechanisms in modeled osteoporosis, we performed RNA sequencing analysis in flushed femurs from TgRANKL mice and wild-type (WT) controls. Our analysis identified 7464 differentially expressed genes and among them 4042 were upregulated and 3422 downregulated in TgRANKL mice compared to WT. Enrichment analysis showed that up-regulated genes were clustered in pathways involving skeletal system development, bone resorption, osteoclast and osteoblast differentiation, Wnt signaling pathway, while downregulated genes were mainly involved in mitochondrial activity and muscle structure. Selected genes from each category were validated using qPCR.

A common characteristic in TgRANKL mice is the progressive development of bone marrow adiposity (BMA). Histological analysis and micro-computed tomography demonstrated that BMA expanded progressively close to resorbed areas. Expression analysis and proteomics in enriched bone marrow mesenchymal stromal cell (BMSC) cultures showed modified metabolic processes including fatty acid metabolism and mitochondrial proteins between TgRANKL and WT mice. Moreover, TgRANKL BMSCs displayed increased adipogenic and decreased osteogenic potential upon differentiation. Furthermore, the effectiveness of an anti-osteoporosis treatment in BMA development was investigated upon treatment of TgRANKL models with alendronate. Notably, alendronate not only improved bone mass (BV/TV, WT: 11.81±1.58 vs Tg5519: 2.00±0.68 vs Tg5519+ALN: 11.40±3.37, $p< 0.05$) but also attenuated BMA expansion at metaphysis (WT: 0.31±0.22 vs Tg5519: 44.41±2.52 vs Tg5519+ALN: 8.27±1.75, $p< 0.001$), indicating a possible involvement of osteoclasts and bone resorption in BMA development. Conclusively, our analysis identified specific markers and deregulated pathways in femurs from osteoporotic TgRANKL models, while also we correlated BMA with BMSC metabolism and osteoclast activity.

doi:10.1016/j.bonr.2020.100461

P127

Development of collagen-based matrix that promotes from mesenchymal stromal cells to differentiate into osteocyte-like cells

Saori Kunii[a], Yoshitaka Horiuchi[b], Nobuhiro Kato[c], Koichi Morimoto[a]
[a]*Genetic Engineering, Kindai University, Kinokawa, Japan*
[b]*Life Science Research Center, Kindai University, Osaka-Sayama, Japan*
[c]*Biomedical Engineering, Kindai University, Kinokawa, Japan*

Background: Osteocytes differentiate from cuboidal-like osteoblasts and are embedded into soft secreted osteoid in mature bone. The regulation of osteocyte differentiation remains poorly understood, however, collagen as a scaffold will have an influence on it. At the ECTS2019 Congress, we showed that low adhesive scaffold type I collagen (LASCol) has marvelous ability to induce from mesenchymal stromal cells (MSCs) to osteoblasts differentiation in short term. In this study, we report the effects of LASCol to promote differentiation from MSCs into osteocyte-like cells followed after osteoblasts.

Methods: Rat MSCs were cultured on LASCol coated-dish or LASCol gel with osteogenic basal medium. The alkaline phosphatase (ALP) and Alizarin red staining of rMMCs cultured on the LASCol coated dish was observed. The expression of mRNAs related to osteocytes differentiation was analysed with qRT-PCR. In addition, Transmission Electron Microscope (TEM) was used to observe the features of cells in LASCol gel. To investigate local properties of the LASCol gel surface, we measured stiffness of LASCol gel by Scanning Probe Microscope (SPM) and surface images were also acquired.

Results: On both the LASCol coated-dish and the LASCol gel, rat MSCs formed spheroid bodies and highly mineralized extracellular matrix was indicated. After 3 and 5 days culture, the osteocyte-related genes such as *Bglap*, *Dmp1*, *Spp1*, and *Phex* significantly increased ($2.4 < \Delta\Delta Ct < 231$). Interestingly, we confirmed osteocyte-like cells in LASCol gel after 40 days culture. After incubation for 1h at 37°C for gel formation, the stiffness of LASCol gel showed an increase depending on concentration (6.8 nN at 10.5 mg/mL). Probably, LASCol would have the strong ability to induce the differentiation of from rMSCs to osteocyte.

Funding: This work was supported by the Adaptable and Seamless Technology Transfer Program through target-driven R&D (AS2715177U to K.M.).

doi:10.1016/j.bonr.2020.100462

P129

OCY454 as a novel osteocyte model to study phosphate metabolism

Danielle Ratsma, Marijke Koedam, Carola Zillikens, Bram van der Eerden
Internal Medicine, Erasmus MC, Rotterdam, Netherlands

Background: Phosphate (P) is essential for many processes including cellular signaling and skeletal mineralization. The main regulator is Fibroblast Growth Factor 23 (FGF23), which is secreted by osteocytes, but the exact mechanism underlying FGF23 regulation is poorly understood. Currently used cell models are inappropriate osteoblast lines or slowly differentiating osteocytes. Here, we propose the novel osteocyte cell line OCY454 as it expresses osteocyte differentiation markers within one week of culturing.

Methods: The immortalized murine cell line OCY454 was kept at 33°C for three days to reach confluence, before being moved to 37°C for differentiation. At 37°C, cells were cultured with 0 or 4 mM β-glycerophosphate (β-GP; P donor). qPCR was used to study the expression of genes of interest at day 0, 7 and 11.

Results: *Fgf23* was detectable in the first week of cell culture. Its regulators Dentin matrix acidic phosphoprotein 1 (*Dmp1*) (36.1-fold, $p=0.0002$), Polypeptide N-acetylgalactosaminyl-transferase 3 (*GalNt3*) (2.65-fold, $p=0.0002$) and Phosphate Regulating Endopeptidase Homolog X-Linked (*Phex*) (2.75-fold, $p=0.029$) were all upregulated after 7 days of culture. Furthermore, 4 mM β-GP significantly increased expression of the negative Fgf23 regulator *Dmp1* (2.8-fold, $p=0.0011$) but decreased expression of positive regulator *GalNt3* (2.7 fold, $p=0.0271$) and *Fgf23* (4.2 fold, $p=0.0230$) at day 11 compared to 0 mM.

Conclusion: The osteocyte model OCY454 appears to be suitable to study P metabolism because of its early expression of *Fgf23* and the dynamic effects of β-GP on genes involved in Fgf23 regulation. Future studies will focus on the yet enigmatic mechanisms underlying FGF23 biology and its interplay with phosphate.

doi:10.1016/j.bonr.2020.100463

P130

Matrix vesicle biomimetics carrying Annexin A5 and Alkaline Phosphatase bind to native collagen produced by human smooth muscle cell transdifferentiated in osteo/chondrocyte cells

Maytê Bolean[a], Benedetta Izzi[b], Soetkin van Kerckhoven[c], Massimo Bottini[d], Ana Paula Ramos[a], José Millán[e], Marc Hoylaerts[f], Pietro Ciancaglini[a]
[a]*Chemistry, University of Sao Paulo, Ribeirão Preto, Brazil*
[b]*Department of Epidemiology and Prevention, IRCCS NEUROMED, Pozzilli, IS, Italy*
[c]*Functiemetingen Pneumologie, UZ Leuven Gasthuisberg, Leuven, Belgium*
[d]*Department of Experimental Medicine and Surgery, University of Rome Tor Vergata, Rome, Italy*
[e]*Sanford Burnham Prebys Medical Discovery Institute, San Diego, United States*
[f]*Department of Cardiovascular Sciences, University of Leuven, Leuven, Belgium*

Vascular smooth muscle cells (VSMCs) transdifferentiated ectopically trigger vascular calcifications, contributing to clinical cardiovascular disease in the aging population. AnxA5 and TNAP play a crucial role in (patho)physiological mineralization. We performed affinity studies between DPPC and 9:1 DPPC:DPPS-proteoliposomes carrying AnxA5 and/or TNAP and different types of collagen matrix: type I, II, I+III and native collagenous extracellular matrix (ECM) produced from VSMCs with or without differentiation, to simulate ectopic calcification conditions. AnxA5-proteoliposomes showed the highest affinity for collagens, specially for type II, reaching 74% binding for 1.8 μg of AnxA5 (protein content into DPPC:DPPS-proteoliposomes). DPPC-proteoliposomes-AnxA5 showed binding of 32%, corresponding to 0.5 mol of AnxA5 bound per mol of coated collagen. TNAP-proteoliposomes bound poorly (not exceeding 20%) in any of the two lipid compositions. The simultaneous presence of TNAP in AnxA5-proteoliposomes disturbed interactions between AnxA5 and collagen. DPPC-proteoliposomes-AnxA5 affinities for ECM from transdifferentiating cells went up 2-fold compared to that from native VSMCs. The affinities of DPPC:DPPS-proteoliposomes were high for ECM from VSMCs with or without differentiation, underscoring a synergistic effect between AnxA5 and DPPS. Co-localization studies uncovered binding of proteoliposomes harboring AnxA5 or TNAP+AnxA5 to various regions of the ECM, not limited to type II collagen. All results were expressed as mean ± SEM. Groups were compared with the one-way ANOVA or Student's t-test ($P < 0.05$). Thus, proteoliposomes as MVs biomimetics are useful in the understanding of mechanisms that regulate the process and essential for the development of novel therapeutic strategies to prevent ectopic mineralization.

Acknowledgments: FAPESP, CNPq and CAPES.

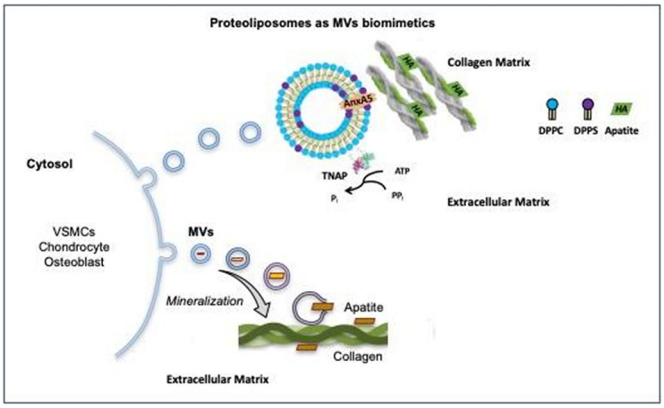

Graphical abstract

doi:10.1016/j.bonr.2020.100464

P131

Linc-ROR promotes MSCs chondrogenesis differentiation and releases osteoarthritis through activation of SOX9 via sponging miR-138 and miR-145

Lu Feng, Zhengmeng Yang, Yucong Li, Gang Li
Department of Orthopaedics and Traumatology, Chinese University of Hong Kong, Shatin, Hong Kong

Long noncoding RNAs (lncRNAs) have gained widespread attention in recent years and was known to be involved in multiple musculoskeletal diseases, including osteoarthritis (OA). Emerging evidences have shown that some lncRNAs play important regulatory roles in chondrogenesis differentiation of mesenchymal stem cell (MSCs), suggesting a potential therapeutic strategy for cartilage repair and osteoarthritis treatment. The present study is to characterize the regulation mechanism of long intergenic non-coding RNA, regulator of reprogramming (linc-ROR) in MSCs chodrogenesis as well as OA. Linc-ROR was found to be down-regulated in articular cartilage tissue sample from OA patients compared with healthy control. Meanwhile, linc-ROR expression level was positively correlated with the expression level of chondrogenic gene SOX9 (R^2 =0.64). Linc-ROR expression level of MSCs was also found to be 6 folds higher at day 21 of chondrogenesis induction compared with the initiating time point. Ectopic expression of linc-ROR significantly accelerated MSCs chondrogenesis. By using bioinformatics prediction and luciferase reporter assays, it was demonstrated that linc-ROR functioned as a miRNA sponge for miR-138 and miR-145, both of which were negative regulators of chondrogenesis key factor SOX9. Further investigations revealed that both miR-138 and miR-145 suppressed MSCs chondrogenesis activity as well as SOX9 expression by around 50%, while co-expression of linc-ROR revealed a rescuing effect of chondrogenesis activity and SOX9 expression to around 80-100%. Furthermore, the linc-ROR overexpressed MSCs were encapsulated into hyaluronic acid (HA) hydrogels and transplanted subcutaneously in nude mice. Linc-ROR overexpressing MSCs also showed a higher *in vivo* chondrogenesis activity and SOX9 expression level compared with negative control. Taken together, linc-ROR modulated MSCs chondrogenesis differentiation by acting as a competing endogenous RNA for miR-138 and miR-145, and activating SOX9 expression. Linc-ROR could be considered as a new therapeutic target for the treatment of OA.

doi:10.1016/j.bonr.2020.100465

P135

Hypertrophy of chondrocytes compromises their mechanical properties

Ekaterina V. Medvedeva[a], Meng Xie[b], Anastasia Akovantseva[c], Peter S. Timashev[a,c,d], Svetlana Kotova[a,c,d], Andrei S. Chagin[a,b]
[a]*Institute for Regenerative Medicine, Sechenov University, Moscow, Russian Federation*
[b]*Department of Physiology and Pharmacology, Karolinska Institutet, Stockholm, Sweden*
[c]*Institute of Photonic Technologies, Research center 'Crystallography and Photonics, Troitsk, Russian Federation*
[d]*Semenov Institute of Chemical Physics, Moscow, Russian Federation*

Chondrocyte hypertrophy is a key aspect of bone elongation. During hypertrophy chondrocytes enormously increase in cellular volume within a very short time, i.e., 20 folds within 12 hours (Cooper KL et al, Nature 2013). We hypothesized that such an abrupt increase in cellular volume might impair mechanical stiffness of these cells. To address this hypothesis, we compared stiffness of proliferative and hypertrophic chondrocytes within the growth plate.

Knowing that various fixations affect mechanical properties of matrix and cells differently, we have employed live thick tissue sections of bones and analysed cell and matrix stiffness within the growth plate using atomic force macroscopy (AFM, cantilever with 5μm glass microsphere). The Young's modulus was calculated according to the Hertzian contact mechanics model. After the measurements cell viability was confirmed by LIVE/DEAD staining.

The AFM measurements revealed that hypertrophy leads to dramatic softening of the cells with Young's modulus decreasing from 13.6±4.7 kPa (proliferative chondrocytes) to 3.1±1.4 kPa (hypertrophic chondrocytes).

These results show that chondrocyte hypertrophy compromises stiffness of the cells and suggest that these cells may be particularly vulnerable to mechanical loading.

doi:10.1016/j.bonr.2020.100466

P137

Activation of caspases and autophagy during cartilage development

Barbora Vesela[a], Petra Bilikova[b], Eva Svandova[a], Alice Ramesova[a], Herve Lesot[b], Eva Matalova[a]
[a]*Faculty of Veterinary Medicine, University of Veterinary and Pharmaceutical Sciences, Brno, Czech Republic*
[b]*Institute of Animal Physiology and Genetics, Academy of Sciences of the Czech Republic, Brno, Czech Republic*

Caspases are proteases acting during inflammation process and apoptosis. The most important caspases activated in apoptotic cascades are caspase-8 and 9 as initiators, the trio of executive caspases, caspase-3, -6 and -7 and caspase-2, which has yet an unclear position. Recently, novel roles of pro-apoptotic caspases in non-apoptotic events such as regulation of autophagy have been reported in different tissues.

Meckel's cartilage is a temporary structure connected with proper mandible development. Recently, autophagy was suggested as an alternative of cell death involved in eliminating the middle segment of Meckel's cartilage. In long bones, formation of the growth plate allows for elongation of the bone and growth plate maturating chondrocytes display an autophagic phenotype. Autophagy in chondrocytes was thus demonstrated as a developmentally regulated process essential for proper bone growth.

This research aimed to: 1) investigate activation of pro-apoptotic caspases within the Meckel's cartilage and long bone development 2) to correlate presence of individual caspases with autophagic markers *in*

vivo, 3) to analyse impact of caspase inhibition on expression of autophagy related molecules in chondrocytes cultures *in vitro*.

Based on temporospatial analysis, caspase-2 and caspase-8 are activated in non-apoptotic regions within the degrading part of the Meckel´s cartilage. Activation of pro-apoptotic caspases was demonstrated to occur also in non-apoptotic growth plate chondrocytes. The co-localization of these caspases with Beclin-1 suggests their possible involvement in the chondrocyte autophagic cell death. Moreover, caspase inhibition in limb derived chondrocytes caused a statistically significant impact on gene expression in the case of the autophagy related molecules and the engagement of individual caspases was uncovered. Thus the presented data open new perspective that are focused on the research into cartilage and bone development.

This work was supported by the Grant Agency of the Czech Republic (19-12023S).

doi:10.1016/j.bonr.2020.100467

P140

Postnatal ablation of IGF2 in chondrocytes doesn't affect normal growth of growth plate and liver

Baoyi Zhou[a], Meng Xie[a], Miguel Constância[b], Andrei S. Chagin[a]
[a]*Department of Physiology and Pharmacology, Karolinska Institutet, Solna, Sweden*
[b]*University of Cambridge, Cambridge, United Kingdom*

Insulin growth factor 2 (Igf2), as a component of growth hormone/insulin growth factor 1 axis, plays a crucial role in multiple systems and organs. Transcriptome profiling of the growth plate revealed that IGF2 among top 10 most abundant genes expressed in the postnatal growth plate both in mice and humans. The functional role of such a high expression of IGF2 by chondrocytes is unclear. To address this question, we have performed conditional ablation of Igf2 in chondrocytes by crossing Col2-CreERT strain with Igf2-floxed strain. Postnatal ablation of Igf2 was performed by injection of tamoxifen at day 3 of age. Hematoxylin and eosin histological staining of tibia growth plate displayed morphology undistinguished from control at postnatal days 14, 18 and 28. Bone length was also unaffected as well as body and liver weights (time points: days 14, 18, 21, and 28). Additionally, Igf1, Igf1r, and Igf2 expressions in the liver (assessed by qPCR) in the mutant mice had no significant differences compared with those in the control mice. We concluded that expression of Igf2 by postnatal chondrocytes has no physiological significance or Igf2 ablation is compensated by yet unknown mechanisms.

doi:10.1016/j.bonr.2020.100468

P141

Oxytocin did not favorably affect the skeletal system of rats with osteoporosis induced by estrogen deficiency and/or type 1 diabetes

Aleksandra Janas, Ewa Kruczek, Piotr Londzin, Urszula Cegieła, Joanna Folwarczna
Department of Pharmacology, School of Pharmaceutical Sciences in Sosnowiec, Medical University of Silesia, Katowice, Sosnowiec, Poland

Oxytocin has been found to take part in the regulation of bone metabolism. It has been proposed that affecting oxytocin pathways may favorably affect osteoporotic bones, especially in female organisms. Moreover, favorable effects of oxytocin on energy metabolism have been reported. The aim of the present study was to investigate the effects of oxytocin on the skeletal system of rats with osteoporosis induced by estrogen deficiency and/or type 1 diabetes (T1D) in rats.

The experiments were performed on mature female Wistar rats, divided into 8 groups (n=8-10). Non-ovariectomized (NOVX), ovariectomized (OVX), T1D NOVX and T1D OVX rats were administered oxytocin (0.1 mg/kg) or the vehicle subcutaneously, once daily for 4 weeks. T1D was induced by a single injection of streptozotocin (60 mg/kg i.p.), 3 days after the bilateral ovariectomy surgery. The oxytocin treatment started one week after the ovariectomy. Serum bone turnover markers (CTX-I and osteocalcin), bone mass and mineralization, histomorphometric parameters (OsteoMeasure system) and mechanical properties (Instron apparatus) of cancellous and compact bone were determined. The results were statistically evaluated by ANOVA tests. Moreover, the oxytocin effects were studied using principal component analysis (PCA).

Estrogen deficiency increased bone resorption and formation in the OVX control rats, and T1D increased bone resorption and decreased bone formation in both NOVX and OVX rats in relation to the appropriate controls. The changes led to worsening of microstructure and mechanical properties of cancellous bone in all three osteoporosis models. Administration of oxytocin (0.1 mg/kg s.c. for 4 weeks) did not favorably affect the investigated skeletal parameters in all the experimental models studied (NOVX, OVX, T1D NOVX and T1D OVX rats). In fact, some bone parameters worsened due to oxytocin administration.

Results of this *in vivo* study do not support the hypothesis on the usefulness of oxytocin as a potential antiosteoporotic drug.

doi:10.1016/j.bonr.2020.100469

P142

Understanding local effects of orexin A and B on bone *in vitro*

Young Eun Park[a], Jian-Ming Lin[a], Karen E. Callon[a], Dorit Naot[a], Brya G. Matthews[b], David S. Musson[a], Jillian Cornish[a]
[a]*Medicine, University of Auckland, Auckland, New Zealand*
[b]*Molecular Medicine and Pathology, University of Auckland, Auckland, New Zealand*

Orexin A and B are neuropeptides involved in sleep control, appetite and energy expenditure. A recent *in vivo* study using transgenic mice discovered orexin also has effects on bone metabolism; acting centrally to enhance bone mass, and locally to reduce bone mass. To better understand the local effects of orexin A and B, we carried out in vitro assays on bone cells at all stages of development.

Primary mouse bone marrow cells were cultured in the presence of orexin A or B in 1) osteogenic media for two weeks, with mineralisation assessed by Von Kossa staining, or 2) adipogenic media for one week, and adipogenesis determined by Oil-Red-O release. Osteoclastogenesis was evaluated by the number of multinucleated TRAP+ve primary mouse bone marrow cells following 48hr treatment. Primary rat osteoblast proliferation was assessed by ^{3}H-thymidine incorporation following 24hr treatment. Osteoblasts were differentiated for three weeks in the presence of orexin A or B, and mineralisation assessed using Von Kossa staining. Osteocyte-rich ex vivo mouse bone was cultured and changes in osteocyte marker gene expression was examined with qPCR and sclerostin secretion measured by ELISA, following 24 or 48hrs treatment.

Orexin A and B (10^{-7}M) increased bone marrow adipogenesis ($p< 0.05$) but did not affect osteoblastogenesis or osteoclastogenesis. Orexin A and B (10^{-8} and 10^{-9}M) significantly increased osteoblast proliferation ($p< 0.01$). Orexin did not have effect on matrix mineralisation by osteoblasts. Orexin did not affect the level of osteocyte marker gene expression or sclerostin secretion.

Our data suggests the negative local effect of orexin on bone observed in vivo might be due to orexin pushing bone marrow towards

adipose tissue over bone, rather than having a direct effect on osteocytes, osteogenesis or osteoclastogenesis.

doi:10.1016/j.bonr.2020.100470

P143
Regulation of the local fibroblast growth factor-23 expression in the intestinal epithelial cells

Mayuree Rodrat[a,b], Kannikar Wongdee[b,c], Narattaphol Charoenphandhu[a,b,d]
[a]*Department of Physiology, Faculty of Science, Mahidol University, Bangkok, Thailand*
[b]*Center of Calcium and Bone Research (COCAB), Faculty of Science, Mahidol University, Bangkok, Thailand*
[c]*Faculty of Allied Health Sciences, Burapha University, Chonbui, Thailand*
[d]*Institute of Molecular Biosciences, Mahidol University, Nakhonpathom, Thailand*

Chronic high-calcium intake and intestinal calcium hyperabsorption often lead to a variety of adverse effects. It is possible that the intestinal epithelial cells possess certain negative feedback mechanisms to restrict calcium absorption in order to prevent toxicity. Calcium-sensing receptor (CaSR) is also expressed in several other tissues related to calcium metabolism, including the intestine. However, the role of CaSR in the regulation of calcium transport across small intestine remains unclear. Although 1,25-dihydroxyvitamin D_3 [$1,25(OH)_2D_3$] and parathyroid hormone (PTH) are well recognized as calciotropic hormones, a few of endocrine and paracrine factors can counterbalance their effects on calcium absorption. Previously, fibroblast growth factor (FGF)-23 expressed in intestinal mucosa has been reported to abolish the $1,25(OH)_2D_3$-enhanced intestinal calcium absorption in mice. We herein hypothesized that CaSR might induce local FGF-23 production in the intestinal epithelial cells and inhibits calcium absorption as part of negative feedback loop. The intestinal-like Caco-2 cells were thus grown on Snapwells for measurement of the transcellular calcium fluxes by Ussing chamber technique. We found that $1,25(OH)_2D_3$ and high luminal calcium completely abolished $1,25(OH)_2D_3$-stimulated calcium transport and induced FGF-23 synthesis and secretion into both apical and basolateral compartments. Western blot analysis revealed an upregulation of FGF-23 protein expression in a dose-dependent manner after exposure to $1,25(OH)_2D_3$ and high calcium. Furthermore, selective CaSR inhibitors fully prevented the negative effect of high calcium exposure on calcium transport, while allosteric CaSR agonists were able to suppress the $1,25(OH)_2D_3$-stimulated calcium transport similar to that observed in high luminal calcium treatment. In conclusions, prolonged exposure to high apical calcium and calcium hyperabsorption probably induces a local production of FGF-23 as a part of negative feedback loop, which, in turn, diminishes calcium absorption in an autocrine/paracrine manner. This phenomenon can help prevent calcium toxicity due to excessive calcium uptake.

doi:10.1016/j.bonr.2020.100471

P144
Diabetes Mellitus: A synonym to functional hypoparathyroidism

Poonji Gupta
ENT, TMMC&RC, Ghaziabad, India

Background: Poor control of blood glucose levels in patients of Diabetes Mellitus often results in low bone mineral density. The reason for this decrease in bone mass is at present uncertain. We evaluated correlation of calcium metabolism with blood glucose levels and normal renal function.

Method: 130 diabetic patients (35 Type 1, 95 Type 2) were enrolled. In all patients plasma calcium (Ca), serum phosphate (PO4), serum parathyroid hormone (PTH), and 24-h urinary calcium (uCa) were determined under both poor and improved control (for at least 7 days) as ascertained by four blood glucose determinations daily.

Results: It was a general observation that Urinary calcium excretion was increased in all diabetic patients in comparison to normal values of excretion in healthy individuals. Improvement of blood glucose level was associated with reduction of uCa both in Type 1 (6.7 ± 1 vs 5.0 ± 0.9 mmol/day) and in Type 2 patients (4.3 ± 0.4 vs 3.1 ± 0.4 mmol/day). It was found that considerably more Type 1 patients (15) had PTH values below the detection limit during poor than during improved control (4). Type 2 patients also showed this difference but to a lesser extent. 33 type 2 patients had PTH level below detection limit during poor control as compared to only 5 patients during good control. Comparison between the two types of diabetes showed that in Type 1 under poor control, Ca and PTH were lower, while uCa was higher, and after improved control, only uCa continued to be higher.

Conclusion: Parathyroid harmone is primary harmone which takes part in calcium metabolism by stimulating calcium absorption from intestines, renal tubules. Whenever calcium level in blood goes down, parathyroid harmones are stimulated to increase level of PTH. This helps in normalizing blood calcium level by increasing calcium absorption from intestines,

doi:10.1016/j.bonr.2020.100472

P146
Consumption of healthcare resources in a bariatric surgery cohort

Maria Del Pilar Ahijado Guzman[a], Raul María Veiga Cabello[b], Miguel Cantalejo Moreira[a], Justo Ruiz Ruiz[c], Antonio Zapatero Gaviria[c]
[a]*Rheumatology, Htal Universitario de Fuenlabrada, Fuenlabrada, Spain*
[b]*Rheumatology, Hospital Central de la Defensa Gómez Ulla, Madrid, Spain*
[c]*Internal Medicine, Htal Universitario de Fuenlabrada, Fuenlabrada, Spain*

Introduction: Bariatric surgery is the set of surgical techniques whose objective is weight reduction.

Objective: To carry out a retrospective observational pilot analysis of a cohort of 140 morbidly obese patients after bariatric surgery, descriptive of the comsuption of healthcare resourses about the locomotor system, among others.

Material and method: Data were collected from the University Hospital of Fuenlabrada of a cohort of morbidly obese people who underwent bariatric surgery from 2009 to the present. Were included as variables current and surgical age, gender, weight before surgery and the last weight available, height, evolution time in years since surgery, and surgical complications (greater if they require re-operative abdominal surgery). And as more specific variables assistance to locomotor, pulmonology and urology doctor`s offices. A descriptive and frequency analysis was performed.

Results: It was a cohort of 48.76 years old operated at 42.88 years old, 25.7% of men compared to 74.3% of women, weigh of 122.14 kg and height of 1.63 m, with a weight loss of 35.88 kg (last available of 86.26 kg) within a period of 5.81 years. 11.4% of patients presented major complications, 37.9% minor, and no deaths were described. 81.4% of patients went to rheumatology doctor`s office due to mechanical problems related to overweight, 3.6% of men to urology consultations due to erectile dysfunction, and 86.4% to pulmonology consultations in relation to obstructive sleep apnea syndrome (OSAS).

Conclusions: It is a study what higlights that bariatric surgery in Fuenlabrada area is mainly performed on morbidly obese women in adulthood, with an expected weight loss of 29.37% over a period of 5.81

years. As expected, there is a high consumption of hospital resources apart from those derived directly from the bariatric surgery protocol.

doi:10.1016/j.bonr.2020.100473

P147

Bone health in women with menstrual and reproductive abnormalities

Piroska Feher[a], Dorina Annar[a], Irina Kalabiska[b], Annamaria Zsakai[a]
[a]*Department of Biological Anthropology, Eotvos Lorand University, Budapest, Hungary*
[b]*Research Center for Sport Physiology, University of Physical Education, Budapest, Hungary*

There have been few epidemiological studies examining the associations between menstrual irregularity and bone health status parameters in premenopausal women. There are several risk factors for skeletal abnormalities beside genetic factors, e.g. malnutrition in quantity and/or quality, endocrine disorders, insufficient vitamin D supply, not reaching the recommended level of physical activity. Abnormalities of reproductive functions can indicate endocrine disorders or abnormalities that presumably significantly influence bone development, maintenance and regeneration.

The study aimed to describe the associations between menstrual pattern, reproductive health status, oestrogen level and bone health (estimated by quantitative ultrasound parameters, bone mass and bone mineral content) in a population-based sample of premenopausal women.

Premenopausal women aged between 18 and 45 years were enrolled to the present analysis (subsample of women with menstrual and reproductive abnormalities - n: 30, control group of women with normal menstrual and reproductive functions - n: 370). Estrogen level was estimated from saliva samples. Bone mineral content (kg) was estimated by InBody 720 analyser. Bone structure was measured by ultrasound osteometer (DTU-One Osteometer). Broadband ultrasound attenuation (BUA, dB/MHz) was used to assess bone structure in the analysis. Bone mass (kg) was estimated by Drinkwater-Ross anthropometric method. Relative bone mass was expressed in the percentage of body mass and stature. Data on menstrual history and reproductive life events were collected by questionnaires during personal interviews.

The results revealed that abnormalities in menstrual pattern and reproductive health status can predict bone quality. This relationship emphasizes the high importance of the regular osteological examinations of women not only with severe reproductive or reproductive abnormalities, but also women with mild but chronic abnormalities of the reproductive system.

doi:10.1016/j.bonr.2020.100474

P148

FGF23 and urinary phosphate excretion for estimation of nephron number: Differences between chronic kidney failure and kidney transplantation

Marzia Pasquali[a], Natalia De Martini[b], Lida Tartaglione[b], Silverio Rotondi[c], Sandro Mazzaferro[a]
[a]*Nephrology, Policlinico Umberto I, Sapienza University, Rome, Italy*
[b]*Sapienza University of Rome, Rome, Italy*
[c]*ICOT, Latina, Italy*

Assuming that FGF23 levels correlate with phosphate excretion per nephron, nephron number can be estimated by measuring FGF23 levels and urinary phosphate excretion (FEP). Kuro-O proposed that the ratio of FEP to serum FGF23 levels should correlate with nephron number and is defined as the nephron index (NI)

The aim of the study is calculating NI as nephron number estimation in patients affected by various degree of chronic kidney disease, both transplanted and not.

In 147 CRF patients (80 kidney transplant recipients) kidney function, mineral metabolism biomarkers and NI were evaluated.

Results: Mean eGFR did not differ between TX and noTX but NI was higher in TX since FEP was higher despite lower FGF23 levels in TX (Table1). No correlation existed between FGF23 and FEP, Ps and eGFR in TX differently from noTX.

Discussion: NI could not be properly defined as nephron number estimation in TX pts. However it may represent higher function of residual nephrons, since higher FEP did not correlate to FGF23 and could be determined by compensatory hyperfiltration (increased single nephron GFR) in transplanted patients.

Conclusions: After kidney transplantation, high NI value could have a functional meaning rather than represent residual number of nephrons.

Table 1

	noTX (n.67)	TX (n.80)	P value
Age (years)	59±15	55±10	0,051
eGFR (ml/min/1.73mq)	50±25	48±16	ns
sCa (mg/dl)	9,4±0,5	10,1±0,8	<0,00001
sP (mg/dl)	3,5±0,6	3,0±0,6	<0,0001
sKlotho (pg/ml)	522±185	477±141	ns
FGF23 (pg/ml)	74,3±52,4	47,3±28,8	<0,0001
1,25D (pg/ml)	25,1±13,4	42,4±15,5	<0,00001
25D (ng/ml)	23,9±11,1	26,1±11,7	ns
PTH (pg/ml)	60,0±32,1	59,3±51,5	ns

doi:10.1016/j.bonr.2020.100475

P149

Evaluation of antidiabetic potential of flavonoid rich fraction of *Hybanthus enneaspermum* in diabetic rats: In-silico molecular docking studies for aldose reductase, α-glucosidase and α-amylase

Dinesh Kumar Patel
Department of Pharmaceutical Science, Sam Higginbottom University of Agriculture, Technology and Sciences, Payagraj, India

Introduction: Diabetes mellitus is a chronic metabolic disease affected a wide range of population all over the world and leads to development of secondary complications. Aldose reductase (AR) enzyme play key role in the development of secondary diabetic cataract and retinopathy via polyol pathway. Hybanthus enneaspermus is used for the treatment of metabolic disorder by some tribal people in the India.

Methods: The flavonoid rich fraction was prepared using ethyl acetate. Oral glucose tolerance test (OGTT) and normoglycemic effect of flavonoid rich fraction of *Hybanthus enneaspermus* (EHE) was evaluated at a dose of 45 and 90 mg/kg, p.o. Further effect of EHE on blood glucose, body weight, antioxidant, lipid and aldose reductase enzyme level were carried out at 45 and 90 mg/kg p.o. per day for 21 days in streptozotocin-induced type-2 diabetic rats. Effect of EHE on glucose uptake by rat hemidiaphragm was investigated. Molecular docking technique was also performed against aldose reductase, α-glucosidase and α-amylase for selected phytoconstituents. Moreover phytochemical analysis was also carried out to know the presence of various phytoconstituents.

Results: EHE contain significant amoun phenolic (71.95 mg/g), tannin (20 mg/g), flavonoid (20 mg/g), flavonol (0.68 mg/g) and saponin content. EHE significantly decreased blood glucose level in diabetic rats. All the tested lipid parameters and enzyme level were significantly restored to the normal level in the EHE treated rats. Moreover, there was a significant increase in the body weight and glycogen contents in the EHE treated rats. Glucose uptake by hemidiaphragm was also enhenced in the presence of EHE. Docking study showed the best binding affinity and

interaction of phytoconstituents with aldose reductase, α-glucosidase and α-amylase.

Conclusion: EHE has very impressive profile as an antidiabetic, antioxidant, lipid lowering capacity and anti-cataract via aldose reductase inhibitors, and it may prove to be effective treatment for the hyperglycemia.

doi:10.1016/j.bonr.2020.100476

P150

Sirtuin 1 deficiency decreases bone mass and increases bone marrow adiposity in a mouse model of chronic energy deficiency

Loïc Louvet, Damien Leterme, Séverine Delplace, Flore Miellot, Pierre Marchandise, Véronique Gauthier, Pierre Hardouin, Christophe Chauveau, Olfa Ghali Mhenni
Laboratoy of Marrow Adiposity and Bone, University of Littoral Côte d'Opale, Boulogne sur mer, France

Sirtuin of type 1 (Sirt1), a class III HDAC, is known to be involved in the regulation of differentiation of skeletal stem cells (SSCs) into osteoblasts and adipocytes. In caloric restriction, it has been shown that the expression and activity of Sirt1 is a tissue-dependent regulation. However, at present, no study has focused on the link between Sirt1, bone marrow adiposity (BMA) and osteoporosis related to anorexia nervosa (AN). Thus, the aims of this work were to (i) determine BMA and bone changes in a mouse model replicating the phenotypes of AN (separation-based anorexia model (SBA)); (ii) determine the expression of Sirt1 in bone marrow stromal cells (BMSCs) extracted from these mice and identify their differentiation capacities and (iiii) delineate the molecular mechanism by which Sirt1 could regulate osteogenesis in an SBA model. Our results demonstrated that SBA protocol induces an increase in BMA and alteration of bone architecture. In addition, BMSCs from restricted mice present a down-regulation of Sirt1 which is accompanied by an increase in adipogenesis at expense of osteogenesis. After a 10-day organotypic culture, tibias from SBA mice displayed low levels of *Sirt1* mRNA which are restored by resveratrol treatment. Interestingly, this recovery of Sirt1 levels also returned the BMA, BV/TV and Tb.Th in cultured tibias from SBA mice to normal levels. Finally, to investigate the molecular mechanisms by which Sirt1 could regulate osteogenesis in the SBA model, the acetylation levels of Runx2 and Foxo1 transcription factors were determined. Our data show that this chronic energy deficiency in female mice causes a decrease in BMSC activity, resulting in critical changes to Runx2 and Foxo1 acetylation levels and thus to their activity. Altogether, these data suggest that Sirt1 could be considered as a potential therapeutic target in osteoporosis related to AN.

doi:10.1016/j.bonr.2020.100477

P151

Transient-receptor-potential-vanilloid-1/Oxytocin receptor mRNA is up-regulated in Soleus muscle and brain while Oxytocin increases in bone after cold stress in mice: The Oxytonic effect of Oxytocin

Claudia Camerino[a,b], Elena Conte[c], Adele Romano[b], Marialuisa De Ceglia[b], Silvana Gaetani[b], Domenico Tricarico[c]
[a]*Department of Biomedical Sciences and Human Oncology, University of Bari, Bari, Italy*
[b]*Department of Physiology and Pharmacology 'V. Erspamer', University of Rome, Sapienza, Rome, Italy*
[c]*Department of Pharmacy-Drug Science, University of Bari, Bari, Italy*

Oxytocin (Oxt) enhances several physiological processes and its involved in energy regulation. We explored the role of specific neuronal nuclei to the "Oxytonic" action of Oxt on slow-twitch muscle and bone after cold stress (CS) in mice, together with the pain sensing Transient-receptor-potential-vanilloid-1 (TRPV1) cation channels. The changes in the expression of Oxytocin receptor (Oxtr) in hypothalamic paraventricular (PVN), supraoptic nuclei (SON) and in the hippocampus (HIPP) were investigated by immunohistochemistry in parallel with measurement of serum Oxt. The expression of *Oxt*/*Oxtr* and *TRPV1* gene in soleus and tibialis *anterioris* (TA) muscles and in bone was investigated by RT-PCR. Mice(n=15) were divided into: controls at room temperature (RT=23°C), exposed to CS at T=4°C for 6 hours(6h) and 5 days (5d). Oxtr level increases by 2-folds (p=0.01) in PVN and by 1.5-fold(p=0.0001) in HIPP after 6h and 5d CS, but decreases by 2-folds (p=0.026) in SON at 5d. The *Oxtr* expression was not affected after 6h but increased by 16-fold after 5d in soleus (p=0.001), but not in TA. The *TRPV1* expression increased by 1.4 and 1.38-fold ($p< 0.05$) after 6h and 5d CS in soleus but not in TA. *Oxt* mRNA was upregulated by 5-folds following 5d CS in bone (p=0.041). The plasmatic levels of Oxt are unaffected after 6h CS but decreases by 0.2-fold(p=0.0141) after 5d CS. The myocardium of 6h CS mice shows positive histopathological signs that are reduced by 3 folds(p=0.021) after 5d CS. In sum, Oxtr was up-regulated in PVN and HIPP after CS, but down-regulated in SON. The up-regulation of Oxtr found in PVN and HIPP and of Oxt in bone at 5d balances the decrease of circulating Oxt. The histopathological signs in the myocardium highlight a similar biphasic pattern of Oxt/Oxtr signaling. Oxt/Oxtr exerts a protective/analgesic/tonic effect on the slow-twitch muscle through brain/bone signaling.

doi:10.1016/j.bonr.2020.100478

P152

Feeding powdered nacre prevents ovariectomy-induced bone loss in the rat

Kim Dung Nguyen[a], Norbert Laroche[a], Arnaud Vanden Bossche[a], Yacine Bertache[a], Marie-Thérèse Linossier[a], Mireille Thomas[a], Sylvie Peyroche[a], Myriam Normand[a], Laurence Vico[a], Marthe Rousseau[a,b]
[a]*Campus Santé Innovation, U1059 INSERM - SAINBIOSE, Saint-Priest-en-Jarez, France*
[b]*CNRS/Lyon University/INSA-Lyon, UMR5510 MATEIS, Lyon, France*

Mother-of-pearl (nacre) influences bone health. Nevertheless, limited studies investigated the effects of oral nacre supplementation in bone loss model. Our aim was to investigate the effect of nutritional supplementation with nacre on ovariectomy-induced osteoporosis in rats.

40 female Wistar rats were sham-operated or ovariectomized and divided into four subgroups: Sham group and OVX group on standard diet, OVX $CaCO_3$ group and OVX Nacre group (supplemented with $CaCO_3$ and Nacre powder respectively, 250 mg/kg body weight/day) for 4 weeks. Changes in body weight and in the uterus were measured. Micro-computed tomography (μCT) of tibias, femurs and 2nd lumbar vertebras, as wells as histological changes in the tibia were analysed. Gene expression was analysed by qRT-PCR. ELISA test was used to evaluate the serum levels of biochemical markers including CTX, OCN and P1NP.

The increase in body weight of the OVX Nacre group was significantly limited after 2 weeks and 4 weeks compared with OVX group. The μCT analysis demonstrated the Nacre group showed an significant improvement in the bone structural parameters in the metaphyseal femur (longitudinal) and in the proximal tibia, femoral head and 2nd lumbar vertebra (*ex vivo*) compared with the other OVX groups. Some genes (e.g. OPN, RANK) are overexpressed in OVX Nacre group compared with OVX and OVX $CaCO_3$ group, while nutritional supplementation of nacre reduced the serum OCN and CTX levels compared with those in OVX group.

Taken together, the results provide evidence for the protective effect of nacre on post-menopausal-induced bone loss.

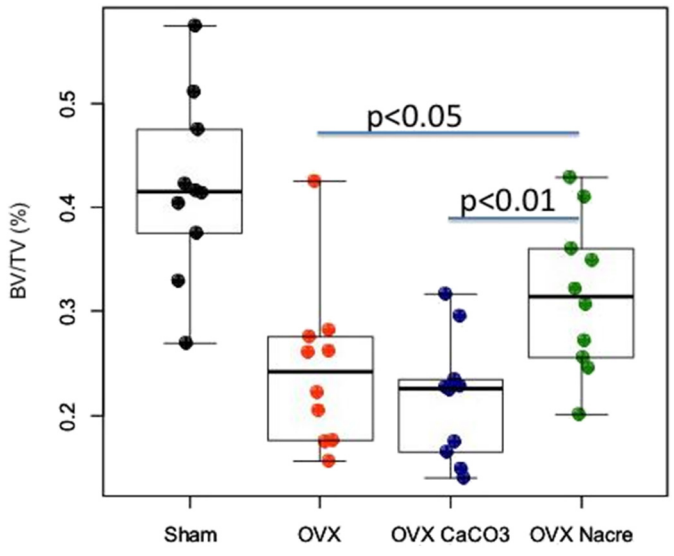

BV/TV of the trabecular bone at the femoral head after 4 weeks of nutritional supplementation.

doi:10.1016/j.bonr.2020.100479

P153

Body composition and anthropometric data - influence of total and uc-dpMGP

Natascha Schweighofer[a,b], Moritz Strasser[c], Christoph W. Haudum[a,b], Albrecht Schmidt[d], Ines Mursic[d], Burkert Pieske[d], Thomas R. Pieber[a,b], Barbara Obermayer-Pietsch[a]

[a]*Dept. of Internal Medicine, Division of Endocrinology and Diabetology, Medical University of Graz, Graz, Austria*

[b]*CBmed, Center for Biomarker Research in Medicine, Graz, Austria*

[c]*Department of Health Studies, Institute of Biomedical Science, FH JOANNEUM, University of Applied Sciences, Graz, Austria*

[d]*Dept. of Internal Medicine, Division of Cardiology, Medical University of Graz, Graz, Austria*

Body composition influences the development of type 2 diabetes mellitus (T2DM) and cardiovascular risk. According to literature, matrix-GLA-protein (MGP) is associated with bone parameters and cardiovascular risk in persons with and without T2DM. We investigated whether uncarboxylated, dephosphorylated MGP (uc-dpMGP), totalMGP or both are associated with body composition and anthropometric parameters in patients with and without T2DM.

We analysed data from the BioPersMed cohort (n=966, 531 females, 435 males, mean age 58 ± 9 years, 255 without and 71 with T2DM), a prospective cohort of asymptomatic subjects at cardiovascular risk. T2DM was defined according to ADA criteria. Uc-dpMGP was measured with IDS-iSYS InaKtif MGP Kit, totalMGP using the Human MGP(Matrix Gla protein) ELISA Kit (Wuhan Fine Biotech Co., Ltd. China). Body composition was determined by Lunar iDXA (GE Healthcare GmbH, Austria).

Total and uc-dpMGP did not correlate with each other in both subject groups.

Uc-dpMGP correlated positively with BMI ($p< 0.001$), weight ($p=0.003$), systolic/diastolic blood pressure ($p=0.021$ and 0.004, respectively), heart frequency ($p=0.011$) and waist and hip circumferences (both $p< 0.001$) in subjects without T2DM and with BMI ($p=0.016$), weight ($p=0.021$) and waist and hip circumferences ($p=0.025$ and 0.046) in T2DM. TotalMGP showed no correlations with these parameters in both subject groups.

Only in subjects without T2DM uc-dpMGP correlated positively with total fat mass ($p< 0.001$), total tissue mass ($p=0.001$), total overall mass ($p=0.002$) and total tissue fat ($p< 0.001$). No correlations were seen with lean, fat free or bone mass. TotalMGP showed no associations with body composition parameters in both subject groups.

Only uc-dpMGP correlated with anthropometric parameters in diabetic and non-diabetic subjects, and with body composition in subjects without diabetes.

Since MGP is expressed in fat tissue, uc-dpMGP might be a modulator of body composition and fat distribution, and thus influence T2DM and cardiovascular risk development.

doi:10.1016/j.bonr.2020.100480

P154

Total versus uc-dpMGP: Associations with cardiovascular parameters

Natascha Schweighofer[a,b], Moritz Strasser[c], Christoph W. Haudum[a,b], Albrecht Schmidt[d], Ewald Kolesnik[d], Burkert Pieske[d], Thomas R. Pieber[a,b], Barbara Obermayer-Pietsch[b]

[a]*CBmed, Center for Biomarker Research in Medicine, Graz, Austria*

[b]*Department of Internal Medicine, Division of Endocrinology and Diabetology, Medical University of Graz, Graz, Austria*

[c]*Department of Health Studies, Institute of Biomedical Science, FH JOANNEUM, University of Applied Sciences, Graz, Austria*

[d]*Department of Internal Medicine, Division of Cardiology, Medical University of Graz, Graz, Austria*

Vascular calcification, modulated i. a. by Matrix-GLA-protein (MGP), is a risk factor for cardiovascular disease. We investigated whether uncarboxylated, dephosphorylated MGP (uc-dpMGP), totalMGP or both are associated with pulse wave velocity (PWV), intima-media thickness (IMT) and relative wall thickness (RWT) in patients with and without type 2 diabetes (T2DM).

We analysed data from the BioPersMed cohort (255 participants without and 71 with T2DM, age 58 ± 9 years,), a prospective cohort of asymptomatic participants at cardiovascular risk. T2DM was defined according to ADA criteria. Uc-dpMGP was measured by IDS-iSYS InaKtif MGP Kit, totalMGP by Human MGP(Matrix Gla protein) ELISA Kit (Wuhan Fine Biotech Co., Ltd., China). Pulse wave analysis was done with a SphygmoCor device (Atcor Medical, Australia), IMT and echocardiograpy with the Vivid 9 device (GE Healthcare Austria GmbH & Co OG, Austria).

Total and uc-dpMGP did not correlate with each other in both participant groups. Uc-dpMGP was associated with BMI ($p< 0.001$), weight ($p=0.003$), systolic/diastolic blood pressure ($p=0.021$ and 0.004, respectively), heart frequency ($p=0.011$) and waist and hip circumferences (both $p< 0.001$) in participants without T2DM and with BMI ($p=0.016$), weight ($p=0.021$) and waist and hip circumferences ($p=0.025$ and 0.046) in participants with T2DM. TotalMGP showed no correlations with these parameters in both participant groups.

In participants without T2DM only uc-dpMGP correlated with PWV and IMT ($p=0.004$ and $p=0.001$, respectively). Elevated uc-dpMGP levels were seen in participants with end organ damage compared to participants without ($p=0.021$). Only uc-dpMGP associated with RWT groups ($p=0.039$) in non-diabetics. Higher uc-dpMGP levels were found in participants with eccentric compared to concentric cardiac hypertrophy.

Uc-dpMGP but not totalMGP was associated with cardiovascular parameters only in participants without T2DM.

Our data implicate that uc-dpMGP is also an active MGP form and might be a cardiovascular risk modulator, which needs further investigation.

doi:10.1016/j.bonr.2020.100481

P155

High fat diet (HFD)-induced obesity augments the deleterious effects of estrogen deficiency in bone. Evidence from post-menopausal mice

Dalia Ali[a], Florence Figeac[a], Michaela Tencerova[b], Nicholas Ditzel[a], Alexander Raunch[a], Clarissa Schmal[a], Moustapha Kassem[a,c]
[a]*Department of Endocrinology and Metabolism, Molecular Endocrinology & Stem Cell Research Unit (KMEB), University of Southern Denmark and Odense University Hospital, Odense, Denmark*
[b]*Molecular Physiology of Bone, Czech Academy of Sciences/Institute of Physiology, Prague, Czech Republic*
[c]*Department of Cellular and Molecular Medicine, University of Copenhagen/ Danish Stem Cell Centre, Copenhagen, Denmark*

Male mice and human studies revealed that high fat diet (HFD)-induced obesity exerted deleterious impact on skeletal stem cells function yet limited studies have paid attention to sexual dysmorphism and its impact on the cellular mechanisms linking obesity, menopause, bone marrow adiposity and bone fragility. Female mice (C57BL/6J) were ovariectomized (OVX) or Sham operated and were fed either HFD or normal diet (ND) for 12 weeks. Mice fed with HFD showed a significant increase in body weight (~86% in HFD and ~122% in HFD-OVX, $p< 0.0005$) and impaired glucose tolerance. MicroCT-scanning revealed negative impact of HFD-induced obesity on Tb.BV/TV (-15±0.004% in HFD, $p< 0.05$ and -37.5±0.005% in HFD-OVX, $p< 0.005$) and Tb-N (-13.8±0.063% in HFD, $p< 0.005$, -23±0.056% in HFD-OVX, $p< 0.0005$) while Tb-Sep increased (+16.2±0.007% in HFD, $p< 0.005$, +31.8±0.008% in HFD-OVX, $p< 0.0005$). In cortical bone, HFD-OVX decreased cortical thickness (-13±0.003%, $p< 0.005$) and increased cortical porosity (+60.7±0.47%, $p< 0.005$). HFD-induced expansion of marrow adipose tissue (MAT) (+60.7±9.9%, $p< 0.05$) was more pronounced in HFD-OVX (+79.5±4.8%, $p< 0.005$). Gene expression analysis of whole bone, revealed that HFD and HFD-OVX exhibited up regulation in adipogenesis (~2-8 fold), inflammation (~2-13 fold) and senescence gene expression markers (~2 fold). HFD-induced obesity lead to bone loss, bone marrow adiposity expansion and up-regulation of inflammatory and senescence associated phenotype marker genes in bone micro-environment. These effects are more pronounced by estrogen deficiency. Thus, obesity is not protective but augments the negative effects of estrogen deficiency on the skeleton.

doi:10.1016/j.bonr.2020.100482

P160

Contribution of PD-L1 expression to the energy metabolism of mesenchymal stromal cells

Antoine Boutin[a], ElHadji Djite[a], Abigaïl Mazzu[a], Didier Pisani[a], Abdel Wakkach[a], Nathalie Mazure[b], Claudine Blin-Wakkach[a], Matthieu Rouleau[a]
[a]*Université Côte d'Azur, CNRS UMR 7370, Laboratoire de PhysioMédecine Moléculaire, Nice, France*
[b]*Université Côte d'Azur, INSERM U1065, C3M, Nice, France*

Bone marrow mesenchymal stromal cells (MSCs) present strong immunosuppressive properties, driving immune responses toward regulation/tolerance. Despite these functions, clinical trials have shown inconsistent efficacy of MSCs due in part to the lack of uniform cell populations. Homogeneous well-characterized cells can be derived *in vitro* from human induced pluripotent stem cells. We recently characterized huiPS-MSCs immunosuppressive properties showing their capacity to induce CD4+ T regulatory cells (Treg).

Immuno-metabolism studies have shown that depriving the microenvironment from glucose (such as an exacerbated glycolytic metabolism in tumor cells) participate to the differentiation of Treg cells. PD-L1 has been involved in controlling such a glycolytic pathway in tumor cells. Because MSCs use PD-L1 to inhibit PD1-expressing T cells, we wondered whether such PD-L1/PD1 interaction could control the energy metabolism of MSCs.

We analyzed the metabolism of MSCs "licensed" by TNF-a required to induce PD-L1 expression. Our results presented in the figure indicate that licensed MSCs might rely less on glycolysis and OxPhos for their energetic metabolism. But, if PD-L1 is stimulated on such licensed MSCs (use of an Fc-PD1 fusion protein), both the glycolysis and respiration of MSCs are largely increased. This indicating that the interaction of PD-L1 with its ligand (PD1) results in a strong metabolic activation of MSCs which could lead to an nutriment-deprived local micro-environment. The molecular pathways involved are under investigation.

Our results bring new insights into the understanding of the metabolic pathways controlled by the PD-L1 receptor on MSCs, contributing to their better characterization for optimal clinical applications.

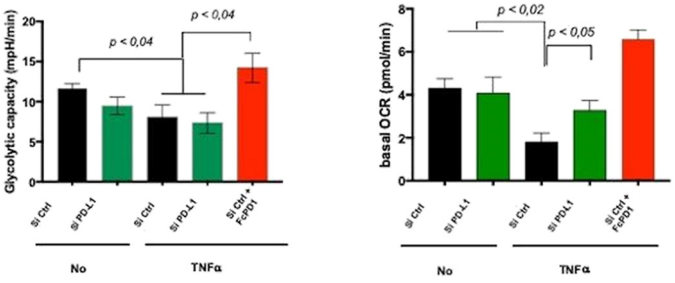

Figure : Strong metabolic activation of MSCs stimulated through PD-L1.
The TNF-α stimulation reduced both the glycolytic (left panel) and the OxPhos (right panel) capacities of MSCs (SeaHorse XFe96 automat, glycolytic capacity and basal oxygen consumption rate - OCR).
Blocking the PD-L1 expression with specific siRNAs showed that the reduction of the basal respiration of MSCs is in part controlled by PD-L1 (right panel, green bars).
If PD-L1 is stimulated by an agonistic Fc-PD1 fusion protein, both the glycolysis capacity and the OCR of MSCs are largely increased (red histogram bars).
(Student t test statistical analyzes on 3 experiments, p value significances are indicated).

doi:10.1016/j.bonr.2020.100483

P161

Characterization and impact on osteogenesis of the extracellular matrix of Bone Marrow Adipocytes in hyperglycemic condition in vitro

Laura Entz[a], Guillaume Falgayrac[b], Christophe Chauveau[a], Gilles Pasquier[b,c], Stéphanie Lucas[a]
[a]*MABLab, ULCO University, Boulogne-sur-Mer Cedex, France*
[b]*MABLab, Lille University, Lille, France*
[c]*Orthopaedic surgery, Lille University Hospital, Lille, France*

Within the bone marrow, the ExtraCellular Matrix (ECM) produced by surrounding cells such as Bone Mesenchymal Stromal Cells (BMSCs) alters osteoblastogenesis. Since Bone Marrow Adipocyte (BMAd) quantity and activity are modified with chronic hyperglycemia, we hypothesize that BMAds produce a specific ECM which, upon exposure to a high concentration of glucose, could be deleterious for bone quality in type 2 diabetes. The aims of this study are to characterize the BMAd ECM and to evaluate its effect on osteogenic differentiation using *in vitro* approaches.

Human primary BMSCs (RoosterBio) were either cultured or differentiated into BMAds or osteoblasts (OB) for 21 days in 5mM (LG)

or 25mM (HG) of glucose. The mRNA expression of several ECM components synthetized by these cells was measured using RT-qPCR. Then BMAd ECMs in LG and HG were devitalized by hypotonic shock for RAMAN spectroscopy characterization and to test osteogenic differentiation of BMSC using mRNA expression.

Among tested genes, fibronectin is down-regulated in BMAds compared to BMSCs (-2fold, $p< 0.05$) and OBs (-5fold, $p< 0.05$). Western-blot analysis confirms this difference. The devitalization protocol was validated through the absence of nucleic acids and triglycerides while proteins could be detected using a silver nitrate-stained gel. For a first donor, intensities of Raman signal of type I collagen at 1653cm^{-1} and 1667cm^{-1}, and, proline and hydroxyproline are increased in BMAd ECM obtained in HG compared to LG condition. Following seeding on BMAd ECM, BMSC adhesion and proliferation were not modified. Osteogenic differentiation on BMAd ECM obtained in HG shows altered expression of osteogenic markers (such as Runx2, Alkaline Phosphatase and Osteocalcin) and fibronectin compared to differentiation on ECM in LG or on plastic.

In summary, BMAds produce a specific ECM which could be modified under HG chronic exposure. Such BMAd ECM could interfere with osteoblast differentiation and mineralization.

doi:10.1016/j.bonr.2020.100484

P162

Ex-situ analysis of bone mineral density and cellular activity in type 1 diabetes mellitus

Liang-Yu Ma[a], Eva Maria Wölfel[a], Kilian Elias Stockhausen[a], Herbert Mushumba[b], Birgit Wulff[b], Klaus Püschel[b], Michael Amling[a], Björn Busse[a], Katharina Jähn[a]
[a]*Department of Osteology and Biomechanics, University Medical Center Hamburg-Eppendorf, Hamburg, Germany*
[b]*Department of Forensic Medicine, University Medical Center Hamburg-Eppendorf, Hamburg, Germany*

Type 1 diabetes mellitus (T1DM) - characterized by insulin deficiency - affects 20-40 million people worldwide. A higher fracture risk with the incidence of hip fracture being 6-fold greater is seen in patients compared to non-diabetic individuals. Studies of bone mineral density (BMD) in T1DM are controversial obscuring fracture risk assessment. BMD is based on coupled bone remodelling activity of bone-resorbing osteoclasts and bone-building osteoblasts. Imbalanced bone remodelling leads to changes in BMD. Therefore, this study aims to analyse BMD and cellular indices of individuals affected by T1DM.

Femoral cortices at mid-diaphysis from 14 individuals (7 Control and 7 T1DM, 47.29±5.12 and 48±7.68 years) and the 12th thoracic (T12) vertebrae from 28 individuals (19 Control and 9 T1DM, 47.11±4.98 and 48.67±6.5 years) were obtained during autopsy. Vertebral BMD was determined by applying dual-energy X-ray absorptiometry (DXA) while cellular indices were analysed via histomorphometry in the anterior quadrant of the femoral cross-section (divided into endo, mid, and peri-cortical region).

DXA results showed equal BMD values for T12 in Controls and T1DM group (0.926±0.200g/cm^2 vs. 0.898±0.134g/cm^2). Histomorphometry revealed low cellular activity of osteoblasts and osteoclasts in both groups. Osteocyte density was similar in both groups with 54.290 ±8.649#/mm^2 in Control and 53.177±17.707#/mm^2 in T1DM ($p=0.655$). The fraction of empty lacunae with 163.074±45.164#/mm^2 in Control and 138.945±43.705#/mm^2 in T1DM was not significantly different ($p=0.338$).

Our results link the quantified values for BMD to cellular activity in healthy individuals and individuals afflicted with T1DM. In contrast to the femoral neck as common skeletal fracture site, the femoral mid-diaphysis is predominantly composed of cortical bone presenting with lower bone turnover. Clearly, the individuals have been on insulin treatment potentially acting bone-anabolic, which might influence bone remodeling processes and thus interfering with fracture risk.

doi:10.1016/j.bonr.2020.100485

P163

Bone Marrow Adipocytes express specific Matrix MetalloProteinases in osteoporotic conditions

Tareck Rharass[a], Laura Entz[a], Adrien Tonione[b,c], Hamanou Benachour[a], Damien Leterme[a], Christophe Chauveau[a], Gilles Pasquier[b,d], Stéphanie Lucas[a]
[a]*MABLab, Marrow Adiposity and Bone Laboratory, ULCO University, Boulogne sur Mer Cedex, France*
[b]*MABLab, Marrow Adiposity and Bone Laboratory, Lille University, Lille, France*
[c]*Rheumatology, Lille University Hospital, Lille, France*
[d]*Orthopaedic Surgery, Lille University Hospital, Lille, France*

Matrix MetalloProteinases (MMPs) are major proteases degrading extracellular matrix. MMPs act as coupling factors in the bone remodeling of pathophysiological conditions but also contribute to the dysregulation of adipose tissues in metabolic diseases. Yet, they remain poorly explored within the specific Bone Marrow Adipocytes (BMAds) which accumulate in post-menopause and type 2 diabetes-related osteoporosis. We thus address the capacity of BMAds to produce MMPs in several models mimicking such conditions.

Human Bone Mesenchymal Stromal Cells (hBMSC, Lonza and Roosterbio) were differentiated into BMAds in either 5mM (LG) or 25mM glucose (HG) for 21 days to test the impact of chronic hyperglycemia. To address the pathophysiological relevance of MMP and TIMP expression, BMAds were isolated from femur and tibia of ovariectomized mice (ethical approval CEEA75-2016071815452669) and from distal femur of post-menopausal women undergoing knee prosthesis surgery (Clinical trial NCT03678831), to be compared to extramedullary adipocytes and remaining Bone Marrow (BM) cells, using real-time-PCR.

The mRNA levels of the two collagenases MMP1 and MMP13 were increased in hBMSC-derived BMAds upon HG exposure (x2.3, $p< 0.05$). Unlike MMP1, the HG-mediated upregulation of MMP13 was restricted to mature BMAds (x2.5, $p< 0.05$) compared to the surrounding non-lipid-laden cells. Following 4 and 14 weeks of ovariectomy, the gelatinase MMP9 and MMP13 expression levels were, respectively, 70- and 67-fold ($p< 0.05$) more expressed in BMAds than in visceral adipocytes. Interestingly MMP13 mRNA was also more expressed in BMAds than in the other BM cells (x39, $p< 0.01$) and tends to increase while insulin resistance develops. The analysis of first clinical samples confirms that BMAds highly express MMP9 and MMP13 compared to subcutaneous adipocytes in post-menopausal patients.

BMAds are a source of specific MMPs which could be metabolically regulated and contribute to bone remodeling processes. Future zymography analyses should clarify the substrate specificities of their proteolytic activities.

doi:10.1016/j.bonr.2020.100486

P164

Time of phenotype onset critical for modelling skeletal effects of T2DM

Tara C. Brennan-Speranza[a], Dean Ross[a], Itamar Levinger[b]
[a]*Physiology, University of Sydney, Sydney, Australia*
[b]*Victoria University, Melbourne, Australia*

Patients with type 2 diabetes (T2DM) have an increased risk of fracture that is not explained by the increased risk of falls. Patients with T2DM have normal-to-high bone mineral density (BMD), despite higher BMD usually being associated with reduced fracture risk. The exact mechanisms behind this observation are not yet known.

Studies investigating skeletal outcomes in T2DM in mice have placed little focus on time-of-onset and often investigate the effect on skeletally immature mice.

We investigated the consequences of a high fat diet (HFD) on skeletal outcomes in C57Bl/6J male mice and the influence that age of onset has on these outcomes using skeletally immature mice (8 weeks) and mature mice (12 weeks).

Differences between the two age groups were uniquely reflected in their respective structural, cellular and molecular parameters. Older mice were protected from the diminished 3D microstructural qualities (uCT) compared to the younger group, with BV/TV, TbTh, and TbN all significantly decreased by the HFD in younger mice (all $p< 0.05$ or lower) but not in older mice. Greater significant differences in cortical thickness and cortical bone volume were observed in younger mice. Cellular morphometry confirmed these results. Tibial RNA expression of type 1 collagen, osteocalcin and sclerostin were all significantly changed by dietary intervention in both age groups.

This data indicates significant negative impacts on bone microarchitecture in mice subject to dietary-induced metabolic challenges and, while younger animals compensate for the metabolic changes more robustly than older animals, the skeleton is not protected. Despite the skeleton in the older animals having achieved peak bone mass before the onset of the dietary challenge the quality of the bone was still compromised, and this, at least in part, may help to explain the increased fracture risk in patients with adult-onset T2DM.

doi:10.1016/j.bonr.2020.100487

P165

Estrogen deficiency alters skeletal and metabolic responses to obesity and weight loss strategies

Maude Gerbaix[a], Maria Papageorgiou[a], Monique Etienne[b], Daniel Courteix[b], Julien Hermet[c], Christophe Montanier[c], Serge Ferrari[a], Lore Metz[b]

[a]*Division of Bone Diseases, Geneva University Hospitals and Faculty of Medicine, Geneva, Switzerland*

[b]*Laboratory of Metabolic Adaptation to Exercise In Physiological and Pathological states (AME2P), Clermont Ferrand, France, Clermont Ferrand, France*

[c]*INRA UMR1019, UNH, Clermont Ferrand, France*

Estrogen deficiency occurring during menopause leads to fat accumulation and bone loss (Ley CJ, 2012). Caloric restriction is effective for obesity management, however, it induces bone loss (Seimon RV, 2019). We aimed to evaluate the effects of estrogen status on metabolic and skeletal adaptations to obesity and energy deficit strategies in mature mice.

Ovariectomized (OVX) and Sham operated C57/Bl6 mice were randomized into 5 groups: Chow diet (20wks), High Fat high fructose diet (HF)(20wks), HF diet (12wks) followed by isocaloric diet (Iso) (8wks), HF diet (12wks) followed by caloric restriction (CR)(8wks) and HF diet followed by caloric restriction + treadmill exercise (CRExo). Body composition (MRI), glucose tolerance (OGTT), tibia microarchitecture (μCT) were measured.

Estrogen deficiency potentiated the effects of HF on body weight (OVX_{HF}:+26g vs. $Sham_{HF}$:+18g, $P< 0.001$), increased fat mass (OVX_{HF}:23% vs. $Sham_{HF}$:15%, $P< 0.01$) and induced glucose intolerance ($AUC_{glucose}$) in both diets (OVX_{chow} vs. $Sham_{chow}$:+6036mg.dl^{-1}.min^{-1}; OVX_{HF} vs. $Sham_{HF}$:+6746mg.dl^{-1}.min^{-1}, $p< 0.05$). Estrogen deficiency decreased tibia Ct.th in both diets ($Sham_{Chow}$:199μm; OVX_{Chow}:188μm; $Sham_{HF}$: 211μm; OVX_{HF}:192; $P_{OVX}< 0.05$) and blunted the positive effect of HF diet on Tb.BV/TV ($Sham_{Chow}$: 2.91%; $Sham_{HF}$:4.28%; OVX_{Chow}:1.19%; OVX_{HF}:1.39%; P_{Diet}, P_{OVX} and $P_{Interaction}< 0.05$).

In obese mice, estrogen deficiency increased fat mass loss induced by CR ($Sham_{CR}$ vs. $Sham_{Iso}$:-1.81g; OVX_{Cr} vs. OVX_{Iso}:-3.96g; P_{CR}, P_{OVX} and $P_{Interaction}< 0.05$), but did not alter glucose tolerance in response to CR. It also blunted the unfavorable CR effect on CT.Th ($Sham_{Cr}$ vs. $Sham_{iso}$: -23μm; OVX_{Cr} vs. OVX_{Iso}:-6μm, P_{CR}; P_{OVX} and $P_{Interaction}< 0.05$). Exercise prevented the deleterious effects of CR on Ct.Th independently of estrogen status ($Sham_{CrExo}$:+19μm vs. $Sham_{Cr}$; OVX_{CrExo}:+18μm vs. OVX_{Cr}, $P_{Cr}< 0.001$; $P_{Exo}< 0.001$).

Our results suggest an important role of estrogens in metabolic and skeletal adaptations to obesity and subsequent caloric restriction. Exercise combined with CR appears to be an effective weight loss strategy to maintain bone health after menopause.

doi:10.1016/j.bonr.2020.100488

P166

Serum irisin in relation to insulin resistance and osteoporosis

Ji Eun Jun[a], You-Cheol Hwang[a], In-Kyung Jeong[a], Kyu Jeung Ahn[a], Ho Yeon Chung[a], Eui-Hyun Kim[b]

[a]*Endocrinology and Metabolism, Kyung Hee Univ Hosp at Gangdong, Seoul, Republic of Korea*

[b]*Endocrinology and Metabolism, Daegu Fatima Hospital, Daegu, Republic of Korea*

Irisin is a muscle-secreted protein which has been proposed to regulate energy homeostasis and bone metabolism. Considering the physiological role of irisin, the aim of this study is to evaluate the association of serum irisin with insulin resistance and osteoporosis.

We conducted a cross-sectional study including 40 female subjects who had never been treated for osteoporosis. We collected the data of clinical characteristics, glycemic and lipid parameters as well as bone turnover markers. The serum irisin and sclerostin levels were measured by commercially available ELISA. The Homeostasis model of assessment-insulin resistance (HOMA-IR) and quantitative insulin sensitivity check index (QUICKI) were calculated as indices of insulin resistance. BMD was measured by dual energy X-ray absorptiometry. Osteocalcin and C-terminal cross-linking telopeptide of type I collagen (CTX) were measured as bone turnover markers.

The mean age of the subjects was 60.6 ± 7.7 years, and mean body mass index (BMI) was 24.8 ± 3.9 kg/m^2. Of the subjects, 25.0% had osteoporosis and 87.5% had type 2 diabetes. Serum irisin levels were inversely correlated with fasting serum insulin levels (ρ =-0.34, $p = 0.032$) and HOMA-IR (ρ = -0.34, $p = 0.030$), while they were positively correlated with QUICKI (ρ = -0.34, $p = 0.030$). However, the association between irisin levels and the indices of insulin resistance lost statistical significance in a multiple linear regression analysis, after adjustment for age and BMI. In addition, serum irisin levels were not associated with osteocalcin, CTX, and sclerostin levels. Serum irisin levels were associated with neither BMD at the lumbar spine, hip and femur neck in the linear regression analyses nor the presence of osteoporosis in logistic regression analyses.

The regulatory role of irisin in relation to glucose homeostasis and bone metabolism still needs to be clarified.

doi:10.1016/j.bonr.2020.100489

P167

Comparative body mass index effect on total and undercarboxilated osteocalcina between normoglucemic premenopausal women and men

Marina Soledad Bonanno[a], Graciela Brito[b], Dana Watson[b], Liliana Zago[c], Carlos Alfredo Gonzalez Infantino[d], Susana Noemí Zeni[a]
[a]*Metabolic Bone Disease Laboratory, INIGEM (UBA/CONICET), Buenos Aires, Argentina*
[b]*Nutrition Department, University of La Matanza (UNLaM), La Matanza, Argentina*
[c]*Nutrition Department, Biochemistry and Pharmacology School, University of Buenos Aires, Buenos Aires, Argentina*
[d]*Nutrition Department, Medical School, University of Buenos Aires, Buenos Aires, Argentina*

We found that body mass index (BMI) through leptin affected osteocalcin (OCN), which in turn influences insulin and glucose homeostasis in men. Now we evaluated such effect in 35 premenopausal women (PMW) comparing the results obtained in these 45 men. All subjects were non-diabetic having normal glucose (80 to 110 mg/dL) and HbA1c (< 5.7%) and were divided according to BMI index in overweight (OW) or type I, II, III obesity (OB) degree. Glucose, HbA1c were measured by standard methods; undercarboxilated OCN (ucOCN) (ng/mL), total OCN (ng/mL), leptin (ng/mL), insulin (uUI/L) and CTX (ng/L) by ELISA, and 25hydroxyvitaminD (25OHD) (ng/mL) by a competitive protein-binding method.

Results: The results (mean ± SD) are summarized in Table 1.

In both genders, ucOCN increased and OCN decreased with BMI increase (P< 0.01) although with some differences by sex: in women OBTIII vs. the remaining groups (P< 0.01); men; ucOCN in OW vs. the three OB types and OCN from OW to OBTIII (p< 0.01). In both genders, leptin increased with BMI increase (p< 0.01) while insulin increased in OBTII and OBTIII vs. OW and OB TI (p< 0.05); and the lowest 25OHD was observed in OB TIII.

Conclusions: The results suggested that BMI effect on ucOCN and OCN present some differences between women and men; although in both genders OCN changes appears to influence insulin levels and glucose homeostasis.

Supported by CONICET/UBA and PROINCE E006 grant of UnLaM.

Table 1

	Glucose	ucOCN	OCN	CTX
OW: M PMW	97.0± 9.0 82.0±6.0	3.9±0.7 1.9±1.4	25.8±15.4 36.1±4 3.8	355±30 160±49
OB TI: M PMW	99.0±8.0 93.0±7.0	4.5±1.1 1.9±1.1	18.8±6.7 35.9±2.7	313±101 294±143
OB TII: M PMW	102 ± 7 91.0±.09	4.8±1.2 2.4±1.8	15.3±4.2 33.9±11.4	318±54 319±150
OBT III: M PMW	106.0±3.0 95.0±11.0	4.3±0.6 4.0±0.8	8.3±4.1 17.9±6.5	344±8 291±145

	25OHD		Leptin		Insulin	
OW: M PMW	21.2±2.4	22.5±2.8	21.0±19.0	9.8±2.5	12.1±3.2	8.0±3.0
OB TI: M PMW	20.7±6.9	24.6±10.6	19.0±11.0	11.1±3.3	12.4±4.1	9.0±4.0
OB TII: M PMW	22.3±7.9	20.6±4.1	27.0±11.0	17.8±4.3	24.2±8.8	12.0±2.0
OBT III: M PMW	16.8±2.8	19.9±13.9	41.0±22.0	43.7±8.8	23.4±4.1	16.0±6.0

doi:10.1016/j.bonr.2020.100490

P168

The effectiveness of vitamin D supplementation in functional outcome and quality of life of lumbar spinal stenosis requiring surgery

Sangbong Ko
Orthopaedic Surgery, Daegu Catholic University Medical Center, Daegu, Republic of Korea

Study design: Retrospective cohort comparative study

Objective: To identify the prevalence of vitamin D deficiency in patients with lumbar spinal stenosis (LSS) requiring surgery, and to compare the differences between the cases whether vitamin D is supplemented and vitamin D is not supplemented in terms of a quality of life during postoperative two year.

Summary of Background Data: Vitamin D supplementation is considered to be associated with good functional outcome. Thus, a few studies have proposed vitamin D supplementation is benefit to the functional outcome in lumbar spinal stenosis requiring surgery.

Methods: All patients with LSS who underwent surgery from March 1, 2015 to August 31, 2016 were enrolled. Among them, 61 patients with vitamin D deficiency were divided into two groups (supplemented group (A) and non-supplemented group (B)). Functional outcomes using Oswestry Disability Index (ODI) and Rolland Morris Disability Index (RMDQ) and quality of life using SF-36 were evaluated at 12month, and 24month follow up periods. Differences in functional score and SF-36 between the vitamin D supplemented and non-supplemented group were compared.

Results: Among the total 102 patients, 78 patients (76.5%) had vitamin D deficiency. Of the 78 patients, 61 patients were included, 27 patients were group A and 27 patients were group B. There was no difference in age and 25-OHD level between the two groups (all 0>0.05). Group A were better functional outcomes at two years after surgery (p< 0.05). On the quality of life, group A were higher score than group B from twelve month later after surgery (p< 0.05).

Conclusions: Vitamin D deficiency was highly prevalent in LSS patients (76.5%). Assessment of serum 25-OHD are recommended in LSS needing surgical intervention and active treatment vitamin D supplementation and maintenance of normal range should be considered for better postoperative functional outcome and quality of life.

doi:10.1016/j.bonr.2020.100491

P169

Vitamin D deficiency and postoperative complications in patients with hip dysplasia undergoing periacetabular osteotomy and the effect of native or active vitamin D supplementation

Taro Mawatari, Misa Osako, Kazuki Kitade, Satoshi Hagio, Takahiro Iguchi, Hiroaki Mitsuyasu, Gen Matsui
Orthopaedic Surgery, Hamanomachi Hospital, Fukuoka, Japan

Purpose: Vitamin D is an important factor for bone health and mineralization, while high prevalence of vitamin D deficiency is reported worldwide. Periacetabular osteotomy (PAO) is accepted as an effective treatment for hip dysplasia in young to middle-aged patients. The purpose of our study was to retrospectively examine the influence of vitamin D deficiency and the effect of vitamin D supplementation on postoperative complications after PAO.

Methods: PAO was performed by a transtrochanteric approach on 81 hips in 62 patients (4 male, 61 female, ave 40.6 years old) with symptomatic hip dysplasia and followed for more than 12 months after surgery. A correlation between postoperative complications and age at surgery, BMI, smoking, preoperative center-edge angle, and serum 25(OH)D levels as well as the effect of native or active vitamin D supplementation were explored.

Results: Average serum 25(OH)D level of 62 patients was 12.8 ng/mL, and none of them were vitamin D sufficient. After the baseline measurement, 13 cases took active vitamin D (0.5 - 2.0 μg/day of alfacalcidol) and 16 cases took varying dose (1,000IU - 5,000IU/day) of native vitamin D (cholecalciferol) supplements. Without vitamin D supplementation, patients whose serum 25(OH)D level was ≤ 11 ng/mL presented delayed union of the greater trochanter osteotomy site (DU) and ischio-pubic stress fracture (SF) occurred in 20.0% and 13.3% of the

patients, respectively. When patients whose serum 25(OH)D was ≤ 11 ng/mL took alfacalcidol, DU and SF occurred in 11.1% and 22.2%, respectively. With relatively high-dose of native vitamin D (cholecalciferol) supplementation, no delayed union and no stress fracture were observed, while one case who quit taking supplements because of the drug eruption end up with the SF.

Discussion & Conclusions: Our study suggests that proactive supplementation of the native vitamin D would be advisable to improve the result of the surgery.

doi:10.1016/j.bonr.2020.100492

P170

Vitamin D status in 1,533 medical examinees at a regional public general hospital

Satoshi Hagio[a], Taro Mawatari[a], Gen Matsui[a], Takahiro Iguchi[a], Hiroaki Mitsuyasu[a], Yasuhiro Mizuki[b]
[a]*Orthopaedic Surgery, Hamanomachi Hospital, Fukuoka, Japan*
[b]*Orthopaedic Surgery, Sasebo Kyosai Hospital, Nagasaki, Japan*

Purpose: The prevalence of vitamin D deficiency is a worldwide concern. The purpose of this study was to clarify the vitamin D status in all the medical examinees.

Methods: We retrospectively reviewed 1533 patients (320 male, 1213 female; mean age, 66 years) who visited our regional public general hospital in Japan (36 departments, 468 beds) and examined their serum 25(OH)D levels. We also gathered available information about other blood chemistry data and bone mineral density. General nutritional status was evaluated using the controlling nutritional (CONUT) score, which is calculated based on the serum albumin concentration, total peripheral lymphocyte count, and total cholesterol concentration. CONUT scores 0-1, 2-4, 5-8, and 9-12 represented normal, mild, moderate, and severe dysnutritional states, respectively.

Results: The average serum 25(OH)D concentration was 15.4 ng/mL; the concentrations were < 10 ng/mL in 308 cases (20%), 10-20 ng/mL in 901 cases (59%), 20-30 ng/mL in 259 cases (17%), and 30- ng/mL in only 65 cases (4%). Regarding gender, 65.9% of male cases and 82.2% of female cases were serum 25(OH)D concentrations < 20 ng/mL, and vitamin D deficiency was very common across all age groups. Serum 25(OH)D levels were higher in October and lower in March. The average CONUT scores were 1.80 in male cases (n=299) and 1.44 in female cases (n=1097). There were no clear relationships between serum 25(OH)D levels and LS- and FN- BMD. Serum 25(OH)D and CONUT scores were only correlated when serum 25(OH)D levels were < 10 ng/mL ($p < 0.05$). Among 65 cases in which the vitamin D level was sufficient, 17 patients were taking native vitamin D supplements.

Discussion & Conclusions: In our study, 97% of the medical examinee were vitamin D insufficiency or deficiency, and 20% was severe deficiency (< 10 ng/mL), and proactive supplementation is advised.

doi:10.1016/j.bonr.2020.100493

P171

Serum folate and vitamin B12 levels and the incidence risk of atherosclerotic events over 12years: The Korean Genome and Epidemiology Study(KoGES)

Ha-Na Kim, Young-Mi Eun, Sang-Wook Song
Department of Family Medicine, St Vincent's Hospital, College of Medicine, The Catholic University of Korea, Suwon-si, Republic of Korea

Atherosclerosis, a common cause of atherosclerotic vascular diseases, is associated with several risk factors including hyperhomocysteinemia, and vitamin B12 and folate are involved in homocysteine metabolism; thus, serum folate and vitamin B12 status may be associated with the risk of atherosclerotic vascular diseases mediated by homocysteine plasma concentrations. Therefore, we hypothesized that low vitamin B12 and folate levels are related to higher risks of atherosclerotic vascular disease and investigated the risk of atherosclerotic vascular events in Korean adults with low serum vitamin B12 and folate levels. This population-based cohort study followed 421 subjects aged 40-69 years for 12 years, 2003-2014. Over the follow-up period, 38 (9.0%) atherosclerotic events occurred. However, serum folate and vitamin B12 levels were not associated with the risk of stroke, coronary artery disease, or myocardial infarction or the development of peripheral arterial disease after adjustment for age, sex, smoking status, alcohol consumption, physical activity, body mass index, serum creatinine, and high-sensitivity C-reactive protein levels and a history of diabetes, hypertension, or dyslipidemia. In conclusion, the incidence of atherosclerotic vascular events in Korean adults aged 40-69 years was not associated with the serum folate or vitamin B12 status.

doi:10.1016/j.bonr.2020.100494

P173

Comparative effectiveness of three methods for body composition assessment in the verification of manifestations of sarcopenia in obese patients

Valeriia Vasileva, Larisa Marchenkova
National Medical Research Center of Rehabilitation and Balneology, Moscow, Russian Federation

Aim of the study was to compare the effectiveness of three methods of body composition assessment such as bioimpedans analysis (BIA), air-replacement bodyplatismography (BodPod) and Dual X-ray absorptiometry Total body program (DXA Total Body) in the verification of reducing of skeletal muscle mass as sign of sarcopenic obesity in obese patients.

Material and methods: The study group included 95 patients aged 21-69 y.o. (average age 53,9±11,05 years) with BMI≥30.0 kg/m2. The control group included 37 patients aged 37-69 y.o (average age 50,73±10,6 years) of the same age without obesity with BMI 20.0-29.9 kg/m2. Body composition was tested using BIA, BodPod and DXA with calculating fat, lean and skeletal muscles mass (kg) and % in all the patients.

Results: According to BIA the groups differ only in fat mass (FM) 42.75 (4.8;6.3) vs. 33.15 (28.4;35.5) kg; p=0.036 and did not differ (p>0.05) in lean (LM), skeletal muscle mass (SMM) and in % of FM and SMM. According to BodPod analyses groups differed in the FM 3.4 [36.81;69.94] vs 31.02 [23.22;38] kg, p=0.007, % FM 45.4 [42.1;53.8] vs 37.7 [28.6;41.1], p=0.003 and % LM - 54.6 [46.2;57.9] vs 62.3 [58.9;71.4], p=0.003, but had statistically equivalent values of LM 55 [49.48;67.77] vs 40.36 [33.12;49.06] kg, p=0.19. According to DXA Total Body analyses statistically significant differences (p< 0.05) have been identified between the groups in FM and % FM of the hands, feet, trunk, total body (p>0.05), but not in LM and % LM (p>0.05).

Conclusions: From methods of body composition assessment, air-replacement bodyplatismography (BodPod) is the most sensitive in the verification of skeletal muscle mass reduction in obese patients. This method shows that patients with obesity have a significantly reduced muscle mass compared with normal weight or overweight subjects.

doi:10.1016/j.bonr.2020.100495

P176

Association between bone mineral density and genetic polymorphisms of Wnt signaling pathway among older adults in Taiwan

Sui-Lung Su
School of Public Health, National Defense Medical Center, Taipei, Taiwan, PR China

Background: Osteoporosis is one of the chronic diseases of the elderly, which is commonly found in the elderly population, and the prevalence rate of osteoporosis increases with age. The cause of osteoporosis is complex, and bone mineral density(BMD) is generally lost with age, some factors will cause loss of bone such as lack of exercise, smoking, drinking, lack of calcium diet, lack of sunbathing. Especially genetic factors may play an important role.

Objective: To explore the association between BMD and the polymorphism of Wnt signaling pathway, and to test the gene-environment interaction. Provide early prevention strategies for high risk groups of bone deficiency.

Material and methods: We performed a case-control study and recruited 764 participants who received health examination at Health Management Center of Tri-Service General Hospital from March 2017to August 2018. Demographic data were obtained by structured questionnaire, and bone mass density was measured by Dual-Energy X-ray Absorptiometry (DEXA). DNA was extracted from a peripheral blood sample, and the genotypes were determined using polymerase chain reaction and iPLEX Gold SNP genotyping methods.Subjects with T-score < -1 was classified as osteopenia case group, t-score ≧-1 was classified as healthy control group. All data analyses were done by using R software version 3.4.2.

Results: In female, after adjusted age and BMI, the frequencies of rs2707466 (WNT16) CT genotype were decreased risk of T-score< -1 than CC genotype (OR=0.60, 95% CI=0.38 - 0.93). T allele were decreased risk of T-score< -1 than C allele (OR=0.60, 95% CI=0.42 - 0.87). CT+TT genotype were decreased risk of T-score< -1 than CC genotype (OR=0.57, 95% CI=0.37 - 0.87).

Conclusion: We found that rs2707466 (WNT16) in female were associated with T-score< -1.

doi:10.1016/j.bonr.2020.100496

P177

Glucocorticoid receptor promotes osteoblast and adipocyte differentiation by recruiting and being recruited to lineage selective enhancers

Martin R. Madsen[a], Moustapha Kassem[b], Susanne Mandrup[a], Alexander Rauch[b]
[a]*Functional Genomics & Metabolism Research Unit, University of Southern Denmark, Odense, Denmark*
[b]*Molecular Endocrinology & Stem Cell Research Unit, University of Southern Denmark, Odense, Denmark*

The glucocorticoid receptor (GR) is a ligand activated hormone nuclear receptor targeted in the treatment of immune and auto-inflammatory disorders. While frequently prescribed, glucocorticoid therapy is associated with several adverse side effects including osteoporosis. In glucocorticoid-induced osteoporosis numbers of bone-forming osteoblast cells are reduced and marrow adipose volume is increased, suggesting that altered differentiation from the common precursor (MSCs) underlies glucocorticoid-induced osteoporosis.

Dexamethasone (dex) is a potent agonist of GR and a common component of both the osteogenic and adipogenic differentiation cocktail when differentiating MSCs *in vitro*. We studied the role of GR in lineage speciation of human telomerase-immortalized mesenchymal stem cells from bone marrow (hMSC-TERT cells) by loss-of-function experiments and withdrawal of dex. By employing global profiling of gene expression, enhancer activity and GR binding early after osteogenic and adipogenic stimulation we identified cell-type selective and common GR dependent programs (Figure A). Importantly, only activation of enhancers was associated with GR binding (Figure B) while lineage context and GR binding intensity were equally important for GR dependent enhancer activity (Figure C). Machine learning algorithms identified known GR interactors such as C/EBP-beta but also novel transcription factors that affect lineage speciation of MSC. Knockdown of either *CEBPB* or *NR3C1* had similar effects on early transcriptional changes due to interaction of C/EBP-beta and GR on the chromatin level with GR recruiting C/EBP-beta to osteoblast-specific and common activated enhancers and vice versa for adipocyte-specific enhancer activation.

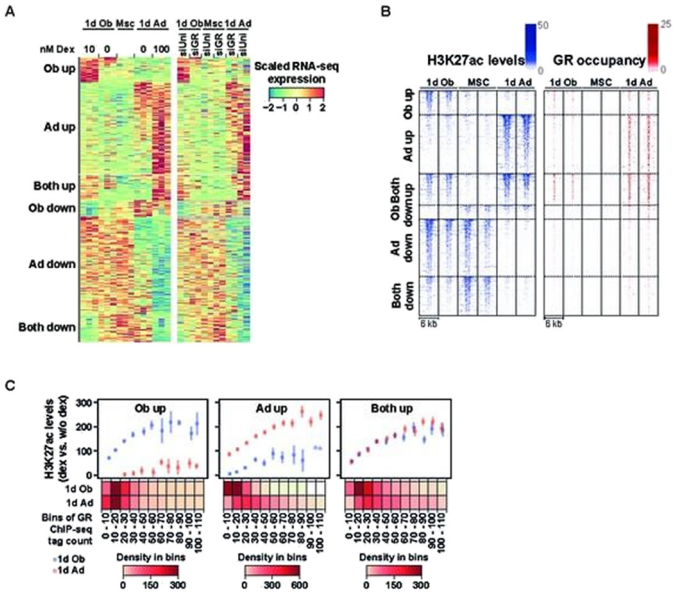

Fig.

doi:10.1016/j.bonr.2020.100497

P178

RUNX2 T-1025C variant is associated with bone-related biochemical parameters and fracture risk in Maltese postmenopausal women

Melissa Marie Formosa, Ritienne Formosa, Angela Xuereb-Anastasi
University of Malta, Msida, Malta

Background & objectives: Runt-related transcription factor 2 (RUNX2) is a major transcription factor involved in osteoblast and chondrocyte differentiation, skeletogenesis and fracture repair. Transactivation of *RUNX2* is under tight regulatory control particularly via promoter 2 (P2). The study aimed to assess the effect of the P2 *RUNX2* T-1025C variant in relation to bone mineral density (BMD) at different anatomical sites, fracture risk and levels of biochemical parameters in the Maltese population.

Methods: Genotyping was performed in 1,045 Maltese postmenopausal women from the Malta Osteoporotic Fracture Study using the TaqMan® fluoregenic 5' nuclease allelic discrimination assay. Genotype-phenotype associations were analysed using the Mann-Whitney statistic whereas odds ratios with 95% confidence intervals were computed using logistic regression analysis adjusted for confounders.

Results: Genotyping was successful in 1,043 samples, with the reference T and alternative C alleles observed at a frequency of 0.92 and 0.08 respectively. Women aged >60 years with the TC genotype had higher total serum calcium (p=0.029) and lower total serum alkaline phosphatase (ALP) levels (p=0.046) relative to women with the TT genotype. Additionally, carriers of the C allele showed higher femoral neck BMD than homozygous carriers of the T allele. Nonetheless, the latter did not reach statistical significance (p>0.05). Homozygosity for the C allele was associated with an almost 5-fold increased fracture risk compared to homozygosity for the T allele, which was not attenuated after adjusting for BMD (adjusted OR: 4.9 [1.2-19.6], p=0.025). This is the first study to report an association with fractures. No association was seen with lumbar spine or total hip BMD.

Conclusion: Results indicate that the *RUNX2* T-1025C is a possible genetic determinant of fracture risk in the Maltese population, as well as calcium and ALP control. This functional variant alters the binding of several transcriptional activators and repressors, possibly affecting bone composition and strength.

doi:10.1016/j.bonr.2020.100498

P179

Phosphate, BMI and body composition in the Rotterdam Study: Mendelian randomization analysis suggests a causal effect of BMI on serum phosphate level

Ariadne Bosman[a], Natalia Campos-Obando[a], Trudy Voortman[b], Arfan M. Ikram[b], Bram C.J. van der Eerden[a], André G. Uitterlinden[a,b], M. Carola Zillikens[a]
[a]*Internal Medicine, Erasmus University Medical Center, Rotterdam, Netherlands*
[b]*Epidemiology, Erasmus University Medical Center, Rotterdam, Netherlands*

Objectives: Observational studies have reported associations between serum phosphate (P) and body mass index (BMI) in specific clinical settings (such as morbid obesity and hypertension) but the nature of this relation in the general population is unclear. This study aimed to investigate whether P and BMI and body composition are related and to explore evidence of causality through bidirectional one-sample Mendelian Randomization (MR).

Methods: 9633 subjects from three cohorts from the population-based Rotterdam Study were included for phenotypic analyses and 8378 subjects were included for MR analyses. Age-adjusted results were meta-analyzed. Outcomes were BMI, waist-to-hip ratio, fat mass, lean mass and fat%, estimated by DXA. Subgroup analysis adjusted for leptin levels was performed. For MR, allele scores with 6 single nucleotide polymorphisms (SNPs) for P and 905 SNPs for BMI were constructed.

Results: An inverse association between P (mg/dL) and BMI was found in both genders (β (95% CI): men: -0.40 (-0.72 to -0.07), p=0.02; women: -1.94 (-2.21 to -1.66), p< 0.001), with a significant sex-interaction (p< 0.05). Results were not explained by potential confounders. Adjustment for leptin attenuated but did not abolish this relation in women. There was a negative relation with fat percentage and fat mass in both sexes, but the latter was abolished in men after adjusting for estradiol and testosterone. Age and sex adjusted MR analyses suggests a causal effect of genetically determined BMI on phosphate (β (95% CI):-0.01 (-0.02 to 0.00), p=0.05), but not vice versa.

Conclusion: In a population-based setting, P was negatively associated with BMI and fat percentage with a stronger effect in women compared to men. Leptin partially explained this relation in women. MR analysis suggests a causal effect of BMI on P and not vice versa. Our results suggest an underlying sex dimorphism in P homeostasis that should be further explored.

doi:10.1016/j.bonr.2020.100499

P180

Short stature and microcephaly in two siblings due to a novel *de novo* IGF1R variant

Alexandra Gkourogianni[a,b], Ingrid Alvarez[a], Sigrun Hallgrimsdottir[a,b], Anna Ek[a], Ola Nilsson[a,b,c]
[a]*Division of Pediatric Endocrinology, Department of Women's and Children's Health, Karolinska Institute and University Hospital, Stockholm, Sweden*
[b]*Center for Molecular Medicine, Karolinska Institute and University Hospital, Stockholm, Sweden*
[c]*School of Medical Sciences, Örebro University and University Hospital, Örebro, Sweden*

Introduction: Heterozygous mutations in the type 1 insulin like growth factor receptor gene (*IGF1R*) cause pre- and postnatal growth failure, microcephaly and IGF-1 resistance.

Case presentation: The, proband is a 3.8 year old girl with SS (height -2.3 SD) (3 SD under MPH), microcephaly (HC -2.5 SD), delayed BA -1.5 years and a history of SGA (BW -2.2 SD, BL -3.2 SD, HC -2.3 SD) without catch-up growth. Her karyotype was normal 46XX. Her brother was also born SGA (GA 40, BW -2.6 SD, BL -2.9 SD, HC -2.2 SD) without catch-up growth. At the age of 1.5 years old his height was -1.2 SD (2 SD under MPH) with relative microcephaly (HC -2.1 SD). Father and mother were unrelated, healthy with normal heights of -0 SD and +2.3 SD (MPH +1.2 SD), respectively. Both siblings presented biochemical signs of IGF-1 resistance, which, together with their clinical characteristics led to suspicion of an *IGF1R* mutation.

Results: A *de novo*, heterozygous, non-synonymous, missense *IGF1R* variant c.3595>G (p.Gly1199Arg) was first detected by Sanger sequencing in the proband and then the same variant was detected in the brother, but in none of the parents. Maternity and paternity was confirmed by SNP arrays.

This variant was not present in Genome Aggregation Database (GnomAD n>120.000 exomes and >15.000 genomes). Finally the variant is predicted to be damaging by all *in silico* tools used.

Conclusions: We detected a novel, heterozygous, *de novo* variant in *IGF1R* associated with short stature, SGA without catch-up growth, microcephaly, and biochemical signs of IGF-1 resistance in two siblings. Gonadal mosaicism is the most likely explanation for the recurrence of this variant in the younger brother.

doi:10.1016/j.bonr.2020.100500

P181

Bone transcriptome sequencing reveals local tissue determinants of bone mineral density

Vid Prijatelj[a,b], Sjur Reppe[c,d], Matthew Dietz[e], Carolina M. Medina-Gomez[b,f], Joost A. Verlouw[b], Andre J. van Wijnen[e], Kaare M. Gautvik[c,d], Eppo B. Wolvius[a], Fernando Rivadeneira[b,f]
[a]*Department of Oral and Maxillofacial Surgery, Erasmus MC, Rotterdam, Netherlands*
[b]*Department of Internal Medicine, Erasmus MC, Rotterdam, Netherlands*
[c]*Institute of Basic Medical Sciences, University of Oslo, Oslo, Norway*
[d]*Department of Clinical Biochemistry, Ullevaal University Hospital, Oslo, Norway*
[e]*Department of Orthopedic Surgery, Mayo Clinic, Rochester, United States*
[f]*Department of Epidemiology, Erasmus MC, Rotterdam, Netherlands*

Background: Osteoporosis (OP) is a chronic disease, affecting structural integrity of the bones. It was thus our aim to establish differentially expressed genes between OP participants and participants with normal total hip bone mineral density (TH-BMD). The analysis was repeated by grouping participants on their genotype information, as per Recall-by-Genotype (RbG) methodology.

Methods: This study was performed on 121 participants (mean chronological age 67.32 years; 16 males). TH-BMD and Total Body(TB)-BMD were established by using Dual-Energy X-ray Absorptiometry (DEXA), with TH-BMD values transformed to T-scores. Bone samples were obtained from either trans-iliacal biopsies or the femoral head distant from the articular surface as part of hip replacement surgery. Sequencing was done using the Illumina Hiseq2000 platform. Genotyping of the iliac samples was done using the Affymetrix Axiom 432 Biobank Genotyping Array. Differential expression analysis was firstly done by grouping participants into OP and those with normal TH-BMD. For the RbG differential expression analysis weighted polygenic risk scores (PRS) were constructed. Differential expression between participants in the upper and lower quintile, based on respective PRS, was repeated.

Results: Higher expressions of sclerostin and dickkopf-1 (*SOST*; *DKK1*) in bone samples of participants with higher BMD were replicated, and multiple novel associations were identified. By replicating the results for *SOST*, the RbG approach was shown to be viable. Expression of selected genes was verified by regressing TB-BMD over their expression. Our results show that local expression of certain Wnt/β-catenin pathway inhibitors is reduced with lower BMD.

Conclusion: By utilizing RNA sequencing, replication as well as novel associations, that further reveal the molecular biology of the bone, were provided. Our results show promise in terms of possible drug repurposing, identification of novel genetic associations, as well as application of genomic risk prediction to differential expression analyses.

doi:10.1016/j.bonr.2020.100501

P183

Dysregulated miRNA expression profile in the presence of *SQSTM1* mutation

Simone Bianciardi[a], Daniela Merlotti[a], Maria Materozzi[b], Christian Mingiano[a], Simone Cenci[b], Luigi Gennari[a]
[a]*Department of Medicine, Surgery and Neurosciences, University of Siena, Siena, Italy*
[b]*Division of Genetics and Cell Biology, San Raffaele Scientific Institute, Milano, Italy*

Mutation of *SQSTM1* gene are a common cause of familial Paget´s disease of bone (PDB) and have been often associated with increased disease severity. In this study we investigated the miRNA-expression profile (Taqman Human MicroRNA Array Card Set v3.0, covering 768 miRNAs) in serum and peripheral blood mononuclear cells (PBMCs) of 20 active PDB patients with (n=10) or without *SQSTM1* (n=10) mutation, as compared to 10 healthy age-matched controls. Data from Array Cards were exported using ViiA7 RUO software and then analyzed using Expression Suite software v1.0.1 (Applied Biosystem). All values were normalized using 3 different housekeeping miRNAs. In PBMCs of PDB cases most miRNAs were up-regulated with respect to controls, and this difference was particularly evident in carriers of *SQSTM1* mutation (with 43 miRNAs reaching statistical significance, with respect to 6 miRNAs in PDB cases without mutation) [Fig. 1A]. This pattern was not replicated in the analysis of circulating miRNAs [Fig. 1B]. In order to uncover a potential role of *SQSTM1* on miRNA expression, we then replicated miRNA-expression profile analysis in bone marrow-derived monocytes (BMMs) from *SQSTM1*-KO mice and p62-P394L knockin mice (P394L-KI, harboring the homolog *SQSTM1* mutation to the P392L mutation observed in human PDB). Of interest, in P394L-KI mice, we evidenced a similar up-regulation of several miRNAs with respect to either *SQSTM1*-KO or WT mice [Fig. 2]. Conversely, there was no difference in the miRNA expression profile between *SQSTM1*-KO and WT mice. Among the different miRNAs, miR-345-5p (a recently discovered regulator of osteogenesis) was more than 2-fold up-regulated in either PDB patients with *SQSTM1* mutation and P394L-KI mice. Further studies are required to validate these findings in larger samples and to address the mechanisms leading to miRNAs up-regulation in the presence of *SQSTM1* mutation and the potential clinical implications.

doi:10.1016/j.bonr.2020.100502

P184

Differential expression analysis of osteoarthritic femoral head bone fragments uncovers underlying transcriptomic determinants

Vid Prijatelj[a,b], Sjur Reppe[c,d], Matthew Dietz[e], Carolina M. Medina-Gomez[b,f], Joost A. Verlouw[b], Cindy G. Boer[b], Joyce B.J. van Meurs[b], Andre J. van Wijnen[e], Kaare M. Gautvik[c,d], Eppo B. Wolvius[a], Fernando Rivadeneira[b,f]
[a]*Department of Oral and Maxillofacial Surgery, Erasmus MC, Rotterdam, Netherlands*
[b]*Department of Internal Medicine, Erasmus MC, Rotterdam, Netherlands*
[c]*Institute of Basic Medical Sciences, University of Oslo, Oslo, Norway*
[d]*Department of Clinical Biochemistry, Ullevaal University Hospital, Oslo, Norway*
[e]*Department of Orthopedic Surgery, Mayo Clinic, Rochester, United States*
[f]*Department of Epidemiology, Erasmus MC, Rotterdam, Netherlands*

Background: Osteoarthritis (OA) is a chronic disease, affecting structural integrity and functionality of the joints. It was our aim to determine whether messenger RNA expression profiles of the OA patients could elucidate further possible genomic determinants of the disease.

Methods: This study was performed on 121 participants (mean chronological age 67.32 years; 16 males)). Bone samples were obtained from either trans-iliacal biopsies or the femoral head fragments collected during hip replacement. Sequencing was done using Illumina Hiseq2000 platform. Differential analysis was performed on two groups consisting of 1) participants that underwent hip replacement surgery due to hip OA (n = 36) and 2) mix of participants (n=85) with hip replacement surgery due to hip fracture or volunteers providing trans-iliacal bone biopsies (neither subgroup had reported osteoarthritis). A prioritization curve was fitted over the differential expression volcano plot. Transcripts plotted above the fitted curve were deemed interesting and subjected to gene set enrichment analyses using WebGestalt.

Results: Results provided replication of findings from previous OA GWAS as well as differential analyses performed on cartilage, including: *MAP2K6*, *PLEC*, *ZNF345*, *LTN1*, *PCYOX1*, *FAM136A*, *SLC39A8*, *SCUBE1*, *FGFR3*, *RNF135* and *MTF1*. Interestingly, *SLC39A8* and *CTSK* shower lower expression in OA subjects (log_2fold change (FC) = -0.699, FDR P= $8.18*10^{-7}$ and log_2FC = -1.41, FDR P= $3.38*10^{-4}$), while *MTF1* showed increased expression (log_2FC = 0.257, FDR P= $1.33*10^{-2}$). Gene set enrichment analyses was performed on 433 transcripts and were concordant with downregulation of processes in mineralized tissues and extracellular matrix processes.

Conclusion: Using RNA sequencing we were able to identify transcriptional profiles of bone tissue that are differentially expressed in osteoarthritis of the hip. Summing our findings to other sources of evidence constitute effective triangulation approaches helping to pinpoint robust evidence of implication of these gene transcripts in the occurrence of OA.

doi:10.1016/j.bonr.2020.100503

P185

Calcium sensing receptor silencing in primary hyperparathyroidism associated with promoter hypermethylation and gain of methylation on histone 3

Priyanka Singh[a], Sanjay Bhadada[a], Ashutosh Arya[a], Naresh Sachdeva[a], Divya Dahiya[b], Jyotdeep Kaur[c], Uma Saikia[d]
[a]*Endocrinology, Postgraduate Institute of Medical Education and Research, Chandigarh, India*
[b]*General Surgery, Postgraduate Institute of Medical Education and Research, Chandigarh, India*
[c]*Biochemistry, Postgraduate Institute of Medical Education and Research, Chandigarh, India*
[d]*Histopathology, Postgraduate Institute of Medical Education and Research, Chandigarh, India*

Introduction: Calcium sensing receptor (CASR) maintains the calcium homeostasis by regulating parathyroid hormone (PTH) secretion in parathyroid glands. Loss of CASR has been reported in parathyroid adenoma and could be regulated by GCM2, as its binding sites present on CASR promoter have not been known. The aim of the study is how promoter methylation and histone methylation of CASR or altered expression of GCM2 can influence the parathyroid tumorigenesis.

Materials and methods: A total of 40 parathyroid adenomas and 10 normal parathyroid tissue were recruited for the study. Quantitative real time polymerase chain reaction (qRT-PCR) was performed for mRNA expression analysis. Immunohistochemistry was performed for protein expression. Bisulphite sequencing PCR (BSP) and chromatin immunoprecipitation-qPCR (ChIP-qPCR) were used to examine promoter methylation and H3K9me3 status.

Results: We observed significantly lower CASR ($p \leq 0.0001$) and GCM2 mRNA expression ($p \leq 0.0001$) as well at protein level. The promoter regions of CASR and GCM2 was displayed significant hypermethylation in 45% (18/40) and 55% (22/40) in sporadic parathyroid adenoma cases respectively. BSP sequencing analysis revealed that methylated CpG at GCM2 binding sites on CASR promoter had maximum methylation (38%) compared to other CpG sites. Analysis revealed that methylation level of GCM2 was correlated inversely with its mRNA expression ($r = -0.45$; $p = 0.003$). On analyzing, H3K9me levels showed significant increased enrichment by 10 folds ($p=0.009$) and 15 folds ($p=0.023$) on CASR and GCM2 promoter regions in sporadic parathyroid adenoma respectively. Correlation analysis displayed H3K9me3 levels correlated with mRNA expression of CASR ($r= 0.60$, $p= 0.003$, $n=23$) and GCM2 ($r= -0.49$, $p= 0.04$, $n=23$) as well.

Conclusion: Our data suggests that promoter and histone methylation of CASR and GCM2 as it may lead to less or no binding on CASR promoter and could be responsible in silencing of CASR in sporadic PHPT.

doi:10.1016/j.bonr.2020.100504

P186

The epigenetic reader Brd4 is required for skeletal development

Christopher Paradise, M. Lizeth Galvan, Sofia Jerez, Eva Kubrova, Roman Thaler, Andre van Wijnen, Amel Dudakovic
Mayo Clinic, Rochester, United States

Lineage-specific differentiation of multi-potent mesenchymal stromal cells (MSCs) is directed by the activation of precise transcriptional networks. Epigenetic mechanisms such as DNA methylation and post-translational histone modifications are utilized to regulate gene expression. Post-translational modifications of histone tails induce chromatin compaction or relaxation to modulate the recruitment of transcriptional machinery. Epigenetic regulators (also knowns as histone code readers, writers, and erasers) are proteins that modify and interact with histone tails to govern chromatin states. We have demonstrated that inhibition of Ezh2, a histone 3 lysine 27 (H3K27) specific methyltransferase, accelerates osteoblastogenesis and is osteo-protective in vivo. Findings from these studies revealed a shift from heterochromatin (H3K27me3) to euchromatin (H3K27Ac) upon Ezh2 inhibition. Based on these observations, our present studies are focused on bromodomain-containing proteins, which are epigenetic regulators responsible for binding (i.e., reading) acetylated lysines. Pharmacological inhibition (+JQ1) or siRNA-mediated knockdown of Brd4 prevents osteoblastic differentiation in pre-osteoblasts and negates the pro-osteogenic effect of Ezh2 inhibition (Ezh2i). In light of these findings, we generated conditional knockout mice that lack Brd4 expression in the mesenchyme ($Brd4^{f/f}$: Prrx1-Cre) and osteo-chondral progenitors ($Brd4^{f/f}$: Osx-Cre). Mesenchymal loss of Brd4 results in smaller mice that are characterized by significantly shortened long bones. Interestingly, we note abnormal growth plate morphology in the juvenile knockout mice (1 and 3 weeks). Osteo-chondral loss of Brd4 (Osx-Cre) also results in smaller mice with shorter limbs; however, the effect on bone length is not as severe. Additional analysis reveals a significant reduction in bone quality in the $Brd4^{f/f}$: Osx-Cre cohort as highlighted by a reduction in trabecular bone formation at 8 weeks of age. Together, our data demonstrate that Brd4 is not only required for proper skeletal development (Prrx1-Cre), but also plays a critical role in regulating bone formation and osteoblastogenesis (Osx-Cre).

doi:10.1016/j.bonr.2020.100505

P188

Body and bone structural, reproductive and cellular ageing of Roma women in Hungary

Dorina Annar[a], Anna Madarasi[b], Piroska Feher[a], Irina Kalabiska[c], Annamaria Zsakai[a]
[a]*Department of Biological Anthropology, Eotvos Lorand University, Budapest, Hungary*
[b]*Peadiatric Pulmonology, Saint Janos Hospital, Budapest, Hungary*
[c]*Research Center for Sport Physiology, University of Physical Education, Budapest, Hungary*

Roma is one of the largest ethnic minority group in Hungary. Most of the Roma population lives in poor conditions in segregated settlements, and experience higher exposure to environmental health hazards: suffer from high rate of unemployment, low wages, poor hygienic conditions. Their health status are mostly poor.

The increased prevalence of chronic illnesses in Roma adults leads to their shortened life expectancy, but it has not been studied yet whether the ageing processes in Roma people are more accelerated than in non-Roma age-peers. Our aim was to study the biological status and ageing of female Roma adults (aged between 35-65, n:20; control non-Roma group for cellular ageing analysis, n:20; Hungarian reference group for body structural and reproductive ageing analysis, n:2500) living in a segregated settlement (Monor) in Hungary. The ageing of body- and bone structural parameters, reproductive- and cellular ageing and their interactions were analysed in Roma and non-Roma women.

Body structure was analysed by body composition estimation. Bone structural estimation was done by quantitative ultrasound technique of

DTU-one osteometer. Reproductive ageing was estimated by collecting data on menstrual and reproductive history by questionnaires. Cellular ageing was estimated by X chromosome loss estimation (FISH probe). Data on actual health status, lifestyle factors (nutritional habits, habitual physical activity level) and the socioeconomic background of Roma families were collected by questionnaires.

The results revealed that Roma women are prone to be more obese, to have higher amount of abdominal body fat, they have worse bone structure and experience longer reproductive period than the national reference values. The evaluation of cellular ageing estimation in Roma and non-Roma women is still in progress, the results of the analysis will be presented during the ECTS congress.

This research was supported by the National Talent Programme of the Hungarian Ministry of Human Capacities (NTP-NFTÖ-19-B).

doi:10.1016/j.bonr.2020.100506

P189

Enhanced BMP-2/BMP-4 ratio in patients with peripheral spondyloarthritis and in cytokine- and stretch-stimulated mouse chondrocytes

Anne Briolay[a], Alaeddine El Jamal[a], Paul Arnolfo[b,c], Benoît Le Goff[b,c], Frédéric Blanchard[b], David Magne[a], Carole Bougault[a]
[a]*CNRS UMR 5246 ICBMS, University of Lyon, Villeurbanne, France*
[b]*INSERM UMR1238, Nantes University, Nantes, France,*
[c]*Rheumatology Department, CHU Nantes, Nantes, France*

Excessive bone formation in the entheses is one of the features of peripheral spondyloarthritis (SpA). Complex pathological mechanisms connecting inflammation, mechanical stress and ossification are probably involved. We focused on Bone Morphogenetic Protein (BMP)-2, -4 and -7 as possible mediators of this process. BMP-2, -4 and -7 concentration was measured by ELISA in synovial fluids (SFs) of SpA (n=56) and osteoarthritic (n=21) patients. Mouse organotypic ankle cultures were challenged by a pro-inflammatory cocktail. Mouse primary chondrocytes, osteoblasts or tenocytes were treated with TNF-α, interleukin (IL)-17 or IL-22 and/or subjected to cyclic stretch, or with recombinant BMP-2 or -4. In SpA SFs, if BMP-7 was barely detectable, BMP-2 concentration was higher and BMP-4 was lower than in osteoarthritic samples, so that BMP-2/BMP-4 ratio augmented 6.5 folds (p=0.001). In SpA patients, TNF-α, IL-6 and IL-17 levels correlated this ratio (n=21, p=0.030, 0.044 and 0.032, respectively). *Bmp-2/Bmp-4* ratio was similarly enhanced by cytokine treatment in explant and cell cultures, at mRNA level. In particular, simultaneous application of TNF-α and cyclical stretch induced a 30-fold increase of the *Bmp-2/Bmp-4* ratio in chondrocytes (p=0.027). Blockade of prostaglandin E_2 and IL-6 production had almost no effect on the stretch-induced regulation of *Bmp-2* or *-4*. Activation of the BMP canonical pathway was selectively detected by phospho-Smad5 immunolabeling in chondrocytes of the sesamoid cartilage zone, which is a location of high mechanical stress. Osteoinductive effects of BMP-4, and to a lesser extend BMP-2, were identified on cultured chondrocytes and tenocytes. Our results first settle that BMP factors are locally deregulated in the SpA joint. An unexpected decrease in BMP-4 could be associated to an increase in BMP-2, possibly in response to mechanical and/or cytokine stimulations. More investigations are needed to decipher how this imbalance could cause abnormal ossification in SpA enthesis.

Acknowledgements: Arthritis Fondation Courtin (2015 and 2018)

doi:10.1016/j.bonr.2020.100507

P192

Enriched osteogenic potential of CD317-negative mesenchymal stromal cell populations in vitro and in vivo

Alasdair G. Kay[a], James Fox[a], Andrew Stone[a], Sally James[a], Elizabeth Kapasa[b], Xuebin Wang[b], Paul G. Genever[a]
[a]*Department of Biology, University of York, York, United Kingdom*
[b]*Division of Oral Biology, University of Leeds, Leeds, United Kingdom*

Bone repair and regeneration therapy using mesenchymal stromal cells (MSCs) is a priority in regenerative medicine. We identified biomarker CD317 that allows discrimination of differentiation-competent MSCs ($CD317^{neg}$) with osteogenic potential from non-differentiating MSCs ($CD317^{pos}$). Here, we investigate the potential impact of $CD317^{pos}$ MSC subpopulations in regenerative therapies.

$CD317^{pos}$ MSCs comprised 0.01-47.41% of primary populations (mean 9.78%±2.33,n=31). Clonal and primary $CD317^{pos}$ MSCs recorded increased interferon-γ index compared to $CD317^{neg}$ (0.987±0.320 vs 0.020±0.005). $CD317^{pos}$ MSCs also showed upregulated gene expression associated with chemokine signalling, leukocyte migration and adhesion (CXCL10, CXCL11 CX3CL1, SSA2, SSA4 and ICAM-1).

$CD317^{pos}$ MSCs co-cultured with primary human CD4+ T cells demonstrated reduced suppression of T-cell proliferative cycles compared with $CD317^{neg}$ clonal and primary lines and primary $CD317^{pos}$ MSCs failed to reduce overall T-cell proliferative capacity (1A). $CD317^{pos}$ clonal MSCs increased T-cell polarisation towards pro-inflammatory Th1 cells (1B). In a zymosan-induced peritonitis mouse model, $CD317^{neg}$ and $CD317^{pos}$ MSCs suppressed leukocyte recruitment ($2.08\pm0.42x10^6$; $3.55\pm1.54x10^6$) compared to control ($9.69\pm1.89x10^6$). Antigen-specific CD8a+ cytotoxic T-cell development was suppressed in spleens of $CD317^{pos}$ MSC-treated mice (2.08±0.50%) but not $CD317^{neg}$ MSC-treated (5.95±0.74%), suggesting a complex interaction between immune cells in response to stromal subtypes.

MSC-loaded scaffolds implanted subcutaneously in immunocompromised mice demonstrated enhanced tissue generation from clonal $CD317^{neg}$ cells, showing evidence of vessel formation by 3 weeks post-implantation, whereas $CD317^{pos}$ MSCs had poor tissue structure suggestive of weak osteogenic capacity in vivo (1C).

Subpopulations of MSCs that do not contribute to tissue formation could detrimentally affect tissue regeneration and offset clinical outcomes in therapeutic applications.

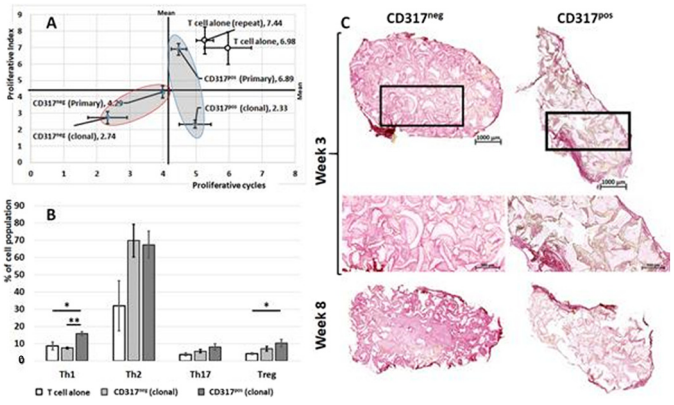

Fig. 1.

doi:10.1016/j.bonr.2020.100509

P193

Proteomic approach in aorta of rheumatoid arthritis-induced 5-LO KO mouse model

Cintia Kazuko Tokuhara[a], Flavia Amadeu Oliveira[b], Talita Ventura[a], Jose Burgos Ponce[c], Joao Paulo Domezi[a], Adriano Pessoa[a], Gabriela Neubern Oliveira[a], Mariana Sanches[a], Vimal Veeriah[b], Mariana Santesso[a], Marilia Afonso Rabelo Buzalaf[a], Rodrigo Cardoso Oliveira[a]

[a]*University of Sao Paulo - Bauru School of Dentistry, Bauru, Brazil*
[b]*Sanford Burnham Prebys Medical Discovery Institute, La Jolla, United States*
[c]*University Center of Adamantina, Adamantina, Brazil*

It has been established that rheumatoid arthritis (RA) mainly affects the joints, however, extra-articular involvement is common. Thus, it is reported that patients with RA have higher risk of mortality in comparison with health people, due mainly to increased cardiovascular disease related to both traditional risk factors and disease-induced chronic inflammation. Leukotrienes (LTs) are lipid mediators derived from arachidonic acid by 5-lipoxygenase (5-LO) pathway and play an important role in the inflammatory response. Thus, we sought to study in detail the role of leukotrienes on protein profile from aorta in rheumatoid arthritis condition. We conducted a quantitative proteomics analysis by using mass spectrometry comparing 5-LO Knockout (KO) and wild type (WT) mice under arthritis-induced condition. 60-days old KO and WT mice were intravenously immunized with 1.5 mg of arthrogen cocktail at day 0 and 10 μg of LPS was intraperitoneally administered at day 3. After 14 days of immunization, mice were euthanized and protein samples from aorta were isolated, purified and processed for proteomics analysis using LC-ESI-MS/MS. Results showed several changes of aorta protein profile between 5-LO KO RA and WT RA. In total, over 1075 proteins were identified by proteomic approach. Among them, 341 proteins were exclusive from 5-LO KO RA and 385 from WT RA and 349 proteins were identified in both groups. Regarding quantitative analysis, 60 and 15 proteins were up and downregulated, respectively in the comparison 5-LO KO RA vs. WT RA. The following proteins histone H4 and nuclear mitotic apparatus protein 1 were increased more than 2-fold in 5-LO KO RA and 15 proteins were decreased more than 2-fold in the same group. Results clearly demonstrated that absence of leukotriene causes significant changes in proteome profile of RA aorta and it may have important functions on metabolism and clinical implications in rheumatoid arthritis.

doi:10.1016/j.bonr.2020.100510

P194

Bone turnover markers in the early stage of rapidly destructive coxopathy

Tadashi Yasuda, Kazuhiro Matsunaga, Takumi Hashimura, Yoshihiro Tsukamoto, Tatsuya Sueyoshi, Satoshi Ota, Satoshi Fujita, Eijiro Onishi

Department of Orthopaedic Surgery, Kobe City Medical Center General Hospital, Kobe, Japan

Serum bone turnover markers are significantly higher in patients with rapidly destructive coxopathy (RDC) than those with osteoarthritis. However, the characteristics of bone turnover makers in the early stage of RDC remain unclear. The purpose of this study was to clarify association of bone turnover markers with the disease progression in the early stage of RDC. This study included 24 female patients with RDC diagnosed with radiographs and computed tomography, which demonstrated chondrolysis >2 mm during 12 months from the disease onset. Serum levels of tartrate-resistant acid phosphatase 5b (TRACP-5b), bone alkaline phosphatase (BAP), matrix metalloproteinase-3 (MMP-3), and C-reactive protein (CRP) were assayed within 12 months from the disease onset. Cortical thickness index (CTI) correlated with bone mineral density of the hip was measured on the radiograph at the onset of hip pain. RDC were classified into two types based on the absence (type 1, n=12) and presence (type 2, n=12) of subsequent femoral head destruction within 12 months after the disease onset. TRACP-5b levels were significantly higher in RDC type 2 (753 ± 316 mU/dl) than in type 1 (526 ± 173 mU/dl) ($P < 0.05$ by Mann-Whitney U test) as well as CRP levels. There were no differences in BAP, MMP-3, age at onset, and CTI between the RDC types. Receiver operating characteristic curve analysis indicated that TRACP-5b may be associated with differentiation between RDC types 1 and 2 in the early stage (the area under the curve, 0.743). The respective sensitivities and specificities were 75.0 % and 75.0 % for TRACP-5b (cutoff, 500 mU/dl). The lack of difference in CTI suggested that high TRACP-5b levels could reflect osteoclast cell activation in hips with RDC type 2 compared with type 1. Serum TRACP-5b may be helpful to differentiate those two types in the early stage of RDC.

doi:10.1016/j.bonr.2020.100511

P195

Major stress linked to pathogenesis of rheumatoid arthritis- a case report

Sekib Sokolovic[a], Sara Dagher[b], Adnan Dautbegovic[b], Eman Jamal[b]

[a]*Clinic for Heart, Blood Vessel and Rheumatic Diseases, University Clinical Center Sarajevo, Sarajevo, Bosnia and Herzegovina*
[b]*Medical Faculty, Sarajevo, Bosnia and Herzegovina*

The case report was described in a 65-year-old female who developed definite rheumatoid arthritis (RA) six years ago. Since the etiology of rheumatoid arthritis is unknown, in this case major life stress occurred as an initial target for the future development of certain disorders including RA. The first health problem she had was gynocological with a hysterectomy 23 years ago and she has had long standing periodontitis. From other co-morbidities she had a myocardial infarction and a PCI procedure 5 years ago, arterial hypertension and hyperlipidemia. She was a heavy smoker with increased smoking after the stress. She delivered three sons, but no abortion was reported. The family history was negative for any inherited cases. Her Disease activity score (DAS) was 6,1 and HAQ score was 2,5 indicating the the severe activity. Laboratory test revealed positive CRP 16,2 mg/l, Sedimenatation rate was 40/70, Rheuma factor was 439,3 IU/ml and vitamin D 24,6 ngl/ml. She was treated with Metotrexat, Sulfasalazin and Glucocorticoids together with NSAIDs and supplements of vitamin D and Omega-3.

Etiology of rheumatoid arthritis is unknown, but major life stress, periodontitis and gingivitis caused by Porphyromonas gingivalis, gastrointestinal tract infection, viral infection, smoking and environmental conditions, including genetic predisposition,

may contribute to the onset of inflammatory joint disease like rheumatoid arthritis or reactive arthritis. In this case, everything was triggered by major life stress in the past. All other co-morbidities can be classified as consequences of major stress that she experienced when she was young.

doi:10.1016/j.bonr.2020.100512

P196

Musculoskeletal complications in patients with hereditary hemochromatosis: A cross-sectional study of 93 patients

Chi Duc Nguyen, Vincent Morel, Adeline Pierache, Georges Lion, René-Marc Flipo, Bernard Cortet, Valérie Canva-Delcambre, Julien Paccou
Lille University Hospital, Lille, France

Objective: To determine the frequency and characteristics of musculoskeletal complications, both arthropathy and osteoporosis, in hereditary hemochromatosis (HH) and related factors.

Methods: In this cross-sectional observational study of 93 patients with HH, demographic and disease-specific variables, genotype, and organ involvement were recorded and a complete rheumatologic investigation was performed. Radiographs of the hands, wrists, knees, and ankles were scored for joint space narrowing, erosions, osteophytes, and chondrocalcinosis. Prevalent (vertebral and non-vertebral) fragility fractures were recorded and bone mineral density (BMD) was systematically evaluated by dual energy x-ray absorptiometry at the lumbar spine (LS), total hip and femoral neck (FN).

Results: The mean age of patients was 60.0 (11.2) years, and 58.0% were men. The frequency of MCP2-3 arthropathy was 37.6% [95% CI 0.28 to 0.48]. MCP2-3 arthropathy was independently associated with older age (OR 1.17 [1.09-1.26] per yr, $p< 0.0001$), male sex (OR 3.89 [1.17-12.97], $p=0.027$) and the presence of the C282Y+/+ genotype (OR 4.78 [1.46-15.68], $p=0.010$). Lumbar spine osteoporosis was present in 8 (8.6%), FN osteoporosis in 4 (4.3%), LS osteopenia in 17 (18.3%), and FN osteopenia in 44 (47.3%) of patients. There was a total of 18 patients with at least 1 prevalent (vertebral or non-vertebral) fragility fractures.The frequency of osteoporosis was 20.4% [95% CI 0.13 to 0.30]. Osteoporosis was independently associated with hepatic cirrhosis (OR 8.20 [1.74-38.68], $p=0.008$).

Conclusion: MCP2-3 arthropathy was found to occur in 37.6% of patients with HH. The association observed between this arthropathy, homozygosity for C282Y, male sex and older age suggests that demographic characteristics and genetic background are likely to be major determinants of this arthropathy and to be more important than severity of iron overload. Osteoporosis was observed in a fifth of patients with HH, independently of the genetic background and severity of iron overload, and was strongly associated with cirrhosis.

doi:10.1016/j.bonr.2020.100513

P197

Incidence of fragility fractures in postmenopausal women with rheumatoid arthritis. A case-control study

Carmen Gómez Vaquero[a], José Manuel Olmos[b], José Luis Hernández[b], Dacia Cerdà[c], Cristina Hidalgo Calleja[d], Juan Antonio Martínez López[e], Luis Arboleya[f], Francisco Javier Aguilar del Rey[g], Silvia Martínez Pardo[h], Inmaculada Ros Vilamajó[i], Xavier Suris[j], Dolors Grados[k], Chesús Beltrán Audera[l], Evelyn Suero-Rosario[m], Inmaculada Gómez Gracia[n], Asunción Salmoral Chamizo[n], Irene Martín-Esteve[m], Helena Flórez[o], Antonio Naranjo[p], Santos Castañeda[q], Soledad Ojeda Bruno[p], Sara García Carazo[r], Alberto Garcia Vadillo[q], Laura López Vives[s], Angels Martínez-Ferrer[t], Helena Borrell Paños[s], Pilar Aguado Acín[r], Raul Castellanos-Moreira[o], Cristian Tebé[u], Núria Guañabens[o], OsteoResSer Working Group of the Spanish Society of Rheumatology
[a]*Hospital Universitari de Bellvitge, Hospitalet de Llobregat, Spain*
[b]*Hospital Marqués de Valdecilla, Santander, Spain*
[c]*Hospital Moisès Broggi, Sant Joan Despí, Spain*
[d]*Hospital Universitario de Salamanca, Salamanca, Spain*
[e]*Hospital Universitario Fundación Jiménez Díaz, Madrid, Spain*
[f]*Hospital Universitario Central de Asturias, Oviedo, Spain*
[g]*Hospital Universitario Virgen de la Victoria, Málaga, Spain*
[h]*Hospital Universitario Mutua Terrassa, Terrassa, Spain*
[i]*Hospital Son Llàtzer, Palma de Mallorca, Spain*
[j]*Hospital General de Granollers, Granollers, Spain*
[k]*Hospital d'Igualada, Igualada, Spain*
[l]*Hospital Universitario Miguel Servet, Zaragoza, Spain*
[m]*Hospital General Mateu Orfila, Maó, Spain*
[n]*Hospital Universitario Reina Sofía, Córdoba, Spain*
[o]*Rheumatology, Hospital Clinic. University of Barcelona, Barcelona, Spain*
[p]*Hospital Universitario de Gran Canaria Dr. Negrín, Las Palmas, Spain*
[q]*Hospital Universitario de La Princesa, Madrid, Spain*
[r]*Hospital Universitario La Paz, Madrid, Spain*
[s]*Hospital de Sant Rafael, Barcelona, Spain*
[t]*Hospital Universitario Doctor Peset, Valencia, Spain*
[u]*Institut d'Investigació Biomèdica de Bellvitge-IDIBELL, Hospitalet de Llobregat, Spain*

Aims: 1. To estimate the incidence of fragility fractures in a population of postmenopausal women diagnosed with rheumatoid arthritis (RA) and compare it with that of the general population; 2. To analyze the risk factors for fracture.

Methods: 330 postmenopausal women with RA from 19 Spanish Rheumatology Departments, randomly selected from the registry of RA patients in each center. The control group consisted of 660 Spanish postmenopausal women from the Camargo Cohort. Clinical fractures during the previous 5 years were recorded. Assessed risk factors for fracture were: sociodemographic characteristics, BMD and variables related to RA.

Results: Median age of RA patients was 64 yrs. vs. 63 yrs. in controls (ns). Evolution of the disease was 8 yrs. 78% and 76% had RF and ACPA+, respectively. 69% of patients were in remission or low activity. 85% had received glucocorticoids and methotrexate and 40% at least one biological DMARD. We identified 105 fractures (87 fragility and 18 traumatic) in 75 patients. Fifty-four patients and 47 controls had at least one major fracture (MF) ($p< 0.001$). Incidence of MF was 296 per 100,000 patient-months (222-383) in patients and 60 (44-79) in controls. Risk factors for MF in RA patients were age, previous fracture, parental hip fracture, postmenopausal period, hip BMD and cumulative dose of glucocorticoids. In controls, risk factors were age, age at menopause and lumbar BMD. Among RA-associated factors, MFs were associated with erosions, disease activity and disability. Previous fracture in RA patients was a strong risk for MF (HR: 10.37 [95% CI: 2.95-36.41]).

Conclusions: Four out of every 100 postmenopausal women with RA have a major fracture per year, more than double that of the

general population. Previous fracture, disease activity and disability associated with RA and the cumulative dose of glucocorticoids are associated with the development of fragility fractures.

doi:10.1016/j.bonr.2020.100514

P198

Adult-onset Still´s disease and Muckle-Wells syndrome: Two sides of the same coin? Case report

Zoran Velickovic
IVa, Institute of Rheumatology, University of Belgrade, Belgrade, Serbia

Adult-onset Still's disease (AOSD), a systemic inflammatory disorder, often represents heterogeneous entity and diagnosis requires the exclusion of a wide range of mimicking disorders. Autoinflammatory diseases are increasingly recognized and are in the differential diagnosis of many disease states, including AOSD. We describe a patient with inflammatory symptoms fulfilling criteria of adult-onset Still disease (AOSD) but also fulfilling a new-proposed diagnostic criteria for Muckle - Wells syndrome (MWS). In the end, it is very tough to differentiate between these two conditions - or maybe one condition with two clinical presentations.

doi:10.1016/j.bonr.2020.100515

P199

Fasciitis diffusa eosinophilica case report

Melanija Rašić
IVa, Institute of Rheumatology, University of Belgrade, Belgrade, Serbia

Eosinophilic fasciitis is a rare sclerodermiform syndrome of unknown etiology. It is characterized by the thickening of the muscular fascia and subcutaneous tissue, with a variable infiltration of eosinophils. Peripheral eosinophilia, poly or monoclonal hypergammaglobulinemia and increased erythrocyte sedimentation rate can be seen. Clinical features begin acutely, with local edema and a painful and symmetrical stiffening of the limbs, progressing rapidly to fibrosis, which can limit joint movements. The diagnosis is confirmed by a deep skin biopsy. Glucocorticoids in high doses is the treatment of choice. We present the clinical characteristics of a 59-year old female patient who could not be diagnosed for a long period and was diagnosed with eosinophilic fasciitis according to muscle biopsy.

doi:10.1016/j.bonr.2020.100516

P201

Thromboembolic safety of tofacitinib and baricitinib: An observational analysis of the WHO VigiBase

Enriqueta Vallejo-Yagüe[a], Stefan Weiler[a,b], Andrea Michelle Burden[a]
[a]*Department of Chemistry and Applied Biosciences, ETH Zurich, Zurich, Switzerland*
[b]*Tox Info Suisse, National Poisons Centre, Associated Institute of the Univerity of Zurich, Zurich, Switzerland*

Objective: The Janus Kinase (JAK) inhibitors baricitinib and tofacitinib are new targeted treatments for rheumatoid arthritis. However, recent concerns regarding the risk of thrombosis has led to warnings by the European Medicines Agency (EMA) and the Food and Drug Administration (FDA). Therefore, we aimed to examine the safety profile of tofacitinib and baricitinib, with focus on thromboembolic events.

Methods: Individual case safety reports (ICSRs) for tofacitinib and baricitinib were retrieved from the World Health Organization global database (VigiBase) in April 2019. The primary outcomes were deep vein thrombosis (DVT) and pulmonary thrombosis (PT) or pulmonary embolism (PE). A disproportionality analysis was conducted by estimating the reporting odds ratio (ROR) and 95% confidence intervals (CIs) to compare the observed versus expected reporting ratio of DVT or PT|PE for tofacitinib or baricitinib. The expected reporting ratio was calculated using all other medicine in VigiBase (worldwide and stratifying by reporting from Europe or the US).

Results: In both tofacitinib (n=40,017) and baricitinib (n=2,138) ICSRs, patients with reported DVT or PT|PE were older and had higher reporting of pro-thrombotic medications (e.g., contraceptives) or indicators of thromboembolic risk (i.e., antithrombotic treatment). The use of tofacitinib was associated with a significant increased reporting for DVT (ROR: 2.37 95% CI 1.23-4.56) and PT|PE (ROR 2.38 95% CI 1.45-3.89) in Europe. Only PT was associated with an elevated reporting risk (ROR: 3.56 95% CI 2.59-4.90) in the US. Similarly, baricitinib was associated with a 3-fold increased risk of reporting for DVT (ROR: 3.47 95% CI 2.18-5.52) or PT|PE (ROR: 3.44 95% CI 2.43-4.88) in Europe, which accounted for 97% of all baricitinib ICSRs.

Conclusion: This study supports the cautious use of JAK inhibitors in patients with rheumatoid arthritis who have a high thrombotic risk profile. Moreover, a potential class effect of JAK inhibitors cannot be ruled out.

doi:10.1016/j.bonr.2020.100517

P202

Screening of musculoskeletal GWAS-discovered lncRNAs in zebrafish

Bodhisattwa Banerjee[a], Ines Föβl[b], Barbara Obermayer-Pietsch[b], David Karasik[a]
[a]*The Azrieli Faculty of Medicine, Bar-Ilan University, Safed, Israel*
[b]*Division of Endocrinology and Diabetology, Medical University Graz, Graz, Austria*

Background: The skeletal system possesses fundamental functions in the human body. Long non-coding RNAs (lncRNAs) are now emerging as critical regulators of major biological processes affecting development, differentiation, and disease. The lncRNA area, in general, just began to be recognized in bone (patho)physiology. Therefore, our study aims to prioritize candidate lncRNAs involved in muscle and bone GWAS and determine the functionality of these lncRNAs in the zebrafish model.

Methods: We have mined the existing GWAS databases and prioritized candidate lncRNAs based on their sequence conservancy in zebrafish and mouse. We performed the expression analysis of three lncRNAs in four tissues (bone, muscle, brain, and liver) of wild type zebrafish using qPCR. Additionally, the expression of the lncRNAs in the skeletal muscle and bony tissues (cranium, operculum) in fish of various ages (3 months, 6 months, 1 year and 1.5 years) was tested. The data were statistically analyzed by Student´s t-test.

Results and discussion: We selected lncRNAs that might have a regulatory function in skeletal phenotypes: *MALAT1*, *GAS5*, and *OIP5-AS1*. Although all three lncRNAs expressed ubiquitously, the *gas5*

expression was significantly elevated in the muscle (p 3.6E-03) compared to the other tissues, whereas the expression of *oip5-as1* was considerably higher (p 0.0027) in the brain. In both muscles and bones, *malat1* and *gas5* lncRNA expression were significantly elevated (p 4.9E-04 and 5.6E-05) in young adults (3 and 6 months) compared to the aged fish (1 and 1.5 y old). Therefore, it might be inferred that some of the lncRNAs are conserved in fish and have a tissue-specific pattern of expression. Also, in the musculoskeletal (MSK) system, the lncRNAs have age-specific functions and expressed differently throughout the lifetime. Further research will be conducted in human plasma and tissue to discover if these candidate lncRNAs are also relevant for the human MSK system.

doi:10.1016/j.bonr.2020.100518

P203

Chronic high-sodium intake elevates blood pressure and reduces bone mass in male Sprague-Dawley rats

Wacharaporn Tiyasatkulkovit[a,b], Siriorn Aksornthong[b,c], Kanikar Wongdee[b,d], Nattapon Panupinthu[b,c], Narattaphol Charoenphandhu[b,c,e]

[a]*Department of Biology, Faculty of Science, Chulalongkorn University, Bangkok, Thailand*

[b]*Center of Calcium and Bone Research, Faculty of Science, Mahidol University, Bangkok, Thailand*

[c]*Department of Physiology, Faculty of Science, Mahidol University, Bangkok, Thailand*

[d]*Faculty of Allied Health Sciences, Burapha University, Chonburi, Thailand*

[e]*Institute of Molecular Biosciences, Mahidol University, Nakhon Pathom, Thailand*

Excessive sodium intake has been associated with a number of non-communicable diseases, including hypertension, cardiovascular accidents and stroke. Recently, an elevated blood pressure in hypertensive patients has been known to increases risk of osteoporosis with low bone mass and fragility fracture. Although high sodium intake is hypothesized to be a risk factor of osteoporosis, the relationship between high salt intake-induced hypertension and a decrease in bone mass is limited and unclear. Therefore, the present study aimed to investigate the effect of chronic high-salt intake on the induction of hypertension and bone microstructural changes in male Sprague-Dawley rats. Two groups of 8-week-old rats were fed normal diet (Control; 0.8% NaCl) or high-salt diet (HSD; 8% NaCl) for 5 months. Blood pressure was monitored by noninvasive tail cuff method. This study has been approved by institutional ethics committee. We observed the elevation of systolic, diastolic and mean arterial pressure, and left ventricular hypertrophy at 5 weeks after HSD treatment. Micro-computed tomography revealed a significant reduction in volumetric bone mineral density (vBMD) and an increased medullary area of the tibial diaphysis in HSD rats ($p< 0.05$). These findings have suggested that excessive sodium intake could induce an elevation of blood pressure, which, in turn, resulted in low bone mass and impaired bone microstructure. Understanding the mechanism by which high-salt diet induces bone structural changes is essential for the prevention of bone loss and fracture in hypertensive patients.

Keywords: bone mineral density, high-salt diet, hypertension, osteoporosis

doi:10.1016/j.bonr.2020.100519

P204

The application of Lugol´s staining for microcomputerized tomografy to visualize and quantify muscles in zebrafish model

Iryna Khrystoforova, Rajashekar Donaka, Chen Schochat-Carvalho, David Karasik

The Azrieli Faculty of Medicine, Bar-Ilan University, Safed, Israel

Teleost zebrafish (*Danio rerio*) is a model for studying human bone biology and bone diseases, such as osteoporosis. The loss of bone mineral density (BMD) is accompanied also with loss of muscle mass; therefore it is important to assess muscle phenotype simultaneously with the measurement of BMD in research model. Several contrast reagents, such as PTA (phosphotungstic acid) and osmium tetroxide have been used to provide contrast to muscles during microCT scanning. Here we validated a Lugol's iodine method, which allows quantifying muscle area and volume by single micro-CT scan in zebrafish, and estimated its effect on BMD. Adult fish (10mpf) were euthanized and fixed for scanning with a BRUKER 1172 micro-CT. Then fish were stained with aqueous Lugol's solution and re-scanned.The enhancement of contrast in soft tissue, especially muscles, was checked. After muscle fiber visualization (region of interest, ROI) we measured its volume and area. BMD was compared before Lugol's staining and after it. Moreover, Lugol stained microCT slices were compared with histological staining by H&E (Fig.1 A-C). Our preliminary results demonstrated no influence of contrast solution on BMD ($p>0.99$).Thus, we are able to measure the area and volume of muscle fibers without histological dissection leaving the specimen intact.

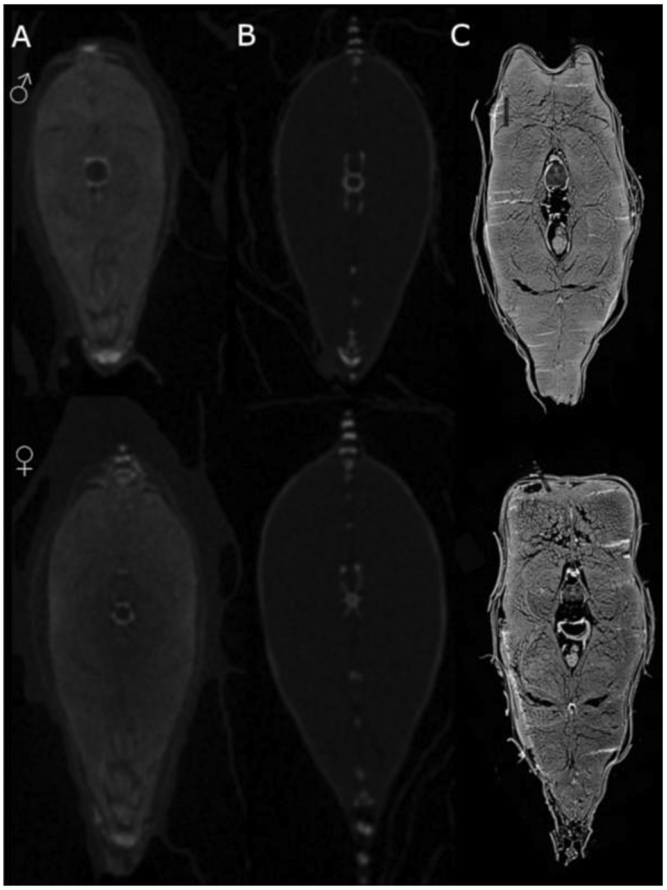

Fig. 1. Reconstructed μCT scan images and H&E staining of zf muscles (Danio rerio).

These results suggest that microCT imaging might be an alternative approach for soft tissue analysis and can be used to visualize structural alterations due to genetic mutation or any other metabolic and physiological perturbation.

Keywords: microCT, zebrafish, contrast agent.

doi:10.1016/j.bonr.2020.100520

P211

The protective effect of IL12/23 p40 neutralizing antibody in sarcopenia induced by chronic inflammatory bowel disease

Jun-Il Yoo[a], Young-Kyun Lee[b], Deog Yoon Kim[c], Yong-Chan Ha[d], KSBMR2020

[a]*Gyeongsang University Hospital, Jinju, Republic of Korea*
[b]*Seoul National University Bundang Hospital, Sungnam, Republic of Korea*
[c]*Kyunghee University, Seoul, Republic of Korea*
[d]*Chung-Ang University College of Medicine, Seoul, Republic of Korea*

Objectives: To determine the improvement of colitis symptom by treatment of Il12/23 p40 neutralizing antibody increase the muscle mass and function of sarcopenia phenotype.

Methods: The experimental colitis model was induced with oral administration of 2% dextran sulfate sodium (DSS) in 8-week-old C57BL/6J male mice for 7 days. During induction of colitis, Il12/23 p40 neutralizing antibody was injected twice at day 3 and 5. The total and hindlimb BMI was measured by Dual-energy X-ray Absorptiometry (DXA). Forelimb grip strength was performed five trials and obtained mean values. The fatigue for running distance of exhaustion was tested using a treadmill system. Cross-sectional area of gastrocnemius and tibialis anterior were determined from the H&E stained slides. Biomarkers associated with muscle regeneration were analysed using quantitative PCR in gastrocnemius and tibialis anteria.

Results: DSS-induced colitis was initiated on day 4 with loss of body weight and increase in DAI score, the highest on day 8 in control group. However, colitis was significantly lessened in treated group of Il12/23 p40 neutralizing antibody. A significant decrease in grip strength, fatigue distance and muscle mass were observed in control mice, and partially rescued in p40 antibody treated mice. But muscle weight and hindlimb BMI index (BMD, BMC, fat, lean and total weight) were not changed. Cross-sectional area of GN and TA were significantly rescued in p40 antibody treated group. The expression of IL12b2 is increased in the muscle of human osteosarcopenia patients, indicating that p40 neutralizing antibody can act directly in muscles.

Conclusion: Our study demonstrates that IL12/23 p40 neutralizing antibody has protective role in experimental colitis-induced muscle atrophy and muscle function.

doi:10.1016/j.bonr.2020.100521

P214

Subchondral perfusion physiology during weight bearing

Michael Beverly[a], David Murray[b]

[a]*OOEC, Botnar Research Centre, NDORMS, University of Oxford, Richmond, United Kingdom*
[b]*University of Oxford, Oxford, United Kingdom*

Objectives: Little is known about the physiology of subchondral perfusion during activity.

The subchondral intraosseous pressure (IOP) may fluctuate with load bearing. We developed an in vitro calf foot model to explore the physiology of subchondral IOP and perfusion during weight bearing.

Methods: Freshly culled week-old calf fore feet were perfused with serum. IOP was measured at three sites in the metacarpal and proximal phalanx through intraosseous needles using pressure transducers and digital recorders. IOP was recorded during perfusion, with and without a tourniquet and with both static skeletal loading and dynamic loading to resemble walking.

Results: Static loading increases subchondral IOP whether the bone is non-perfused, perfused or perfused and with a proximal venous tourniquet. The IOP rise is proportional to the load ($R^2 = 0.984$). With physiological loads subchondral IOP may exceed perfusion pressure.

On removal of a standing load IOP falls to below the pre-load IOP whether non-perfused, perfused or perfused and with a proximal venous tourniquet. Dynamic or walking type loading causes a fluctuating IOP and a falling background IOP.

Conclusion: Subchondral bone act as a perfused tissue in a predictable manner. Superimposed on the background perfusion IOP, physiological loading causes a significant increase in subchondral IOP. This shows that force is transmitted through subchondral bone partly by hydraulic pressure. The falling IOP with repeat loading suggests that there is a subchondral or intraosseous valve or pump. This offers a new understanding of subchondral physiology.

doi:10.1016/j.bonr.2020.100523

P215

The impact of intravenous use of mesenchymal stem cells in a damaged tibia on the indicators of antioxidant system in the calf muscles

Elena Demianenko, Vladyslav Luzin, Pavel Boychenko

State Establishment of Lugansk People's Republic Saint Luka Lugansk State Medical University, Lugansk, Ukraine

Introduction: Bone fractures are accompanied by intensification of free radical oxidation in adjacent muscles as a result of ischemia. The use of mesenchymal stem cells (MSCs) can help reduce oxidative stress.

The aim of the study was to study the dynamics of malondialdehyde (MDA), superoxide dismutase (SOD), catalase in the calf muscles after the formation of tibial defects and the intravenous use of MSCs.

Materials and methods: 90 male rats (4 weeks old) were divided into 3 groups: 1) the control, 2) the comparisons (formed defects of the tibia), 3) experimental groups (5×106 MSCs were administered intravenously 3 days after the formation of bone defects). Indicators were determined in the homogenates of the calf muscles by spectrophotometric method on the 7th, 15th, 30th, 60th and 90th days after the formation of bone defects. To obtain MSCs, rat bone marrow cells were cultured for 14 days in a CO2 incubator.

Results: The level of MDA in the comparison group on the 7th and 15th day exceeded the control value (17.5% and 32.8%). In the experimental group, its level on the 15th day was lower than in group No. 2 by 45.03%. In the comparison group, the activity of SOD was minimal on the 7th day, then increased relative to the control, and again decreased by the 30th day. In the experimental group, the activity of SOD increased as much as possible on the 7th day (14% relative to group No. 2 and 53.5% relative to the control), on the 30th day it did not differ from the control. The dynamics of catalase was similar.

Conclusions: Ischemia in the calf muscles with damage to the tibia is accompanied by a decrease in the activity of antioxidant

enzymes. The use of MSCs contributes to a more rapid restoration of oxidative-prooxidant balance.

doi:10.1016/j.bonr.2020.100524

P216

Ultra high field MRI (150 micron) assessment of the structural elements of the knee entheses in healthy subjects

Damien Roche[a], Constance Michel[b], Pierre Daudé[b], Arnaud Le Troter[b], Christophe Chagnaud[c], Jean-Pierre Mattei[a], Lauriane Pini[b], Maxime Guye[b], David Bendahan[b], Sandrine Guis[a]
[a]*Rheumatology, Aix-Marseille Université, AP-, HM, Marseille, France*
[b]*CRMBM-CEMEREM, UMR CNRS 7339, Aix-Marseille Université, CNRS, Marseille, France*
[c]*Radiology, Aix-Marseille Université, AP-, HM, Marseille, France*

Introduction: Fibrocartilaginous entheses is composed of different histological zones which are commonly referred to the tendon distal extremity (a lamellar tissue with a low cell density, collagen and connective tissue), the fibrocartilaginous zone (with chondrocytes), a progressively mineralized zone and the bone. The MRI visualization of the water content of entheses is challenging given the very short relation time so that entheses has been very poorly assessed using MRI.

Objective: The main objective of the study was to assess the structural elements of the knee entheses based on the quantitative T2* measurements.

Subjects and Methods: Twelve healthy subjects without any osteoarticular pathologies were included in the study after they provided their informed consent. 3D gradient echo sequence with a 4.3 ms echo time and T2* mapping were performed. The lateral internal, external and crossed ligaments, patellar and quadricipital tendons were assessed. T2* measurements were performed specifically on the quadricipital tendon.

Results: As illustrated in the figure, the quadricipital tendon and the bone trabeculation could be visualized on the UHF MR image. The T2* mapping analysis illustrated a large value (16.4 $\pm$ 4 ms) for the subchondral bone and much lower values for the trabecular bone (11 $\pm$ 4.5 ms) and the different zones of the knee entheses (7.7 $\pm$ 1.9 ms).

Discussion: Based on T2* measurements performed using UHF MRI, the different structural elements of the knee entheses were distinguished. This quantitative stratification could be used to assess changes in pathological conditions such as SpA and trauma.

doi:10.1016/j.bonr.2020.100525

P217

Role of sarcopenia in the old patients combined with sagittal imbalance

Ye-Soo Park[a], Jin-Sung Park[b], Byung-Jik Kang[a]
[a]*Orthopaedic Surgery, Guri Hospital, Hanyang University, Guri City, Republic of Korea*
[b]*Orthopaedic Surgery, Samsung Medical Center, Sunngkyunkwan University, Seoul, Republic of Korea*

Objective: The aim of this study was to analyze the association between sarcopenia and sagittal imbalance.

Summary of Background Data: Both sagittal imbalance and sarcopenia affect performance of daily activities and mortality in the elderly; however, little is known regarding their relationship.

Materials and methods: This study included 71 female patients aged between 60 and 85 years. Entire-spine radiography was used to measure radiological parameters. A bioelectrical impedance analyzer was used to measure the skeletal muscle mass index (SMI). Gait velocity (GV), and hand grip strength (HGS) were examined as well. Lumbar spine magnetic resonance imaging (MRI) was employed to measure the functional cross-sectional area (FCSA) and fat signal fraction (FSF) of the paraspinal muscle as well. The subjects were grouped as sagittal imbalance (sagittal vertical axis [SVA] > 50 mm; SI group) and balance (SVA ≤ 50 mm; SB group).

Results: The SI group patients were significantly older and had a lower hip BMD than the SB group patients ($p = 0.001$ and 0.047, respectively). In addition, the SI group showed significantly lower GV, HGS, and SMI than the SB group ($p < 0.001$, < 0.001, and $= 0.002$, respectively). Moreover, the prevalence of sarcopenia was significantly higher in the SI group (56.7%) than in the SB group (17.1%) ($p = 0.001$). The SI group also showed a significantly lower FCSA and higher FSF than the SB group ($p < 0.001$). In the multivariate linear regression analysis, the FSF ($\beta = 1.818$, $p < 0.001$) and SMI ($\beta = -11.571$, $p < 0.001$) were significantly correlated with the SVA ($p < 0.001$).

Conclusion: Sarcopenia and fatty degeneration of paraspinal muscle are closely related to sagittal imbalance in the elderly.

doi:10.1016/j.bonr.2020.100527

P219

Cross cultural adaptation of the Korea sarcopenia quality of life (SarQoL) questionnaire

Yong-Chan Ha[a], Young-Kyun Lee[b], Deog Yoon Kim[c], Jun-Il Yoo[d], KSBMR2020
[a]*Chung-Ang University College of Medicine, Seoul, Republic of Korea*
[b]*Seoul National University Borame Hospital, Seoungnam, Republic of Korea*
[c]*Kyunghee University, Seoul, Republic of Korea*
[d]*Gyeongsang University Hospital, Junju, Republic of Korea*

Purpose: The purpose of this paper was to cross-culturally translate, and validate the sarcopenia quality of life (SarQoL) into the Korean language and setting. In addition, we proved the validity of the SarQOL questionnaire in the revision requirements of the European Working Group on Sarcopenia in Older People (EWGSOP) II version.

Methods: The participants were 341 individuals who were followed up in 2019 in Namgaram-2 Cohort. Questionnaire was back-translated and culturally adapted into Korea according to international guidelines. To validate the Korea SarQoL, we assessed its validity (discriminative power, construct validity), reliability (internal consistency, test-retest reliability) and floor/ceiling effects. The study group was divided into four groups; SARC < 4/SARC_F ≥ 4 and robust grip strength/SARC_F ≥ 4 and robust muscle mass and low grip strength/SARC_F ≥ 4 and low muscle mass and low grip strength. Sarcopenic subjects apart from the Korea SarQoL (SarQoLKR) filled out the Korean versions of two generic questionnaires; Short Form-36 and EuroQoL 5-dimension.

Results: The Korea SarQoL questionnaire was translated without major difficulties. SarQoLKR mean scores were 46.6 $\pm$ 11.04 (range: 36.4-56.9) for sarcopenic subjects and 72.9 $\pm$ 14.1 (range: 71.2-74.6) for non-sarcopenic ones. Results indicated good discriminative power across sarcopenic and non-sarcopenic subjects ($p< 0.001$), high internal consistency (Cronbach's alpha of 0.866) and excellent test-retest reliability ((ICC=0.997, 95% CI 0.995-0.999). Neither a floor nor a ceiling effect was observed.

Conclusion: This study confirmed the reliability and validity of the Korean version of SARQOL. In particular, this is the first study to

demonstrate that the population suspected of sarcopenia is poor in quality of life by SARC-F questionnaire.

doi:10.1016/j.bonr.2020.100526

P220

Effects of osteo-sarcopenia on postoperative functional outcome and subsequent fracture in elderly hip fracture

Kyoung Ho Moon, Gi Cheol Bae
Orthopedic Surgery, Inha University College of Medicine, Incheon, Republic of Korea

Purpose: In this study, we evaluate to determine how muscle mass and bone density affect the postoperative functionaln score and subsequent fracture rate and investigate the correlation between the sarcopenia and osteoporosis by measuring the preoperative psoas muscle index (PMI) and bone mineral density (BMD) in the patients who were followed-up more one year after surgical treatment of hip fracture.operation

Materials and methods: Among the patients, who we was operated for hip -fracture over 65 years old from January 2009 to November 2018, 154 patients who were possibly evaluated with preoperative 3D pelvic bone CT and BMD and followed up postoperatively at least a year. Among these patients, 126 patients were finally included in this study.

We divided into four groups based on PMI and BMD. To analyze the clinical outcomes after surgery, we measured the level of functional activities using the Barthel index and Harris hip HHS score(HSS). Additionally, we compared the rates of.the opposite side hip fracture ratio with patients' characteristics.

The correlation of variables used to analyze with the Chi-square test and Fisher's exact test. Pearson correlation coefficient used to analyze the correlation between the PMI and BMD

Results: Barthel index and HHS score showed a significant difference between the two groups at six weeks, three months, and one year after surgery ($p < 0.001$). Subsequent fracture incidence was significantly higher in the osteo-sarcopenia group than normal group($p = 0.046$). For the more, we found a high level of correlation between BMD and PMI ($a < 0.01$; $R = 0.763$).

Conclusion: In this study, the postoperative functional outcomes in osteo-sarcopenia group showed significantly worse than in normal group and the subsequent fracture rate was significantly higher in osteo-sarcopenia group. Additionally, we found a high correlation between sarcopenia and osteoporosis.

doi:10.1016/j.bonr.2020.100528

P221

Mindfulness and modified medical yoga improve quality of life in persons with osteoporotic vertebral fracture - a randomized controlled trial

Catrin Willerton[a], Paul Enthoven[b], Anna Spångeus[b], Ann-Charlotte Grahn Kronhed[a]
[a]*University of Linköping, Vadstena, Sweden*
[b]*University of Linköping, Linköping, Sweden*

Background: Persons with osteoporotic vertebral compression fractures (VCFs) have decreased health related quality of life (HRQoL). Yoga and mindfulness are methods that can promote well-being.

Objective: The aim of the present study was to explore the effect of mindfulness and modified medical yoga on HRQoL, stress, sleep and pain in persons 60 years or above with an osteoporotic VCF, who were participating in a school of osteoporosis.

Design: This pilot study has a randomized controlled trial (RCT) design.

Materials and Methods: The school was scheduled to once a week for ten weeks. Ten persons were randomised to a theory (T) group and ten persons to a mindfulness/medical yoga (MMY) group. The educational sessions lasted 60 min and were similar for the groups. The MMY-group practiced yoga and mindfulness supervised by an experienced physiotherapist for 60 min. We analysed two intervention arms as follows 1) theory only, and 2) theory and mindfulness/medical yoga. Sleep quality and present stress experience were measured on a Likert scale. EQ-5D, RAND-36 and Qualeffo-41 were used for self-reported HRQoL.

Results: Eight subjects in the MMY-group and seven subjects in the T-group completed the school. The adherence to the intervention program was 89% in the MMY-group and 87% in the T-group. There was no adverse event of the MMY training. After the ten-week intervention period sleep quality ($p< 0.018$), present stress ($p< 0.043$), but not perceived pain were improved in the MMY-group. Regarding HRQoL the social function domain was improved in the MMY-group measured by RAND-36 ($p=0.028$) and Qualeffo-41 ($p=0.012$). Furthermore, the total Qualeffo-41 score was improved in the MMY-group ($p=0.043$).

Conclusion: The present study suggests that mindfulness and modified medical yoga supervised by a skilled physiotherapist may be a feasible way to improve quality of life in older persons with osteoporotic VCFs.

doi:10.1016/j.bonr.2020.100529

P224

Measurements of muscle parameters in computed tomography slices can predict presence of sarcopenia

Ho-Yeon Chung[a], Wan Kyu Eo[b], Soomin An[c]
[a]*Department of Endocrinology and Metabolism, Kyung Hee University, School of Medicine, Seoul, Republic of Korea*
[b]*Department of Medical Oncology/Hematology, Kyung Hee Univ Hosp at Gangdong, Seoul, Republic of Korea*
[c]*College of Nursing Science, Kyung Hee University, Seoul, Republic of Korea*

Background: To evaluate the correlation between measurements of muscle parameters in axial computed tomography (CT) slices and presence of sarcopenia with appendicular skeletal muscle index less than 7.0 kg/m^2 for men and 5.7 kg/m^2 for women by using bioimpedance analysis (BIA).

Methods: In this study, we analyzed data of a cohort of 381 consecutive adult patients who underwent concurrent BIA assessments and abdominal CT scan between January 2014 and July 2014. To assess muscle mass, we analyzed the cross-sectional total skeletal muscle area (SMA) as well as the areas of the paraspinal muscles in a single CT slice at the level of the third lumbar vertebra. Subsequently, the muscle parameters such as SMA, skeletal muscle index (SMI; height-adjusted SMA), SMA to body mass index, paraspinal muscle area (PMA), paraspinal muscle index (PMA adjusted for height squared), and PMA to BMI measurements were correlated with the presence of sarcopenia.

Results: When analysed with multivariable logistic regression model, SMA (odds ratio = 4.32, 95% confidence interval [CI]: 1.43-13.01, $P = 0.009$) and SMI (odds ratio = 3.90, 95% CI: 1.76-8.63, $P = 0.001$)

were strongly associated with the presence of sarcopenia by BIA.

Conclusions: Our data suggest that accurate measurements of sarcopenia can be determined using simple measurements on single-axis CT slices. This could be useful in various medical and scientific environments, where knowledge of the patient´s anthropometric parameters is not readily available.

Keywords: Sarcopenia, Tomography, Body composition

doi:10.1016/j.bonr.2020.100530

P225

Sarcopoenia in an integrated occupational project aimed at elderly patients with femoral fractures due to bony brittleness

Ferdinando D'Amico[a], Rossella D'Amico[b]

[a]*Geriatrics, Hospital of Patti - Health Authority Messina - School of Medicina Messina, Messina, Italy*

[b]*Health Authority Messina, Geriatric Extended Care Network, Messina, Italy*

Objective: 103 elderly patients with femoral fractures have been hospitalized in the Orthogeriatrics. The aim of the integrated rehabilitative OT programme was to evaluate the prevalence of sarcopoenia and to reestablish the functional condition prior to fracture descending from bony brittleness.

Methods: They have been assessed through a multifaceted (orthopedic-geriatric-rehabilitative) approach using MMSE, BADL, IADL, Barthel Index. Osteoporosis and Sarcopoenia were assessed through DEXA Bone Densitometry.

Results: The standing position recovery for 63 patients started within 3 days after prosthesis surgery due to femoral fracture. They were dismissed after a 15/25-day hospitalization. 34 elderly subjects recovering from osteosynthesis regained the sitting position in 2-3 days, load tests were made between 7 and 14 days and they left the unit 30/45 days after admittance. At discharge 10 subjects affected by femoral fracture and sarcopoenia (mean age 78±5) were moved to the Extended Care Unit for lack of assistance at home. There they followed an Occupational Therapy (OT) programme including aims like: 1) performing lower limbs mobilization through specific exercises; 2) working on muscle fibers type 2 to counter-balance the muscle loss. The group including patients following the programme was then compared to one including 8 subjects affected by femoral fracture and sarcopoenia (mean age 77± 6) discharged and going home to their caregivers after femoral fractures. A 6-month individual OT programme at the Extended Care Unit showed: 1) improvement in motor skills detected through scales scores (BADL 3.3/6 > 4.5/6 - IADL 2.5/8 > 5.7/8 - Barthel Index 50/100 > 90/100); 2) improvement both in muscle mass and muscle strength.

Conclusion: Effectiveness of a OT programme focused on walking ability and muscle strength recovery, aimed at patients discharged after femoral fractures and osteosynthesis, was evaluated. The Occupational Therapist approach was customized in order to make the patient regain his self-assurance and independence.

doi:10.1016/j.bonr.2020.100531

P226

Preoperative measurements of muscle parameters in computed tomography slices can predict clinical outcomes in patients with gastric cancer who underwent curative surgical resection

Wan Kyu Eo[a], Soomin Ahn[b], Ho-Yeon Chung[c], Sookyung Lee[d], Sehyun Kim[e], Jungmi Kwon[a]

[a]*Department of Medical Oncology/Hematology, Kyung Hee Univ Hosp at Gangdong, Seoul, Republic of Korea*

[b]*College of Nursing Science, Kyung Hee University, Seoul, Republic of Korea*

[c]*Department of Endocrinology and Metabolism, Kyung Hee University, School of Medicine, Seoul, South Korea, Seoul, Republic of Korea*

[d]*Department of Clinical Korean Medicine, Graduate School, Kyung Hee University, Seoul, Republic of Korea*

[e]*Graduate School, Dankook University, Yongin, Republic of Korea*

Background: Body composition parameters have been suggested to predict outcomes for patients with gastric cancer. However, evidence for an association with long-term survival is still conflicting. This study examined the effect of quantitative and qualitative muscle parameters in computed tomography slices on overall survival (OS) and disease-free survival (DFS) in patients with gastric cancer who underwent curative resection.

Methods: Patients with stages I and II gastric cancer between October 2006 and October 2014 were identified from medical records. Preoperative computed tomography scans at the level of 3rd lumbar vertebra were analyzed to calculate quantitative (e.g., area and adjusted area) and qualitative (e.g., mean attenuation) skeletal muscle parameters. Regarding region of interest, we analyzed the areas of the paraspinal muscles (PSM) as well as the cross-sectional total skeletal muscle (TSM) areas. Both Univariate and multivariate survival analyses were performed using a proportional hazards model, considering with demographic characteristics, and pathologic/laboratory parameters including neutrophil-lymphocyte ratio (NLR), platelet-lymphocyte ratio (PLR), lymphocyte-monocyte ratio (LMR), and prognostic nutritional index (PNI).

Results: The study enrolled 273 patients with gastric cancer. In multivariate analysis, age (Hazard ratio [HR] = 2.36, P = 0.0166), PNI (HR = 0.88, P = 0.0002), and mean attenuation within TSMs (HR = 0.97, P= 0.0368) were associated with OS). In addition, age (HR = 1.98, P = 0.0414), PNI (HR = 0.89, P = 0.0003), and mean attenuation within PSMs (HR = 0.97, P = 0.0236) were associated with DFS.

Conclusion: Mean attenuation within skeletal muscles, along with age and PNI, was an independent prognostic factor for survival.

Keywords: Body Composition; Tomography, Spiral Computed; Stomach Neoplasms; Prognosis

doi:10.1016/j.bonr.2020.100532

P227

Methodology for determining the muscle mass decreasing in young men with type 1 diabetes

Yuliya Dydyshka, Alla Shepelkevich

Department of Endocrinology, Belarusian State Medical University, Minsk, Belarus

Background: According to modern concepts, diabetic myopathy is also a common clinical condition characterized by a lower muscle mass, weakness, and an overall reduced physical capacity.

The aim of our study was to determine the criteria for reducing the content of appendicular muscle mass (AMM) in type 1 diabetes (T1DM) men.

Materials and methods: 35 men with (mean age: 32,4 (24,4 - 37,2) yrs, duration of DM: 13 (7-20) yrs, age of manifestation: 17(13-21) yrs, BMI: 23,67(20,88-25,37), HbA1c: 8,2(7,5-9,1)%) and 24 men controls. In patients with T1DM and in control group revealed comparable (U=130;p=0,423) levels of free testosterone 15.1(9-24) and 19.7(14.75-23.05) nmol/L, (U=130;p=0,423)

respectively, indicating the presence of normagonadal status of the surveyed men. The research involved general clinical examination, serum muscle-specific parameters; DXA body composition parameters were performed on «PRODIGY LUNAR». An appendicular skeletal muscle mass index (ALMI) was measured as appendicular muscle mass (lean mass arms + lean mass legs)/height2.

Results: There were significant differences in T1DM males and control: Lean Arms: 6573 (5915 - 7454) vs 7540 (6658 - 8729)g; (U=248;p=0,017); Lean Legs: 18054 (16361-19794) vs 20455 (18803-22761)g; (U=208; p=0,002); Lean (Arms+Legs) - 25241 (22102-27784) vs 28370 (25541-31367)g; (U=219; p=0,004), Total Body Lean (54082 (48999-60653) vs 60969 (54273-65082)g; U=259; p=0,027), Lean Gynoid Lean (7711 (7155-8843) vs 8423 (8000- 9891)g; U=241; p=0,013. Using ROC analysis determined the cut-off point of the ATM for patients with T1DM (p=0.008) - 8.44 kg/m2.Considering ORs and 95% CIs determined probability of decrease of AMM in young men with T1DM age: OR=5.59 (2,88-10,84; $\chi 2$ =9,16; p=0,025).

Conclusions: Thus, it was determined the significant (p = 0.008) threshold IMM - 8.44 kg/m2, allowing to allocate a group of men with a reduction in the AMM (IMM ≤ 8,44 kg/m2) and people with a normal amount of AMM (IMM> 8.44 kg/m2).

doi:10.1016/j.bonr.2020.100533

P228

Short-term mandibular change, by Norland DXA, in osteoporotic patients treated with Vitamin K

Yun Sun[a], Tom V. Sanchez[b], Ke Qin Pan[a], Chad A. Dudzek[b], Jing Mei Wang[c]
[a]*Department of Radiology, Hospital of Tsinghua University, Beijing, China*
[b]*Department of Research and Development, Norland at Swissray, Fort Atkinson, United States*
[c]*Department of Research and Development, Norland at Swissray, Beijing, China*

Mandibular bone is known as a high-turnover bone that does not change significantly in healthy subjects but undergoes substantial change with disease. The current study examines early changes in the mandible of subjects treated with Vitamin K. Vitamin K may act on osteoporosis by inducing the production and secretion of osteocalcin by osteoblast. Expecting a positive response to Vitamin K treatment to increase bone density at the mandible, the current study examined change in Norland DXA-based mandibular assessment in osteoporotic patients undergoing Vitamin K treatment.

Five subjects underwent three repeated Norland DXA Mandible assessments over 45 to 51 days of Vitamin K treatment for osteoporosis. Scans of the mandible were done as previously reported (Journal of Clinical Densitometry. 21:534-540, 2018) with a documented repeatability of 1.73% and 2.44% for the body and ramus regions, respectively. Follow-up studies were compared to the initial study in an individual with values outside the Least Significant Change Limits of 4.84% (Body) or 6.83% (Ramus) being reflective of significant change.

Three subjects showed significant average increases to 118% of original body or ramus density suggesting a positive response to the treatment program over the evaluation period. The other two subjects showed significant average decreases to 75.6% of original body or ramus density suggesting a lack of response to the treatment program. When viewed by comparison to changes that do not exceed 4.8% for the body or 6.8% for the ramus in healthy subjects the degree of change seen in the five treated subjects suggests that the mandible assessment is reflecting either a positive response or a lack of response to treatment.

In conclusion, the study demonstrates that over the period evaluated the Norland DXA systems fitted with Mandible Assessment document either an early positive response or a lack of response in an osteoporotic treatment.

doi:10.1016/j.bonr.2020.100534

P229

Regional osteoporosis; the impact of monoparesis and hemiparesis on bone density

Atef Michael
Russells Hall Hospital, Dudley, United Kingdom

We present two cases of “regional” osteopenia/osteoporosis.

Case 1: A 59-year-old female fell onto her right femur stump sustaining neck of femur fracture. Her medical history included DM, hypertension, peripheral vascular disease and above knee amputation 30 months earlier. She was mobile with a wheelchair. Examination was unremarkable. X-ray showed markedly osteopenic right femur stump(Fig 1). She was treated conservatively.

Case 2: A 77-year-old male fell sustaining left neck of femur fracture. His medical history included AF, hypertension and intra-cerebral haemorrhage five years previously with residual left hemiplegia. He was mobile with a stick. XR showed osteopenic left femur compared to the right (Fig 2). He had left Dynamic Hip Screw.

Discussion: Movement and weight bearing are the most effective stimuli for increasing bone mineral density. Diseases that affect mobility of a part, e.g. monoparesis, hemiparesis or diparesis can result in osteoporosis of affected part. Following acute immobilization, there is initial rapid loss of bone followed by gradual loss.

Clinicians should be aware of the concept of “regional osteoporosis”, try to reduce its development, perform DXA scan for both limbs and not be falsely reassured by a normal BMD in the non-paretic side. Treatment needs to address the osteoporotic side.

Fig. 1. AKA XR pelvis.

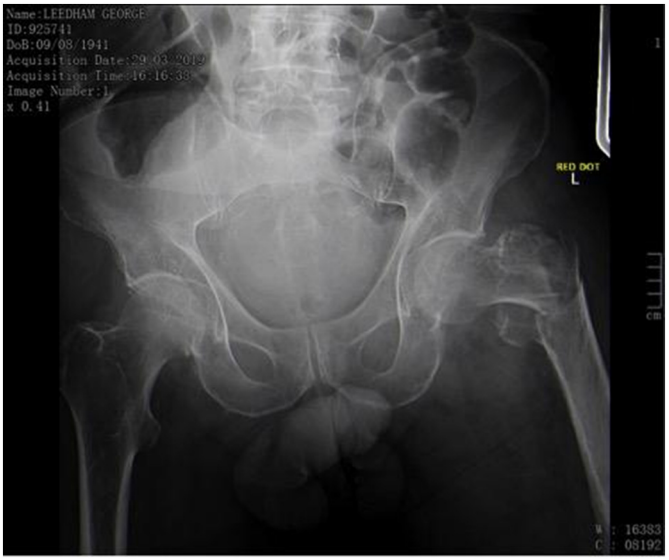

Fig. 2. Hemiplegia XR Pelvis.

doi:10.1016/j.bonr.2020.100535

P231

Static and dynamic balance function in patients with osteoporotic vertebral fractures

Larisa Marchenkova, Ekaterina Makarova, Mikhail Eryomushkin, Ekaterina Chesnikova, Dariya Razvalyaeva, Elena Styazhkina
Rehabilitation Department for Somatic Patients, National Medical Research Center for Rehabilitation and Balneology of Ministry of Health of Russian Federation, Moscow, Russian Federation

The aim was to estimate the static and dynamic balance in osteoporotic patient with vertebral fractures (VFs).

Methods: 90 osteoporotic patients aged 43-80 y.o. were enrolled: 60 patients with at least 1 VF constituted study group and 30 subjects without any fracture were included in control group. Stabilometry, Fukuda-Unterberger and One-leg-standing tests were performed.

Results: Study group was characterized by change vs controls in balance coefficient (BC) (77.2±7.6 vs 85.7±9.4 % with opened eyes, p=0.002, 67.1±9.8 vs 73.4±9.9 % with closed eyes, p=0.03), pressure center of media-lateral (PCML) deviation in sagittal plane (1.2 [-1.1;1.5] vs -1.2 [-1.5;1.2] mm, p=0.025) and PCML displacement in sagittal plane (6.8 [3.1;37.7] vs to 4.8 [1.8;10.7] mm, p=0.01). BC with opened eyes correlated with age (r=0.41, p=0< 0.01) and BMI (r=0.16, p=0< 0.05). PCML deviation in sagittal plane correlated with age (r=-0.42, p=0< 0.01), number of VFs (r=0.40, p=0< 0.001) and femoral neck BMD (r=-0.43, p=0< 0.05), and in frontal plane only with age (r=-0.27, p=0< 0.05). PCML displacement in sagittal plane correlated with age (r=-0.29, p=0< 0.01), number of VFs (r=0.22, p=0< 0.01) and femoral neck BMD (r=-0.38, p=0< 0.05) and in frontal plane with BMI (r=-0.15, p=0< 0.05). Fukuda-Unterberger test showed greater side dislocation in study group vs controls (40° [25.0;45.0] vs 30° [10.0;45.0], p=0.02). Side dislocation correlated with number of VFs (r=-0.30, p< 0.05). Patients with VF lose their balance in One-leg-standing test faster vs controls with open (5.0 [1.0;10.0] vs 7.5 [5.0;10.5] sec, p< 0.05) and with closed eyes (2.0 [0;3.0] vs 3.5 [3.0;5.0] sec, p< 0.05). One-leg-standing test results correlated with age (r=-0.35 with open and r=-0.42 with closed eyes, p< 0.01).

Conclusions: VFs negatively effect on static and dynamic balance. Age, high BMI, low BMD and number of VFs are main factors of balance dysfunction in patients with VFs.

doi:10.1016/j.bonr.2020.100536

P234

Diagnostic trans-iliac bone biopsy: Is there a clinical need? Review of consecutive bone biopsies carried out over 5 years in a UK specialist centre

Linda Skingle[a], Stephen M. McDonnell[b], Phillip Johnston[c], Gavin P.R. Clunie[d], Kenneth E.S. Poole[e]
[a]*Department of Medicine, Cambridge NIHR Biomedical Research Centre, Cambridge, United Kingdom*
[b]*Division of Trauma and Orthopaedic Surgery, University of Cambridge, Cambridge, United Kingdom*
[c]*Department of Trauma and Orthopaedics, Cambridge University Hospitals NHSFT, Cambridge, United Kingdom*
[d]*Department of Rheumatology, Cambridge University Hospitals NHSFT, Cambridge, United Kingdom*
[e]*Department of Medicine, University of Cambridge, Cambridge, United Kingdom*

Clinical diagnostic bone biopsy is indicated in suspected osteomalacia, unusual presentations of various bone diseases and to characterise renal osteodystrophy. Recent guidelines (KDIGO)

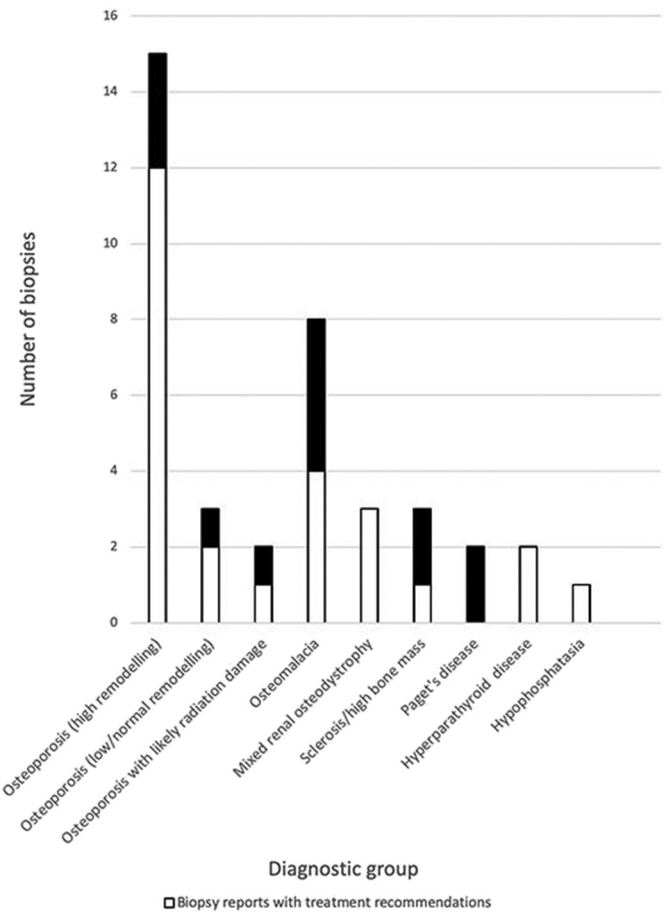

Bar chart showing number of biopsies per diagnostic group (with number of treatment recommendations in white).

highlight two critical biopsy indications i) diagnosis and ii) guiding complex treatment decisions. Here we review our clinical biopsy reports with a view to these two key metrics.

For this assessment we selected only patients from our UK teaching hospital from 2014-2019. The decision to offer biopsy was taken by the Multidisciplinary Team meeting approach. With patients under light general anaesthetic, trephine (7.5mm) trans-iliac cores (with separate Jamshidi marrow sample for decalcification) were taken by orthopaedic surgeons before laboratory embedding into resin, sectioning and staining. Two team members provided microscopic evaluation, diagnosis and clinical advice. Patient demographics and pre-biopsy diagnosis were recorded from the bone biopsy report along with the pathology described and whether treatment advice was given.

There were 46 biopsies (20 male, 26 female, mean age 54.41yrs ± 15.1 SD). Underlying renal disease was the primary indication in 21 cases (45.7%), with 16 other specialist bone indications. In 40 samples (87%) specific pathological features (*figure*) were described and 26 of those reports (65%) contained specific treatment advice.

Bone biopsy has clinical utility for managing our specialist metabolic bone disease patients. Most biopsies exhibited pathology and in 65% of cases this led to new treatment recommendations. To fully assess the clinical utility of bone biopsy we recommend a prospective audit should be carried out to follow the post biopsy course of each patient.

doi:10.1016/j.bonr.2020.100537

P236

Imaging spectroscopy in women with post-surgical hypoparathyrodism

Davide Diacinti[a], Cristiana Cipriani[b], Antonio Iannacone[c], Martina Orlandi[c], Endi Kripa[c], Jessica Pepe[b], Luciano Colangelo[b], Valentina Piazzolla[b], Daniele Diacinti[c], Salvatore Minisola[b]
[a]*Department of Odontostomatological and Maxillo-Facial Sciences, Umberto I Hospital, University Sapienza, Roma, Italy*
[b]*Department of Clinical, Internal, Anesthesiological and Cardiovascular Sciences, 'Sapienza' Rome University, Rome, Italy*
[c]*Department of Radiological Sciences, Oncology and Anatomo-Pathology, University Sapienza, Rome, Italy*

The study was aimed to assess Bone Marrow Fat (BMF) content using Magnetic Resonance Imaging (MRI) Spectroscopy in post-menopausal women with chronic post-surgical hypoparathyroidism.

We enrolled 26 post-menopausal women with chronic post-surgical hypoparathyroidism (mean age 65.3±7 years) and 11 healthy age-matched control women. In all subjects, we assessed Bone Mineral Density (BMD) by dual X-ray absorptiometry (Hologic QDR 4500A, USA) at lumbar spine (L1-L4), femoral neck (FN) and total hip (TH); Trabecular Bone Score (TBS) on the lumbar spine images by the TBS-iNsight software; Vertebral Fracture Assessment (VFA) by iDXA (Lunar, GE, USA). BMF was measured by the 3 Tesla MRI examination of the lumbar spine and the application of the PRESS spectroscopy sequences on L3 vertebral body.

We observed no significant difference in mean BMD values between hypoparathyroid and control women at all sites (L1-L4: 1.045±0.157 g/cm^2 vs 0.757±0.121; FN: 0.907±0.140 vs 0.734 ±0.095; TH: 0.907±0.140 vs 0.817±0.107). Mean TBS values were lower in the hypoparthyroid compared to controls (1.17 ±0.12 vs 1.33±0.10;). BMF was significantly higher in hypoparathyroid compared to control subjects (81.9 ± 4.2 % v. s. 75.3 ± 7.8; $p < 0.01$). 4/26 (15.4%) hypoparathyroid women, had vertebral fractures. No difference in BMF values was observed between hypoparathyroid subjects with and without vertebral fracture. There was no significant association between L1-L4 BMD and BMF, TBS and BMF respectively in the hypoparathyroid subjects.

Our results demonstrate that there is an increase in bone marrow fat in postmenopausal women with post-surgical hypoparathyroidism. Additionally, trabecular microarchitecture is degraded in hypoparathyroid compared to control women. The ongoing enrolment of further subjects will better define perturbations of these parameters relate to skeletal fragility in patients with chronic hypoparathyroidism.

Keywords: Bone Marrow Fat (BMF), Hypoparathyroidism; MRI Spectroscopy; Trabecular Bone Score (TBS)

doi:10.1016/j.bonr.2020.100538

P237

Automated detection of vertebral fractures in CT using 3D convolutional neural networks

Joeri Nicolaes[a,b], Steven Raeymaeckers[c], David Robben[b,d], Guido Wilms[e], Dirk Vandermeulen[b], Cesar Libanati[a], Marc Debois[a]
[a]*UCB Pharma, Brussels, Belgium*
[b]*Medical Image Computing, ESAT-PSI, Department of Electrical Engineering, KU Leuven, Leuven, Belgium*
[c]*Department of Radiology, University Hospital Brussels, Brussels, Belgium*
[d]*icometrix, Leuven, Belgium*
[e]*Department of Radiology, KU Leuven, Leuven, Belgium*

Objective: Develop a fully automated method to identify individual fractured vertebrae in computed tomography (CT) scans.

Background: Despite their frequent occurrence and major associated burden, vertebral fractures remain underdiagnosed and patients under-treated.[1] Spine-containing CT scans provide an opportunity to identify vertebral fractures, yet they commonly go unreported by radiologists.[2]

Automated detection of vertebral fractures would enhance medical care of patients with osteoporosis.

Methods: We built a training database of 90 de-identified CT cases, acquired on three different scanners, containing 969 vertebrae scanned for various indications (average [range] age: 81 [70-101] years; 64% female).[3] We developed a data-driven, automated vertebral fracture detection method that binarily classifies fractured or normal anatomy for each vertebra present in spine-containing CT images.

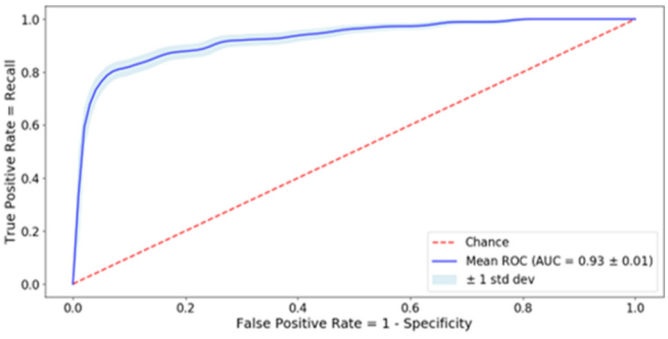

AUC: area under the curve; ROC: receiver operating characteristic

Fig.

Results: We performed a stratified 5-fold cross-validation experiment comparing automated predictions with ground truth readouts from one radiologist resulting in an area under the Receiver Operating Characteristic (ROC) curve of 0.93±0.01.

Conclusions: Our automated vertebral fracture demonstrated the potential for automated early identification of vertebral fractures in patients aged >50 years by opportunistically screening spine-containing CT images. Confirmatory analyses and additional methodological improvements (e.g. automatic Genant grading, fracture location) using more extensive datasets and method validation are ongoing.

References: 1. Johnell O. Osteoporos Int 2006;17:1726-33; 2. Mitchell R. Arch Osteoporos 2017;12:71; 3. University Hospital Brussels Ethical Committee approval: "Designing deep learning algorithms for the automated detection of vertebral fractures", B.U. N. 143201732477.

Acknowledgements: This study was funded by UCB Pharma and Amgen Inc. Medical writing services were provided by Costello Medical.

doi:10.1016/j.bonr.2020.100539

P238

Vertebral fracture and osteoporosis screening from routine CT as an added EXtra - the VORTEX study

Daniel D.G. Chappell[a], Simona D'Amore[b], Keenan Brown[c], Emma Gerety[d], Kenneth E.S. Poole[b]

[a]*Department of Medicine, Cambridge NIHR Biomedical Research Centre, Cambridge, United Kingdom*

[b]*Department of Medicine, University of Cambridge, Cambridge, United Kingdom*

[c]*Mindways Software, Austin, United States*

[d]*Department of Radiology, Cambridge University Hospitals NHSFT, Cambridge, United Kingdom*

Vertebral fractures (VFs) are under-diagnosed in Computed Tomography (CT). There is also a need to develop fracture detection tools that can diagnose osteoporosis. We describe the development of a VF detection tool, SlicePick-MT, that uses quantitative-morphometry to assess suspected VFs in CT datasets collected during a previous audit of 325 patients who had undergone CT scanning for reasons unrelated to osteoporosis.

The detection rate of SlicePick-MT was compared against the current standard, comprising Optasia's ASPIRE™ fracture detection service, which includes a radiologist over-read. Local radiologists verified the Optasia diagnoses. Bone Mineral Density (BMD) in each patient was estimated by spine Quantitative CT(QCT) and hip CT X-ray absorptiometry (CTXA) using Mindways software.

The SlicePick-MT method detected 50 true VF patients compared with 46 VF patients detected by ASPIRE™. SlicePick-MT had a higher sensitivity (98.0%) and specificity (99.6%) than ASPIRE™ (93.9%, 98.4% respectively). Patients with VFs had lower average spine BMD (76.75mg/cm^3 ± 24.58) compared with those without VFs (111.15mg/cm^3 ± 34.97, p>0.0001). Femoral neck BMD was lower in VF patients, 0.600g/cm^2 than non-fracture patients, 0.696g/cm^2 (p>0.005). Spine BMD was a better discriminator of VFs than femoral neck BMD, by Area Under the Curve analysis (AUC, Spine BMD = 0.79, Femoral Neck BMD = 0.7). Eighty-five patients were found to have osteoporosis by either Spine QCT or CTXA of the hip. However, only 30 of these patients were previously known to have osteoporosis.

When applied to routinely-acquired CT datasets, the SlicePick-MT method detected more fractures than the current standard of VF detection. QCT combined with the SlicePick-MT method (the VORTEX pathway) enabled diagnosis of osteoporosis alongside VF detection. There is potential for hospitals to utilise the VORTEX pathway for opportunistic osteoporosis diagnosis, which may reduce the number of future osteoporotic fractures.

doi:10.1016/j.bonr.2020.100540

P239

MRI assessment of bone microarchitecture in Human Bone samples: The issue of air bubbles artefacts

Enrico Soldati[a], David Bendahan[b], Martine Pithioux[c], Jerome Vicente[a]

[a]*IUSTI, AixMarseille University, Marseille, France*

[b]*CRMBM, Marseille, France,*

[c]*ISM, AixMarseille University, Marseille, France*

With the aim of assessing bone microarchitecture, several studies have intended to use MRI, but the issue of air bubbles artefacts has been very scarcely reported.

In the present study, we assessed air bubbles-related artefact in MR images of human bone samples and intended to design a protocol to eliminate them. The method was validated using TSE MRI at 3T and high-resolution X-rays micro tomography (μCT) (fig. 1). Morphological parameters computed from MRI recorded with and without the air bubbles artefacts were compared to those obtained from X-ray micro tomography. The human femurs head were also scanned using MRI at 3T and the corresponding metrics were compared to those obtained using μCT (fig. 2).

The results show that we are able to eliminate the 98.7% of the air bubbles using our protocol in less than 30 minutes. We also show a reduction of the committed error on the calculation of the morphological parameters when comparing the MRI-derived parameters calculated before and after the application of our designed protocol when compared with the ground truth provided by the μCT.

To conclude, we presented an efficient air removal method for the imaging assessment of large humans bone samples.

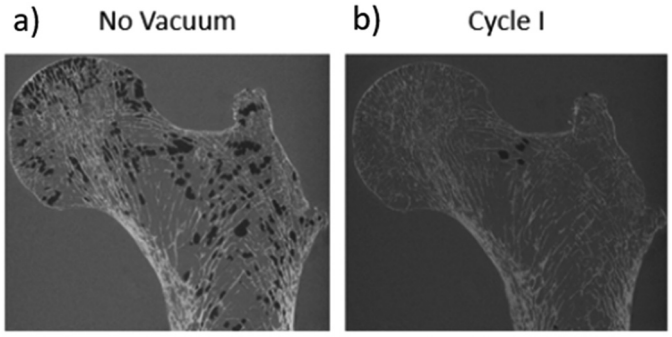

c)

	no vacuum	cycle 1	cycle 2	cycle 3
Vol mm³	12427.07	154.18	103.8	27.72
Vol %	100	1.24	0.83	0.22

a) and b) same coronal plane before and after sample preparation. c) list of air bubbles volumes.

doi:10.1016/j.bonr.2020.100541

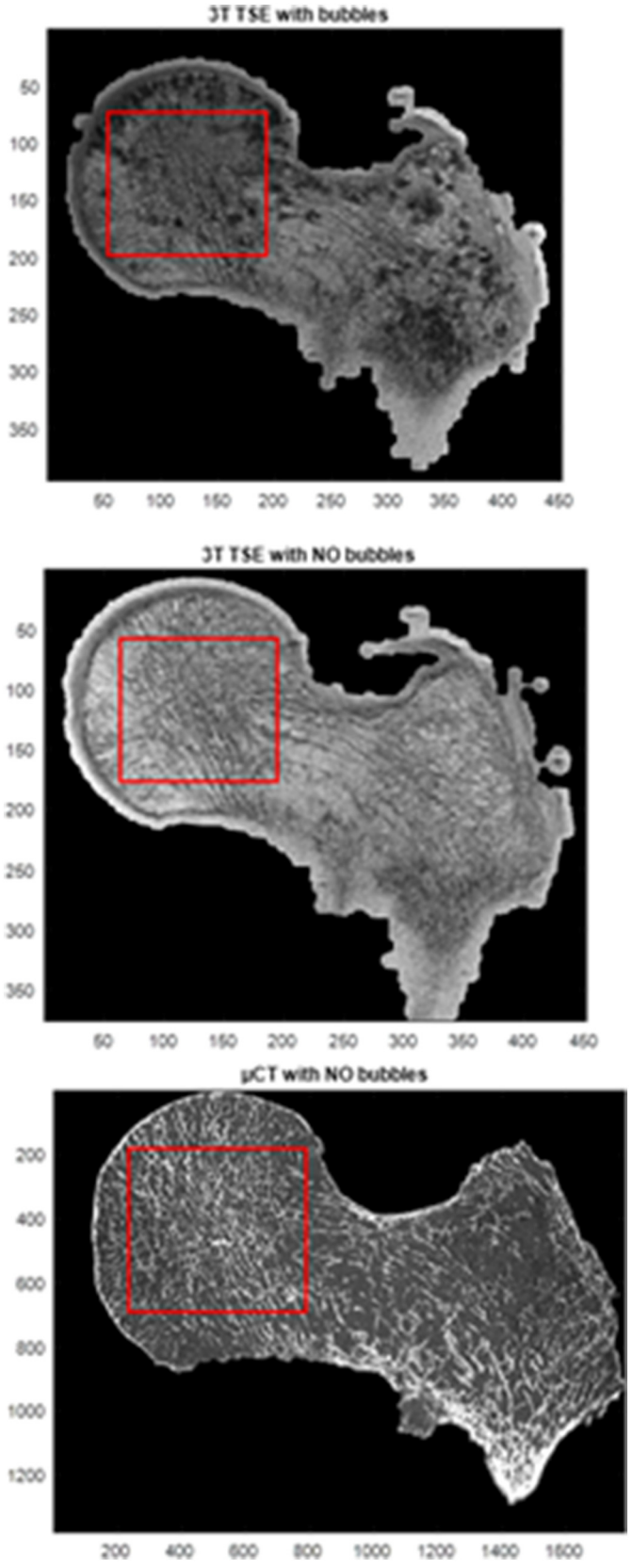

Same coronal plane for the three different acquisitions (before, after sample preparation and µCT.

P240

Trabecular bone microarchitecture: A comparative analysis between high field, ultra high field MRI and X-ray micro CT in humans anatomical samples

Enrico Soldati[a], Martine Pithioux[b], Jerome Vicente[a], David Bendahan[c]
[a]*IUSTI, AixMarseille University, Marseille, France*
[b]*ISM, AixMarseille University, Marseille, France*
[c]*CRMBM, AixMarseille University, Marseille, France*

It has been previously suggested that trabecular bone could be assessed using ultra-high and high-field MRI. In the present study, human femurs head were scanned using with MRI at 3T and 7T MRI and the corresponding metrics were compared to those obtained using high resolution X-ray micro tomography. in the present study four different MRI acquisition were performed i.e. turbo spin echo and gradient echo at 3T and 7T and compared to µCT images. In vivo MRI of human head femur further confirmed that Turbo Spin Echo sequences are less prone to partial volume effects as compared to GRE sequences, in agreement with previous results. Ultra High field (UHF) MRI can provide histomorphometric metrics comparable to those obtained with µCT imaging thereby indicating that UHF MRI could be considered as the new non invasive imaging modality for the assessment of bone microarchitecture and more particularly for osteoporosis risk stratification.

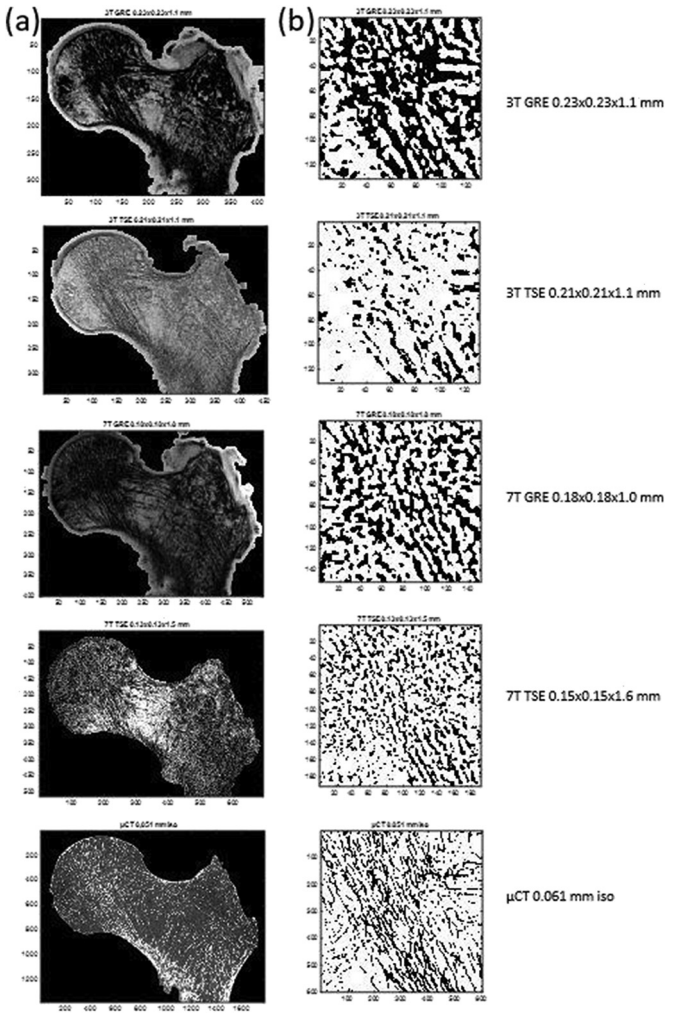

(a) Same coronal planes of MRI acquisitions and µCT. Red squares identify ROI, b) ROI binarized.

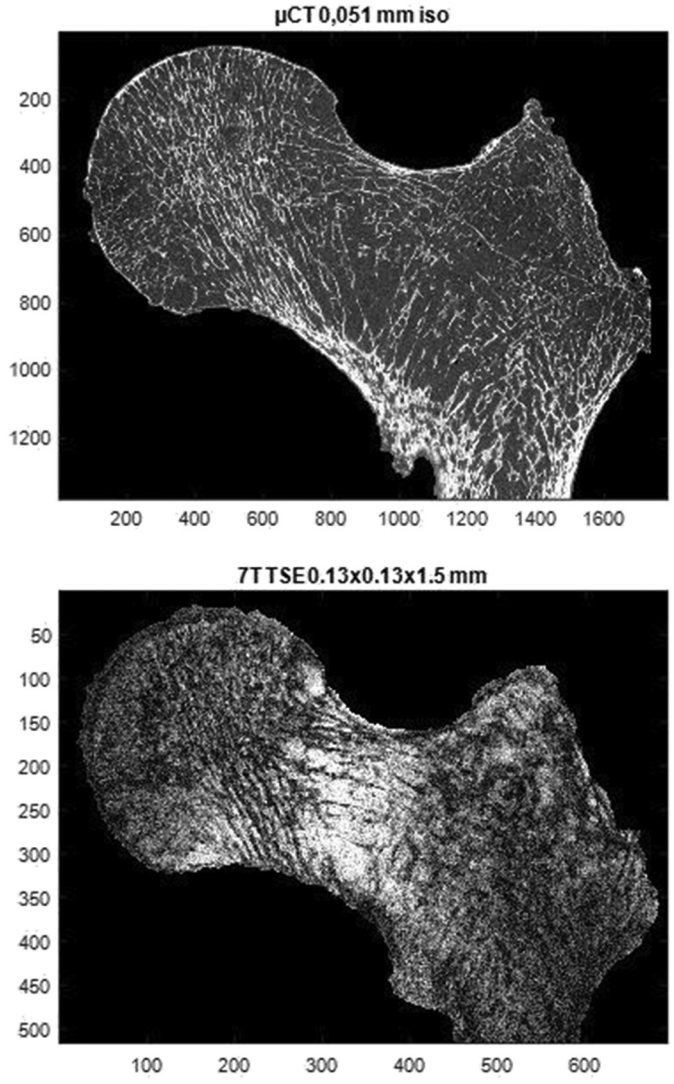

Same coronal plane for 7T TSE MRI and µCT.

	BMD				Tb.Th				Tb.Sp				Tb.N			
	mean	std	err %	p-value	mean	std	err %	p-value	mean	std	err %	p-value	mean	std	err %	p-value
µCT	0,23	0,00	0,00		0,33	0,04	0,00		1,16	0,00	0,00		0,74	0,03	0,00	
3T TSE	0,18	0,02	19,07	0,01	0,66	0,04	100,02	0,0007	2,07	0,25	78,52	0,0032	0,40	0,05	46,68	0,0006
3T GRE	0,52	0,02	126,72	3,6E-05	1,38	0,06	321,50	1,4E-05	1,36	0,06	16,89	0,0036	0,48	0,16	34,77	0,0488
7T GRE	0,39	0,01	71,71	3,7E-06	0,88	0,03	167,88	6,8E-05	1,27	0,02	9,38	0,0015	0,54	0,11	27,49	0,0393
7T TSE	0,22	0,01	3,13	0,44	0,40	0,01	23,33	0,039	1,04	0,08	10,08	0,0055	0,68	0,03	8,75	0,0072

Mean, std, committed error and p-value of the calculated features for MRI and µCT images.

doi:10.1016/j.bonr.2020.100542

P242

Morphodensitometry in patients with diabetes

Karen Vartanyan
Radiotherapy and Radiology, Russian Academy of Advanced Medical Studies, Moscow, Russian Federation

The aim of our study was to use image analysis technology based on morphofunctional approach which include image analysis of x-ray films and results of x-ray osteodensitometry to design a new quantitative method of bone investigation.

Materials and methods: Materials of our pilot study were fragments of x-results from 16 patients with diabetes mellitus type 1.7 patients had a diagnosis of osteopenia and 9 with osteoporosis which were based on routine x-ray and osteodensitometry (OD) methods. We used a information technology based on a dual image analysis of x-rays and OD using computerised morphodensitometry (CMDM). CMDM is a medicobiological oriented densitometric image analysis for evaluation of quantitatve morphofunctional parametres of bone .Using CMDM we evaluated quantitative features MDM of bone (FMDM).

Results: On the first stage of our study using method of multi-variation statistics to study the most informative regions of interest diagnosed by routine methods we can show referance data in arbitrary units, routine methods - 75 $\pm$ 3,osteopenia 61 $\pm$ 6($p< 0.01$), osteoporosis 40 $\pm$ 3($p< 0.01$). FMDM -100 $\pm$ 8, osteopenia - 45 $\pm$ 6 ($p< 0.01$), osteoporosis -20 $\pm$ 5 ($p< 0.001$). As we see the new quantitative parametre FMDM have changed in amplitude more then 10 higher then routine methods.

Conclusion: FMDM is a more specific method of bone assesment. It could be a new diagnostic mareker of bone metabolic control.

doi:10.1016/j.bonr.2020.100543

P243

Usefulness of new technologies based on dual-energy x-ray absorptiometry in patients with growth hormone deficiency or acromegaly

Antonia Garcia-Martin[a,b], Sheila González-Salvatierra[a,b], Beatriz García-Fontana[a,b], María Dolores Avilés-Pérez[a,b], Enrique Moratalla[c], Rafael Nieto[c], Diego Becerra[c], Luis Gracia-Marco[d], Manuel Muñoz-Torres[e]

[a]*Bone Metabolic Unit, Endocrinology and Nutrition Division, Hospital Universitario San Cecilio, Instituto de Investigación Biosanitaria de Granada (Ibs.GRANADA), Granada, Spain*
[b]*CIBERFES, Instituto de Salud Carlos III, Granada, Spain*
[c]*Medicine Nuclear Division, Hospital Universitario San Cecilio, Granada, Spain*
[d]*PROFITH "PROmoting FITness and Health Through Physical Activity" Research Group, Sport and Health University Research Institute (iMUDS), Department of Physical and Sports Education, Faculty of Sport Sciences, University of Granada, Granada, Spain*
[e]*Department of Medicine, Universidad de Granada, Granada, Spain*

Growth hormone (GH) and insulin growth factor 1 (IGF1) have anabolic effects on bone metabolism. GH deficiency (GHD) causes a low bone mineral density (BMD) and high risk of fragility fractures. In patients with acromegaly, an increased risk of vertebral fracturas and controversial data on BMD has been reported. Areal dual-energy x-ray absorptiometry (aDXA) does not capture bone quality or discriminate trabecular and cortical compartment. Recent advances in DXA include software to estimate index of bone microstructure in lumbar spine: Trabecular Bone Score (TBS) and volumetric bone mineral density (vBMD) from hip aDXA scans (3D-DXA). We aimed to explore the hypothesis that TBS and 3D-DXA would be useful in the bone evaluation of patients with GHD and acromegaly. We performed a cross-sectional study in 15 patients with GHD and 20 with acromegaly and we compared TBS values (TBS insight® software) and trabecular and cortical vBMD, cortical surface (sBMD) and cortical thickness (3D-DXA SHAPER software) with 34 age- and sex-matched healthy controls. In table shows results according to the study group. We found differences statistically significant between three groups in cortical vBMD ($p=0,005$) and cortical sBMD ($p=0,012$) but not in TBS values. Patients with GHD showed significantly lower cortical vBMD ($p=0,009$) than healthy controls

while that patients with acromegaly showed significantly higher cortical sBMD (p=0,044), cortical thickness (p=0,042) and TBS values (p=0,045) than healthy controls. According to our results, new techniques applied to DXA provide additional information on bone in states of deficiency or excess of GH.

doi:10.1016/j.bonr.2020.100544

P244

Prevalence of non modifiable and modifiable risk factors of osteoporosis in health care workers of < 40 years at tertiary health centre of remote India

Amit Saraf
TMU, Amritsar, India

Introduction: Osteoporosis is a global problem occurring in every geographic area and affecting 150 million men and women worldwide. Osteoporosis is defined as a reduction of bone mass (or density) or the presence of a fragility fracture. Aim of the study is to gain knowledge of prevalence and identifying risk factors among health care workers and in turn increasing the awareness, education, prevention, and treatment of osteoporosis.

Material and methods: This study is based on International Osteoporosis Foundation (one minute risk test) questionnaire performed on health care workers over the age of 18 years at a tertiary health centre in a remote region of India. A total of 470 health care professionals were included in this study of which 180 were women and 290 men

Results: Non-modifiable risk factors i.e family history was positive in 36.55% male and 48.3% females. H/O Rheumatoid arthritis(M-7.58%, F-11.1%),Corticosteroid use(M-6.89% F-8.33%), H/O Type 1 DM, overactive thyroid, increased PTH(M-8.62% F-5%), Nutritional disorders(M-8.62% F-8.33%), Recurrent falls (m-1.37% f-1.11%). Modifiable risk factors such as Alcohol intake (>2 units/day, M-33.10% F-13.8%),Smoking (M-46.55% F-21.11%), Sun light exposure (< 10 min,M-6.55% F-40.55%), Physical activity (< 30 min/day, M- 14.44% F-42.22%),Allergies to dairy products with no calcium supplementation(M-13.44% F-23.10%) were calculated.

Conclusion: In spite of an awareness of osteoporosis and its risk factors among health professionals, high prevalence of modifiable and non modifiable risk factors was found. Since more than 50% of general population in this part of world is illiterate, a much higher prevalence is expected in then. There is a need to educate this high risk population at the earliest to prevent this disease by implementing national or international health strategies to tackle this increasing global health problem.

doi:10.1016/j.bonr.2020.100545

P245

The assessment of osteoporosis and fracture risk in patients undergoing medical rehabilitation

Larisa Marchenkova, Ekaterina Makarova
Rehabilitation Department for Somatic Patients, National Medical Research Center for Rehabilitation and Balneology of Ministry of Health of Russian Federation, Moscow, Russian Federation

The aim of the study was to evaluate the risk of osteoporosis and related fractures in the patients treating in in-patient rehabilitation department.

Methods: The survey was conducted by means of questionnaire of 600 patients aged >50 y.o. ordinary treated in in-patient department of rehabilitation center. Risk factors for osteoporosis were assessed using IOF "One-minute osteoporosis risk test". 10-year absolute risk for osteoporotic fractures was calculated using Russian scale of FRAX® on-line calculator.

Results: Assessment of osteoporosis risk factors revealed that 58.2% of responders had no risk factors, 6.8% had one risk factor, 3.8% - two, 0.6% - three, 9.1% - four, 21.5% - five or more risk factors. 45.8% of responders had experienced non-traumatic fractures in past, and a fractures occurred during rehabilitation procedures in 4.6% of ones. High 10-year absolute fracture risk was revealed in 38% of all respondents, in particular in 45.7% of women and in 16.6% of men. The average 10-years risk for major osteoporotic fractures was 13.7% [1.6; 48.0] and for the hip fracture - 3.2% [0;16]. 8.6% of patients had 10-year absolute risk for major osteoporotic fractures more than 30%. 42.5% of respondents performed bone densitometry in the past. Osteoporosis was already diagnosed in 34.1% of respondents but only in 56.6% (n=127) of high fracture risk group. Among those who never undergo densitometry there were 43.1% of patients with a high fracture risk. Anti-osteoporoitic treatment received just 31.0% among osteoporotic patients and 12.4% among subjects with high fracture risk.

Conclusions: 45.7% of women and in 16.6% of men aged >50 y.o. ordinary treated in in-patient rehabilitation department had high osteoporotic fracture risk, 41.2% patients had osteoporosis risk factors and 45.8% experienced non-traumatic fractures in past. Data indicate a high probability of non-traumatic fractures in those patients due to concomitant insufficient prescription of anti-osteoporotic medication.

doi:10.1016/j.bonr.2020.100546

P247

Association between self-rated health and 10-year risk of hip fracture in a cohort of older women

Elin Uzunel, Hans Lundin, Per Wändell, Helena Salminen
Neurobiology, Care Sciences and Society, Karolinska Institutet, Huddinge, Sweden

Objective: Fragility fracture of the hip is common and will probably increase in numbers due to increased life expectancy. It is associated with increased morbidity and mortality. By identifying high-risk individuals, fractures can be prevented. Low self-rated health (SRH) has been suggested to be a risk marker for future hip fractures. The aim of our study was to explore the 10-year association between SRH and hip fracture in older community dwelling women.

Methods: This is a prospective cohort study of 351 Swedish women, aged between 69 and 79 years (median 72.4). SRH was assessed at baseline by answering the question “How would you rate your health right now” by putting a mark on a visual-analogue scale (0-100 mm). Data on hip fracture and mortality during the following ten years was collected from health care registers. For statistics we used Cox proportional hazards regression model. SRH was divided into tertiles, where low and intermediate assessed SRH were compared to high SRH regarding the association of future hip fracture.

Results: The age-adjusted hazard ratio (HR) for hip fracture was significantly higher in the low-tertile of SRH (HR: 3.17 (95% CI 1.25-8.01) and intermediate-tertile of SRH (HR: 2.75 (95% CI 1.08-7.04) using high-tertile as reference. HR increased when we added bone mineral density (at the femoral neck) to the model. The total number of hip fractures was 40. The median value of SRH was 62 mm (IQR 50-81 mm).

Conclusion: In our cohort of older women, poor SRH indicated a higher risk of suffering a hip fracture. SRH might be a marker that can add information about the future risk of hip fractures in older women.

Keywords: self-rated health, fragility fractures, hip fracture, osteoporosis, aged women

doi:10.1016/j.bonr.2020.100547

P248

Validation of algorithms to identify osteoporotic hip fractures in the claim database

Young-Kyun Lee[a], Dong Won Byun[b], Deog-Yoon Kim[c], Ha-Young Kim[d], Youjin Lee[e], Yong-Chan Ha[f], Ho-Yeon Chung[c], SNUBH-KSBMR

[a]*Seoul National University Bundang Hospital, Seongnam, Republic of Korea*
[b]*Soonchunhyang University Hospital, Seoul, Republic of Korea*
[c]*Kyung Hee University Medical Center, Seoul, Republic of Korea*
[d]*Wonkwang University Sanbon Hospital, Gunpo, Republic of Korea*
[e]*National Cancer Center, Goyang, Republic of Korea*
[f]*Orthopedic Surgery, Chung-Ang University College of Medicine, Seoul, Republic of Korea*

Background: There remains no standard operational definition for patients with osteoporotic hip fracture in the national claim database. The purpose of the study was (1) to establish the operational definitions to identify osteoporotic hip fracture, and (2) to evaluate the validity of the operational definition in real administrative data from hospital discharge claims.

Methods: Operational definitions were developed by using diagnostic codes for femoral neck and intertrochanteric fractures and procedure codes for hip fracture surgeries. To validate the operational definitions, we conducted a retrospective study of 910 patients who underwent hip surgery from our tertiary hospital in 2018. Osteoporotic hip fracture was defined as a femoral neck and intertrochanteric fracture caused by falling from height level. For validity, we calculated the sensitivity/specificity and positive/negative predictive values of the final operational definition.

Results: Among 910 patients, a total of 298 (32.7%) were identified as true (conceptual) osteoporotic hip fracture in 2018. The operational definition of osteoporotic hip fracture was established by a combination of 2 diagnosis codes and 11 procedure codes. The final operational definition showed a specificity of 99.0% and a positive predictive value of 95.8%.

Conclusion: The proposed operational definition of osteoporotic hip fracture showed satisfactory validity and provided a simple tool to perform research using medical claim databases.

doi:10.1016/j.bonr.2020.100548

P249

Incidence and mortality of subsequent vertebral fractures: Analysis of claims data of the Korea National Health Insurance Service from 2007 to 2016

Young-Kyun Lee[a], Yong-Chan Ha[b], Deog-Yoon Kim[c], Dong Won Byun[d], Youjin Lee[e], Ha-Young Kim[f], Ho-Yeon Chung[c], SNUBH-KSBMR

[a]*Seoul National University Bundang Hospital, Seongnam, Republic of Korea*
[b]*Orthopedic Surgery, Chung-Ang University College of Medicine, Seoul, Republic of Korea*
[c]*Kyung Hee University Medical Center, Seoul, Republic of Korea*
[d]*Soonchunhyang University Hospital, Seoul, Republic of Korea*
[e]*National Cancer Center, Goyang, Republic of Korea*
[f]*Wonkwang University Sanbon Hospital, Gunpo, Republic of Korea*

Objective: The purpose of our study was to determine trends in the incidence and mortality of subsequent vertebral fractures after first-time vertebral fracture in Koreans older than 50 years using the national claims database.

Methods: The national claims data set was analyzed to find all new visits and revisits after 6 months from the last claim to a hospital or clinic for vertebral fractures and revisits in men and women aged 50 years or older between 2007 and 2016. The number of first-time vertebral fractures in 2012 was investigated to determine subsequent vertebral fractures. The incidence, mortality rates, and SMR of subsequent vertebral fractures were calculated. There were no sources of funding and no conflicts of interest associated with this study.

Results: During the 4-year follow-up period, the overall cumulative incidence of subsequent vertebral fractures were 27.53%. According to sex, the cumulative incidence of subsequent vertebral fractures was 20.09% in men and 29.98% in women. The cumulative mortality rate over the first year after subsequent vertebral fractures was 5%. The mortality rates over 1 year were 10.04% for men and 3.81% for women. The overall SMR at the 1-year follow-up after subsequent vertebral fractures was 10.58 (95% confidence interval: 9.29-12.05) in men and 3.88 (95% confidence interval: 3.5-4.3) in women.

Conclusions: Our study showed that subsequent vertebral fractures were more common in women, with an incidence rate of 29.98% over 4 years. However, the mortality rate was higher in men, reaching 10.04% in 1 year. Subsequent vertebral fractures occurred in large numbers, and the mortality rates were relatively high. Thus, first vertebral fracture may be considered as an early warning of high risk for future subsequent vertebral fractures, especially in women.

doi:10.1016/j.bonr.2020.100549

P250

Assessment of self-reported fractures: data from the FRISBEE cohort

Felicia Baleanu[a], Michel Moreau[b], Virginie Kinnard[c], Laura Iconaru[a], Rafik Karmali[a], Serge Rozenberg[d], Michel Rubinstein[e], Marianne Paesmans[b], Pierre Bergmann[f], Jean-Jacques Body[a]

[a]*Department of Endocrinology, CHU Brugmann, Université Libre de Bruxelles, Brussels, Belgium*
[b]*Data Centre, Inst. J. Bordet, Université Libre de Bruxelles, Brussels, Belgium*
[c]*Department of Internal Medicine, CHU Brugmann, Université Libre de Bruxelles, Brussels, Belgium*
[d]*Department of Gynecology, CHU St Pierre, Université Libre de Bruxelles, Brussels, Belgium*
[e]*Department of Nuclear Medicine, Ixelles Hospital, Université Libre de Bruxelles, Brussels, Belgium*
[f]*Department of Nuclear Medicine, CHU Brugmann, Université Libre de Bruxelles, Brussels, Belgium*

Most fracture cohort studies rely on participant self-report of fracture event. This approach may lead to fracture underreporting. The purpose of the study was to assess the rate of non-reported fractures in a well-characterized population-based cohort of 3560 postmenopausal women, aged 60-85 years, included in the Fracture Risk Brussels Epidemiological Enquiry (FRISBEE) study.

Incident low-traumatic or non-traumatic fractures were registered annually during phone calls. In 2018 we reviewed the medical files of 67.9% of our study participants and identified non-reported fractures (false negative (FN) fractures). We also evaluated whether the rate of FN fractures was influenced by baseline patients' characteristics and fracture risk factors.

Over a median follow-up period of 9.2 years, we registered 992 fractures (781 by self-report, confirmed by a radiological report and 211 unreported).

The global FN rate for all fractures was 21.3%, including 22% for MOFs (major osteoporotic fractures), 13.1% for other major fractures and 25.8% for minor fractures. The rate of FN fractures varied by fracture site: for MOFs, it was 2.7% at the hip, 5.3% at the proximal humerus, 7.1% at the wrist and 46.5% at the spine. For other major fractures, the highest rate of FN fractures was found at the pelvic bone (21%), followed by the elbow (17.9%), long bones (10.5%), ankle (6.2%) and knee (5.9%).

Older subjects (OR 1.7; 95% CI, 1.2-2.4; P = 0.003), subjects with early non-substituted menopause (OR 1.8; 95% CI, 1.0-3.3; P = 0.04), with a lower education level (OR 1.5; 95%CI, 1.1-2.2; P = 0.01) and those under drug therapy for osteoporosis (OR 1.5; 95% CI, 1.0-2.2; P = 0.05) were associated with a higher rate of FN.

In conclusion, underreporting of fracture events will influence any model of fracture risk prediction and induce bias when estimating the associations between candidate risk factors and incident fractures.

doi:10.1016/j.bonr.2020.100550

P252

Awareness of osteoporosis and adherence in treatment in Greece

George Trovas, Efthymia Karlafti, Symeon Tournis, Kalliopi Lampropoulou-Adamidou, Eriona Ibro, Ismene Dontas
National and Kapodistrian University of Athens, Athens, Greece

Objectives: Several studies have revealed that adherence to anti-osteoporotic treatment is low, due to low compliance and persistence to anti-osteoporotic treatment. This leads to increased fracture risk. The aim of this retrospective observational study, is to record the opinion of the general population in Greece about osteoporosis and the degree of adherence that Greek patients have to anti-osteoporotic treatment.

Materials and Methods: 2977 individuals, from which 2230 were men (mean age 67.32) and 2747 were women (mean age 63.06) were asked their opinion about osteoporosis, and the importance of the anti-osteoporotic treatment. The participants filled in a questionnaire about the severity of osteoporosis; the importance of anti-osteoporotic treatment, and the importance of non-pharmaceutical measures for bone health (exercise, nutrition). The respondents were asked if they had a medical history of bone fracture, if they had ever had a bone mineral density (BMD) measurement, if they had been diagnosed with osteoporosis, and if they were under any anti-osteoporotic treatment. Moreover, they were asked about the length of time they spent under treatment and their reasons for discontinuation.

Results:

• 39.3% of the participants (1003 people), despite the fact that they think of osteoporosis as a serious disease, have never had a BMD measurement

• 7.9% of the participants who were diagnosed with osteoporosis, have received no treatment

• 43.7% of the participants who were under anti-osteoporotic treatment, received the treatment for 2 years continuously

• 22.7% of the participants with a history of bone fracture have received no treatment

• The main reason for discontinuation of treatment was the fear of side effects (24,5%), and the second most frequent reason was gastrointestinal disturbances (19%)

Conclusions: Despite the fact that the general population in Greece thinks of osteoporosis as a serious disease, low adherence is something that was confirmed in our study.

doi:10.1016/j.bonr.2020.100551

P253

Identification of bone fragility risk by a self-assessment in an orthopaedic surgery unit

Odile Reynaud Levy[a], Xavier Flecher[b], Damien Lami[b], Pierre Olivier Pinelli[b], Mathieu Ollivier[b], Jean Noel Argenson[b]
[a]*APHM, Marseille, France*
[b]*Orthopaedic Surgery, APHM Ste Marguerite, Marseille, France*

Osteoporosis is a general systemic skeletal disorder characterized by a decreased bone formation and an increased bone resorption. It is a major public health subject because of it's high frequency, because of a consequent increase in susceptibility to fracture and because of it's impact on mortality. Bone health screening plays a vital role in the early diagnosis and treatment of this pathology. But this evaluation is long and few practitioners can do it ; so there is an underdiagnosis of osteoporosis, which is a chronic disease. We want to introduce a screening tool to identify individuals at risk for osteoporosis and prioritize them for bone health check-up. We present here the first step before installation of this self- assessment. We tested it's feasibility in a planned orthopaedic surgery unit.

doi:10.1016/j.bonr.2020.100552

P255

Ultrastructure of bone mineral of the hipbone after tibia fracture and oral intake of calcium drugs

Artur Koch'jan[a], Lyudmila Savenko[b], Anna Samokish[b], Dmitry Kolesnikov[b], Anna Govorova[b], Yuliya Vesenko[b]
[a]*SBHI 'Staritskaya CDH', Staritsa, Russian Federation*
[b]*State Establishment of Lugansk People's Republic Saint Luka Lugansk State Medical University, Lugansk, Ukraine*

Aim: Of the study is to test ultrastructure of bone mineral of the hipbone after tibia fracture and to consider possibilities of treatment of fracture sequelae with nutrient Biomin MK.

Material and methods: For the purposes of the experiment we selected 126 male rats with body weight of 135-145 grams and then 3 experimental groups were formed. Group 1 - controls, group 2 - animals with 2.2 mm round reach-through holes in both tibiae, and group 3 comprised animals with fracture that received Biomin MK in dosage of 90 mg/kg. Upon expiration of observation terms (7, 15, 30, 60, 90, and 180 days) the animals were withdrawn from the experiment by means of anesthetized decapitation. Bones were excised and prepared for X-ray scatter analysis.

Results: Fracture of the tibia resulted in instability of mineral crystal lattice with peak found by the 30^{th} and the 60^{th} days. Derangement manifestations were like the following: crystallites enlargement (by 7.09%, 13.78%, 13.86%, 11.90%, and by 8.41% in the period from the 7^{th} up to the 90^{th} day) in comparison with group 1, and microtexture coefficient decrease - by 7.41%, 12.40%, 10.87%, and 10.26% with respect from the 7^{th} up to the 60^{th} day. Biomin MK intake resulted in faster restoration of the crystal lattice features in the period from the 30^{th} to the 90^{th} day - crystallites dimensions decreased in comparison with group 2 by 3.49%, 3.68%, and 3.01%, and microtexture coefficient on the contrary increased by 4.08% by the 30^{th} day.

Conclusion: A simple injury to the tibia results in derangement of the ultrastructure of the bone mineral of the hipbone. Degree of derangements depends on regeneration activities. Biomin MK intake restores deranged ultrastructure of the bone mineral, which is visible in the period from the 30^{th} to the 90^{th} days.

doi:10.1016/j.bonr.2020.100553

P256

Functional validation of the osteoporosis GWAS candidate *FUBP3* in knockout mice

Laura Watts, Bernard Freudenthal, Natalie C. Butterfield, Andrea Pollard, Davide Komla-Ebri, Victoria Leitch, John Logan, Naila Mannan, J.H. Duncan Bassett, Graham R. Williams
Imperial College London, London, United Kingdom

Osteoporosis affects millions of people worldwide, resulting in an enormous healthcare burden and major socioeconomic costs. Bone mineral density (BMD) is a highly heritable quantitative trait and the major risk factor for fracture. We and others have identified non-coding single nucleotide polymorphisms that define an independent locus on chromosome 9 associated with both height and BMD in large scale GWAS. FUBP3 is the closest coding gene and is expressed in osteoclasts and cells of the osteoblast lineage. FUBP3 is a DNA and RNA binding protein and transcriptional regulator of c-myc. Although myc has been implicated in the maintenance of bone mass during aging, the role of FUBP3 in bone is unknown. We hypothesised that FUBP3 represents the causative gene at this locus and investigated its functional role in the skeleton *in vivo*.

FUBP3 deficient mice (*Fubp3*$^{-/-}$, n=6-9 per sex, per genotype, per age, local ethical approval) had short stature at postnatal day 70 (P70) (vs. WT, $p< 0.001$, ANOVA) and P183 (vs. WT, $p< 0.001$, ANOVA). Caudal vertebrae were correspondingly short at P21 (vs. WT, $p< 0.05$, ANOVA), P70 (vs. WT, $p< 0.001$, ANOVA) and P183 (vs. WT, $p< 0.001$, ANOVA). Bone mineral content, measured by x-ray microradiography, was decreased in femurs (vs. WT, $p< 0.05$, Kolmogorov-Smirnov test) and caudal vertebrae (vs. WT, $p< 0.01$, Kolmogorov-Smirnov test), but markedly decreased in lumbar vertebrae (vs. WT, $p< 0.001$, Kolmogorov-Smirnov test). Adult *Fubp3*$^{-/-}$ mice also displayed reduced femoral trabecular thickness and BMD determined by micro-CT (vs. WT, $p< 0.05$, ANOVA).

Together, these data provide functional evidence of a novel role for FUBP3 in bone development and maintenance, defining *FUBP3* as the causative gene associated with BMD at this GWAS locus.

doi:10.1016/j.bonr.2020.100554

P257

The potential for opportunistic identification of vertebral fractures in patients undergoing a CT scan as part of daily clinical practice: Descriptive study using registry data

Michael Kriegbaum Skjødt[a,b], Joeri Nicolaes[c], Christopher Dyer Smith[d], Jonas Banefelt[e], Florence Lebon[c], Cesar Libanati[c], Kim Rose Olsen[f], Cyrus Cooper[g,h], Bo Abrahamsen[a,b,h]
[a]*Department of Medicine, Holbæk Hospital, Holbæk, Denmark*
[b]*OPEN, Open Patient data Explorative Network, Odense University Hospital, Odense, Denmark*
[c]*UCB Pharma, Anderlecht, Belgium*
[d]*Department of Clinical Research, University of Southern Denmark, Odense, Denmark*
[e]*Quantify Research, Stockholm, Sweden*
[f]*Danish Centre for Health Economics, University of Southern Denmark, Odense, Denmark*
[g]*MRC Lifecourse Epidemiology Unit, University of Southampton, Southampton General Hospital, Southampton, United Kingdom*
[h]*NDORMS, Nuffield Department of Orthopaedics, Rheumatology and Musculoskeletal Sciences, University of Oxford, Oxford, United Kingdom*

Objective: The benefits of opportunistic screening for vertebral fractures (VF) using CT scans performed as part of daily clinical practice (*routine CT*) will depend both on the diagnostic performance of the method and on the proportion of referrals already diagnosed with VF or treated for osteoporosis. Our aim was to assess the potential for opportunistic screening for VF in patients undergoing a routine CT locally.

Methods: 2,000 consecutive men and women, aged ≥50 years, undergoing a CT of the thorax, abdomen and/or pelvis from January 2010. Patients were matched 1:3 on age and gender against a background population cohort from the same geographic region and year. Data were retrieved from Danish Health Registers.

Results:

	CT scan population (n=2,000)	Background population controls (n=5,923)
Age, mean (years)	70.2	70.3
Gender, % men	51.6	51.5
Medical history, %[1]		
- Vertebral fracture	1.5	0.6
- Major osteoporotic fracture	14.2	11.7
- Osteoporosis	3.5	3.0
Medications, %		
- Current AOM[2]	6.1	4.0
- Prior AOM[3]	14.0	10.8

1) using hospital ICD-10 diagnosis codes from 1994 or later; 2) in the year prior to the year of the index scan; 3) from 1995 or later.

Conclusion: Patients undergoing a routine CT of the thorax, abdomen and/or pelvis have a low prevalence of prior VF, osteoporosis, and current AOM treatment. With VF estimated to be prevalent in up to 1 in 4 men and women aged 50 years or older, these results indicate a significant potential for opportunistic identification of VF using routine CT scans.

doi:10.1016/j.bonr.2020.100555

P258

Trabecular bone score in subjects with type 1 diabetes and advanced diabetic nephropathy

Simona Kratochvílová, Jana Brunová
Diabetes Centre, Institute for Clinical and Experimental Medicine, Prague, Czech Republic

Introduction: Bone metabolism impairment in terms of low bone mineral density (BMD) is well documented in subjects with advanced diabetic nephropathy. Alterations of bone microstructure contribute to the risk of fracture and trabecular bone score (TBS) measurement offers and additional tool to quantify bone micro-architecture impairment.

Methods: We retrospectively analysed anthropometric, biochemical and densitometric parameters in 176 subjects with type 1 diabetes in advanced stages of diabetic nephropathy (CKD G4-5), candidates for simultaneous pancreas kidney transplantation in years 2011-16 (114 men, 62 women; mean age 41,0±10,1 years; mean glomerular filtration rate 0,25±0,13 ml/s). TBS was evaluated on an apparatus Lunar Prodigy Promo, TBS insight software version 3.0.3.0.

Results: Mean TBS was 1,286±0,125 and was comparable between men and women. TBS was significantly decreased ($^{<}$1,23) in 52 subjects (29,5%) and correlated with lumbar spine BMD (r=0,20; $p^{<}$0,01), femoral neck BMD (r=0,27; $p^{<}$0,001), glomerular filtration rate (r=0,24; $p^{<}$0,01) and vitamin D level (r=0,28; $p^{<}$0,001). No correlation was documented between TBS and age, age of diabetes diagnosis, BMI, PTH nor HbA1c. Significantly lower BMD was registered in subjects on dialysis treatment (n=65) in comparison with subjects in CKD G4 (n=71): 1,260±0,135 vs 1,319±0,115; $p^{<}$0,01 and in subjects with lumbar spine osteoporosis (T-score ≤ 2,5; n=23) in comparison with subjects with normal lumbar spine BMD (n=98): 1,224±0,154 vs. 1,303±0,123; $p^{<}$0,01.

Even 25 subjects (25,5%) with normal lumbar spine BMD had TBS˂1,23.

Conclusions: TBS evaluation offers an additional information about bone metabolism in subjects with type 1 diabetes in advanced stages of diabetic nephropathy. TBS value is low in one third of patients and correlates with renal function and vitamin D level. Further investigation to identify risk factors connected with TBS decrease and its role in fracture prediction is needed.

Supported by MH CZ - DRO (IKEM, IN 00023001)

doi:10.1016/j.bonr.2020.100556

P260

Persistence of fractures in bisphosphonate-treated patients reveals enhanced osteoclast number in trabecular bone despite low remodeling

Bastien Leger[a], Eugenie Koumakis[b], Caroline Marty[a], Patrice Fardellone[c], Catherine Cormier[b], Martine Cohen-Solal[a]
[a]*Hopital Lariboisiere, Inserm U1132 and Université de Paris, Paris, France*
[b]*Department of Rheumatology, Université de Paris, Hopital Cochin, Paris, France*
[c]*Department of Rheumatology, Université d'Amiens, Amiens, France*

Introduction: Osteoporosis (OP) is a systemic bone disease characterized by a low bone resistance which leads to fractures. Bisphosphonates, antiresorptive drugs, are the first line treatment. Fractures may still occur during treatment, suggesting that some patients are non-responders or develop a resistance to bisphosphonates. The aim of the study was to describe the histomorphometric features of bisphosphonate-resistant patients.

Methods: This retrospective study included 33 patients who underwent a bone biopsy while treated by antiresorptive drugs for more than 6 months from 2010 to 2019. Histomorphometric analysis was performed in undecalcified sections of transiliac core biopsy. Measurements included trabecular bone indices and dynamic parameters. Results were compared to home controls.

Results: BV/TV was lower in OP than in controls (11.9±3.48 vs 15-22 %). Osteoclast number was higher in OP (0.68±0.54 vs 0.45± 0.05 µm/mm2) while Osteoblast surface (Ob.S/BS, 0.95±1.15 vs 4±2%) and osteoclast surface (Oc.S/BS, 0.79±0.62 vs 0.88±0.3%) were lower. Conversely, osteoid surface was high (OS/BS, 22.71± 9.91 vs 15±5), suggesting a previous activation of Bone Multicellular Unit (BMU) along the bone surface. Osteoid volume was within the normal range (OV/BV, 2.58±2.51 vs 2±1%).

Discussion: Histomorphometric analysis of bisphosphonate-resistant patients revealed a lower bone cell activity than controls, despite a higher number of osteoclasts. This indicates that bisphosphonates reduces bone remodeling without affecting the osteoclast differentiation or survival. Moreover, mineralization defect is not the cause neither the remaining activation of BMU.

Conclusion: Persistence of osteoclast differentiation / survival in bisphosphonate-resistant patients may play a role in the occurrence fractures. This shed a new light about the contribution of clastokines to bone fragility.

doi:10.1016/j.bonr.2020.100557

P262

Height loss in postmenopausal women with lumbar scoliosis

Nikola Kirilov, Elena Kirilova, Svilen Todorov, Martin Nikolov, Nikolay Nikolov
UMBAL Dr Georgi Stranski, Pleven, Bulgaria

Introduction: With the arrival of the menopause women's bone density starts to decrease. This condition is also known as osteoporosis and may increase the risk of developing a curvature of the spine or scoliosis. Height loss is expected with age, but in some individuals it is more pronounced. Scoliosis in combination with osteoporosis on the other hand plays a major role in the height loss.

Objective: The aim of this study was to investigate how the bone mineral density in combination with lumbar scoliosis affects the height in postmenopausal women.

Material and methods: We studied 28 postmenopausal women with lumbar scoliosis who have undergone dual-energy radiograph absorptiometry (DXA). The subjects were divided into three groups: normal bone mineral density(BMD), osteopenia and osteoporosis according to the result from the DXA scan. The lumbar scoliosis was defined as a curvature with an angle > 10°, measured from the DXA scan image. Each woman was asked for her height before the menopause and then the current one was measured. The difference between these two values was defined as the height loss.

Results: The mean age was 63 years ± 11 SD with minimum of 45 years and maximum of 88. 6 of all 28 (21%) women had normal BMD and mean height loss of 1.33 cm ± 0.51 SD. The women with osteopenia 8 (29%) had height loss of 4.44 cm ± 2.38 SD. Those diagnosed with osteoporosis were 14 (50%) with height loss of 5.14 cm ± 1.35 SD. One-way ANOVA test was conducted to compare the effect of the BMD on the height loss in the groups normal BMD, osteopenia and osteoporosis for postmenopausal women with lumbar scoliosis with [$F(2,25) = 11.975$, $p=0.000$].

Conclusion: There was a significant effect of the BMD values on the height loss.

doi:10.1016/j.bonr.2020.100558

P263

Osteoporosis, bent posture and risk of fall in elderly women

Ferdinando D'Amico[a], Rossella D'Amico[b]
[a]*Geriatrics, Hospital of Patti - Health Authority Messina - School of Medicina Messina, Patti, Italy*
[b]*Geriatric Extended Care Network, Messina, Italy*

Objective: Aim of the study was to evaluate connections among osteoporosis, bent posture and risk of fall in elderly women.

Methods: 97 female subjects (mean age 77 ± 12) have been studied. The clinical protocol included: 1) clinical examination; 2) L2-L4 lumbar DEXA bone densitometry; 3) dorsal-lumbar spine morphometric X-ray examination; 4) BADL- IADL; 5) Conley Scale, risk of fall evaluation; 6) Tinetti Balance and Gait Scale; 7) OWD, occiput- wall distance measurement.

Results: From the Bone densitometry we recorded T Score values ranging between -0.8 and -3.8 DS for all subjects. The dorsal-lumbar spine X-ray examination showed single vertebral fractures in 31 cases and multiple vertebral fractures in 10. All patients were given the Conley Scale (CS), which resulted in 25 women > 2 CS thus showing risk of fall. All subjects were also given the Tinetti Scale (TS). Data highlighted: 1) Balance disorder, score ≤ 10/16 in 27 women; 2) Gait disturbance, score ≤ 8/12 in 22 subjects; 3) Balance disorder and Gait disturbance, total score balance+gait ≤ 19/28 in 12 subjects. Out of 61 cases presenting Balance disorder and/or Gait disturbance, 59 had a bent posture (BP). BP was: 1) mild (35 cases, (OWD < 5 cm);2) moderate (15 cases, OWD 5-8 cm);3) severe (9 cases OWD > 8 cm). Severe BP was detected in 90% women reported with T-Score between -3 and -3.8 (group C). BADL - IADL evaluation highlighted a reduced degree of self-suffiency concerning 24 subjects affected by BP (OWD > 5 cm.)

Conclusion: The study showed a connection among T-Score values assessed through DEXA, postural defects severity, risk of fall and self-sufficiency degree.

doi:10.1016/j.bonr.2020.100559

P264

Phase I/III study to confirm bioequivalence and safe switching of proposed biosimilar denosumab in postmenopausal osteoporosis

Jean-Jacques Body[a], Christie Nie[b], Barbara Vogg[c], Richard Eastell[d]
[a]*Department of Medicine, CHU Brugmann, Université Libre de Bruxelles, Brussels, Belgium*
[b]*Biopharma Clinical Development, Sandoz Inc., Princeton, United States*
[c]*Department of Clinical Development, Hexal AG, a Sandoz company, Holzkirchen, Germany*
[d]*Metabolic Bone Centre, Northern General Hospital, Sheffield, United Kingdom*

Objective: Phase I/III study design to evaluate equivalent efficacy, pharmacodynamics, pharmacokinetics and also comparable safety and immunogenicity of a proposed biosimilar 60-mg denosumab (bsDMAB; GP2411) and its marketed reference biologic (refDMAB) in postmenopausal osteoporosis (PMO).

Methods: PMO was chosen as a sensitive indication to confirm bioequivalence of bsDMAB with its reference. ROSALIA (NCT03974100) is a multinational, randomised, double-blind, parallel arm study enrolling 522 patients 55-80 years of age with an absolute lumbar spine bone mineral density (LS-BMD) T-score between -2.5 and -4.0. In Treatment Period 1, patients are randomised to bsDMAB or refDMAB (60 mg subcutaneous at day 1 and week 26) (Fig. 1). In Treatment Period 2 when patients receive third dose at week 52, half of the women receiving refDMAB will be switched to the biosimilar. All other patients continue their treatment up to week 78. Primary endpoints for equivalence as aligned with regulatory authorities are percent change from baseline in LS-BMD at week 52, the area under the effect versus time curve of bone resorption marker CTX, and standard pharmacokinetic parameters. Adverse events and the development of antidrug antibodies will be monitored throughout the study, with evaluations between weeks 52 and 78 to evaluate the safety of the switch.

Results: Study completion is expected in 2022.

Conclusion: The ROSALIA study design allows the comparison of proposed biosimilar denosumab GP2411 with its reference in terms of efficacy, pharmacodynamics, pharmacokinetics, safety, and immunogenicity. The safety of a single switch will be investigated.

Sponsor: Sandoz

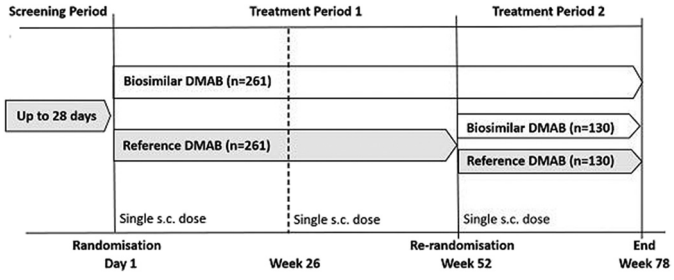

Fig. 1. Study design.

doi:10.1016/j.bonr.2020.100560

P265

Osteoporosis treatment gap in the FRISBEE cohort

Laura Iconaru[a], Celeste Smeys[a], Felicia Baleanu[a], Virginie Kinnard[a], Michel Moreau[b], Silvie Cappelle[a], Murielle Surquin[a], Michel Rubinstein[c], Serge Rozemberg[d], Marianne Paesmans[b], Rafik Karmali[a], Pierre Bergmann[a], Jean-Jacques Body[a]
[a]*CHU Brugmann, Université Libre de Bruxelles, Brussels, Belgium*
[b]*Inst. J. Bordet, Université Libre de Bruxelles, Brussels, Belgium*
[c]*Ixelles Hospital, Université Libre de Bruxelles (ULB), Brussels, Belgium*
[d]*CHU St Pierre, Université Libre de Bruxelles (ULB), Brussels, Belgium*

Despite the availability of efficient drugs to prevent osteoporotic fractures, only a minority of women receives osteoporosis therapy after a fracture, with a treatment gap around 80%. This can have dramatic consequences for patients and the healthcare systems. In this study based on longitudinal data from the FRISBEE ("Fracture RIsk Brussels Epidemiological Enquiry") cohort of 3560 volunteer women aged 60 to 85 years, we evaluated the 1-year treatment gap after a first major incident fragility fracture. There were 386 first validated fragility fractures, 285 major osteoporotic fractures (MOF) and 101 "other major" fractures. The treatment gap was 85.0% (82.8% for MOF versus 91.0 % for "other major" fracture sites) ($p=0.04$), with a lower rate for spine (70.5%) and hip (72.5%) versus shoulder (91.6%) and wrist (94.1%) ($p< 0.0001$). Treatment gap by age groups was 87.9% for women 60-70 years old, 88.2% between 70 and 80 years and 77.8% above 80 years ($p=0.03$), with a greater difference between women who were younger or older than 80 years at inclusion: 88.1% versus 77.8% ($p=0.009$). A diagnosis of osteoporosis ($p=0.01$) and age ($p=0.03$) were the only clinical risk factors (CRFs) significantly associated with treatment initiation. There was no significant difference in the treatment gap according to the fact that fractures were declared by participants (293) or only found in their medical records (93). This study highlights the urgent need of additional education, especially for the medical profession, regarding the risk-benefit balance of treatment.

Keywords: treatment gap, osteoporosis, risk factors, fracture, elderly

doi:10.1016/j.bonr.2020.100561

P266

Severe rebound effect and multiple fractures after denosumab discontinuation in patient with chronic kidney disease stage 5

Sergei Mazurenko[a], Svetlana Feofanova[b]
[a]*Medical Faculty, Saint Petersburg State University, Saint Petersburg, Russian Federation*
[b]*Endocrinology, Leningrad Regional Hospital, Saint Petersburg, Russian Federation*

We report a 46-year old woman with diabetes mellitus type 1, receiving hemodialysis therapy for 7 years. In history it was indicated that she many years took aluminum hydroxide containing antacids to reveal stomach pains. On the 4th year of that practice she suffered fractures of both heel bones. Low BMD was revealed. The patient consulted by endocrinologist and therapy with denosumab 60 mg given subcutaneously every 6 months was started. Four injections of denosumab were performed, the last one in December 2016. Lumbar spine BMD increased after first year of treatment by 7%. However bone mineral of the distal forearm decreased by 16%. The patient stopped the therapy with denosumab. In August 2017 she suffered bilateral femoral neck fracture after falling down from dialysis chair. In 6 months multiple rib and scapular fractures were revealed. Laboratory analysis showed low level of phosphates (0.42 mmol/l), 25(OH) Vit D (22 ng/ml), high level of alkaline

phosphatase and bone metabolites (β-isomers of CTX - 1.620 ng/ml; PINP - 1425 ng/ml. Intact PTH was 12.1 pmol/l (lab reference ranges: 0.7-5.6 pmol/l). This condition was diagnosed as hypophosphatemic osteomalacia and rebound effect of denosumab discontinuation. High doses of alfacalcidol and phosphate-rich diet were prescribed. Seven months later plasma phosphates level raised to 0.79 mmol/l, intact PTH lowered to 5.2 pmol/l, level of calcium raised slightly, but alkaline phosphatase did not change significantly. However bone resorption continued and patient suffered spontaneous fracture of the right arm. To stop this progressive, parathyroid hormone independent, bone loss we had to administer zoledronic acid. Denosumab is not contraindicated for patients with chronic kidney disease, however it should not be used in hemodialysis patients without serious reasons. If one starts therapy with denosumab, one must envisage what to do after its discontinuation.

doi:10.1016/j.bonr.2020.100562

P267

A case of atypical femur fracture during long-term treatment with bisphosphonates

Kira Zotkina
Natoinal Research Almazov Centre, Saint-Petersburg, Russian Federation

Bisphosphonates are used as first-line therapy in the treatment of osteoporosis. In the last decades, the number of cases of atypical femur fractures (AFF) during long-term treatment with bisphosphonates has increased. The aim of this article was to present the case of AFF in the patient who was treated with alendronate for 3.5 years.

A 78-year-old woman, receiving oral bisphosphonate for severe postmenopausal osteoporosis for 3,5 years, suddenly started feeling pain in her right thigh while walking. Three months later, she had got fracture in the middle third of the right femur after falling from her standing height. According to instrumental diagnostics results, this fracture had all criteria of AFF. Blocking intramedullary osteosynthesis with shafts was performed. A retrospective analysis of the magnetic resonance imaging result of right thigh soft tissues conducted before the fracture, showed the presence of an undiagnosed incomplete fracture of the middle third of the right thigh, which subsequently had realized in a complete fracture.

This clinical case demonstrates the complexity of AFF diagnostics. The purpose of the publication is to draw attention of medical specialists to the issue of such rare side effect of bisphosphonates as AFF.

doi:10.1016/j.bonr.2020.100563

P268

The influence of complex supplementation with calcium, vitamins D_3 and B_6 on muscle strength and balance function in patients with osteoporosis after medical rehabilitation

Larisa Marchenkova, Ekaterina Makarova, Mikhail Eryomushkin, Valeria Vasileva
Rehabilitation Department for Somatic Patients, National Medical Research Center for Rehabilitation and Balneology of Ministry of Health of Russian Federation, Moscow, Russian Federation

The aim was to evaluate effect of complex food supplement with calcium and vitamins D_3 and B_6 intake on muscle strength and balance function during 1-year follow-up after rehabilitation course in patients with osteoporosis.

Methods: The study comprised 119 men and women aged 50-80 y. o. with established osteoporosis and high fracture probability by FRAX® model initiating 3-week course of rehabilitation. 41 patients who had already received anti-resorptive therapy were included in the Group 1 (G1), and 78 patients who were never previously treated with anti-osteoporotic medication were randomized in G2 (n=39) or G3 (n=39). The food supplement containing Vitamin D_3 30 mg, Pyridoxine Hydrochloride 4 mg, Calcium Citrate 320 mg and HDBA organic complex 400 mg in daily dosage was administered in G1 and G2 for 12 months. Changes in dynamometry and balance tests were assessed after 3 weeks, and in 6 and 12 months as follow-up.

Results: Achieved higher levels of muscle strength during the rehabilitation course were maintained for up to 12 months in the back extensors and flexors in G1 and G2, and up to 6 months in the lateral back flexors in G1 ($p>0.05$ vs 3 weeks). The effect of medical rehabilitation completely disappeared in G3 after 6 months ($p< 0.05$ vs 3 weeks). Improved vs baseline stabilometry data in balance coefficient and pressure center deviation speed were registered in G1 and G2 in 6 and 12 months ($p>0.05$ vs 3 weeks). Achieved during rehabilitation positive result of balance control measured with One-leg-standing test was maintained only in G1 for 12 months ($p>0.05$ vs 3 weeks), but it significantly ($p< 0.05$) worsened in G3 at follow-up.

Conclusion: Long-term intake of food supplement containing calcium with vitamins D_3 and B_6 can help to maintain the effect of rehabilitation on muscle strength and balance in patients with osteoporosis.

doi:10.1016/j.bonr.2020.100564

P270

Clinical and radiological results of teriparatide treatment in patients with osteoporotic sacral fractures

Stamatios-Theodoros Chatzopoulos[a], Dimitrios Begkas[a], Alexia Balanika[b], Georgios Georgiadis[c], Christos Baltas[d], Alexandros Pastroudis[a]
[a]*6th Orthopedic Department, G.H Asklepieion of Voula, Voula, Greece*
[b]*Computed Tomography Department, G.H Asklepieion of Voula, Voula, Greece*
[c]*4th Orthopedic Department, G.H Asklepieion of Voula, Voula, Greece*
[d]*Radiological Imaging Department, G.H. G. Gennimatas, Athens, Greece*

Aim: The evaluation of clinical and radiological outcomes of teriparatide treatment in patients with osteoporotic sacral fractures (OSF).

Material and method: Between 2015 and 2017, 8 female patients with OSF, were conservatively treated in our department with bed rest (and progressive ambulation within 3 months after the fracture), analgesics, vitamin D supplementation and a daily dosage of 20μg teriparatide. Their follow up was at 1, 3, 6 and 12 months. The evaluation of treatment results was based on clinical (VAS) and radiological (plain X-Rays and Computed Tomography-CT) criteria, bone mineral density (BMD), bone turnover markers (BTM) before and after the initiation of treatment and the incidence of complications.

Results: The mean age of the patients was 72.6 (68-76) years. All of them showed a significant reduction of pain after the initiation of treatment (IoT) and remarkable improvement in their ambulation at 6 months. The mean VAS score was statistically significantly reduced (12.8mm) compared with the initial values (87.6mm) ($p< 0.0001$). The X-Rays and CT showed healing of all the fractures and in addition sclerotic changes in the fracture site in two cases at 6 and 12 months after IoT. The BMD and BTM showed a small increase which was not statistically important. No complications were observed.

Conclusions: Despite the insignificant increase in BMD and BTM, the use of teriparatide in the treatment of OSF resulted in increased

fracture healing, rapid pain reduction and faster mobilization of patients, which led to a decrease in the incidence of potential complications.

doi:10.1016/j.bonr.2020.100565

P271

Outcomes of postoperative teriparatide treatment in patients with cementless bipolar hemiarthroplasty after femoral neck fracture

Dimitrios Begkas[a], Stamatios-Theodoros Chatzopoulos[a], Georgios Georgiadis[b], Christos Baltas[c], Alexia Balanika[d], Alexandros Pastroudis[a]
[a]6th Orthopedic Department, G.H Asklepieion of Voula, Voula, Greece
[b]4th Orthopedic Department, G.H Asklepieion of Voula, Voula, Greece
[c]Radiological Imaging Department, G.H. G. Gennimatas, Athens, Greece
[d]Computed Tomography Department, G.H Asklepieion of Voula, Voula, Greece

Aim: The evaluation of postoperative teriparatide treatment in patients with femoral neck fracture (FNF) treated with cementless bipolar hip hemiarthroplasty (CBHA).

Material and method: This is a retrospective comparative cohort study, which was conducted between 2011 and 2017 and involved 84 patients (40 men and 44 women) with FNF treated with CBHA. Patients were divided into two groups (A and B). Group A (control group) included 42 patients treated with CBHA alone. Group B (study group) included 42 patients treated with CBHA and additionally started teriparatide treatment after surgery. Both Groups were evaluated on the basis of their demographic data, functional (Harris Hip Score - HHS) and radiological results, the incidence of complications and the Health Related Quality of Life score (SF-12 HRQoL).

Results: The average age of the patients was 74.5 (65-87) years. The mean follow up time was 46.4 (24-72) months. Radiologically, group B showed significant decrease in the subsidence of the femoral stem at 6 and 12 months postoperatively ($p=0.003$ and $p=0.008$ respectively). In both groups (A and B) the HHS increased significantly from preoperatively (16.1 and 16.5, respectively) to 12 postoperative weeks (57.9 and 58.6, respectively) and then up to one year postoperatively (86.9 and 87.8 respectively). During the follow-up, there was no difference between the two groups in the incidence of complications, mortality and SF-12 HRQoL.

Conclusions: Teriparatide, reduces significantly the subsidence of the femoral stem in elderly patients that underwent CBHA, however this benefit does not translates in better outcomes in terms of their mobility, complications and health related quality of life.

doi:10.1016/j.bonr.2020.100566

P272

Bisphosphonate drug holiday in treatment planning of dental patients

Jeong Keun Lee[a,b], Hoon Myoung[c]
[a]Oral and Maxillofacial Surgery, Institute of Oral Healrh Science, Ajou University School of Medicine, Suwon, Republic of Korea
[b]Oral and Maxillofacial Surgery, Ajou University Dental Hospital, Suwon, Republic of Korea
[c]Oral and Maxillofacial Surgery, School of Dentistry, Seoul National University, Seoul, Republic of Korea

Osteonecrosis of the jaw (ONJ) was a rare kind of disease until the advent of osteonecrosis-inducing drugs including anti-resorptive agents. Medication-related osteonecrosis of the jaw (MRONJ), named after its causative one, showed its general incidence in Korea as low as 0.04% (one out of 2,300). However its incidence is much more raised in patients under dental care, which concerns most dentists.

The importance of drug holiday in preventing MRONJ is worth of recognition. Drug holiday for Alendronate, Zoledronate are implicated in FLEX study (published in 2006) and HORIZON-PFT study (published in 2012), respectively. Drug holiday is recommended after 5 year intake of Alendronate and 3 year infusion of Zoledranate, respectively. Our study demonstrated drug holiday as a prognostic factor for surgical management of MRONJ, revealing at least 4 months of drug holiday is a must before surgical removal of necrotic bone to avoid poor prognosis. One report pointed out that drug holiday for longer than 2 years was associated with a 39% elevated risk of hip fracture compared with continued bisphosphonate prescription. Conclusively, drug holiday within 2 years may be desirable after recommended time duration of clinical use of bisphosphonates according to each drug type.

AAOMS position paper in 2014 just considers drug holiday less than 2 months and lacks clear declaration of it for prevention of MRONJ. Drug holiday is a must for management of ONJ as an oral and maxillofacial surgeon. The author insists upon clear declaration of drug holiday at the next position statement in near future focusing upon at least 4 months.

Keywords: bisphosphonate, drug holiday, MRONJ

doi:10.1016/j.bonr.2020.100567

P273

Prevalence and incidence of vertebral fractures in institutionalized adults with refractory epilepsy and intellectual disability: A 7-year follow-up study

Jessica Berkvens[a], Marian Majoie[a,b], Kim Beerhorst[c], Sandra Mergler[d,e], Pauline Verschuure[a], Francis Tan[a], Joop van den Bergh[b,f]
[a]Epilepsy Center Kempenhaeghe, Heeze, Netherlands
[b]Maastricht University Medical Center, Maastricht, Netherlands
[c]Zuyderland Medical Center, Heerlen, Netherlands
[d]ASVZ Care and Service Center for People with Intellectual Disabilities, Sliedrecht, Netherlands
[e]Erasmus University Medical Center, Rotterdam, Netherlands
[f]VieCuri Medical Center, Venlo, Netherlands

Purpose: To determine the prevalence and incidence of vertebral fractures (VF) in adults with refractory epilepsy and intellectual disability (ID), residing at a long-stay care facility.

Method: In 2009, all institutionalized adult patients ($n=261$) were invited for a Dual-energy X-ray Absorptiometry (DXA) measurement and Vertebral Fracture Assessment (VFA). In 2016, DXA and VFA were repeated. If evaluable, vertebrae T4-L4 were assessed using quantitative morphometry. Severity of VFs was graded as 1 (mild; 20-25% reduction in height), 2 (moderate; 25-40% reduction) or 3 (severe; >40% reduction) according to the method described by Genant. Prevalent VFs were analyzed at baseline. VFs (grade 1, 2 or 3) present at follow-up, but not at baseline, were considered new VFs. Worsening VFs were defined as VFs with at least one grade deterioration at follow-up, compared to baseline (from grade 1 to 2 or 3, or from grade 2 to 3). All patients were treated with anti-osteoporosis treatment according to the Dutch guideline.

Results: A total of 141 patients (87 male, 61.7%) aged between 18-79 years old (mean 44.8 ± 15.7) at cohort entry could be studied. In 2009, 56 patients (39.7%) had at least one prevalent VF; 40 (28.4%) had ≥1 mild VF, 34 (24.1%) had ≥1 moderate VF and 3 patients (2.1%) a severe VF. 20 of these patients (14.2%) had VFs of

multiple grades. During 7-year follow-up, 39 new VFs occurred in 29 patients (20.6%) and 15 patients (10.6%) had a worsening VF. The combined incidence of new and worsening VFs was 27.7%.

Conclusion: In adults with refractory epilepsy and ID, VFA is challenging due to physical and behavioral aspects, resulting in a substantial proportion of unevaluable vertebrae/scans. Nevertheless, 40% of the patients had a VF at baseline and after 7-years follow-up, 28% had at least one new and/or worsening VF despite adequate anti-osteoporosis treatment.

doi:10.1016/j.bonr.2020.100568

P274

The effect of sequential treatments on circulating microRNAs related to bone metabolism in women with postmenopausal osteoporosis

Elena Tsourdi[a,b], Athanasios D. Anastasilakis[c], Polyzois Makras[d], Athanasios Papatheodorou[d], Martina Rauner[a,b], Lorenz C. Hofbauer[a,b,e], Maria Yavropoulou[f,g]

[a]*Department of Medicine III, Technische Universität Dresden Medical Center, Dresden, Germany*

[b]*Center for Healthy Aging, Technische Universität Dresden Medical Center, Dresden, Germany*

[c]*Department of Endocrinology, 424 General Military Hospital, Thessaloniki, Greece*

[d]*251 Hellenic Air Force & VA General Hospital, Department of Medical Research, Athens, Greece*

[e]*Center for Regenerative Therapies Dresden, Technische Universität Dresden, Dresden, Germany*

[f]*Department of Medical Research, 251 Hellenic Air Force & VA General Hospital, Athens, Greece*

[g]*Endocrinology Unit, 1st Department of Propaedeutic Internal Medicine, National and Kapodistrian University of Athens, UOA, LAIKO General Hospital, Athens, Greece*

Background: Depending on osteoporosis severity a long-term treatment, often as a sequential regimen, may be required. The serum expression of microRNAs (miRs) related to bone metabolism is potentially affected by anti-osteoporotic treatment. Here, we investigated the effect of sequential treatments on microRNA expression profile in the serum.

Methods: This is an observational, open label, non-randomized clinical trial that included 37 postmenopausal women with osteoporosis who were treated with denosumab (Dmab) for 1 year. Patients had been previously treated for 2 years with either teriparatide (n=20), or zoledronate (n=6), or were treatment-naïve (n=11). We evaluated changes in the relative serum expression of selected miRs linked to bone metabolism at 3 and 12 months of Dmab treatment in each group separately.

Results: In the group of patients who were previously treated with teriparatide, the relative expressions of miR-21a-5p, miR-29a and miR-2861 were significantly decreased at 3 months of Dmab treatment (0.2-fold change, $p< 0.001$ for miR-21a-5p; 0.7-fold change, $p< 0.05$ for miR-29a; 0.2-fold change, $p< 0.001$ for miR-2861). Similar changes were identified at 12 months of Dmab treatment. Moreover, the relative expression of miR-23a-3p was also significantly decreased (0.6-fold change $p< 0.001$) at 12 months of Dmab treatment. Previous zoledronate treatment did not affect the relative expression of miRs during Dmab treatment. Moreover, no change was observed during Dmab treatment in previously treatment-naïve women.

Conclusions: Our data indicate that the expression of circulating miRs linked to bone metabolism during Dmab treatment depends on previous treatment status. Patients previously treated with teriparatide depict alterations of the relative expression of miRs related to the expression of key osteoblastic genes such as RUNX-2 (miR-23), collagen type 1 (miR-29a) and HDAC5 gene (miR-2861) during subsequent treatment with Dmab. Our data suggest that teriparatide may influence the subsequent anti-resorptive effect of Dmab on bone metabolism at post-transcriptional level.

doi:10.1016/j.bonr.2020.100569

P275

Can denosumab reduce periprosthetic bone loss after bipolar hip arthroplasty?

Kwangkyoun Kim

Orthopedic Surgery, Konyang University, Daejeon, Republic of Korea

Introduction: Unbalanced load placed on the femur by the implanted stem results in stress shielding, leading to acceleration of bone resorption and a decrease of bone mineral density in the proximal femur. Although effects of bisphosphonate on periprosthetic bone loss after primary total hip arthroplasty have been studied, but there is no study of the effects of denosumab on it. Purpose of this study was to determine whether denosumab is effective in reducing periprosthetic bone loss after cementless bipolar hip arthroplasty.

Material and method: Study was conducted in single institution between Jun 2017 and Sep 2018. We enrolled patients with femur neck fracture treated bipolar hip arthroplasty. Subjects were grouped with denosumab treated and non- treated group. Treated subjects were randomly assigned to receive either 60 mg denosumab subcutaneously every 6 months. Bone mineral density of the periprosthetic femur was measured within 8 days after surgery as a reference baseline, followed by subsequent measurements 3, 6, 12 months postoperatively using dual-energy X-ray absorptiometry. The protocol for analysis of the DEXA scans used radiological zones described by Gruen dividing the periprosthetic femoral bone into seven regions of interest (ROI).

Results: 54 patients completed follow-up protocol at the 6 months. The 21 non-denosumab treated patients showed significant loss of periprosthetic bone mineral density 6 months after bipolar arthroplasty especially in ROI 1, 2, and 7 than in the 33 treated patients (in order, $p = 0.031, 0.017 .0.048$) and no difference in ROI 3-6 (in order, $p = 0.232, 0.295, 0.010$). After 3 month's follow up, the periprosthetic bone mineral density values of the denosumab non-treated group did not show significant loss of periprosthetic bone mineral density in the all ROIs.

Conclusions: These data suggest that denosumab administered following bipolar arthroplasty was effective in preventing first 6 postoperative months periprosthetic bone loss.

doi:10.1016/j.bonr.2020.100570

P277

The effects of bendroflumethiazide on bone mineral density measured using DXA, QCT and VFA; a randomized double-blind placebo-controlled cohort study

Thomas Emmanuel[a], Julius Simoni Leere[b], Christian Kruse[a,b], Trine Holmgaard Poulsen[a], Peter Vestergaard[a,b,c]

[a]*Department of Endocrinology, Aalborg University Hospital, Aalborg, Denmark*

[b]*Department of Clinical Medicine, Aalborg University Hospital, Aalborg, Denmark*

[c]*Steno Diabetes Center North Jutland, Aalborg, Denmark*

Introduction: Thiazide diuretics (TD) are used as anti-hypertensive treatment. TD may prevent osteoporosis. We investigated the effects of

bendroflumethiazide, a commonly used TD, in combination with bisphosphonates on bone mineral density (BMD).

Methods: This was a double-blinded, randomized, placebo-controlled interventional study consisting of four arms. Intervention consisted of 2.5 mg bendroflumethiazide and 573 mg potassium chloride. Newly diagnosed +50-year-old postmenopausal osteoporotic Caucasian women were randomized to either 1) 24 weeks intervention + 24 weeks washout, 2) 24 weeks intervention + 24 weeks placebo, 3) 48 weeks intervention, or 4) 48 weeks placebo. BMD of lower spine (LS) and femoral neck (FN), and total hip (TH) were acquired. VFA was assessed using Genant's semiquantitative method. All measurements were acquired at baseline and at 48 weeks. Danish National Committee #: N-20150022. EudraCT #: 2015-001059-63.

Results: 139 patients were randomized (mean age 64.7 years (SEM 0.6, range 51-79)). 109 (78%) completed the study. Results are seen on Table 1.

	Bendroflumethiazide 24 weeks		Placebo 24 weeks	
	Δ Value, (SEM), percent change	P-score	Δ Value, (SEM), percent change	P-score
†DXA LS-BMD	0.015, (0.0075), 2.7%	0.0639	0.015, (0.0087), 2.6%	0.1054
†DXA TH-BMD	0.0081, (0.0035), 1.4%	**0.0343**	0.012, (0.0039), 1.4%	**0.0098**
†DXA FN-BMD	0.0086, (0.0043), 1.7%	0.0639	0.016, (0.0034), 3.3%	**0.0002**
††QCT LS-BMD	-3.64, (2.68), -4.0%	0.1964	-2.08, (2.46), -2.7%	0.4129
††QCT FN-BMD	0.011, (0.019), 1.4%	0.5716	0.0093, (0.0096), 1.4%	0.3490
	Bendroflumethiazide 48 weeks		**Placebo 48 weeks**	
	Δ Value, (SEM), percent change	P-score	Δ Value, (SEM), percent change	P-score
†DXA LS-BMD	0.020, (0.0060), 2.5%	**0.0019**	0.016, (0.0055), 1.3%	**0.0069**
†DXA TH-BMD	0.0066, (0.0096), 1.4%	**0.0010**	0.011, (0.0028), 1.3%	**0.0007**
†DXA FN-BMD	-0.00035, (0.0046), -0.07%	0.9411	0.012, (0.0040), 1.6%	**0.0071**
††QCT LS-BMD	3.26, (1.63), 4.1%	0.0560	-3.55, (2.01), -4.4%	0.0895
††QCT FN-BMD	0.0059, (0.010), 0.8%	0.5631	0.0022, (0.018), 1.4%	0.9052

Results from BMD measurements. †BMD (g/cm2), ††BMD (mg/cm3).

In summary, some groups saw a significant increase in BMD though no significant difference was found between the Δ values (p-values not shown). VFA showed no new fractures.

Conclusion: Bendroflumethiazide does not increase BMD measured using DXA and QCT after 48 weeks. No significant difference in the increase in BMD was seen for bendroflumethiazide compared to placebo. Longer treatment periods and more patients are needed to further characterize the effects of bendroflumethiazide on bone.

doi:10.1016/j.bonr.2020.100571

P279

Safety and efficacy of denosumab in postmenopausal somen with osteoporosis

Dilsad Sindel, Ekin Ilke Sen, Ayse Yalıman, Sina Arman
Physical Medicine and Rehabilitation, Istanbul University, Istanbul Faculty of Medicine, Istanbul, Turkey

Background and aims: The growing healthcare costs associated with osteoporosis and osteoporotic fractures in postmenopausal women have increased researchers' interests in developing reliable, and efficacious approaches for the treatment of osteoporosis. The aim of this study was to determine the safety and efficacy of denosumab in postmenopausal women.

Methods: We retrospectively reviewed the data of 35 osteoporotic patients who received a single 60-mg subcutaneous dose of denosumab every 6 months for an observation period of 12 months. Bone mineral density (BMD) of the lumbar spine and femur were measured by dual-energy X-ray absorptiometry at baseline and one-year of the study. For safety assessment laboratory examinations including repeated calcium, phosphorus and creatinine level determination were performed. In addition to standard reporting of all adverse events, data were collected by interviews between the visits. Wilcoxon test was used for analysis of dependent variables. All analyses were done using SPSS version 22.0.

Results: The mean age of the patients was 67.4 ± 8.5 years, 73.5% (n=25) of them had received bisphosphonate treatment previously, and the average duration of bisphosphonate usage was 4.7 ± 2.8 years. The BMD at the femoral neck (p=0.034), total hip (p=0.001), and L1-L4 (p=0.020) regions increased significantly with denosumab. There was no statistically significant change in serum calcium, phosphorus, and creatinine levels (p< 0.05). No severe side effects occurred.

Conclusions: Our study highlights the safety and efficacy of denosumab in the treatment of osteoporosis in postmenopausal women, potentially supporting its use to reduce the burden of fractures in this patient population.

doi:10.1016/j.bonr.2020.100572

P281

Effect of the complex physical rehabilitation on postural control in patients with osteoporotic vertebral fractures

Ekaterina Makarova, Larisa Marchenkova
Somatic Rehabilitation, Anti-Aging and Reproductive Health Department, FSBI "National Medical Research Center of Rehabilitation and Balneology" Ministry of Health of Russian Federation, Moscow, Russian Federation

Aim: To evaluate effect of complex physical rehabilitation on postural function in patients with osteoporotic vertebral fractures (VFs).

Materials and methods: Study comprised of 90 osteoporotic patients aged 50-80 (65.4±9.1) with VFs who were randomized as 2:1 into intervention group (group1, n=60) and control group (group2, n=30). Patients in group1 received intensive rehabilitation course including back muscle training #10; sensorimotor training on unstable platform #10; kinesohydrotherapy in a pool #15; physical exercises in a gym #10. Group2 was prescribed only physical exercises in a gym #15. All patients undergo Stabilometry, one leg standing test and Fukuda test at baseline, at the end of rehabilitation and a month after the rehabilitation.

Results: Baseline examination showed no significant differences between groups in stabilometric parameters and coordination tests (p>0.05). There were significant changes in group1 after the rehabilitation course vs baseline in balance function coefficient (BFC) with opened eyes from 77.0±7.6 to 84.1±8.6% (p=0.008) and with closed eyes from 67.1±9.7 to 73.8±9.6% (p=0.007), at the area of statokinesiogram (ASKG) from 176.8±170.2 to 131.9±131,9±210,4†mm2 (p=0.04), pressure center velocity (PCV) from 9.5±4.4 to 12.2±10.1mm/s, (p=0.0004), displacement in Fukuda test from 41.4±21.3 to 32.8±14.5, (p=0.03) and in One leg standing test on both legs with open eyes from 9.7±21.7 to 17.8±31.8sec and from 9.5±15.3 to 17.1±30.1sec respectively (p=0.001). In group2 there was improvement in PCV from 9.2±4.7 to 10.1±3.9mm/s (p=0.05). Positive dynamics in balance tests (BFC with open and closed eyes, PCV, ASKG, displacement in Fukuda test, time for both legs in one leg standing test) were maintained in group1 in month after the rehabilitation treatment. All the postural control parameters were significantly better in group1 vs group2 after 1 month of follow-up (p< 0.01).

Conclusions: The complex physical rehabilitation aimed for trunk muscles and coordination trainings improve the postural function in patients with osteoporotic VFs.

doi:10.1016/j.bonr.2020.100573

P282

The effectiveness of core muscles trainig in patients with osteoporotic compression vertebral fractures

Ekaterina Makarova, Larisa Marchenkova
Somatic Rehabilitation, Anti-Aging and Reproductive Health Department, FSBI "National Medical Research Center of Rehabilitation and Balneology" Ministry of Health of Russian Federation, Moscow, Russian Federation

Aim: To estimate the effect of new complex physical rehabilitation program on core muscles strength in patients with osteoporotic vertebral fractures (VFs).

Materials and methods: Study comprised of 90 osteoporotic patients aged 50-80 (65.4±9.1 years) with low-traumatic VFs who were randomized as 2:1 into intervention group (group1, n=60) and control group (group2, n=30). Patients in group1 received an intensive rehabilitation course including back muscle training with mechanical loads #10; sensorimotor training on double unstable platform #10; kinesohydrotherapy in a pool #15; physical exercises in a gym #10. Group2 was prescribed only physical exercises in a gym #15. All patients undergo tenzodynamometry on BackCheck diagnostic unit (Dr. Wolff, Germany) at baseline, at the end of rehabilitation course and a month after the rehabilitation.

Results: After a rehabilitation course muscle strength increased significantly in trunk extensors (TE) from 15.8±10.1 to 21.7±13.1kg ($p< 0.0001$), trunk flexors (TF) from 14.5±9.1 to 18.9±10.2 kg ($p< 0.001$), left lateral flexors (LLF) from 12.8±7.2 to 17.5±9.6 kg ($p< 0.01$) and right lateral flexors (RLF) from 13.2±7.1 to 17.8± 9.2kg ($p< 0.01$). The maximal improvement of muscle strength was registered in TF +6.5±57.5% above recommended values ($p< 0.001$). TE strength deficiency significantly decreased ($p< 0.001$), but did not reach the recommended values -15.8±25.8%. After the 1-month muscle strength in all examined muscles didn't significantly diminished vs results just after rehabilitation course completion ($p>0.05$). The strength of all the studied muscles were higher ($p< 0.01$) and the muscle deficiency was less in TE ($p< 0.05$) and TF ($p< 0.001$) in group1 vs group2 in a month of follow-up after rehabilitation course.

Conclusions: A new complex physical rehabilitation program leads to increase of muscle strength and elimination of muscle strength deficiency in patients with osteoporotic VFs, and these effects are not attenuate for at least a month after the treatment completion.

doi:10.1016/j.bonr.2020.100574

P283

Investigation on the impact of hops flavonoid extracts on the structural and mechanical properties of rat bone tissue

Anna Nikodem[a], Jarosław Filipiak[a], Agnieszka Matuszewska[b], Beata Nowak[b]
[a]*Mechanical Department, Wroclaw University of Science and Technology, Wroclaw, Poland*
[b]*Department of Pharmacology, Wroclaw Medical University, Wroclaw, Poland*

Determination of impact of new drug therapies, due to the time of action of drugs, mainly uses as a model small animals such as mouse, rat or rabbit. The classical mechnical methods used in engineering are characterized by many limitations which determine the accuracy of the measurement. Therefore, an alternative measurement method that enables a quantitative analysis of a number of parameters defining the structure of bone tissue is high-resolution computer microtomography. The aim of this study is to determine the effect of hops flavonoids on the structural and mechanical properties of bone. The research material consisted of femur bone originating from female Wisnar rats, with an initial weight of 150 ± 20g. and age of 12 weeks. The material was divided into 5 groups: SHAM, control group OVX-C; OVX-E - ovariectomy with supplementation 17-beta-estradiol, OVX-EX - ovariectomy with effluent extract; OVX- XN - ovariectomy, with xanthohumol. Tests of structural properties of bone tissue were carried out using the 1172 SkyScan, Bruker® X-ray microCT The image registration was carried out with a resolution of 9μm, with the 86kV/114mA lamp parameters. To obtain mechanical properties a four-point bending test was carried out, using MTS® 858 MiniBionix machine. In this test the distal and proximal ends of bone, were fixed in sleeves made of Al alloy, embedded with Durakryl Plus® resine. Analysis of structural parameters obtained with microCT showed clear changes in the structure and number of bone trabecuae. These changes concern the geometry of the trabeculae but also their character (SMI). Mechanical results also indicate significant differences between the groups. Xanthohumol turned out to be the best of the compounds tested in terms of both structural and mechanical parameters.

This work has been supported by the National Science Centre, No. 2016/21/B/NZ7/02759.

doi:10.1016/j.bonr.2020.100575

P284

Postoperative acute kidney injury after osteoporotic hip hip fractures in elderly patients

Joon-Soon Kang
Inha University College of Medicine, Incheon, Republic of Korea

Acute kidney injury (AKI) is a rare but serious complication after hip fractures. The aim of this study was to evaluate the incidence and the risk factors of postoperative AKI after osteoporotic hip fractures.

From January 2011 to December 2016, 550 patients who underwent surgery of hip fractures at our institution were retrospectively reviewed. AKI was defined and classified by AKI Network (AKIN) Classification/Staging System. The incidence, mortality, and risk factors of postoperative AKI were investigated. Receiver operating characteristic curve analysis was conducted to evaluate the ability of markers in predicting AKI.

The incidence of postoperative AKI was 4.4% (25 cases). The mean onset of postoperative AKI was 8.0 ± 5.3 days and recovered after 7.0 ± 4.2 days after the occurrence of AKI. Of 25 patients with AKI, 6 patients (24.0%) died within 1 year after surgery. The independent risk factors for postoperative AKI are the estimated blood loss (EBL) (odds ratio (OR) 1.64; 95% confidence interval (CI) 1.33-2.58; $p < 0.01$) and postoperative level of albumin (OR 1.77; 95% CI 1.52-2.74; $p < 0.01$). The cutoff value of the serum albumin was < 2.8 g/dL with a sensitivity of 88.0% and a specificity of 77.1%. The cutoff value of EBL was < 766.5 mL with a sensitivity of 84.0% and a specificity of 66.3%.

In conclusion, postoperative AKI after hip fractures had low incidences (4.4%) but high mortality (24.0%). The postoperative AKI was correlated with blood loss and low postoperative albumin levels.

doi:10.1016/j.bonr.2020.100576

P287

Temporal changes in subchondral bone and cartilage in a post-traumatic osteoarthritis rabbit model

Lingwei Huang[a], Ilari Riihioja[b], Petri Tanska[a], Simo Ojanen[a,c], Sanna Turunen[d], Heikki Kröger[b], Simo Saarakkala[c,e], Walter Herzog[f], Rami Korhonen[a], Mikko Finnilä[a,c]

[a]*Department of Applied Physics, University of Eastern Finland, Kuopio, Finland*

[b]*Department of Orthopedics, Kuopio University Hospital, Kuopio, Finland*

[c]*Research Unit of Medical Imaging, Physics and Technology, University of Oulu, Oulu, Finland*

[d]*Cancer and Translational Medicine Research Unit, University of Oulu, Oulu, Finland*

[e]*Department of Diagnostic Radiology, Oulu University Hospital, Oulu, Finland*

[f]*Human Performance Laboratory, University of Calgary, Calgary, Canada*

Anterior cruciate ligament (ACL) rupture increases the risk for osteoarthritis (OA). This study aims to clarify temporal alterations in subchondral bone (SCB) and articular cartilage in a rabbit model with surgical ACL transection (ACLT).

Operated (ACLT) and contralateral (C-L) knees were harvested two (n=8) and eight (n=6) weeks after ACLT, surgery together with collection of age-matched control (CNTRL, n=8) knees. Each knee was divided into lateral and medial condyles and plateaus, groove and patella. Bone morphology was quantified using micro-computed tomography. Thickness and fixed charged density (FCD) of the cartilage were measured with optical coherence tomography and digital densitometry, respectively.

Trabeculae in ACLT knees were thinner compared to C-L in the lateral plateau (-6.7%;$p=0.007$) and groove (-10.9%;$p=0.015$) two weeks after surgery. At eight weeks, thinner trabeculae compared to C-L were observed at all locations. Trabecular bone volume fraction was decreased in ACLT compared to CNTRL at all locations except for the patella. Subchondral plate was thinner than C-L in the lateral plateau (-26.2%;$p=0.022$), groove (-19.8%;$p=0.005$) and patella (-19.5%; $p=0.001$).

Two weeks after surgery, FCD was reduced at the lateral plateau, the medial condyles, the groove, and the patella in ACLT compared to CNTRL. FCD was lower in the ACLT compared to C-L at all locations except for the lateral plateau. Interestingly, eight weeks after surgery, the FCD was increased in the medial plateau of C-L compared to CNTRL group knees. FCD loss in ACLT was progressive in the condyles, but the initial FCD loss was compensated for in the groove and patella. Also, the cartilage was thicker (50.5%;$p=0.007$) in the lateral plateau of ACLT knees eight weeks after surgery compared to CNTRL.

Summarizing, bone loss and cartilage degeneration occurred in a tissue- and site-specific manner in post-ACLT knees and bone loss spread progressively while some compositional changes of cartilage were recovered.

doi:10.1016/j.bonr.2020.100578

P288

Measurements of bone microarchitecture by histology, microCT and HRpQCT in CKD patients

Eva Benillouche[a], Agnes Ostertag[a], Caroline Marty[a], Pablo Urena Torres[b], Martine Cohen-Solal[a]

[a]*Hopital Lariboisiere, Inserm U1132 and Université de Paris, Paris, France*

[b]*Nephrology, Aura Nord, Saint-Ouen, France*

Introduction: Current available tools such as bone mineral density and biomarkers are insufficient to predict bone fragility in CKD patients. As chronic kidney disease (CKD) patients with fractures have impaired cortical bone, the characterization of bone is therefore crucial to identify patients at high risk.

Objective: we aimed to investigate the cortical and trabecular bone measurements assessing the microarchitecture in bone biopsies comparing histology and microcomputed tomography (μCT) and at the tibia using high resolution peripheral quantitative computed tomography (HRpQCT).

Methods: Nine patients were referred for vertebral or hip fracture (4 with one fracture, 5 with >2). The mean age was 70.3±7.2 years and the mean duration in dialysis therapy of 7.2 years (1-19). Bone microarchitecture was analyzed in transiliac biopsy using histology and in vitro μCT (μCT). Microarchitecture was assessed at the tibia by HR-pQCT. Correlations were performed by Pearson tests.

Results: BV/TV was similar in histology and μCT (0.12±0.03 vs 0.14±0.03%, p NS), while lower in HRpQCT (0.08±0.04%, p< 0.05), but no correlation between histology and μCT (r=0.58, p=0.10). Tb.Th was higher in histology than in μCT or HRpQCT (0.80±0.02, 0.11±0.02, 0.05±0.01 mm respectively, p< 0.01). Conversely, Tb.Sp was not significantly different in histology than in μCT or HRpQCT (0.58±0.12, 0.67±0.11, 0.73±0.43 mm respectively). There was no correlation in Tb.N, Tb.Th and Tb.Sp quantified by histology and μCT, neither with μCT and HRpQCT. However, the mean cortical thickness (Ct.Th) was closed in the 3 methods (0.63±0.25 vs 0.60±0.18 vs 0.59±0.23 mm respectively). Histology Ct.Th was positively correlated to μCT Ct.Th (r=0.75, p< 0.05), but no correlation were found between μCT and HRpQCT Ct.Th (p=0.21).

Conclusions: Neither trabecular or cortical indices measured in bone biopsies correlates with HRpQCT measurement at the tibia. However, cortical thickness is similar throughout the 3 techniques, suggesting an accurate way to measure bone fragility

doi:10.1016/j.bonr.2020.100579

P290

Real-time impedance-based monitoring of the growth and inhibition of osteomyelitis pathogen *Staphylococcus aureus* biofilms treated with novel bisphosphonate-fluoroquinolone antimicrobial conjugates

Parish Sedghizadeh[a], Esmat Sodagar[a], Natalia Tjokro[a], Shuting Sun[b], Adam Junka[c], Philip Cherian[b], Jeffrey Neighbors[d], Graham Russell[e], Charles McKenna[f], Frank Ebetino[b]

[a]*Ostrow School of Dentistry, University of Southern California, Los Angeles, United States*

[b]*BioVinc LLC, Pasadena, United States*

[c]*Pharmaceutical Microbiology and Parasitology, Wroclaw Research Centre EIT, Wroclaw, Poland*

[d]*College of Medicine, Pennsylvania State University, Hershey, United States*

[e]*University of Oxford and University of Sheffield, Sheffield, United Kingdom*

[f]*Chemistry, University of Southern California, Los Angeles, United States*

Osteomyelitis is a limb- and life-threatening orthopedic infection predominantly caused by *Staphylococcus aureus* biofilms. Bone infections are extremely challenging to treat clinically. Therefore, we have been designing, synthesizing, and testing novel antibiotic conjugates to target bone infections. This class of conjugates comprises bone-binding bisphosphonates as biochemical vectors for the delivery of antibiotic agents to hydroxyapatite. In the present study, we utilized a real-time impedance based assay to study the growth of *Staphylococcus aureus* biofilms over time, and to test the antimicrobial efficacy of our novel conjugates on biofilm growth and inhibition in the presence and absence of hydroxyapatite. We tested early and newer generation fluoroquinolone compounds (ciprofloxacin, moxifloxacin, sitafloxacin, and nemonoxacin),

and bisphosphonate-conjugated versions of these antibiotics (bisphosphonate-carbamate-sitafloxacin, bisphosphonate-carbamate-nemonoxacin, etidronate-carbamate-ciprofloxacin, and etidronate-carbamate-moxifloxacin), and found that they were able to inhibit *Staphylococcus aureus* biofilms in a dose-dependent manner. Among the conjugates, the greatest antimicrobial efficacy was observed with bisphosphonate-carbamate-nemonoxacin with an MIC of 1.48 μg/mL. Conjugates demonstrated varying antimicrobial activity depending on the specific antibiotic used for conjugation, the type of bisphosphonate moiety, the chemical conjugation scheme, and the presence or absence of hydroxyapatite. The conjugates designed and tested in this study retained the bone binding properties of the parent bisphosphonate moiety as confirmed by high-performance liquid chromatography. They also retained the antimicrobial activity of the parent antibiotic in the presence or absence of hydroxyapatite, albeit at lower levels due to the nature of their chemical modification. These findings will aid in optimization and testing of this novel class of drugs for future applications to pharmacotherapy in osteomyelitis.

doi:10.1016/j.bonr.2020.100580

P291

Risk factors for avascular bone necrosis in patients with lupus nephritis

Daniela Monova[a], Simeon Monov[b], Dobrina Mluchkova[c], Maria Stambolova[d]
[a]*Department of Internal Medicine, Nephrology and Rheumatology, Medical University - Sofia, Medical Institute, Sofia, Bulgaria*
[b]*Department of Internal Medicine, Clinic of Rheumatology, Medical University - Sofia, Sofia, Bulgaria*
[c]*Department of Imaging Diagnostic, Medical Institute - MVR, Sofia, Bulgaria*
[d]*Department of Internal Medicine, Nephrology and Rheumatology, Medical Institute - MVR, Sofia, Bulgaria*

Objectives: The aim of this study was to investigate the risk factors for symptomatic avascular necrosis of bone (SAVN) in lupus nephritis (LN) patients.

Material and methods: The records of 374 patients (43 males, 331 females) with kidney biopsy-proven LN were reviewed retrospectively. The patients with LN who did not have SAVN were evaluated as a control group. The demographic, clinical, laboratory and management characteristics of two groups of patients were compared and analyzed by logistic regression.

Results: SAVN was present in 17 patients (4 males, 13 females, mean age of 27,4±6,7 years). Among the 17 patients, 28 joints presented SAVN. 12 occurred in hips (2 bilateral), 6-in ankles, 4-in knees, 3-in shoulders and 1- in lumbar spine. In 9 patients SAVN involved 2 or more joints. 14 patients were on steroids at the time of presentation of SAVN. 2 patients were not on steroids and 1 patient did not has documentation of steroid use. Meta-analysis demonstrates a significant increased risk of SAVN in patients with high disease activity and class IV LN ($p< 0,005$). LN patients with SAVN showed an earlier onset age ($p< 0,05$) and received significantly higher total cumulative corticosteroid dose. SAVN was not significantly associated with use of immunosuppressive agents. Serositis, coagulation disorders, vasculitis, cigarette smoking were higher incidence in male with LN and SAVN. Raynaud´s phenomenon, autoimmune thyroiditis, arthritis, Sjögren´s syndrome, antiphospholipid syndrome were higher incidence in female with LN and SAVN.

Conclusion: Many risk factors have been involved in the development of AVN in LN patients. SAVN is prevalent in class IV LN and in younger patients.. Corticosteroids are the principal risk factor, although some cases of SAVN occur in relatively steroid naïve patients. Early detection of AVN is important because the prognosis depends of the stage and location of the lesion.

Keywords: lupus nephritis, avascular bone necrosis

doi:10.1016/j.bonr.2020.100581

P293

Effect of 12-months of isoflavone intake on menopausal symptoms, bone metabolism and risk factors of cardiovascular disease

Byung Yeon Yu[a], Han Jin Oh[b]
[a]*Konyang University Hospital, Daejeon, Republic of Korea*
[b]*Eulji University School of Medicine, Daejeon, Republic of Korea*

Background: Isoflavones are structurally similar to 17-beta estradiol and has “estrogen-like” effect in vivo. The purpose of this study was to investigate the effects of 12 months of isoflavone intake on climacteric symptoms, bone metabolism and risk factors of cardiovascular disease in postmenopausal women.

Methods: Postmenopausal women who were not taking drugs that may affect their estrogen metabolism were randomly recruited. The participants were divided into the isoflavone (18% isoflavone concentration in a 200-ml can; one can per day) and control groups and were studied for 12 months. 51 participants were randomized into each group (isoflavone n=26 versus control n=25).

Results: Climacteric symptoms in the isoflavone group improved significantly by the 12-month follow-up point compared to the baseline levels(, P=0.010), however this improvement did not significantly differ between the two groups

There were no significant differences in the changes in body composition, blood pressure, serum glucose, lipid concentration, c-reactive protein and bone mineral density (lumbar spine, femur neck and total hip) after 12-months between the isoflavone and control groups

Conclusion: In this study, isoflavone supplementation had no significant effect on menopausal symptoms, bone metabolism and cardiovascular risk factors compared to the placebo group after 12 months. Additional large-scale follow-up studies that could verify the effects of isoflavone on postmenopausal women are needed.

doi:10.1016/j.bonr.2020.100582

P294

Bone mass density variability in activity vs remission of the disease in young patients with inflammatory bowel disease: Case series

Iulia Soare[a], Anca Sirbu[a,b], Luminita Cima[a,b], Bogdan Radu Mateescu[c,d], Simona Fica[a,b]
[a]*Endocrinology-University of Medicine and Pharmacy Carol Davila Bucharest, Bucharest, Romania*
[b]*Elias University Hospital, Bucharest, Romania*
[c]*University of Medicine and Pharmacy Carol Davila, Bucharest, Romania*
[d]*Gastroenterology- Colentina Hospital, Bucharest, Romania*

Introduction: Bone mass density in inflammatory bowel disease is influenced by several factors, including malabsorption, malnutrition, glucocorticoid treatment, endocrine disfunctions. Disease activity is another parameter than can influence it, but there are no studies upon how fast these changes can appear. The aim of the

study was to see if there is any precocious difference in the bone mass density depending upon activity of the disease

Patients and methods: 5 young patients (mean age 25 years) with inflammatory bowel disease were prospectively evaluated for one year depending on the moment of the activity of the disease - remission versus active period. The patients were first seen during the remission period (for at least 5 months) and during the active period (in the first 4 weeks). Dual Xray absorptiometry (DXA) of the spine and hip was measured and blood tests were performed. According to ECCO guidelines, Mayo partial score and Harvey-Bradshaw index were used for assessment of the clinical disease activity

Results: During the period of activity of the disease, mean HBI for the patients with CD was 6.3, and c-Mayo for patients with UC was 7.3 (versus 1 and respectively, O during the remission).

During the remission, BMD was higher than during the active period of the disease, both at the spine (mean difference 0.127 g/cm2, mean % BMD 13.6%) and at the hip (mean BMD increase 0.12 g/cm2, mean % BMD hip 14.1%). All the patients received high dose glucocorticoids during the active disease.

Conclusion: Bone mass density can be a precocious modification in young patients with inflammatory bowel disease during the activity of the disease. Close follow up should be offered to these patients and further studies upon larger groups should be continued.

doi:10.1016/j.bonr.2020.100583

P295

Incidence of fractures in a bariatric surgery cohort

Maria Del Pilar Ahijado Guzman[a], Raul María Veiga Cabello[b], Miguel Cantalejo Moreira[a], Justo Ruiz Ruiz[c], Antonio Zapatero Gaviria[c]
[a]*Rheumatology, Htal Universitario de Fuenlabrada, Fuenlabrada, Spain*
[b]*Rheumatology, Hospital Central de la Defensa Gómez Ulla, Madrid, Spain*
[c]*Internal Medicine, Htal Universitario de Fuenlabrada, Fuenlabrada, Spain*

Introduction: Bariatric surgery is the set of surgical techniques whose objective is weight reduction, and it could have complications. One of them may be the increase in the incidence of fractures, secondary to nutritional defects, among others, that could modify bone metabolism with an increase in remodeling.

Objective: To carry out a retrospective observational pilot analysis of a cohort of 140 morbidly obese patients after bariatric surgery, of a total of 304, descriptive of axial and peripheral fractures, among other variables.

Material and method: Data were collected from the University Hospital of Fuenlabrada of a cohort of morbidly obese people who underwent bariatric surgery from 2009 to the present. Were included as variables age in years, sex, body mass index (BMI) before surgery, evolution time since surgery in years, incidence of sleep apnea syndrome (OSAS), incidence and type of fracture, osteoporotic or not, and axial or peripheral. A descriptive and frequency analysis, and a chi-square contingency table between incidence of fracture, and gender, OSAS, or childhood obesity, were performed.

Results: A 48.76 years old cohort was observed, 25.7% men/74.3% women, 30.8% childhood obesity, BMI of 45.65 kg / m^2, and 45% with a diagnosis of OSAS. A 15% of fractures were noted: 66.66% considered as osteoporotics (40.76% axial, 50.31% peripheral, and 8.93% of both) in a time of evolution of 5.81 years, and without relationship with gender, OSAS or childhood obesity ($p = 0.7$, $p = 0.15$, $p = 0.16$)

Conclusions: It is a study what higlights that bariatric surgery in Fuenlabrada area is mainly performed on morbidly obese women in adulthood. There is a high rate of OSAS, and an increase in the incidence of fractures unrelated to gender, OSAS or childhood obesity, despite the fact that in the bariatric surgery protocol densitometric osteoporosis is an exclusion criterion.

doi:10.1016/j.bonr.2020.100584

P296

Tophaceous Pseudogout in the middle finger mimicking soft tissue tumor

Nestor Avgoustidis[a], Nikolaos Kougkas[a], Elias Drakos[b], Ioannis Galanakis[c], Katerina Pateromichelaki[a], Sofia Pitsigavdaki[a], Ioannis Papalopoulos[a], Argyro Repa[a], Prodromos Sidiropoulos[a]
[a]*Rheumatology, University Hospital of Heraklion, Heraklion, Greece*
[b]*Pathology, University of Crete, Medical School, Heraklion, Greece*
[c]*Orthopaedic Surgery, University Hospital of Heraklion, Heraklion, Greece*

When CPPD crystals are deposited in a massive state, the condition is designated as tophaceous pseudogout. Reports of tophaceous pseudogout occurring in the upper limb are rare. We report a case of tophaceous pseudogout in the middle finger. Patient has provided informed consent for clinical case publication.

Fig. 1. Cloudy-calcified mass on the radio-volar side of right middle finger.

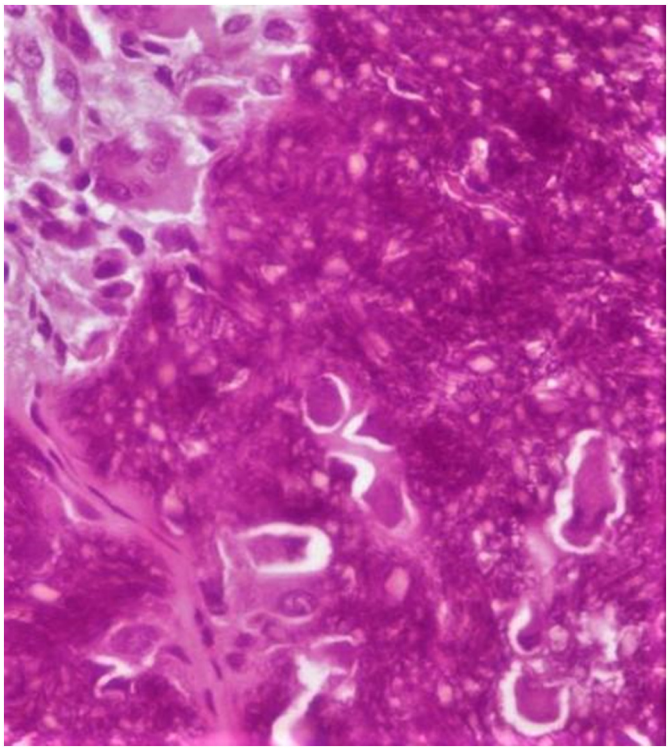

Fig. 2. Eosin and heamatoxylin stain; original magnifications: X400.

78 year old female presented in our outpatient department with a mass in the right middle finger, which had first occurred 6 months ago. Plain X-ray has revealed a cloudy-calcified mass (Fig. 1). Laboratory tests were unremarkable

She was referred to orthopaedic department for excision of the underlying lesion. Histological report was consistent with tophaceous pseudogout. Microscopic analysis of the lesion shows heavily calcified purple areas,rhomboid crystals are observed in the calcified areas, showing positive birefringence under compensated polarized light. (Fig 2). At one year follow-up, no obvious signs of recurrence were observed. Most publications on tophaceous pseudogout are case reports and frequently occurred in middle aged and elderly patients, with a female predominance.

Differential diagnosis is broad including: tophaceous gout, calcified tumors, synovial chondromatosis, chondrosarcoma, chondroma, but differentiation from a malignant tumor is extremely important because misdiagnosis might lead to overtreatment and unnecessary laboratory and imaging investigations.

doi:10.1016/j.bonr.2020.100585

P297

Diagnostic value of Trabecular Bone Score (TBS) in Kidney Transplant (Tx)

Marzia Pasquali[a], Lida Tartaglione[b], Silverio Rotondi[c], Natalia De Martini[b], Daniele Diacinti[d], Sandro Mazzaferro[a]
[a]*Nephrology, Policlinico Umberto I, Sapienza University, Rome, Italy*
[b]*Policlinico Umberto I, Sapienza University, Rome, Italy*
[c]*ICOT, Latina, Italy,*
[d]*Radiology, Policlinico Umberto I, Sapienza University, Rome, Italy*

Introduction, aim: TBS estimates fractures(FX) risk, but few data are available in Tx.

Methods: In 60Tx pts and in 60 controls(C) we assayed BMD, TBS, fractures and aortic calcifications (AC).

Results: Tx-pts (47±13y.o., Tx since 6,0±5,4y, eGFR 50±18ml/min), had high PTH (132±136ng/ml) and Ca (9,8±0,9mg/dl) and low 25vitD (21±10ng/ml). Compared to C, Tx-pts had lower Neck-Tscore (-1,43± 1,27 vs -0,39±1,05;p< .0001) and TBS (1.321±0.114 vs 1.404±0.047; p=.0001) and higher prevalence of Fx (13vs2;p< 0.001). Both in Tx (1.150±0.048 vs 1.364±0.081;p< .001) and in C (1.408±0.03 vs 1.292± 0.16;p< .001) TBS was lower in FX than in non-FX. In non-FX, TBS was lower in Tx (1.364±0.081) than in C (1.408±0.03; p< .001), similarly to Neck-Tscore(-1.32±1.3 vs -0.36±1.05;p< .01). 32/60 Tx had AC and TBS was lower in those with AC (1.281±0.11 vs 1.366±0.09; p=.002), while Neck-Tscore was not. In Tx, TBS was correlated with age (r=-0.28;p< 0.02) and Lumbar-Tscore (r=0,25;p< 0.049). Importantly, TBS was negatively correlated with AC (-0.33;p< 0.009). Regression analysis showed TBS predicts FX in Tx (OR 0.96, 95% CI 0.92-0.98); ROC curve AUC was 0.98 for identification of prevalent FX. In a subgroup of 26Tx with follow-up 9.1±1.8y, we recorded no difference in the two time-spaced evaluations of Neck-Tscore, TBS and in the number of cases with FX or AC. However, AC score increased (from 1,9±5 to 7,5±5, p< 0.004).

Conclusions: Tx-pts had TBS values indicative of pathologic bone microarchitecture. TBS was lower than C even in cases without FX. TBS could be an early marker of FX risk in Tx-pts. Importantly,TBS was negatively correlated with the score of AC (link: bone health-calcification risk).

doi:10.1016/j.bonr.2020.100586

P298

Increased PTH maintains bone mineral density in patients with CKD

Pierre-Emmanuel Cailleaux[a], Agnes Ostertag[a], Pascal Houillier[b], Marie Metzger[c], Martin Flamant[b], Pablo Urena Torres[d], Martine Cohen-Solal[a]
[a]*Hopital Lariboisiere, Inserm U1132 and Université de Paris, Paris, France*
[b]*Department of Physiology, Université de Paris, Paris, France*
[c]*Epidémiologie Rénale et Cardiovasculaire, INSERM U-1018 and Université Saint-Quentin, Villejuif, France*
[d]*Nephrology, Aura Nord, Saint-Ouen, France*

Introduction: Patients with chronic kidney disease (CKD) have an increased risk of fragility fractures. Bone mineral density (BMD), a key element to predict patients at risk of fracture in non-CKD patients, is now recommended by KDIGO guidelines. Parathyroid hormone (PTH) levels are associated with bone loss in non-CKD patients. It is unknown whether PTH levels predict bone loss in early CKD.

Objective: We aimed to study the predictive value of PTH levels of bone loss in CKD patients.

Methods: The NephroTest cohort included adults with CKD stages 1 to 5 followed for a mean duration of 4.34±2.03 years. Glomerular filtration rate (mGFR, 51Cr-EDTA) and serum mineral biomarkers were measured in all and BMD in a subset. We used descriptive analysis for cross-sectional data and linear mixed effects model to investigate the relationship between PTH and the changes in BMD.

Results: 858 patients (mean age 58.9±15.2, sex ratio men/women 2:1, BMI 26.8±5.3kg/m²) underwent at least two successive BMD measurements. At baseline, CKD grades were 19% G1-2, 24.4% G3a, 31.2% G3b and 19.7% G4. Cross-sectional analysis revealed that serum PTH levels increased significantly with the severity of CKD (p< 0.001), so were serum phosphate concentrations (p< 0.001). BMD decreased

significantly throughout CKD at the femoral neck (p-value < 0.001) and total hip (p-value < 0.001), but not at the lumbar spine Investigating longitudinal bone loss, the adjusted PTH concentrations at baseline had a negative relationship with BMD at femoral neck (slope=-0.022, p< 0.01), at total femur (slope=-0.026, p< 0.01) and at the lumbar spine (slope=-0.030, p< 0.01), with a non-significant relationship at the radius (slope=0.011, p=0.07).

Conclusion: CKD was associated with low femoral neck BMD, which was inversely associated with baseline PTH level. This suggests that the increase in PTH levels in CKD would be a compensatory mechanism preserving BMD with time.

doi:10.1016/j.bonr.2020.100587

P299

Investigation of whole body vibration intervention to reduce rates of disuse-related bone loss after spinal cord injury

Sylvie Coupaud[a], Mariel Purcell[b]
[a]*Biomedical Engineering, University of Strathclyde, Glasgow, United Kingdom*
[b]*Queen Elizabeth National Spinal Injuries Unit, NHS Greater Glasgow & Clyde, Glasgow, United Kingdom*

Significant bone loss occurs in the long bones of the paralysed limbs of patients with complete spinal cord injury (SCI). Patient-specific rates of decreases in bone mineral density (BMD) can be calculated from pQCT scan series performed at fracture-prone sites (around the knees and ankles), to detect the onset of disuse-related osteoporosis within months of injury and implement targeted, early intervention.

Study objectives were: 1) Early detection and intervention to reduce bone loss in the paralysed limbs after SCI; 2) Preliminary evaluation of Whole Body Vibration (WBV) as a physical intervention to reduce rates of bone loss.Ethical approval was provided by the National Health Service to recruit patients with motor-complete SCI at neurological levels C4 and below. Baseline pQCT scans (XCT3000, Stratec) were performed in the tibia and femur within 6 weeks, and repeated at 4 months post-SCI. Changes in trabecular BMD, total BMD, and bone mineral content were calculated. Participants with FAST bone loss (≥ 3% decrease in BMD at the distal tibia and/or femur) were offered WBV intervention. 27Hz side-alternating WBV (Galileo, Novotec) was applied 3 times per week for four months (FAST-WBV group). The REF group underwent standard rehabilitation only. Rates of bone loss were calculated for FAST-WBV and REF groups, and compared between time-points (Baseline, 4 months, 8 months, 12 months post-SCI).

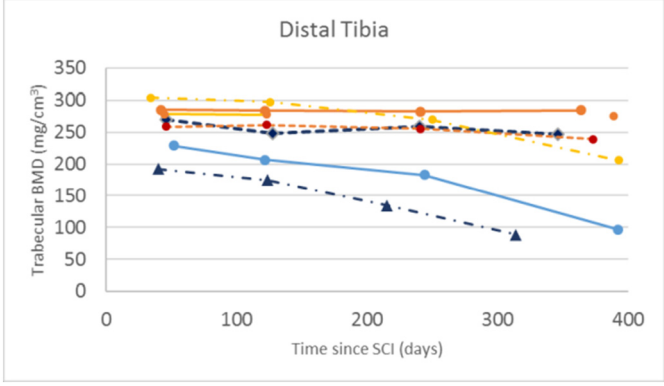

Fig. 1. BMD changes at the distal tibia (yellow lines: REF group; blue lines: FAST-WBV group).

Overall, rates of bone loss at fracture-prone sites were not significantly reduced in the FAST-WBV group (n=3). Data evaluating WBV as an intervention to reduce bone loss were inconclusive, based on small participant numbers.

doi:10.1016/j.bonr.2020.100588

P301

A 2 years longitudinal data of bone health in adolescent patients with axial spondyloarthritis

Shin-Hee Kim[a], Kwi Young Kang[b]
[a]*Catholic University of Korea, Incheon, Republic of Korea*
[b]*Internal Medicine, Catholic University of Korea, Incheon, Republic of Korea*

Objective: The present study examined bone mineral density (BMD) and trabecular bone score (TBS) in adolescent patients with axial spondyloarthritis (axSpA) at baseline and 2 years follow-up and investigated the association between systemic inflammation and bone health over 2 years.

Method: We analyzed clinical characteristics of 43 adolescent axSpA patients. Baseline assessment included age, disease duration, treatment agents, clinical, radiologic and laboratory data. BMD at the lumbar spine, femoral neck, and total hip and TBS were measured by dual energy X-ray absorptiometry at baseline and 2 years follow-up. Multivariate linear regression analyses were performed to identify factors independently associated with BMD and TBS. We analyzed associations between BMD change and reduction of inflammatory markers.

Result: The average age was 17.9±1.6 years and mean disease duration was 2.2 ± 2.2 years. At baseline, BMI, ESR, and spinal structural damage were associated with Z score in the lumbar spine in multivariate analysis. TBS was associated with ESR and severity of sacroiliitis. After 2 years, lumbar spinal BMD and Z scores of the lumbar spine and femoral neck were increased. Change of BMD in the lumbar spine was correlated with the reduction of ESR ($r = 0.40$, $p=0.02$). Z score changes in the lumbar spine and total hip were correlated with the reduction of ESR ($r = 0.37$, $P = 0.04$ and $r = 0.37$, $P = 0.05$). BMD change in the total hip was correlated with the reduction of CRP ($r = 0.38$, $P = 0.03$). Z score change in the femoral neck, total hip was correlated with the reduction of CRP ($r = 0.32$, $P = 0.08$. $r = 0.40$, $P = 0.03$).

Conclusions: In adolescent axSpA patients, bone health was associated with systemic inflammation and severity of structural damage. Reduction of systemic inflammation was associated with improvement of bone health.

doi:10.1016/j.bonr.2020.100589

P302

Regulation of the expression and activity of YAP in osteosarcoma stem cells by Calpain-6

Joëlle Tchicaya Bouanga, Emilie Chotard, Martine Cohen-Solal, Dominique Modrowski
UMR-1132, BIOSCAR, INSERM, Paris, France

Lung metastases reduced the survival of patients with osteosarcoma. To evade the tumor and home in distant tissues, cancer cells have to adapt to various environments. This should involve specific regulations of mechano-transduction especially YAP a key effector of the Hippo pathway. We previously reported that calpain-6 expressing cells have cancer stem cell characteristics associated with higher metastatic abilities. Using immunofluorescence and FACS analyses, we

now show that in osteosarcoma cells but also in bone tumors, calpain-6 expression was associated with high levels of YAP. Western blots showed that YAP protein was increased by 40% in calpain-6 overexpressing (Calp6+) cells as compared to cells expressing calpain-6 shRNA (Calp6 KD) although the expression of YAP mRNA was unchanged. Consistently, Calpain-6 inhibited LATS activation in serum-starved cells. Moreover, a proteinase K protection assay showed that a large amount of GSK3 and Axin were trapped in intracellular vesicles in Calp6 + as compared to calp6 KD cells. Thus, calpain-6 stabilizes YAP through modulation of the Hippo pathway and by regulating the fate of the β-catenin destruction complex. Unexpectedly, high YAP expression was not always found associated with a strong TEAD transcriptional activity and CTGF expression, especially when the cells were cultured at very high density. In vitro, exposure to 1μM verteporfin induced the proliferation and then detachment of both Calp6 + and KD cells. In mice that were orthotopically implanted with K7M2 osteosarcoma cells, IP injections of verteporfin (6 mg/Kg) significantly reduced bone tumor development, since 5/17 mice developed a bone tumor, whereas, 11/16 solvent-treated mice did. However the 5 verteporfin-treated mice with a bone tumor developed huge lung metastases. Together our results suggest that YAP has distinct roles in osteosarcoma stem-like cells in primary tumors and in metastatic sites where it could be involved in cancer cell dormancy.

doi:10.1016/j.bonr.2020.100590

P303

Effects of bisphosphonates on osteoporosis induced by Duchenne muscular dystrophy: A prospective study

Wenbin Zheng[a], Yi Dai[b], Jing Hu[a], Dichen Zhao[a], Ou Wang[a], Yan Jiang[a], Weibo Xia[a], Xiaoping Xing[a], Mei Li[a]
[a]*Department of Endocrinology, Key Laboratory of Endocrinology, National Health and Family Planning Commission, Peking Union Medical College Hospital, Chinese Academy of Medical Sciences and Peking Union Medical College, Beijing, China*
[b]*Department of Neurology, Peking Union Medical College Hospital, Chinese Academy of Medical Sciences and Peking Union Medical College, Beijing, China*

Objective: Duchenne muscular dystrophy (DMD) is a severe X-linked progressive neuromuscular disease, with increased risk of osteoporosis and bone fractures. We prospectively evaluate the effects of oral and intravenous bisphosphonates on bone of children with DMD.

Methods: In this study, a total of 52 children with DMD were included. They were divided into zoledronic acid (ZOL), alendronate (ALN) and control group according to bone mineral density (BMD) and a fragility fracture history. 17 patients received ZOL and 18 patients took ALN. 17 patients in control group only took calcium, vitamin D and calcitriol. During the treatment, BMD, serum levels of alkaline phosphatase (ALP) and cross-linked C-telopeptide of type I collagen (β-CTX) were evaluated.

Results: After 24-month treatment, the percentage change of BMD at lumbar spine was 23.2 ± 9.7% and 23.6 ± 8.8% in ZOL and ALN group, with significant increase of BMD Z-scores in these two groups (all $P < 0.01$ vs baseline). The increases did not differ between ZOL and ALN groups, but significantly greater than control group ($P < 0.01$). Serum β-CTX and ALP levels were decreased by 44.4 ± 18.0% and 31.9 ± 26.7% in ZOL group, and 36.0 ± 20.3% and 25.8 ± 14.4% in ALN group, respectively (all $P < 0.01$ vs baseline).

Conclusions: Zoledronic acid and alendronate had similar protective effects to increase bone mineral density and reduce bone resorption in children with DMD, which were superior to treatment of calcium, vitamin D and calcitriol.

Keywords: Duchenne muscular dystrophy; osteoporosis; zoledronic acid; alendronate

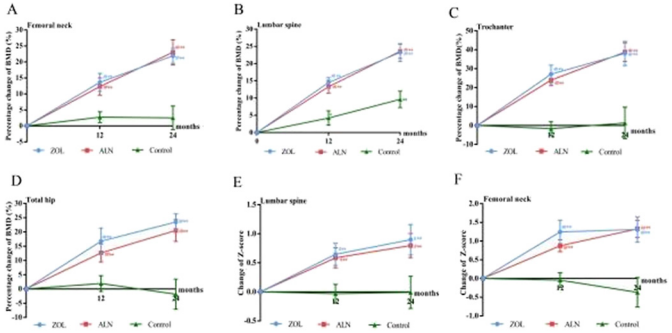

Changes of bone mineral density and its Z-score at femoral neck and lumbar spine during treatment.

doi:10.1016/j.bonr.2020.100591

P304

Bone density as indicator of fracture risk in children with chronic diseases

Silvia Vai[a], Francesca Broggi[a], Carla Colombo[b], Luciana Ghio[b], Alberto Edefonti[b], Fabrizia Corona[b], Gabriella Nebbia[b], Maria Luisa Bianchi[a]
[a]*Experimental Laboratory for Children's Bone Metabolism Research, Istituto Auxologico Italiano IRCCS, Milano, Italy*
[b]*Pediatric Clinic, University of Milano, Milano, Italy*

BMD is considered a predictor of the risk of fragility fractures in adults, but there are insufficient data for children and adolescents.

The aim of this prospective study was to evaluate whether BMD can be used to estimate the risk of fragility fractures (i.e. for minor trauma) in children affected by chronic diseases.

We previously reported that in 1,200 children/adolescents (654 F, 546 M, age 2-19 years), 71% of those with fractures had a Z-score ≤-2. Following this observation, we prospectively studied 698 patients (aged 3-18 years at baseline) affected by various chronic diseases (renal diseases, systemic connective diseases, cystic fibrosis, liver diseases, Duchenne Muscular Dystrophy) for 5 years. Spine and total body (TB) BMC and BMD were measured with DXA (Hologic).

During the 5-year follow-up, 164 patients had one or more fractures for minor trauma. The average Z-score was -2.6±1.7. It was < -2 in 101 cases (61.6%), and between -2 and -0.9 in the remaining 63 (38.4%).

A strong association between the baseline BMD and the 5-year fracture risk was observed ($p < 0.001$), and the risk markedly increased with a Z-score < -2.

For each 1 SD decrease of TB BMD, we observed a 2.1-fold increase in the risk of a peripheral fracture; and for each 1 SD decrease of spine BMD, a 2.8-fold increase in the risk of a vertebral fracture.

The risk of a new fracture was increased 1.8-fold after a previous fracture.

There was an increased risk of fractures if the BMD increase was < 5% per year. GCs doubled the risk of fractures if the Z-score was < -1.5. No gender differences were observed.

In conclusion, in young patients affected by chronic diseases, BMD seems predictive of the risk of fragility fractures over the next 5 years.

doi:10.1016/j.bonr.2020.100592

P305

Detailed analysis of TNAP expression in zebrafish paves the way for establishment of a novel *in vivo* model reflecting the rare disease hypophosphatasia

Angela Borst[a], Barbara Ohlebusch[a,b], Rabea Blümel[a], Eva Klopocki[a], Franz Jakob[c], Daniel Liedtke[a], Stephanie Graser[c]
[a]*Institute for Human Genetics, Biocenter, Würzburg, Germany*
[b]*Zoological Institute, University of Cologne, Cologne, Germany*
[c]*Orthopedic Department, University of Würzburg, Würzburg, Germany*

Hypophosphatasia (HPP) is a rare, hereditary disease caused by mutations in the *ALPL* gene, which is encoding the ectoenzyme "tissue-nonspecific alkaline phosphatase" (TNAP). HPP can lead to severe functional defects in dental and bone mineralization processes. Besides that, the rare disease can be accompanied by craniosynostosis as well as neurological disorders like epileptic seizures, anxiety, and depression. In this project, we established the zebrafish (*Danio rerio*) as a novel *in vivo* model system for detailed investigations and visualization of tissue-specific effects of HPP within the context of craniosynostosis and neuronal symptoms.

For elucidation of *alpl* expression in zebrafish, whole mount *in situ* hybridization (ISH), qPCR and combined *alpl*-ISH/Proliferating cell nuclear antigen (PCNA) immunostaining was performed at different developmental stages and in whole brains from adult zebrafish. Moreover, visualization of alkaline phosphatase activity was established via ELF97® Phosphatase staining on brain sections from adult zebrafish. In future experiments we plan to perform *in vivo* Alizarin red (AR) staining and confocal imaging for the detection of craniosynostosis and abnormal skeletal development in the HPP-zebrafish model.

Interestingly, *alpl*-ISH signals could be detected in all embryonal stages that have been analyzed as well as in adult brain sections. Zebrafish embryos showed prominent TNAP expression in brain, nephros, retina, and fin. In the adult zebrafish brain, *alpl* mRNA and enzymatic activity was detected in more restricted areas, among others in the amygdala, which implies its connection to anxiety disorders. Furthermore, we successfully established AR staining of developing skull bone structures for analysis of pathological closure of the cranial sutures.

In summary, we developed a zebrafish model system for functional analyses of HPP symptoms related to the nervous system and craniosynostosis. Establishment of diverse molecular techniques paves the way for future tissue-specific investigations and helps providing new molecular insights into consequences of *alpl* mutations *in vivo*.

doi:10.1016/j.bonr.2020.100593

P306

Deciphering the skeletome: Contributions from mouse forward genetics ENU mutagenesis campaigns

Robert Brommage
Independent Scientist, Texas, United States

N-ethyl-N-nitrosourea (ENU) is a chemical super-mutagen that increases spontaneous mutation rates by ~100-fold, predominantly through point mutations. Many groups have utilized forward genetic ENU mutagenesis campaigns to produce mutant mice having altered phenotypes in areas of interest, including bone. Next generation genome sequencing protocols have replaced traditional methods involving positional cloning to rapidly identify the exact gene mutations responsible for aberrant phenotypes. In addition to LoF mutations, ENU mutagenesis can also produce activating GoF, hypomorphic and dominant-negative mutations. When gene knockout produces lethality hypomorphic ENU mutations can allow phenotypic analyses on viable mutant mice.

Mutations in 75 genes identified through mouse ENU mutagenesis campaigns influence skeletal morphological patterning (*Ankrd11, Arsb, Col2a1, Colgalt1 Cplaine1, Ctnnb1, Eif3c, Ednra, Etv5, Fbn2, Fgfr1, Fgfr2, Flnb, Fras1, Frem1, Frem2, Gja1, Gnptab, Hmx1, Hoxd12, Ift140, Impa2, Intu, Kif7, Lmbr1, Lrp6, Mks1, Nell1, Npr3, Nubp1, Nubp2, Plzf, Ptch1, Rdh10, Shh, Smpd3, Sufu, Tapt1, Tent5a, Ttc21b, Trip11, Tulp3, Twist, Wdr19, Wdr35, Xylt1*), bone mass (*Col1a1, Crh, Enpp1, Gh, Lrp5, Ostm1, Phospho1, Ptpn6, Rankl, Tcirg1, Zdhhc13*), mineral homeostasis (*Alpl, Ap2s1, Asgr1, Casr, Galnt3, Gna11, Gnas, Jak1, Klotho, Phex, Trpv5, Umod*), bone inflammation (*Fgr, Gdf5, Plcg2, Pstpip2*), and/or ectopic calcification (*Car2, Polg2*).

Although most ENU mutants have phenotypes similar to those observed in gene knockout mice, ENU mutagenesis yielded hypomorphic (*Ptch1*), activating (*Casr, Crh, Fgr, Jak1, Plcg2*) and dominant-negative (*Gdf5, Gja1, Tcirg1*) mutations.

Forty-one ENU mutant mouse lines have skeletal defects mimicking human rare bone disease genetic disorders described in the *International Skeletal Dysplasia Society* 2019 Skeletal Disorder Nosology database (Mortier GR et al., American Journal of Medical Genetics. 179:2393-2419; 2019).

Characterizing additional ENU mutants should add to our knowledge of *Skeletome* genes affecting bone mass, architecture, mineralization and strength.

doi:10.1016/j.bonr.2020.100594

P307

Identifying causal genes for families with history of osteoporosis and/or atypical femur fractures by building a common workflow

Wei Zhou, Denise van de Laarschot, Annemieke Verkerk, Carola Zillikens
Erasmus Medical Center, Rotterdam, Netherlands

Object: We aim to identify causal genes for families and sporadic cases with a history of osteoporosis and/or atypical femur fractures (AFF). To facilitate analyses, we are building a common workflow using a bioinformatics pipeline to select for genetic variants from whole exome sequencing data.

Methods: We performed whole exome sequencing on a family including seven members with osteoporosis, three of which have AFF. We hypothesize that 1) osteoporosis and AFF have separate causal genes, 2) a gene on top of an osteoporosis gene causes AFF and 3) more than one gene causes osteoporosis, and in combination predispose to AFF. In this regard, variants were filtered for rare (MAF $< =0.001$) exonic nonsynonymous variants and indels and splicing variants assuming a dominant mode of inheritance using a customized R package based on a model for the familial osteoporosis and a separate model for AFF. We used different in-house and publicly available databases to prioritize variants for the identification of candidate genes. Experiments were designed for further functional validation.

Results: We created an R package to customize the variants filtering. After filtering, 34 variants in 34 genes were left in the model for osteoporosis and 81 variants in 63 genes were left in the model for AFF. Prioritization was performed using gene and protein information from different resources, which resulted in several genes that require further experimental validation.

Conclusion: Our workflow facilitates the identification of causal genes for families with osteoporosis and/or AFF. Further experimental validation for selected candidate genes is needed.

doi:10.1016/j.bonr.2020.100595

P308

Exploitation of circulating CD34+ cells and non-genotoxic conditioning to overcome major limitations to treatment for autosomal recessive osteopetrosis

Valentina Capo[a], Sara Penna[a,b], Ivan Merelli[c], Matteo Barcella[a], Serena Scala[a], Luca Basso-Ricci[a], Elena Draghici[a], Eleonora Palagano[d,e], Erika Zonari[a], Paolo Uva[f], Roberto Cusano[f], Alessandro Aiuti[a], Francesca Ficara[d,e], Cristina Sobacchi[d,e], Bernhard Gentner[a], Anna Villa[a,d]
[a]San Raffaele Telethon Institute for Gene Therapy, IRCSS San Raffaele Scientific Institute, Milan, Italy
[b]DIMET, University of Milano-Bicocca, Monza, Italy
[c]Institute for Biomedical Technologies, National Research Council, Segrate, Italy
[d]CNR-IRGB, Milan Unit, Milan, Italy
[e]Humanitas Clinical and Research Center - IRCCS, Rozzano, Italy
[f]CRS4, Science and Technology Park Polaris, Pula, Italy

Autosomal recessive osteopetrosis (ARO) is a rare genetic disease, affecting osteoclast differentiation or function. Most patients present mutations in *TCIRG1* gene, encoding the a3 subunit of V-ATPase proton pump, necessary for bone resorption. Symptoms include dense and brittle bones, limited bone marrow cavity, anaemia and progressive nerve compression, leading to death in the first decade of life. To date, the treatment with allogeneic hematopoietic stem cell transplantation is hampered by availability of HLA-matched donors, toxicity of conditioning regimens and significant transplant-related morbidity.

We studied possible solutions to overcome these major limitations.

First, we dissected the features of CD34+ cells circulating at high frequency in ARO patients. We observed that their peripheral blood has a cellular composition that resembles bone marrow. Preliminary analysis of CD34+ cell transcriptome indicated the expression of hematopoietic stem and progenitor genes, similarly to conventional stem cell sources. Thus, circulating CD34+ cells could be exploited as an autologous cell source for gene therapy protocols.

Second, we plan to study the efficacy of non-genotoxic conditioning regimens in the osteopetrotic *oc*/*oc* murine model, to reduce transplant-related complications and mortality while ensuring efficient engraftment of donor- or gene corrected autologous- cells. In particular, saporin (SAP) toxin will be conjugated to anti-CD45 or anti-cKit antibodies to obtain SAP-CD45 or SAP-cKit antibody-drug conjugates. We aim to selectively deplete hematopoietic stem and progenitor cells, sparing off target organs. Due to the short life span of *oc*/*oc* mice, newborn pups will be conditioned and then transplanted with WT or lentiviral vector transduced ARO Lin- cells.

Overall, we provided evidence that autologous CD34+ cells could be an effective source of HSPC for gene correction, avoiding the search for a HLA-matched donor. The application of non-genotoxic conditioning will further reduce the treatment burden for autosomal recessive osteopetrotic patients.

doi:10.1016/j.bonr.2020.100596

P309

Investigation of the bone damage in mucopolysaccharidosis type I Hurler Syndrome: Pathophysiological mechanisms and the impact of *ex vivo* gene therapy

Sara Penna[a,b], Stefania Crippa[a], Valentina Capo[a], Ludovica Santi[a], Roberto Bosotti[a], Mara Riminucci[c], Alessandro Corsi[c], Marta Serafini[b], Bernhard Gentner[a], Alessandro Aiuti[a], Maria Ester Bernardo[a], Anna Villa[a,d]
[a]San Raffaele-Telethon Institute for Gene Therapy, IRCSS San Raffaele Scientific Institute, Milan, Italy
[b]University of Milano-Bicocca, School of Medicine and Surgery, Monza, Italy
[c]Department of Molecular Medicine Sapienza University, Rome, Italy
[d]CNR-IRGB, Milan Unit, Milan, Italy

Hurler syndrome is the most severe form of mucopolysaccharidosis type 1 (MPSIH), one of the most frequent autosomal recessive lysosomal storage diseases. MPSIH is caused by mutations in *IDUA* (alpha-L-iduronidase), a molecule involved in the catabolism of glycosaminoglycans. MPSIH patients experience severe symptoms such as dysostosis multiplex, cognitive impairment, heart disease, respiratory problems, hepatosplenomegaly and reduced life expectancy. Despite several therapeutic interventions have been developed, including enzyme replacement therapy (ERT) and allogeneic hematopoietic stem cell transplantation (HSCT), the delivery of sufficient enzyme to the bones and consequent correction of bone defects remains an unmet clinical need. A phase I/II clinical trial based on *ex vivo* HSC gene therapy (GT) is ongoing at our institution. Preliminary results showed supraphysiologic IDUA levels in peripheral blood (PB) and improved joint mobility. However, the pathogenesis of bone defects in MPSIH is still debated. We investigated the role of mesenchymal stromal cells (MSCs) and osteoclasts in bone remodeling. As expected, IDUA activity was absent in MPSIH-MSCs. In parallel, we differentiated osteoclasts from peripheral blood or bone marrow of MPSIH patients pre- and post-GT. Osteoclast differentiation and bone resorption activity were not affected by IDUA absence. Notably, we observed supraphysiologic IDUA levels in osteoclasts and in culture media after GT at different time points. We hypothesized that osteoclasts can deliver IDUA enzyme in the bone microenvironment, cross-correcting MSCs and their progeny. Dissecting this mechanism, we observed a robust expression of Sortilin-1 and LAMP-1 presumably responsible for IDUA uptake in MSCs exposed for 16h to GT osteoclast-conditioned medium. To confirm the detoxification of the bone cells, we plan to develop a 3D *in vitro* bone model to mimic the bone physiology of healthy donors and patients. Morover, we will analyze bone biopsies obtained from MPSIH patients pre- and one year post-GT by transmission electron microscopy and immunohistochemistry.

doi:10.1016/j.bonr.2020.100597

P310

Skeletal deterioration in *COL2A1*-related spondyloepiphyseal dysplasia occurs prior to the development of osteoarthritis

Tim Rolvien[a], Timur A. Yorgan[b], Uwe Kornak[c], Irm Hermans-Borgmeyer[d], Stefan Mundlos[c], Tobias Schmidt[b], Andreas Niemeier[e], Thorsten Schinke[b], Michael Amling[b], Ralf Oheim[b]
[a]Department of Orthopedics, University Medical Center Hamburg-Eppendorf, Hamburg, Germany
[b]Department of Osteology and Biomechanics, University Medical Center Hamburg-Eppendorf, Hamburg, Germany
[c]Institute of Medical Genetics and Human Genetics, Charité-Universitätsmedizin, Berlin, Germany
[d]Center for Molecular Neurobiology, University Medical Center Hamburg-Eppendorf, Hamburg, Germany
[e]Department of Biochemistry and Molecular Cell Biology, University Medical Center Hamburg-Eppendorf, Hamburg, Germany

Spondyloepiphyseal dysplasia, a combination of progressive arthropathy with variable signs of skeletal dysplasia, can be a result of mutations in the collagen, type II, alpha 1 (*COL2A1*) gene. The skeletal phenotype (e.g., density, microstructure) in this disorder has hitherto not been studied. A 50-year-old female patient and her

8-year-old son with flattening of vertebral bodies and early-onset osteoarthritis presenting at our department were genetically tested using a custom designed gene bone panel including 386 genes. Bone microstructure and turnover were assessed using high-resolution peripheral quantitative computed tomography (HR-pQCT) and serum bone turnover markers, respectively. Furthermore, the bone and cartilage phenotype of male mice heterozygous for the loss-of-function mutation of *Col2a1* (*Col2a1*$^{+/d}$) was analyzed compared to wildtype littermates using μ-CT and histomorphometry. We identified a dominant *COL2A1* mutation (c.620G>A p.(Gly207Glu)) indicating spondyloepiphyseal dysplasia in the female patient and her son, both being severely affected by skeletal deterioration. Although there was no osteoarthritis detectable at first visit, the son was affected by trabecular osteopenia, which progressed over time. In an iliac crest biopsy obtained from the mother, osteoclast indices were remarkably increased. *Col2a1*$^{+/d}$ mice developed a moderate skeletal phenotype expressed by reduced cortical and trabecular parameters at 4 weeks (Ct.Th 82.7±11.2 μm *vs.* 108.1± 15.2 μm, $p< 0.005$; BV/TV 6.93±2.5 % *vs.* 11.55±2.42 %., $p< 0.05$). Importantly, no articular defects could be observed in the knee joints at 4 weeks, while osteoarthritis measured by OARSI score was only detectable in 12-week-old mice. In conclusion, our results indicate that collagen type II deficiency in spondyloepiphyseal dysplasia leads to skeletal deterioration with early onset in humans and mice that occurs prior to the development of osteoarthritis.

doi:10.1016/j.bonr.2020.100598

P311

Phenotypic characterization of human primary mandibular osteoblasts from patients with fibrous dysplasia of bone

Johan Sergheraert[a,b], Marie-Laure Jourdain[a,b], Julien Braux[a,b], Christine Guillaume[a], Halima Kerdjoudj[a], Sébastien Laurence[b], Fabien Bornert[c], Sophie C. Gangloff[a], Frédéric Velard[a], Cédric Mauprivez[a,b]
[a]*EA4691 BIOS, Université de Reims Champagne Ardenne, Reims, France*
[b]*CHU Reims, Pôle de Médecine Bucco-Dentaire, Reims, France*
[c]*CHU de Strasbourg, Strasbourg, France*

Objectives: Fibrous dysplasia of bone (FD) is a rare genetic disease that normal bone is progressively replaced by fibroosseous lesions. Hypertrophic cranio-facial lesions may be responsible of pain, nervous compression and/or aesthetics injuries. The pathogenesis of these lesions has been poorly studied and the clinical management is only symptomatic. The aim of this study is to characterize primary culture of human mandibular osteoblasts from patients presenting fibrous dysplasia compared to healthy patients.

Results and discussion: FD cells exhibited an increase in their proliferative capacities compared to cell controls (doubling time 4.6 vs 2.3 days, $p< 0.05$), accordingly to the literature based on appendicular osteoblast culture [Marie and coll, 1997]. At day 21, FD culture decreased their ALP activity (23.86 vs 50.64 mIU/L/μg total protein, $p< 0.05$) and osteocalcin expression as compared to cell controls, suggesting an altered process of osteogenic differentiation. Furthermore, a decrease in extracellular calcium deposits in FD cells culture (230.99 vs 423.18 μg/mL, $p>0.05$) tends to indicate defective mineralization abilities. These original data are consistent with histologically observed defects in iliac bone sections [Terpstra and coll, 2002]. The osteoclastogenic activity may be raised in FD culture by decreasing the secretion of OPG compared to healthy culture (D14 : 32,27 vs 84.47 ng/mL, $p< 0.05$; D21 : 18,63 vs 95.58 ng/mL, $p< 0.05$). In both conditions, no expression of RANK-L was detected in supernatants or at the cell membrane surface.

Conclusion: These preliminary results suggest that cells from mandibular FD lesions were highly proliferative with an immature phenotype, compared to controls. In contrast to appendicular skeleton, oro-facial dysplasic lesions exhibit a high bone resorption activity which could explain hypertrophic lesions. Comparative study between mandibular and appendicular osteoblast culture will sustain present results and allow therapeutic adaptation corresponding to the type of lesions.

doi:10.1016/j.bonr.2020.100599

P312

S1P serum concentration is increased in CFTR-F508DEL patients: A novel biomarker of cystic fibrosis related bone disease

Johan Sergheraert[a], Marie-Laure Jourdain[a], Christine Guillaume[a], Julien Braux[a], Cédric Mauprivez[a], Dominique Hubert[b], Sandra Audonnet[c], Sophie C. Gangloff[a], Jacky Jacquot[a], Frédéric Velard[a]
[a]*EA4691 BIOS, Université de Reims Champagne Ardenne, Reims, France*
[b]*Service de Pneumologie, CRCM, Hôpital Cochin, Paris, France*
[c]*URCACyt, Université de Reims Champagne Ardenne, Reims, France*

Objectives: Personalized therapies and progresses in treatments increase life expectancy of patients suffering from cystic fibrosis (CF). Comorbidities like CF-related bone disease (CFBD) complexifies the pathology burden, even early in life (Jacquot *et al.*, 2016). Bone remodeling is a dynamic and constant process involving osteoblasts and osteoclasts. This process is under the control of many soluble factors among which sphingosine-1-phosphate (S1P). In CFTR-G551D patients we evidenced an increase of RANK+ (critical receptor involved in OC fusion and activity) circulating osteoclast precursors (Velard *et al.*, 2018). This work aims to determine if S1P may be considered as a biomarker for CFBD in CFTR-F508del patients.

Results: In serum from CFTR-F508del patients (n=5), S1P level is elevated as compared to non-CF controls (n=6) (9.1 *vs* 5.8ng.mL^{-1}, $p< 0.05$). We also evidenced that CF patients (n=12) exhibit increase RANK+ monocytes (57% *vs* 38%, $p< 0.05$) with higher receptor coverage on each cells compared to healthy donors (n=13) (90% increase, $p< 0.05$). Of particular interest, F508del CFTR corrector-treated patients (Orkambi®, n=5) demonstrated a significant ($p< 0.05$) 40% reduced serum S1P concentration independently of patients inflammatory status as compared to untreated patients (serum IL-6, -8 and TNF-α levels were not impacted and remained higher than in non-CF donors $p< 0.05$ for all three cytokines).

Discussion: S1P plays a major role in bone homeostasis thanks to its involvement in osteoblasts/osteoclasts communication. Disruption in S1P concentration in CF patients serum, associated with rise of RANK^{high} monocytes precursors of osteoclasts, may indicate S1P as a potential biomarker of early CFBD in CFTR-F508del patients. Moreover, the modulation of serum S1P in Orkambi treated patients lead us to speculate that this mediator might be CFTR-regulated. Thus S1P regulation could affect bone hometostasis and be part of increased bone resorption observed in CFBD suffering patients.

doi:10.1016/j.bonr.2020.100600

P315

Visualization of asfotase alfa-binding to sites of calcification in vivo

Flavia Amadeu de Oliveira, Sonoko Narisawa, Massimo Bottini, José Luis Millán
Sanford Burnham Prebys Medical Discovery Institute, La Jolla, United States

Hypophosphatasia (HPP) is a rare genetic metabolic disorder, caused by loss-of-function mutation(s) in the *ALPL* gene encoding tissue-nonspecific alkaline phosphatase (TNAP), that mainly affects

skeletal and dental mineralization. A mineral-targeted form of recombinant tissue-nonspecific alkaline phosphatase, asfotase alfa, was approved as enzyme replacement therapy for pediatric-onset hypophosphatasia in 2015. Only two reports to-date have shown some evidence of binding of this drug to mineralizing tissues using histochemistry and immunohistochemistry. Here, we sought to expand on those earlier studies by directly visualizing the *in vivo* binding of asfotase alfa conjugated with AnaTag HiLyte Fluor 750 or Alexa Fluor 647 fluorescent dye to sites of skeletal and dental mineralization and of ectopic calcification. We utilized 40 days-old *Tagln-Cre; Hprt*$^{ALPL/Y}$ mice (N=8), a model of severe medial vascular calcification, *Tie2-Cre; Hprt*$^{ALPL/Y}$mice (N=8), a model of severe intimal calcification, and sibling WT *Hprt*^{ALPL} mice devoid of soft-tissue calcification (N=8). A single dose of 8 mg/Kg labeled asfotase alfa was injected via the retro-orbital route. Skeletal tissues and soft organs were imaged *ex-vivo* 2-days after the injection. Strong fluorescence signal was observed in all skeletal tissues (calvaria, jaw, mandibles, vertebra and long bones) from mutants and WT. Fluorescence analysis of histological sections from bones revealed strong binding of asfotase alfa to the extracellular matrix. Asfotase alfa binding to sites of ectopic calcification in the heart, aorta and renal artery were found in both the *Tagln-Cre; Hprt*$^{ALPL/Y}$ and *Tie2-Cre; Hprt*$^{ALPL/}$mice but not in WT mice. In addition, the asfotase alfa binding was also seen in the kidney stroma and brain of the *Tie-Cre; Hprt*$^{ALPL/Y}$ mice. Our results show that labeled asfotase alfa administered *in vivo* binds not only to sites of skeletal and dental mineralization but also to sites of ectopic calcification.

doi:10.1016/j.bonr.2020.100601

P316

Regulation of TAZ by DEPTOR controls mesenchymal progenitors lineage commitment in response to PTH1R signaling

Fabiana Csukasi[a], Ivan Duran[a], Michaela Bosakova[b], Maya Barad[a], Jorge H. Martin[a], Daniel H. Cohn[a], Pavel Krejci[b], Deborah Krakow[a]
[a]*University of California Los Angeles, Los Angeles, United States*
[b]*Masaryk University, Brno, Czech Republic*

Skeletal elements are established from mesenchymal progenitors that form cartilage, which will be replaced by bone. These mesenchymal progenitors (or mesenchymal stem cells, MSCs) can differentiate into bone, cartilage and fat. Multiple signaling pathways are involved in lineage commitment such as BMPs, Hh and Wnt. Less studied is the role played by PTH/PTHrP; deletion of PTH1R in mice resulted in increased bone marrow fat. Two human skeletal dysplasias result from mutations in *PTH1R*; Jansen Metaphyseal Chondrodysplasia (JMC), which results from constitutive action of PTH1R and Blomstrand Chondrodysplasia (BOCD), caused by loss-of-function mutations. The specific molecular mechanisms by which these mutations mediate their effects remain unknown. Two key transcription factors (TF), RUNX2 and PPARγ, drive MSCs differentiation into osteoblasts or adipocytes, respectively. TAZ, a member of the Hippo pathway, is a known regulator of these TF, coactivating and corepressing RUNX2 and PPARγrespectively to promote bone formation and inhibit fat accumulation. We previously showed that DEPTOR, an mTOR inhibitor, accumulates in patients with JMC and demonstrated that PTH1R signaling controls DEPTOR degradation. Here, we show that JMC patients accumulate fat in the bone, whereas BOCD patients show chondrocytes immersed in the bone, indicating aberrant and distinct MSC differentiation caused by different mutations in the *PTH1R*receptor. DEPTOR directly interacts with TAZ; knockdown of DEPTOR in MSC cells results in a decrease in TAZ, RUNX2 and PPARγproteins following osteogenic induction. Moreover, TAZ and PPARγtranscriptional activity are also decreased, consistent with decreased bone formation in BOCD patients. Knockdown of DEPTOR also increased SOX9 transcriptional activity, supporting increased chondrocyte formation in BOCD. Our results revel a previously undescribed crosstalk between the mTOR component, DEPTOR, and the Hippo pathway effector, TAZ, and demonstrate their role in the regulation of mesenchymal progenitors lineage commitment in response to PTH1R signaling.

doi:10.1016/j.bonr.2020.100602

P319

A skeletal focal adhesion pathway initiated by LAMA5 regulates skeletogenesis

Fabiana Csukasi[a], Pavel Krejci[b], Deborah Krakow[a], Ivan Duran[a,c]
[a]*University of California Los Angeles, Los Angeles, United States*
[b]*Masaryk University, Brno, Czech Republic*
[c]*University of Malaga, Malaga, Spain*

In addition to its structural role in skeletogenesis, extracellular matrix (ECM) allows for communication between cells to control their differentiation, proliferation, migration and survival. Alterations in extracellular proteins cause a number of skeletal disorders and one mechanism attributed to these disorders results from the deleterious effects of mutated proteins on ECM structure. The consequences of abnormal ECM on cell communication, still remains poorly understood. Herein, we describe two novel unclassified types of bent bone dysplasias caused by mutations in the focal adhesion genes *LAMA5* and *VINCULIN*. These cases uncover a new mechanism of disease that is driven by alteration of the ECM-cell interactions between alpha5-containing Laminins, Vinculin, and Integrin mediated focal adhesion signaling surrounding blood vessels in the skeleton. This signaling pathway responds through a non-canonical and tissue specific pathways regulated by PYK2 and the specific-SRC kinase FYN. This newly described mechanism underlies the importance of vasculature-associated signals that promote skeletogenesis and the mechanism of disease related to ECM-cell interaction in skeletal disorders.

doi:10.1016/j.bonr.2020.100603

P320

Compound heterozygosity of mutations located in the first and third β-propeller domain of LRP4 causes sclerosteosis in a Spanish patient

Yentl Huybrechts[a], Ellen Steenackers[a], Neveen Hamdy[b], Geert Mortier[a], Guillermo Martinez[c], Milagros Sierra Bracamonte[c], Natasha Appelman-Dijkstra[b], Wim Van Hul[a], Eveline Boudin[a]
[a]*Department of Medical Genetics, University of Antwerp and University Hospital of Antwerp, Edegem, Belgium*
[b]*Department of Endocrinology, Leiden University Medical Center, Leiden, Netherlands*
[c]*Endocrinology and Nutrition Resident, 12 de Octubre University Hospital, Madrid, Spain*

Sclerosteosis is a rare autosomal recessive skeletal dysplasia that is characterized by progressive hyperostosis in both the axial and appendicular skeleton. In addition to the hyperostosis, patients with sclerosteosis often present with syndactyly of the fingers and tall stature. Initially, it was shown that loss-of-function mutations in *SOST* (encoding sclerostin) are the genetic cause of sclerosteosis. However, currently, it is known that hypomorphic mutations in the sclerostin binding partner LRP4 can also cause sclerosteosis. We have previously described three mutations in LRP4 which are all located in

the cavity of the third β-propeller domain and result in an impaired LRP4-sclerostin binding.

With this report, we provide evidence that mutations outside the third β-propeller domain of LRP4 can also cause sclerosteosis. In a Spanish patient who demonstrates increased thickness of the skull and sclerosis of the axial skeleton, we've identified two compound heterozygous mutations in LRP4. One variant (p.R1170Q) is residing in the cavity of the third β-propeller domain and is known to be disease-causing. The other variant (p.R632H) is located in the first β-propeller domain of LRP4. *In silico* and segregation analyses support the pathogenicity of this variant. In addition, the high serum levels for sclerostin observed in this patient suggest that both mutations affect the LRP4-sclerostin binding. Furthermore, a Wnt luciferase reporter assay shows that the p.R632H variant interferes with the normal inhibition of the Wnt signaling pathway by sclerostin.

In conclusion, identification of a disease-causing mutation in the first β-propeller domain of LRP4 broadens the mutational spectrum of sclerosteosis-causing mutations. Additional studies are needed to further elucidate the mechanism whereby the p.R632H mutation affects the LRP4 function and to investigate the role of the first β-propeller domain in LRP4 during bone formation.

doi:10.1016/j.bonr.2020.100604

P321

Supporting rare and common disease research in mineralized tissues

Jason Wan
NIH/NIDCR, Bethesda, United States

Today's research climate is one of a multidisciplinary, team-based approach with many findings in one scientific discipline crossing over into others and mutually benefitting the advancement of both areas. In calcified tissues, there are several examples of reciprocal findings in systemic diseases to local manifestations and birth defects of such cross-fertilization of ideas and knowledge. Rare diseases, which number roughly 7,000, could be rare in some areas while common in others. Common diseases, which affect a great many people at once, have their own dedicated investigators and funding. Whether rare or common, these diseases are a burden upon the individuals living with them and in total affect a large percentage of the population. Funding agencies around the world support research on all continents [see figure]. For example, funding in rare disease by the largest public supporter of research in the United States has steadily increased over the past four years from $3,679 M USD in 2015 to $5,459 M USD in 2019. Preclinical and translational studies of calcified or mineralized tissues cover a wide range of topics from genetics to biomechanics, and range in scale from the atomic and molecular to tissues and organisms. This poster will detail the investments in rare and common diseases affecting mineralized tissues and encourage researchers and clinicians to forge and continue collaborations that benefit the community.

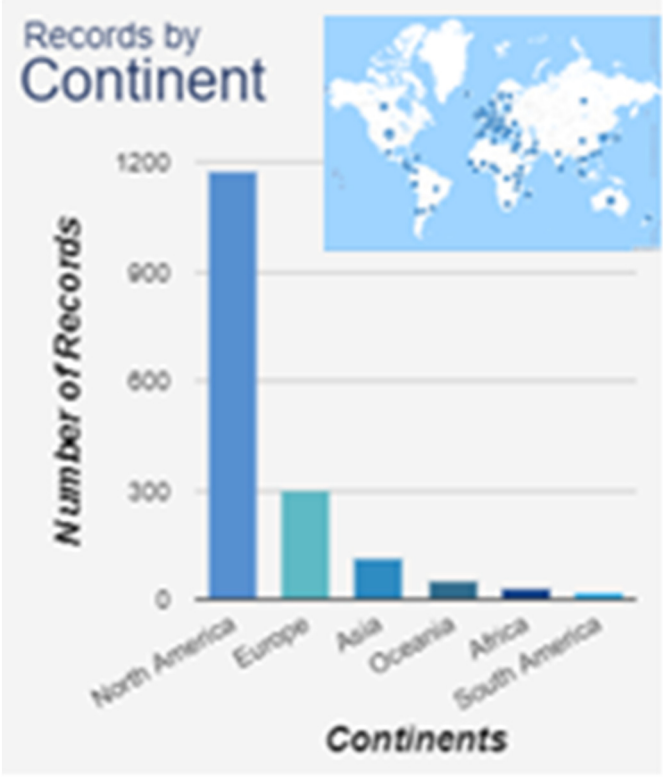

Fig. 1. Rare Disease projects by Continent in 2017 from World RePORT (worldreport.nih.gov).

doi:10.1016/j.bonr.2020.100605

P323

Fate of intracellular retained mutant collagen

Roberta Besio[a], Nadia Garibaldi[a], Nicoletta Gabriella Giannini[b], Saïd Bendahhou[b], Antonella Forlino[a]
[a]*Dept of Molecular Medicine, University of Pavia, Pavia, Italy*
[b]*CNRS, Université de Nice-Sophia Antipolis, Nice, France*

In classical dominant osteogenesis imperfecta (OI), caused by mutations in the α1 and α2 chains of type I collagen, the delay in type I collagen folding due to glycine substitution is responsible for a prolonged exposure of the chains to the endoplasmic reticulum (ER) enzymes in charge of post-translational modifications. Thus, in OI cells overmodified collagen molecules are synthesized. Intracellular retention of mutant collagen has been reported in OI affecting cellular homeostasis and contributing to OI pathology. Here, using OI patient fibroblasts carrying glycine substitutions by various amino acids in different locations along the α1(I) chain, we focused our attention on how this altered collagen is degraded and on ER homeostasis. Indeed, we demonstrated that retained collagen molecules are responsible for ER enlargement and activation of the unfolded protein response. Autophagy upregulation was detected in OI cells suggesting that the retained mutant collagen could be eliminated through this route. To clarify the nature of the degradation pathway for mutant type I collagen, α1(I) expression was evaluated by western blot on patient and control cells treated with proteasome and autophagosome or autophagolysosome inhibitors (MG132, wortmannin and chloroquine, respectively). The increased intracellular α1(I) in patient cells compared to controls following the incubation with chloroquine ($p < 0.05$), but not with wortmannin or MG132, supported the conclusion that mutant type I collagen with structural defects is degraded in fibroblasts mainly via autophagy independent action of phosphatidyl inositol 3 kinases. Furthermore, the contribution of altered collagen on ER function is currently evaluated and will provide further insights on molecular bases of OI.

Funding: Italian Ministry 697 of Education, University and Research (MIUR) [Dipartimenti di Eccellenza (2018-2022)] to AF and Fondazione Cariplo 2016-0417 to RB

doi:10.1016/j.bonr.2020.100606

P325

A natural history study of fibrodysplasia ossificans progressiva (FOP): 12-month outcome results

Robert J. Pignolo[a], Geneviève Baujat[b], Matthew A. Brown[c], Carmen De Cunto[d], Maja Di Rocco[e], Edward C. Hsiao[f], Richard Keen[g], Mona Al Mukaddam[h], Kim Hanh Le Quan Sang[i], Andrew Strahs[j], Rose Marino[j], Frederick S. Kaplan[h]

[a]*Department of Medicine, Mayo Clinic, Rochester, United States*
[b]*Departement de Genetique, Institut IMAGINE and Hôpital Necker-Enfants Malades, Paris, France*
[c]*Guy's & Thomas' NHS Foundation Trust and King's College London NIHR Biomedical Research Centre, London, United Kingdom*
[d]*Pediatric Rheumatology Section, Department of Pediatrics, Hospital Italiano de Buenos Aires, Buenos Aires, Argentina*
[e]*Unit of Rare Diseases, Department of Pediatrics, Giannina Gaslini Institute, Genoa, Italy*
[f]*Division of Endocrinology and Metabolism, the UCSF Metabolic Bone Clinic, the Institute of Human Genetics, and the UCSF Program in Craniofacial Biology, Department of Medicine, University of California-San Francisco, San Francisco, United States*
[g]*Centre for Metabolic Bone Disease, Royal National Orthopaedic Hospital, Stanmore, United Kingdom*
[h]*Departments of Orthopaedic Surgery & Medicine, The Center for Research in FOP and Related Disorders, Perelman School of Medicine, University of Pennsylvania, Philadelphia, United States*
[i]*Hôpital Universitaire Necker-Enfants Malades, Paris, France*
[j]*Clementia Pharmaceuticals Inc., Newton, United States*

Background: FOP is a rare bone disease characterised by episodic flare-ups and heterotopic ossification (HO) leading to disability and early death. We present 12-Month results of a 3-year, ongoing, prospective, longitudinal, global natural history study (NHS; NCT02322255) investigating the progression of FOP, and its impact on HO formation and physical functioning.

Methods: HO volume was assessed in patients with FOP by low-dose whole-body computed tomography (WBCT), interpreted by a blinded, central laboratory. Functional outcome measures included: Cumulative Analogue Joint Involvement Scale (CAJIS; 0-30 [higher score=greater severity]); FOP Physical Function Questionnaire (FOP-PFQ; percent total score). For all outcomes, Change from Baseline (CfB) at Month 12 was evaluated.

Results: 93/114 enrolled patients (aged 4-56 years; mean age 17 years; 56% male) had data and evaluable WBCT scans at Baseline and Month 12. 37 (40%) formed new HO (24/37 [65%] reported ≥1 flare-up; mean 2.3 flare-ups/year) and 56 (60%) did not form new HO (24/56 [43%] reported ≥1 flare-up; 1.8 flare-ups/year). Mean volume of new HO was 22,958mm^3 (SD=68,743mm^3) across all patients and 57,706mm^3 (SD=100,079mm^3) in those who formed new HO. Mean new HO volume in those who reported flare-ups was 39,718mm^3 (SD=91,969mm^3), and 5,081mm^3 (SD=14,582mm^3) in those who did not. Mean CfB in CAJIS and FOP-PFQ was minimal (CAJIS: 0.6 [SD=2.4], FOP-PFQ: 4.4% [SD=11.2]) and similar across individuals whether they formed new HO or not.

Conclusions: Volume of HO increased over 12 months, but most patients did not form new HO. These results demonstrate that new HO formation can be quantified by WBCT over 12 months, suggesting flare-ups may impact volume of HO formation. 12 months was insufficient to observe significant worsening of CAJIS and FOP-PFQ.

Study sponsor: Clementia, an Ipsen company.

The authors thank the patients, their families, IFOPA, investigators and clinical research teams who participated in this programme.

doi:10.1016/j.bonr.2020.100607

P327

Metformin treatment in a pre-school boy with pseudohypoparathyroidism type 1A and morbid obesity

Noah Gruber[a,b], Kineret Mazor-Aronovitch[a,b], Yael Levy-Shraga[a,b]

[a]*Pediatric Endocrinology and Diabetes Unit, The Edmond and Lily Safra Children's Hospital, Sheba Medical Center, Ramat Gan, Israel*
[b]*The Sackler Faculty of Medicine, Tel-Aviv University, Tel-Aviv, Israel*

Background: Early onset obesity is one of the features of pseudohypoparathyroidism type 1A (PHP1A). Metabolic consequences, sleep apnea and asthma were described in these patients. Weight control can be very challenging as patients may not respond to standard approaches of dietary management and exercise. To date, specific reports concerning specialized management of obesity in these patients are sparse.

Objective: To describe the effect of metformin treatment in a child with PHP1A.

Case presentation: The patient was born at 36 weeks gestation weighting 3.5kg. At the fifth day of life, blood tests revealed TSH-76 mIu/l (normal range 0.7-9.8) and FT4-9.9 pmol/l (7-16). Levothyroxine treatment was initiated with good response. However, excessive weight gain ensued and at 6 months he weighed 11.3 kg (+3.3 SDS). Therefore, a further workup was performed and found an elevated PTH-129 pg/ml (normal 16-87), calcium-9.7 mg/dl, phosphor-6.7 mg/dl. Sequence analysis of the *GNAS* gene revealed a novel heterozygous frameshift mutation (c.518_521delACTG). Treatment with calcium carbonate and alfacalcidiol was initiated at the age of 1.4 years. His weight continued to raise excessively and he developed obstructive sleep apnea and hyperactive airways disease. At the age of 5.5 years, his weight was 51.1kg (+4.5 SDS), height 118.7cm (+1.3 SDS), BMI 36.7kg/m² (+3.9 SDS), and blood pressure was elevated 112/76. He had acanthosis nigricans. Blood test results: fasting glucose 84 mg/dl, HbA1C-4.1% and elevated insulin 63.9 mu/l (normal 1-10). Treatment with metformin was initiated at a dose 500 mg/day and was increased gradually to 1200 mg/day. After 16 months of metformin treatment, his BMI-SDS decreased to +3.2 SDS, the blood pressure normalized (93/56) and his fasting insulin decreased to 30 mu/l.

Conclusion: Metformin treatment may be considered in children with PHP1A and morbid obesity with complications. Further studies are needed to evaluate the metabolic consequences of PHP1A and the treatment.

doi:10.1016/j.bonr.2020.100608

P328

Measuring outcomes in ultra-rare bone diseases: Methodology of the palovarotene fibrodysplasia ossificans progressiva clinical development programme

Robert J. Pignolo[a], Geneviève Baujat[b], Matthew A. Brown[c], Carmen De Cunto[d], Maja Di Rocco[e], Edward C. Hsiao[f], Richard Keen[g], Mona Al Mukaddam[h], Andrew Strahs[i], Donna R. Grogan[i], Rose Marino[i], Frederick S. Kaplan[h]

[a]*Department of Medicine, Mayo Clinic, Rochester, United States*
[b]*Departement de Genetique, Institut IMAGINE and Hôpital Necker-Enfants Malades, Paris, France*
[c]*Guy's & Thomas' NHS Foundation Trust and King's College London NIHR Biomedical Research Centre, London, United Kingdom*
[d]*Pediatric Rheumatology Section, Department of Pediatrics, Hospital Italiano de Buenos Aires, Buenos Aires, Argentina*
[e]*Unit of Rare Diseases, Department of Pediatrics, Giannina Gaslini Institute, Genoa, Italy*
[f]*Division of Endocrinology and Metabolism, the UCSF Metabolic Bone Clinic, the Institute of Human Genetics, and the UCSF Program in Craniofacial*

Biology, Department of Medicine, University of California-San Francisco, San Francisco, United States
[g]*Centre for Metabolic Bone Disease, Royal National Orthopaedic Hospital, Stanmore, United Kingdom*
[h]*Departments of Orthopaedic Surgery & Medicine, The Center for Research in FOP and Related Disorders, Perelman School of Medicine, University of Pennsylvania, Philadelphia, United States*
[i]*Clementia Pharmaceuticals Inc., Newton, United States*

Background: Fibrodysplasia ossificans progressiva (FOP) is an ultra-rare genetic disease characterised by soft and connective tissue 'flare-ups', and heterotopic ossification (HO) leading to disability and early mortality. Palovarotene (PVO) is a selective retinoic acid receptor gamma agonist under investigation for treatment of FOP.

Objective: Describe the PVO in FOP clinical development programme, a methodological approach addressing the challenges of conducting clinical trials in underexplored rare bone diseases.

Methods: The programme consists of an ongoing, non-interventional natural history study (NCT02322255), a multicentre, randomised, double-blind, placebo-controlled, adaptively designed phase II trial (PVO-1A-201; NCT02190747) and its ongoing open-label extension (PVO-1A-202; NCT02279095) (Table). Flare-ups (defined as ≥2 of: pain, swelling, stiffness, decreased range of motion, redness, warmth) are evaluated, with outcomes assessed at flare-up Days 1 and 84 and/or longitudinally. HO incidence and volume are determined by low dose whole body computed tomography using standardised procedures. Other clinical, functional and patient-reported outcomes are also assessed. Studies were approved by independent ethics committees. Learnings informed design of the ongoing phase III MOVE trial (NCT03312634).

Conclusions: Novel methodological approaches are needed to expedite availability of disease-modifying treatments for serious, ultra-rare diseases. HO is the main cause of disability in patients with FOP. This clinical development programme could be used as an example to inform development of new treatments in rare bone diseases.

The authors thank the patients, their families, IFOPA, investigators and clinical research teams who participated in this programme.

Study sponsor: Clementia, an Ipsen company.

Table 1
Study designs

	Natural history study	PVO-1A-201
Adult/ Paediatrics	Both (0-65 years)	Both (≥6 years)
PVO dosing regimen	N/A	Episodic (2/4 wks)
PVO dose (mg)	None	5/2.5 10/5 Placebo
Randomisation	N/A	Age ≥15 years: 0:3:1 Age ≥6 years: 3:3:2

	PVO-1A-202 Part A	PVO-1A-202 Part B	PVO-1A-202 Part B	PVO-1A-202 Part C
Adult/ Paediatrics	Both (≥6 years)	Skeletally immature[a]	Skeletally mature	Both
PVO dosing regimen	Episodic (2/4 wks)	Episodic (≥4/8 wks)	Chronic (daily) + Episodic (≥4/8 wks)	
PVO dose (mg)	10/5	20/10	Chronic 5 + Episodic 20/10	
Randomisation	N/A	N/A	N/A	

PVO doses were weight-adjusted. [a] <18 years of age with <90% skeletal maturity on hand/wrist radiography. PVO: palovarotene; wks: weeks

doi:10.1016/j.bonr.2020.100609

P329

Cherubism: A systemic skeletal disease? About a case report

Anne Morice[a], Manon Ricquebourg[b], Aline Joly[a], Gérard Maruani[c], Emmanuel Durand[d], Louise Galmiche[e], Jeanne Amiel[f], Yoan Vial[g], Kahina Belhous[h], Marie Piketty[i], Martine Cohen-Solal[j], Ariane Berdal[k], Corinne Collet[b], Arnaud Picard[a], Natacha Kadlub[a], Amélie Coudert[l]
[a]*Service de Chirurgie Maxillo-faciale, Université de Paris Hopital Necker - Enfants Malades APHP, Paris, France*
[b]*Service de Biochimie APHP Hôpital Lariboisière, BIOSCAR INSERM U1132 Université de Paris, Paris, France*
[c]*Service de Physiologie, Université de Paris Hopital Necker - Enfants Malades APHP, Paris, France*
[d]*IR4M - Université Paris-Sud, CNRS, Orsay, France*
[e]*Service d'Anatomopathologie et cytologie, Université de Paris Hopital Necker - Enfants Malades APHP, Paris, France*
[f]*Département de Génétique Médicale, Université de Paris Hopital Necker - Enfants Malades APHP, Paris, France*
[g]*Département de Génétique, APHP Hôpital Robert Debré, INSERM UMR 1131, Institut de Recherche Saint-Louis, Université de Paris, Paris, France*
[h]*Service d'imagerie médicale pédiatrique, APHP - Hôpial Necker - Enfants Malades, Paris, France*
[i]*Service des Explorations Fonctionnelles, APHP - Hôpial Necker - Enfants Malades, Paris, France*
[j]*BIOSCAR INSERM U1132 Université de Paris APHP Hôpital Larinoisière, Paris, France*
[k]*Université de Paris, POM CRC INSERM U1138 - Equipe 5, Paris, France*
[l]*BIOSCAR INSERM U1132 APHP Hôpital Larinoisière Université de Paris UFR Odontologie, Paris, France*

Cherubism is a rare autosomal dominant genetic condition caused by mutations in the *SH3BP2* gene. This disease is characterized by a jaws osteolysis with the bone replaced by soft tissue rich in fibroblasts and containing multinuclear giant cells. SH3BP2 is a ubiquitous adaptor protein yet the mutation consequences are only so far described in the patient face. Cherubism mouse models have been generated and unlike in patients, the knock-in mice exhibit a systemic bone loss phenotype together with a systemic inflammatory phenotype. Taken these data into account, we decided to search for a systemic cherubism phenotype potentially affecting a 6 year-old patient with an aggressive cherubism. Thereby we report here the first case of cherubism with systemic manifestations. A bone densitometry showed low bone density (total body Z-score = - 4.6 SD). Several markers of bone remodelling (CTx, BALP, P1NP) as well as inflammation markers (TNFα and IL-1) were elevated. The presence of another mutation in genes already involved in low bone mass phenotype was ruled out by a genes panel analysis. If this systemic skeletal cherubism phenotype should be confirmed, it would simplify the treatment of the severe cherubism patients and lower the second thoughts about using a systemic treatment such as those recently published (tacrolimus or imatinib) for a previously believed jaw localised disease

doi:10.1016/j.bonr.2020.100610

P330

Osteogenesis imperfecta type XIX due to a novel *MBTPS2* mutation: A case report

Tatiana Grebennikova, Anatoly Tiulpakov, Kristina Kulikova, Galina Melnichenko, Zhanna Belaya
Endocrinology Research Center, Moscow, Russian Federation

Osteogenesis imperfecta (OI) is a genetically heterogeneous disease. In 2016, Lindert et al. identified OI type XIX (MIM#:300294) which is characterized by *MBTPS2* mutation with X-linked recessive inheritance,

prenatal fractures and generalized osteopenia with severe short stature in adulthood, as well as variable scoliosis and marked anterior angulation of the tibia. The OMIM database contains the description of only two families with OI type XIX.

A 18-year-old male (height,164 cm; weight,56 kg) was hospitalized with pain in bones and joints. He had three low-traumatic hip fractures at the age of 1, 13 and 14. The patient received calcium and vitamin D supplements for a long time. At the age of 17 y.o, zoledronic acid 4 mg iv was administered. On DXA scans we found low bone mineral density: -2.6 Z-score at the lumbar spine and -3.8 Z-score at the femoral neck. On CT scans, there were Th11 and Th12 vertebral compression fractures. Serum calcium,phosphate, alkaline phosphatase,creatinine, vitamin D, PTH, testosterone,TSH, HbA1c and osteocalcin were within the reference ranges, but C-terminal telopeptide of type I collagen was slightly elevated 0.93 ng/ml (0.1-0.85). The patient´s mother (41-years-old; height,148 cm; weight,84 kg) had several fractures before puberty, she has got blue sclerae, osteopenia (-2.8 Z-score DXA lumbar spine, -1.9 Z-score at the femoral neck). His sister (9-year-old) has scoliosis and genu valgus without fractures. His father and brothers did not have any fractures. A whole exome sequencing revealed X-linked mutation in the gene *MBTPS2*:p.G494R, which confirms OI type XIX in the proband. His mother and sister are carriers of the mutation. We continued to treat the patient with intravenous 5 mg of zoledronic acid once a year.

Conclusion: This is the first description of genetically confirmed OI type XIX in Russia. The type of mutation probably explains the mild phenotype of this patient.

doi:10.1016/j.bonr.2020.100611

P331

Is it feasible to use 3D-printed titanium implant for radiated mandible reconstruction?

Jinwoo Kim, Michidgerel Odkhuu, Jung-Hyun Park
Oral and Maxillofacial Surgery, Ewha Womans University, Seoul, Republic of Korea

This clinical case presents a novel method of mandible reconstruction with 3D-printed titanium implant. A 53-year old male who suffered osteoradionecrosis due to the radiation after squamous cell carcinoma resection resection. The 3D titanium printed implant with pre-mounted dental implant fixtures was simulated and fabricated with SLM method. The implant was successfully inserted and the discontinuous mandible defect was rehabilitated without postoperative infection or foreign body reaction during follow-ups, until a year. The 3D-printed titanium implant can be considered as a good new alternative method for radiated mandible reconstruction. (Surgical protocol is available at https://www.youtube.com/watch?v=rd7FkbESRpA)

Fig.

doi:10.1016/j.bonr.2020.100612

P332

Frequency and causes of high bone mass

Aurore Nottez[a], Sami Kolta[b], Georges Lion[a], Camille Ternynck[a], Isabelle Legroux-Gérot[a], Marie-Christine Vantyghem[a], Bernard Cortet[a], Julien Paccou[a]
[a]*Lille University Hospital, Lille, France*
[b]*APHP - Cochin, Paris, France*

Introduction: A finding of high bone mass (HBM) on routine DXA scanning is not infrequent. This study was performed to assess the frequency and causes of HBM within the general population referred for DXA scanning in a tertiary centre hospital.

Material and methods: DXA databases were initially searched for individuals with a BMD T- or Z-score≥+4 at any site within the lumbar spine or hip, at the Lille University Hospital (France) from April 1st, 2008 to April 30st, 2018.

Results: At the lumbar spine, 18,229 bone density tests were performed in women and 10,209 in men. At the hip, 17,390 tests were performed in women and 9,857 in men. The total number of patients who performed at least one bone density test was 14,745 with 64.2% of female. Among these patients, 211 of them had a T- and/or Z-score ≥+4 at any site, i.e. a frequency of 1.43% [1.25%-1.64%]. DXA scans and medical records of 92 men and 119 women with high BMD were screened to assess causes. An artefactual cause was found in 75% of patients with HBM (mostly degenerative disease of the spine) and an acquired cause of focal HBM was only found in 2 patients with sclerotic bone metastases from prostate cancer. An acquired cause of generalized HBM was found in 15% of patients with a vast majority of renal osteodystrophy (n=11), hematological disorders (n=9; e.g. myeloproliferative syndromes and mastocytosis) and diffuse bone metastases from solid cancer (n=5). Of the remaining causes, rare hereditary diseases (e.g. osteopetrosis...), and unexplained high BMD were found in 10 and 6 cases respectively.

Conclusion: The frequency of high BMD (T- or Z-score≥+4 at any site) was higher than expected. Further works are needed to differentiate artefactually HBM from hereditary or acquired high BMD and to investigate unexplained high BMD.

doi:10.1016/j.bonr.2020.100613

P333

STOPFOP: A European phase II clinical trial using saracatinib to treat FOP

Bernard J. Smilde[a], Richard Keen[b], Clemens Stockklausner[c], Dong Liu[d], Alex Bullock[e], Anette von Delft[e], Natasja M. van Schoor[f], Paul B. Yu[g], E. Marelise W. Eekhoff[a]
[a]*Department of Internal Medicine, Amsterdam University Medical Center, Amsterdam, Netherlands*
[b]*Department of Rheumatology, Royal National Orthopaedic Hospital, London, United Kingdom*
[c]*Department of Paediatrics, Klinikum Garmisch-Partenkirchen, Garmisch-Partenkirchen, Germany*
[d]*Research and Development, AstraZeneca, Boston, United States,*
[e]*Nuffield Department of Medicine, University of Oxford, Oxform, United Kingdom*

[f]Department of Epidemiology and Biostatistics, Amsterdam University Medical Center, Amsterdam, Netherlands
[g]Department of Medicine, Brigham and Women's Hospital, Boston, United States

Background: Fibrodysplasia ossificans progressiva (FOP) is a genetic, progressive and devastating disease characterized by severe heterotopic ossifications (HO), contractures and early death. There are no approved medications yet. Our STOPFOP team identified AZD0530 (saracatinib) as a potent inhibitor of the ALK2-kinase which plays a key role in this rare bone disease. AZD0530 was proven to be effective in FOP mouse models. The EU Innovative Medicines Initiative provided funding to investigate the repurposing of AZD0530, originally designed for ovarian cancer treatment, to treat patients with FOP.

Methods: This is a phase 2a study, designed as European, multicentre, 6-month double blind randomized controlled trial of AZD0530 versus placebo, followed by a 12 month trial comparing open-label extended AZD0530 treatment with control data from a previous trial. We will include 20 FOP patients, aged 18-65 years, with the classic FOP mutation (R206H). Endpoints are objective change in heterotopic bone volume measured by low-dose whole-body computer tomography (CT) , [18F] NaF PET activity and patient reported outcome measures.

Discussion: Drug repurposing - using existing clinical molecules for new disease indications - represents an ideal solution for limiting risks in early clinical studies. This is especially useful in rare diseases with limited study populations. Using existing assets may also allow more affordable pricing once an indication is approved.

With positive study outcome, AZD0530 may provide a rapidly translatable therapy for FOP due to the availability of extensive safety data from 28 registered clinical trials with AZD0530 involving over 600 patients.

Trial registration: EudraCT number 2019-003324-20

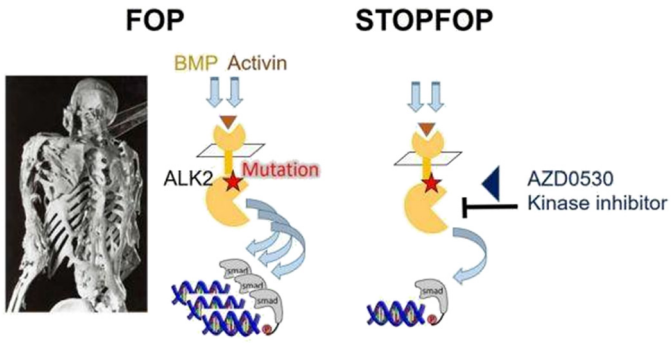

Fig. 1. Working mechanism of AZD0530 (saracatinib).

doi:10.1016/j.bonr.2020.100614

P334

Beyond toothache: A new perspective on Eagle syndrome

Sanne Treurniet[a], Jeroen Jansen[b], Leo van Ruijven[c], Ton Langeveld[b], Tim Forouzanfar[d], Nathalie Bravenboer[e], Marelise Eekhoff[a]
[a]Endocrinology, Amsterdam University Medical Center, Amsterdam, Netherlands
[b]Otolaryngology, Leiden University Medical Center, Leiden, Netherlands
[c]Oral Cell Biology and Functional Anatomy, ACTA-University of Amsterdam and VU University, Amsterdam, Netherlands
[d]Oral and Maxillofacial Surgery, Amsterdam University Medical Center, Amsterdam, Netherlands
[e]Clinical Chemistry, Bone and Calcium Metabolism Lab, Amsterdam University Medical Center, Amsterdam, Netherlands

Introduction: A 44-year old woman presented with pain and nerve compression in the face due to Eagle syndrome. Eagle syndrome was diagnosed after many years of unexplained pain in the jaw and neck. The Eagle syndrome is due to elongation of the styloid process or calcification of the stylohyoid ligament. In this patient Eagle syndrome was diagnosed on both sides of the neck, which is very rare. Previously performed surgery, at the age of 39, to relieve complaints was not successful. At the age of 42, a second surgery took place to remove bone formed by the Eagle syndrome on the right side of the neck. Two years later, surgical removal of the calcified tissue on the left side of the neck was performed successfully.

Method: Preoperatively a [18F]NaF PET/CT scan was conducted. Histologic examination and microCT was performed on removed tissue.

Results: [18F]NaF PET/CT scan prior to surgery showed no increased uptake of [18F] NaF in the styloid hyoid region, indicating active bone formation was not present at this site. The tissue removed during surgery is classified as calcified tissue. Histologic examination and microCT revealed cortical and trabecular bone and some areas of cartilage tissue.

Conclusion: The molecular mechanism leading to calcification in the styloid region in Eagle syndrome is still unknown. This case-report suggested an endochondral process of bone formation. Further examination of the calcified tissue will take place to investigate the properties of this material.

doi:10.1016/j.bonr.2020.100615

P335

A novel mutation in *PLS3* causes extremely rare X-linked osteogenesis imperfecta

Jing Hu, Lu-Jiao Li, Wen-Bin Zheng, Di-Chen Zhao, Ou Wang, Yan Jiang, Xiao-Ping Xing, Weibo Xia, Mei Li
Department of Endocrinology, National Health Commission Key Laboratory of Endocrinology, Peking Union Medical College Hospital, Chinese Academy of Medical Sciences and Peking Union Medical College, Beijing, China

Introduction: Osteogenesis imperfecta is a phenotypically and genetically heterogeneous bone dysplasia, characterized by low bone mineral density (BMD) and multiple fractures. We investigate the pathogenic mutation and the phenotypes of a family with rare X-linked inherited OI.

Methods: We designed a novel targeted next generation sequencing panel with all candidate genes of OI to detect the pathogenic mutation and confirmed it by Sanger sequencing. We investigated the phenotypes of OI by evaluating BMD, bone fractures, and bone turnover biomarkers. We summarized the characteristics of patients with *PLS3* mutation according to the previous literature to explore the genotype-phenotypic correlation of this rare disorder.

Results: The proband, a twelve-year-old boy, experienced long bone fractures, multiple vertebral fractures and blue sclera. The family history of fractures and blue sclera was positive. All affected individuals in the family shared a novel frameshift mutation (c.1106_1107insGAAA) in exon 10 of *PLS3*. The proband and his brother were hemizygous, while their mother was a heterozygous carrier. The mutation was predicted to cause a premature termination of mRNA translation (p.Phe369Leufs*5), which would contribute to the skeletal disorder. During 12 months of zoledronate treatment, BMD of the two patients was remarkably increased while the serum β-CTX level was decreased. The compressed vertebral bodies were reshaped.

Conclusion: X-linked OI could be induced by variants in coding and non-coding region of *PLS3* with no obvious hot-spot mutation. Frequent fractures were hallmarks of the disease and BPs were beneficial for X-linked OI patients.

Keywords: X-linked osteogenesis imperfecta; *PLS3*; novel mutation; zoledronate

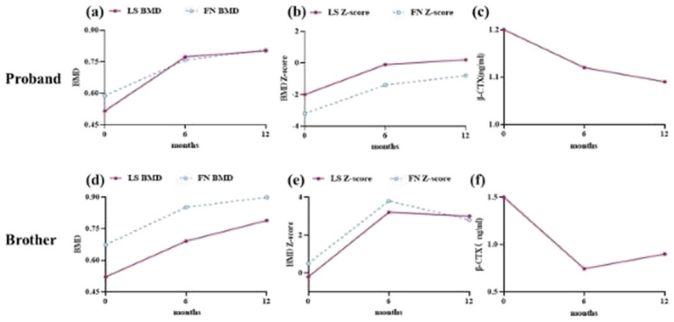

Changes in BMD, BMD Z-score and serum β-CTX level after zoledronate infusion.

doi:10.1016/j.bonr.2020.100616

P336

Autosomal recessive hypophosphatemic rickets Type 1 caused by different *DMP1* mutations in three Chinese families

Xiaolin Ni, Xiang Li, Qi Zhang, Mei Li, Xiaoping Xing, Ou Wang, Yan Jiang, Weibo Xia
Peking Union Medical College Hospital, Chinese Academy of Medical Sciences and Peking Union Medical College, Beijing, China

Inherited hypophosphatemic rickets (HR) consists of a group of inherited diseases. Recently, autosomal recessive hypophosphatemic rickets type 1 (ARHR1), as an extremely rare type of autosomal recessive form of HR was reported to be caused by homozygous mutation of dentin matrix protein 1(*DMP1*) gene. Here we described three pedigrees presented with lower limb deformity and short stature, characterized with hypophosphatemia, elevated alkaline phosphatase (ALP), high to normal intact parathyroid hormone (iPTH), high intact fibroblast growth factor (iFGF23). We performed an oral phosphate test on patients, and compared the result with XLH and ADHR, ARHR1 revealed a better gastrointestinal phosphate absorption and stronger stimulation of iPTH and iFGF23. Serum sclerostin level elevated in ARHR1. Radiographs showed short and deformed long bones, degenerative arthritis in spine and coexistence of osteomalacia and osteosclerosis in pelvis and hand. Areal bone mineral density (aBMD) of axial bone by DXA was relatively high rather than decreased as expected for osteomalacia, while volumetric BMD (vBMD) and microstructure of distal radius and tibia detected by HR-pQCT was obviously damaged in ARHR1 patients. Mutation analysis of DMP1 revealed a novel homozygous splicing mutation c.54+1 G >C in Family 1, a reported splicing mutation c.184-1 G >A in Family 2, and a novel nonsense mutation c.94C >A (p.E32X) in Family 3. Minigene assay proved the pathogenicity of novel splicing mutation to alter the splicing of exon 2. In conclusion, we reported 3 unrelated pedigrees with ARHR1 from Chinese population and identified 2 novel *DMP1* mutation. Our findings expanded the phenotypic and genotypic spectrum of ARHR1 and provided unique insights into the further study.

doi:10.1016/j.bonr.2020.100617

P337

Adult osteosclerotic metaphyseal dysplasia with progressive osteonecrosis of the jaws and abnormal osteoclast resorption pattern due to a LRRK1 splice site mutation

Antonia Howaldt[a], Anna-Floriane Hennig[a], Tim Rolvien[b], Uta Rössler[a], Nina Stelzer[a], Sebastian Böttger[c], Jozef Zustin[b], Ralf Oheim[b], Sven Geißler[a], Michael Amling[b], Hans-Peter Howaldt[c], Uwe Kornak[a,d]
[a]*Charité-Universitatsmedizin Berlin, Berlin, Germany*
[b]*University Medical Center Hamburg-Eppendorf, Hamburg, Germany*
[c]*University Hospital Gießen and Marburg, Giessen, Germany*
[d]*Institute for Human Genetics, Universitatsmedizin Gottingen, Gottingen, Germany*

We report on a 34 year old patient patient with sandwich vertebrae, platyspondyly, osteosclerosis of the tubular bones, pathologic fractures, and anemia. In the third decade, he developed osteonecrosis of the jaws, which was progressive in spite of repeated surgical treatment over a period of 11 years. An iliac crest bone biopsy revealed an elevated trabecular density (BV/TV [%] 32.2 vs. 21.5±14.8) and the presence of hypermineralized cartilage remnants leading to an overall increase in mineralization (CaMean [wt%] 25.65 vs. 21.8). We also found large multinucleated osteoclasts with abnormal morphology and inadequate bone resorption. Together, these findings were reminiscent of an osteoclast-rich osteopetrosis like autosomal recessive osteopetrosis type 2. However, no mutations in CLCN7 nor TCIRG1 were detected by Sanger sequencing. Subsequent whole exome sequencing identified the novel homozygous splice-site mutation c.261G>A in the gene LRRK1. The mutation co-segregated with the phenotype in the family. cDNA sequencing showed nearly complete skipping of exon 3 leading to a frameshift (p.Ala34Profs*33), very likely leading to a loss of function. LRRK1 encodes a protein kinase and was recently described as the cause for osteosclerotic metaphyseal dysplasia (OSMD; OMIM # 615198). Osteoclasts differentiated in vitro from the patient's peripheral blood monocytes formed very quickly and became unusually large. These cells formed large areas with superficial pseudo-resorption but excavated only few resorption pits (resorption pit surface [%] 0.8±0.6 vs. 6±0.4; p< 0.01). Phosphorylation of L-plastin at position Ser5 was strongly reduced in patient-derived osteoclasts, thus corroborating a loss of function of the mutated LRRK1 kinase protein (0.26±0.1 vs. 1±0.08; p< 0.01). Our analysis indicates a strong overlap of LRRK1-related OSMD with other forms of intermediate osteopetrosis, but an exceptional abnormality of osteoclast resorption. Like in other osteoclast pathologies an increased risk for progressive osteonecrosis of the jaws should be considered.

doi:10.1016/j.bonr.2020.100618

P339

Primary hyperparathyroidism - related osteitis fibrosa cystica: Exceptional finding nowadays

Mara Carsote[a], Anda Dumitrascu[b], Claudiu Tupea[c], Ana Valea[d], Marian Romeo Smarandache[e], Marioara Cristina Corneci[f], Dumitru Ioachim[g], Monica Livia Gheorghiu[a]
[a]*Endocrine, C. Davila University of Medicine and Pharmacy & C.I.Parhon National Institute of Endocrinology, Bucharest, Romania*
[b]*Radiology, C.I. Parhon National Institute of Endocrinology, Bucharest, Romania*
[c]*Endocrine, C.I. Parhon National Institute of Endocrinoogy, Bucharest, Romania*
[d]*Endocrine, I. Hatieganu University of Medicine and Pharmacy & Clinical County Hospital, Cluj-Napoca, Romania*

[e]Surgery, C.I.Parhon National Institute of Endocrinology, Bucharest, Romania
[f]ATI, C. Davila University of Medicine and Pharmacy & C.I.Parhon National Institute of Endocrinology, Bucharest, Romania
[g]Hystology, C. Davila University of Medicine and Pharmacy & C.I.Parhon National Institute of Endocrinology, Bucharest, Romania

Introduction: Atypical aspects of primary hyperparathyroidism (PHP) like osteitis fibrosa cystica (OGC) are not currently seen especially in patients with normal renal function. We introduce such a case.

Method: This is a clinical case report.

Case presentation: A 56-year old female with negative family history is admitted as emergency for acute hypercalcemia. Her medical records reveal high blood pressure since last 10 years, non-traumatic forearm fracture 15 years ago; menopause since the age of 53. The blood tests show: total calcium 14.6mg/dL (N:8.4-10.3), phosphorus 2.3 mg/dL (N:2.5-4.5), PTH 1107pg/mL (N:15-65), alkaline phosphatase 660U/L (N: 38-105), normal calcitonin, meta/normetanephrines. Computed tomography showed multiple tumour-like bone lesions with cortical disruption at the level of right ribs I,II, III of 1.8 cm maximum diameter, left ribs IV, V, VI of maximum 4 cm, left scapula of 5 cm, bilateral iliac and coxae bones of maximum 9 cm. A tumour of 2.4/4 cm at right cervical area next to right thyroid lobe is suggestive for a parathyroid adenoma which was removed (right inferior parathyroidectomy) and post-operatory histological confirmed. Post-operatory PTH was11 pg/mL. The patient was offered daily 1μg alphacalcidol and 2 g calcium but 2 weeks later she developed acute hypocalcemia (total calcium of 5.5 mg/dL) requiring intravenous calcium and a new dosage of vitamin D replacement, most probably related to the recovery of bone cystic lesions.

Discussion: As limit of the case study we mention no direct histological report of bone anomalies but clinical and paraclinical data are highly suggestive making biopsy unnecessary. We also mention the fact that calcitriol and PTH therapy were not available at the moment for severe hypoparathyroidism.

Conclusion: Even the subject was admitted twice as emergency for hyper, respective hypocalcemia, OFC is a long standing complication of PHP representing an exceptional finding in real life medicine nowadays.

doi:10.1016/j.bonr.2020.100619

P340
Health-related quality of life in paediatric patients with Osteogenesis imperfecta

Adalbert Raimann[a,b], Eva Pairitsch[a], Diana-Alexandra Ertl[a,b], Gabriele Haeusler[a,b]
[a]Medical University of Vienna, Vienna, Austria
[b]Vienna Bone and Growth Centre, Vienna, Austria

Background: Children and adolescents with Osteogenesis imperfecta (OI) often face strong impact on physical, emotional and social wellbeing. Quality of life (QoL) assessment represents a crucial tool for the comprehension of disease-associated burdens. This study aimed to characterize the QoL of paediatric patients with OI and to identify determinants and risk factors for health-related QoL.

Methods: This cross-sectional data evaluation included children and adolescents with genetically confirmed OI aged from 0.4 to 17 years. Paediatric Quality of Life Inventory (PedsQL TM) was performed as part of regular clinical visits. Patients were grouped according to sex, deforming vs. non-deforming type, bisphosphonate treatment and migration background. Pearson correlation coefficient was used to measure relationship between individual core dimensions of health. Multivariate analysis of variance was used to identify differences between patient groups. The level of statistical significance was set at $p < 0.05$.

Results: 25 children with OI (f:m=10:15, deforming: non-deforming type 8:17) were included. There was no difference between total QoL and individual life quality dimension (physical, emotional, social, educational QoL) between the type of OI, sex, established bisphosphonate treatment or migration background. Regarding QoL determining factors, sitting height z-scores exhibited a strong negative correlation with physical functioning in both children with deforming and non-deforming OI ($R=-0.82$, $p < 0.001$).

Conclusion: In this single-centre paediatric cohort, patients with deforming and non-deforming types of OI reported a comparable affection of total and specific QoL. Neither sex, bisphosphonate treatment nor migration background affected QoL significantly. Sitting height z-scores were a strong predictor of QoL, indicating an important role of vertebral affection on life quality.

Prospective assessment of QoL in pediatric patients with OI may aid to earlier identification of functional impairments and to allow targeted support and sustain health dimensions beyond physical outcomes.

doi:10.1016/j.bonr.2020.100705

Bone Reports 13 (2020) 100301

Contents lists available at ScienceDirect

Bone Reports

journal homepage: www.elsevier.com/locate/bonr

New Data Abstracts

POSTER

NDO01

A genome-wide association study in mice reveals a role for *Rhbdf2* in skeletal homeostasis

Roei Levy[a], Clemence Levet[b], Keren Cohen[a], Matthew Freeman[b], Richard Mott[c], Fuad Iraqi[d], Yankel Gabet[a]

[a]*Anatomy & Anthropology, Sackler Faculty of Medicine, Tel Aviv University, Tel Aviv, Israel*

[b]*Dunn School of Pathology, Oxford, United Kingdom*

[c]*UCL Genetics Institute, University College London, London, United Kingdom*

[d]*Clinical Microbiology and Immunology, Sackler Faculty of Medicine, Tel Aviv University, Tel Aviv, Israel*

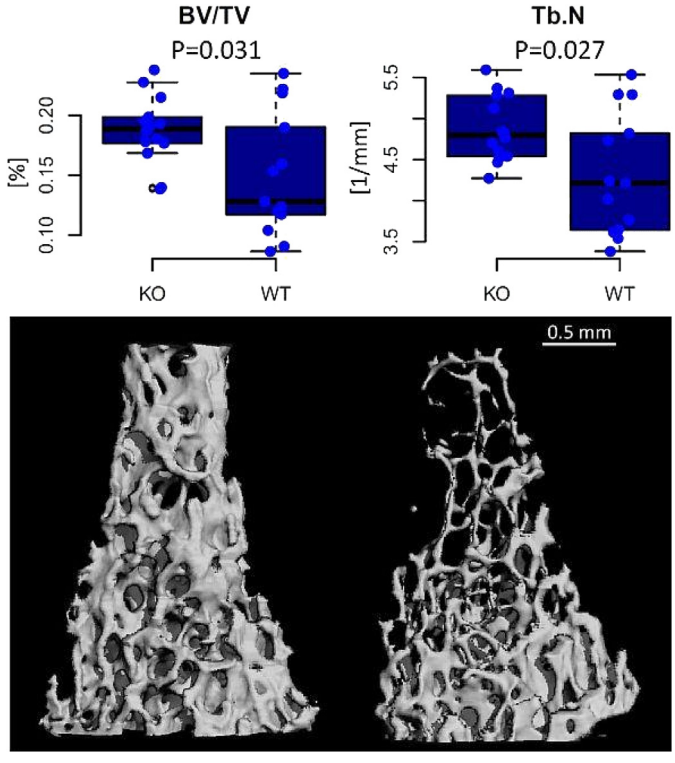

Figure. High trabecular bone mass in *Rhbdf2* knockout mice. µCT analysis in the femora of 11-week-old KO (left) versus WT (right) male mice. Quantitative morphometric parameters presented as box-and-whisker plots, denoting the median and interquantile range. Bottom, representative trabecular bone #d reconstructions for *Rhbdf2* knockout (left) and wild-type (right) mice.

Low bone mass and an increased risk of fracture are predictors of osteoporosis. Individuals who share the same bone-mineral density (BMD) vary in their fracture risk, suggesting that microstructural architecture is an important determinant of skeletal strength. Here, we utilized the rich diversity of Collaborative Cross mice to identify causal genes contributing to bone microarchitecture. Using micro-computed tomography, we examined key structural features that pertain to bone quality in the femoral cortical and trabecular compartments of male and female mice, in a total of 34 genetically distinct lines. We estimated the broad-sense heritability to be 50-60% for all examined traits, and we identified five quantitative trait loci (QTL) significantly associated with six traits. BV/TV and Tb.N contained a marked peak at a locus of ~0.45 Mb between 116.5 and 116.9 Mb on chromosome 11, with peak log*P* values of 7.6 and 6.8. We then refined each QTL by combining information inferred from the ancestry of the mice and the top two genes likely associated with BV/TV and Tb.N were *Aanat* and *Rhbdf2*. We selected 4 extreme lines based on their BV/TV values and collected total bone RNA. We found that although the expression of *Aanat* was undetectable, *Rhbdf2* expression showed a strong inverse correlation with BV/TV ($r=-0.92$). Finally, we found that *Rhbdf2* knockout in mice results in a highly significant increase in BV/TV and Tb.N (+25%, $p=0.027$ and +13%, $p=0.021$, respectively, $n>13$, Figure). Our results indicate that *Rhbdf2* plays a decisive role in bone mass accrual and microarchitecture.

doi:10.1016/j.bonr.2020.100302

NDO02

Proteo-transcriptomic analysis of osteogenic differentiation of valve interstitial cells from patients with calcific aortic valve disease

Arseniy Lobov[a], Daria Semenova[a,b,c], Aleksandra Kostina[a], Artem Kiselev[b], Arsenii Zabirnyk[d], Jarle Vaage[d,e,f], Anna Malashicheva[a,b,c]

[a]*Laboratory of Regenerative Biomedicine, Institute of Cytology of the Russian Academy of Science, Saint Petersburg, Russian Federation*

[b]*Institute of Molecular Biology and Genetics, Almazov Federal Medical Research Centre, Saint Petersburg, Russian Federation*

[c]*Department of Embryology, Saint-Petersburg State University, Saint Petersburg, Russian Federation*

[d]*Department of Molecular Medicine, University of Oslo, Oslo, Norway*

[e]*Institute of Clinical Medicine, University of Oslo, Oslo, Norway*

[f]*Department of Emergency and Critical Care, Oslo University Hospital, Oslo, Norway*

Calcific aortic valve disease (CAVD) is one of the most common cardiac disorder, which may progress to heart dysfunction due to valve calcification. Key pathogenic processes of CAVD are osteogenic

changes of valve interstitial cells (VIC). The mechanisms that trigger osteoblastic transformation in the heart valve are not well understood and only avaliable tretment of CAVD is surgery.

Our previous data show higher sensitivity of VICs from the CAVD patients to osteogenic differentiation (OD) compared to healthy VICs. Here we analyzed VICs from healthy and diseased valves for their differences in osteogenic potential at (1) transcriptomics level at the early stages of differentiation (n=12) and (2) proteomics level at later stages (n=15). VICs were isolated from aortic valves of CAVD patients or from healthy hearts at transplantation, OD was induced by osteogenic medium; transcripts were analyzed 48h after the OD induction while proteomes were analyzed at the 10th day. Total RNA and total protein extracts were analyzed using RNA-seq and shotgun proteomics respectively.

All four comparison groups (control and differentiated VICs from healthy or diseased valves) formed distinct clusters in 3D PLS-DA based on both data (38% and 37% of explained variance for transcriptomics and proteomics data respectively). We identified key molecular markers of osteogenic differentiation in both VICs from healthy and diseased valves after the induction of OD ($P < 0.05$, $FC > 2$). Nevertheless, we observed differential patterns of protein and transcript changes during OD of VICs from diseased or healthy donors. The difference included proteins involved in OD: IGFBP-5 and components of HIF-1 signal pathway (HIF1A, VEGFA, EGLN3; $p < 0.05$).

The data suggest intrinsic differences in sensitivity to proosteogenic stimuli in the aortic valve interstitial cells of healthy persons and of the patients with CAVD.

The project was funded by RFBR research grant 19-29-04082.

doi:10.1016/j.bonr.2020.100303

ND-P01

Microstructural effects of collagen membrane from bovine pericardium in bone defects

Jéssica Suzuki Yamanaka[a], Ana Clara Oliveira[a], Bruna Leonel Carlos[a], Ana Paula Macedo[a], Pedro Babo[b], Raphael Canadas[b], Rui Reis[b], Vitor M. Correlo[b], Antonio Carlos Shimano[a]
[a]*University of São Paulo, Ribeirão Preto, Brazil*
[b]*University of Minho, Guimarães, Portugal*

Techgraft® is a membrane of collagen derived from bovine pericardium produced by Baumer® SA and could be a great alternative biomaterial to application in guided bone regeneration. Therefore, the purpose of this study was to evaluate its microstructural effects in regeneration of bone defect in rat tibia.

Methods: It was an experimental in vivo study approved by the Ethics Committee on Animal Experiments of the University of São Paulo (188/2017). Eighty male Sprague Dawley rats were submitted to surgical procedure to create a bone defect on tibia. Thus, animals were assigned into four groups according treatments: without intervention (CONT), autograft (AG), collagen membrane (CM) and collagen membrane and autograft (CM+AG). Groups were subdivided in two subgroups (n=10) according experimental time (21 and 42 days). In sequence, tibiae were collected and micro-ct analysis was carried out. Data were analyzed using ANOVA test, adopting a 5% significance level.

Results: The membrane induced bone formation in proximity of membrane, in top levels, and increased trabecular appearance of newly formed bone, while autograft groups showed more bone in bottom of defect. BV/TV was lower in CM group compared to other treated groups ($p< 0{,}001$), but all treated groups, including CM, had higher BV/TV than control group ($p< 0{,}005$) at 21 days. At 42 days just CM+AG group showed difference of CONT ($p=0{,}021$). At 21 days AG group had increased trabecular thickness compared to other groups ($p< 0{,}05$); trabecular number was higher in CM+AG group than other groups ($p< 0{,}05$) and higher in CM group than CONT ($p< 0{,}001$); trabecular separation was higher in CONT group than treated groups ($p< 0{,}05$). At 42 days only trabecular number showed significance difference between CM+AG and CONT group ($p=0{,}014$).

Conclusion: The treatment of defects with membrane was positive, but more effective when associated to autograft.

doi:10.1016/j.bonr.2020.100304

ND-P02

Coated latex membrane with calcium β-triphosphate in bone healing of tibia of osteopenic rats

Bruna Leonel Carlos[a], Ana Clara Oliveira[a], Ana Paula Macedo[a], Jessica Suzuki Yamanaka[a], Rondinelli Donizetti Herculano[b], Antônio Carlos Shimano[a]
[a]*Universidade de São Paulo, Ribeirão Preto, Brazil*
[b]*Universidade Estadual Paulista, Araraquara, Brazil*

Bone repair in osteoporotic bones is complicated due to the poor bone quality. Therefore, it is essential to investigate strategies to improve this process. The aim of this study was to evaluate the influence of the latex membrane coated with calcium β-triphosphate in the tissue repair of bone defect performed in the tibia of osteopenic rats, using analysis of bone mineral density (BMD) and mechanical tests. This study was approved by the ethics committee on animal testing of the Medical School of Ribeirão Preto under the Protocol 094/2017. In this study, 40 Sprague-Dawley rats were used. Osteopenia was induced in all animals through ovariectomy and a vitamin D-deficient diet, except in animals of the sham surgery group. After 90 days of ovariectomy, a bone defect of 2.5 mm in diameter was made in the distal third of the animals´ left tibia. The defects received the following treatments per group ($n = 8$): C and SHAM: without specific treatment; L: covered with latex membrane; CBT: filled with calcium β-triphosphate; CBTL: covered with latex membrane coated with calcium β-triphosphate. After 14 days, the animals were killed, and the left tibiae were designated for analysis. BMD was evaluated at the defect site, and the mechanical properties of maximum strength and stiffness were obtained through the mechanical shear test. There was a statistically significant difference for BMD with $p = 0.005$. The CBT (0.141 ± 0.027), L ($0.147 \pm 0{,}0306$) and SHAM ($0.178 \pm 0{,}017$) groups, were the same as each other and presented the highest values of BMD, being different from C (0.113 ± 0.030). The CBTL (0.137 ± 0.023) group had intermediate values. For maximum strength and relative stiffness, there were no statistical differences between groups. In conclusion, natural latex and β-TCP improved BMD at the site of the bone defect, but more analysis is needed to obtain conclusive results.

doi:10.1016/j.bonr.2020.100305

ND-P03

Effects of electroacupuncture on bone defect regeneration in tíbias of ovariectomized rats

Ana Clara Oliveira[a], Jéssica Suzuki Yamanaka[a], Ricardo Tadeu Lopes[b], Ana Paula Macedo[a], Bruna Leonel Carlos[a], Antônio Carlos Shimano[a], Aline Azevedo[a]
[a]*Universidade de São Paulo, Ribeirão Preto, Brazil*
[b]*Universidade Federal do Rio de Janeiro, Rio de Janeiro, Brazil*

Background: Osteoporosis is an osteometabolic disease characterized by low bone mass, deterioration of bone tissue microarchitecture,

delayed bone regeneration, and increased risk of fractures. The use of electroacupunture (EA) for postmenopausal osteoporosis treatment is recent and has been positive for bone quality improvement.

Objective: To verify the effects of EA on the regeneration process in the bone defect in the tibias of ovariectomized rats.

Methods: 48 female Sprague-Dawley rats (aged six weeks) were subdivided into four groups (n=12): OVXDEA: ovariectomy (OVX) + bone defect. + EA; OVXD: OVX + bone defect, without EA; SDEA: SHAM surgery + bone defect + EA; SD: SHAM surgery + bone defect, without EA. OVX surgery was performed. After 90 days, the tibial bone defect was performed bilaterally. EA protocol started after 24h of the bone defect, and used the Zusanli (ST36) Sanyinjiao (SP6) acupoints. Therapy occurred once a day for 20 minutes, for three cycles of 10 days, with one day intervals between them. After euthanasia, bone microarchitecture evaluation by computed bone microtomography (Micro-CT) was performed. Statistical significance between groups were tested using analysis of variance (ANOVA); ($P< 0.05$ was considered statistically significant). The OVXD group had lower values for micro-CT, being statistically significant.

Conclusions: It can be concluded that EA may present the improvement of boné microarchitecture in the bone defect model in osteopenic tibias. Further studies in this area are suggested.

doi:10.1016/j.bonr.2020.100306

ND-P04

A novel mouse model to study fracture healing at the proximal femur

Melanie Haffner-Luntzer[a], Birte Weber[b], Charles Lam[c], Verena Fischer[a], Miriam Kalbitz[b], Anita Ignatius[a], Ralph S. Marcucio[c], Theodore Miclau[c]
[a]*Institute of Orthopedic Research and Biomechanics, University Medical Center Ulm, Ulm, Germany*
[b]*Department of Traumatology, Hand-, Plastic-, and Reconstructive Surgery, University Medical Center Ulm, Ulm, Germany*
[c]*Orthopedic Trauma Institute, Department of Orthopedic Surgery, University of California, San Francisco, United States*

The majority of fractures especially in elderly and osteoporotic patients occurs in metaphyseal bone due to the susceptibility of trabecular bone to microstructural damage. While these injuries are important from a clinical standpoint, adequate small animal models to study them are lacking. Therefore, the aim of the current study was to develop a novel mouse model to study metaphyseal fracture healing at the proximal femur. 12 weeks old female C57BL/6J mice were used for the study (n=6 per group; $p< 0.05$). We successfully combined an open osteotomy approach to the proximal femur with a closed approach for intramedullary stabilization. No animals were lost due to surgical issues or anesthesia. All animals displayed normal limb loading and a physiological gait pattern within the first three days after fracture. µCT analysis revealed successful implementation of the osteotomy between the lesser and the third trochanter in all animals. Bony bridging score increased significantly between d14 and d21 (0.2 vs. 3.5). Bone volume ratio also increased significantly between d14 and d21. Total callus volume decreased significantly between d14 and d21. Histomorphometric analysis of Safranin O-stained sections revealed that all fractured healed via endochondral ossification, whereas relative amount of cartilage decreased and relative amount of bone increased between d14 and d21. All fracture calluses at d21 displayed less than 10% of cartilage tissue, indicating successful cartilage-to-bone transition between d14 and d21. TRAP staining showed high osteoclast abundance and activity at the rims of the fracture callus at d14 and throughout the whole fracture callus at d21 after fracture, indicating that fracture callus remodelling has already started at d21 after fracture. Our novel model provides a fast, reliable and inexpensive way to study metaphyseal fracture healing in mice. Future studies using osteoporotic mice might help to unravel molecular mechanisms of delayed osteoporotic fracture healing.

doi:10.1016/j.bonr.2020.100307

ND-P05

Effects of the escitalopram oxalate on densitometric parameters at the intact and bone callus in growing and young adult rats

Roberta Shimano[a], Ariane Zamarioli[a], Ana Paula Macedo[b], José Batista Volpon[a]
[a]*Department of Orthopedics and Anesthesiology, University of Sao Paulo, Ribeirão Preto, Brazil*
[b]*Department of Dental Materials and Prosthesis, University of Sao Paulo, Ribeirão Preto, Brazil*

Objective: to assess the effect of the escitalopram oxalate intake on densitometric analysis at the intact femur and at the fracture callus in growing and young adult rats.

Methods: Four-week-old and 8-week-old Hannover rats (n=28) were distributed into four groups: GP: growing and placebo; AP: adult and placebo; GE: growing and escitalopram; and AE: adult and escitalopram. Daily administration of 2.0 mg/kg of escitalopram (or saline solution) were orally administered for 35 days. Additionally, a fracture at the right femur was produced in all animals on day 21. Densitometric analysis (BMD and BMC) was performed at the distal metaphysis and at the neck of the intact femur, and in the whole bone callus. Analysis of variance with Bonferroni adjustment was made for comparisons ($p\leq0.05$).

Results: both the BMD at the distal femur ($p=0.039$) and BMC femoral neck ($p=0.043$) were higher in adult than growing animals. The drug-treated growing and young adult animals showed significantly lower BMC ($p=0.042$) and BMD ($p=0.027$) at the distal femur, which infer a negative effect of the drug on bone mass. This decrease in bone density did not differ among immature and mature animals ($p=0.207$). Conversely, the escitalopram oxalate intake did not affect the callus density in either group ($p=0.184$).

Conclusion: the escitalopram oxalate administration equally impaired bone density at the intact femur both in immature and mature animals. However, bone callus density remained unchanged with the pharmacological agent.

doi:10.1016/j.bonr.2020.100308

ND-P06

Different prostate cancer bone metastasis models respond differently to treadmill exercise

Hector Arredondo[a], Alexandria Sprules[b], Colby Eaton[a], Ning Wang[a]
[a]*Oncology and Metabolism, University of Sheffield, Sheffield, United Kingdom*
[b]*Sheffield Hallam University, Sheffield, United Kingdom*

Background: Prostate cancer (PCa) is a leading cause of death in men with a predilection to metastasize into bone, when the disease is considered to be uncurable. Exercise has been suggested to improve the health of patients with PCa but no current studies on its effects on PCa bone metastasis.

Hypothesis: Treadmill exercise can prevent the progression of PCa bone metastasis.

Methods: Human xenograft PCa cell line PC3 and murine syngeneic RM1-BM cells were intracardiacally injected (~1x10 cells/injection) into BALB/c nude (n=8) and C57BL/6J mice (n=12),

respectively. The following day, the mice were subjected to treadmill exercise (12 meters/minute, 5° inclination, 30 minutes/day, 5 days/week) for 3 weeks. Bioluminescence assay was used to track skeletal tumour growth weekly and micro-CT was used to analyse bone morphometrics ex vivo. Naïve mice (n>6) were subject to the same treadmill protocol and used to assess the osteogenic response. Animal procedures were ethically approved by The University of Sheffield, UK.

Results: In the xenograft model, the treadmill exercised mice developed significantly higher tumour burden ($p< 0.05$, Mann-Whitney test) in their hindlimbs compared to sedentary controls. The bone structure was not improved by treadmill exercise according to micro-CT analysis. In contrast, the syngeneic model showed significantly lower tumour burden in exercised mice compared to controls ($p< 0.05$, Mann-Whitney test) and a tendency to significantly improved survival curve ($p=0.07$, Gehan-Breslow-Wilcoxon test). The trabecular thickness (Tb.Th) was found significantly higher compared to controls ($p< 0.001$, unpaired t-test). In the naïve baseline study, the trabecular BV/TV had a 7.5% increase in C57BL/6J but 8.5% reduction in BALB/c nude mice, compared between exercised to sedentary controls.

Conclusion: Treadmill exercise alleviates PCa growth in bones of syngeneic RM1-BM/C57BL/6J but not the xenograft PC3/BALB/c nude model, a possible consequence of different osteogenic response to treadmill by the two mouse strains.

doi:10.1016/j.bonr.2020.100309

ND-P07

Estrogen-mediated downregulation of HIF-1a signaling in B lymphocytes influences postmenopausal bone loss

Xianyi Meng[a], Zhen Lin[a], Iga Janowska[b], Shan Cao[a], Koshiro Sonomoto[a], Darja Andreev[a], Karl Xaver Knaup[c], Michael Sean Wiesener[c], Marta Rizzi[b], Georg Schett[a], Aline Bozec[a]

[a]*Department of Internal Medicine 3, Friedrich-Alexander-University Erlangen-Nürnberg (FAU) and Universitätsklinikum Erlangen, Erlangen, Germany*

[b]*Department of Rheumatology and Clinical Immunology, Medical Center-University of Freiburg, Faculty of Medicine, University of Freiburg, Freiburg, Germany*

[c]*Department of Internal Medicine 4, Friedrich-Alexander-University Erlangen-Nürnberg (FAU) and Universitätsklinikum Erlangen, Erlangen, Germany*

In the bone marrow, B cells and bone resorbing osteoclasts co-localize and form a specific microenvironment. How B cells functionally influence osteoclasts and bone architecture is poorly understood.

We demonstrate that hypoxia-inducible factors-1a (HIF-1 a) signaling in bone marrow B cells regulates postmenopausal osteoporosis through RANKL-mediated osteoclast formation. Deletion of HIF-1 a in B cells prevents estrogen deficiency-induced bone loss in mice, whereas B cell-specific *Vhl* knockout mice with prolonged HIF-1 a signaling in B cells showed enhanced RANKL production and osteoclast formation. Using high-throughput analyses, we show that estrogen controls HIF-1 a protein stabilization and its downstream *Rankl* transcription through HSP70 induction. Moreover, administration of the HSP70 inducer, Geranylgeranylacetone (GGA), conferred a remarkable protection again ovariectomy-induced bone loss. Interestingly, positive correlation of *RANKL*, and *HIF1A* gene expression in human bone marrow B cells and a reduction of *HSP70* gene expression in circulating B cells from postmenopausal patients, suggesting the HSP70/HIF-1 a axis might serve as new therapeutic targets against osteoporosis.

Hence, these data describe a previously unrecognized role of HIF-1 a signaling for RANKL production by bone marrow B cells, which controls bone homeostasis and osteoclastogenesis.

doi:10.1016/j.bonr.2020.100310

ND-P08

Type 2 diabetes impairs mesenchymal stem cells functions and differentiation

Jonathan Ribot[a], Rebecca Landon[a], Cyprien Denoeud[a], Guilhem Frescaline[a], Morad Bensidhoum[a], Graciela Pavon-Djavid[b], Hervé Petite[a], Fani Anagnostou[a,c]

[a]*Laboratory of Bioingénierie et Biomécanique Ostéo-articulaires - UMR CNRS 7052, Paris 7-Denis Diderot University, Paris, France*

[b]*Laboratory for Vascular Translational Science, Cardiovascular Bioengineering - INSERM U1148, Paris 13 Sorbonne University, Paris, France*

[c]*Department of Periodontology, Service of Odontology,-Pitié Salpetrière Hospital, et Hôtel-Dieu Hospital AP-HP, Paris 7-Denis Diderot University, U.F.R. of Odontology, Paris, France*

Objective: Bone marrow-mesenchymal stem cells (BMMSCs) have the capacity to proliferate and to differentiate into multilineage. They play a key role in osteogenesis and angiogenesis. Type 2 Diabetes Mellitus (T2DM) changes the bone marrow microenvironment and is associated with bone fragility and impaired bone healing. The present study focused to characterize the T2DM-microenvironment impact on BMMSCs select functions pertinent to bone repair.

Materials and methods: BMMSCs were harvested from Zucker Diabetic fatty (ZDF) rats (13-weeks-old; early diabetes) and their LEAN littermates (ZL) as controls. Formation of fibroblastic-like colonies, proliferation, apoptosis and migration were analyzed using established methods. Adipogenic differentiation of BM-MSCs was determined by oil red O staining and adipogenic genes expression. Osteogenic differentiation by alkaline phosphatase activity, calcium content and marker genes expression. Angiogenic potential was evaluated by angiogenic markers expression using matrigel plug *in vitro* et *in vivo*.

Results: The results obtained showed that the ZDF-BMMSCs were fewer, with limited clonogenicity (by 45%; $p< 0.05$), proliferation (by 50%; $p< 0.001$), migration capability (by 25%; $p< 0.05$) and increased apoptosis rate (by 60%; $p< 0.001$), than their ZL counterparts. Compared to ZL-BMMSCs, the ZDF-BMMSCs cultured in adipogenic medium, exhibited enhanced adipogenic differentiation (upregulation of PPARG, adiponectine and FABP4) while in osteogenic medium, their potential to differentiate into the osteoblast phenotype was less impacted. Moreover, ZDF-BMMSCs expressed differentially angiogenic genes, specifically 10 genes were upregulated and 11 genes were downregulated, and exhibited impaired vascular formation *in vivo*.

Conclusion: The results of the present study provide evidence that BMMSCs harvested from a T2DM microenvironment were dysfunctional. They may partially explain the altered bone tissue homeostasis and compromised repair in diabetic patients and set the basis for a rationally designed BMSC-based therapy.

doi:10.1016/j.bonr.2020.100311

ND-P09

SLIT2/ROBO1-axis intensifies inflammation, M1 macrophage polarization, and alveolar bone loss in periodontitis, possibly via the activation of MAPK pathway

Liping Wang[a], Zheng Jing[a], Janak Lal Pathak[a], Lijing Wang[b], Linhu Ge[a]

[a]*Key Laboratory of Oral Medicine, Guangzhou Institute of Oral Disease, Affiliated Stomatology Hospital of Guangzhou Medical University, Guangzhou, China*

[b]Vascular Biology Research Institute, School of Life Science and Biopharmaceutics, Guangdong Pharmaceutical University, Guangzhou, China

SLIT2, a member of neuronal guidance cues, has been reported to regulate inflammation and cancer progression. SLIT2/ROBO1-axis facilitates the proliferation of osteosarcoma cells and inhibits their apoptosis. This study aims to explore the expression pattern of SLIT2 in periodontitis and its role in disease progression and bone loss. Gingival tissue of 20 periodontitis patients and 20 healthy-controls was obtained. Ligature-induced periodontitis (LIP) mice-model was developed in Slit-Tg and wildtype-mice. The effect of SLIT2 overexpression on inflammation, M1 macrophage polarization, and alveolar bone loss in periodontitis was analyzed extensively. Ethical approval was obtained for the use of human tissue samples and animals. The selected significance level was $P< 0.05$. In periodontitis-affected gingival-tissue (PAT), SLIT2 expression was 4.4-fold higher compared to healthy-volunteers. LIP enhanced SLIT2 expression in PAT and blood circulation of wildtype-mice by 4.8-, and 5.0-fold, respectively. In Slit2-Tg-mice PAT, SLIT2 expression was 1.5-fold higher compared to wildtype-mice. Micro-CT and histomorphometric analysis revealed a 1.3-fold higher cement-enamel-junction to the alveolar-bone-crest (CEJ-ABC) distance and alveolar bone loss in LIP Slit2-Tg-mice compare to LIP wildtype-mice. Results from RNA-sequencing, RT-qPCR, and ELISA showed a higher expression of *Cxcr2, il-8,* TNFα, IL-6, and IL-1β in Slit2-Tg-mice PAT compared to wildtype-mice. Slit2-Tg-mice PAT showed a higher number of osteoclasts, M1 macrophages, and the upregulation of Robo1 expression. Slit2-Tg-mice PAT showed upregulation of M1 macrophage marker CD16/32 and osteoclastogenic markers Acp5, Ctsk, and Nfatc1, but osteogenic markers (ALP, OPN, OCN) remained unchanged. Immunohistochemistry unveils the higher vasculature and infiltration of CD45+ inflammatory cell in Slit2-Tg-mice PAT. RNA-sequencing, GO-pathway enrichment analysis, and western blot analysis revealed the activation of the MAPK signaling pathway in Slit2-Tg-mice PAT. In conclusion, SLIT2/ROBO1-axis intensifies inflammation, M1 macrophage polarization, osteoclastogenesis, and alveolar bone loss in periodontitis, possibly via activation of MAPK signaling, suggesting the role of SLIT2/ROBO1-axis on inflammation-mediated bone loss.

doi:10.1016/j.bonr.2020.100312

ND-P10

Effects of running exercise on bone histological parameters in Wistar rats: Comparison between continuous and intermittent running

Celine Bourzac[a,b], Stephane Pallu[b,c], Morad Bensidhoum[b], Rkia Wazzani[b], Hugues Portier[b,c]
[a]Clinique équine, Ecole Nationale Veterinaire d'Alfort, Maisons-Alfort, France
[b]Laboratoire B3OA UMR CNRS 7052 INSERM U1271, Universite de Paris, Paris, France,
[c]COST, Universite d'Orléans, Orléans, France

This study aims to investigate the effects of running exercise on bone histological parameters in Wistar rats. We hypothesized that intermittent running would improve histological quality of cortical bone.

Thirty male Wistar rats were divided in three groups (n=10): sedentary control (SC), continuous running (CR, 45 min at moderate speed) and intermittent running (IR, 5 min at moderate speed, then 2 min of intensive running and 1 min of passive recovery). Training lasted for 8 weeks, 5 days/week, 45 min/day. After sacrifice, tibiae were harvested and included in PMMA. The diaphysis cortical bone surface, osteocyte lacunae occupancy rates (LOR), mean number of apoptotic osteocyte lacunae (cleaved caspase-3) per region in cortical, intermediate and trabecular bone, and mean surface for osteoclastic marking (TRAP) were assessed by histological and immunohistological stainings, using Image J and VHX softwares. Experimental protocols were approved by the local Animal Ethical Committee.

Comparisons were made using a Kruskal-Wallis test, then a Mann-Witney test when applicable, with significance set at $p< 0.05$.

Compared to SC, CR significantly reduced mean cortical surface and LOR, and increased the mean TRAP-positive surface and the mean number of apoptotic lacunae. In contrast, IR significantly increased LOR and decreased the mean number of apoptotic lacunae. TRAP activity was similar between cortical, intermediate and trabecular bone in the CR group, whereas mainly localized in the cortical bone in the IR group.

Continuous running drove cortical bone toward resorption, while intermittent running reduced bone resorption and enhanced cortical bone formation.

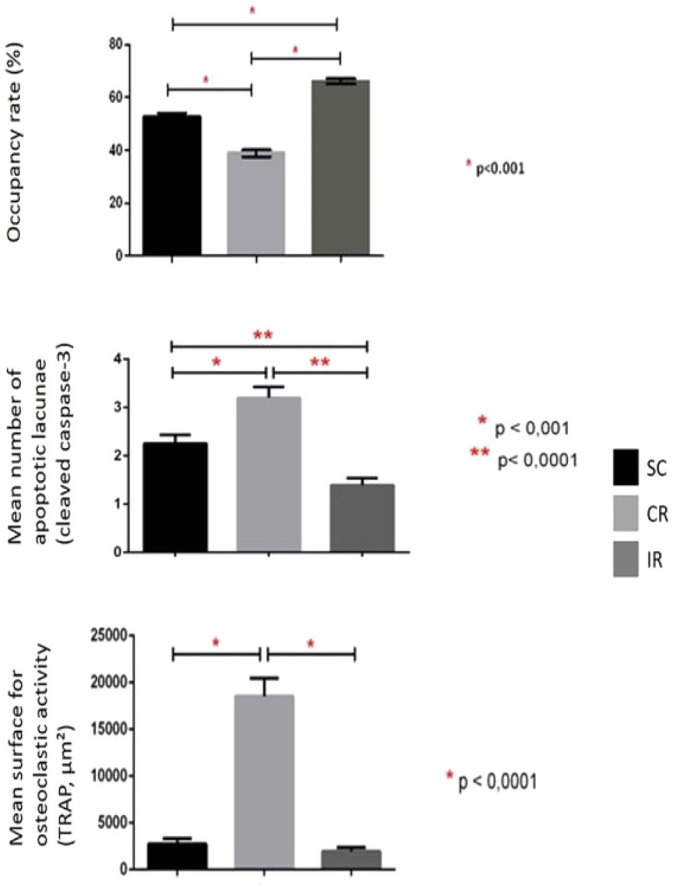

Effects of running exercise on lacunae occupancy rate, apoptotic and osteoclastic activities.

doi:10.1016/j.bonr.2020.100313

ND-P11

The adjustment of bone mineral density measurements for body weight and its impact on the diagnosis of osteoporosis

Xiaoguang Cheng[a], Glen Blake[b], Ling Wang[a], Karen Hind[c]
[a]Department of Radiology, Beijing Jishuitan Hospital, Beijing, China
[b]School of Biomedical Engineering & Imaging Sciences, King's College London, St Thomas' Hospital, London, United Kingdom

[c]Department of Sport and Exercise Sciences, Durham University, Durham, United Kingdom

Background: Although the diagnosis of osteoporosis using DXA T-scores is known to preferentially target patients with lower body weight, there is growing evidence that obesity is not protective against fractures. We compared the effects of body weight on BMD assessments and the diagnosis of osteoporosis by QCT and DXA, respectively.

Methods: The participants were 964 men and 682 women referred for low dose chest CT and a DXA examination as part of their employers' health check-up programs. The ethics committee approved the study and no additional radiation was involved. QCT vBMD was measured in the L1 and L2 vertebrae and DXA aBMD in the spine (L2-L4) and hip. After adjustment of gender and age, vBMD and aBMD residuals were plotted against weight and slopes determined by linear regression.

Results: Slopes of vBMD residuals against weight for spine QCT were not significantly different from zero in men ($P = 0.82$) or women ($P = 0.30$). In contrast, slopes for aBMD residuals were highly statistically significant ($P < 0.001$) for all DXA sites. Although the overall percentage of women and men > 50 years diagnosed with osteoporosis was similar for QCT and DXA, for QCT cases were evenly distributed over the body weight tertiles, while for DXA they were preferentially in the lower weight groups. Adjustment of DXA aBMD for weight using slopes of 0.005 g cm^{-2} kg^{-1} for men and 0.006 g cm^{-2} kg^{-1} for women brought DXA findings into closer alignment with QCT. FRAX 10-year fracture risks gave higher risks at lower weight.

Conclusions: Our study highlights clinically important differences between DXA and QCT in their correlation with body weight and its effect on the diagnosis of osteoporosis. The ability of weight corrected aBMD to predict fracture risk warrants further study.

doi:10.1016/j.bonr.2020.100314

ND-P12

In vivo cortical parameter measurement at the one-third distal radius using HR-pQCT and ultrasonic axial transmission

Donatien Ramiandrisoa[a], Sylvie Fernandez[b], Claudio Araya[c], Martine Cohen-Solal[d], Jean-Gabriel Minonzio[c,e,f]
[a]Bleu Solid, Pomponne, France
[b]Department of rheumatology, Hôpital Lariboisière, Inserm U1132, USPC Paris-Diderot, Paris, France
[c]Escuela de Ingeniería Civil en Informática, Universidad de Valparaiso, Valparaiso, Chile
[d]Department of rheumatology, Hôpital Lariboisière, USPC Paris-Diderot, Paris, France
[e]Centro de Investigación y Desarrollo en Imgeniería en Salud, Universidad de Valparaiso, Valparaiso, Chile
[f]Laboratoire Imagerie Biomédicale, Sorbonne Université, Paris, France

Osteoporosis is a skeletal disease leading to bone fragility and increasing the risk of fractures. Current clinical gold standard, Dual-energy X-ray Absorptiometry, is limited by its projection technique and poor spatial resolution. High Resolution-peripheral Quantitative Computed Tomography (HRpQCT) is able to provide estimates of cortical thickness (Ct.Th) and volumetric bone mineral density (Ct.vBMD) highly correlated to cortical porosity (Ct.Po). Recent studies showed that measurement ultrasonic guided waves can provide estimates of Ct.Th and Ct.Po using axial transmission (AT). The aim of this study is to compare AT parameters, (Ct.Th, Ct.Po) with HR-pQCT measurements (Ct.Th, Ct.vBMD) performed at the site-matched (one-third distal) and conventional (distal) radius locations. In this preliminary study, measurements were performed in a small population but largely representative of age and sex distribution. Sixty six subjects (34 females, 26 males, 19 to 87 years, Body Mass Index between 17 and 30 $kg.m^{-2}$) were recruited from the rheumatology department. AT measurement failed for two subjects. Highly significant ($p < 10^{-5}$) Pearson correlations were found between Ct.Th estimates obtained by the two methods at the one-third distal ($R^2 = 0.84$, RMSE = 0.25mm) and at the distal location ($R^2 = 0.57$, RMSE = 0.40mm). A weak correlation between Ct.Po and vBMD was observed at the one-third distal radius ($R^2 = 0.11$, RMSE = 2.8%, $p = 0.02$), while no correlation existed with the distal Ct.vBMD, partly due to thin cortical thickness (< 0.5 mm) limitation. Note that the site matched correlation between Ct.Po and vBMD increased ($R^2 = 0.50$, RMSE = 1.7%, $p < 10^{-6}$), while keeping the 45 patients associated with the highest quality factor of the AT measurements. This study shows the potential of AT measurements to provide in vivo cortical thickness and porosity estimates. These parameters may improve the identification of patients at high risk of fracture.

doi:10.1016/j.bonr.2020.100315

ND-P13

A short-chain fructo-oligosaccharide promotes peak bone mass and maintains skeleton in ovariectomized rats by an osteogenic effect

Konica Porwal[a], Subhashis Pal[a], Chirag Kulkarni[a], Priya Singh[a], Shivani Sharma[a], Ashim Mullick[b], Naibedya Chattopadhyay[a]
[a]Endocrinology, CSIR-Central Drug Research Institute, Lucknow, India
[b]Tata Chemicals Innovation Centre, Pune, India

Fructooligosaccharide (FOS) is a prebiotic reported to have beneficial skeletal effect in young rats, senescent model of mouse and in children suffering from celiac disease. We studied the skeletal effect of FOS in ovary intact (sham operated) and ovariectomized (OVX) rats (Institutional Animal Ethics Committee approval no:/2018/136 dated 17.9.2018). FOS given at the human equivalent dose (1.85g/kg per oral) to adult female Sprague Dawley sham and OVX rats for 12 weeks. FOS had no effect on body weight gains, body composition and metabolic parameters. In the sham+FOS group, bone mineral content (BMC) in the femur metaphysis and serum procollagen type 1 N-terminal propeptide (P1NP) were higher than the sham+veh group [BMC (g-HA) - 1.16±0.13 (sham+veh) vs. 3.07±0.19 (sham+FOS), p< 0.001 and P1NP (ng/ml) - 2.00±0.3 (sham+veh) vs. 3.74±0.14 (sham+FOS), p< 0.001). In the sham+FOS group, compressive energy to failure of femur head was higher than the sham+veh group [energy (mJ), 165.3±7.3 (sham+veh) vs. 296.4±36.8 (sham+FOS), p< 0.01). FOS treatment to OVX rats resulted in the increase in BMD of femur metaphysis over the OVX+veh group [BMD (g/cm^3) - 0.319±0.025 (sham+veh), 0.177±0.009 (OVX+veh) and 0.23±0.009 (OVX+FOS); p< 0.001 sham+veh vs. OVX+veh and p< 0.01 OVX=veh vs. OVX+FOS). FOS treatment to OVX rats restored the compressive energy to failure at femur head [energy (N) - 165.3±7.3 (sham+veh), 98.13±5.54 (OVX+veh and 211.56±28.86 (OVX+FOS)]. Serum P1NP in the FOS+veh group (3.18±0.26) was higher than the sham+veh (2.00±0.3) and OVX+veh (0.32±0.05) groups [p< 0.001 between sham+veh vs. OVX+veh and p< 0.01 between sham+veh vs. OVX+FOS]. FOS treatment to OVX rats failed to suppress the OVX-induced increase in serum CTX-1. FOS had no effect on the apparent calcium absorption in the sham and OVX rats. We conclude that FOS promotes peak bone mass and protects bone against OVX-induced bone loss by an osteoanabolic mechanism.

doi:10.1016/j.bonr.2020.100316

ND-P14

Site-specificity of bone quality in a patient with osteogenesis imperfecta (OI) type V undergoing total hip arthroplasty

Julian Stürznickel[a], Maximilian Delsmann[a], Oliver Semler[b], Frank Timo Beil[c], Christian Netzer[d], Michael Amling[a], Ralf Oheim[a], Tim Rolvien[a,c]

[a]Department of Osteology and Biomechanics (IOBM), University Medical Center Hamburg-Eppendorf, Hamburg, Germany
[b]Children's Hospital, University of Cologne, Germany, Cologne, Germany
[c]Department of Orthopedics, University Medical Center Hamburg-Eppendorf, Hamburg, Germany
[d]Institute of Human Genetics, University of Cologne, Cologne, Germany

Introduction: Autosomal dominant mutations in *IFITM5* are known to cause the rare type of OI V, associated with increased fracture risk and hyperplastic callus formations. While these complications result in challenges regarding the clinical management of these patients, previous studies of bone biopsies indicated exuberant primary bone formation. We here demonstrate the detailed skeletal status of a 32 years-old female patient with OI V undergoing total hip arthroplasty (THA).

Methods & Results: The patient presented with multiple vertebral and peripheral fractures, dwarfism, and multilocular heterotopic ossifications (HO). Skeletal assessment consisted of dual-energy x-ray (DXA) and high-resolution peripheral quantitative computed tomography (HR-pQCT) and revealed a Z-score -2.7 at femoral neck as well as trabecular bone loss.

After resection of the femoral head (FH) and HO during successful THA, we analyzed both bone specimens by undecalcified histology and microCT as well as quantitative backscattered electron imaging (qBEI). This revealed lower osteoid levels, reduced bone turnover, decreased trabecular number (Tb.N), and loss of connectivity density (Conn.Dens) in the FH compared to the HO. Additional qBEI-analysis revealed higher and more homogenous mineralization as well as lower osteocyte lacunar number (N.Ot.Lc) in the FH compared to the HO.

Discussion: Patients with OI V caused by IFITM5 mutations are characterized by trabecular bone loss, which is caused by loss of secondary spongiosa due to impaired differentiation of chondrocytes to osteoblasts as well as hyperplastic callus formations. Severe skeletal deformities (i.e., scoliosis/dwarfism) pose challenges in surgical management. The obtained histological and qBEI data are in line with previously detected high mineralization and high osteocyte lacunar density in OI V, indicating exuberant primary bone formation. Importantly, analysis of both FH and HO specimens revealed severe trabecular loss in the FH and increased bone mass and turnover in HO, indicating a disturbed control of bone formation and matrix mineralization.

doi:10.1016/j.bonr.2020.100317

ND-P15

Establishing the first pan-European Registry for rare bone and mineral disorders: EuRR-Bone

Corinna Grasemann[a], Marina Mordenti[b], Inês Alves[c], Rebecca Skarberg[d], Ondrej Soucek[e], Marco Roos[f], M. Kassim Javaid[g], S. Faisal Ahmed[h,i], Agnès Lignart[j], Klaus Mohnike[k], Wolfgang Högler[l], Luca Sangiorgi[b,m], Natasha M. Appelman-Dijkstra[i]

[a]Ruhr-University Bochum, Bochum, Germany
[b]IRCCS Istituto Ortopedico Rizzoli, Bologna, Italy
[c]ERN Bond EPAG Representative ANDO Portugal, Lisabon, Portugal
[d]ERN Bond EPAG Representative OIFE, Eindhoven, Netherlands
[e]Fakulti Nemocnice Motole, Prague, Czech Republic
[f]Leiden University Medical Center, Leiden, Netherlands
[g]University of Oxford, Oxford, United Kingdom
[h]University of Glasgow, Glasgow, United Kingdom
[i]Endocrinology, Leiden University Medical Center, Leiden, Netherlands
[j]Assistance Publique - Hopitaux de Paris, Paris, France
[k]Otto-von-Guericke-University Magedeburg, Magdeburg, Germany
[l]Johannes Kepler University Linz and Kepler University Hospital, Linz, Austria
[m]ERN BOND Coordinator, Bologna, Italy

The European Registry for Rare Bone and Mineral Conditions (EuRR-Bone) will be the first pan-European registry for Rare Bone and Mineral Conditions(RBMCs), that constitute a complex group of diseases for which the need of adequate care and shared treatment pathways is pivotal. EuRR-Bone aims to establish a full registry of all diseases covered in the European Reference Network on Rare Bone Diseases(ERN BOND), focussing on >150 rare diseases affecting bones, cartilage and dentin and>40 conditions affecting phosphate and calcium metabolism.

The lack of natural history data across rare bone diseases is substantial, and the quality of care and expertise varies across regions and countries. Depending on age, first symptoms and local healthcare processes, a wide variety of specialists can be involved in the care and follow-up. Until recently, the cross-disciplinary alignment was limited: each discipline had its own network, conference, guidelines and registries.

EuRR-Bone consists of a core group of ERN BOND healthcare providers, affiliated centres and other experts. In addition, patients have been requesting better registry resources to facilitate more research. Their engagement in the planning of EuRR-Bone has therefore been essential and they will play a central role. EuRR-Bone will work closely with the European Registry for Rare Endocrine Conditions project(EuRRECa) to develop: an e-reporting programme that will capture new clinical encounters, a centralised core registry aligned with ERN BOND scope.Clinician and patient facing platforms, will be developed with disease-specific modules on Achondroplasia, Fibrous Dysplasia/McCune Albright syndrome, Osteogenesis Imperfecta and Hypophosphatemia. Finally, EuRR-Bone aims to explore linkages between EuRR-Bone and local, disease-specific registries. EuRR-Bone will take the lead to organise and harmonise data, hopefully improving healthcare for RBMCs, aiming to scale this approach for all rare bone and calcium disorders, favouring both healthcare and research progress as EuRR-Bone will be an open platform for all centres, including non-ERN members.

doi:10.1016/j.bonr.2020.100318

ND-P16

Osteogenesis imperfecta: Fracture characteristics during pregnancy and post-partum

Eugenie Koumakis[a], Azeddine Dellal[b], Marc Debernardi[b], Bernard Cortet[c], Françoise Debiais[d], Rose-Marie Javier[e], Thierry Thomas[f], Nadia Mehsen-Cetre[g], Martine Cohen-Solal[h], Elisabeth Fontanges[i], Michel Laroche[j], Karine Briot[b], Christian Roux[b], Catherine Cormier[k]

[a]Rheumatology Department, Reference Center for Rare Sekeletal and Bone Diseases, Cochin Hospital, Paris, France
[b]Cochin Hospital, Paris, France
[c]Rheumatology Department, Lille, France
[d]Rheumatology Department, Poitiers, France
[e]Rheumatology Department, Strasbourg, France
[f]Rheumatology Department, Saint-Etienne, France
[g]Rheumatology Department, Bordeaux, France
[h]Rheumatology Department, Lariboisière Hospital, Paris, France
[i]Rheumatology Department, Lyon, France
[j]Rheumatology Department, Toulouse, France
[k]Rheumatology Department, Cochin Hospital, Paris, France

Objectives: Fracture occurrence during pregnancy and post-partum, and the determinants of these fractures, are not well known in Osteogenesis imperfecta (OI). The aim of this study was to characterize the fractures that occurred during pregnancy and the post-partum period in a cohort of women suffering from OI.

Materials and methods: Retrospective multicentric study including 50 OI patients (83 pregnancies) from the Reference Center for Rare Bone Diseases of Cochin Hospital, Paris, and patients from other French Reference Centers recruited via the GRIO.

Results: 12 patients (24%) (14 pregnancies/83) had a fracture during pregnancy or in the 6 months following delivery. Among these patients, 2 presented fractures for 2 consecutive pregnancies, and 2 other patients presented fractures during pregnancy and also during the post-partum period. Therefore 16 pregnancy-related fracture events were analyzed. The localization of fractures were: spine (4/16), proximal femur (6/16), pelvis or ribs (3/16), ankle (1) and wrist (1).

Patients characteristics: Mean age was 32,7±3,1 in the fracture group, compared with 29,3±5,0 years-old in the non-fractured group (p=0.002). Patients had OI type 1 in 77.1% of cases, type III in 14.3% of cases, and other OI subtypes in 8.6%. All patients who displayed fractures in the post-partum period were breastfeeding, compared with 47% of patients with no fractures (p=0.03). Fracture during pregnancy or post-partum was not associated with the severity of OI childhood. Bone mineral density was lower in patients with pregnancy-related fractures compared with other patients : spine Z-score -2.9±1.6DS vs -1,48±1,67 (p=0.03), and total hip Z-score -2,05±0,74 vs -0,53±1,36 (p=0.04). At least one concomitant risk factor was identified in 81.8% of fractured patients.

Conclusion: OI management during pregnancy and post-partum should aim for the optimal control of modifiable risk factors. Breastfeeding should be avoided especially in women with low bone mass or other risk factors.

doi:10.1016/j.bonr.2020.100319